Methods in Molecular Biology 1483

Springer Protocols

Philippe Schmitt-Kopplin *Editor*

Capillary Electrophoresis

Methods and Protocols

Second Edition

Humana Press

METHODS IN MOLECULAR BIOLOGY

Series Editor
John M. Walker
School of Life and Medical Sciences
University of Hertfordshire
Hatfield, Hertfordshire, AL10 9AB, UK

For further volumes:
http://www.springer.com/series/7651

Capillary Electrophoresis

Methods and Protocols

Second Edition

Edited by

Philippe Schmitt-Kopplin

Helmholtz Zentrum Munchen, Neuherberg, Germany

Humana Press

Editor
Philippe Schmitt-Kopplin
Helmholtz Zentrum Munchen
Neuherberg, Germany

ISSN 1064-3745 ISSN 1940-6029 (electronic)
Methods in Molecular Biology
ISBN 978-1-4939-6401-7 ISBN 978-1-4939-6403-1 (eBook)
DOI 10.1007/978-1-4939-6403-1

Library of Congress Control Number: 2016952998

Cover Illustration: Capillary Electrophoresis, from small to macromolecules.

Printed on acid-free paper

This Humana Press imprint is published by Springer Nature
The registered company is Springer Science+Business Media LLC New York

Preface

In modern "omics" times, capillary electrophoresis (CE) still finds its place as a powerful high-resolution separation tool with many advantages in terms of small sample consumption, green chemistry environmental-friendly technology, and versatility. CE found its place orthogonally in classical chromatographic, spectrometric, and spectroscopic approaches for the analysis of small to macromolecules and even particles or living cells. The high flexibility of CE is in the many types of applications, and this aspect is illustrated in this new edition of the book *Capillary Electrophoresis: Methods and Protocols*. The goal of this book edition was again to actualize the approaches and relevant applications and techniques from the first edition and present in a few chapters the state of the art in these CE applications and developments. The readers should be able to find essential references in the various fields presented and have some selected methods illustrated as protocols. The combination of focused mini-review and application notes may be very useful for beginners and students to get a quick overview of the field.

Capillary electrophoresis found its place with routine applications in biology, biotechnology, food sciences, and the environment with possible quantitative analysis of various inorganic/organic ions in relevant sensitivity. We present in this edition the principal methods in CE separation involving CZE, MEKC, MECC, NACE, and corresponding hyphenated techniques to organic mass spectrometry and ICP-MS and techniques of single-cell analysis as well as derivatization, enantioseparation, or the use of ionic liquids that are newly highlighted. The use of CZE for the separation of living cells is also highlighted. In terms of applications, various methods for the analysis of small ions, organic acids, amino acids, and (poly)saccharides to peptides are shown with pollutants and biomarkers in food and health. Overall, the book covers a wide field of interest which I hope will again be used for applications.

I thank my colleagues and friends for having participated in the setup of this new edition and for having given shape to the new edition.

Neuherberg, Germany — *Philippe Schmitt-Kopplin*

Contents

Preface . . . . . *v*
Contributors . . . . . *ix*

PART I PRINCIPLES AND INSTRUMENTAL

1 The CE-Way of Thinking: "All Is Relative!" 3
Philippe Schmitt-Kopplin and Agnes Fekete

2 A Semiempirical Approach for a Rapid Comprehensive Evaluation of the Electrophoretic Behaviors of Small Molecules in Free Zone Electrophoresis 21
Philippe Schmitt-Kopplin and Agnes Fekete

3 Derivatization in Capillary Electrophoresis 37
M. Luisa Marina and María Castro-Puyana

4 Statically Adsorbed Coatings for High Separation Efficiency and Resolution in CE–MS Peptide Analysis: Strategies and Implementation 53
Martin Pattky, Katalin Barkovits, Katrin Marcus, Oliver H. Weiergräber, and Carolin Huhn

5 Micellar Electrokinetic Chromatography of Aminoglycosides 77
Ulrike Holzgrabe, Stefanie Schmitt, and Frank Wienen

6 Microemulsion Electrokinetic Chromatography 91
Wolfgang Buchberger

7 Nonaqueous Capillary Electrophoresis Mass Spectrometry 111
Christian W. Klampfl and Markus Himmelsbach

8 Ionic Liquids in Capillary Electrophoresis 131
Ulrike Holzgrabe and Joachim Wahl

9 CZE–CZE ESI–MS Coupling with a Fully Isolated Mechanical Valve 155
Felix J. Kohl and Christian Neusüß

10 Capillary Electrophoresis-Inductively Coupled Plasma Mass Spectrometry 167
Bernhard Michalke

11 Use of CE to Analyze Solutes in Pico- and Nano-Liter Samples from Plant Cells and Rhizosphere 181
A. Deri Tomos

PART II APPLICATIONS FROM SMALL TO MACROMOLECULES

12 Analysis of Small Ions with Capillary Electrophoresis 197
Jatinder Singh Aulakh, Ramandeep Kaur, and Ashok Kumar Malik

13 Metal Ions Analysis with Capillary Zone Electrophoresis 217
Ashok Kumar Malik, Jatinder Singh Aulakh, and Varinder Kaur

14 Bioanalytical Application of Amino Acid Detection by Capillary Electrophoresis 249
Daniela Fico, Antonio Pennetta, and Giuseppe E. De Benedetto

15 Enantiomer Separations by Capillary Electrophoresis 277
Gerhard K.E. Scriba, Henrik Harnisch, and Qingfu Zhu

16 Capillary Electrophoresis of Mono- and Oligosaccharides 301
Mila Toppazzini, Anna Coslovi, Marco Rossi, Anna Flamigni, Edi Baiutti, and Cristiana Campa

17 Use of Capillary Electrophoresis for Polysaccharide Studies and Applications 339
Amelia Gamini, Anna Coslovi, Mila Toppazzini, Isabella Rustighi, Cristiana Campa, Amedeo Vetere, and Sergio Paoletti

18 Separation of Peptides by Capillary Electrophoresis 365
Gerhard K.E. Scriba

19 Microbial Analysis of *Escherichia coli* ATCC, *Lactobacteria* and *Saccharomyces cerevisiae* Using Capillary Electrophoresis Approach 393
Paweł Pomastowski, Viorica Railean-Plugaru, and Bogusław Buszewski

20 Capillary Electrophoretic Analysis of Classical Organic Pollutants 407
Ashok Kumar Malik, Jatinder Singh Aulakh, and Varinder Kaur

21 Capillary Electrophoresis in Metabolomics 437
Tanja Verena Maier and Philippe Schmitt-Kopplin

22 Capillary Electrophoresis in Food and Foodomics 471
Clara Ibáñez, Tanize Acunha, Alberto Valdés, Virginia García-Cañas, Alejandro Cifuentes, and Carolina Simó

23 Capillary Electrophoresis in Wine Science 509
Christian Coelho, Franck Bagala, Régis D. Gougeon, and Philippe Schmitt-Kopplin

Index *525*

Contributors

Tanize Acunha • *Foodomics Laboratory, CIAL, CSIC, Madrid, Spain; CAPES Foundation, Ministry of Education of Brazil, Brasilia, DF, Brazil*

Jatinder Singh Aulakh • *Department of Chemistry, Punjabi University, Patiala, Punjab, India*

Franck Bagala • *Institut Universitaire de la Vigne et du Vin, Université de Bourgogne, AgroSupDijon, Dijon, France*

Edi Baiutti • *Bracco Imaging SpA—CRB Trieste, Trieste, Italy*

Katalin Barkovits • *Functional Proteomics, Medical Proteome-Center, Ruhr-Universität Bochum, Bochum, Germany*

Wolfgang Buchberger • *Institut für Analytische Chemie, Universität Linz, Linz, Austria*

Bogusław Buszewski • *Department of Environmental Chemistry and Bioanalytics, Faculty of Chemistry, Nicolaus Copernicus University, Torun, Poland; Interdisciplinary Centre of Modern Technology, Nicolaus Copernicus University, Torun, Poland*

Cristiana Campa • *GSK Vaccines, Manufacturing Science & Technology, Bellaria di Rosia, Sovicille (Siena), Italy*

María Castro-Puyana • *Department of Analytical Chemistry, Physical Chemistry, and Chemical Engineering, Faculty of Biology, Enviromental Sciences, and Chemistry, University of Alcalá, Alcalá de Henares, Mardid, Spain*

Alejandro Cifuentes • *Foodomics Laboratory, CIAL, CSIC, Madrid, Spain*

Christian Coelho • *Institut Universitaire de la Vigne et du Vin, UMR PAM Université de Bourgogne, AgroSupDijon, Dijon, France*

Anna Coslovi • *GSK Vaccines, Manufacturing Science & Technology, Bellaria di Rosia, Sovicille (Siena), Italy*

Giuseppe E. De Benedetto • *Laboratorio di Spettrometria di Massa Analitica ed Isotopica, Dipartimento di Beni Culturali, Università degli Studi del Salento, Lecce, Italy*

Agnes Fekete • *Lehrstuhl fuer Pharmazeutische Biologie, Julius-Maximilians-Universitaet Wuerzburg, Wuerzburg, Germany*

Daniela Fico • *Laboratorio di Spettrometria di Massa Analitica ed Isotopica, Dipartimento di Beni Culturali, Università, Edificio M, Lecce, Italy*

Anna Flamigni • *Bracco Imaging SpA—CRB Trieste, Trieste, Italy*

Amelia Gamini • *Department of Chemistry and Pharmaceutical Sciences, University of Trieste, Trieste, Italy*

Virginia García-Cañas • *Foodomics Laboratory, CIAL, CSIC, Madrid, Spain*

Régis D. Gougeon • *Institut Universitaire de la Vigne et du Vin, Université de Bourgogne, AgroSupDijon, Dijon, France*

Henrik Harnisch • *Department of Pharmaceutical Chemistry, University of Jena, Jena, Germany*

Markus Himmelsbach • *Institut of Analytical Chemistry, Johannes Kepler University Linz, Linz, Austria*

Ulrike Holzgrabe • *Institut für Pharmazie und Lebensmittelchemie, Universität Würzburg, Würzburg, Germany*
Carolin Huhn • *Institute for Physical and Theoretical Chemistry, Eberhard Karls Universität Tübingen, Tübingen, Germany*
Clara Ibáñez • *Foodomics Laboratory, CIAL, CSIC, Madrid, Spain*
Ramandeep Kaur • *Department of Chemistry, Punjabi University, Patiala, Punjab, India*
Varinder Kaur • *Department of Chemistry, Panjab University, Patiala, Punjab, India*
Christian W. Klampfl • *Institut of Analytical Chemistry, Johannes Kepler University Linz, Linz, Austria*
Felix J. Kohl • *Department of Chemistry, Aalen University, Aalen, Germany*
Tanja Verena Maier • *Research Unit Analytical BioGeoChemistry, Helmholtz Center Munich—Germany Research Center for Environmental Health GmbH, Neuherberg, Germany*
Ashok Kumar Malik • *Department of Chemistry, Punjabi University, Patiala, Punjab, India*
Katrin Marcus • *Functional Proteomics, Medical Proteome-Center, Ruhr-Universität Bochum, Bochum, Germany*
M. Luisa Marina • *Department of Analytical Chemistry, Physical Chemistry, and Chemical Engineering, Faculty of Biology, Environmental Sciences and Chemistry, University of Alcalá, Alcalá de Henares, Mardid, Spain*
Bernhard Michalke • *Research Unit Analytical BioGeoChemistry, Helmholtz Center Munich—Germany Research Center for Environmental Health GmbH, Neuherberg, Germany*
Christian Neusüß • *Department of Chemistry, Aalen University, Aalen, Germany*
Sergio Paoletti • *Department of Life Sciences, University of Trieste, Trieste, Italy*
Martin Pattky • *Institute for Physical and Theoretical Chemistry, Eberhard Karls Universität Tübingen, Tübingen, Germany*
Antonio Pennetta • *Laboratorio di Spettrometria di Massa Analitica ed Isotopica, Dipartimento di Beni Culturali, Università degli Studi del Salento, Lecce, Italy*
Paweł Pomastowski • *Department of Environmental Chemistry and Bioanalytics, Faculty of Chemistry, Nicolaus Copernicus University, Torun, Poland; Interdisciplinary Centre of Modern Technology, Nicolaus Copernicus University, Torun, Poland*
Viorica Railean-Plugaru • *Department of Environmental Chemistry and Bioanalytics, Faculty of Chemistry, Nicolaus Copernicus University, Torun, Poland; Interdisciplinary Centre of Modern Technology, Nicolaus Copernicus University, Torun, Poland*
Marco Rossi • *Bracco Imaging SpA—CRB Trieste, Trieste, Italy*
Isabella Rustighi • *Department of Life Sciences, University of Trieste, Trieste, Italy*
Stefanie Schmitt • *Institut für Pharmazie und Lebensmittelchemie, Universität Würzburg, Würzburg, Germany*
Philippe Schmitt-Kopplin • *Research Unit Analytical BioGeoChemistry, Helmholtz Center Munich—Germany Research Center for Environmental Health GmbH, Neuherberg, Germany*
Gerhard K.E. Scriba • *Department of Pharmaceutical Chemistry, University of Jena, Jena, Germany*
Carolina Simó • *Foodomics Laboratory, CIAL, CSIC, Madrid, Spain*
A. Deri Tomos • *Ysgol Gwyddorau Bioleg, Prifysgol Bangor, Bangor, Gwynedd, UK*
Mila Toppazzini • *GSK Vaccines, Manufacturing Science & Technology, Bellaria di Rosia, Sovicille (Siena), Italy*

Alberto Valdés • *Foodomics Laboratory, CIAL, CSIC, Madrid, Spain*
Amedeo Vetere • *Broad Institute, Cambridge, MA, USA*
Joachim Wahl • *Institut für Pharmazie und Lebensmittelchemie, Universität Würzburg, Würzburg, Germany*
Oliver H. Weiergräber • *Institute for Complex Systems-6, Forschungszentrum Jülich, Jülich, Germany*
Frank Wienen • *Institut für Pharmazie und Lebensmittelchemie, Universität Würzburg, Würzburg, Germany*
Qingfu Zhu • *Department of Chemistry, Wichita State University, Wichita, KS, USA*

Part I

Principles and Instrumental

Chapter 1

The CE-Way of Thinking: "All Is Relative!"

Philippe Schmitt-Kopplin and Agnes Fekete

Abstract

Over the last two decades the development of capillary electrophoresis instruments lead to systems with programmable sampler, separation column, separation buffer, and detection devices comparable visually in many aspects to the setup of classical chromatography.

Two processes make capillary electrophoresis essentially different from chromatography and are the basis of the *CE-way of thinking*, namely, the injection type and the liquid flow within the capillary. (1) When the injection is made hydrodynamically (such as in most of the found applications in the literature), the injected volumes are directly dependent on the type and size of the separation capillary. (2) The buffer velocity is not pressure driven as in liquid chromatography but electrokinetically governed by the quality of the capillary surface (separation buffer dependant surface charge) inducing an electroosmotic flow (EOF). The EOF undergoes small variations and is not necessarily identical from one separation or day to the other. The direct consequence is an apparent nonreproducible migration time of the analytes, even though the own velocity of the ions is the same.

The effective mobility (field strength normalized velocity) of the ions is a possible parameterization from acquired timescale to effective mobility-scale electropherograms leading to a reproducible visualization and better quantification with a direct relation to structural characters of the analytes (i.e., charge and size—see chapter on semiempirical modelization).

Key words Hydrodynamic injection, Electroosmotic flow, Effective mobility, Mobility scale

1 Introduction

It is already more than two decades that Jorgenson and Lukacs [1, 2] presented zone electrophoresis in open-tubular glass capillaries and capillary electrophoresis. This chapter does not aim to repeat the fundamentals on CE that can be found very easily in many good books and review articles [3–11], but to concentrate on some essential specificities of CE relative to liquid chromatographic techniques. In liquid chromatography, the injection volume is determined by the syringe volume or the injection loop size, and the solvent velocity in the column determined by the pressure governed with the pumps. The well-known instrumental setup of CE is remembered in Fig. 1; the main differences to chromatography are the

Philippe Schmitt-Kopplin (ed.), *Capillary Electrophoresis: Methods and Protocols*, Methods in Molecular Biology, vol. 1483,
DOI 10.1007/978-1-4939-6403-1_1,

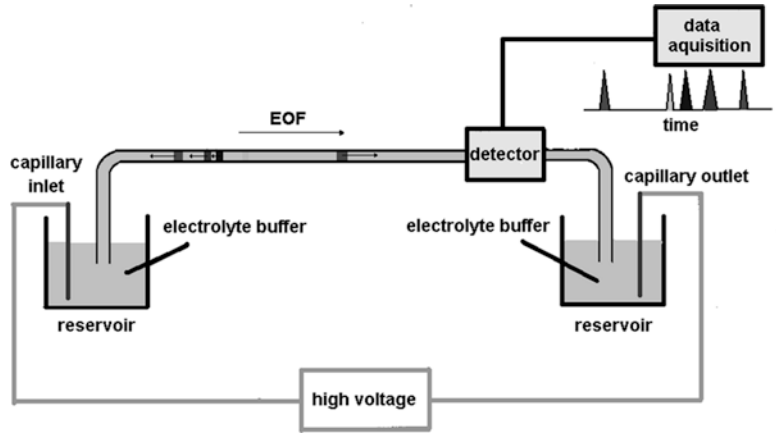

Fig. 1 Schematic representation of capillary electrophoresis

column-setup-dependant injection volumes and *separation-buffer-dependant liquid flux* in the column. These two specificities are detailed in this chapter with some practical aspects and implications.

2 The Injection Mode

The hydrodynamic injection mode is far the most used injection type in CE; the electrokinetic injection sometimes can offer higher selectivity and even sensitivity but is seldom used because being very sensitive to the constitution and quality of the sample. In the hydrodynamic injection mode, pressure forces a small portion of the sample into the open tube capillary plunging in the sample vial. A difference in pressure is applied across the capillary by pressurizing the sample vial and the injected sample volume is proportional to the following solution parameters:

$$V_{inj} = \frac{\Delta P \cdot d^4 \cdot t}{\eta \cdot L} \tag{1}$$

(with ΔP the difference in pressure across the capillary, d is the capillary inner diameter, t the time of pressure application, η the viscosity, and L the capillary length)

Too large sample zones may result in the distortions of the signals in the detector because the sample zone does not reach equilibrium before being detected. The general rule in CE is that the sample plug should never exceed 3–4% of the total column length. Table 1 gives a representative overview of the column volume and the respective injected volumes when applying 0.5 psi for one second to different column dimensions. The injection volume is directly

Table 1
Calculated total volumes, volumes injected per second hydrodynamic injection at 0.5 psi for different columns lengths and i.d.

Column	Total volume	Volume injected	In 1 s
Ld/Lt[a]	i.D. 50 μm	i.D. 75 μm	i.D. 100 μm
30/37	0.7 μl/1.8 nl	1.6 μl/9 nl	2.9 μl/28.6 nl
40/47	0.9 μl/1.4 nl	2.1 μl/7.1 nl	3.6 μl/22.5 nl
50/57	1.1 μl/1.1 nl	2.5 μl/5.8 nl	4.5 μl/18.5 nl
60/67	1.3 μl/0.9 nl	2.9 μl/5 nl	5.2 μl/15.8 nl
70/77	1.5 μl/0.8 nl	3.4 μl/4.3 nl	6 μl/13.7 nl

[a]Length to detector (Ld), total length (Lt)

proportional to the injection time: 10% of the column is thus filled when applying 10 s pressure to a 37 column of 100 μm i.D.

It is important to remember these rules when adapting some methods from the literature to various instruments when the injection pressure conditions and/or column lengths are not necessarily identical.

Additionally, it should be noted that identical injection times with different column i.d. or length lead not only to different column volumes but also to different local sample concentrations when passing the detector. This is in particularly important when analyzing analytes with concentration dependent aggregation properties such as polymeric materials or natural organic matter.

3 The Driving Force: The Electroosmotic Flow

3.1 Origin and Implications

Electroosmosis is fundamental process in CE. The electroosmotic flow (EOF) is a direct consequence of the surface charge on the wall of the uncoated fused silica capillary.

The wall of the fused silica capillary contain silanol groups (pK_a between 3 and 5 depending on the quality of the charge production), which ionize as a function of the pH of the electrolyte solution. This dissociation to silanate ions (SiO^-) produces a negatively charged wall. An electrical double layer is established at solid/liquid interface to preserve electroneutrality.

An externally imposed tangential flow of the medium over the surface leads to a distortion of the ions to create a "streaming potential." This process is reversible and when a voltage is applied, the counter ions and their associated solvating water molecules migrate toward the cathode. The produced movement of ions and the associated water molecules result in a flow of solution toward

the detector. This flow effectively pumps solute ions along the capillary generally toward the detector called as electrically driven pump.

The electroosmotic flow (μ_{eo}) is directly dependant on the chemistry of the buffer such as the viscosity η and its dielectric constant ε:

$$\mu eo = \frac{\varepsilon\zeta}{4\pi\eta r} \tag{2}$$

ζ is the zeta potential measured at the plane of shear close to the liquid–solid interface and is thus directly related to the pH of the buffer. Since ζ is related to the inverse of the charge per unit surface area, the number of valence electrons, and the square root of the concentration of the electrolyte, an increase in the concentration of the electrolyte decreases EOF; strongly adsorbed cations will have the same effects. The direct implication of these effects is that the liquid flow through the capillary depends both on pH and capillary size. Some flows are illustrated in theoretical (Table 2) and real values (Fig. 2).

The EOF is generated by the entire surface and therefore produces a constant flow rate all along the capillary. As a consequence, the electrophoretic flow profile is plug-like in nature. Because analytes are swept at the same rate in the capillary sample, dispersion is minimized. This is an advantage compared to the flow encountered in pressure-driven systems such as liquid chromatography (LC) where frictional forces at the liquid–solid interface, such as the packing and the walls of the tubing, result in substantial pressure drops. Even in an open tube, frictional forces are severe

Table 2

Theoretical buffer flow (nl/min) in 50 cm long capillaries of different internal diameters (i.d. in μm) as a function of the observed time of the EOF (*a t_{eof} of 2.0 min corresponds to a buffer velocity of 25 cm/min)*

t_{eof} (min)	i.d. 100 μm (nl/min)	i.d. 75 μm (nl/min)	i.d. 50 μm (nl/min)	i.d. 20 μm (nl/min)
2.0	1964	1105	491	79
2.5	1571	884	393	63
3.0	1309	736	327	52
3.5	1122	631	280	45
4.0	982	552	245	39
4.5	873	491	218	35
5.0	785	442	196	31
5.5	714	402	178	29
6.0	655	368	164	26
6.5	604	340	151	24

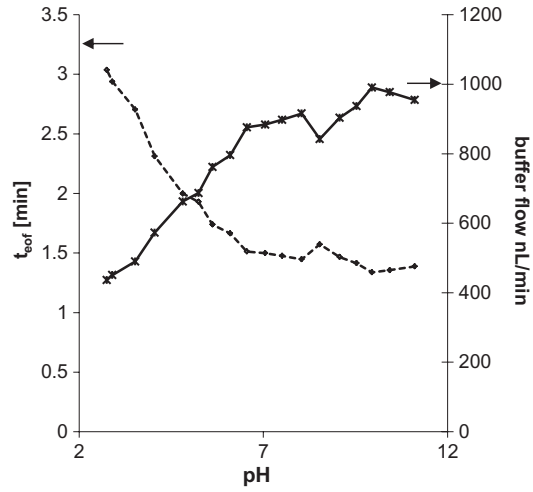

Fig. 2 Real t_{eof} and corresponding buffer flow in a 37 cm capillary, 20 kV

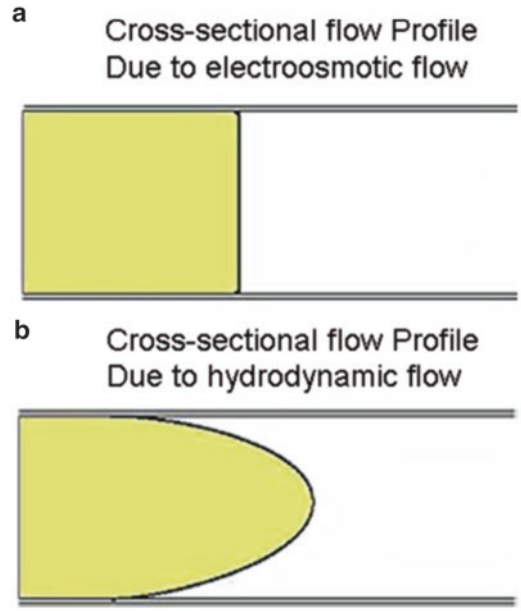

Fig. 3 Flow profiles in electrophoretic and pressure-driven separation columns

enough at low flow rates to result in laminar or parabolic flow profiles (Fig. 3). In laminar flow the solution is pushed from one end of the column and the solution at the edges of the column is moving slower than the solution in the middle of the column, which

results in different solute speeds across the column. Therefore, laminar flow broadens peaks as they travel along the column.

4 "All Is Relative!" or the CE-Mode-of-Thinking

4.1 Qualitative/Quantitative Implications of μ-Scale Transformations

The "*CE-mode-of-thinking*" as it was already called by Whatley [12] is a prerequisite handling CE problems and reaching the goal of robust results. Reaching good reproducibility in migration times (qualitative aspects) and in peak integration (quantitative aspects) is part of these goals: the low reproducibility in these parameters is very often related to little changes in EOF due to uncontrollable alterations of the capillary surface, leading to not always understandable migration time shifts, especially when analyzing real samples (matrix effects). A first step to increase qualitative and quantitative precision is the choice and standardization of the proper operating, calibrating, and equilibrating conditions, leading to stable EOF and reproducible migration times. This goal can be reached with different experimental setups as, for example, adequate rinse steps or voltage preconditioning techniques [13].

The standardization/normalization of raw electrophoretic data sets cannot only be accomplished by experimental optimization, but also by how which they are visualized and analyzed. Software available to control and process signals of the CE were mainly derived from existing classical chromatography techniques and allowed the description of the signal variation only as a function of time. Electrophoretic separations, however as seen before, are not based on the same separation processes as in chromatography and the time-based plots are not necessarily representative of the fundamental parameter controlling mobility which is the velocity of the sample per unit of field strength (not linear with time). An extensive study demonstrated recently the high reproducibility that is afforded by using effective mobility (thus independent of small EOF changes), allowing taking this parameter as a robust reproducibility tool instead of migration times [14]. Only recently has available software adapted to these needs, allowing high precision calculations of the now automated mobility and effective mobility calculations of selected peaks with CE-adapted integration algorithm [15]. This qualitative improvement allows the effective mobility value of a component at given separation pHs (combined with its UV–visible spectrum, and the use of a spectral library as obtained by diode array detectors) to be used as a decision-making tool for accurate peak assignments [16, 17]. Hudson et al. clearly showed the advantages of this alternative for the use of CE-DAD (instead of the classical GC/NPD technique) in forensic toxicology when screening for the "general unknown," among basic drugs in body fluids [18, 19].

Various attempts to normalize total raw electrophoretic data for improved qualitative comparison have already proposed, including plotting the signals versus the *quantity of electric charge* [20], the *1/time domain* [21], using *migration indices* [22], and *migration time ratios* [23], or using dimensionless parameters like the *reduced mobility* [24, 25]. These transformations increase significantly the reproducibility in the calculated parameters but cannot be used directly for the quantification of the analytes. The transformation of the entire time-scaled electropherograms to the corresponding effective mobility scale (using EOF markers or internal standards of known/calculated mobility) is another recent approach for normalizing CE data sets and opens news possibilities in qualitative as well as in quantitative data treatment. This last approach has been followed in our group for several years in different applications [26–28].

4.2 The Mobility Scale Transformation

It is essential to identify some basic rules of CZE [29] that support the proposed x-scale transformation. Each molecule has a specific effective mobility as a function of its own physicochemical characteristics (charge, size) within a given separation buffer (pH and ionic strength governing its charge and hydrodynamic radius). The measured electrophoretic mobility, μ_{mes}, ($cm^2/V\ s$ or $cm^2/V\ min$) is calculated from the measured electrophoretic velocity, v_e, (cm/s or cm/min) and the applied electric field strength E (V/cm), taking account of the migration time (t_{mes}), length of the capillary to the detector (L_d), the total length of the capillary (L_t), and the applied voltage (V):

$$\mu mes = \frac{ve}{E} = \frac{LdLt}{tmV} \tag{3}$$

The measured migration time (t_m) and the corresponding measured mobility do not reflect the velocity (directly correlated to the effective electrophoretic mobility, μ_{eff}) of the analytes in the separation system because they are also dependent on the electroosmotic flow acting as pump for the buffer toward the cathode (see CZE setup in Fig. 4). The effective mobility can thus be regarded as a V/cm-normalized velocity of the molecules in the capillary obtained by changing the reference system from the observer (time measurement of signals through the detection device) to the buffer system itself; this absolute value becomes independent of the used column lengths, voltages, and even buffer velocity fluctuations (EOF changes). The effective electrophoretic mobility (μ_{eff}) of the analytes is calculated by subtracting the electroosmotic flow (μ_{eof}) from the measured electrophoretic mobility (μ_{mes})—*EOF-correction*—and is used as an absolute electrophoretic value. Its value is negative in sign for anions and positive for cations:

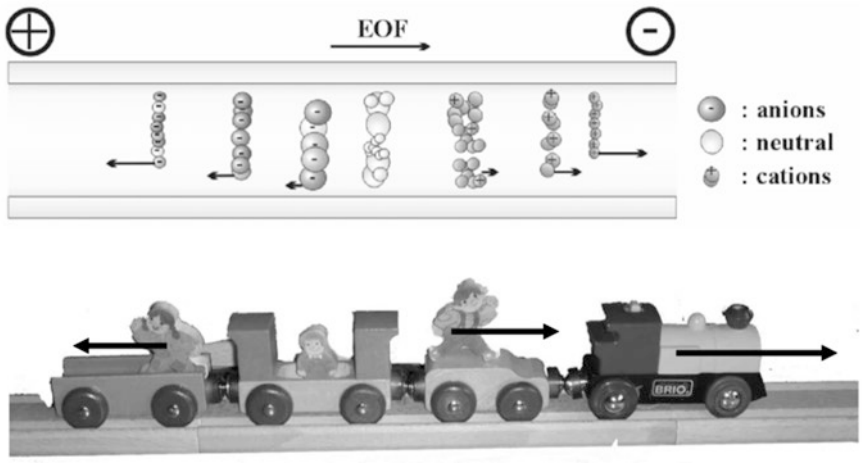

Fig. 4 Capillary zone electrophoresis standard setup; the sample is injected at the anode; the EOF is governing a liquid flow toward the cathode and the sample is separated based on the differences in velocities of the ions in the capillary. Comparison of the setup to a train with a given velocity in which persons are running with always the same own velocity in the same direction than the train (anions), the contrary direction (cations) … or are sitting in the train (neutrals)

$$\mu_{\text{eff}} = \mu_{\text{mes}} - \mu_{\text{eof}} \tag{4}$$

$$\mu_{\text{eff}} = \frac{L_d \cdot L_t \cdot \left(t_{\text{eof}} - t_m\right)}{V \cdot t_m \cdot t_{\text{eof}}} \tag{5}$$

During measurements, the detection signals (from UV/Vis, LIF, MS, etc.) are plotted against time—signal $=f(t_m)$. Transforming the data into the μ-scale does not give any loss in information because of the bit-to-bit correspondence similar to the transformation into the 1/t domain or in infrared spectroscopy from wavelength to frequency terms [21]. The input parameters for the transformation in μ_{eff}–scale are only L_d ,L_t, V, and t_{eof} (the EOF peak is determined manually after addition of mesityl oxide) according to Eq. 5—signal $=f(\mu_{\text{eff}})$.

If an internal standard with known (or measurable) mobility μ_{int} (time t_{int}) is used, the transformation is similar by calculating first t_{eof} from Eq. 5 and substituting the value of t_{eof} to Eq. 5 to obtain the signal as a function of μ_{eff}. A software was written for these two alternatives; normal spreadsheet calculation software can be used as well. Thus, one obtains [6] as:

$$\mu_{eff} = \mu_{\text{int}} + \frac{Ld \cdot Lt\left(t_m - t_{\text{int}}\right)}{V \cdot tm \cdot t_{\text{int}}} \tag{6}$$

4.3 EOF-Dependant Migration Time Fluctuations

No better sentence fits better with the CE-mode-of-thinking than Albert Einstein's "*all is relative*." How explain better the need effective mobility transformation than with: all is relative to the endoosmotic flow!

When assuming only little changes in the viscosity of the buffer (a parameter that is nearly impossible to measure systematically in the laboratory), i.e., when operating at constant temperature, Eq. 5 governs the changes of the migration time (t_m) of a component with the EOF (t_{eof}) as a function of the column lengths (L_d and L_t), the applied voltage (V), and the effective mobility (μ_{eff}) of the analyzed molecule (μ_{eff} has a constant value in the same separation buffer). Illustrated in Fig. 5 is the relationship between these key parameters in plots of migration time (t_m) versus the time of the endoosmotic flow (t_{eof}). The four chosen μ_{eff} correspond to four components bearing charges of 1, 2, 3 and, respectively, 4 (for example, fully ionized benzoic, phthalic, trimellitic, and pyromellitic acid in alkaline pH). Clearly small fluctuations in the EOF from one measurement to another can have big effects on the migration time of components. For example, at 25 kV and with a 60/67 cm column, the change in EOF from 2.2 to 2.6 min would induce a shift in the migration time of a highly charged molecule from 13.4 min to over 60 min.

Molecules with lower mobility, however, would not be affected as much (Fig. 5). This effect is increased for higher applied voltages and lower column lengths.

Small variations in the EOF affecting the migration time of a component (and thus the reproducibility of the observed electropherogram) may occur when analyzing samples from real matrices [30] or trying to follow variations in mobility of samples by addition of some ligands in the separation buffer within affinity capillary electrophoresis studies [31, 32].

However under identical separation buffer conditions, the effective mobility of a component is by definition constant and independent of any changes in EOF. As a response to this fact we proposed a representation of the primary data in the mobility scale (μ-scale) [16, 26, 33]. The plots of the measured signal in the $1/$ time domain (also possible in an online mode) have already been proposed by other authors as useful way of representation of electropherograms [21]. Even though the difference between two peaks becomes a linear function of their difference in mobility in the $1/t$ domain, variations may occur when the EOF is not stable within a measurement series, so that different separation conditions (column length, voltage) cannot be compared directly.

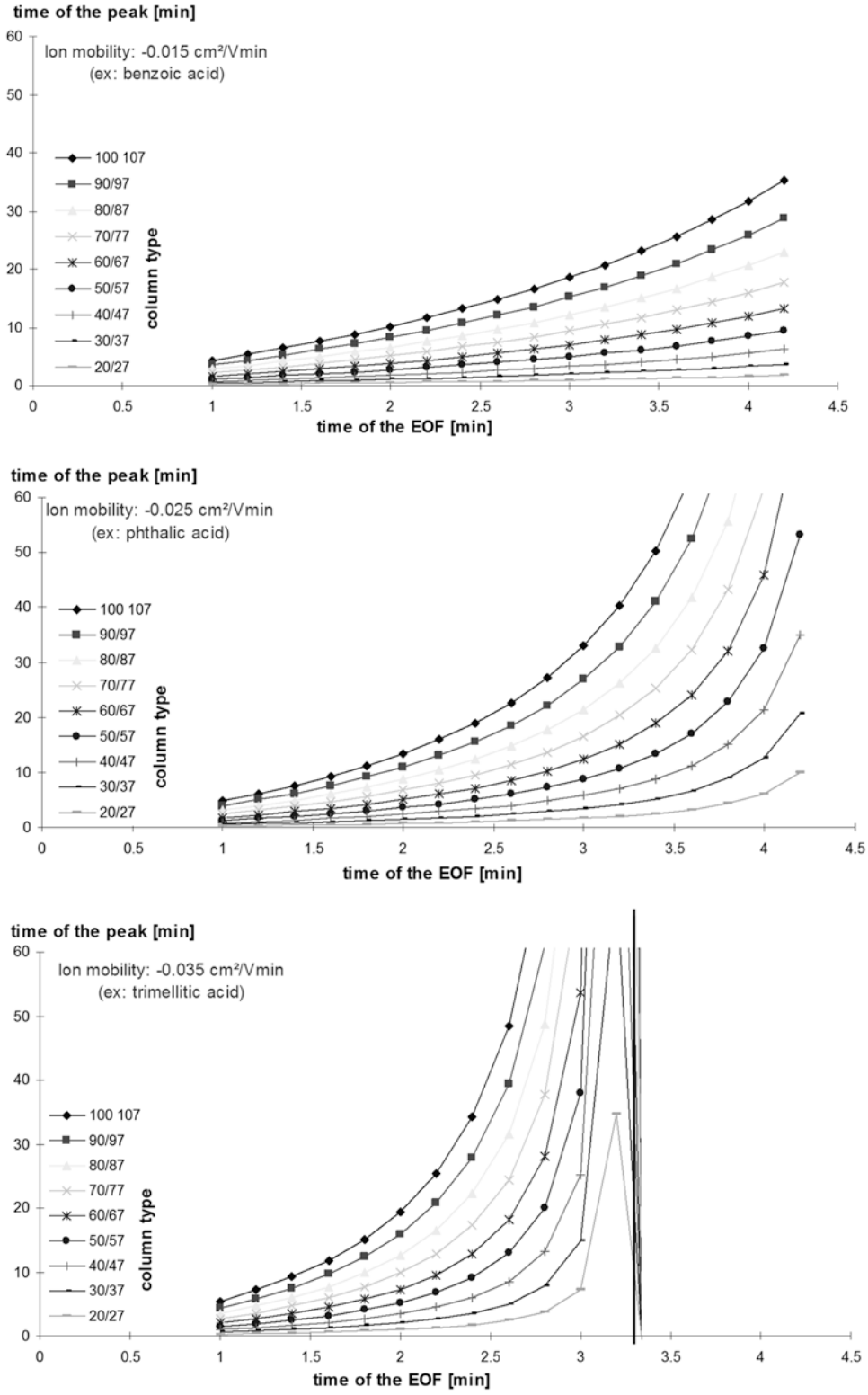

Fig. 5 Theoretical implication on migration times by changes in EOF times for different experimental column lengths (constant voltage separation of 25 kV) for three substances of different effective mobility (corresponding from their mobility to mono-, di-, and tricarboxylated benzenes)

5 Qualification and Quantification Implications

Improvements on the performance characteristics of capillary electrophoretic separations when applying μ-scale transformation according to Eq. 5 are illustrated with an example. Derivatives of benzotriazoles and benzothiazole used as corrosion inhibitor in metalworking fluid were determined with CE under highly basic condition (25 mM CAPS pH 11.75, 15 % acetonitrile) [34]. Because of the alkaline separation medium needed for deprotonization of the analytes, the system is sensitive to any changes of the local activity of the buffer and the silanol groups on the capillary surface. To increase the method robustness necessary for routine application, mobility scale transformation was tested since (1) easy to use, (2) fast, (3) no additional measurements are needed, and (4) the measurements can be compared directly even they were made different days and different instruments since the effective mobility independent on the capillary length and applied voltage. An electropherogram and effective mobility scale of the five analytes is shown in Fig. 6. The X-axis of the mobility scale is minus-scaled which manifests that the analytes were separated as anions. Because the data acquisition rate is linear with time, and the mobility is a function of $1/t$, an increased number of data points will be found from cations to anions in the μ-scale electropherograms. For fast moving cations, a high data acquisition

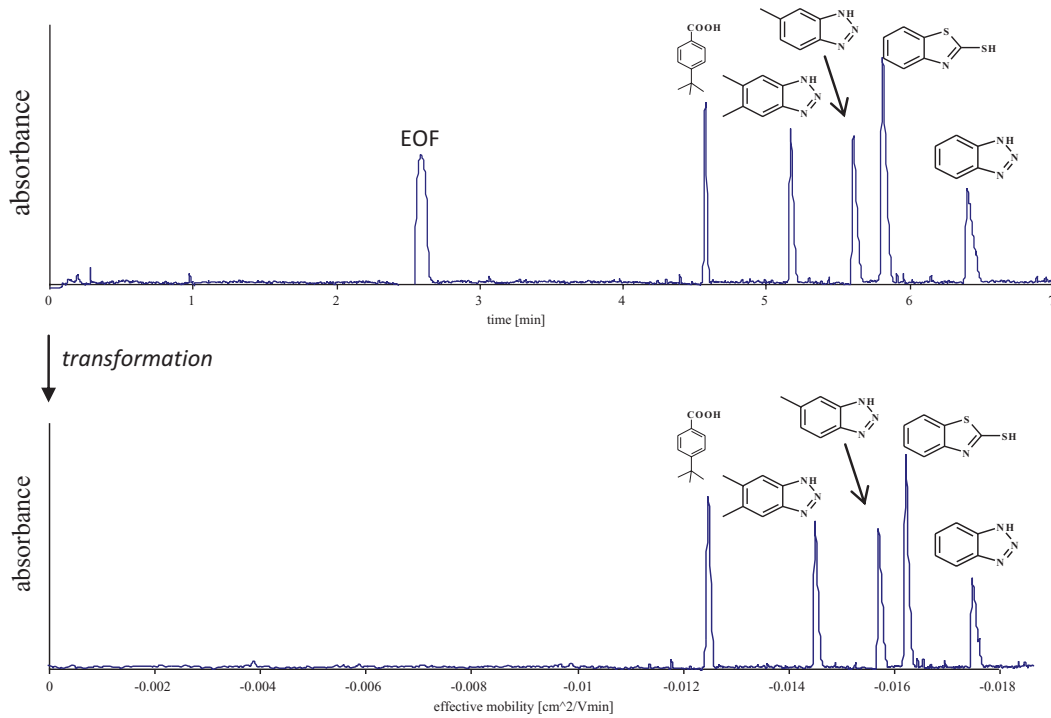

Fig. 6 Electropherogram in time and transformed μ-scale of the anionic analytes

rate should thus be chosen to get good visual peak separation, quantification, and reproducibility. The transformed μ-scale can be handled the same way as the electropherogram in terms of peak integrations. Thus, the needed qualification and quantification parameters can be easily determined and thus the μ-scale is fitting tool for validation and routine application.

A reliable peak assignment requires high precision of identification parameter and sharp and resolved peaks. Thus, the within run, day-to-day, and capillary-to-capillary reproducibility of migration time and effective mobility, experimental theoretical number plate, symmetry factor, and resolution were determined before and after μ-scale transformation as shown in Table 3. The experimental number plates (N) decreased more than third in the migration window of 2 min and it was linearly dependent ($r^2 = 0.925$) on the time. The experimental number of plates increased from 77,000 to 289,000 thousand in timescale to 230,000 to 408,000 thousand after μ-scale transformation. Additionally, when N were determined from effective mobilities, they were independent of the migration of the

Table 3
Performance characteristics of identification using time- and μ-scale

		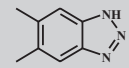	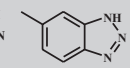	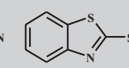	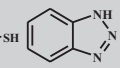
Migration time (min)	4.57	5.17	5.60	5.81	6.40
μ_{eff} (*cm2/V min*)	*–0.0124*	*–0.0144*	*–0.0157*	*–0.0162*	*–0.0174*
N^* from timescale	289,644	176,096	134,367	144,427	77,816
N from μ-scale*	*408,080*	*313,269*	*333,943*	*404,880*	*228,975*
A_S from timescale	*1.50*	*2.22*	*2,60*	*2,60*	*5*
A_S from μ-scale	*1.44*	*2.10*	*2.46*	*2.31*	*4.78*
Resolution R_s from timescale	9.55	5.27	2.22	5.20	
Resolution Rs from μ-scale	*13.16*	*6.85*	*2.97*	*6.57*	
Run-to-run RSD from timescale	2.77%	3.04%	3.37%	3.67%	3.77%
Run-to-run RSD from μ-scale	*0.47%*	*0.34%*	*0.29%*	*0.80%*	*0.26%*
Day-to-day RSD from timescale	4.86%	5.51%	6.01%	6.26%	6.97%
Day-to-day RSD from from μ-scale	*0.81%*	*0.87%*	*0.97%*	*0.90%*	*1.10%*
Cap to cap from timescale	5.27%	5.34%	6.01%	6.32%	6.63%
Capillary to capillary from μ-scale	*1.91%*	*1.36%*	*1.61%*	*1.57%*	*1.45%*

N^* apparent theoretical number plate obtained experimentally, A_S symmetry factor, R_s resolution *RSD* relative standard deviation

analytes (no correlation was found between N and mobilities). Because the endoosmotic flow and the effective mobility of the components are the driving force in most CE separation techniques, the peak width of the analytes is migration time dependent. Cations moving with the EOF will show sharp peaks, and anions (moving against the buffer flux in the capillary) become wider with higher migration times in the time domain. In mobility scale, peak widths become very similar for all analytes including cations to anions, showing that this distortion effect is not only due to diffusion but mainly results from the endoosmotic flow effect (the final velocity through the detection window becomes slower by increasing absolute effective mobility for anions). As a direct consequence of this dependency, a higher reproducibility is found after mobility scale transformation. The within-day precision of the identification was 10–15 times higher when effective mobilities were used as identification parameter determined from μ-scale. The same phenomenon was concluded in the case of day-to-day and capillary-to-capillary precision. The day-to-day and capillary-to-capillary RSDs decreased from 5–7 to 1–2% (the RSD between capillaries have to be lower than 4–6% for fused-silica tubes with 50–250 μm i.d. as described in the literature). Thus, the absolute values of the determined mobilities from 1 day and capillary to the other can be applied and therefore the CE instrument and separation capillary can be effectively controlled.

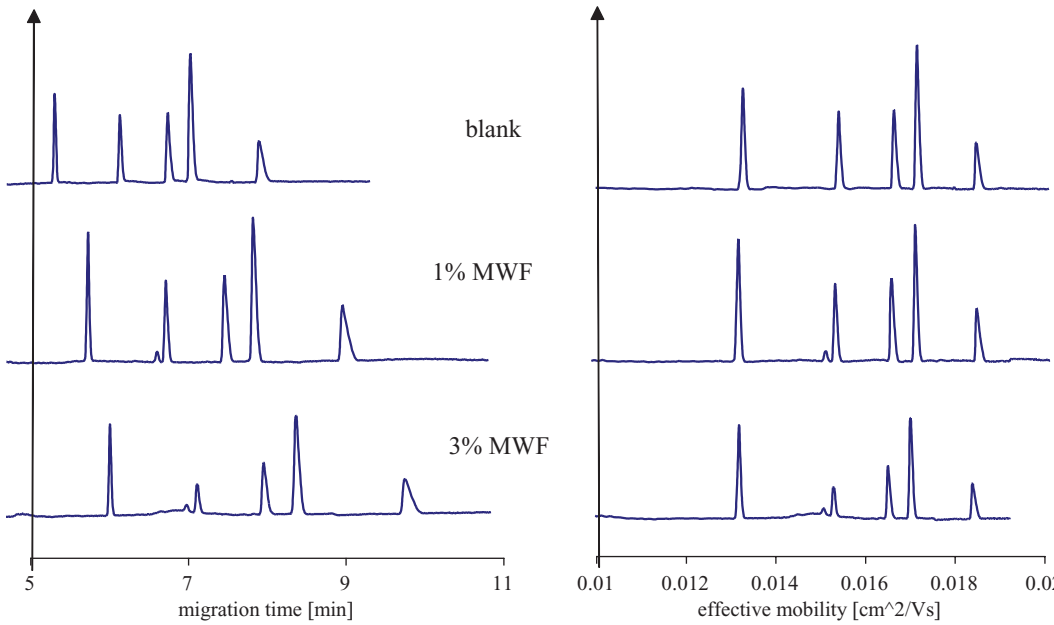

Fig. 7 Electopherogram in time and μ-scale of spiked standard solution of MWF emulsion

The applicability of the mobility scale was also tested when highly complex mixture was analyzed. The standard solution was spiked with metalworking fluid (MWF) which is a stable emulsion of oil and water. As shown in Fig. 7, systematic shifting in the migration time of the solutes was observed in the function of MWF content. It can be caused by different unpredictable factors such as small difference in the viscosity of the injected sample or by matrices differentiating the surface of the capillary wall and thus the activity of the silanol groups resulting in changes in the endoosmotic flow. Therefore, additional measurements or cleanup steps in the sample preparation would have to be added for reliable identification of the target compounds from real samples. When the electropherograms were transformed into μ-scale, the effective mobility became independent on the metalworking fluid content. Therefore, we can conclude that the matrices affected the EOF and not directly the electrophoretic mobility of the solutes.

The applicability of the μ-scale was also tested on quantification was also checked through the validation. Thus, the quantification performance characteristics were also determined from the transformed scale. The precision, linearity, detection limit, and accuracy were identically determined from electropherogram and μ-scale, since no systematic differences between the RSDs of the peak area, the regression coefficient, the limit of detection, and the recoveries were observed. Significant difference in the slope of the calibration curve was determined as shown in Fig. 8 when taking the areas calculated from timescale. To explain this phenomenon, the absorption coefficient of the benzotriazole derivatives was determined in the separation electrolyte with

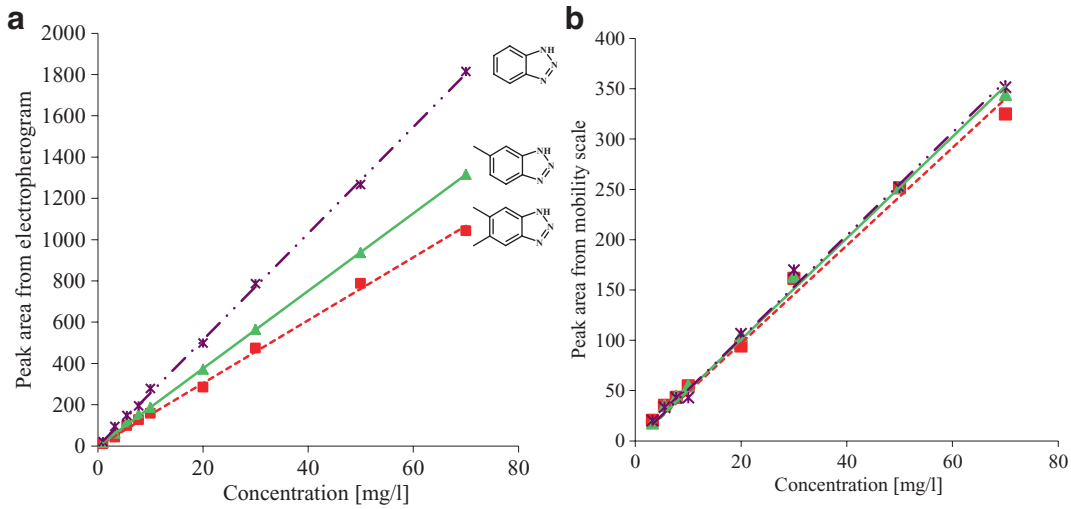

Fig. 8 Calibration curves determined from electropherograms in (**a**) time and (**b**) μ-scale

UV-spectrophotometer since the absorbance depends on the length of the light, absorption coefficient concentration and only this parameter has influence on the slope of the calibration curve. Since the coefficient values were similar, the differences in the slope values determined from electropherogram can be caused by the differences of the time the plug migrating through the detection window. This difference is eliminated by the mobility scale transformation; therefore, the slopes of the benzotriazole derivatives became similar when determined from μ-scale. The μ-scale can be therefore used not only for identification but for quantification without any restrictions.

6 Concluding Remarks on Mobility Transformations

For possible routine analysis, capillary electrophoresis techniques need to give comparable qualitative and quantitative results from run-to-run and day-to-day measurements. Modern technology allows these goals to be reached by new instrumentation. However, for electrophoretic separations where the migration time of an analyte is directly related to the electroosmotic flow (as affected by the matrices), "*chromatographic mode of thinking*" and data processing need to be readapted. Representing electropherograms in the μ-scale brings both qualitative and quantitative advantages. Conversion of the primary time-scaled data to the mobility scale (μ-scale) leads to a better interpretation of electropherograms in terms of separation processes. The benefits include better direct comparison of electropherograms and an easier "peak tracking" when trying to identify single components with complex matrices, especially when the UV–visible signatures of the components are also available. Peak integration also is often more precise when done in μ-scale as compared to the time especially when wide ranges of concentration and voltage are involved. The same data treatment can be done when comparing measurements done with columns of different lengths or upscaling methods from one instrument to the other. Furthermore, this data presentation was proven to be necessary when describing the distribution of effective mobility for polydisperse samples such as charged synthetic polymers and NOM. This transformation is also applicable to other CE techniques where changes in the EOF can alter the stability of migration times, such as CGE, MEKC, and ACE.

It is certainly unusual for the *chromatography-mode-thinkers* to make the transformation from the timescale into the μ-scale but probably "trivial" for *CE-mode-thinkers* who are used to induce differences in the velocities of the molecules they want to separate. The fact is that software to process electrophoretic-based CE data is needed.

References

1. Jorgenson JW, Lukacs KD (1981) Zone electrophoresis in open-tubular glass capillaries. Anal Chem 53:1298–1302
2. Jorgenson JW, Lukacs KD (1983) Capillary zone electrophoresis. Science 222:266–272
3. Shintani H, Polonski J (1997) Handbook of capillary electrophoresis applications, vol 737. Blackie Avademic & Professional, London
4. Rhighetti PG (1996) Capillary electrophoresis in analytical biotechnology, vol 551, CRC series in analytical biotechnology. CRC Press, Boca Raton
5. Li SFY (1993) Capillary electrophoresis. Principles, practice and applications. J Chrom Libr 52:582, Elsevier, Amsterdam
6. Kuhn R, Hoffstetter-Kuhn S (1993) Capillary electrophoresis: principles and practise. Springer, Heidelberg, Berlin
7. Khaledi MG (1998) High-performance capillary electrophoresis: theory techniques, and applications, vol 1050. Wiley, Chichester
8. Guzman NA (1993) Capillary electrophoresis technology, vol 64, Chromatographic science series. Marcel Decker Inc., New York, p 857
9. Baker DR (1995) Capillary electrophoresis, vol 244. Wiley, New York
10. Chankvetadze B (1997) Capillary electrophoresis in chiral analysis. Wiley, Chichester, p 555
11. Deyl Z, Miksik I, Tagliaro F, Tesarova E Editors, (1998) Advanced chromatographic and electromigration methods in biosciences. ELSEVIER, 1125 pages.
12. Whatley H (1999) Making CE work—poonts to consider. LC-GC Europe 12:762–766
13. Shihabi ZK, Hinsdale M (1995) Some variable affecting reproducibility in capillary electrophoresis. Electrophoresis 16:2159–2163
14. Chapman J, Hobbs J (1999) Putting capillary electrophoresis to work. LC-GC Europe 12:266–279
15. Faler T, Engelhardt H (1999) How to achieve higher repeatability and reproducibility in capillary electrophoresis. J Chromatogr A 853:83–94
16. Schmitt-Kopplin P, Fischer K, Freitag D, Kettrup A (1998) Capillary electrophoresis for the simultaneous separation of selected carboxylated carbohydrates and their related 1,4-lactons. J Chromatogr A 807:89–100
17. Hudson JC, Malcom MJ, Golin M (1998) Advancements in forensic toxicology. Page Setter Beckman Coulter, p 2
18. Hudson JC, Golin M, Malcom M (1995) Capillary zone electrophoresis in a comprehensive screen for basic drugs in whole blood. Can Soc Forensic Sci 28:153–164
19. Hudson JC, Golin M, Malcom M, Whiting CF (1998) Capillary zone electrophoresis in a comprehensive screen for drugs of forensic interest in whole blood: an update. Can Soc Forensic Sci 31:1–29
20. Iwata T, Koshoubu J, Kurosu Y (1998) Electropherograms in capillary zone electrophoresis plotted as a function of the quantity of electric charge. J Chromatogr A 810:183–191
21. Mammen M, Colton IJ, Carbeck JD, Bradley R, Whitesides GM (1997) Representing primary electrophoretic data in the 1/time domain: comparison to representations in the time domain. Anal Chem 69:2165–2170
22. Lee TT, Yeung ES (1991) Facilitating data transfer and improving precision in capillary zone electrophoresis with migration indices. Anal Chem 63:2842–2848
23. Yang J, Bose S, Hage DS (1996) Improved reproducibility in capillary electrophoresis through the use of mobility and migration time ratios. J Chromatogr A 735:209–220
24. Kenndler E (1996) Effect of electroosmotic flow on selectivity, effiency and resolution in capillary zone electrophoresis expressed by the dimensionless reduced mobility. J Capillary Electrophor 3:191–198
25. Kenndler E (1998) Dependence of analyte separation on electroosmotic flow in capillary zone electrophoresis: quantitative description by the reduced mobility. J Microcolumn Sep 10(3):273–279
26. Schmitt-Kopplin P, Garmash AV, Kudryavtsev AV, Perminova IV, Hertkorn N, Freitag D, Kettrup A (1999) Mobility distribution description of synthetic and natural polyelectrolytes with capillary zone electrophoresis. J AOAC Int 82:1594–1603
27. Schmitt-Kopplin P, Menzinger F, Freitag D, Kettrup A (2001) Improving the use of CE in a chromatographer's world. LC-GC Europe 14:284–388
28. Schmitt-Kopplin P, Garmash AV, Kudryavtsev AV, Menzinger F, Perminova IV, Hertkorn N, Freitag D, Petrosyan VS, Kettrup A (2001) Quantitative and qualitative precision improvements by effective mobility-scale data transformation in capillary electrophoresis analysis. Electrophoresis 22:77–87
29. Whatley H (1997) Mobility determinations in capillary electrophoresis. Tech Inform Beckman
30. Garrison AW, Schmitt P, Martens D, Kettrup A (1996) Enantiomeric selectivity in the environmental degradation of Dichlorprop as determined by high performance capillary electrophoresis. Environ Sci Technol 30:2449–2455

31. Schmitt-Kopplin P, Burhenne J, Freitag D, Spiteller M, Kettrup A (1999) Developement of capillary electrophoresis methods for the analysis of fluoroquinolones and applications to the study of the influence of humic substances on their photodegradation in aqueous phase. J Chromatogr A 837:253–265
32. Schmitt P, Trapp I, Garrison AW, Freitag D, Kettrup A (1997) Binding of s-triazines to dissolved humic substances: electrophoretic approaches using affinity capillary electrophoresis (ACE) and micellar electrokinetic chromatography (MEKC). Chemosphere 35:55–75
33. Schmitt-Kopplin P, Garrison AW, Perdue EM, Freitag D, Kettrup A (1998) Capillary electrophoresis in humic substances analysis, facts and artifacts. J Chromatogr A 807:101–109
34. Breuer D, Fischer K, Hansen K, Fekete A, Lahaniatis M, Ph S-K (2003) Benzotriazole (1,2,3-benzotriazole, 5-methyl-1H-benzotriazole, 5,6-dimethylbenzotriazole). In: Kettrup A (ed) Analytische methoden band 1, Deutschen Forschungsgemeinschaft, Senatskommosion zur Prüfung gesundheitsschädlicher Arbeitsstoffe-Arbeitsgruppe "Analytische Chemie" p 13

Chapter 2

A Semiempirical Approach for a Rapid Comprehensive Evaluation of the Electrophoretic Behaviors of Small Molecules in Free Zone Electrophoresis

Philippe Schmitt-Kopplin and Agnes Fekete

Abstract

A phenomenological model is proposed for the evaluation of relative electrophoretic migration of charged substances present in mixtures and for the rapid pH optimization prior CZE method development. The simple and robust model is based on the Offord model that takes account of the chemical structure. The effective charge and the molecular mass of the molecule are needed; the charge can easily be calculated from pK_a obtained from known sources or simulated with existing pK-calculation programs. A first example was chosen with the separation of hydroxy-s-triazines to illustrate the applicability of this simple approach for determination of the first buffer-pH conditions prior experimental method optimization when separation of different ions is needed. In a second example, the confirmation of aminoalcohols in the CZE method development of unsaturated hexahydro-triazines and oxasolidines.

Key words Semiempiric model, Mobility simulation, Separation optimization, S-triazines, Aminoalcohols, Formaldehyde releasers

1 Introduction

Especially within the fields of *Genomics, Proteomics,* and *Peptidomics*, models for a better understanding of the free zone electrophoresis of DNA fragments (few bp up to several thousands of bp), proteins, or peptides were developed. These models intended an optimization of the separation conditions, a prognosis of electrophoretic separations of these mixtures, and identification of structures based on standardized experimental separation conditions (i.e., small peptide structures obtained after tryptic digestion) [1–5].

Since the introduction of CE in the 1980s, different simulations of the capillary zone electrophoretic processes were proposed. Some of the simulations aimed at the evaluation of equilibrium (binding toward ions and mobility pH dependency) in CZE [6] and can also be used for optimization of separation parameters [7, 8]. Others principally aimed at understanding peak

Philippe Schmitt-Kopplin (ed.), *Capillary Electrophoresis: Methods and Protocols*, Methods in Molecular Biology, vol. 1483,
DOI 10.1007/978-1-4939-6403-1_2,

anomaly/shape [9], peak sharpening effects [10], anomalous spikes, boundary structures using the Kohlrausch regulating function [11], and allow correct interpretation of experimental CZE results [12]. A last approach allowed the determination of physical–chemical parameters that can be deduced from the electrophoretic behavior under variable experimental conditions (dissociation constants pK_a [13, 14], isoelectric points pI [14], hydrophobicities Log(P) [15], charge [16, 17], binding constants [18]).

We propose to simulate electrophoretic mobilities with a *simple and robust guideline for a rapid method development in CE* based on a model involving easily accessible structural data of the analyte (pK, molecular mass). On the other hand, screening of unknown components through a series of CE experiments at different pH allows the evaluation determination of charge variations of these analytes. The proposed model was verified for low molecular weight components.

2 Semiempirical Models

Semiempirical models were already described from the mid-sixties to predict the mobilities of peptides in electrophoretic separation systems and to obtain information on their amide groups [19]. These descriptions were rapidly adapted to capillary electrophoretic separations of polypeptides and proteins [20]. The effective mobility of an analyte can be generally described with a charge-to-size model where the size of the molecules is approximated by their molecular mass M. It was found to be a continuous function of $M^{-1/3}$ to $M^{-2/3}$, depending on the magnitude of M and the ionic strength of the buffer.

The mobility of an analyte in free solution is defined as the ratio of its electric charge Z (Z= q.e, with e the charge on an electron and q the valency) to its electrophoretic friction coefficient f (Eq. 1).

$$\mu = \frac{qe}{f} \tag{1}$$

All models are based on Eq. 1, with two parameters needing to be estimated: the net charge and the frictional coefficient.

$$\zeta = \frac{Z}{4\pi\varepsilon R\left(1+\kappa R\right)} \tag{2}$$

(R is the sphere radius, k^{-1} the Debye length, ε the permittivity, and Z the particle charge)

Charge estimation: The ζ potential of charged spherical particle is expressed with Eq. 2:

The charge Z can be estimated from the pK of the analytes as a function of the pH with the Henderson–Hasselbalch equation. However for a series of analyzed components, the pK values found in literature databases are often not comparable or useable for the chosen experimental conditions (measured at different ionic strength, temperatures, or in different solvents). In this case, several simulation programs are available and can be used; some were tested within this study. Best results (relative values) are obtained when taking a homogeneous set of values (i.e., calculated with identical programs or from the same database).

Frictional coefficient (f) estimation: This parameter (f) corresponds to the drag (viscous) force the particle experiences when moving with a given velocity under an electrical field and its estimation is more ambiguous than for charge. An approach would be usable to derive it from the Nernst–Einstein equation:

$$D = \frac{kT}{f} \tag{3}$$

(D is the diffusion coefficient, k the Boltzmann constant, T the temperature)

$$\mu = \frac{qe}{kT} \times D \tag{4}$$

(k is the Boltzmann constant, T the temperature, z the charge, μ the mobility)

Because this relationship is rarely used, diffusion coefficients (D) can be determined [21] with Eq. 4 when the mobility and the charge are known:

$$f = 6\pi\eta R \tag{5}$$

(η is the viscosity, R the radius of the ion)

A first approximation of f can be used for spherical shaped and rigid ions through the Stokes Eq. 5:

$$\mu = \frac{qe}{6\pi\eta R} \tag{6}$$

This leads to mobility Eq. 6:

The resulting approximations, however, are very imprecise because R is often unknown and can only be determined on basis of diffusion, sedimentation, or electrophoretic mobility. Moreover,

the solvent/water and ions moving with the analyte are not taken into account. This effect can be estimated taking account of the Debye theory presented earlier and the nature of the solution contiguous to the ion (ionic strength, counterions). The ion cloud can influence the mobility and lead to *relaxation* effects. Cifuentes and Poppe (1997) combined the relaxation effects and electrophoretic retardation effects into a reducing effect on the mobility. They presented a model in which the effects of the deformation of the ion cloud around the moving ion was included and leads to formation of an electric force that counteracts the applied field [2]. In the case of large moving ions (compared to the buffer ions), the relation could be reduced to Eq. 7:

$$\mu = A \times \frac{qe}{6\pi\eta R^2} \tag{7}$$

(with A is a constant)

Theoretical approaches give much insight into the mobility of smaller ions, but fail for highly charged and larger ions. Following a more empirical approach is therefore often the best strategy [2].

3 Mobility Prediction from Structural Data

Many empirical models can be found in literatures that were developed that fit the experimental and predicted data for very specific compounds classes (mainly peptides). These mobility expressions usually include in the formula the charge (Z) of the analyte, its molecular mass (M), or the number of amino acids (n). These formulations include:

Grossman's Eq. (8) [4]:

$$\mu = A \times \frac{\log(Z+1)}{n^B} \tag{8}$$

(Z the charge, A and B are constants, n number of amino acids)

Offords approach (Eq. 9) [5, 19, 22]:

$$\mu = A \times \frac{Z}{M^{2/3}} \tag{9}$$

(Z the charge, A constants, M molecular mass)

$$\mu = A \times \frac{Z}{M^{\mathrm{m}}} \tag{10}$$

$$\mu = A \times \frac{Z}{BM^{1/3} + CM^{2/3}} \tag{11}$$

(Z the charge, A, B, C and m constants, M molecular mass)

Compton's Eqs. (10) and (11) [3, 20]:

Cifuentes and Poppe conducted this development further and came up with a relation giving the best mobility prediction for peptides (Eq. 12) with a combination of Eqs. 8 and 9 [1, 2, 23].

$$\mu = A \times \frac{\log(1 + BZ)}{M^{C}} \tag{12}$$

(Z is the charge, A and B are constants, M is the molecular weight)

An interesting approach is the one of Fu and Lucy [24] that integrated the effects of hydration using the McGovan hydration increments [25] to further improve the prediction. It is however limited to monoamines and the equations are far from being phenomenological.

4 Experimental Approach

4.1 A Semiempirical Model for Small Molecules

For the development of a general mobility model, we wanted to stay as close as possible to the phenomenological approach (Eq. 7). Any purely mathematical data linearization and curve fitting would improve the prediction but would limit the possibility of data interpretation with the particular samples used for the fitting (see equations earlier).

Originally we wanted to use the equation for anionic NOM (natural organic matter); we chose substances similar in structure and mobility, like phenolic, aliphatic, and sugar acids. The relation $\mu = f$(charge, size) had to be tested over different pH ranges to be able to interpret mobility changes versus pH as derived from charge and size effects.

The first problem was to find a homogeneous data set of pK values. The values found in literature often varied in the range of 50%, due to the use of different solvents and temperatures. We chose to simulate pK with three available pK-simulation software programs and to compare the obtained values within the phenomenological models. We estimated all pKs with the Pallas 3.1 [26], ACD-Labs pK calculator 3.5, and the SPARC chemical reactivity model (the latter was available thanks to Dr. S.W. Karickhoff, Dr. A.W. Garisson, and Dr. J.M. Long, USEPA Athens Georgia USA [27, 28]). For a given pH, different charged states are calculated in each of the three pK calculation possibilities; when calculating the hydration effect with the McGovan increment method this had to be taken in account.

The Stoke's radius can be obtained by treating the molecule as a sphere and using the van der Waals volumes calculated by molecular modeling (Alchemy III and ACD Sotware). From the volumes, the corresponding radii were calculated assuming spherical shapes. Since the size data obtained in this way is not always available, it was important to compare these models with systems using the molecular mass only.

The tested models are listed in Fig. 1. From all tested combinations (3 different p*K* sources, size modeled with *M*, *r*, *s*, *v* and the hydration effect H), we selected the one that gave the best regression coefficient. Hydration factors were calculated for each substance and added to the molecular weight (weight factor taken from the table in [25] as a function of the present structures (calculations needed to be done at each pH to take account of the partial ionization of the acidic groups) [24, 25]. These values are given in Table 1 for selected data combinations and include phenolic acids only. Other attempts to include additional molecular

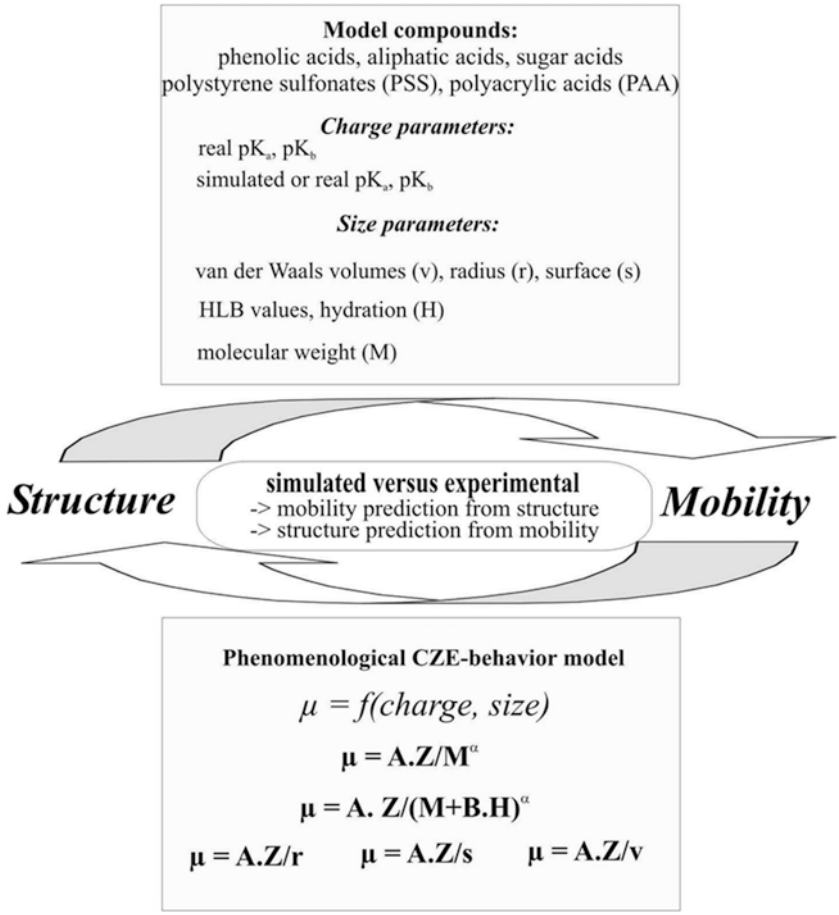

Fig. 1 The applied approach for the phenomenological model

Table 1

pK_a (calculated from the Pallas Software package) and molecular weight of selected aliphatic, phenolic, and sugar acids

Aliphatic acids	pK_a (Pallas)	Molecular weight	Phenolic acids	pK_a (Pallas)	Molecular weight
Formic acid	3.55	46.0	Phenol	9.92	94.1
Acetic acid	4.56	60.1	Catechol	9.53, 12.67	110.1
Oxalic acid	0.99, 6.68	74.0	Resorsinol	9.33, 11.27	110.1
Propionic acid	4.76	74.1	Benzoic acid	4.2	122.1
Glycolic acid	3.75	76.1	*o*-Hydroxybenzoic acid	4.07, 9.72	122.1
Butyric acid	4.63	88.1	Methylcatechol	9.96, 12.69	124.1
Pyruvic acid	2.26, 2.26	88.1	Transcinnamaldehyde	13.15	132.2
Glyoxylic acid	1.18	90.0	2,4-Hydroxybenzaldehyd	7.33, 9.3	138.1
Lactic acid	3.75	90.1	m-Hydroxybenzoic acid	2.66, 10.03	138.1
Valerianic acid	4.84	102.2	*p*-Hydroxybenzoic acid	4.58, 10.03	138.1
Malonic acid	2.77, 5.38	104.1	*p*-Hydroxyphenyl acetic acid	4.497.85	152.2
Glyceric acid	3.41	106.1	Protocatechoic acid	4.45, 9.94, 12.17	154.1
Fumaric acid	4.09, 4.69	116.1	alpha-Methylcinnamic acid	5.17	162.2
Levulinic acid	4.69	116.1	*m*-Coumaric acid	4.39, 9.59	164.2
Succinic acid	4, 5.24	118.1	*o*-Coumaric acid	4.63, 9.87	164.2
Erythronic acid-1,4-lacton	12.38	118.1	*p*-Coumaric acid	4.63, 9.58	164.2
Tartronic acid	2.31, 4.64	120.1	Phthalic acid	2.95, 5.41	166.1
Malic acid	3.16, 4.59	134.1	4-Tertiobuthylcatechol	10.03, 12.71	166.2
Threonic acid	3.86	136.1	Vanillic acid	4.47	168.2
Adipic acid	4.37, 5.06	146.2	Gallic acid	4.32, 8.86, 10.68	170.1
Tartaric acid	2.7, 3.99	150.1	Ascorbic acid	3.94, 12.78	176.1
Galactonic acid-1,4-lacton	12.13	178.2	*t*-3,4,-Dimethoxycinamic acid	4.54	176.2

(continued)

Table 1
(continued)

Aliphatic acids	pK_a (Pallas)	Molecular weight	Phenolic acids	pK_a (Pallas)	Molecular weight
Isosacharin	3.19	180.2	4-Hydroxy, 3-methoxycinamaldehyde	9.63, 13.31	178.2
Citric acid	2.39, 4.01, 4.9	192.1	Coffeic acid	4.57, 9.5, 12.04	180.2
Mannonic acid-1,4-lactone	3.16, 12.73	192.1	Coniferyl alcohol	10.09	180.2
2-Keto-gluconic acid	3.08	194.1	Homovanillic acid	4.43, 7.85	182.2
5-Keto-gluconic acid	3.26	194.1	Ferulic acid	4.58, 9.58	194.2
Gluconic acid	3.27	196.2	Syringic acid	4.36, 10.03	198.2
Galactaric acid	2.92, 3.63	210.2	Trimellitic acid	2.81, 4.16, 4.76	210.1
Glucaric acid	2.92, 3.64	210.2	2,6-Naphthalene dicarboxylic acid	3.67, 4.51	216.2
			Sinapic acid	4.53, 9.58	224.2
			Pyromellitic acid	1.86, 3.03, 4.5, 5.67	254.2
			Quercetin	8.9, 9.95, 11.23, 12.83	302.2
			Conidendrin	9.8, 10.36	356.4
			Matairesinol	9.98, 10.06	358.4
			Pinoresinol	9.92, 10.53	358.4
			Hydroxymatairesinol	9.95, 10.05	374.4
			Rutin	8.92, 10.1, 11.38, 12.63	610.5

characteristics such as the hydrophobicity (Log*P*) or the ovality of the molecules were not successful.

The requirement to the separation buffer was to be noncomplexing toward the analytes so that the measured mobility could be attributed to structural effects only. Borate is, for example, a buffer that interacts with diol groups and therefore induces some mobility shifts as a function of the binding strength. For all the tested combinations, we compared the experimental data (all data sets were

Table 2

Selected best R^2 results from the data linearization using different models for charge (pK_a from ACD, Pallas, SPARCS) and size (molecular weight Mw, van der Walls radius r^2, hydration factor H corrected van der Waals radius R^2)

					H from ACD		H from SPARC		H from PALLAS	
pK_a\Size	$Mw^{2/3}$	$Mw^{2/3}$ hydr. Corrected	r^2 Alchemy	r^2 ACD	hydr. R^2 Alchemy	hydr. R^2 ACD	hydr. R^2 Alchemy	hydr. R^2 ACD	hydr. R^2 Alchemy	hydr. R^2 ACD
ACD	0.9151	0.8689	0.9146	0.8847	0.8776	0.8747	0.8587	0.853	0.8581	0.8522
SPARC	0.94	0.8786	0.9395	0.9163	0.8754	0.8761	0.8866	0.8877	0.861	0.8599
PALLAS	0.9384	0.9134	0.9355	0.9097	0.9191	0.9187	0.9086	0.907	0.9213	0.9208

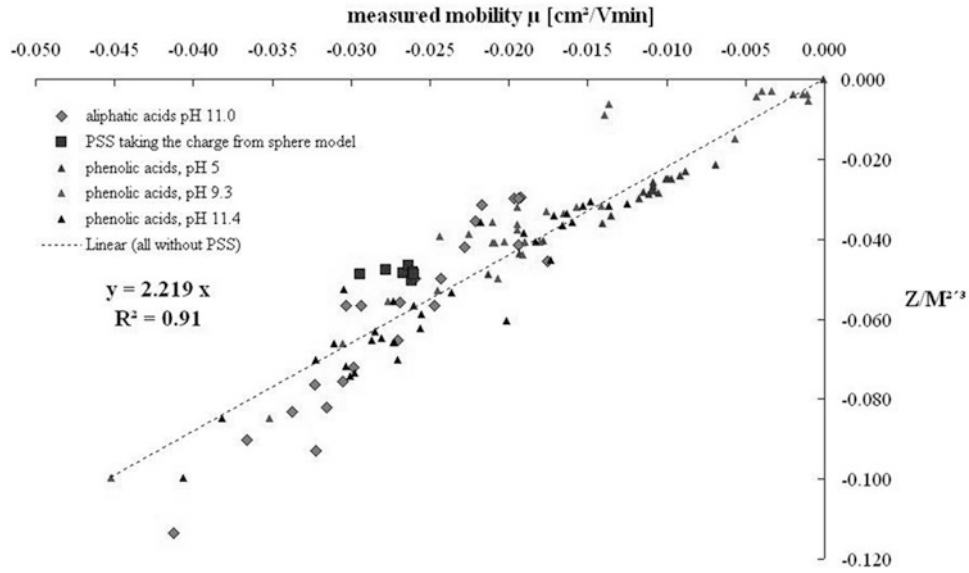

Fig. 2 All experimental data sets involving phenolic acids at three different pH and aliphatic acids at pH 11

calculated with the phenolic compounds at three pHs) with simulated mobility values involving the van der Waals volumes/surface/radius and additional hydration volumes. The simplest model (already proposed by Offord in 1966) was found to be the best with a linearity of $R^2 = 0.9384$ (*see* Table 2).

Including the experimental data of the aliphatic acids into the Offord model, the data also fit into the linearity (Fig. 2). Aliphatic acids were measured at pH 11.0 using CTAB to invert the EOF and 2,6-naphthalenedicarboxylic acid as a UV absorbing background electrolyte [29]. Acetic acid was used as an internal standard for mobility correction.

The shape and the size of the molecules are thus directly responsible for their mobility. Assuming a homogeneous density of the molecules and a spherical shape, the radius is proportional to the power of 1/3. This hypothesis was verified for all the model phenolic acids studied earlier and found the relation ($r = 0.59385.\ M^{1/.3}$ with $R^2 = 0.901$), where r was obtained from the calculated volumes of the phenolic acids with Alchemy 2000 software.

When substituting this relation in the Stoke's Eq. 6, the proportionality of the mobility to $M^{-2/3}$ is verified. It was also found previously by many authors that Offord's model is verified for peptides [2, 5, 22].

This result signifies that surface charge density governs the mobility of these analytes. However, a universal model could never been verified between all available data sets because the dependency on $M^{-\alpha}$ (α between 1/3 and 2/3) was a function of the used amino acid residues and the composition of the separation buffer (complexing or noncomplexing, ionic strength effects on the Debye length). In the studies presented here, we systematically used noncomplexing (acetate and carbonate buffers) at the same ionic strength (25 mM) and in all calculations structural data was used from the same source (identically simulated).

This best empiric relation for mobility found with all tested combinations, which can systematically be used in CZE method developments is:

$$\mu = A \times \frac{Z}{M^{2/3}} \tag{13}$$

with $A = 2.219$ in our experimental conditions for these analytes.

More information on mobility variation with pH is gained with this approach than using the simple relation between the mobility and the pK of the substances, which can only be taken as a preliminary assessment of separation [30]. The Offord model can be used in a general manner to simulate systematically the electrophoretic mobility of the components of interest over the pH range. An example of theoretical evolution of the mobilities by pH is illustrated for aliphatic and phenolic acids in Fig. 3. Different pH zones can be differentiated (arrows) in which the mobilities of the components are governed alone by COOH groups (carboxylic acidity, pH 5) or OH and COOH group (total acidity, pH 11.4). At a pH around 9, the phenols (low mobility) can be additionally distinguished from the phenolic acids (high mobility).

4.2 Simulation and Separation of Hydroxy-s-Triazines as Cations and Anions in CZE

An example of the application of this approach is given for the optimization of the separation of 12 hydroxy-s-triazines, all hydroxylated metabolites of s-triazine pesticides presenting different side chain substituents (Table 3). Based on Eq. 13, the pK_a and the molecular mass values in Table 3, an evolution of the

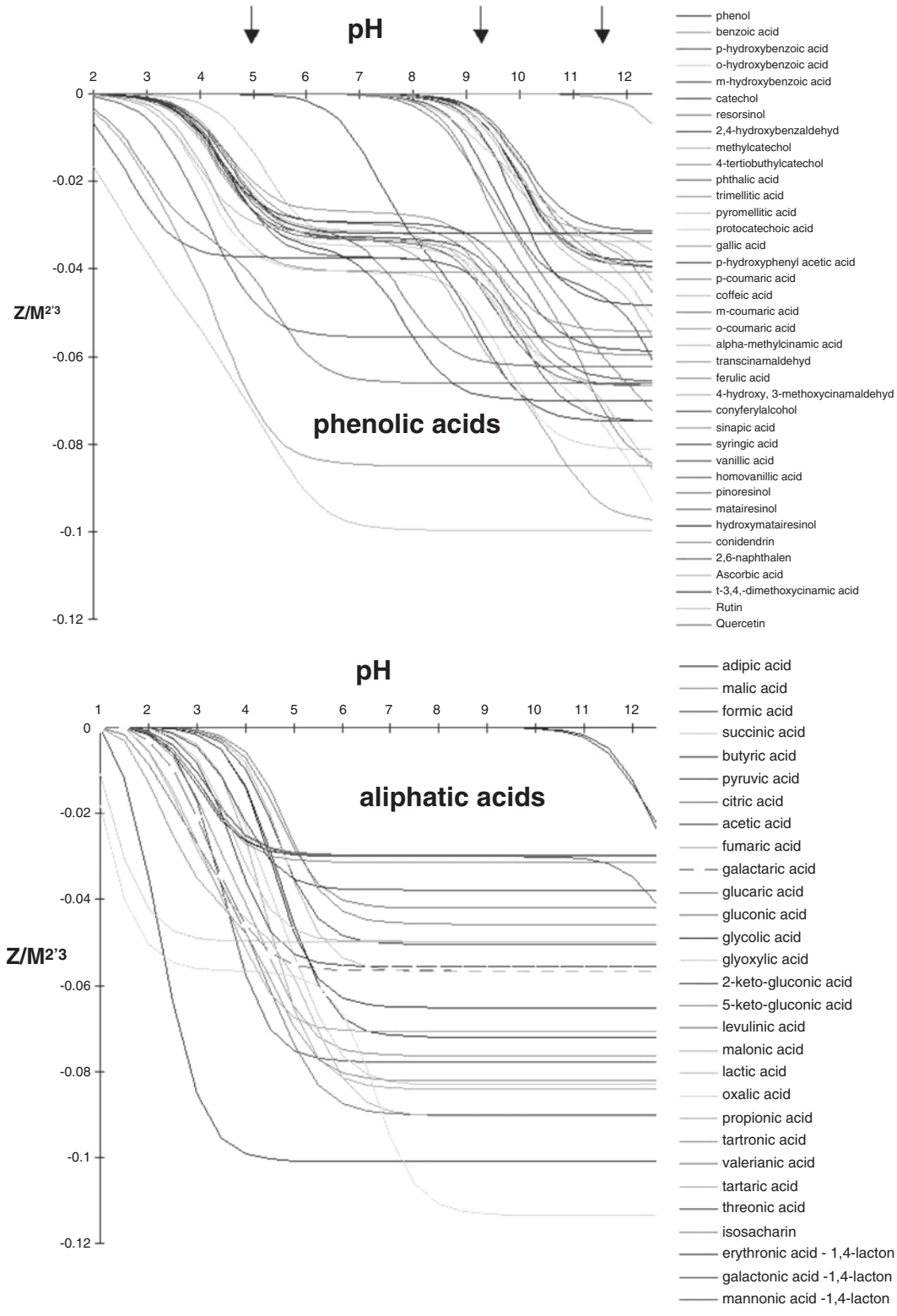

Fig. 3 Theoretical mobility evolution by pH using the Offord model for phenolic and aliphatic acids. Important in this figure is not to recognize the different traces but actually to see the potential of the simulation in rapidly recognizing the best pH for the optimal separation of components in mixtures

Table 3

Substituted hydroxy-s-triazines (1-12 in Fig. 4), their mass *M* and acidic pK_a and basic pK_b

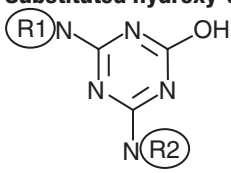

R1, R2		M	pK_a	pK_b
H, H	1	127	4.44	9.54
H, Et	2	155	4.64	9.93
H, iPr	3	169	4.71	9.96
H, tBu	4	183	4.91	10.34
Et, Et	5	183	4.94	10.31
H, mAr	6	233	3.96	9.48
Et, iPr	7	197	4.95	10.39
Et, tBut	8	211	5.2	10.88
iPr, iPr	9	211	5.01	10.88
iPr, Ar	10	245	4.24	9.78
H, Ar	11	203	4.02	9.49
iPr, mAr	12	275	4.29	9.73

theoretical mobility can be calculated as a function of pH. The resulting curves are shown in Fig. 4.

From Fig. 4 it can easily been seen that the optimum separation pH is at low or high pH values; at neutral pH the mobility of the analytes is zero (all analytes migrate with the EOF) due to the zwitterionic character of the substances. Indeed the electropherograms shown in Fig. 4 verify nicely this separation selectivity.

Actually the knowledge of the variations in electrophoretic mobility by pH can be used to determine precisely pK_a values as illustrated with the same analytes in ref. [14] and in the review chapter on pharmaceuticals of Marsh et al.

4.3 Confirmation of Aminoalcohol in the CZE-Indirect Detection of Formaldehyde Releasers

Unsaturated triazines and oxasolidines used as biocides in metalworking fluid were separated at neutral pH condition since they are not stable under acidic medium; they hydrolyze releasing formaldehyde and different derivatives of corresponding aminoalcohols. According to Offord's model, the $Z/M^{2/3}$ values of the analytes calculated at pH 7 are differed from each other, meaning that they can be separated with capillary electrophoresis. However after separation with a noncomplexing buffer, the measured mobilities did

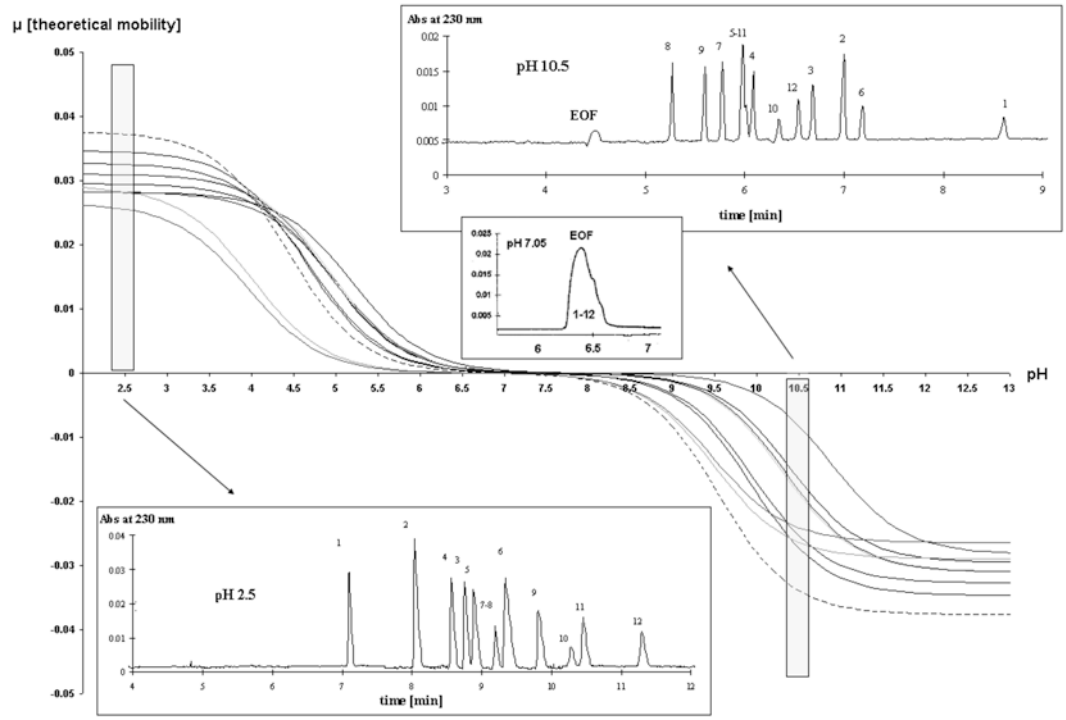

Fig. 4 Theoretical evolution of the mobility by pH for the substituted hydroxy-s-triazines in Table 3

not check up with the corresponding $Z/M^{2/3}$ values (all measured mobilities were much lower than the estimated ones). Moreover, two substances migrated together in spite the fact that their calculated $Z/M^{2/3}$ was totally different (linear correlation between the theoretical and measured values was as low as $r^2 = 0.320$). Since the hydrolysis products of these two analytes are identical we calculated the $Z/M^{2/3}$ of all possible aminoalcohols and compared them to their measured mobility. Strong linear correlation ($r^2 = 0.995$) was found between the calculated and measured mobility of the aminoalcohols as shown in Fig. 5.

Thus, applying this semiempirical approach it was possible to verify that the selected hexahydro-triazines and oxasolidines were rapidly hydrolyzed under the separation condition and thus the hydrolysis products were detected. This hypothesis was verified with CE/MS and NMR studies not shown here. Consequently, these biocides can be indirectly identified with capillary electrophoresis if the sample does not contain the hydrolysis product (derivatives of aminoalcohols).

5 Conclusion

The Offord model (effective mobility linearly correlated to $Z/M^{2/3}$) was verified as the simplest and most accurate approach to rapidly simulate the relative mobility of ions in free zone electrophoresis

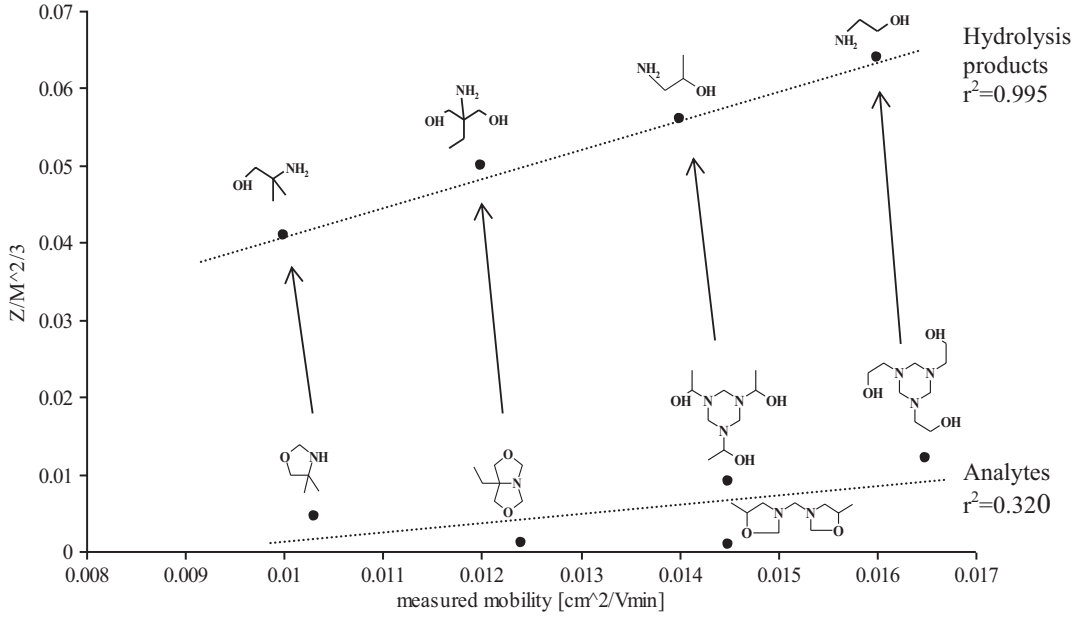

Fig. 5 Comparison of the measured mobility and Offord model ($Z/M^{2/3}$) of the selected unsaturated triazines and oxasolidines and their hydrolysis products

based on their chemical structure. The charge can easily be calculated from the p*K* values (as from the literature, databases, or calculated by simulation programs) and the mass can be used to evaluate the frictional force. The accuracy of the model is robust enough to give at least a good estimation of a starting pH when developing methods to separate known substances in mixtures or to confirm charge-to-mass ratios of known/unknown structures in method development.

Acknowledgement

H. Neumeir and B. Look are thanked for their technical assistance and their kind support during the past years.

References

1. Cifuentes A, Poppe H (1995) Effect of ph and ionic strength of running buffer on peptide behavior in capillary electrophoresis: theoretical calculation and experimental evaluation. Electrophoresis 16:516–524
2. Cifuentes A, Poppe H (1997) Behavior of peptides in capillary electrophoresis: effect of peptide charge, mass and structure. Electrophoresis 18:2362–2376
3. Chen N, Wang L, Zhang YK (1993) Correlation free-solution capillary electrophoresis migration times of small peptides with physicochemical properties. Chromatographia 37:429–432
4. Grossman PD, Colburn JC, Lauer HH (1989) A semiempirical model for the electrophoretic mobilities of peptides in free-solution capillary electrophoresis. Anal Biochem 179:28–33

5. Rickard EC, Strohl MM, Nielsen RG (1991) Correlation of electrophoretic mobilities from capillary electrophoresis with physicochemical properties of proteins and peptides. Anal Biochem 197:197–207
6. Havel J, Janos P (1997) Evaluation of capillary zone electrophoresis equilibrium data using the CELET program. J Chromatogr A 786:321–331
7. Britz-McKibin P, Chen DDY (1997) Prediction of the migration behavior of analytes in capillary electrophoresis based on three fundamental parameters. J Chromatogr A 781:23–34
8. Sahota RS, Khaledl MG (1994) Target factor modeling of migration behavior in capillary electrophoresis. Anal Chem 66:2374–2381
9. Ermakov SV, Bello MS, Righetti PG (1994) Numerical algorithms for capillary electrophoresis. J Chromatogr A 661:265–278
10. Gas B, Vacik J, Zelensky I (1991) Computer-aided simulation of electromigration. J Chromatogr 545:225–237
11. Kohlrausch F (1897) Ueber Concentrations-Verschiebungen durch Electrolyse im Inneren von Lösungen und Lösungsgemischen. Annalen der Physik und Chemie B 62:210–239
12. Ermakov SV, Mazhorova OS, Zhukov MY (1992) Computer simulation of transient states in capillary zone electrophoresis and isotachophoresis. Electrophoresis 13:838–848
13. Gluck SJ, Steele KP, Benkö MH (1996) Determination of acidity constants of monoprotic and diprotic acids by capillary electrophoresis. J Chromatogr A 745:117–125
14. Schmitt P, Poiger T, Simon R, Garrison AW, Freitag D, Kettrup A (1997) Simultaneous ionization constants and isoelectric points determination of 12 hydroxy-s-triazines by capillary zone electrophoresis (CZE) and capillary electrophoresis isoelectric focusing (CIEF). Anal Chem 69:2559–2566
15. Freitag D, Schmitt-Kopplin P, Simon R, Kaune A, Kettrup A (1999) Interactions of hydroxy-s-triazines with SDS-micelles by micellar electrokinetic capillary chromatography (MEKC). Electrophoresis 20:1568–1577
16. Gao J, Gomez FA, Härter R, Whitesides GM (1994) Determination of the effective charge of a protein in solution by capillary electrophoresis. Proc Natl Acad Sci 91:12027–12030
17. Menon MK, Zydney AL (1998) Measurement of protein charge and ion binding using capillary electrophoresis. Anal Chem 70:1581–1584
18. Schmitt P, Trapp I, Garrison AW, Freitag D, Kettrup A (1997) Binding of s-triazines to dissolved humic substances: electrophoretic approaches using affinity capillary electrophoresis (ACE) and micellar electrokinetic chromatography (MEKC). Chemosphere 35:55–75
19. Offord RE (1966) Electrophoretic mobilities of peptides on paper and their use in the determination of amide groups. Nature 211:591
20. Compton BJ (1991) Electrophoretic modeling of proteins in free solution zone capillary electrophoresis and its application to monoclonal antibody microheterogeneity analysis. J Chromatogr 559:357
21. Nikodo AE, Garnier JM, Tinland B, Ren H, Desruisseaux C, McCormick LC, Drouin G, Slater GW (2001) Diffusion coefficient of DNA molecules during free solution electrophoresis. Electrophoresis 22:2424–2432
22. Cross RF, Cao J (1997) Salt effects in capillary zone electrophoresis 1. Dependence of electrophoretic mobilities upon the hydrodynamic radius. J Chromatogr A 786:171–180
23. Cifuentes A, Poppe H (1994) Simulation and optimization of peptide separation by capillary electrophoresis. J Chromatogr A 680:321–340
24. Fu S, Lucy CA (1998) Prediction of electrophoretic mobilities. 1. Monoamines. Anal Chem 70:173–181
25. McGowan JC (1990) A new approach for the calculation of HLB values of surfactants. Analyse 27:229–230
26. Fekete J, Morovjan G, Csizmadia F, Darvas F (1994) Method development by an expert system: advantages and limitations. J Chromatogr A 660:33–46
27. Hilal SH, Karickhoff SW (1995) A rigorous test for SPARC's chemical reactivity models: estimation of more than 4300 ionization pk_as. Quant Struct Act Relat 14:348–355
28. Karickhoff SW, McDaniel VK, Melton C, Vellino AN, Nute DE, Carreira LA (1991) Predicting chemical reactivity by computer. Environ Toxicol Chem 10:1405–1416
29. Dabek-Zlotorzynska E, Dlouhy JF (1994) Capillary zone electrophoresis with indirect UV detection of organic ions using 2,6-naphthalenedicarboxylic acid. J Chromatogr A 685:145–153
30. Souza SR, Tavares MFM, de Carvalho LRF (1998) Systematic approach to the separation of mono- and hydroxycarboxylic acids in environmental samples by ion chromatography and capillary electrophoresis. J Chromatogr A 796:335–346

Chapter 3

Derivatization in Capillary Electrophoresis

M. Luisa Marina and María Castro-Puyana

Abstract

Capillary electrophoresis is a well-established separation technique in analytical research laboratories worldwide. Its interesting advantages make CE an efficient and potent alternative to other chromatographic techniques. However, it is also recognized that its main drawback is the relatively poor sensitivity when using optical detection. One way to overcome this limitation is to perform a derivatization reaction which is intended to provide the analyte more suitable analytical characteristics enabling a high sensitive detection. Based on the analytical step where the CE derivatization takes place, it can be classified as precapillary (before separation), in-capillary (during separation), or postcapillary (after separation). This chapter describes the application of four different derivatization protocols (in-capillary and precapillary modes) to carry out the achiral and chiral analysis of different compounds in food and biological samples with three different detection modes (UV, LIF, and MS).

Key words Derivatization, Capillary electrophoresis, In-capillary, Precapillary, Ultrasound-accelerated derivatization, Microwave-accelerated derivatization, Amino acids, Food samples, Biological samples, Fluorescein isothiocyanate (FITC), O-phthalaldehyde (OPA), Butanol

1 Introduction

Despite the impressive potential of CE to achieve analytical separations in a great variety of research fields, its main drawback is the relatively poor detectability in terms of sensitivity, particularly when UV detection is employed. This fact is attributable to both the short on-column optical path length (controlled by the capillaries internal diameters) and the low amount of sample injected. Different approaches such as the use of alternative detection systems, sample concentration procedures, and derivatization reactions have been developed during the last years in order to increase the sensitivity in CE. Derivatization is without doubt one of the best options to achieve a high sensitive detection of many compounds that cannot be detected because of the lack of structural properties necessary for the production of a signal compatible with the CE detector. Thus, derivatization is mostly a detection-oriented modification of the original structure of an analyte by adding a

Philippe Schmitt-Kopplin (ed.), *Capillary Electrophoresis: Methods and Protocols*, Methods in Molecular Biology, vol. 1483,
DOI 10.1007/978-1-4939-6403-1_3,

chromophore, fluorophore, or electrophore group (the latter to a lesser extent) in order to provide the suitable structural features to increase the detection sensitivity. Along with an increase in detectability, the derivatization step also improves the selectivity.

Even though in most cases, derivatization with a suitable reagent is carried out with the purpose of enhancing the detectability, it can also be used to improve other aspects. For instance, derivatization can provide the analyte with a more appropriate charge-to-mass ratio, improve the electrophoretic behavior (peak shapes or interaction with chiral selectors), change hydrophobicity to use MEKC separations, convert enantiomers into diastereomers which can be separated under achiral conditions, or give analytes (such as carbohydrates) more suitable properties for mass spectrometry detection [1–5].

To convert compounds into products with more favorable CE detection characteristics, a wide variety of reagents exists, but in any case, derivatization relies with the presence of a reactive group, such as amino, hydroxyl, carboxylate, thiol, aldehyde, etc., in the analyte. An ideal derivatizing reagent should contain strong chromophore, fluorophore, or electrophore groups reacting rapidly and quantitatively with the analyte to form stable derivatives without interference side products. A broad number of reagents have been applied to derivatize different compounds in CE analysis. *o*-phthaldialdehyde (OPA) [6–8], 9-fluorenylmethylchloroformate (FMOC) [9–11], fluorescein isothiocyanate (FITC) [12–14], naphthalene-2,3-dicarboxaldehyde (NAD) [15–17], or dansylcloride (DNS) [18–20] is among the reagents most employed. Excellent reviews published during the last two decades provide extensive documentation matching functional groups and reagent for use in the development of CE methodologies (*see* Table 1).

Derivatization reactions in CE can be divided in three different modes based on their place in the final analytical setup: before (precapillary), during (in-capillary), or after (postcapillary) the electrophoretic separation. The most appropriate mode depends on parameters such as the reason why the derivatization step is introduced, the number of samples to analyze, the properties of the analyte and the reagent, etc. [24]. Precapillary derivatization mode can be carried out either off-line (manual) or at-line (automated). Even though the current tendency is to perform more in-capillary derivatizations, the precapillary mode is still frequently used. This fact is due to the high flexibility in the reaction conditions (i.e., it is possible to carry out reactions requiring extreme conditions) and the wide availability of reagents that can be employed. The main drawbacks of this approach are the possible formation of side products, a loss in sensitivity due to the dilution of the sample, and the fact that it is often time consuming. To overcome the long time usually required to carry out a precapillary derivatization, it is highly desirable to develop novel strategies for accelerating those slow derivatization reactions. In any case, it should be taken into account

Table 1
Review papers on derivatization in capillary electrophoresis published in the last two decades (1994–2014)

Subject	Publication year	Reference
General strategies and selection of derivatization reactions for LC and CE	1994	[21]
Improved detection and derivatization in CE	1994	[22]
Pre-, on-, and postcolumn derivatization in CE	1997	[23]
Derivatization in CE	1998	[24]
Postcolumn derivatization for fluorescence and chemiluminescence detection in CE	1998	[25]
Derivatization trends in CE	2000	[26]
Derivatization trends in CE: an update	2002	[27]
Luminol-type chemiluminescence derivatization reagents for LC and CE	2002	[28]
Derivatization of inorganic ions in CE	2003	[29]
Derivatization in the current practice of analytical chemistry	2003	[30]
Recent progress in derivatization methods for LC and CE analysis	2003	[31]
Derivatization of biomolecules for chemiluminescent detection in CE	2003	[32]
CE using chemical and physicochemical reactions	2005	[33]
Sample preconcentration with chemical derivatization in CE. Capillary as preconcentrator, microreactor, and chiral selector for high-throughput metabolite screening	2006	[34]
Derivatization of carbohydrates for analysis by chromatography, electrophoresis, and mass spectrometry	2011	[4]
Derivatization strategies for the determination of biogenic amines in wines by chromatographic and electrophoretic techniques	2011	[35]
Ultraviolet derivatization of low-molecular-mass thiols for HPLC and CE analysis	2011	[36]
Derivatization of hydroxyl functional groups for LC and capillary electroseparation	2013	[37]

that using precapillary derivatization, peak shapes, efficiency, and separation selectivity will be changed (either positively or negatively) what means that not only the detectability of the analytes but also the separation characteristics will be changed [24, 29]. Using a postcolumn derivatization, the native analytes are separated and derivatized afterward. This implies that interferences from side products and band broadening caused by multiple reactions can be

avoided. However, effects such as negative effects on peak efficiency, loss of analyte, incomplete reactions, and high baseline noise originate that this derivatization mode is less used. Regarding in-capillary derivatization mode, it has received a considerable attention in the last years due to its remarkable advantages over pre- and postcapillary derivatization modes. Among these advantages are a low consumption of reagents and samples, high derivatization efficiency, and short reaction time (it is generally accepted that derivatization must be performed with reactions that are complete in seconds). Comparing with pre- and postcapillary approaches, sample dilution is reduced to minimum using in-capillary procedures. Moreover, it allows automation which minimizes the sample preparation work for CE users. As limitations, it can be pointed out that the derivatization should be fast and quantitative what limits the choice of derivatizing reagents. Figure 1 depicts the in-capillary derivatization strategies that can be performed in CE. Both at-inlet and zone-passing strategies (Fig. 1a, b, respectively) involve the injection of separate plugs of sample and reagent before the application of voltage. In the former, sample and derivatization reagent are injected (either by tandem or sandwich mode) to the inlet of a

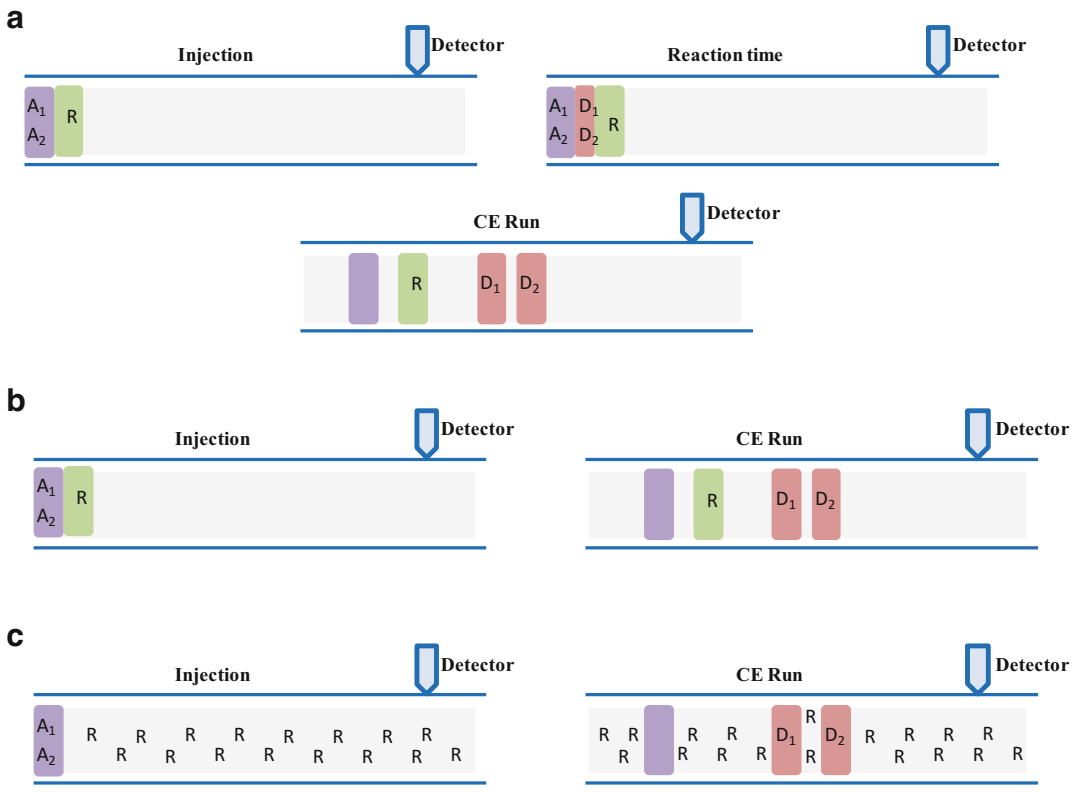

Fig. 1 In-capillary derivatization strategies: at-inlet (**a**), zone-passing (**b**), and throughout mode (**c**). *R* reagent, *A* analyte, *D* derivative formed from analytes

capillary where they are mixed by diffusion and allowed to react during a specific time required to complete the reaction. In the latter, the derivatization reaction takes place (normally in the middle of the capillary) by passing either an analyte or a reagent zone through the other under an electric field. In this case, sample, buffer, and reagent plugs can be injected in different modes; tandem, sandwich, and mixed tandem (reagent–buffer–sample). To carry out this zone-passing approach, it is imperative a good derivatization yield in the short period of contact between the analyte and the reagent plug. In the throughout-capillary approach, the derivatization reagent is added to the background electrolyte (BGE) and the analyte is injected directly into de capillary, so that the reaction occurs within the capillary (Fig. 1c).

Since it is out of the scope of a single chapter to describe all the reported procedures, four representative derivatization strategies employed in the achiral and chiral CE analysis of different compounds in food and biological samples will be herein described. The first example shows an in-capillary protocol with a suitable reagent to enhance the UV sensitivity of amino acids [38]. The second and third examples describe the use of two different devices to carry out an accelerated precapillary derivatization using FITC as derivatization reagent for protein and nonprotein amino acids [39, 40]. The last example shows a simple precapillary derivatization strategy enabling to improve the ionization efficiencies of nonprotein amino acids in CE-MS analysis [41].

2 Materials and Equipment

2.1 In-Capillary Derivatization by CE–UV for the Separation and Determination of Amino Acids in Beer Samples

1. Analytes: Histidine (His), alanine (Ala), glycine (gly), tyrosine (Tyr), valine (Val), arginine (Arg), isoleucine (Ile), phenylalanine (Phe), tryptophan (Trp), glutamine (Glu), lysine (Lys) (from Sigma-Aldrich).
2. Sample preparation: Filter beer samples through 0.2 μm membranes prior to use.
3. Derivatization reagent: *o*-phthalaldehyde (OPA) (Sigma-Aldrich). Prepare 10 mM OPA by dissolving 1.6 μg in a mixture of methanol (16 μL) and 2-mercaptoethanol (24 μL) following by diluting with 20 mM borate buffer to 1.192 mL (*see* **Note 1**).
4. BGE: 20 mM borate buffer (prepared by dilution from a stock solution of 100 mM at pH 10.0) containing as additives 40 mM 1-butyl-3-methyl-imidazolium tetrafluoroborate ([BMIm] BF_4), 40 mM SDS, and 2.5 mM β-CD (*see* **Notes 2** and **3**).
5. CE–UV instrument and capillary: Commercial CE system (CL1020 Beijing Cailu Science Apparatus) equipped with UV detector working at 340 nm. Normal polarity (electric field at 200 V/cm) and constant room temperature. Uncoated fused

silica capillary of 50 cm total length (48 cm to the detector) × 50 μm i.d. (from Hebei Yongnian Optical Fiber Factory) (*see* **Note 4**).

2.2 Ultrasound-Assisted Derivatization of Ornithine for Its Enantiomeric Determination in Dietary Food Supplements by CE–UV

1. Analyte: DL-ornithine (from Fluka).
2. Sample: Dissolve an appropriate amount of dietary food supplements in Milli-Q water. Filter through 0.45 μm pore size disposable nylon filters and dilute this solution in borate buffer 100 mM (pH 10.0) to obtain an appropriate concentration (*see* **Note 5**).
3. Derivatization reagent: Fluorescein isothiocyanate (FITC) (from Fluka). Prepare a FITC solution in acetone at the concentration necessary to obtain a FITC/ornithine ratio of 30 (*see* **Note 6**).
4. BGE: 100 mM borate buffer at pH 10.0 containing 1 mM γ-CD (*see* **Note 2**).
5. CE–MS instrument and capillary: HP^{3D} CE instrument (Hewlett-Packard) equipped with an on-column DAD working at 240 nm. Normal polarity (20 kV) and constant room temperature. Uncoated fused silica capillary of 50 cm total length (48 cm to the detector) × 50 μm i.d. (from Composite Metal Services) (*see* **Note 4**).

2.3 Microwave-Assisted Derivatization CE–LIF Method for the Determination of Histidine, 1- and 3-Methylhistidine in Human Urine

1. Analytes: Histidine, 1-methylhistidine, and 3-methylhistidine (from Sigma).
2. Samples: Human urine samples collected from two healthy volunteers (a female and a male). Before derivatization centrifuge (during 10 min) and filter through a 0.45 mm cellulose acetate membrane the human urine.
3. Derivatization reagent: Fluorescein isothiocyanate (FITC) (from Aldrich). Prepare a stock solution of 10 mM FITC in acetone, stored at −18 °C and diluted to the desired concentration with acetone before use. The buffer solution used for derivatization is 20 mM sodium carbonate and 20 mM sodium bicarbonate at pH 9.4 (*see* **Note 5**).
4. BGE: 22 mM sodium tetraborate at pH 10.5 containing 32% (v/v) acetonitrile (*see* **Note 2**).
5. CE–MS instrument and capillary: MDQ CE system equipped with a LIF detection system (Beckman Coulter). The excitation light from an argon ion laser (3 mW) is focused on the capillary window by means of a fiber-optic connection. LIF detection wavelength was fixed at 488 nm (488 and 520 nm band-pass filters are used as excitation and emission filters, respectively). Normal polarity (25 kV) and constant room temperature. Uncoated fused silica capillary of 50.2 cm total length (40 cm to the detector) × 75 μm i.d. (Yongnian Ruifeng Chromatogram Equipment) (*see* **Note 4**).

2.4 Simple Derivatization of Nonprotein Amino Acids for Their Determination as Novel Markers for the Detection of Adulteration in Olive Oils by CE–MS

1. Analytes: γ-aminobutyric acid and β-alanine (from Sigma) and pyroglutamic acid, alloisoleucine, ornithine, and citrulline (from Fluka).
2. Sample preparation: Mix 40 g of vegetable oils and extra virgin olive oils with 160 mL methanol:chloroform (2:1 v/v) and left at −20 °C overnight. After centrifugation (4000 × *g*, 15 min, 4 °C) collect de upper phase. Wash the bottom phase with 100 mL methanol/chloroform/water (2:1:0.8 v/v/v) combined the upper phase with those obtained previously. Wash the mixed fraction (40 mL chloroform and 100 mL water), centrifuge (4000 × *g*, 15 min, 4 °C) and evaporate the aqueous phase to dryness in a concentrator at 80 °C.
3. Derivatization reagent: hydrogen chloride/1-butanol solution (from Fluka) (*see* **Note 7**).
4. BGE: 0.1 mM formic buffer at pH 2.0 (*see* **Note 2**).
5. CE–MS instrument and capillary: HP^{3D} CE instrument (Agilent Technologies) coupled through an orthogonal electrospray interfase (ESI, model G1607A from Agilent Technologies) to an ion-trap mass spectrometer (model 1100 Agilent Technologies). Normal polarity (25 kV) and constant temperature (25 °C). Uncoated fused silica capillary of 60 cm to the MS detector × 50 μm i.d. (from Composite Metal Services) (*see* **Notes 4** and **8**).

3 Methods

The methods described herein outline the use of different derivatization protocols to determine compounds such as protein and nonprotein amino acids in food and biological samples. In the first example, an in-capillary (zone-passing mode) approach using OPA as reagent to derivatize eleven protein amino acids is carried out [38]. The derivatization step is needed to enhance the sensitivity detection by providing a suitable chromophore group to the amino acids. Combining the in-capillary derivatization with a CE–UV methodology based on a multiple buffer additive strategy, in which an ionic liquid has been used to enhance the selectivity of CE analysis, trace amounts of amino acids can be determined in seven beer samples. The second and third methodologies herein described are based on the use of an ultrasound probe and microwave radiation to carry out an accelerated precapillary derivatization of ornithine (a nonprotein amino acid) (Elena) or histidine, 1-methylhistidine and 3-methylhistidine (Zhou) with FITC. In the first case, the ornithine derivatization is reduced 96 times (from 16 h to 10 min) by using an ultrasound probe to accelerate the derivatization reaction [39]. In the second case, using a microwave precapillary strategy it is possible to reduce the derivatization

reaction of histidine and its metabolites to only 150 s [40]. Both derivatization procedures can be successfully applied to the determination of ornithine in dietary food supplements by CE–UV [39] or to the determination of histidine and its metabolites in human urine by CE–LIF [40]. The last example of this chapter describes a simple derivatization protocol of nonprotein amino acids and their determination by CE–MS^2 [41]. In this work, the purpose of the derivatization strategy is to use the carboxylic groups of nonprotein amino acids to carry out the derivatization improving not only the ionization efficiency but also the mass differentiation among the analytes increasing the selectivity. After determining and identifying the six nonprotein amino acids studied in vegetable oil samples it was possible to propose some of them as novel markers for the detection of adulterations in olive oils.

3.1 In-Capillary Derivatization by CE–UV for the Separation and Determination of Amino Acids in Beer Samples

1. Between analyses the capillary is rinsed with BGE during 2 min to obtain an adequate repeatability.
2. In-capillary derivatization by sandwich mode: injection of OPA reagent (10 cm, 3 s), injection of sample (10 cm, 3 s), injection of OPA (10 cm, 3 s) (*see* **Note 9**).
3. After the second injection of OPA reagent, insert the inlet capillary in a vial containing the BGE and apply a separation potential of 200 V/cm to start the electrophoretic process.
4. Figure 2 shows the corresponding electropherograms obtained by the CE–UV analysis of OPA-amino acids in different beer samples (*see* **Note 10**).

3.2 Ultrasound-Assisted Derivatization of Ornithine for Its Enantiomeric Determination in Food Supplements by CE–UV

1. To maintain an adequate repeatability between injections the capillary is rinsed at 1 bar with acetone (3 min), 0.1 M NaOH (4 min), Milli-Q water (2 min), and BGE (4 min) (*see* **Note 11**).
2. To carry out the precapillary derivatization mix 1 mL of food supplement solution diluted in borate buffer at pH 10.0 with 2 mL FITC in acetone at the concentration necessary to obtain a FITC/ornithine ratio of 30.
3. Use an ultrasound probe (microprobe (model CV-18) coupled to a sonicator device Sonic Vibra-Cell (model VCX-130)) to accelerate the derivatization reaction. Fix the tip of the probe at 3 mm from the bottom of the solution, 10 min of continuous sonication at amplitude of 100% without pulses (*see* **Notes 12** and **13**).
4. Inject the sample previously derivatized by pressure (50 mbar for 5 s) in the CE–UV system.
5. Apply a separation voltage of 20 kV to start the electrophoretic process.
6. Figure 3 depicts the electropherograms corresponding to a dietary food supplement derivatized with FITC spiked and nonspiked with 0.1 mM DL-ornithine.

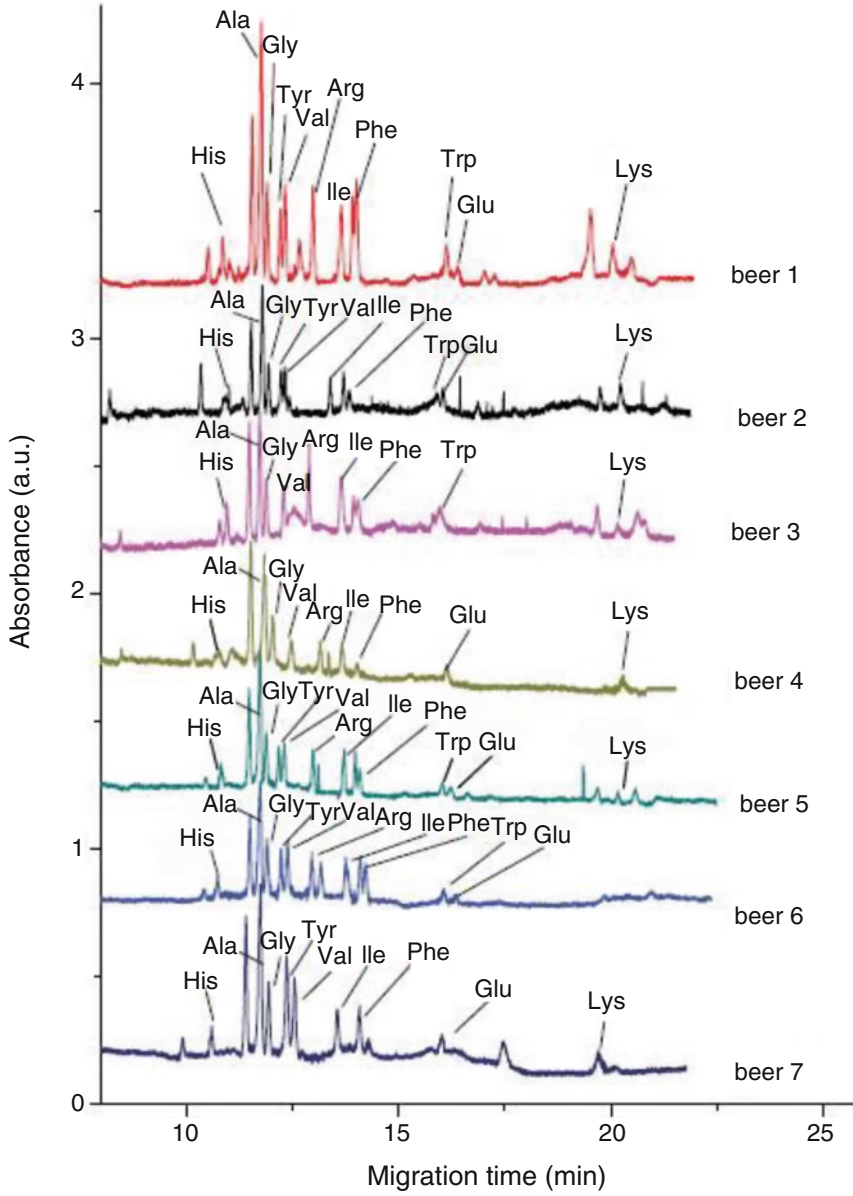

Fig. 2 Electropherograms of CE–UV analysis of OPA-amino acids in seven beer samples. BGE: 20 mM borate containing 40 mM [BMIm]BF_4, 40 mM SDS and 2.5 mM β-CD; in-capillary derivatization by sandwich injection; separation electric field strength, 200 V/cm, UV detection, 340 nm. (Reprinted from [38] with permission from Wiley-VCH)

3.3 Microwave-Assisted Derivatization CE–LIF Method for the Determination of Histidine, 1- and 3-Methylhistidine in Human Urine

1. Rinse the capillary with distilled water (5 min), HCl (5 min), distilled water (2 min), and buffer (5 min) at the beginning of each run to maintain a good reproducibility.
2. To carry out the precapillary derivatization mix sequentially 10 μL of sample, 165 μL of derivatization buffer, and 25 μL of 2 mM FITC solution into a 1.5 mL microcentrifuge vial. Then seal the vial by a small piece of parafilm and place it in a domestic

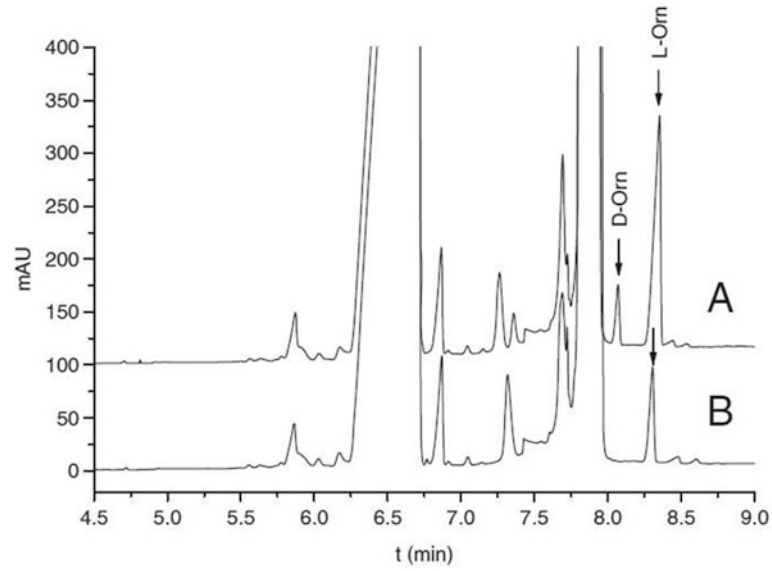

Fig. 3 Electropherograms corresponding to (**a**) the dietary food supplement previously derivatized with FITC and spiked with 0.1 mM DL-ornithine and (**b**) the same sample without spiking 0.1 mM DL-ornithine. CE conditions: BGE, 100 mM borate buffer at pH 10 with 1 mM γ-CD; ultrasound accelerated precapillary derivatization with FITC, applied voltage, 20 kV; temperature, 25 °C. (Reprinted from [39] with permission from Wiley-VCH)

microwave oven together with a conical flask containing 20 mL water (*see* **Note 14**).

3. Apply microwave irradiation energy of 700 W during 150 s to carry out the derivatization reaction (*see* **Note 15**).
4. After cooling to ambient temperature, dilute the reaction mixture 20 times with distilled water for CE analysis.
5. Inject the sample by pressure (3.45 KPa for 3 s) in the CE–LIF system.
6. Apply a separation voltage of 25 kV to start the electrophoretic process.
7. Figure 4a depicts a comparison of different derivatization modes with that described in this protocol.
8. Figure 4b shows the electropherograms of human urine samples collected from volunteers under the described condition of derivatization and separation.

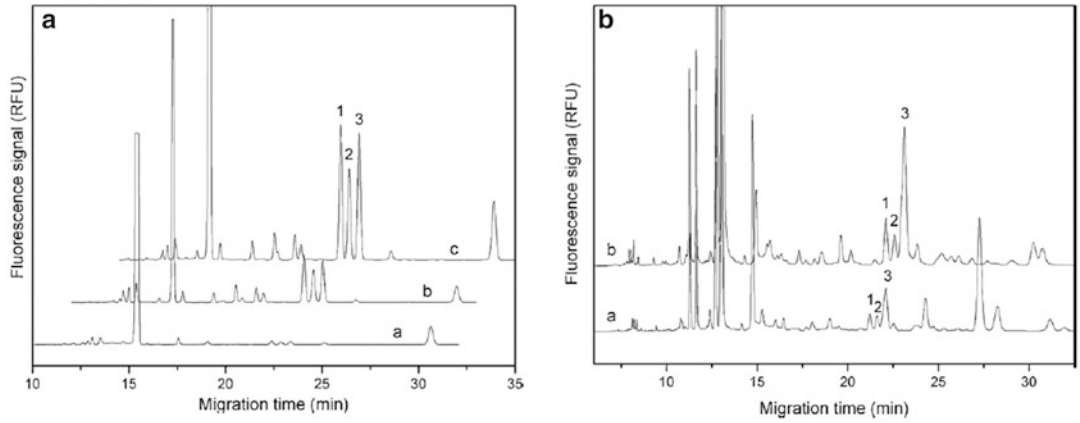

Fig. 4 **(a)** Comparison of different derivatization methods: (a) derivatization at 20 °C for 150 s, (b) derivatization in a boiling water bath for 150 s, (c) derivatization in a microwave oven for 150 s at 700 W. **(b)** Electropherogram of human urine from female (a) and male volunteer. CE conditions: BGE, 22 mM sodium tetraborate (pH 10.5) with 32 % acetonitrile; microwave accelerated precapillary derivatization with FITC (150 s at 700 W), applied voltage, 25 kV; temperature, 25 °C. (Reprinted from [40] with permission from Elsevier)

3.4 Simple Derivatization of Nonprotein Amino Acids for Their Determination as Novel Markers for the Detection of Adulteration in Olive Oils by CE–MS

1. Between injections, rinse the capillary at 1 bar for 2 min with buffer.
2. Insert the capillary in the ESI interface. The capillary tip position should be approximately 1 mm from the nebulizing capillary.
3. Prepare the sheath liquid isopropanol: water (50:50 v/v) with 0.1 % formic acid and degas it by sonication (*see* **Note 16**).
4. Use a chromatographic syringe (SGE syringe of 10 mL from Supelco) to introduce the sheath liquid in the CE–MS system at a flow rate of 3.3 μL/min (*see* **Note 17**).
5. Set the drying gas flow and temperature at 3 L/min and 300 °C, respectively. Also set the nebulizer pressure at 2 psi (*see* **Note 18**).
6. Fix the data collection settings of the ion trap for tandem MS (MS^2) analysis: positive ion mode (spray voltage at 4.5 kV); scan range from 50 to 280 m/z, CE–MS^2 in MRM mode using a fragmentation amplitude of 1.0 V and a width of 4 m/z.
7. To carry out the precapillary derivatization add 1 mL of butanol derivatization reagent to the evaporated extract of the samples and shake in a vortex. The reaction is carried out in an oven at 80 °C during 30 min. After 5 min in a freezer to stop the reaction evaporate to dryness the derivatization reagent excess in a concentrator at 80 °C. Reconstitute the sample in 500 μL of acetonitrile:water (40:60 v/v) (*see* **Note 19**).
8. Inject the sample previously derivatized by pressure (50 mbar for 50 s) in the CE–MS system.
9. Apply a voltage of 25 kV to start simultaneously the electrophoretic process and data collection on MS.

10. By using this methodology was possible to determine γ-aminobutyric acid, β-alanine, pyroglutamic acid, alloisoleucine, and ornithine in soybean, corn, and sunflower oils (citrulline was not detected in the oils studied). However, only γ-aminobutyric acid, β-alanine, and pyroglutamic acid were determined in extra virgin olive oil samples whereas ornithine, alloisoleucine, and citrulline were not detected. This implies that both ornithine and alloisoleucine can be proposed as marker of adulteration of olive oils with soybean, corn, or sunflower oils.
11. Figure 5 depicts the CE–MS^2 extracted ion electropherogram (EIE) and the mass spectra for ornithine and alloisoleucine obtained under the described experimental conditions in soybean oil samples, extra virgin oil sample, and a mix of both.

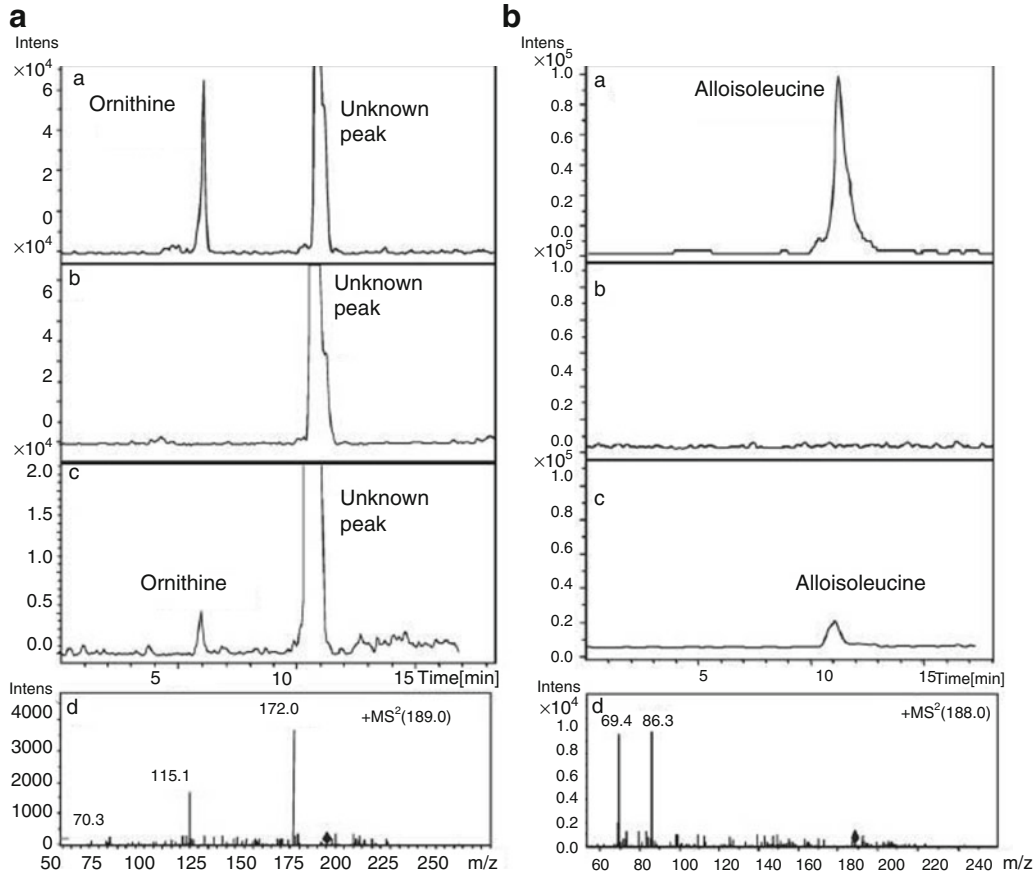

Fig. 5 CE–MS^2 extracted ion electropherogram for ornithine (**a**) and alloisoleucine (**b**) in (a) soybean oil sample, (b) extra virgin oil sample, (c) oils mixture of both samples (i.e. extra virgin oil sample containing 2 or 5 % of soybean oil to ornithine or alloisoleucine, respectively) and (d) MS^2 spectra of both nonprotein amino acids in the oil mixture. CE conditions: BGE, 0.1 M formic acid at pH 2.0; precapillary derivatization with butanol, applied voltage, 25 kV; temperature, 25 °C. ESI conditions: positive ion mode (4.5 kV); sheath liquid, isopropanol:water (50:50 v/v) with 0.1 % formic acid at 3.3 μL/min; drying gas flow, 3 L/min; drying gas temperature, 300 °C; nebulizer pressure, 2 psi. MS^2 conditions at MRM mode, fragmentation amplitude at 1.0 V, and isolation width at 4 m/z; (Reprinted from [41] with permission from Elsevier)

4 Notes

1. OPA is a fluorescence reagent which reacts with primary amines of amino acids. This derivatization reagent can be used not only for fluorescence labeling, but also for UV detection of amino acids at 340 nm since it has no absorbance at this wavelength. OPA derivatization reaction exhibits good performance in alkaline borate buffer.
2. Filter all buffer and solutions to prevent blockage of the CE capillary.
3. A multiple buffer additive strategy is employed to achieve an efficient separation of all the OPA-amino acids studied. The effect and optimum concentration of each additive added to the buffer is exhaustively investigated.
4. Before the first use, capillary must be conditioned. A standard protocol to do that is the following: flush at 1 bar with 1 M NaOH for 30 min, followed by milli-Q water for 5 min, and the BGE for 60 min. In case that acidic separation buffer was required to carry out the separation, it is recommended to flush the capillary with 0.1 M HCl during 5 min before the BGE. Moreover, at the beginning of each day, the capillary should be conditioned by flushing 1 M NaOH during 5 min, Milli-Q water for 5 min, and BGE for 30 min. In the same way, it is strongly recommended to rinse the capillary at the end of the day with 0.1 M NaOH (5 min) followed by Milli-Q water (5 min).
5. The derivatization reaction of amino compounds with FITC is carry out at alkaline medium to favor the amine deprotonation.
6. Convenient FITC/ornithine ratios of 30 are necessary to reach the optimum sensitivity [42].
7. The butylation of compounds containing mono and dicarboxylic acid groups not only improves greatly the ionization efficiencies (and therefore the sensitivity) but also improves the mass differentiation among the analytes increasing the selectivity.
8. Due to the use of 1 M NaOH during capillary conditioning, it is imperative to keep the capillary end out of the ionization source.
9. The capillary inlet is briefly dipped into a water vial to avoid cross-contamination after each of the three consecutive injections.
10. The detection of the studied amino acids do not show interferences from biogenic amines which are commonly found in beer samples and that can react readily with OPA.
11. The washing step with acetone is crucial to remove conveniently FITC from the capillary. It allowed the solubilization of FITC which improves reproducibility. Moreover, during

this conditioning either the ESI voltage and nebulizer pressure should be switched off to prevent the entrance of NaOH into the source.

12. Parameters such as distance between the ultrasound probe and the bottom of the solution, and the sample volume must be constant because their variation can modify the effectiveness and reproducibility of the sonication.
13. By using this procedure it is not necessary to protect the solutions from the light.
14. Use a microwave with small amount of load, i.e., with a small amount of substance to "heat" may cause damage in the magnetron (essential part of a microwave oven). For this reason, a conical flask containing certain amount of water is used for protecting the microwave.
15. Microwave irradiation energy, microwave irradiation time, and FITC concentration are parameters that should be properly optimized to achieve an efficient derivatization.
16. The choice of sheath liquid, needed to ensure the electric circuit and permit the CE separation, has a significant effect in sensitivity. Usually, the organic component is ≥50% to favor the transfer of the analytes from the liquid into the gas phase. A portion of the acid or base used in the BGE is also added to the sheath liquid. It is strongly recommended degassing the sheath liquid to eliminate the formation of air bubbles avoiding drops in current.
17. The sheath liquid flow should be enough to form a stable aerosol in the ESI source.
18. The nebulizer pressure is set at low pressure since higher values could cause a suction effect.
19. The samples are reconstituted in acetonitrile:water (40:60 v/v) to achieve a stacking sample preconcentration.

Acknowledgments

The authors thank the Ministry of Economy and Competitiveness (Spain) for research project CTQ2013-48740-P. M.C.P. also thanks this Ministry for her "Ramón y Cajal" research contract (RYC-2013-12688).

References

1. Martínez-Girón A, García-Ruiz C, Crego AL et al (2009) Development of an in-capillary derivatization method by CE for the determination of chiral animo acids in dietary supplements and wine. Electrophoresis 30:696–704
2. Martínez-Girón A, Dominguez-Vega E, García-Ruiz C et al (2009) Enantiomeric separation of ornithine in complex mixtures of amino acids by electrokinetic chromatography with off-line derivatization with 6-aminoquinolyl-N-hydrox

ysuccinimidyl carbamate. J Chromatogr B 875:254–259
3. Vshivkov S, Pshenichnov E, Golubenko Z et al (2012) Capillary electrophoresis to quantitate gossypol enantiomers in cotton flower petals and seed. J Chromatogr B 908:94–97
4. Harvey DJ (2011) Derivatization of carbohydrates for analysis by chromatography; electrophoresis and mass spectrometry. J Chromatogr B 879:1196–1225
5. Fernandez de la Osa MA, Torre M, García-Ruiz C (2012) Determination of nitrocellulose by capillary electrophoresis with laser-induced fluorescence detection. Anal Chimica Acta 745:149–155
6. Shen C-C, Tseng W-L, Hsieh M-M (2012) Selective extraction of thiol-containing peptides in seawater using Tween 20-capped gold nanoparticles followed by capillary electrophoresis with laser-induced fluorescence. J Chromatog A 1220:162–168
7. Akamatsu S, Mitsuhashi T (2012) Development of a simple capillary electrophoretic determination of glucosamine in nutritional supplements using in-capillary derivatization with o-phthalaldehyde. Food Chem 130:1137–1141
8. Su Y-S, Lin Y-P, Cheng F-C et al (2010) In-capillary derivatization and stacking electrophoretic analysis of gamma-aminobutyric acid and alanine in tea samples to redeem the detection after dilution to decrease matrix interference. J Agric Food Chem 58:120–126
9. Sánchez-Hernández L, Castro-Puyana M, García-Ruiz C et al (2010) Determination of L- and D-carnitine in dietary food supplements using capillary electrophoresis-tandem mass spectrometry. Food Chem 120:921–928
10. Fradi I, Servais A-C, Lamelle C et al (2012) Chemo and enantioselective method for the analysis of amino acids by capillary electrophoresis with in-capillary derivatization. J Chromatogr A 1267:121–126
11. Sánchez-Hernández L, Dominguez-Vega E, Montealegre C et al (2014) Potential of vancomycin for the enantiomeric resolution of FMOC-amino acids by capillary electrophoresis-ion-trap mass spectrometry. Electrophoresis 35:1244–1250
12. Tezcan F, Uzasci S, Uyar G et al (2013) Determination of amino acids in pomegranate juice and fingertprint for adulteration with apple juices. Food Chem 141:1187–1191
13. Zhao DY, Lu MH, Cai ZW (2012) Separation and determination of B vitamins and essential amino acids in health drinks by CE-LIF with simultaneous derivatization. Electrophoresis 33:2424–2432
14. Lin W-C, Liu W-L, Tang W-Y et al (2014) Determination of amino acids by microemulsion electrokinetic chromatography laser induced fluorescence method. Electrophoresis 35:1751–1755
15. Kanetal K, Ogura T, Imasaka T (2011) Analysis of proteins in biological samples by capillary sieving electrophoresis with postcolumn derivatization/laser-induced fluorescence detection. Electrophoresis 32:1061–1067
16. Kao Y-Y, Liu K-T, Huang M-F et al (2010) Analysis of amino acids and biogenic amines in breast cancer cells by capillary electrophoresis using polymer solutions containing sodium dodecyl sulfate. J Chromatogr A 1217:582–587
17. Nandi P, Scott DE, Desai D et al (2013) Development and optimization of an integrated PDMS based-microdialysis microchip electrophoresis device with on-chip derivatization for continuous monitoring of primary amines. Electrophoresis 34:895–902
18. Qi L, Yang G (2009) On-column labeling technique and chiral ligand-exchange CE with zinc(II)-L-arginine complex as chiral selector for assay of dansylated D, L-amino acids. Electrophoresis 30:2882–2889
19. Béni S, Sohajda T, Neumajer G et al (2010) Separation and characterization of modified pregabalins in terms of cyclodextrin complexation, using capillary electrophoresis and nuclear magnetic resonance. J Pharm Biomed Anal 51:842–852
20. Giuffrida A, Messina M, Contino A et al (2013) Optimisation methodology in the chiral and achiral separation in electrokinetic chromatography in the case of a multicomponent sample of dansyl amino acids. J Pharm Biomed Anal 85:55–60
21. Krull IS, Deyl Z, Lingeman H (1994) General strategies and selection of derivatization reactions for liquid chromatography and capillary electrophoresis. J Chromatogr B 659:1–17
22. Szulc ME, Krull IS (1994) Improved detection and derivatization in capillary electrophoresis. J Chromatogr A 659:231–245
23. Bardelmeijer HA, Waterval JCM, Lingeman H et al (1997) Pre-, on- and post-column derivatization in capillary electrophoresis. Electrophoresis 18:2214–2227
24. Bardelmeijer HA, Lingeman H, de Ruiter C et al (1998) Derivatization in capillary electrophoresis. J Chromatogr A 807:3–26
25. Zhu R, Kok WT (1998) Post-column derivatization for fluorescence and chemiluminescence detection in capillary electrophoresis. J Pharm Biomed Anal 17:985–999
26. Waterval JCM, Lingeman H, Bult A et al (2000) Derivatization trends in capillary electrophoresis. Electrophoresis 21:4029–4045
27. Underberg WJM, Waterval JCM (2002) Derivatization trends in capillary electrophoresis: an update. Electrophoresis 23:3922–3933

28. Yamaguchi M, Yoshida H, Nohta H (2002) Luminol-type chemiluminescence derivatization reagents for liquid chromatography and capillary electrophoresis. J Chromatogr A 950:1–19
29. Padarauskas A (2003) Derivatization of inorganic ions in capillary electrophoresis. Electrophoresis 24:2054–2063
30. Rosenfeld JM (2003) Derivatization in the current practice of analytical chemistry. Trends Anal Chem 22:785–798
31. Fukushima T, Usui N, Santa T et al (2003) Recent progress in derivatization methods for LC and CE analysis. J Pharm Biomed Anal 30:1655–1678
32. García-Campaña AM, Gámiz-Gracia L, Baeyens WRG et al (2003) Derivatization of biomolecules for chemiluminescent detection in capillary electrophoresis. J Chromatogr B 793:49–74
33. Taga A (2005) Capillary electrophoresis using chemical and physicochemical reactions. Chromatography 26:13–17
34. Ptolemy AS, Britz-McKibbin P (2006) Sample preconcentration with chemical derivatization in capillary electrophoresis. Capillary as preconcentrator, microreactor and chiral selector for high-throughput metabolite screening. J Chromatogr A 1106:7–18
35. Hernández-Cassou S, Saurina J (2011) Derivatization strategies for the determination of biogenic amines in wines by chromatographic and electrophoretic techniques. J Chromatogr B 879:1270–1281
36. Kusmierek K, Chwatko G, Glowacki R et al (2011) Ultraviolet derivatization of low-molecular-mass thiols for high performance liquid chromatography and capillary electrophoresis analysis. J Chromatogr B 879:1290–1307
37. Escrig-Doménech A, Simó-Alfonso EF, Herrero-Martínez JM et al (2013) Derivatization of hydroxyl functional groups for liquid chromatography and capillary electroseparation. J Chromatogr A 1296:140–156
38. Tian M, Zhang J, Mohamed AC et al (2014) Efficient capillary electrophoresis separation and determination of free amino acids in beer samples. Electrophoresis 35:577–584
39. Domínguez-Vega E, Martínez-Girón A, García-Ruiz C et al (2009) Fast derivatization of the non-protein amino acid ornithine with FITC using an ultrasound probe prior to enantiomeric determination in food supplements by EKC. Electrophoresis 30:1037–1045
40. Zhou L, Yan N, Zhang H et al (2010) Microwave-accelerated derivatization for capillary electrophoresis with laser-induced fluorescence detection: a case study for determination of histidine, 1- and 3-methylhistidine in human urine. Talanta 82:72–77
41. Sánchez-Hernández L, Marina ML, Crego AL (2011) A capillary electrophoresis-tandem mass spectrometry methodology for the determination of non-protein amino acids in vegetables oils as novel markers for the detection of adulteration in olive oils. J Chromatogr A 1218:4944–4951
42. Li H, Wang E, Chen J (2003) Determination of amino acid neurotransmitters in cerebral cortex of rats administered with baicalin prior to cerebral ischemia by capillary electrophoresis-laser induced fluorescence detection. J Chromatogr B 788:93–101

Chapter 4

Statically Adsorbed Coatings for High Separation Efficiency and Resolution in CE–MS Peptide Analysis: Strategies and Implementation

Martin Pattky, Katalin Barkovits, Katrin Marcus, Oliver H. Weiergräber, and Carolin Huhn

Abstract

Coatings are necessary to prevent protein and peptide adsorption to the capillary surface and obtain high intermediate precision. In this protocol, we first present our basic strategy to address peptide separation using three different coatings: one neutral and two cationic coatings, the latter largely differing in their induced electroosmotic mobility. In detail, we will describe how we apply the statically adsorbed coatings to obtain very high plate numbers and high repeatability.

With some model examples, we clearly describe the scope of the method for the analysis of peptide samples: tryptic digests are addressed as well as small glycoproteins and glycopeptides largely differing in their effective electrophoretic mobility. We also show that the method is suitable for a fast screening of peptide samples despite a high matrix load comprising of up to 500 mmol/L sodium chloride. We demonstrate that this basic CE–MS method is rather independent of the polarity of the analytes with a very fast near-baseline separation of very hydrophobic Aβ peptides related to the onset of Alzheimer's disease. These examples will give an impression, which coating is most suitable for a specific analytical application.

Special attention is paid to difficult aspects of the coating procedure and the CE–MS method, e.g., the potential of cross-contamination when changing the coatings.

Key words Resolution, Coatings, Proteins, Peptides, Electroosmotic flow velocity, Mass spectrometry

1 Introduction

The analysis of peptide digests is currently dominated by chromatography, especially nanoLC–MS, and relies almost exclusively on tryptic digests. The advantage of using trypsin is its ability to cut C-terminal to the most basic amino acids lysine and arginine which gives rise to peptides with a rather homogeneous distribution of basic amino acids. Without missed cleavages, an overall low charge by the low number of cationic side groups per peptide prevails, which is ideal for the analysis using LC–MS as the polarity range is mostly acceptable which results in a low risk to have peptides

Philippe Schmitt-Kopplin (ed.), *Capillary Electrophoresis: Methods and Protocols*, Methods in Molecular Biology, vol. 1483,
DOI 10.1007/978-1-4939-6403-1_4,

without retention on the column. Though strongly hydrophobic peptides may still be present as, e.g., well known for peptides from the Alzheimer related peptides of Aβ [1, 2]. Many groups have now shown that CE–MS is likewise suitable for the analysis of complex proteomic samples [3] and can also be applied for biomarker discovery, e.g., for urinary peptides [4]. Whereas LC–MS provides a very high robustness with standard protocols for peptides partly with posttranslational modifications such as phosphorylation or glycosylation, CE–MS offers specific advantages: extremely small sample volumes may be analyzed. We routinely work with 7–10 μL sample solution, from which more than ten injections can be made. With the small capillaries compared to chromatographic columns, loadability is an issue in CE, if no preconcentration strategies are used. However, we have to keep in mind that in contrast to LC there is no on-column dilution of the sample, instead, mostly a shortening of the sample plug is possible. With the significantly higher separation efficiencies—we routinely achieve about 300,000 plates when cationic coatings are used—the peak intensities are clearly higher when the same amount of sample is injected as in LC. CE thus has intrinsically lower detection limits, when we look only at the absolute injected amount of analyte. Despite the relatively low loadability in the nanoliter range, we can achieve detection limits for peptides in the nanomolar range with CE–MS.

We have developed a standard CE–MS method using a very low pH (2.2) background electrolyte of 3:1 acetic acid:formic acid (each 1 mol/L, Buffer A) except when higher ionic strength is required and where the concentration is doubled (Buffer B). This low pH guarantees that all peptides migrate as cations. So far, we have not observed any peptide sample we could not analyze with this method.

Another advantage is the often high matrix tolerance of CE. For bare fused silica capillaries, relatively harsh rinsing steps may be used; for adsorbed coatings recoating procedures may be applied to obtain a fresh surface for further analysis. Salt as sample matrix is not critical up to a certain value. Below we will show that the analysis of samples with up to 500 mmol/L NaCl is possible for screening purposes (i.e., identification of peptides, but not quantification) (*see* Subheading 1.3).

In our work, we prefer a short CE run (5–10 min) with our standard peptide CE–MS method for the screening of samples from peptide synthesis instead of direction infusion experiments. In most cases, no sample preparation other than dilution is necessary to obtain high quality MS or MS/MS spectra and to minimize quenching effects upon some separation of the peptides. Isobaric compounds may be discriminated. Especially fast inorganic salt compounds including sodium, potassium but also chloride and phosphate are well separated from the peptide signals. Rinsing steps between analyses can be automized so the whole analysis will take between 10 and 15 min analysis time for each sample. No further manual steps are required and automation is possible.

Most of this screening can be done with a neutral coating as it provides the largest range of mobilities and thus a quick overview. With the (possibly prior) knowledge on the electrophoretic mobility, it may be advantageous to use, e.g., polybrene coating with its fast cationic EOF for extremely fast analytes. In a second step, we conduct a fine-tuning of the resolution choosing one out of three coatings according to the absolute effective electrophoretic mobility as well as the range of analyte mobilities for the sample as will be discussed later (*see* Subheading 1.5).

1.1 Coating Strategies

A large body of work has been published on capillary coating strategies [5], both for CE with optical detection, but also explicitly for the higher demands of CE–MS [6]. We can discriminate coatings via the charge on the coating being anionic, cationic, or neutral. Alternatively, coating classes may be distinguished based on the way the coating adheres to the surface: *dynamic coatings* can most easily be applied just being added to the background electrolyte (BGE). As they are in large excess, they will nearly always win the competition with the analyte for binding sites on the silanol surface of the capillary and thus prevent reversible or irreversible adsorption of the analytes. Also, harsh rinsing conditions may be applied as fresh dynamic coating agent is delivered upon rinsing with BGE. Dynamic coatings include small- to medium-sized amines and polyamines (e.g., putrescine, spermine), polysugars (methylhydroxy ethyl cellulose, hydroxyethylcellulose), polymers of medium chain length (otherwise sieving effects become present) such as polybrene or polyethylene oxides or detergents. None of these dynamic coatings is compatible with mass spectrometric detection.

Covalent coatings are synthesized directly in the capillary by various protocols. One of the oldest is the polyacrylamide coating by Hjertèn [7], which has several variants now. The great disadvantage can be that its surface is relatively hydrophobic and may lead to adsorption of hydrophobic proteins. The most favorite coating is polyvinylalcohol (PVA), which may be covalently attached [8–10], but may also be applied as static coating followed by a heating step, where the PVA crystallizes. PVA provides an ideal surface with its very high hydrophilicity, so that it is commercialized by several vendors. The disadvantage of covalent coatings is the often limited stability at very basic pH, the often tedious procedures for their manufacture, and the relatively high price for commercial capillaries compared to bare fused silica capillaries. But for many applications they are long-term stable.

In our work we prefer, what we call *statically adsorbed coatings*. A brilliant overview was given by Lucy et al. [5]. They are derived from polymers with rather long chain length and adhere to the capillary surface by physical effects, including hydrogen bridges and hydrophobic interaction (i.e., entropic effects) for neutral coatings,

but predominantly ionic interaction for cationic polymers. With the large number of attachment sites for long polymer chains, very stable coatings can be obtained, if a suitable coating protocol can be established. We learnt from our work that a good coating quality often requires some time to bind to the surface. Especially the cationic coatings have to overcome ionic repulsion during the coating process. On total we will show, how three coatings, two cationic of different induced EOF velocity, and one neutral coating can be chosen for optimal overall resolution of analyte signals.

In this chapter, we will first present some application examples of our CE–MS method. They will show the advantages but also some of its limitations. But we will demonstrate how impressive the tuning possibilities with regard to capillary coatings can be. In the second part of the chapter, all details of our coating procedure are presented. The Notes section will further point to practical aspects which will be helpful to start the method.

1.2 Separation Efficiency and Peak Capacity

In CE–MS with normal capillary lengths (we use 60 cm), we commonly achieve a separation within 15 min, only a few peptides, e.g., very small dipeptides, single amino acids, or very basic peptides may be found at higher migration times in case of cationic coatings. Most analytes are detected in a time window of about 10 min (*see* Fig. 1). Due to the extremely high separation efficiency, a high peak capacity is obtained. Comparing 4–9 s peak base width (for all but the late migrating analytes) with common peak widths in LC, a similar peak capacity with chromatographic methods would correspond to a separation window of about 30 min in conventional LC.

In Fig. 1a, a commercial tryptic digest of four proteins (BSA, PYGM Rabit, ENO1 Yeast, and ADH1 Yeast) was analyzed with OHNOON coating. Extremely sharp signals can be obtained with a high quality coating. The plate numbers, of course, depend on the diffusion coefficient of the analytes, but plate numbers of more than 400,000 were reached with our method for all three coatings [11]. About 500 signals were recorded within less than 5 min as presented in the electropherogram in Fig. 1a. MS/MS protein identification using a fast Q-TOF instrument is possible with this sample and high mascot score values between 200 and 600 were obtained for all four proteins. For MS/MS the impressive separation efficiency is critical with regard to the speed of the MS/MS cycles. With appropriate settings for threshold and release time, high quality spectra can be obtained with standard MS1 and MS2 times of 333 and 200 ms, respectively. An example is given in Fig. 1b.

1.3 Matrix Tolerance

Matrix components can have a negative impact on both ionization efficiency and analyte separation [12, 13] when chromatographic or electrophoretic separation techniques are used, especially with regard to sodium analyte adducts or sodium acetate clusters formed

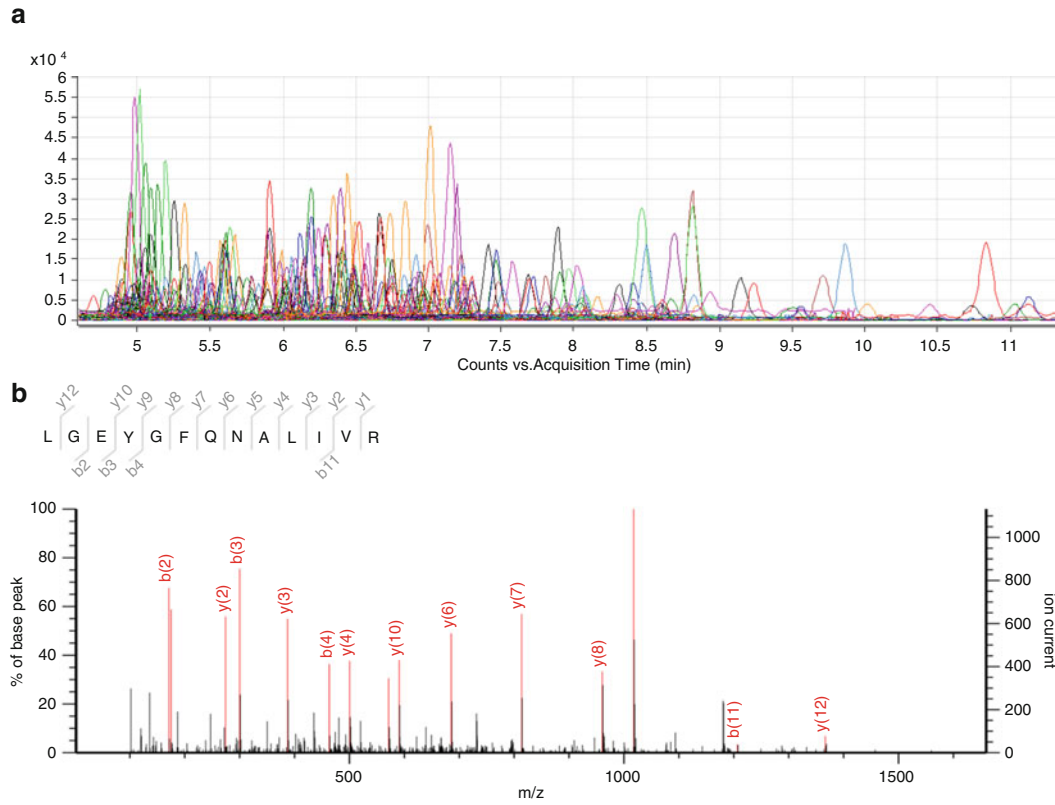

Fig. 1 (**a**) Excerpt of the electropherogram from the analysis of a commercial tryptic protein digest of four model proteins (BSA, PYGM Rabit, ENO1 Yeast, and ADH1 Yeast) separated in 3:1 acetic acid:formic acid (each 1 mol/L, Buffer A); samples were injected for 15 s at 100 mbar, standard CE method with OHNOON coating, −30 kV; (**b**) representative MS/MS spectrum for the peptide LGEYGFQNALIVR in another CE–MS/MS run

when a running buffer containing acetic acid is chosen [14]. In contrast to chromatographic approaches, a high salt content in the sample may have a positive or a negative impact on the separation performance in CE with de/stacking or sample-induced transient isotachophoretic phenomena [15–19]. Despite the impact of the ionic strength of the sample solution described earlier, CE–MS analysis can be performed without further sample pretreatment when samples with moderate salt content are investigated [20–22].

As an example for the analysis of samples with very high salt concentration, we here show the CE–MS analysis of two oligopeptide samples of the recombinant human chemokine CCL16 containing sodium chloride in a concentration up to 500 mmol/L for dissolution and prevention of aggregation. The chemoattractant cytokines (chemokines) form a family of secretory proteins which typically comprise about 75 amino acid residues with two disulfide bonds in their mature forms. Chemokines play an important role in activation and chemoattraction of leukocytes and other cell types; these functions are mediated by specific G-protein-coupled

receptors on the surface of target cells. Posttranslational modifications of chemokines have been described to increase or reduce their biological function. The polypeptide CCL16 investigated here contains an extension of about 25 amino acids at the C-terminus of the chemokine core structure. The exact function of this segment still has to be fully elucidated and is subject to further investigation. Enzymatic degradation upon long-term storage at 4 °C was assessed with CE–MS and the results are given in Figs. 2 and 3. In both cases, a very broad sodium zone (represented by the most abundant sodium acetate cluster), with its sharp boundaries clearly indicating isotachophoresis, was obtained. Peptide signals were well separated and were identified based on their mass differences to the CCL16 peptide confirming the assumed enzymatic degradation. In both samples, degradation at the C-terminus was more pronounced compared to the N-terminus.

Comparing the results for the two samples, Sample B clearly contains a higher amount of sodium (broader isotachophoretic peak).

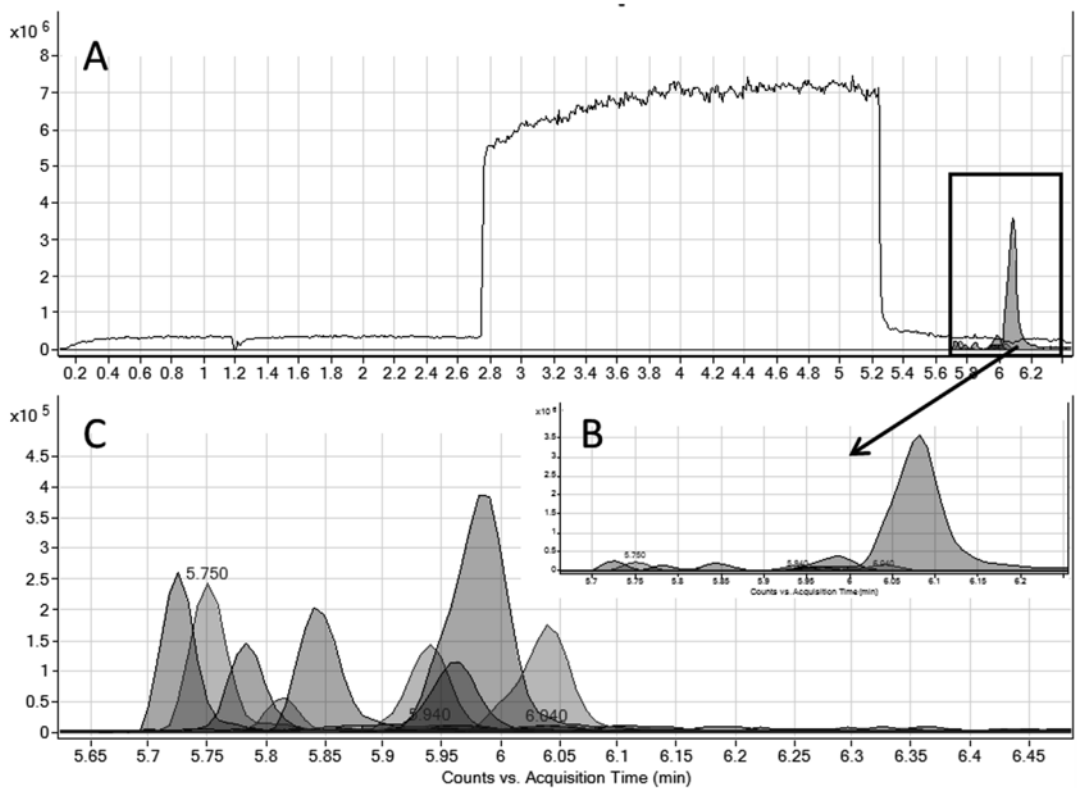

Fig. 2 CCL16 Sample A; standard BGE with LN coating, +30 kV; injection 3 s at 50 mbar; Buffer A; (**a**) The extracted ion electropherogram (EIE) of the most abundant sodium acetate cluster mass 268.998 is shown; (**b**) the EIEs for all assigned peptide masses are shown (the mass of intact CCL16 is detected at 6.08 min); (**c**) enlarged view of (**b**) excluding the EIE of intact CCL16

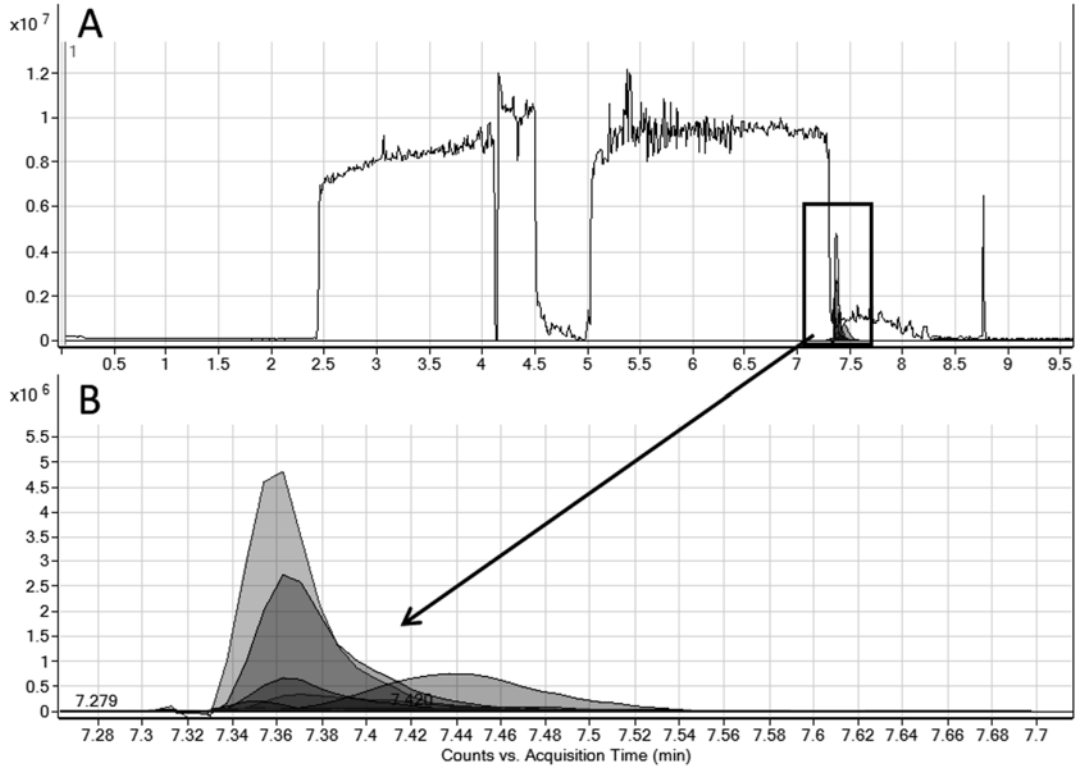

Fig. 3 CCL16 Sample B; standard BGE with LN coating, +30 kV; injection 3 s at 50 mbar; Buffer A; (**a**) the EIE of the most abundant sodium acetate cluster mass 268.998 is shown; (**b**) the EIEs for all assigned peptide masses are shown (enlarged view of (**a**), excluding the sodium acetate signal)

While a partial resolution of the different peptides could be achieved for Sample A, the transformation of the t-ITP stack into a CE-based peptide separation was not completed for Sample B. Here, the analytes could only be separated from the sodium zone which indicates that a sample salt concentration of 500 mmol/L or higher may be inappropriate for CE–MS analysis when a proper separation of the analytes themselves is required.

These results show that the CE–MS method is well suited for a fast screening of unknown samples with high ionic strengths, if transient leader ions are present. Both samples were successfully investigated without further sample pretreatment and valuable qualitative information was obtained within less than 10 min separation time for both samples. The neutral coating allowed for a very fast analysis of the investigated peptides due to their high effective electrophoretic mobility. However, for larger sample cohorts, frequent MS-source cleaning may be required.

1.4 Peptide Polarity

With the use of tryptic peptides, mostly a limited polarity range is obtained. This is ideal for LC–MS. Likewise, a rather good

distribution of basic amino acids is achieved and thus a rather homogeneous charge distribution. Currently, it is unknown, if this is not even a disadvantage for CE separation as only a limited mobility window is present. In any case, the situation changes, when native or therapeutic peptides are envisaged, where the polarity is predetermined. At least one charge (at the N-terminus) is present on each peptide so that all peptides will be amenable to CE. However, the distribution of hydrophilic vs. hydrophobic amino acids may become problematic for chromatographic techniques. An example are the very hydrophobic Aβ peptides being in charge for Alzheimer plaque formation in brain, which are notoriously difficult to analyze with RP-HPLC [1, 2]. Aβ 1–42 with the amino acid sequence DAEFRHDSGY EVHHQKLVFF AEDVGSNKGA IIGLMVGGVV IA contains a high number of hydrophobic amino acids and thus shows a very high retention in RPLC. When this larger peptide is subjected to enzymatic digestion, the situation is even worse as the C-terminus is solely composed of hydrophobic amino acids at positions 29–42, while the N-terminus contains 5 basic amino acids (arginine, lysine, and 3 histidines) at positions 1–16. As a consequence, a full sequence coverage for tryptic or Lys-C peptides cannot be obtained with RP-HPLC [23]. It has to be pointed out that the N-terminal peptides from Aβ digests with trypsin or Lys-C cannot be covered by RPLC together with the C-terminal one, as they comprise the hydrophilic amino acids.

We tested our standard CE–MS method with OHNOON for Lys-C digested Aβ 1–40 and 3 intact Aβ peptides, slightly varying in the length at the C-terminus. The results are given in Fig. 4 for intact Aβ. Baseline separation was obtained in less than 10 min. No tailing and thus no hydrophobic interaction was visible.

With the same CE–MS method, also extremely hydrophilic peptides containing a large number of basic amino acids can be

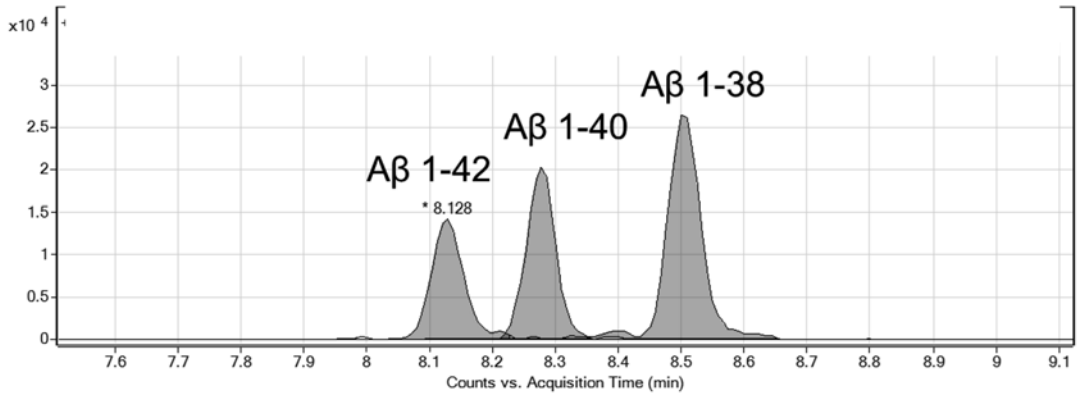

Fig. 4 CE–MS separation of three intact Aβ peptides (1–42, 1–40, 1–38) with an OHNOON coated capillary. Standard BGE, −30 kV separation voltage; sample injection 5 s at 50 mbar, Buffer A

characterized. For example, we analyzed a therapeutic peptide with five arginines and a pI of >11 [24]. We here used polybrene coating to account for the extremely large effective electrophoretic mobility of this peptide in our standard BGE. In contrast, LC–MS failed even when using HILIC columns [24].

To summarize, we can clearly show that CE–MS is able to comprise all peptides in one run as at least one (N-terminal) charge will be present. CE–MS is independent of the polarity of the peptide species, which makes it ideal for the study of protein digests with peptides of varying polarity and thus for diagnostic and therapeutic peptides.

1.5 Resolution and Coatings

When using coatings, the first aspect to be addressed is the reduction of adsorption phenomena and thus a higher robustness, just like procedures such as end-capping for chromatographic columns. However, with the surface modification, also the EOF is modified, which strongly influences the resolution, which is proportional to the square root of $1/(\bar{\mu} + \mu_{eo})$ and thus the difference between the analytes' mean effective electrophoretic mobility $\bar{\mu}$ and the electroosmotic mobility μ_{eo} [6]. With a neutral coating, this term reduces to $\bar{\mu}$, but for counterelectroosmotic migration of analytes, that is, with cationic coatings when using a low pH BGE, very small values and thus high resolution may be obtained. In contrast, for coelectroosmotic migration, very low resolution has to be expected.

For peptide analysis, we consider all three coatings. Figure 5 demonstrates the differences in overall analysis time and resolution obtained from this comparison. Of course, for LN, the migration order is reversed compared to the cationic coatings. Analysis time for the coatings is polybrene < LN < OHNOON. Each coating has an optimal resolution for different peptides, which is highest for those peptides having an effective electrophoretic mobility closest to μ_{eo}. Of course, for LN this accounts for the slowest peptides but for the fastest with PB and OHNOON. Highest resolution would be obtained with the effective electrophoretic mobilities of the two analytes of one pair bracketing the electroosmotic mobility. The analytes, however, would then show an overall migration in opposite directions. With this knowledge we can now adapt the coating strategy according to the analyte mobility in combination with the analysis time: for highest effective electrophoretic mobility analytes, PB is a good choice, for slow analytes, OHNOON may be preferred, whereas LN is ideal for analytes of intermediate effective electrophoretic mobility. If mixtures with a broad analyte characteristic are to be analyzed we mostly choose OHNOON, whereas we select LN coating for prescreening experiments.

As an example for analytes with intermediate to fast effective electrophoretic mobility, we analyzed intact RNase B (pI of RNase $A \sim 9.63$), which is decorated with high mannose glycans and thus

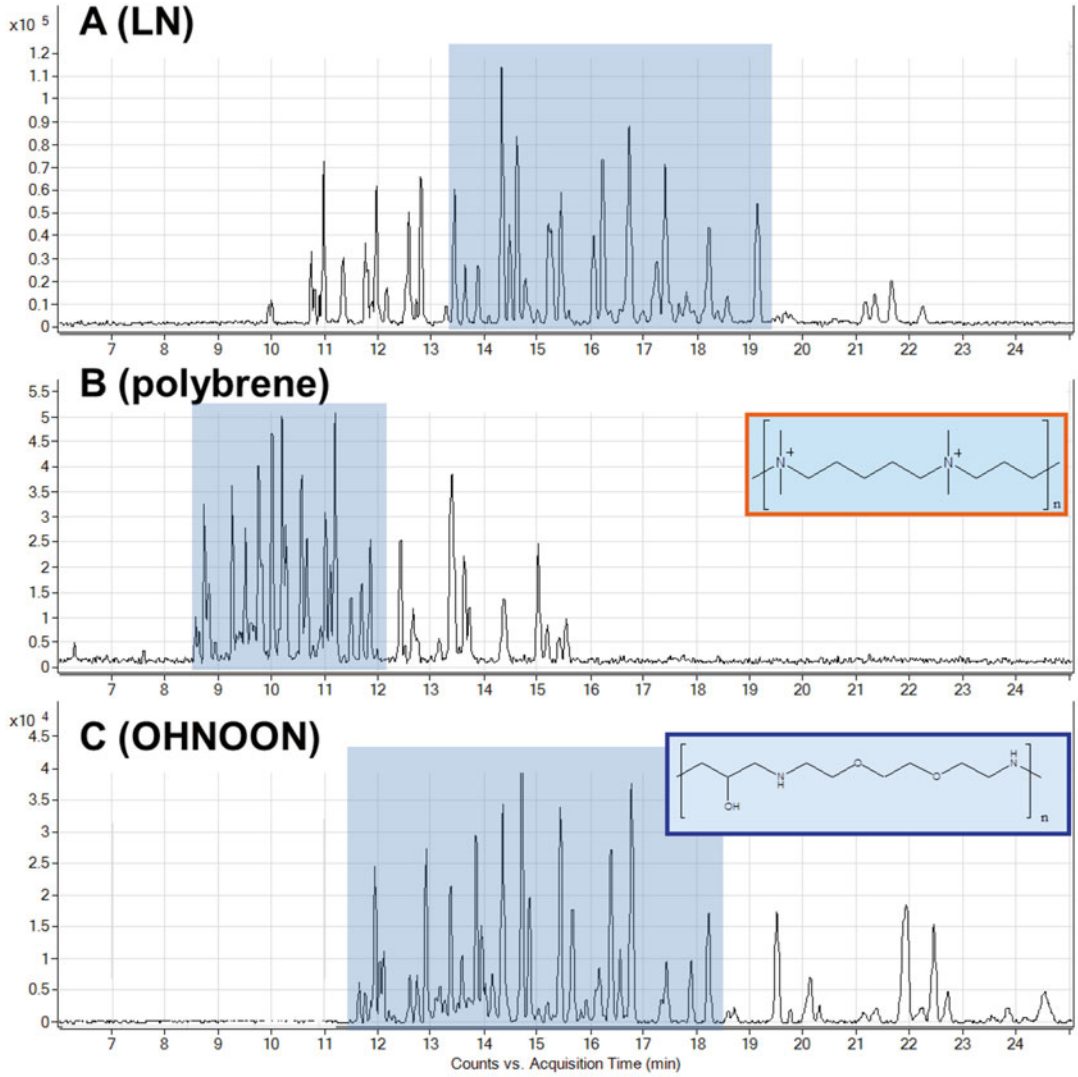

Fig. 5 Separation of a tryptic BSA digest with 80 cm capillaries using Buffer B. Analytes were injected for 5 s at 50 mbar. The separation voltage was +30 kV for the neutral and −30 kV for the cationic coatings. The standard coating procedure was used. (**a**) (LN), (**b**) (polybrene), and (**c**) (OHNOON) show the base peak electropherogram (BPE) constituted of the masses of all major BSA signals

has isoforms differing in the number of mannoses [5–9]. High mannose glycopeptides or small intact proteins like the RNase are relatively easy to separate [25], however, only at optimized EOF conditions. As visible in Fig. 6, LN provides fast analysis with insufficient resolution. As there are clear differences in the effective electrophoretic mobilities, another coating strategy will be helpful: using polybrene, similarly fast separations can be obtained with acceptable resolution. Only with the slow EOF for OHNOON coating, however, very high resolution and near-baseline

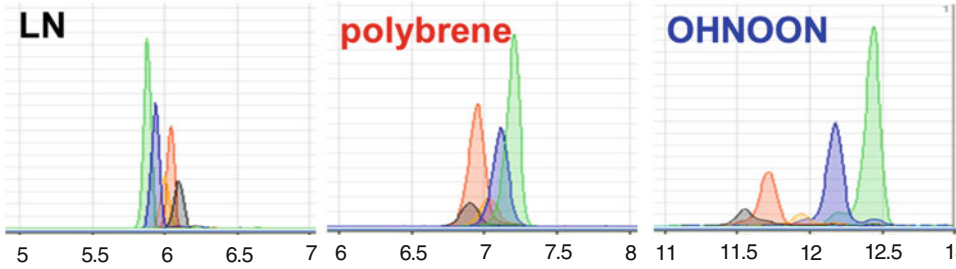

Fig. 6 Intact RNAse B with high mannose glycan isoforms. Buffer A, the separation voltage was +30 kV for the neutral and −30 kV for the cationic coatings; samples were injected for 5 s at 50 mbar

separation is possible. In contrast, the analysis time is nearly doubled. This example impressively shows the fine-tuning possibilities with an appropriate coating strategy.

Small glycopeptides from immunoglobulin (IgG) purified from human plasma using ProtG are an interesting example for low mobility analytes. Twenty micrograms of IgG were tryptically digested. Compared to the peptide backbone, the glycans constitute relatively large hydrophilic substituents, which strongly reduce the peptide electrophoretic mobility by increasing the hydrodynamic radius. Sialic acids additionally neutralize cationic charges and further reduce the migration velocity. With LN coating, too long migration times evolve and diffusional band broadening reduces both resolution and sensitivity. With cationic coatings, extremely fast analysis is possible with separation times less than 3.5 min for polybrene and less than 5.5 for OHNOON (Fig. 7). Again, resolution is lower for polybrene. With OHNOON a partial separation of peptide isoforms differing in the number of galactoses is obtained. It has to be noted that no separation for the IgG subforms (IgG 1, 2, and 4) based on the peptide moiety was obtained.

2 Materials

Capillaries: bare fused silica capillaries with 50 μm inner diameter, length 60 or 80 cm.

Electrode cleaning: ethanol, if necessary aqueous ammonia (1 mol/L)

Background electrolyte: acetic acid:formic acid, 3:1, each 1 or 2 mol/L (Buffer A and Buffer B).

Sheath liquid composition: isopropanol:water, 1:1 plus 1% acetic acid.

Reference standard: We use a tryptic digest of bovine serum albumin as reference material (prepared at larger amount and

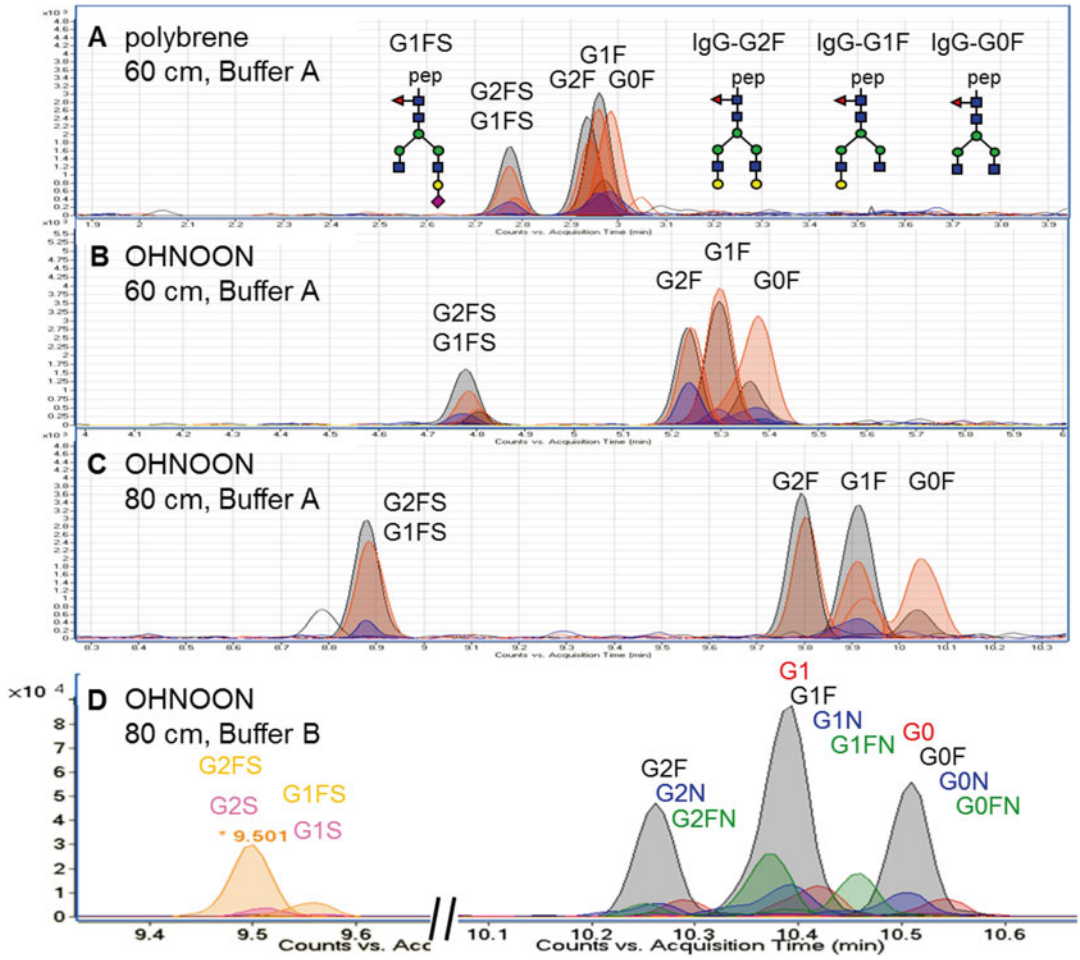

Fig. 7 Glycopeptides in human IgG (tryptic digest); Buffer A was used in (**a**)–(**c**), Buffer B in (**d**), the separation voltage was −30 kV. (**a**) polybrene, 60 cm capillary, (**b**) OHNOON, 60 cm cap., (**c**) OHNOON, 80 cm cap., and (**d**) enlarged view, OHNOON, 80 cm cap., Buffer B. Note the increase in migration time and analyte resolution from **a** to **d**

frozen in aliquots). Also, commercial standards may be analyzed or ideally spiked tryptic digests as internal standards.

Tryptic digest: Chemicals required are acetonitrile, ammonium bicarbonate, trypsin, glacial acetic acid, iodoacetamide, dithiothreitol, RapidGest, ice. Materials required are stove (37 and 60 °C). Ninety-six well plates made of polypropylene (from NUNC) can be used.

OHOON coating synthesis: ethylenedioxy-diethylamine, epichlorohydrin, glacial acetic acid, ice bath, flask (250 mL), and stirrer.

Commercial coatings: LN coating EOTROL (concentrate) from Target Discovery (Palo Alto, CA, USA), polybrene (>95%, MW = 15,000).

3 Methods

3.1 Coating Materials

1. The commercial LN coating is a polyacrylamide derivative, which adheres to the capillary surface by hydrophobic interactions. According to the vendor, it can be removed by highly concentrated sodium hydroxide solution. This coating can well be applied for a large range of applications. Many colleagues report a higher robustness, when separations are conducted with additional 10 mbar pressure. This is helpful for the electrospray interface as no EOF transports BGE to the MS. The need for additional pressure during the separation can easily be assessed when frequent spikes occur for MS detection (with the capillary being installed properly).
2. The commercial polybrene solution (>95 %) has a relatively high charge density and thus induces a very high electroosmotic flow. With our standard BGE, the electroosmotic mobility is -6.2×10^{-4} cm^2/V s. The EOF velocity is almost pH independent due to the presence of quaternary ammonium groups. The great advantages of polybrene are very fast measurements and a very high robustness of the CE–MS coupling as the EOF transports a significant amount of BGE to the interface. However, for some applications, the EOF is too fast to allow for high resolution and a higher noise level is obvious in MS detection.
3. OHNOON coating was optimized with regard to a moderate charge density and thus moderate induced EOF, which in our standard BGE is -5.2×10^{-4} cm^2/V s. In addition, instead of alkyl spacers as in polybrene, we chose ether functionalities to increase the hydrophilicity of the coating and reduce possible hydrophobic interactions. The coating is not commercially available but can be produced in a very simple synthesis according to a similar procedure originally published elsewhere [26]. We prepared different batches, which gave rise to suitable coatings with similar EOF. One batch of 20 mL proved to be sufficient for 5 years of work proving the excellent stability of the polymer when stored at 4 °C. The OHNOON coating was synthesized according to [11]: 7.51 g (0.05 mol) 2,2′-(ethylenedioxy)-diethylamine was dissolved in water and the flask was positioned in an ice bath. Then, 4.65 g (3.94 mL, 0.05 mol) epichlorohydrin were added dropwise to the stirred solution. Within 48 h of continuous stirring, the solution thickened and water (10 mL) was added, followed by seven additional days of stirring, until the reaction was complete. Afterwards, the pH of the polymer solution was adjusted to 8 with 2 mol/L acetic acid and diluted with water to a total volume of 50 mL, yielding the viscous coating stock solution, containing 0.2 g/mL of the coating agent (calculated as free base). The name OHNOON was derived just from reading the functionalities in the polymer repeating unit including the hydroxy, 2 amine, and two ether functions.

3.2 Coating Procedures

3.2.1 Capillary Conditioning and Coating Application

First of all, the capillary has to be cut to a suitable length. We routinely use 60 cm capillaries for CE–MS coupling (*see* **Note 1**). If we use a BGE of 2 mol/L, the capillary length has to be increased or the separation voltage decreased to avoid excessive Joule heating. From our observation, a good capillary cut being smooth is vital, especially on the MS side (*see* **Notes 2** and **3**). We remove the polyimide coating at both ends at a length of 3 mm using a simple lighter (*see* **Note 4**).

The capillary conditioning is critical to fully clean and activate the silanol surface of the capillary. The rinsing processes are programmed as a CE method, also including the coating step itself, so the whole procedure can be conducted automatically and unattended (Table 1). During rinsing, the capillary outlet is immersed in BGE (*see* **Note 5**).

Table 1

Protocol for capillary conditioning and application

Solution	Time	Pressure/voltage
Methanol	600 s	1 bar
1 mol/L HCl	600 s	1 bar
1 mol/L NaOH	1500 s	1 bar
Distilled water	600 s	1 bar
Coating solution[a]	1800 s	1 bar
For OHNOON additional rinsing with 1:10 diluted coating solution (*see* **Note 6**)	600 s	1 bar
Incubation in coating solution (*see* **Note 7**)	Overnight, at least 5 h	
BGE	20–300 s	5 bar (*see* **Note 8**)
Test on permeability (watching the capillary end upon pumping with 1 bar)		
BGE	600 s	1 bar
Conditioning at ±30 kV (depending on the coating type)	600 s	±30 kV
Rinsing with fresh BGE	600 s	1 bar
Cleaning spray shield and ESI tip (*see* **Note 9**) with isopropanol or sheath liquid	Optional; recommended whenever increased MS background is observed	

[a]Polybrene 5 % solution; LN EOTROl, dilution 1:5; OHNOON, dilution 1:5

For coating application, different dilutions for the different coatings are used: For polybrene, a 5% aqueous polymer solution can be made and used directly. For LN and OHNOON we prefer a 1:5 diluted solution for the coating application in order to avoid clogging. The coating is left in the capillary overnight (*see* **Note 7**). Short incubation times (e.g. 3 h) lead to significantly lowered separation efficiency [11].

3.2.2 Rinsing Out Coating Solution and Capillary Conditioning

Having ensured the permeability of the capillary, the coating solution is rinsed out with BGE at 1 bar for 600 s (*see* **Note 8**). Make sure that you avoid rinsing steps with NaOH and organic solvents from now on. For polybrene and LN coating it was stated that highly concentrated NaOH solution will remove the coating. Afterwards, the capillary is inserted into the electrosprayer and installed at the MS. We strongly recommend an electrophoretic conditioning for at least 20 min at + or –30 kV (depending on the coating charge). During this time, the ESI voltage should still be switched off to prevent contamination of the MS: in this early time period one can observe a very large signal intensity in the mass spectrometer of various compounds. These signals diminish over time (typically 5–10 min) and can be related to compounds still present on the capillary surface, which leek into the BGE. Additionally, many compounds from the fingertips of the operator as well as from the removal of the polyimide layer will be present until they are rinsed away by the sheath liquid and the BGE (*see* **Note 10**).

A fresh inlet vial with BGE is now installed and the capillary is rinsed at 1000 mbar for 600 s. In the last step before use, the sprayshield and the sprayer are quickly wiped with isopropanol to avoid contamination. We recommend waiting for additional 180 s after cleaning of the electrosprayer until the MS is switched on to ensure minimum contamination of the transfer capillary with the coating polymer. The first measurements may still show some drifting phenomena, which quickly diminish [11]. We use a tryptic digest of BSA which was prepared according to the protocol described in Subheading 3.5 in a 96-well plate. After digestion, the wells were combined and aliquots were frozen for further use.

These are our criteria for a successful coating when using capillaries of 60 cm length (50 μm i.d.), BSA samples as described later and the CE and MS parameters given as follows: The current observed for ±30 kV has to be stable at 33 ± 2 μA for Buffer A. Increasing the acid concentration by a factor of 2 (Buffer B) requires to use longer capillaries and/or reduce the separation voltage (we use 80 cm capillaries at ±30 kV or 60 cm capillaries at ±25 kV) to avoid excessive Joule heating (*see* **Note 12**).

First of all, the migration times of the EOF are recorded. In general, the EOF was very repeatable and low RSDs intra- and interday were obtained. The EOF migration time for OHNOON

was at 3.7–3.9 with a 60 cm capillary and Buffer A (*see* **Note 13**), for polybrene at 2.9–3.2 min. The electroosmotic mobility of LN coated capillaries was negligible.

An important criterion was the separation efficiency. For 60 cm capillaries, plate numbers of 200,000–350,000 corresponding to peak base widths of 4–8 s were obtained for most analytes with migration times below 10 min. We here want to stress that very often, repeatable EOF and high separation efficiency were observed simultaneously. We did not observe bleeding effects. However, recoating steps were shown to be beneficial for the long-term stability of the capillary coatings (*see* **Note 13**).

3.3 CE–MS Method

CE: The BGE usually consists of acetic acid (1 mol/L):formic acid (1 mol/L) in a ratio of 3:1 (Buffer A) leading to a current of 33 ± 2 μA (*see* **Note 12**). Sometimes, also a 2 mol/L (each) solution was used as the basis (Buffer B). The current was, of course, significantly increased reaching more than 40 μA. For these measurements, the voltage was decreased or the capillary prolonged (80 cm or 25 kV for the 60 cm capillaries). Our standard injection parameters are 50–100 mbar for 5 s. The usual run time for 60 cm capillaries and 30 kV separation voltage is 15 min, if OHNOON is used. For LN somewhat higher migration times may be observed for very low mobility analytes. With polybrene, fast runs are possible. However, for the 2 mol/L BGEs and the 80 cm capillaries, 30 min are required to cover all peptides of the sample for OHNOON and LN coating.

SL: The sheath liquid of the standard method consists of 50:50 water:isopropanol with 1 % glacial acetic acid added for higher conductivity (*see* **Note 14**). Acetic acid and protons are thus present in the sheath liquid to provide counterions for the electrophoretic run. The sheath liquid is delivered via an LC pump at a flow rate of 400 μL/min (*see* **Note 15**). If required we add tune masses for internal calibration to the sheath liquid, e.g., 10–20 μL purine and 20–50 μL of the Agilent tune mass HP-1221 solution to 100 mL sheath liquid. The signal intensity of these internal standards should exceed 10,000 counts (*see* **Note 16**).

MS: For our QTOF a fragmentor voltage of 175 V is commonly used, higher voltages up to 215 V can be used when larger peptides are to be analyzed. The capillary voltage is set to 4000 V. The data frequency is critical due to the very high peak efficiency. Our compromise between intensity and accurate description of the signal is 2 Hz.

3.4 Control Sample

We use a tryptic digest of BSA to characterize the quality of the coating. Standard electropherograms for all coatings are given in Fig. 8. A good coating quality is characterized by peak base widths in the range of 4–8 s for the majority of the peaks with migration times below 10 min when Buffer A is used, including a significant

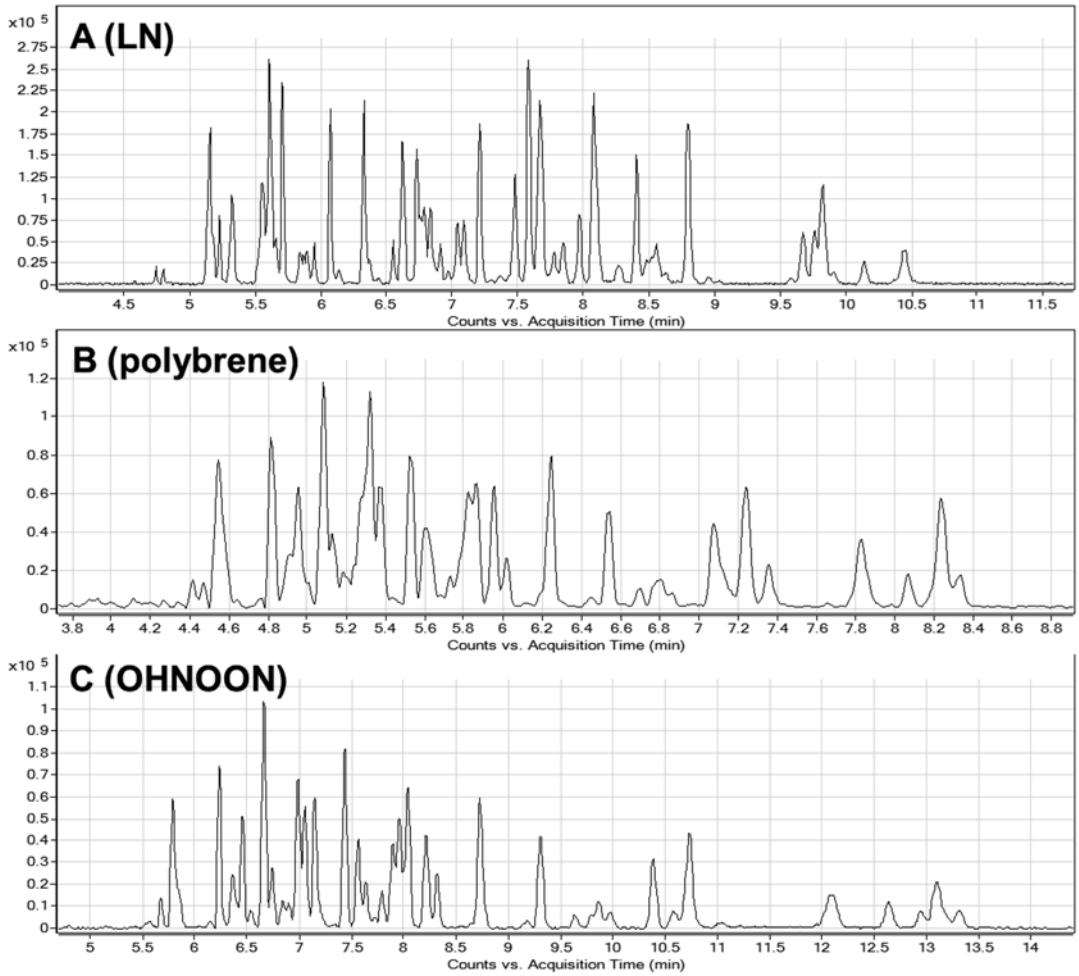

Fig. 8 CE–MS electropherogram of a BSA tryptic digest under standard CE–MS conditions for a 60 cm capillary with Buffer A, coated with (**a**) LN, (**b**) polybrene and (**c**) OHNOON coating. Note the sharp peaks for all analytes with migration times below 10 min

number of signals with peak base widths in the range of 6 s or below (*see* **Note 17**). As described in [11] drifting migration times may be observed for the first measurements. When stabilization of the migration times is observed, RSD values for the migration times in the range of 0.5% should be observed for analytes with migration times below 10 min; RSD values in the range of 0.2–0.3% are commonly achieved in our lab.

3.5 Tryptic Digestion

Tryptic digestion of BSA is performed based on a modified protocol given by Selman et al. [27]. We use the same protocol also for other standard proteins and protein samples of unknown composition. We use 96-well plates from vwr (NUNC 442587) for the procedure.

1. The commercial trypsin (sequencing grade modified trypsin) is dissolved with 100 µL ice-cold aqueous acetic acid solution (20 mmol/L) (57.2 µL glacial acetic acid in 50 mL distilled water). The solution is then diluted to 2000 µL using a 15:85 mixture of acetonitrile and distilled water. All solutions are stored on ice.
2. 2 µL of the protein solution (for protein standards usually 10 mg/mL protein in water) are added to 15 µL RapidGest solution (0.1%, which is prepared dissolving the content of one vial of RapidGest from the vendor in 1 mL aqueous NH_4HCO_3 (50 mmol/L)) (*see* **Note 18**).
3. 1.3 µL aqueous dithiothreitol solution (50 mmol/L from dissolving 7.71 mg in 1 mL NH_4HCO_3 solution (50 mmol/L)) are added and the mixture is incubated for 60 min at 60 °C (*see* **Note 18**).
4. Then, 4 µL aqueous iodoacetamide solution (50 mmol/L obtained by dissolving 9.248 mg in 1 mL water) are added. The incubation is accomplished for 30 min at room temperature in darkness as iodoacetamide is photosensitive. A fresh solution is always recommended.
5. Now, 20 µL of the trypsin solution are added (20 µg dissolved in 2000 µL), which equals 200 ng trypsin per vial. The mixture is then incubated for 8 h or overnight at 37 °C.

3.6 Cleaning Electrodes and Prepunchers

Care has to be taken not to contaminate fresh capillaries with coating from previous runs. When changing the coating type it is vital to clean the electrodes and the prepuncher, where especially cationic coatings are deposited. We achieve this simply by removing the inlet electrode and the prepuncher from the CE instrument. The hollow electrodes from Agilent have to be penetrated with a fused silica capillary to allow the ethanol to replace the air inside the electrode. Then the electrode is rinsed with ethanol several times using a pipette. The electrode is then completely immersed in ethanol in a small beaker. It is necessary to fill ethanol into the electrode for Agilent machines (and to rinse with a pipette) to make sure that the inner cylinder is filled with solution and to remove crude coating adherences. The prepuncher can simply be immersed in ethanol. Then, ultrasonication for 15–20 min is applied. The electrode is then rinsed four times with fresh ethanol (inside and outside), the prepuncher is immersed once in fresh ethanol and the solution is allowed to drain. After drying the electrode is reinstalled. We recommend using gloves for this step to avoid contaminating the electrode surface (*see* **Note 19**). Please note that electrode cleaning is especially required when switching to bare fused silica capillaries or when switching from cationic to neutral coating.

4 Notes

1. With a CE–MS system from Agilent, also 55 cm capillaries may be used. Other instrument configurations may require longer capillaries. For short capillaries, make sure to restrict the electrophoretic current to 40 μA to avoid damages on the ESI needle and reduce Joule heating effects. We prefer to work with short capillaries, simply because the analysis time increases with the square of the capillary length—L^2 and mostly no pronounced gain in resolution is obtained for longer capillaries. However, in order to ensure maximum analyte resolution and to increase plate numbers, we used 80 cm capillaries successfully.
2. To our experience, best cuts are obtained with a ceramic cutter, at an angle of 35–45° to the capillary, cutting with its edge. Alternatively, commercial cutters may be employed.
3. For the control of the quality of the cut, we normally install the capillary in the ESI sprayer and check the capillary end with the lens we otherwise use to control the capillary positioning in the ESI needle.
4. Removing the polyimide serves two main purposes. (a) Polyimide is known to swell over time in the presence of organic solvents. This can potentially lead to an irregularly shaped capillary outlet which reduces electrospray stability. To a lesser extent, the same accounts for the capillary inlet. (b) Even though polyimide is relatively stable, small amounts of the polymer can be washed out over time, potentially leading to interferences with MS detection. With regard to the swelling phenomena described earlier we remove the polyimide coating to reduce the risk of mass spectrometric interferences.
5. We immerse the capillary outlet in a BGE vial during rinsing. This acidic solution helps to prevent an MS contamination later on (especially from sodium ions) and reduces the risk of evaporation followed by crystallization and capillary blockage.
6. The extra rinse with a 1:10 coating solution was observed to be necessary due to the high viscosity of the more concentrated solution. After the overnight incubation process, frequent blockage of the capillary was observed, which can easily be prevented with a less concentrated solution.
7. We observed large differences in the separation efficiency when the incubation time for the coating was only 3 h compared to an overnight coating procedure. We assume that only the evolution of multiple binding sites for each polymer strain leads to a high surface coverage and thus an optimal shielding of the silica surface. This holds true especially for the cationic coatings, where ionic repulsion will be present between polymer chains.

8. The high-pressure step at 5 bar (you may have to use the external pressurization options, depending on the vendor of the instruments) is necessary as we otherwise frequently observed capillary blockage, mainly in case of OHNOON with the highest viscosity.
9. We clean the capillary tip, the ESI needle tip, and spray shield quickly by rinsing with isopropanol or with sheath liquid to avoid coating solution entering the MS and adsorb onto the inner wall of the glass transfer capillary at the MS inlet. The cleanliness may be observed monitoring the total ion current in the MS at a glance until an acceptable noise level is reached (typically within 3–10 min).
10. For our system, the total ion current measured at 2 Hz and at 400 μL/min sheath liquid flow rate reaches $1 \times E^7$, when +30 kV are applied (5,000,000–7,500,000, for −30 kV) after some time. Measurements are then possible without quenching problems.
11. The first three measurements may show some migration time shift, when freshly prepared capillaries are used or a recoating step was made. Migration times asymptotically stabilize relatively quickly in most cases. When a recoating step was applied (compare *see* **Note 13**), shifting phenomena are sometimes present for more than five measurements, especially when the capillary was rinsed with coating solution for a relatively long time (>10 min). Accordingly, we recommend short recoating procedures (flush time 3–5 min), longer recoating steps are only required in "severe" cases, e.g., when the capillary was not used for more than a week. It should be noted that the quality of the analytical run is not negatively affected even if the shifting phenomena are observed for a longer time period, so only surface effects are present.
12. In general, we restrict the current to below 40 μA for our system. First to avoid excessive Joule heating and second to reduce the risk to harm the ESI needle.
13. Especially for freshly coated capillaries, the separation performance and migration time stability may decrease after 10–20 consecutive runs. Capillary recoating steps were extremely useful to increase the long-term stability of the capillary coating. Capillary recoating is simply accomplished via rinsing the capillary for 3–10 min with coating solution, followed by a 300–600 s rinse with BGE and 600 s capillary conditioning at ±30 kV. While recoating may be necessary with polybrene coated capillaries more frequently, 2–3 recoatings steps at the first 2–3 days of use often were found to be "sufficient" to provide very stable capillary coatings which then could be used for 1 week without further recoating.

14. This EOF value is expected for our OHNOON coating. We did not observe large differences upon OHNOON production batches, but changes are possible. The reference method thus has to be defined thoroughly in the beginning.
15. A higher percentage of 70% isopropanol may be helpful to increase the ionization efficiency of some peptides in case of cationic coatings. For the neutral LN coating, a higher organic content of the sheath liquid frequently results in poor electrospray stability.
16. Surprisingly, the sheath liquid flow rate shows a relatively low impact on signal intensity, e.g., when the flow rate is varied between 4 and 6 μL/min. Often, the electrospray flow rate can be varied in order to ensure stable electrospray conditions.
17. In case of a higher noise level in the mass range of purine, higher concentrations of this standard will be necessary. Slightly higher ion counts (20,000–50,000) can be beneficial to assure maximum mass accuracy.
18. Migration time stability: peak base widths *below* 6 s for the fast migrating analytes and RSD values for the migration time below 0.5% (typically 0.2–0.3%) characterize a "very" high quality coating. However, stable measurements can also be performed with slightly broader signals (minimum peak base width 6–7 s) and slightly less stable migration times (RSD up to 1%). Higher values indicate inaccurate separation conditions, challenging sample composition/analyte properties or a poor coating quality.
19. More DTT/iodoacetamide and/or a RapidGest solution of higher concentration (factor of 4) may be necessary if the protein contains many disulfide bridges or is difficult to denature.
20. In rare cases, but mostly for cationic coatings, this cleaning procedure was not sufficient. This can easily be seen from the current profile, which diminishes quickly if a cationic surface is created and the EOF is reversed. Sheath liquid is then sucked into the capillary decreasing the conductivity through the capillary. In this case, we recommend to take the electrode and prepuncher out once more and to leave the electrode in ethanol for 3–5 h followed by ultrasonication for 30 min. The electrode is then left for 20–30 min in aqueous ammonia ($c = 1$ mol/L). Please make sure that the inner cylinder is filled. Make sure that the electrode is not left in ammonia for a longer time period and do not use more aggressive solvents in order to protect the electrode from oxidation. For the same reason, the electrode and prepuncher have to be washed with water immediately after removal from the ammonia solution. Note: It may be necessary to include the cleaning step with ammonia in the routine method.

References

1. Condron M, Monien B, Bitan G (2008) Synthesis and purification of highly hydrophobic peptides derived from the C-terminus of amyloid β-protein. Open Biotechnol J 2:87–93
2. Du C, Ramaley C, McLean H, Leonard SC, Miller J (2005) High-performance liquid chromatography coupled with tandem mass spectrometry for the detection of amyloid beta peptide related with Alzheimer's disease. J Biomol Techn 16:354–361
3. Zhao SS, Zhong X, Tie C, Chen DDY (2012) Capillary electrophoresis-mass spectrometry for analysis of complex samples. Proteomics 12(19–20):2991–3012. doi:10.1002/pmic.201200221
4. Kolch W, Neusüß C, Pelzing M, Mischak H (2005) Capillary electrophoresis-mass spectrometry as a powerful tool in clinical diagnosis and biomarker discovery. Mass Spectrom Rev 24(6):959–977
5. Lucy CA, MacDonald AM, Gulcev MD (2008) Non-covalent capillary coatings for protein separations in capillary electrophoresis. J Chromatogr A 1184(1–2):81–105
6. Huhn C, Ramautar R, Wuhrer M, Somsen GW (2010) Relevance and use of capillary coatings in capillary electrophoresis–mass spectrometry. Anal Bioanal Chem 396:297–314
7. Hjertén S (1985) High performance electrophoresis elimination of electroendoosmosis and solute adsorption. J Chromatogr 347:191–198
8. Xu L, Dong X-Y, Sun Y (2009) Electroosmotic pump-assisted capillary electrophoresis of proteins. J Chromatogr A 1216(32):6071–6076
9. Kitagawa F, Inoue K, Hasegawa T, Kamiya M, Okamoto Y, Kawase M, Otsuka K (2006) Chiral separation of acidic drug components by open tubular electrochromatography using avidin immobilized capillaries. J Chromatogr A 1130(2):219–226, doi: http://dx.doi.org/10.1016/j.chroma.2006.03.077
10. Ou J, Li X, Feng S, Dong J, Dong X, Kong L, Ye M, Zou H (2006) Preparation and evaluation of a molecularly imprinted polymer derivatized silica monolithic column for capillary electrochromatography and capillary liquid chromatography. Anal Chem 79(2):639–646. doi:10.1021/ac061475x
11. Pattky M, Huhn C (2013) Advantages and limitations of a new cationic coating inducing a slow electroosmotic flow for CE-MS peptide analysis: a comparative study with commercial coatings. Anal Bioanal Chem 405(1):225–237. doi:10.1007/s00216-012-6459-8
12. Chiu C-W, Chang C-L, Chen S-F (2012) Evaluation of peptide fractionation strategies used in proteome analysis. J Sep Sci 35(23):3293–3301. doi:10.1002/jssc.201200631
13. Hall TG, Smukste I, Bresciano KR, Wang Y, McKearn D, Savage RE (2012) Identifying and overcoming matrix effects in drug discovery and development. In: Prasain J, Dr Jeevan Prasain (eds) Tandem mass spectrometry—applications and principles, ISBN: 978-953-51-0141-3, InTech, DOI: 10.5772/32108. http://www.intechopen.com/books/tandem-mass-spectrometry-applications-and--principles/identifying-and-overcoming-matrix-effects-in-drug-discovery-and-development. DOI: 10.5772/32108
14. Kamerke C, Pattky M, Huhn C, Elling L (2013) Synthesis of nucleotide-activated disaccharides with recombinant β3-galactosidase C from Bacillus circulans. J Mol Catal B: Enzym 89:73–81
15. Huhn C, Pyell U (2010) Diffusion as major source of band broadening in field-amplified sample stacking under negligible electroosmotic flow velocity conditions. J Chromatogr A 1217(26):4476–4486
16. Burgi DS, Chien RL (1991) Optimization in sample stacking for high-performance capillary electrophoresis. Anal Chem 63(18):2042–2047
17. Chien RL, Helmer JC (1991) Electroosmotic properties and peak broadening in field-amplified capillary electrophoresis. Anal Chem 63(14):1354–1361
18. Chien RL, Burgi DS (1992) On-column sample concentration using field amplification in CZE. Anal Chem 64(8):489A–496A. doi:10.1021/ac00032a002
19. Boden J, Bächmann K (1996) Investigation of matrix effects in capillary zone electrophoresis. J Chromatogr A 734(2):319–330
20. Cao P, Moini M (1998) Analysis of peptides, proteins, protein digests, and whole human blood by capillary electrophoresis/electrospray ionization-mass spectrometry using an in-capillary electrode sheathless interface. J Am Soc Mass Spectr 9(10):1081–1088
21. Wahl JH, Gale DC, Smith RD (1994) Sheathless capillary electrophoresis-electrospray ionization mass spectrometry using 10 μm I.D. capillaries: analyses of tryptic digests of cytochrome c. J Chromatogr A 659(1):217–222
22. Zhang B, Foret F, Karger BL (2000) A microdevice with integrated liquid junction for facile peptide and protein analysis by capillary elec-

trophoresis/electrospray mass spectrometry. Anal Chem 72(5):1015–1022

23. Watanabe K-I, Ishikawa C, Kuwahara H, Sato K, Komuro S, Nakagawa T, Nomura N, Watanabe S, Yabuki M (2012) A new methodology for simultaneous quantification of total-Aβ, Aβx-38, Aβx-40, and Aβx-42 by column-switching LC/MS/MS. Anal Bioanal Chem 402(6):2033–2042. doi:10.1007/s00216-011-5648-1
24. Pattky M, et al. (2015) Structure characterization of unexpected covalent O-O-sulfonation and ion pairing on an extremely hydrophilic peptide with CE-MS and FT-ICR-MS. Anal Bioanal Chem 407:6637–6655
25. Pattky M, Huhn C (2010) Protein glycosylation analysis with capillary-based electromigrative separation techniques. Bioanal Rev 2(1):115–155. doi:10.1007/s12566-010-0018-6
26. Hardenborg E, Zuberovic A, Ullsten S, Soderberg L, Heldin E, Markides KE (2003) Novel polyamine coating providing non-covalent deactivation and reversed electro-osmotic flow of fused-silica capillaries for capillary electrophoresis. J Chromatogr A 1003(1–2):217–221
27. Selman MH, McDonnell LA, Palmblad M, Ruhaak LR, Deelder AM, Wuhrer M (2010) Immunoglobulin G glycopeptide profiling by matrix-assisted laser desorption ionization Fourier transform ion cyclotron resonance mass spectrometry. Anal Chem 82(3):1073–1081

Chapter 5

Micellar Electrokinetic Chromatography of Aminoglycosides

Ulrike Holzgrabe, Stefanie Schmitt, and Frank Wienen

Abstract

The components of the aminoglycosides, e.g., gentamicin, sisomicin, netilmicin, kanamycin, amikacin, and tobramycin, and related impurities of these antibiotics can be separated by means of micellar electrokinetic chromatography (MEKC). Derivatization with *o*-phthaldialdehyde and thioglycolic acid is found to be appropriate for these antibiotics. The background electrolyte was composed of sodium tetraborate (100 mM), sodium deoxycholate (20 mM), and β-cyclodextrin (15 mM) having a pH value of 10.0. This method is valid for evaluation of gentamicin, kanamycin, and tobramycin. It has to be adopted for amikacin, paromomycin, neomycin, and netilmicin.

Key words MEKC, Bile salts, Background electrolyte, Cyclodextrins, Aminoglycosides, Gentamicin, Kanamycin, Tobramycin

1 Introduction

Micellar electrokinetic chromatography, denoted as MEKC and often called micellar electrokinetic capillary chromatography (MECC), was originally developed by Terabe [1] for separation of neutral compounds which cannot be achieved by capillary zone electrophoresis. Applying an ionic surfactant such as sodium dodecylsulfate in a concentration higher than the critical micelle concentration and a high pH value makes a separation possible based on the differential partition of the analytes between the running buffer and the surfactant micelles.

The micelles form a pseudostationary phase moving with the migration velocity and direction which is different to the background electrolyte. Hence, the MEKC can be regarded as a hybrid of chromatography and capillary electrophoresis and terms such as electrolyte solution and mobile phase, migration time and retention time, and elution and migration are equally used.

The separation of the analytes is possible between the migration velocity of the electrolyte solution, which is at high pH values

Philippe Schmitt-Kopplin (ed.), *Capillary Electrophoresis: Methods and Protocols*, Methods in Molecular Biology, vol. 1483,
DOI 10.1007/978-1-4939-6403-1_5,

identical to the electroosmotic flow (EOF), and the effective migration velocity of the surfactant micelles. Thus, analytes only staying in the electrolyte solution cannot be separated. They migrate with the EOF at the time t_{eo}. Analytes residing exclusively in the micelles are also not separable and elute from the capillary at the migration time of the micelles t_{mc}. In the case the complexation constants between the various analytes and the micelles are different a separation can be achieved within a characteristic migration t_a, in which $t_{eo} < t_a < t_{mc}$ (*see* Fig. 1; modified after [2]). The migration order of neutral analytes is mostly related to their hydrophobicity; due to the hydrophobicity of the micelle core the more hydrophobic analytes migrate slower than less hydrophobic analytes. For details of the physicochemical background, see the excellent reviews by Pyell [3] and Terabe [4].

The selectivity of the separation depends sensitively on the differences of distribution constants between the electrolyte solution and the micelles for neutral analytes to be resolved, and in the case of ionized analytes on the differences of distribution constants between both phase and the effectively electrophoretic mobility. Favorable kinetic properties result in high efficiency and a reasonable peak capacity, especially for systems with a narrow migration window. Therefore, the choice of the surfactant system is of high importance for a satisfying separation. Separations can be further optimized by varying the pseudostationary phase/mobile phase ratio and by adding different concentrations of modifiers such as organic solvents, urea, complexing agents, e.g., cyclodextrins, etc., to the system. The modifier often reduces the distribution constant and widens the migration window. The buffer concentration, the ionic strength, and the pH may also enlarge the migration window for a better separation.

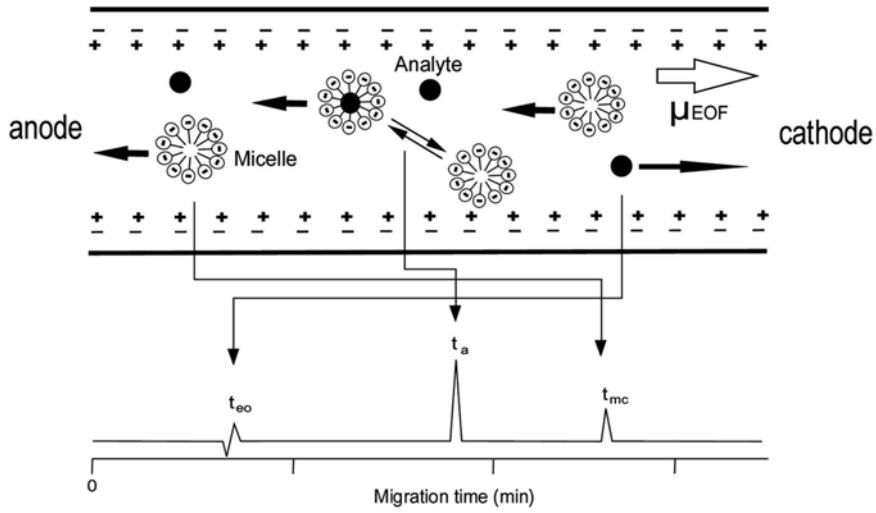

Fig. 1 Schematic representation of the separation mechanism of micellar electrokinetic chromatography (MEKC) using anionic micelles. t_{eo} = migration time of a neutral "unretained" analyte, t_a = "retention" time in MEKC, t_{mc} = migration time of a micelle

1.1 Micelle-Forming Agents

The surfactants are the selectivity determining factor. They can be categorized as anionic surfactants like sulfates, sulfonates or carboxylates, bile salts, cationic surfactants containing quaternary ammonium head groups, and nonionic surfactant. Moreover, two different surfactants, ionic and nonionic, can be applied forming mixed micelles which may result in a different selectivity and an improved resolution [4, 5]. Table 1 gives an overview over the often used micelle-forming agents. The surfactants used in MEKC should have a low critical micelle concentration, because high surfactant concentration would create an excessive current and high solution viscosity. The surfactant concentrations appropriate for MEKC are 10–200 mM. The surfactants must be available in a

Table 1
Surfactant employed in MEKC and their critical micelle concentration in distilled water at room temperature

Surfactant	CMC (mM)
Anionic surfactants	
Sodium dodecyl sulfate (SDS) Sodium tetradecylsulfate (STS)	8.1 2.1
Sodium dodecyl sulfonate	7.2
Sodium hexadecyl sulfate	2.1
Sodium *N*-lauroyl-*N*-methyl-β-alaninate (ALE)	9.8 (40 °C)
Sodium *N*-lauroyl-*N*-methyltaurate (LMT)	8.7 (35 °C)
Lithium perfluorooctanesulfonate (LIPFOS)	6.7
Bile salts	
Sodium cholate (Chol)	13–15
Sodium deoxycholate (DChol)	4–6
Sodium taurocholate (TC)	10–15
Sodium taurodeoxycholate (TDChol)	6
Cationic surfactants	
Tetradecyltrimethylammonium bromide (TTAB)	3.5
Cetyltrimethylammonium bromide (CTAB)	0.92
Zwitterionic surfactants	
N-Dodecyl-*N,N*-dimethylammonio-3-propanesulfonate	3.3
3-(3-Cholamidopropyl)dimethylammonio-3-propanesulfonate (CHAPS)	8
Non-ionic surfactant	
Polyoxyethylene[23]dodecanol (Brij 35)	0.09
Polyoxyethylene[20]sorbitanmonolaurate	0.95

pure form, should have a good solubility, a low UV absorbance, and should be stable over the pH range necessary for the electroosmotic flow, i.e., pH 6–9.

Due to the small detection cell volume the detection limits are always low in comparison to HPLC. The sensitivity can be enhanced by sample stacking which is based on differences in the electric conductivity of bordering zones. As the ions move across the boundary separating regions of different electric field strength they will be focused in a narrower zone than injected initially. In addition, sweeping can be applied which is the "picking and accumulation of analyte molecules by the pseudostationary phase that penetrates the sample zone" [4, 6]. This also results in a focusing of the sample and, thus, in an increase in sensitivity. Further techniques improving the detection sensitivity were recently summarized by El Deeb et al. [7].

1.2 Gentamicin

MEKC has been shown to be highly suitable for the separation of very complex mixtures of analytes with similar electrophoretic mobility of the components which are often neutral but can also be ionic. Thus, MEKC is appropriate to separate the components and impurities of aminoglycosides, such as gentamicin. Whereas the aminoglycosides kanamycin, neomycin, and paromomycin are characterized by one main component accompanied by some minor components of less than 5% content, gentamicin consists of four major components, i.e., GM C1, C1a, C2, and C2a, and some minor components such as GM C2b, 2-deoxystreptamine (DSA), garamine (GA), sisomicin, and netilmicin, the latter two being antibiotics on their own. Additionally, according to the ICH guidelines, impurities of a level higher than 0.1% being the limit allowed for a small-molecule drugs have to be evaluated (Scheme 1).

Due to the close structural relationship and the missing chromophor of the aminoglycosides, the evaluation of the composition and related substances is still a challenge for both HPLC [8–14] and capillary zone electrophoresis (CZE) [15–18] applying precolumn or precapillary derivatization, evaporative light scattering detection, pulsed electrochemical detection, and mass detection.

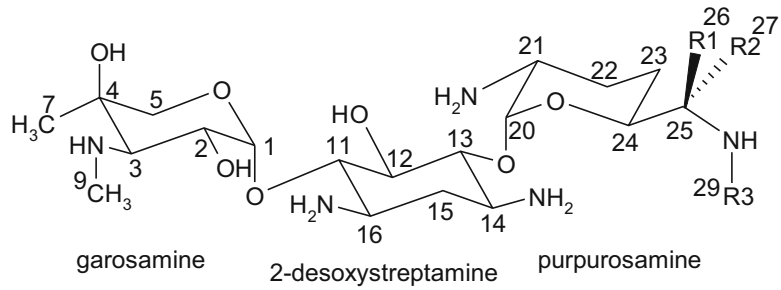

Scheme 1 Gentamicin (R^1, R^2, R^3 = H or CH_3)

Recently, a MEKC method was developed and validated [19–21] which is capable of separating and quantifying both the components of gentamicin and the impurities after a derivatization with the *o*-phthaldialdehyde/thioglycolic acid system. The method is characterized by high selectivity and efficiency.

2 Materials

2.1 Apparatus

CE experiments were carried out on a HP^{3D}-CE (Agilent Technologies, Waldbronn, Germany) equipped with a DAD detector. The capillaries were purchased from Polymicro (BGB Analytik, Schloßböckelheim, Germany). The fused-silica capillaries were of 50 μm internal diameter and effective length of 24.5 cm. The samples were loaded by pressure injection applying 50 mbar for 5 s on the anode side and detection at 340 nm was performed at the cathode side. Electrophoresis was carried out at 25 °C and a voltage of 12 kV (*see* **Note 1**).

2.2 Reagents and Chemicals

1. Chemicals used were of analytical grade.
2. Gentamicin sulfate, netilmicin sulfate, and sisomicin (CRS) were purchased from Promochem (Wesel, Germany), 2-deoxystreptamine dihydrochloride (DSA) and garamine hydrochloride (GA) were gifts from Merck (Darmstadt, Germany); gentamicin C2b sulfate (also as known as sagamicin and micronomicin) was purchased from Pharm Chemical (Shanghai Lansheng Corporation, China).
3. The GM components C1, C1a, and C2/C2a were separated from a commercial sample of GM by column chromatography and analyzed by TLC, CE, and ^{1}H NMR [22] (*see* **Note 2**).
4. *o*-Phthaldialdehyde (OPA) (for fluorescence, ≥99%), DChol (MicroSelect ≥99%), picric acid, sodium tetraborate decahydrate (TB, 99.5%), and boric acid were purchased from Fluka/Riedel de Haen (Seelze, Germany), TGA (Reag. Ph. Eur., ≥99.0%), methanol (HPLC grade) and isopropanol from Merck (VWR-International, Darmstadt, Germany), and acetonitrile (HPLC grade) from Carl Roth (Karlsruhe, Germany). β-CD was a gift from the Consortium für Elektrochemische Industrie (München, Germany).

2.3 Buffers

1. All BGE solutions were prepared using ultrapure Milli-Q water and filtered with a 0.22-μm polyvinylidenefluoride filter (both Millipore, Milford, MA, USA).
2. In order to prepare the BGE, adequate amounts of TB, DChol, and β-CD were weighed in a flask, 80% of the water needed was added and the components dissolved using an ultrasonic bath.

3. The required pH value was adjusted with NaOH solution (1.0 M). After water was added, the pH value was checked and adapted, if necessary.

2.4 Derivatization Reagent

1. The samples were dissolved in high purity water solution (2.0 mg/ml) containing picric acid (IS, 7 mg/ml).
2. *o*-Phthaldialdehyde (OPA) reagent: 650 mg of OPA were dissolved in 2.0 ml of methanol and approx. 15 ml of boric acid solution (pH 10.4, 30 mM). After ultrasonification the solution was adjusted to pH 10.4 using potassium hydroxide solution (8 M). Thioglycolic acid (1.300 ml) was added and pH was adjusted again to 10.4 with potassium hydroxide solution (8 M).
3. This solution was diluted to 25.0 ml with boric acid solution (pH 10.4, 30 mM).
4. The solution can be stored at 4 °C for at least 48 h.

3 Methods

Previously, the European Pharmacopoeia (EP 5) [23] tried to limit the impurities of gentamicin by a HPLC method utilizing a styrene–divinylbenzene copolymer column and a pulsed amperometric detector (PAD). However, the method suffered from several drawbacks, e.g., the pulsed amperometric detection is not very robust, the run time of a chromatogram is longer than 70 min, and the main components of gentamicin elute partially longer than 10 min. Currently, the EP 8 determines the components and limits the impurities by means of a slightly modified method making use of a simple RP18-HPLC but still utilizes the PAD. Whereas the peak shape has improved, the run time is still 80 min and the gentamicin components elute after 25 min [24, 25]. Thus, a capillary zone electrophoretic (CZE) method is an alternative. The method developed by Kaale et al. [17] was a good starting point for the development of the MEKC method presented here.

Because the aminoglycosides are lacking of any chromophores or fluorophores and most direct detection methods turned out to be not very robust, a derivatization using *o*-phthaldialdehyde and thioglycolic acid was chosen. Of note, Kaale et al. have also developed a corresponding in-capillary derivatization [26].

Having derivatized gentamicin the obtained molecules are neutral and, thus, suitable to be separated by MEKC. Applying the optimized CZE conditions (30 mM tetraborate buffer, 7.0 mM β-CD, 12.5% methanol) several micelle-forming agents, i.e., SDS, SChol, SDChol, STC, Brij35, CTAB, and TAB, were checked each at a concentration of 25 mM (*see* **Note 3**). The sodium cholic acids and especially the SDChol revealed the best separation. Variation of the background electrolyte (BGE) concentration between 10

and 125 mM tetraborate (TB) resulted in the best resolution of all components at 100 mM. In previous experiments the kind and concentration of the cyclodextrins (various neutral and negatively charged CDs) was varied and the cheap β-CD found to be appropriate. Applying increasing concentrations of β-CD lowered the run time and gave a very good peak shape. Thus, the highest possible β-CD concentration was chosen (15 mM). Finally the pH of the BGE was adopted. In a range of 9.5–10.5, the pH of 10.0 gave the best separation. Organic modifiers such as methanol, isopropanol, or acetonitrile did not improve of the separation. For quantification purposes an internal standard has to be used. Picric acid was already successfully applied in CZE [15, 17] and was also suitable for the MEKC method.

In order to assign the peaks of the electropherogram they have to be spiked with reference substances. Even though the method was found to be precise and robust with regard to the migration time (*see* Fig. 2), additional impurities may change the electropherogram in a way that the assignment fails.

The method was applied to various lots of gentamicin collected from the European and American market. As can be seen form the comparison of Fig. 2, displaying a pure sample, and Fig. 3, showing a sample with high number of impurities of high concentration, the method is appropriate to evaluate the quality of gentamicin.

The method developed here is also appropriate for other aminoglycosides such as kanamycin and tobramycin and with slight variation of the conditions for amikacin, paromomycin, neomycin, and netilmicin [19].

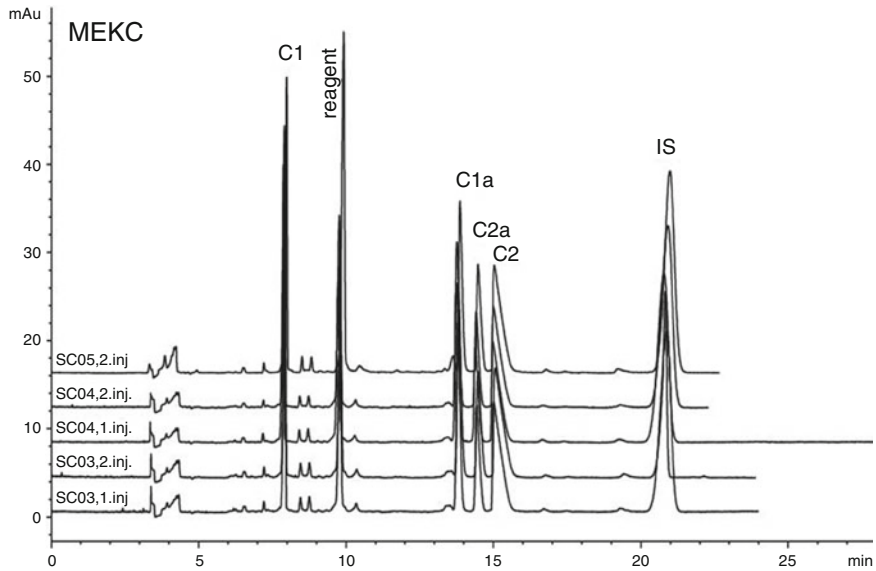

Fig. 2 Electropherograms of the same sample, but different derivatization reactions (SCO 3, 4 and 5), injected once or twice

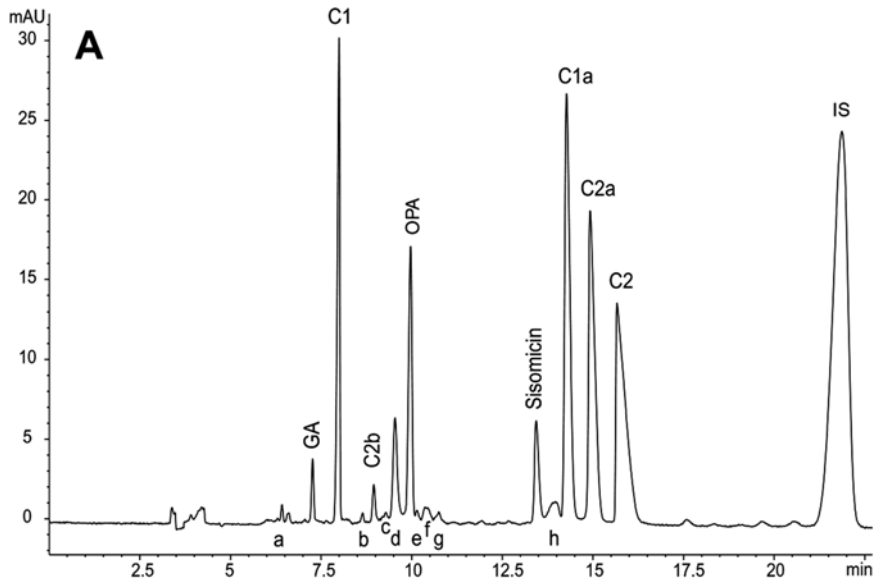

Fig. 3 Electropherogram of a sample of low purity showing sisomicin in addition to additional unknown impurities a–h

3.1 Derivatization

The derivatization with *o*-phthaldialdehyde and thioglycolic acid described earlier was already optimized by Kaale et al. [15]. The reaction can be performed either in methanol or isopropanol.

A volume of 0.45 ml of the sample solution was mixed with 0.25 ml of methanol and 0.16 ml of the OPA reagent (*see* **Note 4**). This solution was vortexed and heated in a water bath at 60 °C for exactly 4 min (*see* **Note 5**) and diluted to 1.0 ml with methanol. After cooling to room temperature the solution was poured in a vial appropriate for CE. The measurement should start immediately.

3.2 Running Buffer

Optimized separation conditions for CE are the following:

1. The BGE was composed of a TB (100 mM, pH 10.0), DChol (20 mM), and β-CD (15 mM) (*see* **Notes 6** and **7**).
2. The pH value has to be adapted to 10.0 (*see* **Note 8**).
3. The samples were loaded by pressure injection applying 50 mbar (=0.0145 psi) for 5 s on the anode side and detection at 340 nm (*see* **Note 9**) was performed at the cathode side.
4. The electrophoresis was carried out at 25 °C and a voltage 12 kV.
5. In order to prove the absence or presence of netilmicin, the voltage has to be increased (*see* **Note 1**).

3.3 Rinsing Procedure

In order to avoid crystallization of the components of running buffer, derivatization reagent and the derivatized samples and in order to increase the reproducibility the capillary has to be rinsed carefully. Thus, between two runs, the capillary was rinsed with water for 2 min (8 bar; = postconditioning) and with NaOH solution

(0.1 M) and water for 1.5 min (5 bar), respectively, and with HCl solution (1.0 M) and water for 2.0 min (5 bar), respectively, and with the BGE for 3 min (8 bar; = pre-conditioning) (*see* **Note 10**).

4 Notes

1. Variation of the voltage results in a change of the electropherogram. For evaluation 12 kV was chosen. Applying 14 V the potential impurity netilmicin can be quantified, because a baseline separation from the reagent peak can be achieved (*see* Fig. 4). However, netilmicin is not expected to be found in gentamicin drug substance and was not found in any of the samples studied.
2. Since gentamicin is composed of many components peak identification by reference substances is necessary.
3. As can be seen from Fig. 5 the choice of micelle-forming acids determines fundamentally the separation.
4. The OPA reagents can be stored at 4 °C for 48–72 h to prevent additional peaks in the electropherograms which are not coming from gentamicin components [19].

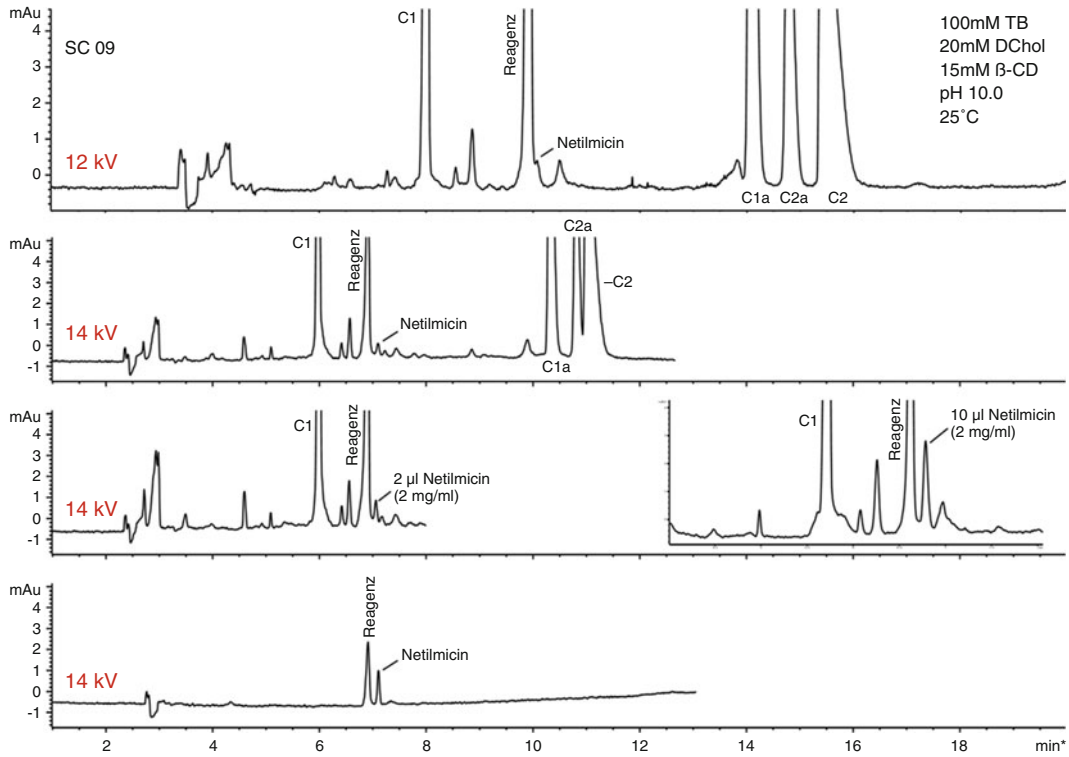

Fig. 4 (**a**) Electropherogram of a sample spiked with netilmicin; voltage 12 kV, (**b**) electropherogram of a sample spiked with netilmicin; voltage 14 kV, (**c**) electropherogram of a sample spiked with increasing amounts of netilmicin; voltage 14 kV, (**d**) electropherogram of netilmicin

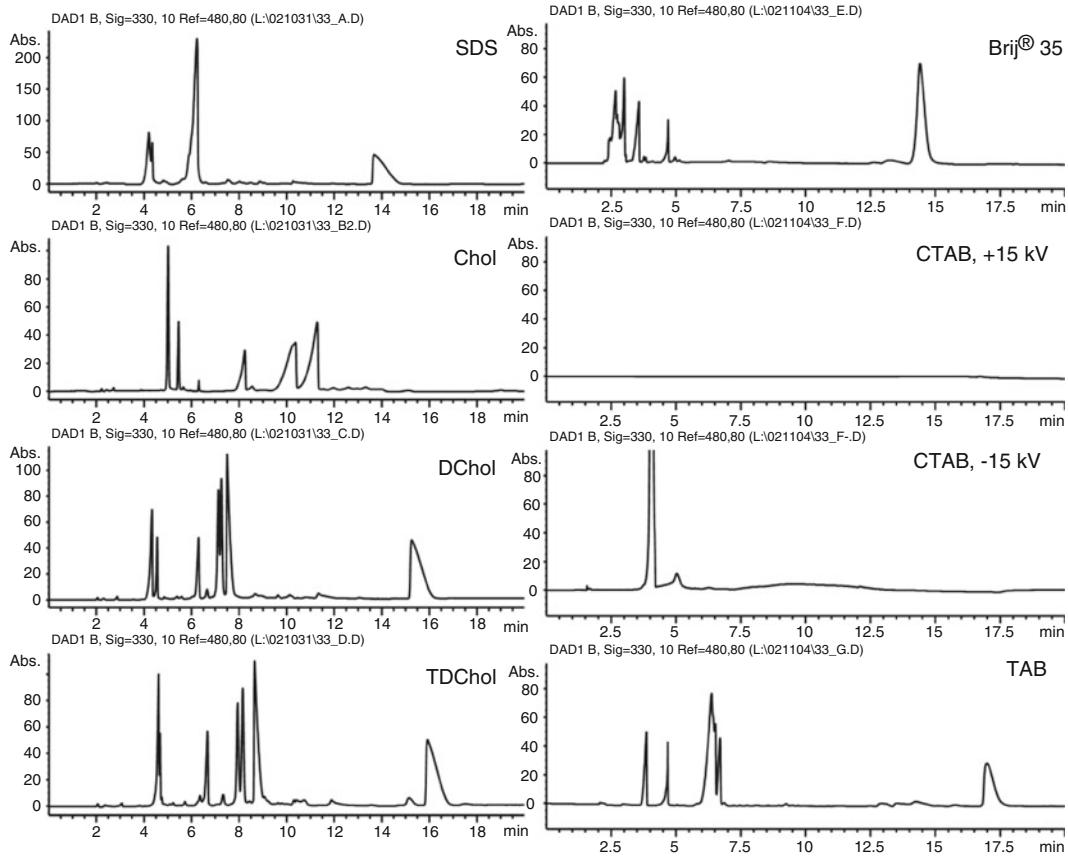

Fig. 5 Electropherograms obtained with various surfactants using the same conditions: 30 mM TB, 25 mM surfactant, pH 10.0, voltage 15 kV. Abbreviations of the surfactant can be found in Table 1; *TAB* tetramethylammonium bromide

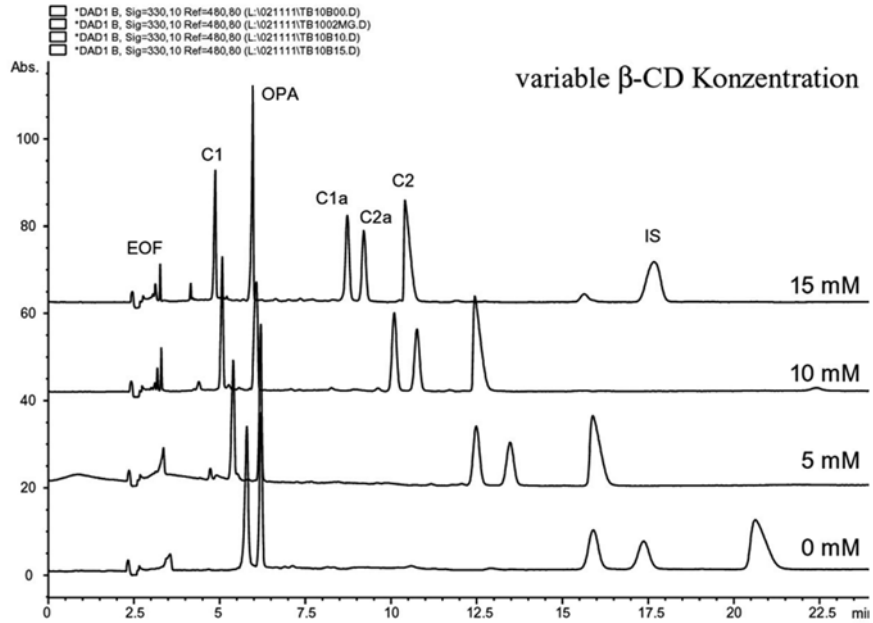

Fig. 6 Electropherogram obtained with increasing amounts of β-CD under the same conditions 100 mM TB, 25 mM TDChol, pH 10.0, voltage 15 kV, temperature 20 °C

5. The reaction is completed after 4–5 min at 60 °C. The reaction time and temperature has to be checked carefully.
6. Best separations were achieved when using 125 mM of TB. However, the current is very high at the TB concentration and often the buffer reagent precipitates during the course of measurements. Therefore, a buffer concentration of 100 mM was chosen, finally.
7. Higher β-CD concentration results in a shorter migration time and a rather sharp peak shape which can be impressively seen in Fig. 6. Since the solubility of β-CD in water is limited, the concentration of β-CD was set to 15 mM.
8. Whereas at pH 9.5 the internal standard comigrates with some components of gentamicin and the separation of all peaks is poor, at pH 10.5 the migration time increased substantially and the peaks became very broad (*see* Fig. 7 = 1.1–10), Thus,

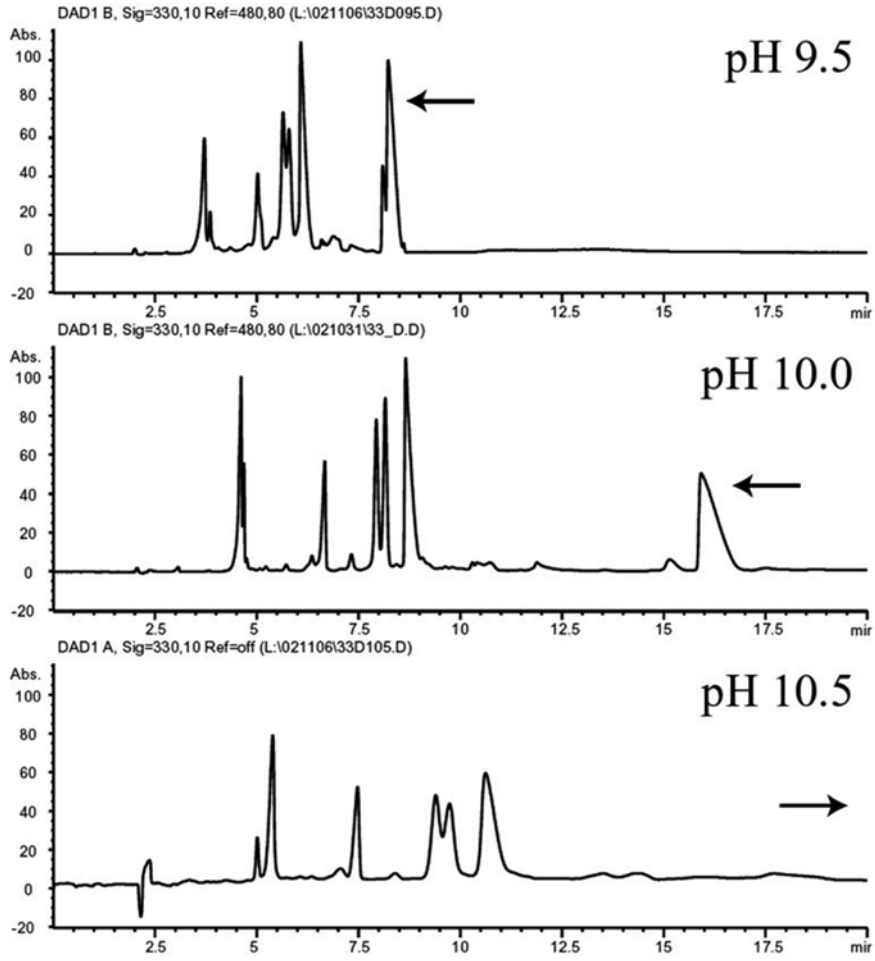

Fig. 7 Electropherogram obtained at different pH value under the same conditions: 100 mM TB, 25 mM TDChol, voltage 15 kV, temperature 20 °C

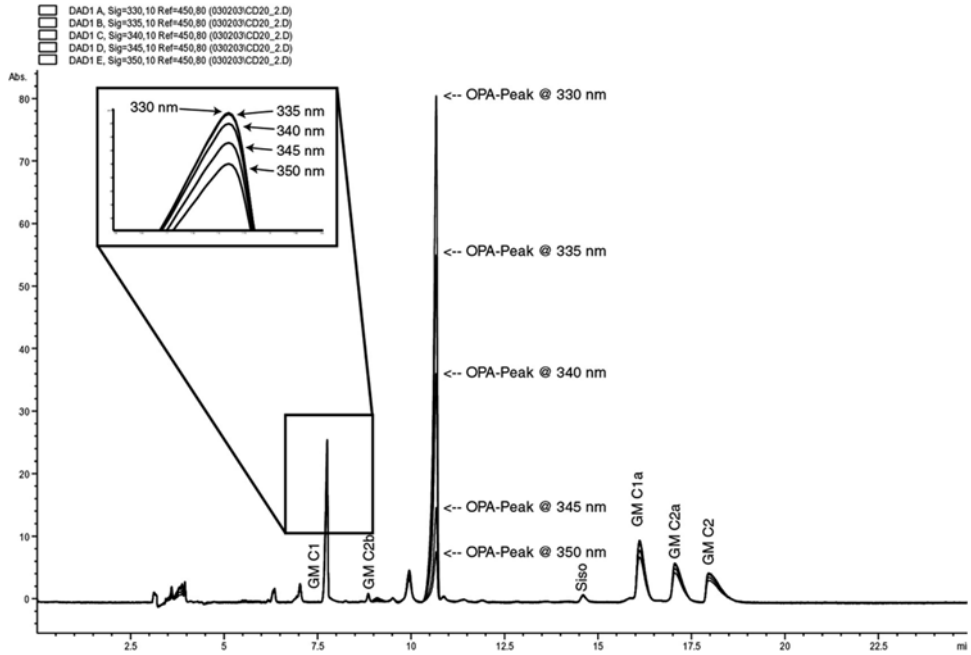

Fig. 8 Variation of the detection wave length between 330 and 350 nm

pH 10.0 turned out to be a good compromise with regard to migration time and peak sharpness.

9. It is important to find a suitable detection wave length. On the one hand, the OPA reagent peak should be as small as possible to avoid covering of the substance peaks by the reagent peak. On the other hand, the substance peaks should be as large as possible in order to increase the sensitivity. As can be seen in Fig. 8 at 340 nm the reagent peak has relatively low intensity and the sample peaks are of high intensity. In addition, all electropherograms were registered at the reference wave length of 450 nm in order to visualize artifacts of the separation which may be caused by the instrument and are found in the entire UV spectrum. The artifacts are filtered off automatically.
10. Other rinsing procedures using SDS/acetonitrile mixtures which are often described in the literature [27] turned out to be insufficient with respect to reproducibility.

Acknowledgement

Thanks are due to the Federal Institute of Drugs and Medical Devices, Bonn, Germany, for financial support. Furthermore thanks to Dr. A. Kirsch, Merck, Darmstadt, Germany, for providing the impurities GA and DSA and samples.

References

1. Terabe S, Otsuka K, Ando T (1985) Electrokinetic chromatography with micellar solution and open-tubular capillary. Anal Chem 57:834–841
2. Watanabe T, Terabe S (2000) Analysis of natural food pigments by capillary electrophoresis. J Chromatogr A 880:311–322
3. Pyell U (2000) Micellar electrokinetic chromatography. In: Meyers EA (ed) Encyclopaedia of analytical chemistry, vol 13. Wiley, Chichester, UK, pp 11042–11383
4. Terabe S (2009) Capillary separation: micellar electrokinetic chromatography. Ann Rev Anal Chem 2:99–120
5. Poole CF (2003) The essence of chromatography. Elsevier, Amsterdam, p 644, Chapter 8.3
6. Quirino JP, Terabe S (1999) Sweeping of the analyte zones in electrokinetic chromatography. Anal Chem 71:1638–1644
7. El Deeb S, Dawwas HA, Gust R (2013) Recent methodological and instrumental development in MEKC. Electrophoresis 34:1295–1303
8. Seidl G, Nerad HP (1988) Gentamicin C: separation of C1, C1a, C2, C2a and C2b components by HPLC using isocratic ion-exchange chromatography and post column derivatization. Chromatographia 25:169–171
9. Kaine LA, Wolnik KA (1994) Forensic investigation of gentamicin sulfates by anion-exchange ion chromatography with pulsed electrochemical detection. J Chromatogr A 674:255–261
10. Getek TA, Vestal ML (1991) Analysis of gentamicin sulfate by high-performance liquid chromatography combined with thermospray mass spectrometry. J Chromatogr 554:191–203
11. Adams E, Roelants W, De Paepe R, Roets E, Hoogmartens J (1998) Analysis of gentamicin by liquid chromatography with pulsed electrochemical detection. J Pharm Biomed Anal 18:689–698
12. Clarot I, Chaimbault P, Hasdebteufel F, Netter P, Nicolas A (2004) Determination of gentamicin sulfate and related compounds by high-performance liquid chromatography with evaporative light scattering detection. J Chromatogr A 1031:281–287
13. Ghinami C, Giuliani V, Menarini A, Abballe F, Travaini S, Ladisa T (2007) Electrochemical detection of tobramycin or gentamicin according to the European Pharmacopoeia analytical method. J Chromatogr A 1139:53–56
14. Li B, Adams E, Van Schepdael A, Hoogmartens J (2006) Analysis of unknown compounds in gentamicin bulk samples with liquid chromatography with ion trap mass spectrometry. Rapid Commun Mass Spectrom 20:393–402
15. Kaale E, Leonard S, Van Schepdael A, Roets E, Hoogmartens J (2000) Capillary electrophoresis analysis of gentamicin sulfate with UV detection after pre-capillary derivatization with 1,2-phthalic dicarboxaldehyde and mercapto acid. J Chromatogr A 895:67–79
16. Wienen F, Deubner R, Holzgrabe U (2003) Composition and impurity profile of multisource raw material of gentamicin—a comparison. Pharmeuropa 15:273–279
17. Kaale E, Van Schepdael A, Roets E, Hoogmartens J (2001) Development and validation of a simple capillary zone electrophoresis method for the analysis of kanamycin sulfate with UV detection after pre-capillary derivatization. J Chromatogr A 924:451–458
18. Curiel H, Vanderaerten W, Velez H, Hoogmartens J, Van Schepdael A (2007) Analysis of underivatized gentamicin by capillary electrophoresis with UV detection. J Pharm Biomed Anal 44:49–56
19. Wienen F, Holzgrabe U (2003) A new micellar electrokinetic capillary chromatography method for separating of the components of the aminoglycoside antibiotics. Electrophoresis 24:2948–2957
20. Deubner R, Holzgrabe U (2004) Micellar electrokinetic capillary chromatography, high performance liquid chromatography and nuclear magnetic resonance—three orthogonal methods for characterization of critical drugs. J Pharm Biomed Anal 35:459–467
21. Kühn K-D, Weber C, Kreis S, Holzgrabe U (2008) Evaluation of the stability of gentamicin in different antibiotic carriers using a validated MEKC method. J Pharm Biomed Anal 48:612–618
22. Deubner R, Wienen F, Holzgrabe U (2003) Assignment of the major and minor components of gentamicin for evaluation of batches. Magn Reson Chem 41:589–598
23. (2004) European Pharmacopoeia. 5th ed., European Directorate for Quality of Medicines, Strasbourg, France
24. (2014) European Pharmacopoeia. 8th ed., European Directorate for Quality of Medicines, Strasbourg, France, (see also knowledge data base)
25. Li B, Van Schepdael A, Hoogmartens J, Adams E (2011) Mass spectrometric characterization of gentamicin components separated by the new European Pharmacopoeia method. J Pharm Biomed Anal 55:78–84

26. Kaale E, Van Goidsenhoven E, Van Schepdael A, Roets E, Hoogmartens J (2001) Electrophoretically mediated microanalysis of gentamicin with in-capillary derivatization and UV detection. Electrophoresis 22:2746–2754

27. Kunkel A, Wätzig H (1999) Micellar electrokinetic capillary chromatography as a powerful tool for pharmacological investigations without sample pretreatment: a precise technique providing cost advantages and limits of detection to the low nanomolar range. Electrophoresis 20:2379–2389

Chapter 6

Microemulsion Electrokinetic Chromatography

Wolfgang Buchberger

Abstract

Microemulsion electrokinetic chromatography (MEEKC) is a special mode of capillary electrophoresis employing a microemulsion as carrier electrolyte. Analytes may partition between the aqueous phase of the microemulsion and its oil droplets which act as a pseudostationary phase. The technique is well suited for the separation of neutral species, in which case charged oil droplets (obtained by addition of an anionic or cationic surfactant) are present. A single set of separation parameters may be sufficient for separation of a wide range of analytes belonging to quite different chemical classes. Fine-tuning of resolution and analysis time may be achieved by addition of organic solvents, by changes in the nature of the surfactants (and cosurfactants) used to stabilize the microemulsion, or by various additives that may undergo some additional interactions with the analytes. Besides the separation of neutral analytes (which may be the most important application area of MEEKC), it can also be employed for cationic and/or anionic species. In this chapter, MEEKC conditions are summarized that have proven their reliability for routine analysis. Furthermore, the mechanisms encountered in MEEKC allow an efficient on-capillary preconcentration of analytes, so that the problem of poor concentration sensitivity of ultraviolet absorbance detection is circumvented.

Key words Microemulsion, Electrokinetic chromatography, Capillary electrophoresis, Pseudostationary phase, Hydrophobic interaction

1 Introduction

Microemulsion electrokinetic chromatography (MEEKC) covers variants of capillary electrophoresis (CE) employing a microemulsion as carrier electrolyte. Contrary to other CE techniques, MEEKC allows the separation of neutral analytes. In addition, this technique is also suited for separation of charged species, whereby separation selectivities may be achieved which are significantly different from those obtained by commonly used CE techniques for separation of ionic analytes. Microemulsions have been discovered more than 70 years ago by Hoar and Schulman [1] and have been introduced for CE separation techniques in 1991 by Watarai [2]. Since then the numbers of applications of MEEKC have increased steadily, which has been documented in review papers that have been published regularly within the last few years [3–8].

Philippe Schmitt-Kopplin (ed.), *Capillary Electrophoresis: Methods and Protocols*, Methods in Molecular Biology, vol. 1483,
DOI 10.1007/978-1-4939-6403-1_6,

1.1 Fundamentals

Microemulsions are dispersions of two immiscible liquids and may consist either of oil droplets suspended in water (oil-in-water [o/w] microemulsions) or of water droplets suspended in an oil phase (water-in-oil [w/o] microemulsions). MEEKC separations are mostly carried out in oil-in-water microemulsions. Typically, they consist of octane droplets dispersed in an aqueous buffer containing surfactants to coat the octane droplets and lower the surface tension between the two liquids. Furthermore, a short-chain alcohol like *n*-butanol (called a cosurfactant) is added which also lowers the surface tension. Under such conditions, a stable microemulsion is generated with droplet sizes below 10 nm. It is optically transparent and looks like a single-phase solvent although it is a two-phase system. As mentioned earlier, o/w microemulsions are the most common form of microemulsions used in MEEKC. Therefore, the following discussions will mostly focus on this type, and w/o microemulsions will be treated only shortly in part 1.4.

Sodium dodecyl sulfate (SDS) is commonly used as surfactant for stabilization of the microemulsion droplets. At the interface between the aqueous phase and the oil phase, the dodecyl chain is oriented toward the inner of the oil droplet, whereas the negatively charged sulfate group is oriented toward the aqueous phase. The cosurfactant such as *n*-butanol will also attach to the surface of the oil droplet with the butyl group toward the oil phase and the alcohol group toward the aqueous phase. As a result of the presence of the anionic surfactant, the oil droplets will acquire a negative charge and will exhibit an electrophoretic mobility in the direction of the anode. The aqueous phase is generally buffered at an alkaline pH. In fused-silica capillaries, alkaline buffers generate an electroosmotic flow (EOF) toward the cathode. Provided that the pH is high enough, the magnitude of the EOF exceeds the electrophoretic mobility of the oil droplets (which is directed against the EOF). Therefore, the EOF will sweep the oil droplets to the cathode. The apparent mobility of the oil droplets is directed to the cathode and has a magnitude that is lower than that of the EOF.

Highly hydrophilic neutral analytes injected at the anodic side of the capillary will reside predominantly in the aqueous phase so that they will be transported to a detector positioned at the cathodic side of the separation capillary by the EOF according to the electroosmotic mobility. The time at which they reach the detector after injection may be called t_{EOF}. Conversely, highly hydrophobic analytes will reside predominantly in the oil droplets, will be transported to the cathodic detection side according to the apparent mobility of the droplets, and will reach the detector after the time t_{ME}. Analytes of medium polarity will undergo partitioning equilibria between the aqueous phase and the oil phase, and will reach the detector at a time t, which is between t_{EOF} and t_{ME}. Obviously, MEEKC separates neutral analytes according to their hydrophobicities. The technique offers a limited separation time window

governed by t_{EOF} and t_{ME}. These two parameters may be determined by injection of methanol as EOF marker (t_{EOF}) and octanophenone or dodecyl benzene as microemulsion marker (t_{ME}).

The partitioning equilibria of analytes established between the aqueous phase and the oil droplets indicate that chromatographic principles are involved in the separation (justifying the word "chromatography" in MEEKC). Therefore, the oil droplets may be called a pseudostationary phase. In analogy to chromatography, one can define retention factors k for the analytes:

$$k = \frac{t_r - t_{EOF}}{t_{EOF} - \left(\frac{1 - t_r}{t_{ME}} \right)}$$

In case of a true stationary phase as encountered in liquid chromatography, t_{ME} would become infinite and t_{EOF} would be the dead time. The equation given earlier would turn into the well-known definition of k being the ratio of net retention time to dead time.

A schematic presentation of the MEEKC separation process is given in Fig. 1. Additional details can be found in recently published review papers (see for example [9]). It should be pointed out that the separation mechanisms encountered in MEEKC are similar to those in micellar electrokinetic chromatography (MEKC), which uses micelles (aggregates of surfactant molecules) as pseudostationary phase. Advantages of MEEKC over MEKC may include the fact that oil droplets exhibit a reduced rigidity compared to micelles so that hydrophobic analytes can more easily penetrate the surface and enter the core of the pseudostationary phase. Furthermore, MEEKC may offer a somewhat larger separation time window, because the total charge of the droplets (and thereby t_{ME}) can be manipulated by employing mixed surfactants composed of charged and neutral species in different compositions.

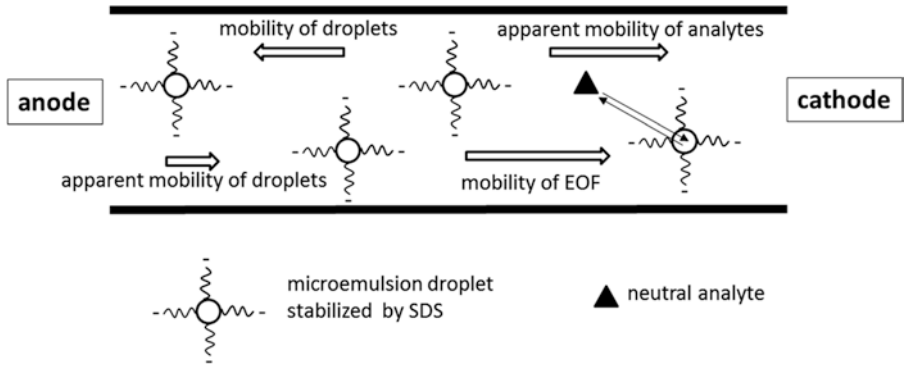

Fig. 1 Principle of the separation process in microemulsion electrokinetic chromatography for a neutral analyte in an alkaline microemulsion stabilized by an anionic surfactant like sodium dodecyl sulfate

Instead of alkaline buffers, acidic buffers are used occasionally. In such a case the EOF is very low and is no longer able to transport an anionic pseudostationary phase (droplets stabilized by SDS) to the cathodic detection side. Therefore, one has to switch the polarity and the detection must be at the anodic side of the capillary.

Besides anionic surfactants like SDS, also cationic surfactants like cetyltrimethylammonium bromide (CTAB) may be employed for stabilization of the oil droplets. Such surfactants will not only lead to positively charged droplets, but they also act as EOF modifiers due to the generation of a positively charged inner surface of the fused-silica capillary, resulting in a reversed direction of the EOF. Therefore, the detector must be positioned at the anodic end of the capillary when working with such cationic surfactants.

MEEKC separations of ionic analytes involve somewhat more complex mechanisms, because the apparent mobility of the analytes is governed by both their electrophoretic mobilities and their interactions with the pseudostationary phase. Generally, nonionic surfactants can be used leading to a neutral pseudostationary phase, but cationic or anionic pseudostationary phases may be suited as well. In the latter case, one has to take into account a possible repulsion of the charged analyte from the charged pseudostationary phase if both are anionic (or if both are cationic). In case of analytes with a charge opposite to the pseudostationary phase, additional ion-pairing equilibria at the surface of the droplets may have an impact on the separation. In addition, ion pairing between the charged analyte and excess of surfactant may occur in the aqueous phase, which may favor the partitioning reaction into the oil droplet.

Last, but not least, one should keep in mind that depending on the pH of the microemulsion the analytes may be in a neutral form or in a protonated/deprotonated form. Therefore, different types of microemulsions (neutral or charged) may be recommendable, and different separation selectivities can be expected. This is demonstrated in Fig. 2, which shows the separation of closely related methyl derivatives of quinoline that are used as raw materials for industrial production of agrochemicals and pharmaceuticals [10]. Chromatogram A presents the separation of methylquinolines at pH 9.4 (neutral analytes) using a negatively charged oil phase, and B presents the separation of the same set of analytes at pH 4.0 (protonated analytes) using a neutral oil phase [10]. In case A, the separation selectivity is solely governed by the partitioning between the aqueous phase and the oil droplets, whereas in case B separation selectivity is significantly different because it is affected by both partitioning and electrophoretic behavior of the analytes. It is worth mentioning that a buffer of pH 4 without oil droplets (corresponding to a pure capillary zone electrophoretic mode) would not lead to any satisfactory separation.

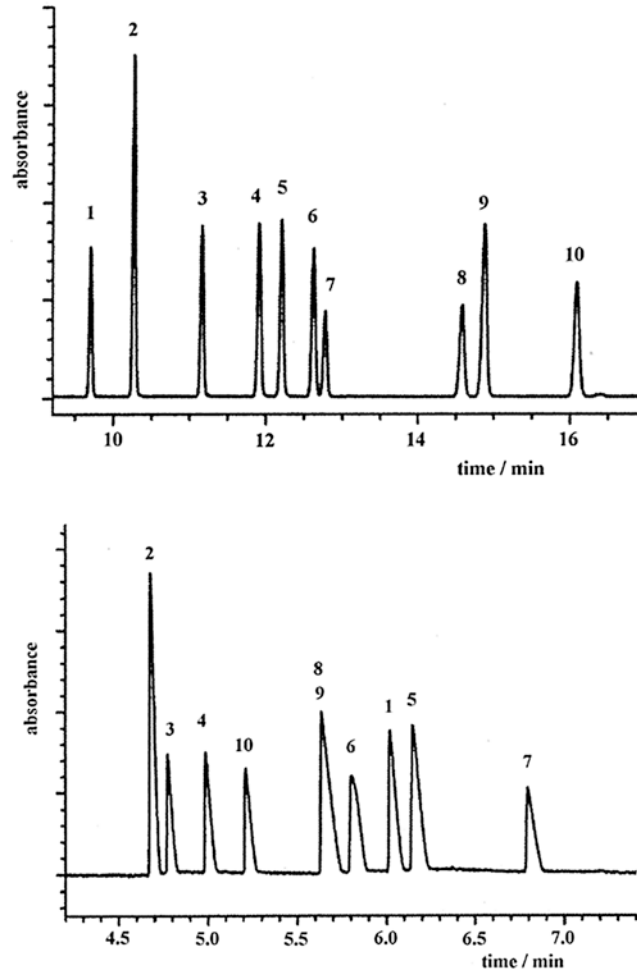

Fig. 2 MEEKC separation of methylquinolines at pH 9.4 using a negatively charged oil-in-water microemulsion consisting of SDS, *n*-butanol, *n*-octane, and borate buffer (**a**), and at pH 4 using a neutral oil-in-water microemulsion consisting of Brij35, *n*-butanol, *n*-heptane, and acetate buffer (**b**). Peaks: 1 = quinoline, 2 = isoquinoline, 3 = 2-methylquinoline, 4 = 4-methylquinoline, 5 = 3-methylquinoline, 6 = 6-methylquinoline, 7 = 8-methylquinoline, 8 = 4,8-dimethylquinoline, 9 = 2,8-dimethylquinoline, 10 = 2,4,8-trimethylquinoline. UV detection at 214 nm. Adapted from ref. [10]

1.2 Optimization of the Separation of Neutral Analytes

Variables to be optimized with respect to manipulation of migration order and optimization of separation selectivity of neutral analytes include the kind of oil phase, the kind of surfactant and cosurfactant, the addition of water-miscible solvents, and the use of specific additives such as cyclodextrins, carbon nanotubes, and others, that introduce extra effects for the separation of certain analytes.

1.2.1 Oil Phase

The concentration of the oil phase in the carrier electrolyte is typically around 1 % or less. Frequently, *n*-alkanes like hexane, heptane, or octane are employed as oil phase, with octane often being

preferred. As an alternative, ethyl acetate has been selected because of its lower surface tension which allows lower concentrations of surfactant for stabilization. Other compounds occasionally reported for preparation of microemulsions include cyclohexane, toluene, 1-chloropentane, alcohols of medium chain length like 1-hexanol or 1-octanol, and propylene glycol monomethylester acetate. More recently, ionic liquids have been investigated as oil phase, whereby 1-butyl-3-methylimidazolium hexafluorophosphate may be promising [11–13]. Even vegetable oils and artificial oils made of alkane and alcohol may have some potential [14]. Different partitioning coefficients provided by the different oil phases may lead to somewhat different separations, but major changes in migration order are not likely. Unfortunately, it is often still a matter of trial and error to find the best oil phase. In any case, octane may be a good start.

For separation of enantiomers, a chiral oil phase may be used. Chiral alkyl tartrates have been investigated for this purpose [15, 16]. Resolution between enantiomers was obtained if borate buffers were employed, whereas phosphate or Tris buffers did not lead to any enantioseparation. The authors attributed this phenomenon to the formation of a complex between borate and the alkyltartrate.

1.2.2 Surfactants

Surfactants are a key component in the microemulsion. They have a direct impact on stability of the oil droplets by lowering the surface tension, and they affect size and charge of the droplets, magnitude, and direction of the EOF. Anionic or cationic surfactants as well as mixtures of them with nonionic surfactants have been employed for separation of neutral analytes. One should keep in mind that the addition of ionic surfactants can lead to a significant increase of electric conductivity of the carrier electrolyte, which may limit the applied voltage in order to avoid excessive Joule heating.

The most common surfactant for MEEKC is sodium dodecyl sulfate (SDS), which is typically used at concentrations around 3%. Alternative anionic surfactants include lithium dodecyl sulfate (which leads to somewhat lower electric currents), bile salts like sodium cholate, or sulfosuccinates like sodium bis(2-ethylhexyl) sulfosuccinate.

Cationic surfactants reported for use in MEEKC are based on quaternary ammonium salts like dodecyltrimethyl ammonium chloride, tetradecyltrimethyl ammonium bromide, or cetyltrimethyl ammonium chloride/bromide. As mentioned in the part on fundamentals, the behavior of these salts as EOF modifiers must be taken into account.

The use of mixtures of surfactants may provide various benefits. The combination of SDS and Brij-35 (a nonionic surfactant) allows the manipulation of the charge of the droplets and thereby manipulation of the separation time window.

Chiral surfactants have been introduced for MEEKC separations of enantiomers, such as R- and S-dodecoxycarbonylvaline

(DDCV) [17–19]. This approach can also be combined with the use of a chiral oil phase (see previous part) which has been demonstrated for the use of DDCV together with dibutyltartrate or diethyltartrate [20, 21].

1.2.3 Cosurfactant

The variations of nature and concentration of the cosurfactant may be exploited for fine-tuning of the separation (see for example [22]). Short chain alcohols are frequently used as cosurfactants, with 1-butanol at a concentration of around 6% being the most common one. It has been suggested that such solvents do not only act as cosurfactants, but that a significant portion of it can partition into the oil droplet, especially as the amount of cosurfactant present in the microemulsion exceeds that of the actual oil phase [23]. Thereby, the chromatographic properties of the pseudostationary phase are modified and with it the k values of the analytes affected. General rules for selection of appropriate cosurfactants are still difficult to establish.

Chiral separations may benefit from the use of chiral 2-alkanols like R(−)-2-pentanol, R(−)-2-hexanol or R(−)-2-heptanol as cosurfactants [24]. A synergistic effect has been observed when (S)-2-hexanol was employed together with a chiral surfactant [25]. In addition, even three-chiral-component microemulsions (R- or S-DDCV, S-2-hexanol, and R- or S-diethyltartate) have been investigated and compared with one- and two-chiral-component microemulsions [26].

Interestingly, it has also been claimed that a stable microemulsion prepared by hexane and SDS in an ammonium acetate solution can be generated without the use of any cosurfactant [27], but such an approach has not made its way to a wider range of applications.

1.2.4 Water-Miscible Solvents

For certain applications, water-miscible organic solvents may be added to the microemulsion [23]. In this way, the partitioning equilibria of the analytes between the aqueous phase and the oil phase may be manipulated. This aspect is of major significance when analytes with very poor solubility in water are separated. Such analytes would not partition at all into a purely aqueous phase and would therefore reach the detector after the time t_{ME}. A typical example for the benefits of water-miscible solvents is the analysis of highly hydrophobic polymer stabilizers [28]. Depending on the type of water-miscible solvent, there are upper limits for its use in MEEKC. Exceeding these limits will result in a disintegration of the microemulsion. It has been reported that methanol may be used up to 8% (v/v), acetonitrile up to 12%, whereas 2-propanol may be used at considerably higher concentrations [29]. One should not forget the well-known side effect of organic solvents on the magnitude of the EOF which depends on the dielectric constant of the liquid phase, on the viscosity, and on the zeta potential of the capillary wall (all these parameters are directly affected by amount and type of an organic solvent in the aqueous phase of the microemulsion).

1.2.5 Other Additives

The addition of cyclodextrins to the carrier electrolyte is a well-established approach for chiral separations in capillary zone electrophoresis. The formation of transient diasteromeric complexes with cyclodextrins can also be exploited in MEEKC as an interaction in addition to the partition equilibrium between aqueous and oil phase, whereby either neutral cyclodextrins or cyclodextrins modified by charged groups (sulfated cyclodextrin) may be suited [30–32].

More recently, carbon nanotubes dispersed in the microemulsion have been investigated in order to establish additional interactions that might improve the separation selectivity in MEEKC [33–35].

Some experiments have been done with water-soluble ionic liquids as additives. In case of an anionic surfactant, the cation of the ionic liquid may interact and may partly neutralize the negative charge, thereby changing the properties of the pseudostationary phase [36].

1.3 Optimization of the Separation of Ionic Analytes

In the simplest case, ionic analytes are separated by using an oil phase stabilized by nonionic surfactants. In this case, the principles for optimization of the separation are similar to those mentioned earlier for separation of neutral analytes in a charged microemulsion. Nonionic surfactants most often employed are Brij-35, Tween-20, or Triton X-100. In addition, a less common nonionic surfactant, Pluronic F-127 has seen suggested [37] (which is an amphiphilic block copolymer consisting of ethylene oxide and propylene oxide), although so far only in combination with SDS for separation of neutral analytes. Most recently, zwitterionic surfactants like *N*-dodecyl-*N*,*N*-dimethyl-3-ammonio-1-propanesulfonate (DAPS) have been studied [38].

As mentioned in the Introduction, the use of charged microemulsions may lead to additional attraction or repulsion of ionic analytes to/from the droplets. This attraction/repulsion may be manipulated by using a mixture of a cationic and an anionic surfactant (see for example [39]). Oppositely charged analytes/droplets or analytes/excess surfactant in aqueous phase may also undergo interactions by ion-pair formation. A systematic treatment of such complex additional interactions is somewhat difficult so that generally valid strategies for optimization of separation selectivity are still limited.

1.4 Water-in-Oil Microemulsions

Although MEEKC is almost exclusively done in oil-in-water microemulsions, a few attempts have been made to apply water-in-oil microemulsions. Altria et al.[40, 41] introduced w/o microemulsions typically composed of 10% SDS, 80% butanol (or 78% butanol and 2% octane), and 10% aqueous buffer (or slight modifications of this composition). Similar compositions have been used later by other groups [42–45], but up to now the number of applications of w/o microemulsions in MEEKC is quite limited.

1.5 Sample Preconcentration by Sweeping

Spectroscopic detection techniques generally suffer from poor detection limits due to the short detection path length provided by the inner diameter of the separation capillary. Preconcentration effects occurring under proper injection conditions may help to improve detection limits. CE separation techniques based on pseudostationary phases may allow a preconcentration step called sweeping. It is generally defined as the picking and accumulating of analytes by a charged pseudostationary phase that penetrates the sample zone during application of a voltage. Most work on sweeping was done using micelles as pseudostationary phase (see, for example, the review in [46]), and the same principles work for microemulsions as well. Therefore, this chapter will not go into details regarding the theory of sweeping. In the simplest case, efficient preconcentration can be achieved with an microemulsion consisting of an oil phase stabilized by a negatively charged surfactant and an aqueous phase of low pH. The sample solution that does not contain the pseudostationary phase is injected hydrodynamically at the cathodic end of the capillary. After injection, the anionic pseudostationary phase will migrate from the cathodic carrier electrolyte vial into the capillary and through the sample zone (because of the low pH, the EOF can be neglected). In the sample zone, neutral analytes undergo partitioning and are focused into a narrow zone. As a result of the focusing effect, quite high volumes of sample may be injected without peak broadening (making possible a more than 1000-fold increase in sensitivity). Nevertheless, too long injection zones (without pseudostationary phases) may lead to instabilities of the system after applying voltage. Therefore, electrokinetic injection techniques have been used instead of hydrodynamic injection (which allows the selective injection of anions or cations without generating an excessively long zone of sample) followed by the sweeping step. Details of quite sophisticated combinations of injection techniques and sweeping would go beyond the scope of this chapter but can be found in recent review papers [3, 4, 7].

1.6 Detection

In common with other CE modes, the most widely used detection technique for MEEKC is UV–visible absorbance detection. Besides, fluorescence detection (with a xenon lamp or a laser as light source) may be the alternative for analytes that show native fluorescence or can be transformed into fluorescent derivatives prior to injection. A typical example for the latter approach is the separation of amino acids after derivatization with fluorescein isothiocyanate (FITC) [47].

Mass spectrometric (MS) detection may be most attractive as it provides the confirmation of peaks for target analytes or the structure elucidation of unknown peaks. Capillary zone electrophoresis can be hyphenated with MS via an electrospray ionization (ESI) source using a sheath–liquid interface which allows the realization of a makeup flow of a few μL/min to make flow

rates better compatible with commercial ESI sources and at the same time allows the application of the high voltage of the CE separation [48]. Unfortunately, the high concentrations of surfactants used in MEEKC make the technique hardly suited for coupling with ESI which would suffer from severe ionization suppression. Instead of ESI, atmospheric pressure photoionization (APPI) was found to tolerate components of a microemulsion much better [49–51]. A microemulsion consisting of 0.8 % octane, 2 % SDS, 6.6 % butanol, and 90.6 % of 20 mM ammonium hydrogencarbonate buffer (pH 9.5) allowed the quantitative analysis by APPI-MS of various pharmaceuticals down to the sub-µg/ml range without dedicated sample preconcentration during injection [49].

More recently, MEEKC has also been hyphenated with MS detection by an inductively coupled plasma interface, thereby allowing element-selective detection. This approach has been used for the analysis of anticancer platinum complexes [52].

1.7 Applications

The following discussion cannot give an exhaustive compilation of applications reported so far, but intends to give an idea of the broad variety of classes than can be separated. In Table 1 the focus is put on those applications that demonstrate a separation of a larger number of analytes, whereas applications dealing with just a single analyte are not included. The separations done by MEEKC range from pharmaceutical drugs to vitamins, agrochemicals, polycyclic hydrocarbons, natural products, derivatized sugars, derivatized amino acids, proteins, fatty acids, nucleosides, and chiral compounds. Actually, it is possible to use a single set of operating conditions for different applications. A microemulsion consisting of 0.8 % (w/w) octane, 6.6 % (w/w) 1-butanol, 3.3 % SDS, and 89.3 % (w/w) 10 mM sodium tetraborate buffer may be successful for a large number of different analytes and is often a quite successful starting point. In cases where this composition does not lead to satisfactory results, fine-tuning is possible by variation of the components of the microemulsion according to the principles discussed earlier.

Besides its benefits for analytical chemistry, MEEKC has frequently been employed as a simple tool for assessment of hydrophobicity (expressed as octanol–water partition coefficient $P_{o/w}$) [75–77]. The following linear relationship exists between $P_{o/w}$ and log k (k being the retention factor as mentioned earlier):

$$\log P_{o/w} = a \log k + b$$

Slope and intercept of this line can be obtained from experiments with solutes of known octanol–water partition coefficients.

Table 1
Selected applications of microemulsion electrokinetic chromatography

Analytes	Carrier electrolyte	Ref.
Fat-soluble vitamins	0.8% *n*-octane/6.6% 1-butanol/6.0% SDS/20.0% 2-propanol/66.6% 25 mM phosphate buffer pH 2.5	[53, 54]
Water- and fat-soluble vitamins	20 mM borate buffer pH 8.7 containing 1.2% SDS, 21% *n*-butanol, 18% acetonitrile, 0.8% hexane	[55]
Water- and fat-soluble vitamins	0.81% *n*-octane/6.61% 1-butanol/3.31% SDS/89.27% 10 mM sodium tetraborate	[56]
Derivatized amino acids	87.24% 30 mM phosphate buffer pH 6, 2.16% SDS, 6% 1-butanol, 0.6% cyclohexane, 4% acetonitrile	[47]
Derivatized sugars	0.81% *n*-octanol/6.61% 1-butanol/3.31% SDS/89.27% 5 mM borate buffer pH 8	[57]
Derivatized fatty acids	0.66% *n*-heptane/6.55% 1-butanol/4.87% cholate/87.93% 10 mM borate buffer pH 10.2	[58]
5-Lipoxygenase metabolites	20 mM borate buffer pH 9 containing 3% SDS, 0.5% octane, 5% 1-butanol and 15 mM α-cyclodextrin	[59]
Green tea catechins	1.13% *n*-heptane/7.66% cyclohexanol/2.89% SDS/88.09% 50 mM sodium phosphate pH 2.5	[22]
Rhubarb anthraquinones and bianthrones	0.5% di-*n*-butyl tartrate/1.2% *n*-butanol/0.6% SDS/97.7% 10 mM borate buffer pH 9.2	[60]
Plant hormones	97.2% 10 mM borate buffer pH 9.2, 1.0% ethyl acetate, 0.6% SDS, 1.2% *n*-butanol	[61]
Food-grade antioxidants	0.6 g octane, 6.6 g 1-butanol, 3.3 g SDS, 69.3 g 25 mM phosphate buffer pH 3, 20 g 2-propanol	[62]
Preservatives in food	0.8% *n*-octane/6.6% 1-butanol/3.3% SDS/89.3% borate buffer pH 9.5	[63]
Food colorants	0.81% *n*-octane/6.61% 1-butanol/3.31% SDS/10% acetonitrile/79.27% 50 mM phosphate buffer pH 2.0	[64]
Lignin degradation products	0.91% *n*-heptane/6.61% *n*-butanol/1.66% SDS/90.92% 20 mM sodium tetraborate	[65]
Sun protection agents	0.8% *n*-octane/6.6% 1-butanol/2.25% SDS/ 0.75%/ Brij35/17.5% 2-propanol/72.1% 10 mM borate buffer pH 9.2	[66]
Anticancer platinum complexes	0.82% heptane/6.48% 1-butanol/1.44% SDS, 91.26% 20 mM phosphate buffer pH 7.4	[52]
Nitrofuran antibiotics	10 mM borate buffer pH 9.7 containing 0.82% octane, 3.48% SDS, 6.48% *n*-butanol	[67]
Fluoroquinolone antibiotics	8 mM phosphate/borate buffer pH 7.3 containing 1% heptane, 100 mM SDS, 10% *n*-butanol	[68]

(continued)

Table 1
(continued)

Analytes	Carrier electrolyte	Ref.
Nonsteroidal anti-inflammatory drugs	0.8% ethyl acetate, 6.6% *n*-butanol, 6% acetonitrile, 1.0% SDS, 85.6% 10 mM borate buffer pH 9,2	[69]
Endocrine disrupting compounds	25 mM phosphate buffer pH 2, 80 mM octane, 900 mM butanol, 200 mM SDS, and 20% propanol	[70]
Phthalate esters	60 mM borate buffer pH 9 containing 0.5% *n*-octane, 100 mM sodium cholate, 5% 1-butanol	[71]
Triazine herbicides	10 mM borate buffer pH 9.5 containing 2.5% SDS, 0.8% ethyl acetate, 6% *n*-butanol	[72]
Aromatic carboxylic acids	50 mM phosphate buffer pH 2 containing 3.7% SDS, 0.975% octane, 5% cyclohexanol	[73]
Polycyclic aromatic hydrocarbons	90% of 0.81% *n*-octane/6.61% *n*-butanol/3.31% SDS/89.27% 10 mM sodium tetraborate; 10% ethanol	[74]

2 Materials

1. *Microemulsion for general applications using a negatively charged oil phase*: mix 3.3 g SDS and 6.6 g 1-butanol, and then add 0.8 g *n*-octane and 89.3 g 10 mM borate buffer pH 9.4 (prepared from a 10 mM boric acid adjusted to pH 9.4 with NaOH). The mixture is placed in an ultrasonic bath for 30 min to obtain a clear solution. Afterward, the microemulsion is filtered through a 0.45 μm membrane filter.
2. *Microemulsion for highly hydrophobic analytes using a negatively charged oil phase*: mix 2.25 g SDS, 0.75 g Brij 35 (*see* **Note 1**), and 6.6 g 1-butanol, and then add 0.8 g *n*-octane, 25 g 2-propanol, and 64.6 g 10 mM borate buffer pH 9.4 (prepared from a 10 mM boric acid adjusted to pH 9.4 with NaOH). The mixture is placed in an ultrasonic bath for 30 min to obtain a clear solution. Afterward, the microemulsion is filtered through a 0.45 μm membrane filter.
3. *Microemulsion for general applications using a neutral oil phase*: mix 3.32 g Brij 35 and 6.62 g 1-butanol, and then add 0.82 g *n*-heptane and 89.2 g 25 mM acetate buffer pH 4.0 (prepared from a 25 mM acetic acid adjusted to pH 4.0 with NaOH). The mixture is placed in an ultrasonic bath for 30 min to obtain a clear solution. Afterward, the microemulsion is filtered through a 0.45 μm membrane filter (*see* **Note 2**).
4. *Microemulsion for on-capillary preconcentration by sweeping using a negatively charged oil phase*: mix 3.3 g SDS and 6.6 g

1-butanol, and then add 0.8 g *n*-octane and 89.3 g 50 mM phosphoric acid pH 2.0. The mixture is placed in an ultrasonic bath for 30 min to obtain a clear solution. Afterward, the microemulsion is filtered through a 0.45 μm membrane filter.

5. CE instrument "7100 CE System" (Agilent, Waldbronn, Germany), or equivalent, equipped with an ultraviolet (UV) absorbance detector, high voltage supply up to +/−30 kV, and autosampler for both hydrodynamic and electrokinetic injection.
6. Fused-silica capillaries (Polymicro Technologies, Phoenic, AZ) with inner diameter and outer diameter of 50 and 360 μm, respectively, a length from inlet to detector of 51.5 cm, and a length from inlet to outlet of 60 cm (*see* **Note 3**).
7. Sample vials for autosampler of CE instrument.

3 Methods

3.1 General Procedure for Conditioning New Fused-Silica Capillaries

1. Four vials are filled with 1 M NaOH, water, 0.1 M NaOH, and 0.2 M HCl, respectively.
2. The vials are placed into appropriate positions of the autosampler for rinsing the capillary.
3. The capillary is rinsed with 1 M NaOH for 10 min, with water for 5 min, with 0.2 M HCl for 10 min, with water for 1 min, with 0.1 M NaOH for 10 min, and with water for 10 min.

3.2 Separation of Neutral Analytes Using a Negatively Charged Oil Phase

1. Two vials are filled with 0.1 M NaOH and microemulsion, respectively, for rinsing the capillary (the microemulsion is prepared according to the procedure given in Subheading 2, **item 1**.).
2. Two carrier electrolyte vials (for inlet and outlet side) are filled with the microemulsion.
3. Sample solutions and calibration solutions are filled into vials (*see* **Note 4**).
4. All vials are put into appropriate positions of the autosampler.
5. The capillary is rinsed with 0.1 M NaOH for 5 min and with microemulsion for 5 min.
6. The first sample or calibration solution is injected using hydrodynamic injection at a pressure of 50 mbar for 5 s (*see* **Note 5**), and the separation is started by applying a voltage of +25 kV (*see* **Note 6**).
7. The capillary is rinsed with 0.1 M NaOH for 1 min and with microemulsion for 1 min.
8. **Steps 6** and **7** are repeated for the next sample or calibration solution.

3.3 Separation of Highly Hydrophobic Analytes Using a Negatively Charged Oil Phase

1. Two vials are filled with 0.1 M NaOH and microemulsion, respectively, for rinsing the capillary (the microemulsion is prepared according to the procedure given under Subheading 2, **item 2**).
2. Two carrier electrolyte vials (for inlet and outlet side) are filled with the microemulsion.
3. Fill vials with sample solutions and calibration solutions, prepared in the microemulsion as solvent.
4. All vials are put into appropriate positions of the autosampler.
5. The capillary is rinsed with 0.1 M NaOH for 5 min and with microemulsion for 5 min.
6. The first sample or calibration solution is injected using hydrodynamic injection at a pressure of 50 mbar for 3 s, and the separation is started by applying a voltage of +30 kV.
7. The capillary is rinsed with 0.1 M NaOH for 1 min and with microemulsion for 1 min.
8. **Steps 6** and 7 are repeated for the next sample or calibration solution.

3.4 Separation of Positively Charged Analytes Using a Neutral Oil Phase

1. Two vials are filled with 0.1 M NaOH and microemulsion, respectively, for rinsing the capillary (the microemulsion is prepared according to the procedure given under Subheading 2, **item 3**).
2. Two carrier electrolyte vials (for inlet and outlet side) are filled with the microemulsion.
3. Vials are filled with sample solutions and calibration solutions.
4. All vials are put into appropriate positions of the autosampler.
5. The capillary is rinsed with 0.1 M NaOH for 5 min and with microemulsion for 5 min.
6. The first sample or calibration solution is injected using hydrodynamic injection at a pressure of 50 mbar for 5 s (*see* **Note 5**), and the separation is started by applying a voltage of +25 kV (*see* **Notes 6** and 7).
7. The capillary is rinsed with 0.1 M NaOH for 1 min and with microemulsion for 1 min.
8. **Steps 6** and 7 are repeated for the next sample or calibration solution.

3.5 Separation of Neutral Analytes with On-Capillary Preconcentration by Sweeping

1. Two vials are filled with 0.1 M NaOH and microemulsion, respectively, for rinsing the capillary (the microemulsion is prepared according to the procedure given in Subheading 2, **item 4**).
2. Two carrier electrolyte vials (for inlet and outlet side) are filled with the microemulsion.

3. Vials are filled with sample solutions and spiked sample solutions.
4. All vials are put into appropriate positions of the autosampler.
5. The capillary is rinsed with 0.1 M NaOH for 5 min and with microemulsion for 5 min.
6. The first sample solution is injected using hydrodynamic injection at a pressure of 100 mbar for 150 s (*see* **Note 8**), and the separation is started by applying a voltage of –20 kV (*see* **Note 6**).
7. The capillary is rinsed with 0.1 M NaOH for 1 min and with microemulsion for 1 min.
8. **Steps 6** and **7** are repeated for the next sample or spiked sample solution (*see* **Note 9**).

4 Notes

1. The partial substitution of SDS by Brij 35 results in lower charge of the oil droplet and thereby in a lower velocity. This leads to a decrease of the analysis time. For a specific separation, one can try to vary the ratio of SDS/Brij 35 to achieve optimal analysis time.
2. This microemulsion prepared in a buffer of pH 4.0 is suited for the separation of analytes that undergo protonation or deprotonation reactions at this pH, so that positively or negatively charged compounds are formed to some extent. The pH can be changed if necessary.
3. Shorter or longer capillaries can be used if necessary to optimize resolution and analysis time.
4. If the analytes are not easily soluble in water, the sample and calibration solutions can be prepared in the microemulsion as solvent. One should avoid pure organic solvents for the samples and the calibration solutions because these can disrupt the microemulsion adjacent to the zone of injected sample, leading to distorted peak shapes. It is recommended that an internal standard be added to both the sample and the calibration solutions.
5. Somewhat longer injection times can be used to achieve lower detection limits. Peak distortion will occur at too long injection times.
6. It may be advantageous to use somewhat lower or higher separation voltages depending on the length of the capillary.
7. The positive voltage applied is suited for cationic analytes. In the case of anionic analytes, it may be necessary to use a negative voltage (depending on the electrophoretic mobility of the analyte in relation to the electroosmotic mobility).

8. Depending on the analytes, this injection time may need to be decreased in order to avoid deterioration of peak shapes.
9. The incorporation of the online preconcentration effect makes quantitation by standard addition instead of external standards preferable.

References

1. Hoar TP, Schulman JH (1943) Transparent water-in-oil dispersions: the oleopathic hydromicelle. Nature 152:102–103
2. Watarai H (1991) Microemulsion capillary electrophoresis. Chem Lett 391–394
3. Yang H, Ding Y, Cao J, Li P (2013) Twenty-one years of microemulsion electrokinetic chromatography (1991-2012): a powerful analytical tool. Electrophoresis 34:1273–1294
4. Yu L, Chu K, Ye H, Liu X, Yu X, Chen G (2012) Recent advances in microemulsion electrokinetic chromatography. Trends Anal Chem 34:140–151
5. Ryan R, Altria K, McEvoy E, Donegan S, Power J (2013) A review of developments in the methodology and application of microemulsion electrokinetic chromatography. Electrophoresis 34:159–177
6. Ryan R, McEvoy E, Donegan S, Power J, Altria K (2011) Recent developments in the methodology and application of MEEKC. Electrophoresis 32:184–201
7. Ryan R, Donegan S, Power J, McEvoy E, Altria K (2009) Recent advances in the methodology, optimisation and application of MEEKC. Electrophoresis 30:65–82
8. McEvoy E, Marsh A, Altria K, Donegan S, Power J (2007) Recent advances in the development and application of microemulsion EKC. Electrophoresis 28:193–207
9. Ryan R, Donegan S, Power J, Altria K (2010) Advances in the theory and application of MEEKC. Electrophoresis 31:755–767
10. Schöftner R, Buchberger W (2003) Systematic investigations of different capillary electrophoretic techniques for separation of methylquinolines. J Sep Sci 26:1247–1252
11. Cao J, Qu H, Cheng Y (2010) The use of novel ionic liquid-in-water microemulsion without the addition of organic solvents in a capillary electrophoretic system. Electrophoresis 31:3492–3498
12. Wang Y, Li F, Yang FQ, Zuo HL, Xia ZN (2012) Simultaneous determination of α-, β- and γ-asarone in Acorus tatarinowii by microemulsion electrokinetic chromatography with [BMIM]PF_6 as oil phase. Talanta 101:510–515
13. Li F, Yang FQ, Xia ZN (2013) Simultaneous determination of ten nucleosides and related compounds by MEEKC with [BMIM]PF_6 as oil phase. Chromatographia 76:1003–1011
14. Siren H, Vesanen S, Suomi J (2014) Separation of steroids using vegetable oils in microemulsion elekctrokinetic capillary chromatography. J Chromatogr B 945–946:199–206
15. Hu S, Chen Y, Zhu H, Zhu J, Yan N, Chen X (2009) In situ synthesis of di-n-butyl L-tartrate-boric acid complex chiral selector and its application in chiral microemulsion electrokinetic chromatography. J Chromatogr A 1216:7932–7940
16. Hu S-Q, Chen Y-L, Zhu H-D, Shi H-J, Yan N, Chen X-G (2010) Effect of molecular structure of tartrates on chiral recognition of tartrate-boric acid complex chiral selectors in chiral microemulsion electrokinetic chromatography. J Chromatogr A 1217:5529–5535
17. Pascoe R, Foley JP (2002) Rapid separation of pharmaceutical enantiomers using electrokinetic chromatography with a novel chiral microemulsion. Analyst 127:710–714
18. Mertzman MD, Foley JP (2004) Effect of surfactant concentration and buffer selection on chromatographic figures of merit in chiral microemulsion electrokinetic chromatography. Electrophoresis 25:3247–3256
19. Mertzman MD, Foley JP (2004) Effect of oil substitution in chiral microemulsion electrokinetic chromatography. Electrophoresis 25:723–732
20. Kahle KA, Foley JP (2007) Two-chiral-component microemulsion electrokinetic chromatography-chiral surfactant and chiral oil: part 1. Dibutyl tartrate. Electrophoresis 28:1723–1734
21. Kahle KA, Foley JP (2007) Two-chiral component microemulsion EKC—chiral surfactant and chiral oil. Part 2: diethyl tartrate. Electrophoresis 28:2644–2657
22. Pomponio R, Gotti R, Luppi B, Cavrini V (2003) Microemulsion electrokinetic chromatography for the analysis of green tea catechins: effect of the cosurfactant on the separation selectivity. Electrophoresis 24:1658–1667

23. Klampfl C (2003) Solvent effects in microemulsion electrokinetic chromatography. Electrophoresis 24:1537–1543
24. Zheng ZX, Lin J-M, Chan W-H, Lee AWM, Huie CW (2004) Separation of enantiomers in microemulsion electrokinetic chromatography using chiral alcohols as cosurfactants. Electrophoresis 25:3263–3269
25. Kahle KA, Foley JP (2006) Chiral microemulsion electrokinetic chromatography with two chiral components: improved separations via synergies between a chiral surfactant and a chiral cosurfactant. Electrophoresis 27:896–904
26. Kahle KA, Foley JP (2007) Influence of microemulsion chirality on chromatographic figures of merit in EKC: results with novel three-chiral-component microemulsions and comparison with one- and two-chiral-component microemulsions. Electrophoresis 28:3024–3040
27. Nozal L, Arce L, Simonet BM, Rios A, Valcarcel M (2006) Microemulsion electrokinetic chromatography separation using hexane-in-water microemulsion without cosurfactant: comparison with MEKC. Electrophoresis 27:4439–4445
28. Hilder EF, Klampfl CW, Buchberger W, Haddad PR (2001) Separation of hydrophobic polymer additives by microemulsion electrokinetic chromatography. J Chromatogr A 922:293–302
29. Altria KD, Clark BJ, Mahuzier P-E (2000) The effect of operating variables in microemulsion capillary chromatography. Chromatographia 52:758–768
30. Borst C, Holzgrabe U (2013) Cyclodextrin-mediated enantioseparation in microemulsion electrokinetic chromatography. Meth Mol Biol 970:363–375
31. Borst C, Holzgrabe U (2008) Enantioseparation of DOPA and related compounds by cyclodextrin-modified microemulsion electrokinetic chromatography. J Chromatogr A 1204:191–196
32. Borst C, Holzgrabe U (2010) Comparison of chiral electrophoretic separation methods for phenethylamines and application on impurity analysis. J Pharm Biomed Anal 53:1201–1209
33. Cao J, Qu H, Cheng Y (2010) Separation of flavonoids and phenolic acids in complex natural products by microemulsion electrokinetic chromatography using surfactant-coated and carboxylic single-wall carbon nanotubes as additives. Electrophoresis 31:1689–1696
34. Cao J, Dun W, Qu H (2011) Evaluation of the addition of various surfactant-suspended carbon nanotubes in MEEKC with an in situ-synthesized surfactant system. Electrophoresis 32:408–413
35. Cao J, Li P, Chen J, Tan T, Dai H-B (2013) Enhanced separation of compound Xueshuantong capsule using functionalized carbon nanotubes with cationic surfactant solutions in MEEKC. Electrophoresis 34:324–330
36. Ni X, Yu M, Cao Y, Cao G (2013) Microstructure of microemulsion modified with ionic liquids in microemulsion electrokinetic chromatography and analysis of seven corticosteroids. Electrophoresis 34:2568–2576
37. Hsieh S-Y, Wang CC, Wu SM (2013) Microemulsion electrokinetic chromatography for analysis of phthalates in soft drinks. Food Chem 141:3486–3491
38. Cao W, Hu S-S, Li X-Y, Pang X-Q, Cao J, Ye L-H, Dai H-B, Liu X-J, Da J-H, Chu C (2014) Highly sensitive analysis of flavonoids by zwitterionic microemulsion electrokinetic chromatography coupled with light-emitting diode-induced fluorescence detection. J Chromatogr A 1358: 277–284
39. Cao J, Dun WL (2011) Separation and sweeping of flavonoids by microemulsion electrokinetic chromatography using mixed anionic and cationic surfactants. Talanta 84:155–159
40. Altria KD, Broderick MF, Donegan S, Power J (2004) The use novel water-in-oil microemulsions in microemulsion electrokinetic chromatography. Electrophoresis 25:645–652
41. Broderick M, Donegan S, Power J, Altria K (2005) Optimisation and use of water-in-oil MEEKC in pharmaceutical analysis. J Pharm Biomed Anal 37:877–884
42. Nyunt KTN, Prutthiwanasan B, Suntornsuk L (2013) Microemulsion electrokinetic chromatography of β-carotene and astaxanthin. J Liq Chrom Rel Techn 36:671–686
43. Bitar Y, Holzgrabe U (2007) Impurity profiling of atropine sulfate by microemulsion electrokinetic chromatography. J Pharm Biomed Anal 44:623–633
44. Cao J, Chen J, Yi L, Li P, Qi L-W (2008) Comparison of oil-in-water and water-in-oil microemulsion electrokinetic chromatography as methods for the analysis of eight phenolic acids and five diterpenoids. Electrophoresis 29:2310–2320
45. Huang H-Y, Liu W-L, Singco B, Hsieh S-H, Shih Y-H (2011) On-line concentration sample stacking coupled with water-in-oil microemulsion electrokinetic chromatography. J Chromatogr A 1218:7663–7669
46. Terabe S (2009) Capillary separation: micellar electrokinetic chromatography. Ann Rev Anal Chem 2:99–120
47. Lin W-C, Liu W-L, Tang W-Y, Huang C-P, Huang H-Y, Chin T-Y (2014) Determination

of amino acids by microemulsion electrokinetic chromatography laser induced fluorescence method. Electrophoresis 35:1751–1755

48. Klampfl CW, Buchberger W (2010) Recent advances in the use of capillary electrophoresis coupled to high-resolution mass spectrometry for the analysis of small molecules. Curr Anal Chem 6:118–125
49. Himmelsbach M, Haunschmidt M, Buchberger W, Klampfl CW (2007) Microemulsion electrokinetic chromatography with on-line atmospheric pressure photoionization mass spectrometric detection. Anal Chem 79:1564–1568
50. Himmelsbach M, Haunschmidt M, Buchberger W, Klampfl CW (2007) Microemulsion electrokinetic chromatography with on-line atmospheric pressure photoionization-mass spectrometric detection of medium polarity compounds. J Chromatogr A 1159:58–62
51. Schappler J, Guillarme D, Rudaz S, Veuthey J-L (2008) Microemulsion electrokinetic chromatography hyphenated to atmospheric pressure photoionization mass spectrometry. Electrophoresis 29:11–19
52. Bytzek AK, Reithofer MR, Galanski M, Groessl M, Keppler BK, Hartinger CG (2010) The first example of MEEKC-ICP-MS coupling and its application for the analysis of anticancer platinum complexes. Electrophoresis 31:1144–1150
53. Pedersen-Bjergaard S, Naess O, Moestue S, Rasmussen KE (2000) Microemulsion electrokinetic chromatography in suppressed electroosmotic flow environment. Separation of fat-soluble vitamins. J Chromatgr A 876:201–211
54. Oledzka I, Kowalski P, Baluch A, Baczek T, Paradziej-Lukowicz J, Taciak M, Pastuszewska B (2014) Quantification of the level of fat-soluble vitamins in feed based on the novel microemulsion electrokinetic chromatography (MEEKC) method. J Sci Food Agric 94:544–551
55. Yin C, Cao Y, Ding S, Wang Y (2008) Rapid determination of water- and fat-soluble vitamins with microemulsion electrokinetic chromatography. J Chromatogr A 1193:172–177
56. Altria KD (1999) Application of microemulsion electrokinetic chromatography to a wide range of pharmaceuticals and excipients. J Chromatogr A 844:371–386
57. Miksik I, Gabriel J, Deyl Z (1997) Microemulsion electrokinetic chromatography of diphenylhydrazones of dicarbonyl sugars. J Chromatogr A 772:297–303
58. Miksik I, Deyl Z (1998) Microemulsion electrokinetic chromatography of fatty acids as phenacyl esters. J Chromatogr A 807:111–119
59. Abromeit H, Werz O, Scriba GKE (2013) Separation of 5-lipoxygenase metabolites using cyclodextrin-modified microemulsion electrokinetic chromatography and head column field-amplified sample stacking. Chromatographia 76:1187–1192
60. Sun S-W, Yeh P-C (2005) Analysis of rhubarb anthraquinones and bianthrones by microemulsion electrokinetic chromatography. J Pharm Biomed Anal 36:995–1001
61. Chen Z, Lin Z, Zhang L, Cai Y, Zhang L (2012) Analysis of plant hormones by microemulsion electrokinetic capillary chromatography coupled with on-line large volume sample stacking. Analyst 137:1723–1729
62. Darji V, Boyce MC, Bennett I, Breadmore MC, Quirino J (2010) Determination of food grade antioxidants using microemulsion electrokinetic chromatography. Electrophoresis 31:2267–2271
63. Huang H-Y, Chuang C-L, Chiu C-W, Yeh J-M (2005) Application of microemulsion electrokinetic chromatography for the detection of preservatives in foods. Food Chem 89:315–322
64. Huang H-Y, Chuang C-L, Chiu CW, Chung M-C (2005) Determination of food colorants by microemulsion electrokinetic chromatography. Electrophoresis 26:867–877
65. Javor T, Buchberger W, Tanzcos I (2000) Determination of low-molecular-mass phenolic and non-phenolic lignin degradation compounds in wood digestion solutions by capillary electrophoresis. Microchim Acta 135:45–53
66. Klampfl CW, Leitner T (2003) Quantitative determination of UV filters in sunscreen lotions using microemulsion electrokinetic chromatography. J Sep Sci 26:1259–1262
67. Jiang T-F, Lv Z-H, Wang Y-H, Yue M-E, Lian S (2009) Separation and determination of nitrofuran antibiotics in turbot fish by microemulsion electrokinetic chromatography. Anal Sci 25:861–864
68. Wei S, Lin J, Li H, Lin J-M (2007) Separation of seven fluoroquinolones by microemulsion electrokinetic chromatography and application to ciprofloxacin, lomefloxacin determination in urine. J Chromatogr A 1163:333–336
69. Macia A, Borrull F, Calull M, Aguilar C (2005) Separation and on-column preconcentration of some nonsteroidal anti-inflammatory drugs by microemulsion electrokinetic capillary chromatography using high-speed separations. Electrophoresis 26:970–979
70. Fogarty B, Dempsey E, Regan F (2003) Potential for microemulsion electrokinetic chromatography for the separation of priority endocrine disrupting compounds. J Chromatogr A 1014:129–139

71. Lin Z, Zhang J, Cui H, Zhang L, Chen G (2010) Determination of phthalate esters in soil by microemulsion electrokinetic chromatography coupled with accelerated solvent extraction. J Sep Sci 33:3717–3725
72. Li R-H, Liu D-H, Yang Z-H, Zhou Z-Q, Wang P (2012) Vortex-assisted surfactant-enhanced-emulsification liquid-liquid microextraction for the determination of triazine herbizides in water samples by microemulsion electrokinetic chromatography. Electrophoresis 33:2176–2183
73. Huang H-Y, Wei M, Lin Y-R, Lu P-H (2009) Determination of organic impurities in mother liquors from oxidative terephthalic acid synthesis by microemulsion electrokinetic chromatography. J Chromatogr A 216:2560–2566
74. Altria KD (2000) Background theory and applications of microemulsion electrokinetic chromatography. J Chromatogr 892:171–186
75. Poole SK, Durham D, Kibbey C (2000) Rapid method for estimating the octanol-water partition coefficient by microemulsion electrokinetic chromatography. J Chromatogr B 745:117–126
76. Henchoz Y, Romand S, Schappler J, Rudaz S, Veuthey J-L, Carrupt P-A (2010) High-throughput log P determination by MEEKC coupled with UV and MS detections. Electrophoresis 31:952–964
77. Jiang X, Xia Z, Deng L, Wei W, Chen J, Xu J, Li H (2012) Evaluation of accuracy for the measurement of octanol–water partition coefficient by MEEKC. Chromatographia 75:347–352

Chapter 7

Nonaqueous Capillary Electrophoresis Mass Spectrometry

Christian W. Klampfl and Markus Himmelsbach

Abstract

The term nonaqueous capillary electrophoresis (NACE) commonly refers to capillary electrophoresis with purely nonaqueous background electrolytes (BGE). Main advantages of NACE are the possibility to analyze substances with very low solubility in aqueous media as well as separation selectivity that can be quite different in organic solvents (compared to water)—a property that can be employed for manipulation of separation selectivities. Mass spectrometry (MS) has become more and more popular as a detector in CE a fact that applies also for NACE. In the present chapter, the development of NACE–MS since 2004 is reviewed. Relevant parameters like composition of BGE and its influence on separation and detection in NACE as well as sheath liquid for NACE–MS are discussed. Finally, an overview of the papers published in the field of NACE–MS between 2004 and 2014 is given. Applications are grouped according to the field (analysis of natural products, biomedical analysis, food analysis, analysis of industrial products, and fundamental investigations).

Key words Nonaqueous capillary electrophoresis, Mass spectrometric detection

1 Introduction

Only 3 years after the introduction of capillary electrophoresis (CE) by Jorgenson and Lukacs [1], the first paper on CE employing a nonaqueous electrolyte (tetraethyl ammonium perchlorate/hydrochloric acid in acetonitrile) was published [2]. From that time on nonaqueous capillary electrophoresis (NACE) was distinguished from aqueous CE by the use of background electrolytes (BGE) based on purely organic solvents. This definition will also be followed in the present review. Some of the most convincing reasons for favoring NACE over CE with aqueous BGEs are [3, 4] as follows:

- Improved solubility of large number of analytes.
- Improved separation selectivity.
- Lower electric current allowing the use of higher separation voltages.
- Higher plate numbers.

Philippe Schmitt-Kopplin (ed.), *Capillary Electrophoresis: Methods and Protocols*, Methods in Molecular Biology, vol. 1483,
DOI 10.1007/978-1-4939-6403-1_7,

Due to these features NACE has faced increasing interest over the last decade with more than 200 publications since 2004 (found in SciFinder). This is also reflected in several review papers discussing theoretical aspects [3–6] as well as listing applications of NACE [7–10]. Thereby, similar as in aqueous CE in most cases spectrophotometric detection is employed and only a fraction (less than one quarter) of NACE applications describe the use of mass spectrometric (MS) detection. There is only one review article so far, specifically dedicated to NACE–MS which was published by Scriba in 2007 [11]. Nevertheless, most review articles focusing on CE–MS in general also include sections dealing with NACE–MS [12–17].

1.1 BGE Systems for NACE

BGEs for NACE commonly consist of an electrolyte (either a salt and acid/base or mixtures thereof), additives, and a solvent or solvent mixture. In the subsequent sections, these BGE constituents will be discussed focusing on their role in NACE–MS with respect to both, separation and detection.

1.2 Solvents for NACE and NACE–MS

One main asset of NACE is the possibility to select from a large range of different solvents. Table 1 gives an overview of physicochemical properties of solvents frequently used in NACE in comparison with water. As can be seen from these data, relevant physicochemical properties vary substantially between solvents and it seems obvious that the choice of solvent can be a valuable tool for manipulating separations. Separation of analytes in electrophoresis is governed by differences in their electrophoretic mobility μ_{ep}, i.e., their ability to migrate according to their ionic radius/charge ratio.

Table 1
Properties of solvents at 25 °C [9]

Solvent[a]	ε	η (mPa s)	ε/η (mPa^{-1} s^{-1})	T_{boil} (°C)	γ (N m^{-1})	pK_{auto}
Water	78.4	0.89	88.1	100.0	0.0718	14.0
Methanol	32.7	0.55	59.5	64.5	0.0223	16.9
Ethanol	24.6	1.08	22.8	78.2	0.0219	19.1
1-Propanol	20.5	1.94	10.6	97.1	0.0231	19.4
2-Propanol	19.9	2.04	9.8	82.2	0.0212	21.1
Acetonitrile	35.9	0.34	105.6	81.6	0.0283	32.2
Formamide	109.5	3.30	33.2	210.5	0.0582	16.8
N-Methylformamide	182.4	1.65	110.5	199.5	0.0395	10.7
N,*N*-Dimethylformamide	36.7	0.80	45.9	153.0	0.0364	23.1
Dimethylsulfoxide	46.5	1.99	23.4	189.0	0.0430	31.8

[a] ε, relative permittivity; η, viscosity coefficient; T_{boil}, boiling point; γ, surface tension; pK_{auto}, autoprotolysis constant

These parameters (ionic radius and charge) are both influenced substantially by the type of solvent employed. Different solvents lead to changes in the size of the solvated ion thereby influencing its ionic radius; dielectric constants ε and acid base properties of the solvent affect the degree of protonation/deprotonation and with it the charge of the analyte. In addition to that, also the viscosity (η) of the solvent determines migration velocities and subsequently the speed of separation. Actually the ratio of ε/η (given in Table 1) can be seen as good parameter for comparing solvents or solvent mixtures with respect to ion mobilities, whereby lower ε/η values imply slower migration of the ions [11]. An in-depth discussion of solvent effects in NACE would be beyond the scope of this book chapter, but more comprehensive information is available from several review articles [3, 4, 18, 19].

Focusing on the situation in NACE–MS, when choosing an appropriate solvent not only factors related to separation have to be observed, but also the effect of the chosen solvent on the performance of the MS detector. When using a triaxial sheath flow interface (as done in the majority of NACE–MS applications published so far) the effluent from the separation capillary is substantially diluted by the sheath liquid (which will be discussed later), so the sprayed solution should mainly consist of the sheath liquid and conditions were thus supposed to be dominated by its composition. Nevertheless, the solvent used for NACE still influences the efficiency of the electrospray process and thereby important parameters like signal-to-noise (S/N) ratio and limit of detection (LOD). This has been discussed in more detail in two interesting papers, focusing on solvent properties and their role in detection in NACE–MS [19, 20]. Studies employing an organic/aqueous (isopropanol:water = 4:1) sheath liquid and BGEs based on several solvents (methanol, acetonitrile, dimethylsulfoxide, formamide, *N*-methylformamide, and *N,N*-dimethylformamide) revealed substantial differences in the LODs obtained. Only methanol and acetonitrile provided similar results for the tested analytes (2-aminobenzimidazole, procaine, propranolol, and quinine) as observed with aqueous electrolytes; for the other solvents less favorable LODs were recorded. In the case of 2-aminobenzimidazole, the LOD with formamide and *N*-methylformamide in the BGE was more than 300-fold higher than the one obtained with methanol, acetonitrile, or the aqueous BGE [19]. A consequence of these findings may be the fact that when browsing the applications listed in Table 2 the majority of NACE–MS applications is performed using BGEs containing methanol, acetonitrile, or mixtures of these two solvents.

1.3 Electrolyte Systems for NACE–MS

Focusing on electrolyte systems for NACE, the impact of the solvent employed has to be considered first. One major prerequisite is the solubility of the selected electrolyte system in nonaqueous solvent systems. Some of the most popular buffer systems in aqueous

Table 2
Applications of nonaqueous capillary electrophoresis–mass spectrometry (since 2004)

	Method details	Ref.
Plants and natural products		
Crude root bark extracts from an African Ancistrocladus species	BGE: 100 mM ammonium acetate in methanol/acetic acid 60/40 v/v Ion trap MS with ESI in positive ion mode Sheath liquid: 2-propanol/water 1/1 v/v *Remark:* comparison with HPLC	[21]
β-Carboline alkaloids extracted from dried leaves	BGE: 40 mM $(NH_4)_2CO_3$ in methanol/glacial acetic acid 80/20 v/v Ion trap MS with ESI in positive ion mode Sheath liquid: 2-propanol/water 1/1 v/v *Remark:* combined detection system laser-induced fluorescence and MS; comparison with aqueous CE	[32]
Isoquinoline alkaloids in Fumaria officinalis	BGE: 60 mM ammonium acetate and 2.2 M acetic acid in acetonitrile/methanol 9/1 v/v Ion Trap MS with ESI in positive ion mode Sheath liquid: water/2-propanol 1/1 v/v	[33]
Nicotine-related alkaloids in chewing gums, beverages, and tobaccos	BGE: 50 mM ammonium formate in acetonitrile/methanol 50/50 v/v, apparent pH 4.0 Ion Trap MS with ESI in positive ion mode Sheath liquid: isopropyl alcohol/water 80/20 v/v	[36]
Alkaloids in Central European Corydalis species	BGE: 50 mM ammonium acetate and 1 M acetic acid in methanol/acetonitrile 1/9 v/v	[34]
Quinolizidine alkaloids in the roots of Sophora flavescens Ait. and S. tonkinensis Gagnep	BGE: 50 mM ammonium acetate and 0.5% acetic acid in methanol/acetonitrile 7/3 v/v Quadrupole MS with ESI in positive ion mode Sheath liquid: 0.5% acetic acid in methanol/water 80/20 v/v *Remark:* Field-amplified sample stacking with electromigration injection	[37]
Pyrrolo- and pyrido[1,2-a] azepine alkaloids in Stemona	BGE: 50 mM ammonium acetate, 1 M acetic acid, and 10% methanol in acetonitrile Ion Trap MS with ESI in positive ion mode Sheath liquid: water/2-propanol 1/1 v/v	[35]
Cinchona alkaloids in cinchona bark	BGE: 80 mM formic acid, 20 mM acetic acid, and 30 mM ammonium formate in methanol/ethanol/acetonitrile 50:35:15 v/v/v QTOF MS with ESI in positive ion mode Sheath liquid: 0.1% formic acid in 2-propanol/water 8/2 v/v	[38]
Alkaloids from psychoactive plant extracts	BGE: 58 mM ammonium formate and 1 M acetic acid in acetonitrile QTOF and Ion Trap MS with ESI in positive ion mode	[39]

(continued)

Table 2
(continued)

	Method details	Ref.
Alkaloids from a plant extract of Mitragyna speciosa	BGE: 60 mM ammonium formate and in acetonitrile/acetic acid 1000/35 v/v QTOF MS with ESI in positive ion mode Sheath liquid: 5% acetic acid in 2-propanol/water 66/34 v/v *Remark:* design of experiments to study the influence of the background electrolyte on separation and detection in NACE–MS	[20]
Mesembrine alkaloids in Sceletium tortuosum	BGE: 75 mM ammonium acetate in acetonitrile/glacial acetic acid 9/1 v/v Ion Trap MS with ESI in positive ion mode Sheath liquid: 5% acetic acid in 2-propanol/water 66/34 v/v	[40]
Matrine and oxymatrine in Sophora flavescens	BGE: 30 mM ammonium acetate and 1% acetic acid in methanol/acetonitrile 85/15 v/v Ion Trap MS with ESI in positive ion mode Sheath liquid: 2-propanol/water 2/1 v/v	[59]
Alkaloids isolated from Amaryllidaceae plants	BGE: 40 mM ammonium acetate and 0.5% acetic acid in methanol/acetonitrile 2/1 v/v Ion Trap MS with ESI in positive ion mode Sheath liquid: water/2-propanol 1/1 v/v	[60]
Biomedical analysis		
Lidocaine and its metabolites in human plasma	BGE: 70 mM ammonium formate and 2 M formic acid in acetonitrile/methanol 6/4 v/v Quadrupole MS with ESI in positive ion mode Sheath liquid: 2% formic acid in water/2-propanol 1/1 v/v	[41]
Peptaibol alamethicin F30 isolated from the culture broth of Trichoderma viride	BGE: 12.5 mM ammonium formate in methanol Ion trap and TOF MS with ESI in positive ion mode Sheath liquid: 1% formic acid in 2-propanol/water 1/1 v/v *Remark:* comparison with aqueous CE	[42]
Determination of salbutamol enantiomers in urine	BGE: 0.75 M formic acid, 10 mM ammonium formate, and 15 mM Heptakis(2,3-di-O-acetyl-6-O-sulfo)-β-cyclodextrin in methanol Ion Trap MS with ESI in positive ion mode Sheath liquid: 0.1% formic acid in 2-acetonitrile/water 3/1 v/v	[28]
Amino acid sequences of alamethicins F30	BGE: 12.5 mM ammonium formate in methanol Ion trap and TOF MS with ESI in positive ion mode Sheath liquid: 1% formic acid in 2-propanol/water 1/1 v/v	[43]
Phospholipids extracted from rat peritoneal surface	BGE: 20 mM ammonium acetate and 0.5% acetic acid in acetonitrile/methanol 60/40 v/v Ion Trap MS with ESI in negative ion mode Sheath liquid: 50 mM ammonium acetate in acetonitrile/methanol 60/40 v/v	[44]

(continued)

Table 2
(continued)

	Method details	Ref.
Three anesthetic drugs in human plasma	BGE: 2 M formic acid and 70 mM ammonium acetate in acetonitrile/methanol 60/40 v/v Quadrupole MS with ESI in positive ion mode Sheath liquid: 2% formic acid in methanol/water 8/2 v/v *Remark:* microextraction by packed sorbent in combination with CE	[45]
20 Antidepressants in plasma samples	BGE: 60 mM ammonium acetate and 1 M acetic acid in acetonitrile/water/methanol 100/1/0.5 v/v/v TOF MS with ESI in positive ion mode Sheath liquid: methanol/water 9/1 v/v	[47]
Amphetamine and related compounds in equine plasma	BGE: 25 mM ammonium formate and 1 M formic acid in acetonitrile/methanol 2/8 v/v Ion Trap MS with ESI in positive ion mode sheath liquid: 0.5% formic acid in water/2-propanol 1/1 v/v	[48]
Identification of fentanyl derivatives	BGE: 200 mM ammonium acetate in glacial acetic acid/acetonitrile 1/9 v/v Ion Trap MS with ESI in positive ion mode Sheath liquid: 2-propanol/water 1/1 v/v	[49]
Five fluoroquinolones in Urine	BGE: 20 mM ammonium acetate in acetonitrile/methanol 50/50 v/v adjusted to pH 4 with formic acid Quadrupole MS with ESI in positive ion mode Sheath liquid: 2% formic acid in acetonitrile/methanol 50/50 v/v *Remark:* microextraction by packed sorbent in combination with CE	[46]
Pregabalin in human urine	BGE: 10 mM ammonium formate and 0.05% acetic acid in methanol QTOF MS with ESI in positive ion mode Sheath liquid: 10 mM ammonium formate and 0.05% acetic acid in methanol	[61]
Nonsteroidal anti-inflammatory drugs (NSAIDs) and glucuronides in urine samples	BGE: 5 mM ammonium acetate in acetonitrile/methanol 80/20 v/v Quadrupole MS with ESI in negative ion mode Sheath liquid: 2-Propanol/water/NH_4OH 49.5/49.5/1 v/v/v *Remark:* comparison of a sheath liquid and sheathless interface	[30]
Food		
Phenolic compounds from olive oil	BGE: 25 mM ammonium acetate in methanol/acetonitrile 1/1 v/v, apparent pH adjusted to 5.0 with acetic acid TOF MS with ESI in negative ion mode Sheath liquid: 5 mM sodium hydroxide and 0.2% formic acid in water/2-propanol 1/1 v/v	[31]

(continued)

Table 2
(continued)

	Method details	Ref.
Analyses of clenbuterol, salbutamol, and terbutaline in pork	BGE: 18 mM ammonium acetate in methanol/acetonitrile/glacial acetic acid 66/33/1 v/v/v TOF MS with ESI in positive ion mode Sheath liquid: 5 mM ammonium acetate in methanol/water 80/20 v/v	[51]
Glycerophospholipids in olive fruit and oil	BGE: 100 mM ammonium acetate and 0.5% acetic acid in methanol/acetonitrile 60/40 (v/v) Ion Trap MS with ESI in positive ion mode Sheath liquid: 0.5% acetic acid in methanol/water 8/2 v/v	[50]
Environmental and industrial		
Detection of hexamethonium–perchlorate association complexes	BGE: 2-propanol/acetone 2/1 v/v Ion trap MS with ESI in positive ion mode Sheath liquid: methanol	[52]
Separation and characterization of ionizable organic polymers nonsoluble in water	BGE: 1 M acetic acid, 20 mM ammonium acetate in methanol/acetonitrile 87.5/12.5 v/v Ion Trap MS with ESI in positive ion mode Sheath liquid: methanol/acetonitrile 87.5/12.5 v/v	[53]
Degradation products of the herbicide oxasulfuron	BGE: 50 mM ammonium acetate and 1.2 M acetic acid in acetonitrile/methanol 9/1 v/v Ion Trap MS with ESI in positive ion mode Sheath liquid: 1% acetic acid in water/methanol 1/1 v/v	[54]
Characterization of nonderivatized Brij 58 oligomers	BGE: 20 mM NH4I in methanol Ion Trap MS with ESI in positive ion mode Sheath liquid: 25 mM ammonium acetate in methanol/water 95/5 v/v *Remark:* EOF reversal with hexadimethrine bromide	[27]
Six pharmaceutical compounds and their respective process-related impurities	BGE: 10 mM ammonium acetate and 100 mM acetic acid in methanol/acetonitrile with varying ratios Ion trap MS with ESI Sheath liquid: 0.1% formic acid in methanol/water 50/50 v/v	[55]
Separation of basic drugs, including their enantiomers	BGE: 10 mM HP-β-CD or 10 mM HDMS-β-CD in methanol containing 10 mM ammonium and 0.75 M formic acid Ion trap MS with ESI in positive ion mode Sheath liquid: 0.1% formic acid in acetonitrile/water 75/25 v/v *Remark:* Nonaqueous electrokinetic chromatography using anionic cyclodextrins;	[56]

(continued)

Table 2
(continued)

	Method details	Ref.
Separation of 10 acidic drugs, including their enantiomers	BGE: 20 mM PA-β-CD in methanol containing 20 mM ammonium acetate or 5 mM IPA-β-CD in methanol containing 40 mM ammonium acetate Ion trap MS with ESI in negative ion mode Sheath liquid: 5 mM ammonium acetate in acetonitrile/water 75/25 v/v *Remark:* Nonaqueous electrokinetic chromatography using cationic cyclodextrins; polyacrylamide and polyvinylamide coated capillaries were used	[26]
Organotin compounds in water samples	BGE: 50 mM ammonium acetate and 1 M acetic acid in acetonitrile/methanol 80/20 v/v QTOF MS with ESI in positive ion mode Sheath liquid: 0.2% formic acid in 2-propanol/water 1/1 v/v *Remark:* speciation of organotin compounds	[57]
Fundamental investigations		
2-Aminobenzimidazole, procaine, propranolol, and quinine	BGE: 10 mM ammonium acetate in 7 different solvents Ion Trap MS with ESI in positive ion mode Sheath liquid: 0.1% formic acid in 2-propanol/water 4/1 v/v *Remark:* assessment of the influence of the solvent on selectivity, separation speed, and peak efficiency for a given set of model compounds	[19]
2,4-Dinitrophenol, pentachlorophenol, 3,4-dichlorocinnamic acid, 2-methyl-4,6-dinitrophenol, 2,3,4,5-tetrachlorophenol	BGE: 25 mM ammonium formate in methanol, apparent pH adjusted to 8.0 with 25 mM NH_4OH Triple quadrupole MS with ESI in negative ion mode Sheath liquid: 2 mM ammonium acetate in 2-propanol/water 80/20 v/v *Remark:* Large volume stacking using an EOF pump	[58]
Separation of carvedilol enantiomers	BGE: 0.75 M formic acid, 10 mM ammonium acetate and 10 mM sulfated β-CD in methanol Ion Trap MS with ESI in positive ion mode Sheath liquid: 0.1% formic acid in 2-propanol/water 3/1 v/v *Remark:* addition of different single-isomer sulfated β-CD derivatives	[29]

CE such as phosphate and borate are hardly soluble in nonaqueous media. Second, the critical parameter giving an idea about the dissociation of an electrolyte is the relative permittivity ε of the solvent. As can be seen from Table 1, for most solvents employed in NACE, ε is lower than in the case of water. As a consequence of this fact, comparing a given concentration of an electrolyte substance in water and in a nonaqueous solvent (such as methanol or acetonitrile) its conductivity will be lower in the nonaqueous

medium. For this reason, relatively high concentration of electrolyte substances can be employed in NACE without reaching the limiting electrical current. This can clearly be seen from the applications listed in Table 2, where electrolyte systems containing 100 mM ammonium acetate and 40% of acetic acid could be used without any problems with excessive current [21].

Comparing NACE with spectrophotometric detection and NACE–MS, it can be observed that using MS as detector has a clear impact on the selection of components that can be included in the BGE, whereby no significant difference exists between aqueous and nonaqueous electrolyte systems. The MS detector is far more prone to interferences caused by physicochemical properties of electrolyte ingredients than a photometric one. Unfortunately, the need to ensure compatibility with MS reduces the number of selectable electrolyte ingredients substantially. Focusing on MS with the most commonly used ionization technique, namely, electrospray ionization (ESI) [22] the use of volatile BGE components is mandatory. This prerequisite excludes a series of substances which are of very popular in CE, such as buffers based on phosphate or borate (although these two are not employed in NACE due to solubility issues in the commonly employed organic solvents), capillary coatings based on alkylammonium salts or sulfonate/sulfate additives. BGEs mostly used in CE–MS are based on formic acid, acetic acid (and their ammonium salts), carbonate, and solutions of ammonia or alkylamines if strongly alkaline conditions are needed. Here the situation in NACE–MS is quite similar. Nevertheless, there are some reports on the use of other BGE systems containing nonvolatile ingredients and their impact on ionization in ESI–MS exist [23]. In-depth information about requirements for MS-compatible CE electrolytes, in general, can be found in a comprehensive review article published by Pantuckova et al. [24].

1.4 pH in Nonaqueous Systems

A crucial parameter in optimizing the BGE for CE in general is the selection of the appropriate pH value, as this factor influences the direction and magnitude of the electro endoosmotic flow as well as the degree of protonation/deprotonation of the analytes and with it the direction and magnitude of their electrophoretic mobilities. Whereas measuring and adjusting the pH is a more or less simple task in aqueous systems, the concept of pH measurement and adjustment cannot be transferred easily to nonaqueous conditions. Several approaches to overcome this problem have been suggested so far [11]. One option is to measure pH in nonaqueous solvents employing the same procedure as in aqueous media. This leads to the so-called apparent pH a value that is quite often used to describe nonaqueous buffer systems. Nevertheless, it has to be taken into account, that this “apparent pH” only allows comparison between BGEs based on the same solvent. An alternative is pH calculation using the Henderson–Hasselbalch equation. This approach can only be used if the pK values of the employed acid or

base in the respective solvent are available. A comprehensive discussion on the issue of pH measurement and adjustment in nonaqueous solvents has been published by Porras and Kenndler [6].

1.5 Capillary Coatings and Additives

Capillary coatings are quite popular in CE. They are used, for example, to reduce analyte/capillary wall interactions or to suppress or even reverse the electro endoosmotic flow, just to name a few reasons for their application [25]. Dynamic coating (i.e., the coating substance is added to the BGE) and static coating (the coating is attached to the capillary wall either by covalent bonds or by strong electrostatic interaction) can be distinguished. When moving from aqueous conditions to NACE it has to be ensured that the coating is still stable even when purely organic BGEs are employed. Furthermore, most substances used for dynamic coating are not compatible with MS. So either capillaries with covalently bonded coatings are employed in NACE–MS [26] or substances like hexadimethrine bromide that show strong interactions with the capillary wall even under completely nonaqueous conditions [27].

The group of additives for CE comprises a wide range of quite different substances. These can be micelle-forming agents, ion-pairing reagents, chiral selectors, and so on just to name a few. Also in the case of additives analyte/additive interactions have to be reevaluated when moving from aqueous to nonaqueous media. Similar as in the case of substances employed for capillary coating, most of the additives commonly employed in CE are not compatible with MS detection. A strategy to combine NACE with nonvolatile additives such as cyclodextrins with MS detection is to select conditions where these additives migrate toward the capillary inlet [26, 28, 29]. So no disadvantageous suppression effects are encountered as the cyclodextrins are not reaching the MS ion source.

1.6 Sheath Liquids for Nonaqueous Capillary Electrophoresis–Mass Spectrometry

From the NACE–MS papers listed in Table 2, only in one case a sheathless interface is employed for CE–MS coupling [30]. In this study, a recently developed sheathless interface was compared to a conventional triaxial sheath flow interface with respect to its performance in NACE–MS of acidic compounds. In all other studies, the addition of an appropriate sheath liquid is required for guaranteeing a stable electrospray. The sheath liquid serves as a makeup flow (to reach the minimum flow rates needed for the ESI source), it is needed to close the electric circuit of the CE system (as no second electrolyte vial is present in CE–MS coupling), and its composition should enhance ionization efficiency and probably overcome less favorable characteristics of the BGE (with respect to ionization). When comparing sheath liquid compositions used in aqueous CE–MS and those for NACE–MS not real difference can be detected. In most cases a mixture of water and an alcohol (mainly methanol or 2-propanol) or acetonitrile together with small amounts of a volatile salt (often ammonium acetate or formate) and/or a MS compatible acid or base (formic acid,

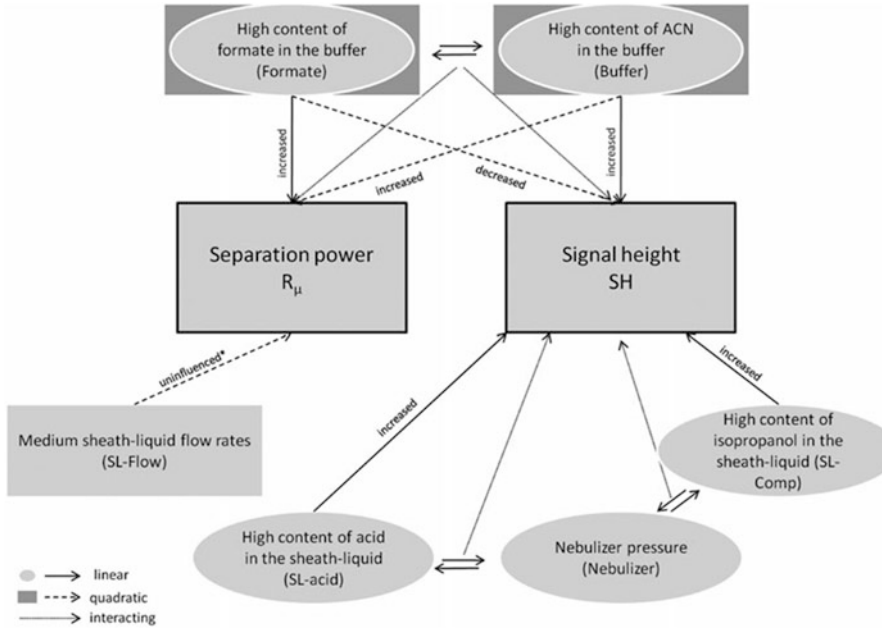

Fig. 1 Visualizationof the interactions and influences of the process parameters on the response variables. CE parameters are shown on top, MS parameters are shown below the response variables. Reproduced from [20] with permission

acetic acid, or ammonia, respectively) are the best choice. An example demonstrating a further functionality of the sheath liquid was presented by Gomez-Caravaca et al. [31]. By adding 2.5 mM of NaOH to sheath liquid, sodium formate clusters were formed that could be directly used for mass calibration of the TOF instrument.

1.7 Optimization of NACE–MS Parameters

When searching for the best operational parameters for NACE–MS experiments, mutual interference between several experimental parameters like BGE composition, composition of the sheath liquid, sheath liquid flow rate, or nebulizer pressure has to be taken into account. Posch et al. have published an in-depth study discussing the possibility to use a design of experiments approach to study the influence of the background electrolyte on separation and detection in NACE–MS [20]. A scheme depicting potential interactions and influences is shown in Fig. 1. In this work it was proven that at high electro endoosmotic flow conditions, separation can be optimized without inferences from the MS detection system.

2 Applications

Table 2 gives an overview of NACE–MS applications published since 2004. Applications are grouped according to the field of application and listed in chronological order. In this table, relevant

information concerning the type of analytes investigated and/or the field of application, BGE and sheath liquid composition, and the type of MS instrument/ionization source used is provided. Additionally, remarks on characteristic features of the work are given.

2.1 NACE–MS of Plants and Natural Products

The analysis of plants and natural products is one of the main fields of application of NACE–MS. Unger et al. compared HPLC with CE and NACE for the analysis of crude extracts from Ancistrocladus species [21]. Although the highest number of resolved components was achieved by HPLC, NACE allowed the separation of cis/trans isomers (that could not be resolved using HPLC) whereas conventional CE with an aqueous electrolyte led to comigration of all analytes. Huhn et al. designed a CE system allowing simultaneous laser-induced fluorescence and MS detection [32]. Employing this setup, β-carbolines from an Ayahuasca sample were analyzed, whereby distinctly different migration orders were achieved in NACE compared to CE with an aqueous BGE. The group of Stuppner used NACE–MS with a BGE based on mixed solvents (acetonitrile/methanol=9/1) for the investigation of several plant extracts [33–35]. A NACE–MS method for the analysis of alkaloids in tobacco and chewing gums was developed by Chiu et al. [36]. In their paper they investigated a series of nonaqueous BGEs differing in apparent pH, methanol/acetonitrile ratio, as well as type and concentration of electrolyte employed. The combination of NACE–MS and field amplified sample stacking for the high-sensitivity analysis of quinolizidine alkaloids was presented by Wang et al. [37]. Buchberger et al. achieved the separation of cinchona alkaloids extracted from cinchona bark [38]. Employing a rather complex nonaqueous BGE based on formic acid, acetic acid, and ammonium formate in a mixture of methanol/ethanol and acetonitrile, a series of diastereomeric compounds could be separated. The group of Huhn published a series of papers on the use of NACE–MS for the analysis of forensically interesting alkaloids from several plant species [20, 39, 40]. In one of these papers (as discussed earlier) the use of a "design of experiment" for optimization of NACE–MS parameters is discussed [20].

2.2 NACE–MS for Bioanalytical Applications

A second major field of application of NACE–MS is biomedical analysis. Anderson et al. described a NACE–MS method for the determination of lidocaine and its metabolites in human plasma [41]. Alamethicin peptides from Trichoderma viride were analyzed by Psurek et al. employing NACE–MS [42, 43]. Comparing the results obtained with aqueous and nonaqueous conditions revealed improved separation efficiency for the nonaqueous BGE as well as substantial selectivity changes. The latter might be attributed to changes in the shape of the peptide when switching from aqueous to nonaqueous conditions. Cyclodextrin-mediated NACE–MS was employed for the determination of salbutamol enantiomers in urine by Servais et al. [28]. The developed method allowed the baseline separation of the two enantiomers in less than 12 min. Due to their

low solubility in aqueous media, phospholipids are not easily accessible to CE–MS analysis. Gao et al. investigated the potential of different nonaqueous BGE systems for the NACE–MS analysis of these compounds [44]. Morales-Cid et al. developed sophisticated automated instrumentation, including sample pretreatment steps such as packed sorbent microextraction and microdialysis for the analysis of drugs in body fluids by NACE–MS [45, 46]. Although both, aqueous and nonaqueous electrolytes were studied, the NACE approach was selected due to the increased sensitivity obtained. Employing the right mixture of methanol and acetonitrile allowed to adjust selectivity and to reduce analysis times. A series of antidepressants were separated by NACE and subsequently detected using MS by Sasajima et al. [47]. As can be seen from Fig. 2, great improvement in separation was achieved when moving from an aqueous BGE to a nonaqueous one. Interestingly, the BGE finally selected for this analytical problem can no longer be seen as a purely nonaqueous one, as it contains 1 % of water. Amphetamines in race-horse plasma were analyzed by Li et al. [48]. Fentanyl derivatives were separated using NACE by Rittgen et al. [49]. The analysis of these compounds gains more and more interest as clandestine fentanyl laboratories produce these substances for the illegal drug market. An interesting study comparing not only CE with aqueous

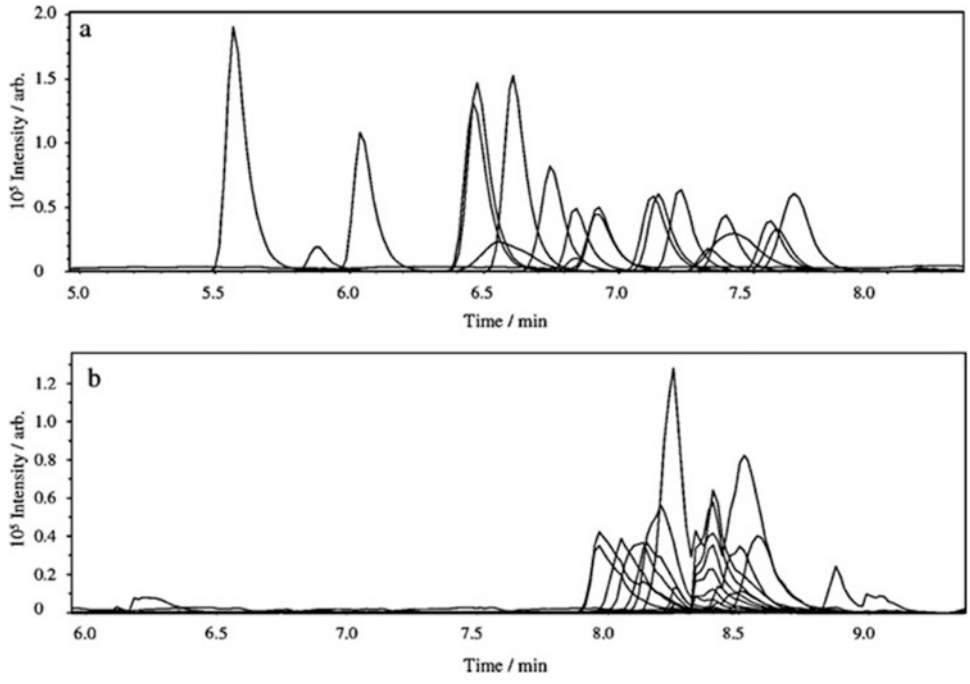

Fig. 2 Separation of 20 antidepressants—comparison between NACE and aqueous CE. BGE, (**a**) 50 mM ammonium acetate and 1 M acetic acid in acetonitrile, (**b**) 1 M formic acid in water; all other parameters are identical. Reproduced from [47] with permission

and nonaqueous conditions, but also two different types of ESI interfaces for CE–MS coupling was published by Bonvin et al. [30]. As can be seen from Fig. 3, switching from an aqueous BGE to NACE substantially improved the resolution of the investigated test substances. In addition, sensitivity obtained with NACE–MS was 5–10 times better than in CE–MS, although also a substantially higher noise level was observed with the nonaqueous BGE.

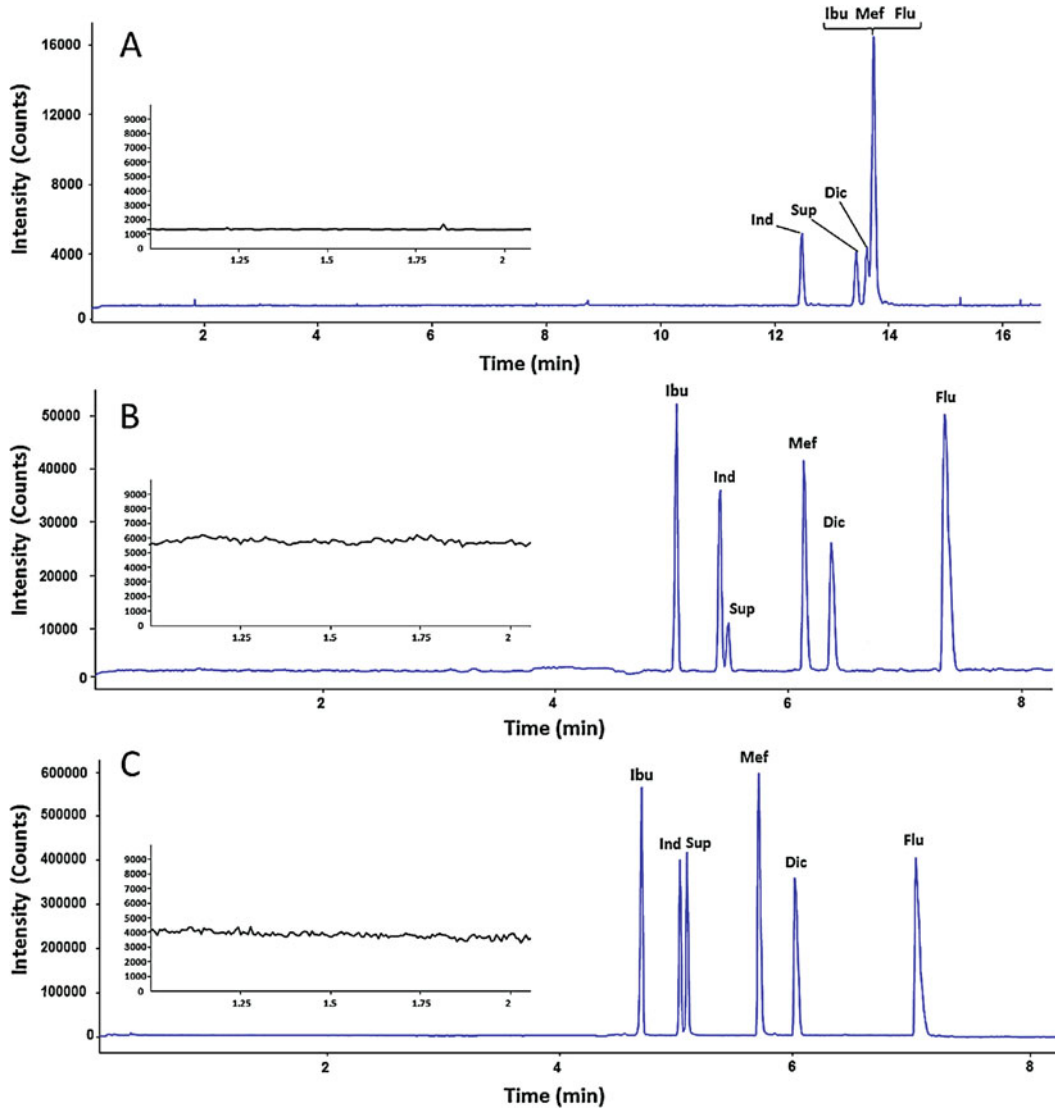

Fig. 3 CE–MS electropherograms of acidic compounds in negative ESI obtained for selected nonsteroidal anti-inflammatory drugs (dissolved at 1 μg/mL in ACN-MeOH 60:40 (v/v)) with the sheath liquid interface in (**A**) aqueous CZE mode; BGE: ammonium acetate 50 mM, pH 8.5 and (**B**) NACE mode; BGE: ammonium acetate 5 mM in ACN-MeOH 80:20 (v/v). (**C**) CE–MS electropherograms with the sheathless interface in NACE mode; BGE: ammonium acetate 5 mM in ACN-MeOH 80:20 (v/v). Peaks: *Ind*: Indomethacin; *Sup* Suprofen; *Dic* Diclofenac, *Ibu* Ibuprofen, *Mef* Mefenamic acid, *Flu* Flufenamic acid. Reproduced from [30] with permission

2.3 NACE–MS in Food Analysis

Nonaqueous conditions are definitely favorable when it comes to the CE analysis of samples with low solubility in water. This fact has been exploited in two studies describing the NACE–MS analysis of olive oils and olive fruit with respect to phenolic compounds [31] and phospholipids [50]. β-Agonists in pork meat were analyzed by NACE–MS and HPLC–MS [51].

2.4 NACE–MS for the Analysis of Technical Products and Environmental Samples

Groom and Hawari investigated the formation of complexes including hexamethonium perchlorate (substances frequently used as rocket fuel) in both aqueous and polar nonaqueous solvents [52]. The resulting complexes were resolved employing NACE and detected by ESI–MS. A characteristic of this work is the rather unusual BGE based on a mixture of 2-propanol and acetone. Organic polymers are often insoluble in aqueous media. For this reason separation methods working in nonaqueous solution are preferable for the analysis of such samples. Simo et al. demonstrated the suitability of NACE–MS for the analysis of synthetic polymers (poly (*Nε*-trifluoroacetyl-l-lysine)) [53]. Thereby, structures containing up to 38 monomers could be resolved. Scrano et al. developed a NACE–MS method allowing the identification and quantitation of two novel degradation products originating from the photolytic reaction of oxasulfuron [54]. Another polymer-related application of NACE–MS has been published by Morin et al. [27]. The separation of the neutral polyethylene oxide surfactant was based on its complexation with ammonium in methanol as solvent. More than 25 oligomers of this surfactant could be characterized. Aqueous CE, open-tubular capillary electrochromatography and NACE, all coupled to MS, were compared with respect to their potential for the impurity profiling of drugs by Vassort et al. [55]. The results obtained within this study suggest that some of the previously developed CE–MS methods should be replaced by NACE–MS due to improved separation capabilities. Additionally, NACE appears attractive as a large portion of drug candidates are poorly soluble in water. Electrokinetic chromatography with cyclodextrins in nonaqueous media was employed for the analysis of various acidic drugs by Mol et al. [26, 56]. The effect of the cationic cyclodextrins on the ESI process was studied, whereby the separation voltage applied led to migration of these components in direction of the inlet vial, thereby not interfering with the ionization process. A fast NACE–MS method for the speciation of organotin compounds, substances commonly employed as antifouling agents, was presented by Malik et al. [57]. The use of a homemade CE instrument allowed applying separation voltages as high as 35 kV together with the use of short capillaries—thereby reducing analysis times to 2.5 min.

2.5 NACE–MS: Fundamental Investigations

Several papers discussing fundamental issues with respect to the coupling of NACE with MS have been published so far. Steiner and Hassel performed in-depth investigations on the influence of

solvent properties on separation and detection [19]. They compared a series of solvents with respect to analysis times, separation efficiency, as well as performance in combination with ESI–MS detection. Some of the findings from this paper have already been discussed in the previous section on "Solvents for NACE and NACE–MS." The potential of large volume sample stacking in combination with NACE–MS was investigated by Kim et al. whereby a 400-fold enrichment of anionic analytes was achieved [58]. Technical obstacles arising from the long sample matrix plug were solved by supplying a backup run buffer from the outlet vial of the CE system. Cyclodextrins are widely used in electrokinetic chromatography for selectivity manipulations. Unfortunately they can cause adverse effects in ESI–MS detection due to the occurrence of ionization suppression. Nonaqueous electrokinetic chromatography with either anionic [56] or cationic [26] cyclodextrins has successfully been coupled to MS detection. In a further paper, Servais et al. discussed the influence of BGE composition and type of cyclodextrin used on the detector response observed in cyclodextrin-mediated NACE–MS [28].

3 Materials

In this section instrumentation and materials for a typical NACE–MS application are discussed. Some of these points are also valid for normal CE–MS with aqueous BGE.

3.1 BGE for NACE–MS

BGE ingredients have to comply with both, requirements from NACE and requirements from ESI–MS. From the wide range of solvents employed in NACE with spectrophotometric detection only a few are also used in combination with MS: these are alcohols (methanol, ethanol) and acetonitrile. Electrolyte ingredients (salts, acids, or bases) have to be soluble in the selected solvent and have to be compatible with ESI–MS. So in most cases low molecular weight organic acids (formic acid, acetic acid) and/or their ammonium salts are employed.

3.2 Sheath Liquid for NACE–MS

Sheath liquids used in NACE–MS are almost identical to those in aqueous CE–MS. Although purely nonaqueous sheath liquids can be used (methanol, propanol, or acetonitrile/alcohol mixtures) most sheath liquids in NACE contain 20–50% water together with a small amount of acid/base or a volatile salt to enhance ionization.

3.3 CE Instrumentation

"7100 CE System" (Agilent), Beckman PA 800 (SCIEX Separations) or equivalent, equipped with an ultraviolet (UV) absorbance detector, high voltage power supply up to +–30 kV, and autosampler for both hydrodynamic and electrokinetic injection. Also a special capillary cartridge for hyphenation with MS is

needed. Due to the higher volatility of organic solvents (compared to aqueous BGEs) a cooling option for the tray, housing the sample and the electrolyte vials is advisable.

3.4 CE–MS Interface

The majority of CE–MS applications are performed using a triaxial sheath flow interface like the one available from Agilent (G1607A or G1607B). For supplying the sheath liquid ideally an HPLC pump with a 1:100 flow splitter is employed. A second option is the use of a syringe pump (e.g., from Harvard Apparatus, South Natick, MA, USA) whereby an increased baseline noise due to flow rate fluctuations must be taken into account.

3.5 MS Instrument

In most cases, MS instruments that offer commercially available dedicated interfaces for CE–MS coupling are preferable. Apart from that, MS instruments with an ionization source where the sprayer needle is grounded, whereas high voltage is applied to the MS orifice, as is the case in Agilent and Bruker instruments, for example, substantially facilitate CE–MS coupling. As CE is a highly efficient separation technique resulting in narrow peaks a sufficiently fast MS instrument is advantageous. In recent times, TOF and Q/TOF instruments have become the most frequently used instruments in CE–MS coupling.

3.6 Fused-Silica Capillaries

For example, from Polymicro Technologies (Phoenic, AZ) with inner diameter and outer diameter of 50 and 360 μm, respectively, and sufficient length to introduce the capillary into the MS interface. The capillary length can vary significantly due to the different layout of the available CE–MS systems and may be in the range between 60 cm and more than 100 cm. If coated capillaries are employed, stability of the coating in nonaqueous BGEs has to be ensured.

References

1. Jorgenson JW, Lukacs KD (1981) Zone electrophoresis in open-tubular glass. Anal Chem 53:1298–1302
2. Walbroehl Y, Jorgenson JW (1984) On-column absorption UV-detector for open tubular capillary zone electrophoresis. J Chromatogr 315:135–143
3. Kenndler E (2014) A critical overview of nonaqueous capillary electrophoresis. Part I: mobility and separation selectivity. J Chromatogr A 1335:16–30
4. Kenndler E (2014) A critical overview of non-aqueous capillary electrophoresis. Part II: separation efficiency and analysis time. J Chromatogr A 1335:31–41
5. Kenndler E (2009) Organic solvents in CE. Electrophoresis 30:S101–S111
6. Porras SP, Kenndler E (2004) Capillary zone electrophoresis in non-aqueous solutions: pH of the background electrolyte. J Chromatogr A 1037:455–465
7. Riekkola M-L (2002) Recent advances in nonaqueous capillary electrophoresis. Electrophoresis 23:3865–3883
8. Weinberger R (2006) Non aqueous capillary electrophoresis. Am Lab 38:49–50
9. Geiser L, Veuthey J-L (2009) Nonaqueous capillary electrophoresis in pharmaceutical analysis. Electrophoresis 30:36–49
10. Szumski M, Buszewski B (2013) Non aqueous capillary electrophoresis. Springer Series Chem Phys 105:203–213
11. Scriba GKE (2007) Nonaqueous capillary electrophoresis-mass spectrometry. J Chromatogr A 1159:28–41

12. Zhong X, Zhang Z, Shan J, Li L (2014) Recent advances in coupling capillary electrophoresis-based separation techniques to ESI and MALDI-MS. Electrophoresis 35:1214–1225
13. Kleparnik K (2013) Recent advances in the combination of capillary electrophoresis with mass spectrometry: from element to single-cell analysis. Electrophoresis 34:70–85
14. Bonvin G, Schappler J, Rudaz S (2012) Capillary electrophoresis-electrospray ionization-mass spectrometry interfaces: fundamental concepts and technical developments. J Chromatogr A 1267:17–31
15. Pioch M, Bunz S-C, Neususess C (2012) Capillary electrophoresis/mass spectrometry relevant to pharmaceutical and biotechnological applications. Electrophoresis 33:1517–1530
16. Desiderio C, Rosetti DV, Iavarone F, Messana I, Castagnola M (2010) Capillary electrophoresis-mass spectrometry: recent trends in clinical proteomics. J Pharm Biomed Anal 53:1161–1169
17. Klampfl CW (2009) Capillary electrophoresis-mass spectrometry: a rapidly developing hyphenated technique. Electrophoresis 30:S83–S91
18. Fillet M, Servais A-C, Crommen J (2003) Effects of background electrolyte composition and addition of selectors on separation selectivity in nonaqueous capillary electrophoresis. Electrophoresis 30:1499–1507
19. Steiner F, Hassel M (2005) Influence of solvent properties on separation and detection performance in non-aqueous capillary electrophoresis–mass spectrometry of basic analytes. J Chromatogr A 1068:131–142
20. Posch TN, Müller A, Schulz W, Pütz M, Huhn C (2012) Implementation of a design of experiments to study the influence of the background electrolyte on separation and detection in non-aqueous capillary electrophoresis–mass spectrometry. Electrophoresis 33:583–598
21. Unger M, Dreyer M, Specker S, Laug S, Pelzing M, Neusüß C, Holzgrabe U, Bringmann G (2004) Analytical characterisation of crude extracts from an African ancistrocladus species using high-performance liquid chromatography and capillary electrophoresis coupled to ion trap mass spectrometry. Phytochem Anal 15:21–26
22. Hommerson P, Khan AM, de Jong GJ, Somsen GW (2011) Ionization techniques in capillary electrophoresis-mass spectrometry: principles, design, and application. Mass Spectrom Rev 30:1096–1120
23. Hommerson P, Khan AM, de Jong GJ, Somsen GW (2007) Comparison of atmospheric pressure photoionization and ESI for CZE-MS of drugs. Electrophoresis 30:203–214
24. Pantuckova P, Gebaur P, Bocek P, Krivankova L (2009) Electrolyte systems for on-line CE-MS: detection requirements and separation possibilities. Electrophoresis 28:1444–1453
25. Huhn C, Ramautar R, Wuhrer M, Somsen GW (2010) Relevance and use of capillary coatings in capillary electrophoresis-mass spectrometry. Anal Bioanal Chem 396:297–314
26. Mol R, de Jong GJ, Somsen GW (2008) Coupling of non-aqueous electrokinetic chromatography using cationic cyclodextrins with electrospray ionization mass spectrometry. Rapid Commun Mass Spectrom 22:790–796
27. Morin CJ, Geulin L, Mofaddel N, Desbene AM, Desbene PL (2008) Analysis of neutral surfactants by non-aqueous medium capillary electrophoresis hyphenated to mass spectrometry (ion trap). J Chromatogr A 1198–1199:226–231
28. Servais A-C, Fillet M, Mol R, Somsen GW, Chiap P, de Jong GJ, Crommen J (2006) On-line coupling of cyclodextrin mediated nonaqueous capillary electrophoresis to mass spectrometry for the determination of salbutamol enantiomers in urine. J Pharm Biomed Anal 40:752–757
29. Servais A-C, Fillet M, Mol R, Rousseau A, Crommen J, Somsen GW, de Jong GJ (2010) Influence of the BGE composition on analyte response in CD-mediated NACE-MS. Electrophoresis 31:1157–1161
30. Bonvin G, Schappler J, Rudaz S (2014) Non-aqueous capillary electrophoresis for the analysis of acidic compounds using negative electrospray ionization mass spectrometry. J Chromatogr A 1323:163–173
31. Gomez-Caravaca AM, Carrasco-Pancorbo A, Segura-Carretero A, Fernandez-Gutierrez A (2009) NACE-ESI-TOF MS to reveal phenolic compounds from olive oil: introducing enriched olive oil directly inside capillary. Electrophoresis 30:3099–3109
32. Huhn C, Neusüß C, Pelzing M, Pyell U, Mannhardt J, Pütz M (2005) Capillary electrophoresis-laser induced fluorescence-electrospray ionization-mass spectrometry: a case study. Electrophoresis 26:1389–1397
33. Sturm S, Strasser E-M, Stuppner H (2006) Quantification of Fumaria officinalis isoquinoline alkaloids by nonaqueous capillary electrophoresis–electrospray ion trap mass spectrometry. J Chromatogr A 1112:331–338
34. Sturm S, Seger C, Stuppner H (2007) Analysis of Central European Corydalis species by non-aqueous capillary electrophoresis–electrospray

ion trap mass spectrometry. J Chromatogr A 1159:42–50

35. Sturm S, Schinnerl J, Greger H, Stuppner H (2008) Nonaqueous capillary electrophoresis-electrospray ionization-ion trap-mass spectrometry analysis of pyrrolo- and pyrido[1,2-a] azepine alkaloids in Stemona. Electrophoresis 29:2079–2087
36. Chiu C-W, Liang H-H, Huang H-Y (2007) Analyses of alkaloids in different products by NACE-MS. Electrophoresis 28:4220–4226
37. Wang S, Qu H, Cheng Y (2007) NACE-ESI-MS combined with on-line concentration for high-sensitivity analysis of quinolizidine alkaloids. Electrophoresis 28:1399–1406
38. Buchberger W, Gstottenmayr D, Himmelsbach M (2010) Determination of cinchona alkaloids by non-aqueous CE with MS detection. Electrophoresis 31:1208–1213
39. Posch TN, Martin N, Pütz M, Huhn C (2012) Nonaqueous capillary electrophoresis–mass spectrometry: a versatile, straightforward tool for the analysis of alkaloids from psychoactive plant extracts. Electrophoresis 33:1557–1566
40. Roscher J, Posch TN, Pütz M, Huhn C (2012) Forensic analysis of mesembrine alkaloids in Sceletium tortuosum by nonaqueous capillary electrophoresis mass spectrometry. Electrophoresis 33:1567–1570
41. Anderson MS, Lu B, Abdel-Rehim M, Blomberg S, Blomberg LG (2004) Utility of nonaqueous capillary electrophoresis for the determination of lidocaine and its metabolites in human plasma: a comparison of ultraviolet and mass spectrometric detection. Rapid Commun Mass Spectrom 18:2612–2618
42. Psurek A, Neusüß C, Pelzing M, Scriba GKE (2005) Analysis of the lipophilic peptaibol alamethicin by nonaqueous capillary electrophoresis-electrospray ionization-mass spectrometry. Electrophoresis 26:4368–4378
43. Psurek A, Neusüß C, Degenkolb T, Brückner H, Balaguer E, Imhof D, Scriba GKE (2006) Detection of new amino acid sequences of alamethicins F30 by nonaqueous capillary electrophoresis–mass spectrometry. J Pept Sci 12:279–290
44. Gao F, Zhang Z, Fu X, Li W, Wang T, Liu H (2007) Analysis of phospholipids by NACE with on-line ESI-MS. Electrophoresis 28:1418–1425
45. Morales-Cid G, Cárdenas S, Simonet BM, Valcárcel M (2009) Direct automatic determination of free and total anesthetic drugs in human plasma by use of a dual (microdialysis–microextraction by packed sorbent) sample treatment coupled at-line to NACE–MS. Electrophoresis 30:1684–1691
46. Morales-Cid G, Cárdenas S, Simonet BM, Valcárcel M (2009) Fully automatic sample treatment by integration of microextraction by packed sorbents into commercial capillary electrophoresis–mass spectrometry equipment: application to the determination of fluoroquinolones in urine. Anal Chem 81:3188–3193
47. Sasajima Y, Lim LW, Takeuchi T, Suenami K, Sato K, Takekoshi Y (2010) Simultaneous determination of antidepressants by non-aqueous capillary electrophoresis-time of flight mass spectrometry. J Chromatogr A 1217:7598–7604
48. Li XQ, Uboh CE, Soma LR, Guan FY, You YW, Kahler MC, Judy JA, Liu Y, Chen JW (2010) Simultaneous separation and confirmation of amphetamine and related drugs in equine plasma by non-aqueous capillary-electrophoresis-tandem mass spectrometry. Drug Test Anal 2:70–81
49. Rittgen J, Pütz M, Zimmermann R (2012) Identification of fentanyl derivatives at trace levels with nonaqueous capillary electrophoresis-electrospray-tandem mass spectrometry (MSn, n = 2, 3): analytical method and forensic applications. Electrophoresis 33:1595–1605
50. Montealegre C, Sánchez-Hernández L, Crego AL, Marina ML (2013) Determination and characterization of glycerophospholipids in olive fruit and oil by nonaqueous capillary electrophoresis with electrospray-mass spectrometric detection. J Agric Food Chem 61:1823–1832
51. Anurukvorakun O, Buchberger W, Himmelsbach M, Klampfl CW, Suntornsuk L (2010) A sensitive non-aqueous capillary electrophoresis-mass spectrometric method for multiresidue analyses of beta-agonists in pork. Biomed Chromatogr 24:588–599
52. Groom CA, Hawari J (2007) Detection of hexamethonium-perchlorate association complexes using NACE-MS. Electrophoresis 28:353–359
53. Simó C, Cottet H, Vayaboury W, Giani O, Pelzing M, Cifuentes A (2004) Nonaqueous capillary electrophoresis–mass spectrometry of synthetic polymers. Anal Chem 76:335–344
54. Scrano L, Bufo SA, Menzinger F, Schmitt-Kopplin P (2006) Novel degradation products of the herbicide oxasulfuron identified by capillary electrophoresis—mass spectrometry. Environ Chem Lett 4:225–228
55. Vassort A, Shaw PN, Ferguson PD, Szücs R, Barrett DA (2008) Comparison of CZE, open-tubular CEC and non-aqueous CE coupled to electrospray MS for impurity profiling of drugs. Electrophoresis 29:3563–3574
56. Mol R, Servais A-C, Fillet M, Crommen J, de Jong GJ, Somsen GW (2007) Non-aqueous electrokinetic chromatography-electrospray ionization mass spectrometry using anionic cyclodextrins. J Chromatogr A 1159:51–57

57. Malik AK, Grundmann M, Matysik F-M (2013) Development of a fast capillary electrophoresis-time-of-flight mass spectrometry method for the speciation of organotin compounds under separation conditions of high electrical field strengths. Talanta 116:559–562
58. Kim J, Chun M-S, Choi K, Chung DS (2009) Large volume stacking using an EOF pump in NACE-MS. Electrophoresis 30:1046–1051
59. Zhang J, Chen Z (2012) Determination of matrine and oxymatrine in Sophora flavescens by nonaqueous capillary electrophoresis-electrospray ionization-ion trap-mass spectrometry. Anal Lett 46:651–662
60. Zhang Y, Chen Z (2013) Nonaqueous CE ESI-IT-MS analysis of Amaryllidaceae alkaloids. J Sep Sci 36:1078–1084
61. Rodríguez J, Castañeda G, Muñoz L (2013) Direct determination of pregabalin in human urine by nonaqueous CE-TOF-MS. Electrophoresis 34:1429–1436

Chapter 8

Ionic Liquids in Capillary Electrophoresis

Ulrike Holzgrabe and Joachim Wahl

Abstract

Recently, a great interest was drawn toward ionic liquids (ILs) in analytical separation techniques. ILs possess many properties making them excellent additives in capillary electrophoresis (CE) background electrolytes (BGE). The most important property is the charge of the dissolved ions in BGE enabling the cations to interact with deprotonated silanol groups on the capillary surface and thereby modifying the electroosmotic flow (EOF). Ionic and/or proton donor–acceptor interactions between analyte and IL are possible interactions facilitating new kinds of separation mechanisms in CE. Further advantages of ILs are the high conductivity, the environmentally friendliness, and the good solubility for organic and inorganic compounds. The most commonly used ILs in capillary electrophoresis are dialkylimidazolium-based ILs, whereas for enantioseparation a lot of innovative chiral cations and anions were investigated.

ILs are reported to be additives to a normal CE background electrolyte or the sole electrolyte in CE, nonaqueous CE (NACE), micellar electrokinetic chromatography (MEKC), and in enantioseparation. An overview of applications and separation mechanisms reported in the literature is given here, in addition to the enantioseparation of pseudoephedrine using tetrabutylammonium chloride (TBAC) as IL additive to an ammonium formate buffer containing β-cyclodextrin (β-CD).

Key words Ionic liquids, NACE, MEKC, Enantioseparation, Cyclodextrin

1 Introduction

Ionic liquids are defined as (semi-)organic salts with a melting point below 100 °C. The ionic bond of a salt is stronger than the van der Waals forces in normal solids and liquids. For that reason, salts are usually solid and melt at higher temperatures than other solids. The low melting point of the ILs is explained by a lower degree of symmetry of cation and/or anion, by high conformational freedom and an effective charge delocalization [1, 2]. On the other hand, the high Coulombic forces between the ions in ILs lead to lower vapor pressures compared with molecular liquids of a similar molecular weight [3]. Katritzky et al. assumed in 2002 that there is the possibility to form 10^{18} cation/anion combinations building an ionic liquid [4]. More specifically, a room-temperature ionic liquid (RTIL) is a salt with a melting point below ambient

Philippe Schmitt-Kopplin (ed.), *Capillary Electrophoresis: Methods and Protocols*, Methods in Molecular Biology, vol. 1483,
DOI 10.1007/978-1-4939-6403-1_8,

temperature. The first RTIL, ethylammonium nitrate (melting point: 14 °C), was described in 1914 by Walden [5]. In most cases, ILs consist of a nitrogen-containing organic cation and an inorganic or less frequently organic anion. The anion is often fluorinated because in this case the negative charge weakens the hydrogen bond to the cation and as a result lowers the melting point [6]. The structural formulas of widely used ILs are shown in Fig. 1. Other frequently used anions are halides, hydroxide, sulfate, acetate, and nitrate.

In the past few years, the interest in ionic liquids increased. One special advantage of ILs is that they can be designed as requested. It is possible to modify the melting point, the viscosity, the miscibility, and the electrochemical behavior by altering the combination of cations and anions. In most cases, the choice of the anion determines the solubility in water. Water-immiscible ILs often contain PF_6^- or bis(trifluoromethylsulfonyl)imide anions, whereas BF_4^- provides a high water miscibility. Other advantages are a high thermal stability, a negligible vapor pressure, and therefore an ecological friendliness. Furthermore, they are little or inflammable and can be designed to be protic or aprotic solvents. Some physicochemical properties can be explained by the structure of the cation or the anion. It is also known that a change in cation–anion combination can influence the physicochemical properties strongly. For example, the hydrophobicity, density, viscosity, surface tension, and solubility are characteristics depending on the chain length of alkyl substituents of the IL cation. It has to be mentioned that impurities in ILs can affect their physicochemical

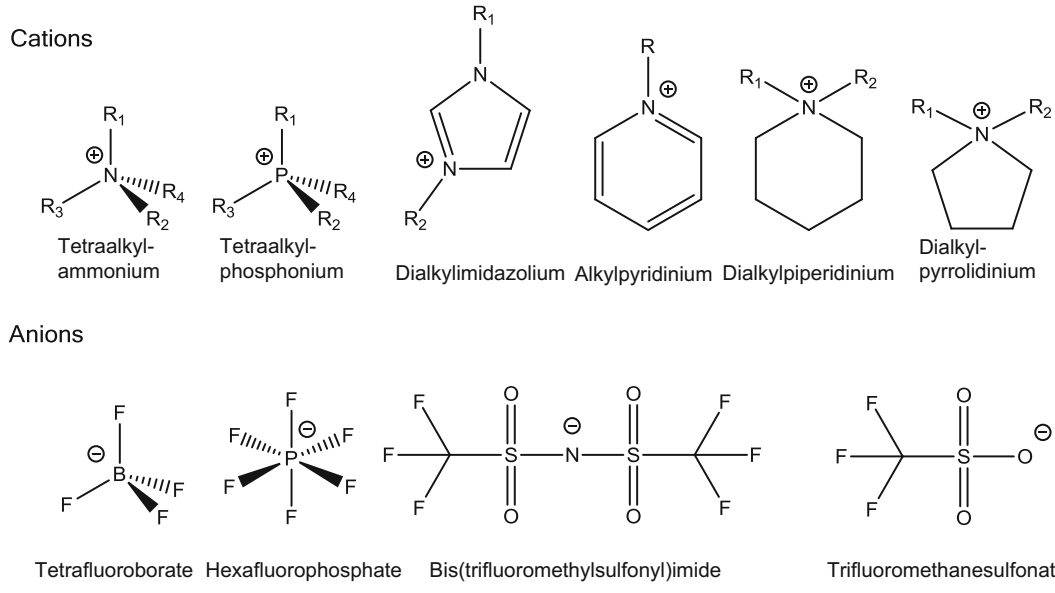

Fig. 1 Structures of widely used cations and anions in ionic liquids

properties. For example, it was observed that halide impurities can narrow the potential windows because they can be easier oxidized than other IL anions [7].

In the last few years, ILs get an increasing relevance as reaction media and catalyst in organic and inorganic synthesis, for example, in peptide and oligosaccharide synthesis [8, 9]. Considerable advantages are, for example, efficient transfer of microwaves, excellent heat transfer, increased reactivity, and easy product recovery. In biochemical reactions ILs can improve the activity, stability, and enantioselectivity of enzymes. ILs are applied in photoelectrochemical solar cells, as electrolytes in rechargeable lithium-ion batteries, in double-layer capacitors, and in fuel cells. ILs can be used to enhance solubility of poor water-soluble pharmaceutical drugs to improve their bioavailability [10]. Furthermore, ILs can be applied for extraction purpose, for example, in liquid–liquid extraction, liquid-phase microextraction, and solid-phase microextraction.

2 Ionic Liquids in Chromatography

ILs can also be used in analytical chemistry. In gas chromatography ILs make it possible to separate complex mixtures of polar and nonpolar compounds [11, 12]. With their thermal stability, wetting ability, high viscosity, and their controllable solvation interactions they are an ideal stationary phase. The thermal stability of ILs depends on many factors, the stability of anions, for example, increases by ascending charge delocalization [12]. For this reason, a lot of anions contain fluorine atoms. Tsunashima et al. reported a higher stability for benzyl-substituted phosphonium ionic liquids in comparison to the analogous ammonium ionic liquids [13]. Even chiral ionic liquid stationary phases are reported in gas chromatography [14]. The first commercially available ionic liquid GC column, based on 1,9-di(3-vinylimidazolium)nonane bis(trifluoromethylsulfonyl)imide, was launched in 2008.

ILs are employed as additives in HPLC mobile phases to suppress interactions between basic analytes and free silanol groups on silica-based reversed phases. Better peak shapes, improved resolution, and shorter retention times can be achieved by addition of ILs to the mobile phase without having an influence on the pH, which is in contrast to observation made for triethylamine. ILs as additives to the mobile phase can also affect the analyte retention mechanism through interactions with both stationary and/or mobile phase. However, one important disadvantage of ILs used in HPLC is their high viscosity leading to unfavorable high back pressure [15].

Columns with covalent IL coatings, such as butylimidazolium bromide, are reported too [16]. Due to their low vapor pressure, leading to low column bleeding, ILs are employed as column material in mass spectrometry. Thereby, a better identification and quantification of samples is achieved.

RTILs, based on α-cyano-4-hydroxycinamic and sinapic acid anions, are tested as a new class of matrix in MALDI-MS, because they are nonvolatile in vacuum, they adsorb laser light, and they dissolve samples even more homogeneous than solid matrices [17]. Because of the higher homogeneity the results for quantification and determination of molecular weight in MALDI-MS are improved. Even in an ion chromatography–ion association electrospray ionization mass spectrometry (IC/IA-ESI-MS) method for determination of perchlorate ILs showed an advantage [18].

3 Ionic Liquids in Capillary Electrophoresis

With regard to ILs in capillary electrophoresis, it has to be noticed that they may not be used directly as solvent because their high viscosity and high conductivity is leading to high currents and high Joule heating. In BGE solutions they do not exist as an IL, but as dissolved cations and anions. Therefore, ILs in CE should better be called solutions of ionic liquids. In capillary electrophoresis ILs could be used as main electrolyte, as electrolyte additive and for dynamic coating of the capillary surface. ILs have a lot of advantages making them excellent additives in CE background electrolytes, e.g., high solubility, heat stability, good electrical conductivity, and remarkable influence on the EOF.

The application of ILs in capillary electrophoresis had its origin in the 1980s by using surfactants like cetyltrimethylammonium bromide (CTAB) and tetradecyltrimethylammonium bromide (TTAB) to control the electroosmotic flow in CZE [19, 20]. Using these surfactants a change of the EOF direction can be achieved which enables the separation of low molecular weight carboxylic acids. Furthermore, it was shown that a reduction of EOF leads to better separation of analytes of nearly similar mobilities. Based on observations in liquid chromatography, Garner and Yeung, reported an electrochromatography by dynamic ion exchange using CTAB [21]. They performed a CZE with a polyimide coated capillary on which the CTAB adsorbed and formed a double layer. This double-layer leads to a direction change of the electroosmotic flow because the stationary phase surface gets charged positively. Beside the coulombic interactions between the negative charged analytes and this positive charged double layer, a small amount of an ion pair between the analytes and CTAB can be formed, which builds hydrophobic interactions with the coated stationary phase [22]. Expectedly, for neutral analytes the reversed electroosmotic mobility in hydrophobic coated capillaries increased by an increasing concentration of CTAB in buffer due to the higher positive charge on capillary surface. The increase of mobility achieves a maximum when the hydrophobic surface is saturated with CTAB [23].

It is important to note that CTAB and TTAB are no ionic liquids, because their melting points are above 100 °C, but these studies can be considered as a precursor for studying ionic liquids in CE. Furthermore, separation mechanisms and electrophoretic behavior of analytes are comparable between ILs and these surfactants.

3.1 Ionic Liquid Coated Capillaries

In 2000, the first capillary with a covalent bond IL was reported [24]. The covalent coating with (dialkyl-)imidazolium reversed the EOF. In contrast to bare fused silica, an increase of the buffer pH value can reduce the velocity of the anodic EOF because a higher amount of noncoated silanol groups gets charged negative. The enhanced migration time leads to an increase in resolution of several analytes like carboxylic acids and sildenafil and its metabolite [24, 25]. The positively charged (dialkyl-)imidazolium cations can act as a kind of anion exchanger for buffer and analyte anions and therefore a further separation system is implemented in the capillary electrophoresis system. A covalent coating of silanol groups with IL cations has few advantages like a repulsion of positively charged analytes (e.g., sildenafil, inorganic cations [26], DNA [27]), a stable EOF, coating without deterioration for up to 96 h [27], and the compatibility with MS detection.

3.2 Ionic Liquids in Capillary Electrophoresis

The first real ILs used for aqueous capillary electrophoresis separation were 1-alkyl-3-methylimidazolium based. In 2001, Yanes et al. separated different phenolic compounds in grape seed extracts using an IL as only background electrolyte [28]. The direction of the EOF was observed to be toward the anode because the imidazolium cations coated the capillary wall silanol groups leading to a positive surface charge. It was found that the polyphenols associate either with the free or the coated imidazolium cations because uncharged polyphenols migrated after the EOF. A comparison between the change in EOF and the change in polyphenol mobility showed that the interaction with free imidazolium dominates. With increasing IL concentrations the EOF leveled off, the effective electrophoretic mobility ($\mu_{\text{catechin}}-\mu_{\text{EOF}}$) of catechin increased even above this plateau. The stability of the EOF at high IL concentrations indicates a saturation of the capillary wall with adsorbed IL. These separations were improved for a lot of different compounds in the last few years. Interestingly, not only the migration time gets shorter by increasing IL concentration, even the separation between the peaks gets better. By changing the alkyl group in the cation from ethyl to butyl a better separation could be achieved because longer migration times lead to more interactions with imidazolium cations. Interestingly, an increasing chain length in cathodic detection mode, using same IL concentrations, also causes a decrease in EOF [29–31]. Summarizing it can be seen that in both cathodic and anodic detection mode, a longer alkyl chain

leads to a decrease in EOF, longer migration times, and better separation but also to poorer peak shape. Effects of the alkyl chain length on EOF are shown in Table 1.

When using low IL concentrations in combination with a traditional buffer system, the EOF is directed toward the cathode. An increase in IL concentration leads to a decrease of the EOF velocity. Higher migration times often lead to improved resolutions due to a higher number of interactions between analyte and the separation system. Further increasing the IL concentration resulted in higher migration time, and occurring of peak tailing decreases the resolution. The EOF can decrease thus far, that a better separation of negative charged analytes can be achieved in reversed mode (shorter migration times, better peak shape) compared to methods without IL addition. To this end inorganic or small organic anions with extremely high electrophoretic mobilities, like nicotinic acid and its isomers, can be separated using ILs [32]. Because of their high electrophoretic mobility these anions cannot be detected at the cathode in normal mode. In this reversed mode (EOF still cathodic) an increasing IL concentration leads to a decrease in migration time but an increase in resolution and peak shape. Depending on the type of IL a further increase of IL concentration can lead to a change in EOF direction, e.g., for the separation of benzoic acid and chlorophenoxy acid herbicides [33], and anions can be separated in a coelectroosmotic mode at the anodic capillary end [34, 35]. Interestingly, this change in direction is reversed again by raising the pH value, because the silanol groups get deprotonated [33]. Effects of IL concentration and BGE pH on the EOF are also shown in Table 1 and Fig. 2.

The separation of inorganic cations can also be improved by addition of ILs to the BGE. Because of their weak UV activity these cations have to be detected in indirect mode using cationic chromophors (protonated form). For that reason separation and detection of inorganic cations is limited to low pH values. By covalent coating the capillary with a imidazolium-based IL and using this IL as BGE additive a constant mobility of inorganic cations can be achieved in a pH range from 3 to 11 [26].

For the separation of anionic analytes, such as aromatic acids, and basic proteins an additional improvement of separation can be

Table 1
Effects of IL concentration, pH, and alkyl chain length of the IL cation on the EOF

EOF-direction	IL-concentration ↑	pH ↑	Alkyl-chain length ↑
Cathodic	EOF ↓ (inversion possible)	EOF ↑	EOF ↓
Anodic	EOF ↑ to plateau	EOF ↓ (inversion possible)	EOF ↓

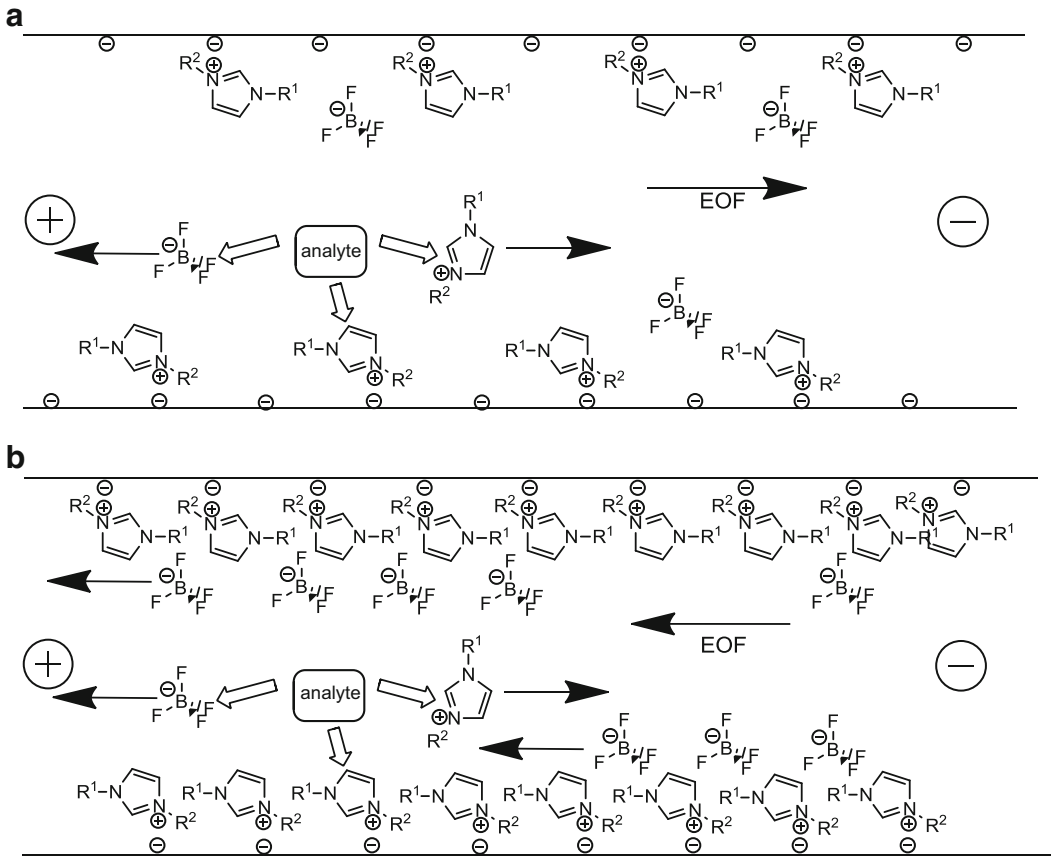

Fig. 2 Possible interactions between analyte and IL cations (coated or in BGE) and IL anions. Due to the better capillary surface coating and therefore higher positive surface charge and due to the higher amount of anions migrating to the anode, increasing concentrations of ILs reverse the direction of the EOF. (**a**) Low IL concentration → cathodic EOF; (**b**) high IL concentration → anodic EOF

achieved by using a polymeric ionic liquid (poly(1-vinyl-3-butylimidazolium bromide)) for dynamical capillary coating because it reduces the problematic adsorption of analytes to the capillary wall. The authors hypothesized a higher rate of capillary surface coverage by polymeric ILs compared to IL monomers [36–38].

First studies on interaction mechanisms between IL and analytes were conduced by Yue and Shi [39] who used different 1-alkyl-3-methylimidazolium cations to separate flavonoids. They observed that the H-2 of the imidazolium cation is essential for a hydrogen bonding interaction with the analytes. This observation was proved by a 2-methylated imidazolium cation showing no separation and was confirmed by other studies [40]. When 1-butyl-2-methyl-3-methylimidazolium tetrafluoroborate was added to the BGE no resolution of aryl propionic acids could be achieved. They also reported that the counterion plays a role in separation. By exchanging counterions (BF_4^-, PF_6^-, Br^-, I^-) differences in

migration time, separation, and peak shape can be observed. Interestingly, the resolution increases with a decreasing melting point of the ILs. This phenomenon can be explained by weaker interactions (hydrogen bonds) between IL cation and IL anion leading to a higher amount of free cation that may interact with capillary surface and analyte. The same observation was made in NACE where weaker association between the ions leads to a higher current because of an increasing capillary coating [41]. Cabovska et al. investigated the interaction between halophenols and 1-ethyl-3-methylimidazolium cations and found a larger hydrophobic surface of the analyte to elevate the affinity [42].

Using ILs in combination with classical buffers often leads to poor baseline stability. This can be explained by high UV absorption of imidazolium and pyridinium cations. Better results can be achieved by using contactless conductivity detection or electrochemiluminescence (ECL) [43–46]. By addition of ILs into buffer, the ECL intensity increases because of the enhanced conductivity of the BGE, which makes, in comparison to BGE without IL, the electrical resistance of the sample solution passing the detector much higher. Alkylimidazolium-based ILs can be used as chromophors in indirect UV detection, for example, in separation of carbohydrates and inorganic cations both lacking a chromophor [30].

An ideal application for ILs in capillary electrophoresis is the separation of basic compounds, because the ILs suppress the adsorption of these analytes to the capillary surface which results in a better separation efficiency and repeatability [47]. This beneficial effect can even be observed in a BGE containing no IL when the capillary was dynamical coated by rinsing with IL prior to the separation [48].

Associations between ILs and analytes can theoretically be a result of hydrogen bonding, hydrophobic bonding, ion–ion, ion–dipole, or ion-induced-dipole interactions. The associations between IL cations and analytes seem to be more specific and important for separation in comparison to associations between IL anions and analytes. It goes without saying that the choice of the IL cation plays an important role due to its association with the analyte and furthermore to its capillary wall coating effect. Analyte molecules can associate with IL molecules coated on capillary surface and/or IL molecules in bulk solution. Possible interactions of an analyte molecule with the IL and the influence of the IL concentration on the EOF are displayed in Fig. 2.

3.3 Ionic Liquids in Micellar Electrokinetic Chromatography (MEKC) and Micro emulsion Electro kinetic Chromato graphy (MEEKC)

In 2003, the first MEKC method using ILs was reported [49]. By using chiral poly(sodium oleyl-L-leucylvalinate) (poly-SOLV) as surfactant the first enantioseparation of several binaphthyl derivatives in IL modified capillary electrophoresis was reported, too. An increase in cathodic EOF was reported at low concentrations of 1-alkyl-3-methylimidazolium ILs. This can be explained by an increase of current. However, generally by further increasing the IL concentration in MEKC a decrease in cathodic EOF can be

observed as a result of capillary coating. No general statement can be made whether ILs are leading to better or worse separation in MEKC. The next step was made by Rizvi and Shamsi who for the first time used an amino acid-derived cationic IL as chiral selector [50]. They synthesized undecenoxycarbonyl-L-leucinol bromide and undecenoxycarbonyl-L-pyrrolidinol bromide for the application in a MEKC enantioseparation of bromophenylacetate and 2-(2-chlorophenoxy)propanoate anions (structures *see* Fig. 3). The application of these ILs reversed the EOF (cathode to anode) and, by changing the pH value, an electrostatic interaction between IL cations and analyte anions was found. At low pH values the two anionic analytes mentioned earlier are not separated because the protonated acids cannot interact electrostatically with the IL cations. Similarly, the analysis of uncharged aryl-propionic acids in anodic detection mode did not provide any enantioseparation by using this chiral IL as single chiral selector [51]. However, enantioseparation of the acidic analytes was achieved after the addition of a cyclodextrin (CD) in cathodic detection mode. An overview over ILs, additives, and analytes is given in Table 2.

Tian et al. achieved a great improvement in separation and resolution of poorly water-soluble lignans using 1-butyl-3-methylimidazolium tetrafluoroborate and sodium dodecyl sulfate (SDS) [52]. Theoretically, it seems obvious that the imidazolium

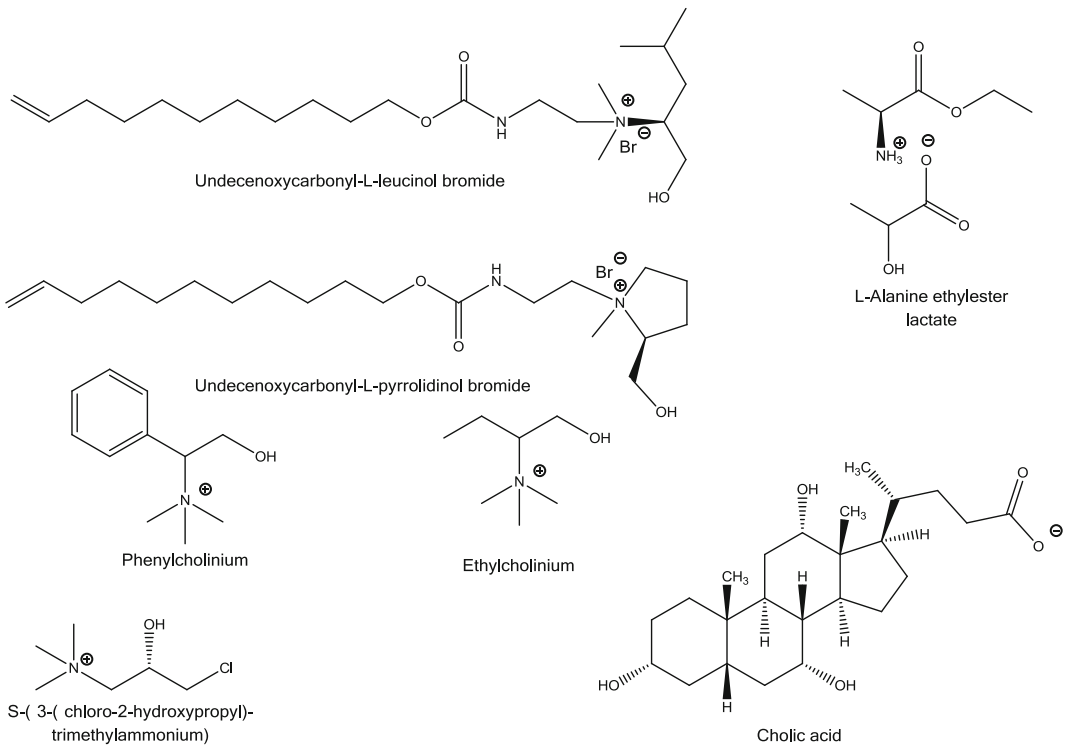

Fig. 3 Structures of reported chiral IL cations and anions

Table 2

Method details to the reported separations in MEKC, MEEKC, enantioseparation, and NACE

Ionic liquid	BGE additives	Analyte	Technique	Reference
1-Alkyl-3-methylimidazolium	SDS, poly-SOLV	Alkyl aryl ketones, Phenols, chiral Binaphthyl derivatives	MEKC	[49]
Undecenoxycarbonyl-L-leucinol bromide, Undecenoxycarbonyl-L-pyrrolidinol bromide	–	Enantioseparation of Bromophenylacetic acid, 2-(2-Chlorophenoxy) propanoic acid	MEKC	[50]
Undecenoxycarbonyl-L-leucinol bromide	CD	Aryl-propionic acids	MEKC	[51]
1-Tetradecyl(dodecyl)-3-methylimidazolium	–	Phenols, Benzenes	MEKC	[53]
1-Butyl-3-methylimidazolium hexafluorophosphate	SDS	Phenolic acids	MEEKC	[54]
1-Alkylimidazolium tetrafluoroborate	Poly-SOLV	Enantioseparation of Binaphthyl derivatives; Warfarin, Coumachlor, Benzoin derivatives	MEKC	[55]
S-(3-(Chloro-2-hydroxypropyl) trimethylammonium)	Cholic acid	Enantioseparation of Aryl-propionic acids, Atenolol, Propranolol, Warfarin	CE	[58]
Undecenoxycarbonyl-L-leucinol bromide	CD	Aryl-propionic acids	MEKC	[60]
Ammonium-based, Pyrrolidinium-based, 1-Ethyl-3-methylimidazolium L-lactate	CD	Enantioseparation of Miconazole, Econazole, Ketoconazole, Itraconazole	coated capillary	[61]
L/D-Alanine methyl(ethyl, tert-butyl) ester lactate, bis(trifluoromethylsulfonyl)imide	–	Enantioseparation of Binaphthyl derivatives	CE	[65]
6-O-2-Hydroxypropyltrimethyl ammonium-β-cyclodextrin tetrafluoroborate	–	Different enantiomers	CE	[66]
1-Butyl-3-methylimidazolium hexafluorophosphate, acetate, trifluoroacetate	–	2 Brønsted bases (Janus Green, Brilliant Cresyl Blue), Sudan Black, 2 Brønsted acids (Thymolphthalein, Phenolphthalein)	NACE	[69]

(continued)

Table 2
(continued)

Ionic liquid	BGE additives	Analyte	Technique	Reference
1-Butyl-3-methylimidazolium trifluoroacetate, acetate, hexafluorophosphate, bis(trifluoromethylsulfonyl)imide	–	Phenols, Carboxylic acids	NACE	[70]
1-Butyl-3-methylimidazolium tetrafluoroborate, trifluoroacetate, heptafluorobutanoate	–	(Poly-)phenols	NACE	[71]
1-Butyl-3-methylimidazolium trifluoroacetate, heptafluorobutanoate	–	Phenols	NACE	[72]

cations are electrostatically and hydrophobically attracted by the negative charged SDS micelle exterior, which neutralizes the micelle surface. Thereby, the repulsion between the negatively charged hydrophilic "SDS heads" is reduced leading to a change in charge, shape, and size of micelles and a decrease of the critical micelle concentration. It was reported that lignans could be resolved from other compounds in real samples at low IL and surfactant concentrations.

In 2008, Borissova et al. reported a new long-chain alkylimidazolium IL that acts simultaneously as IL and micelle former [53]. They showed that these alkylimidazolium ILs build micelles like other surfactants and that the CMC decreases with increasing length of hydrophobic tail. Furthermore, they found not only separation of neutral hydrophobic benzene derivatives due to analyte–micelle interaction but also of phenols due to electrostatic analyte–IL interaction as mentioned earlier.

In 2010, Cao et al. reported a MEEKC method using the hydrophobic IL 1-butyl-3-methylimidazolium hexafluorophosphate instead of oil to form an IL/W microemulsion by addition of SDS [54]. For the separation of phenolic acids they observed a decrease in EOF by addition of the IL, too. The use of IL/W microemulsions introduces some new separation mechanisms compared to O/W microemulsions. There are possible associations between analyte and coated IL and IL in emulsion droplets by hydrogen bonding and Coulombic force.

3.4 Ionic Liquids in Capillary Electrophoresis: Enantioseparation

As mentioned before, the first MEKC enantioseparations using ILs as additive in BGE were performed by Mwongela et al. [49, 55]. They investigated the resolution of several enantiomers (shown in Table 2) in a BGE consisting of chiral poly-SOLV micelles and added 1-alkyl-3-methylimidazolium cations to the solute. The enantioselectivity can

be either achieved by a chiral selector, like CD, or by the chiral IL itself. Francois et al. investigated the enantioselective power of choline-derived ILs (*see* Fig. 3). No enantioseparation of 2-arylpropionic acids was found when these ILs were the sole chiral additives to BGE, but the addition of cyclodextrins revealed a synergistic effect between the two chiral selectors [56]. However, not only synergistic effects between ILs and CDs are possible. Mofaddel et al. reported detrimental interactions between the two additives leading to a decrease in resolution of binaphthyl derivatives enantiomers [57]. Tran and Mejac observed that ibuprofen enantiomers can be separated in a BGE consisting of a chiral IL cation S-(3-(chloro-2-hydroxypropyl)trimethylammonium) and chiral cholic acid, but neither with the acid nor with the IL cation solely added to water [58]. Structures of the chiral selectors are shown in Fig. 3. This observation shows that there can be cooperative interactions between two chiral selectors, the chiral cation and anion, and the analyte. Salbutamol, cimaterol, and formoterol cannot be enantioseparated by using β-CD in phosphate buffer only, but by addition of several ammonium, imidazolium, and pyridinium-based ILs [59].

Taken together it can be seen that interactions between ILs and CDs in enantioseparation can be synergistic, neutral, or antagonistic. Of note, the synergistic effects in the IL-chiral selector system result in optimal separation by much lower concentrations of chiral selectors, like β-cyclodextrin. An antagonistic effect can be explained by the inclusion of the IL ions in the CD cavity in a kind of competitive inhibition. A lot of interactions in enantioseparation using ILs seem to be possible. Beside the inclusion of the enantiomers into the cavity of CDs, the IL or an IL–analyte complex can also be included in this cavity. The analytes might associate with IL cations either coated on capillary wall or free in BGE. Furthermore, associations with the negative counterions are possible. Additionally, it seems to be possible that the analyte–CD inclusion complex or analyte–IL–CD inclusion complex can interact with IL ions. For example, Wang et al. measured the binding constants between the three compounds analyte, CD, and IL in MEKC [60]. They found that the enantioseparation was achieved because of the competition between the IL and the analyte for the CD cavity.

A proof of the interactions between IL and CD without the effect of capillary surface coating was performed by using a polyacrylamide-coated capillary [61]. An enhancement in chiral resolution by addition of IL to the CD containing BGE could be achieved in this capillary. Due to the interaction between IL cations and the analyte–cyclodextrin complex, the migration time was shortened, indicating that IL cations take part in the analyte–CD inclusion complex leading to higher electrophoretic mobility. A BGE containing only IL and no CD did not decrease the migration time indicating that there is no interaction between analyte and IL. Furthermore, these observations were manifested by NMR spectroscopy. Possible interactions between these three compounds are shown and listed in Fig. 4.

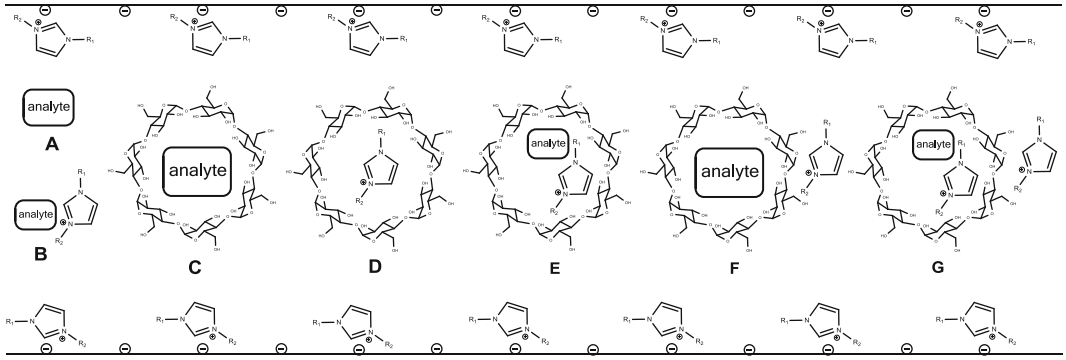

Fig. 4 Possible interactions between analyte, IL, and CD. (**a**) Sole analyte. (**b**) Analyte IL interaction. (**c**) Analyte included in CD. (**d**) IL included in CD. (**e**) Analyte and IL included in CD. (**f**) Analyte included in CD interacting with IL. (**g**) Analyte and IL included in CD interacting with IL. Furthermore, complexes **a**–**g** can interact with IL cations coated on capillary surface and with IL anions

A ligand-exchange enantioseparation of amino acids using an amino acid ionic liquid was reported by Liu et al [62]. Using 1-alkyl-3-methylimidazolium L-proline and copper leads to an adsorption of imidazolium cations on capillary surface. The L-proline anions associated with the imidazolium cations and the copper cations with the L-proline anions. The separation of the amino acid enantiomers was achieved by formation of ternary mixed-metal complexes with different complex stability constants. Similar observations were made by using amino acids as cationic part of ILs in combination with inorganic and organic anions [63]. Mu et al. reported better enantioseparation of amino acids using an L-proline trifluoroacetate IL compared with a BGE containing L-proline and trifluoroacetic acid. Other complexes investigated in ligand-exchange CE are composed of zinc, L-arginine, L-lysine, and different imidazolium cations. An enantioseparation could also be achieved in nonaqueous media. Ma et al. separated rabeprazole and omeprazole enantiomers by using an ephedrine-based IL ((+)-*N,N*-dimethylephedrinium-bis(trifluoromethylsulfonyl) imide) as both chiral selector and BGE in acetonitrile–methanol mixtures [64]. The first aqueous method with a chiral IL as sole chiral selector was developed by Stavrou et al. in 2013 [65]. They observed the enantioseparation of binaphthyl derivatives by addition of alanine ester-based ILs (for details and structure *see* Table 2 and Fig. 3) in a tris-borate buffer. In 2013, the first IL based on a CD was reported: an ammonium-β-CD cation was combined with tetrafluoroborate [66]. A lot of different structures are used as chiral IL-ions, for example, amino acids (as cations or as anions), ephedrine-based cations, surfactant-based and CD-based structures. In the last years, two synergistic system with vancomycin-based and glycogen-based chiral selectors instead of CDs were reported [67, 68]. It has to be noticed that enantioseparation strongly depends on composition and pH of the BGE. Chiral ILs

can be simultaneously used as chiral selectors and electrolyte in CE. Advantages of amino acid-based ILs are high biocompatibility, environmental friendliness, stable chirality, weak UV absorption, and low costs.

3.5 Ionic Liquids in Nonaqueous Capillary Electrophoresis (NACE)

ILs are also applied in nonaqueous capillary electrophoresis. First, they were used as additives to acetonitrile as charge carrier to stabilize the electric field [69–71]. Dialkylimidazolium-based ILs are especially suitable due to their good miscibility with acetonitrile. A separation of 5 hydrophobic dyes (details in Table 2) could be achieved by addition of 1-butyl-3-methylimidazolium ILs to acetonitrile in cathodic detection mode, while no separation can be seen in 100 % acetonitrile [69]. The authors supposed that the analytes get charged in presence of the IL by building heteroconjugates. Two compounds being Brønsted bases (Janus Green, Brilliant Cresyl Blue) interact with the dialkylimidazolium cation and migrate faster than the two Brønsted acids (Thymolphthalein, Phenolphthalein) interacting with the anions. The analyte being neither a proton donor nor an acceptor migrates in middle, with the EOF. The separation mechanism of these compounds and a schematic electropherogram is shown in Fig. 5. A similar observation was made when studying the migration order of different phenols, being positional isomers, and carboxylic acids. The migration order depends on the p*K*a value, which has an influence on the degree of heteroconjugation [72]. When methanol or water is given to the solute the separation diminishes, because these solvents can act as proton donor and acceptor effecting the breakdown of existing heteroconjugates [70]. Further investigations on separation concept with different anionic counterions confirm the existence of an interaction between Brønsted acids and IL anions by estimation of mobilities [71].

The influence of different anionic counterions on 1-ethyl-3-methylimidazolium cations was tested for flavonoids [41]. By using BF_4^- no anodic mobility of the analytes was observed, whereas the addition of Cl^- and HSO_4^- led to a mobility toward the anode. This observation verifies a specific interaction between IL anions and the analyte, the heteroconjugation between Cl^- and HSO_4^- on one side and the flavonoids on the other side is much stronger than between BF_4^- and flavonoids. With rising concentration of IL the cathodic EOF is diminished in nonaqueous capillary electrophoresis, too. Like in aqueous CE, a change in EOF direction in nonaqueous CE can be achieved by addition of ILs [64]. Furthermore, Francois et al. demonstrated that there is an affinity of 2-arylpropionic acids to dialkylimidazolium cations in solute as well as to dialkylimidazolium cations coated on capillary surface, indicating a coating of the capillary surface in NACE, too [73]. Interestingly, the separation of 1-alkyl-3-methylimidazolium cations in pure acetonitrile showed in low concentrations (0–2 mM) a retention

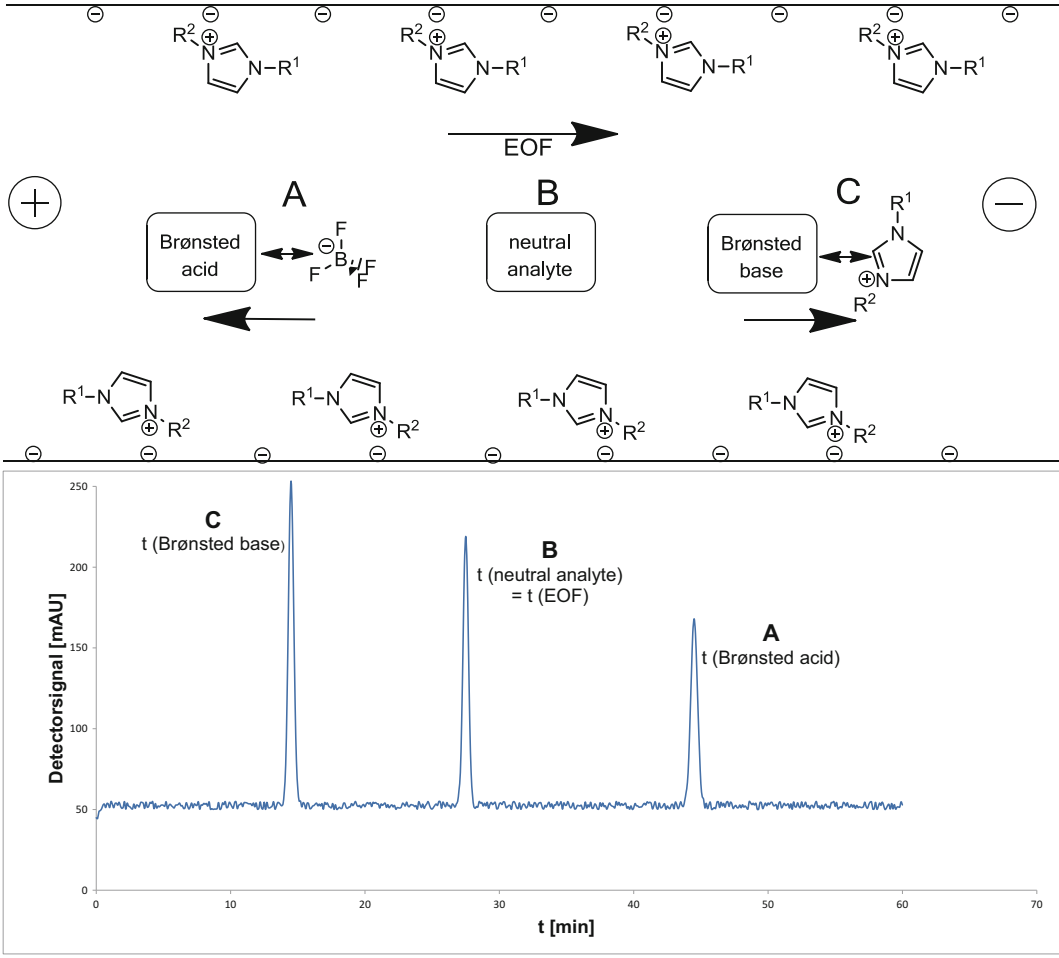

Fig. 5 Schematic separation mechanism and schematic electropherogram of three analytes in NACE. (**a**) Brønsted acids are building a heteroconjugate with IL anions and migrate toward the anode → slower than the EOF. (**b**) Neutral analytes do not interact with the IL and migrate with the EOF. (**c**) Brønsted bases are building a heteroconjugate with IL cations and migrate toward the cathode → faster than the EOF

against an EOF marker, which disappears by increasing concentrations, pointing to the formation of ion pairs at low concentrations. Thus, a good and stable separation could only be achieved at higher concentrations of ILs [43].

Seiman et al. investigated the behavior of the EOF in nonaqueous solvents containing 1-butyl-3-methylimidazolium trifluoroacetate. They observed two different effects [44]: In the first group (acetonitrile, ethanol, propylene carbonate, dimethylformamide), the EOF decreased by increasing IL concentrations whereas in group two (methanol, nitromethane) upon addition of low concentrations the EOF increased and passed a maximum before it decreased. This can be explained by different conductivities and viscosities between the several solvents used in this investigation.

4 Conclusions

1. ILs can be applied to coat the capillary surface covalently or dynamically, as single separation medium or binary pseudostationary phase in combination with micelles, CDs, or chiral selectors.
2. The electroosmotic flow can be controlled by addition of different concentrations of ILs to the BGE.
3. The direction of the EOF in CE depends on the concentration and character of the IL. In low concentrations the EOF heads to the cathode. Increase of IL concentration leads to decrease of EOF in cathodic detection mode, because the silanol groups on the capillary surface get shielded. Addition of even higher concentrations of IL to the BGE leads to a change in EOF direction. In anodic detection mode the EOF increases by further raising the IL concentrations (*see* Table 1).
4. Some observations suggest that the velocity and reversal of the EOF depends on the alkyl chain length of the IL cation. In cathodic detection mode longer alkyl chains effect a decrease and reversal of EOF in lower IL concentrations than shorter alkyl chains. This can be explained by the hydrophobicity of long chain ILs forming a more stable bilayer and thereby the negative charged silanol groups get better shielded. In anodic detection mode an increase in alkyl chain length also causes a decrease in EOF velocity due to the lower positive charge density (*see* Table 1).
5. By interaction between silanol groups and IL cations the stationary phase gets more hydrophobic. Therefore, hydrophobic analytes interact more with the stationary phase.
6. A practical problem in working with ILs in capillary electrophoresis is the equilibrium of IL in solution and coated on capillary. So a few runs can be necessary until the silanol groups on capillary surface are saturated and measured data gets reproducible [28, 59]. The number of runs is depending on the character of IL.
7. Both IL cation and IL anion play an important role in separation and enantioseparation, whereas interactions between IL cation and analytes seem to be more specific due to the additional adsorption on capillary surface. However, a change in both ions can lead to a change in migration order, peak shape, and migration time [33, 59].
8. ILs are very interesting for the separation of anions with high electrophoretic mobilities. Because of the change in EOF direction anions can be detected in anodic detection mode. The migration time decreases and thereby peak shape and

resolution can improve. Furthermore, ILs have an advantage in separation of basic compounds because they suppress the adsorption of this analytes to capillary wall silanol groups.

9. The melting point of an IL allows predictions of the separation with this IL in capillary electrophoresis. A low melting point indicates a weak association between IL cation and IL anion leading to more free ions in solution. Therefore, longer migration times, better separation and resolution, and better peak shapes are observed by using ILs with low melting points. The melting point of an IL often depends on the ability of an anion to build a hydrogen bond to its cationic counterion.

5 Enantioseparation of Pseudoephedrine

Many currently used pharmaceutical drugs are chiral. It is known that the biological activity, the toxicology, and pharmacokinetic parameters of enantiomers can be different. For some drugs it is important to ensure the enantiomeric purity. Therefore, the development of effective methods for enantioseparation is important. Pseudoephedrine is an active compound of ephedrae herba and a popular ingredient in cold medicines. A method using the benefits of ILs to improve the enantioseparation of pseudoephedrine is reported herein. A comparison to other methods separating pseudoephedrine enantiomers developed by our group is also given.

5.1 Materials

5.1.1 Apparatus

CE experiments were carried out on a Beckman P/ACE System MDQ instrument (Beckman Coulter, Fullerton, USA) equipped with a DAD detector. The uncoated fused-silica capillaries (BGB Analytik, Schloßböckelheim, Germany) had a total length of 60.2 cm (effective length 50 cm) and an internal diameter of 50 μm. The samples were injected hydrodynamically with 0.5 psi for 5 s on the anodic end of the capillary. The separation was carried out at 25 °C and a voltage of +20 kV. The detection wavelength was set to 194 nm.

To check the pH of the buffer solutions a PHM220 pH meter from MeterLab (Villeurbanne, France) was used. For the preparation of homogenous sample solutions a 2510-Branson-Sonicator (Heinemann Ultraschall- und Labortechnik, Schwäbisch Gmünd, Germany) was used.

5.1.2 Reagents and Chemicals

1. All chemicals used were of analytical grade.
2. Tetrabutylammonium chloride (TBAC), (1*S*,2*S*)-(+)-pseudoephedrine, (1*R*,2*R*)-(−)-pseudoephedrine, ammonium formate, and formic acid were purchased from Sigma Aldrich (Steinheim, Germany), 0.1 M NaOH and 0.1 M HCl from VWR (Darmstadt, Germany), and β-cyclodextrin from Wacker (Munich, Germany).

5.1.3 Buffers and Samples

1. All buffer and sample solutions were prepared using ultrapure Milli-Q water (Millipore, Milford, MA, USA) and filtered through a 0.2 μm pore-size CA-filter (cellulose acetate) (Carl Roth, Karlsruhe, Germany) prior to use.
2. The running buffer consisted of an aqueous solution of 50 mM ammonium formate, 12 mM β-cyclodextrin, and a step-wise raising amount of TBAC.
3. Ammonium formate was dissolved in water and the pH value was adjusted to 3.0 with formic acid and NaOH.
4. β-Cyclodextrin and TBAC were dissolved in this formate buffer using an ultrasonic bath. The pH value was checked and adapted with 0.1 M NaOH and formic acid, if necessary.
5. Pseudoephedrine samples were prepared dissolving 5.0 mg (1*S*,2*S*)-(+)-pseudoephedrine and 5.0 mg (1*R*,2*R*)-(−)-pseudoephedrine in 10.0 ml water. The solution was stored at 8 °C.

5.1.4 Rinsing Procedure

New capillaries were conditioned at 25 °C by rinsing with 0.1 M NaOH for 20 min, water for 5 min, 0.1 M HCl for 10 min, and again with water for 10 min.

To avoid current breakdown and to achieve repeatable migration times and a stable baseline a steady dynamically capillary coating with TBAC is necessary. To achieve repeatable separations the capillary was rinsed with water for 5 min, isopropyl alcohol for 10 min, water for 5 min, 0.1 M NaOH for 5 min, water for 5 min, 0.1 M HCl for 5 min, and again with water for 10 min at the beginning of each working day. At the end of each sequence of experiments the capillary was rinsed with water for 5 min, isopropyl alcohol for 20 min, water for 5 min, 0.1 M NaOH for 10 min, water for 5 min, 0.1 M HCl for 5 min, and water for 10 min. Before a new sample was injected the capillary was conditioned by flushing with BGE for 5 min.

All capillary wash cycles were performed at a pressure of 30 psi.

5.2 Methods

To investigate the influence of the IL concentration on the separation of pseudoephedrine enantiomers the concentration of TBAC in a 50 mM ammonium formate buffer containing 12 mM β-cyclodextrin was step-wise raised up to 200 mM. Electropherograms are displayed in Fig. 6.

As can be seen in Table 3 and in Fig. 7, an enhancement in resolution and a prolongation of migration time, due to capillary coating, was observed. In this concentration range no change in EOF direction occurred. When the concentration of TBAC exceeds 150 mM no further enhancement of the resolution can be observed. In contrast, due to the increased migration time and peak broadening at a concentration of 200 mM TBAC a deterioration of the resolution can be seen.

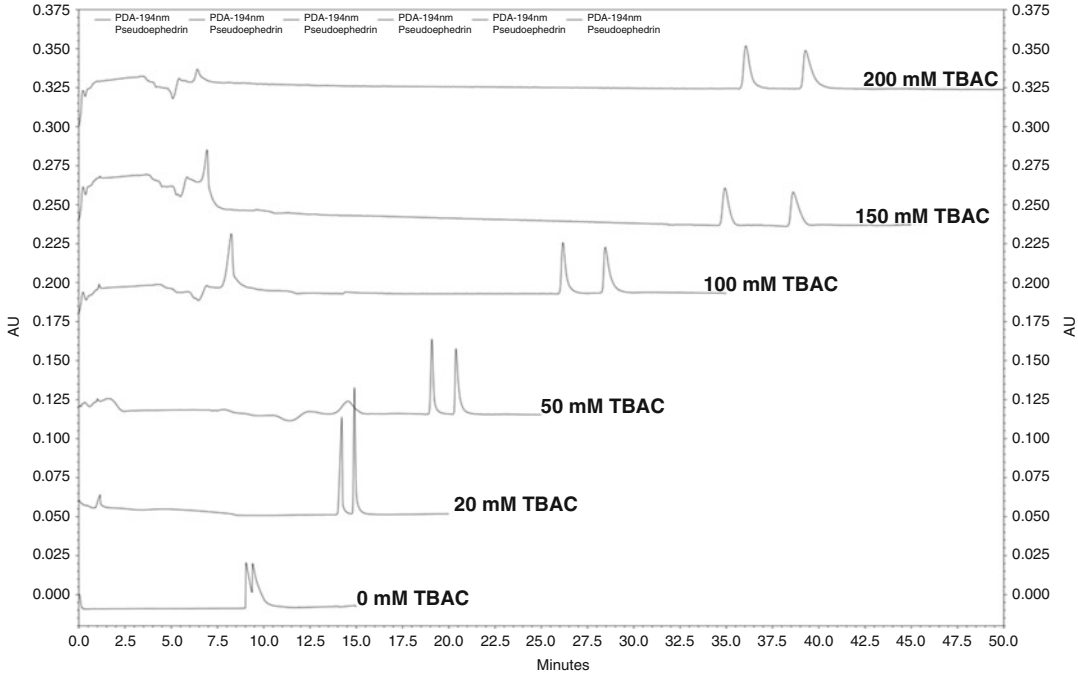

Fig. 6 Electropherograms showing the separation of pseudoephedrine enantiomers adding TBAC. Separation conditions: 50 mM ammonium formate buffer, pH 3.0, 12 mM β-cyclodextrin; voltage: +20 kV; temperature: 25 °C; detection wavelength: 194 nm; fused silica capillary (60.2/50 cm, 50 μm); sample conc.: 0.5 mg/ml

Table 3

Migration time and resolution of pseudoephedrine enantiomers

TBAC (mM)	t_1 (min)	t_2 (min)	Rs
0	9.0	9.4	0.68
20	14.2	14.9	3.27
50	19.1	20.4	4.60
100	26.2	28.5	4.66
150	34.9	38.6	5.01
200	36.1	39.3	4.44

Separation conditions are the same as in Fig. 6

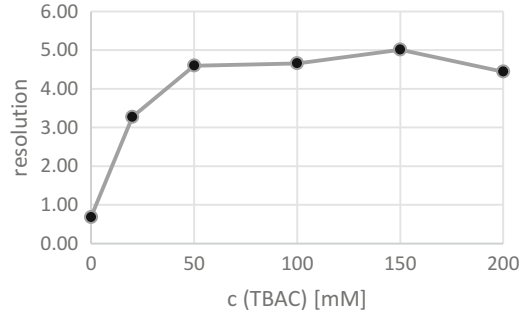

Fig. 7 Plot of the chiral resolution of pseudoephedrine. Separation conditions are the same as in Fig. 6

Summarizing it can be seen that the addition of TBAC to a β-cyclodextrin containing BGE has a synergistic effect on the enantioseparation of pseudoephedrine. By addition of 150 mM TBAC and 12 mM β-CD to the formate buffer, a higher resolution of pseudoephedrine enantiomers can be achieved, compared to a CE method (phosphate buffer, 12 mM β-CD, pH = 3) developed by our group (Rs = 3.1) [74]. Our group also reported a MEEKC method using 4.0% sulfated β-CD, 0.5% ethyl acetate, 1.0% SDS, 4.0% 1-butanol, 2.8% propan-2-ol in 20 mM phosphate buffer pH 2.5 for the enantioseparation of pseudoephedrine [75]. The IL-modified CE method yields to resolutions comparable to those achieved with this method (Rs = 5.7).

References

1. Rocha MA, Coutinho JA, Santos LM (2012) Cation symmetry effect on the volatility of ionic liquids. J Phys Chem B 116:10922–10927
2. Krossing I, Slattery JM, Daguenet C, Dyson PJ, Oleinkova A, Weingärtner H (2006) Why are ionic liquids liquid? A simple explanation based on lattice and solvation energies. J Am Chem Soc 128:13427–13434
3. Fuller J, Carlin RT, De Long HC, Haworth D (1994) Structure of 1-ethyl-3-methylimidazolium hexafluorophosphate: model for room temperature molten salts. J Chem Soc Chem Commun 299–300
4. Katritzky AR, Jain R, Lomaka A, Petrukhin R, Karelson M, Visser AE, Rogers RD (2002) Correlation of the melting points of potential ionic liquids (imidazolium bromides and benzimidazolium bromides) using the CODESSA program. J Chem Inf Comput Sci 42:225–231
5. Walden P (1914) Über die Molekulargrösse und elektrische Leitfähigkeit einiger geschmolzenen Salze. Bulletin de l'Académie Impériale des Sciences de St-Pétersbourg 1–11:405–422
6. Bonhôte P, Dias A, Papageorgiou N, Kalyanasundaram K, Grätzel M (1996) Hydrophobic, highly conductive ambient-temperature molten salts. Inorg Chem 35:1168–1178
7. O'Mahony AM, Silvester DS, Aldous L, Hardacre C, Compton RG (2008) Effect of water on the electrochemical window and potential limits of room-temperature ionic liquids. J Chem Eng Data 53:2884–2891
8. Tietze AA, Heimer P, Stark A, Imhof D (2012) Ionic liquid applications in peptide chemistry: synthesis, purification and analytical characterization processes. Molecules 17:4158–4185
9. Galan MC, Jones RA, Tran AT (2013) Recent developments of ionic liquids in oligosaccharide synthesis: the sweet side of ionic liquids. Carbohydr Res 375:35–46
10. Moniruzzaman M, Kamiya N, Goto M (2010) Ionic liquid based microemulsion with pharmaceutically accepted components: formulation and potential applications. J Colloid Interface Sci 352:136–142
11. Yao C, Anderson JL (2009) Retention characteristics of organic compounds on molten salt and ionic liquid-based gas chromatography stationary phases. J Chromatogr A 1216:1658–1712
12. Poole CF, Lenca N (2014) Gas chromatography on wall-coated open-tubular columns with ionic liquid stationary phases. J Chromatogr A 1357:87–109
13. Tsunashima K, Niwa E, Kodama S, Sugiya M, Ono Y (2009) Thermal and transport properties of ionic liquids based on benzyl-substituted phosphonium cation. J Phys Chem B 113:15870–15874
14. Ding J, Welton T, Armstrong DW (2004) Chiral ionic liquids as stationary phases in gas chromatography. Anal Chem 76:6819–6822
15. Poole CF, Kersten BR, Ho SSJ, Coddens ME, Furton KG (1986) Organic salts, liquid at room temperature, as mobile phase in liquid chromatography. J Chromatogr A 352:407–425
16. Sun Y, Stalcup AM (2006) Mobile phase effects on retention on a new butylimidazolium-based high-performance liquid chromatographic stationary phase. J Chromatogr A 1126:276–282
17. Armstrong DW, Zhang L, He L, Gross M (2001) Ionic liquids as matrixes for matrix-assisted laser desorption/ionization mass spectrometry. Anal Chem 73:3679–3686

18. Martinelango PK, Anderson JL, Dasgupta PK, Armstrong DW, Al-Horr RS, Slingdby RW (2005) Gas-phase ion association provides increased selectivity and sensitivity for measuring perchlorate by mass spectrometry. Anal Chem 77:4829–4835
19. Tsuda T (1987) Modification of electroosmotic flow with cetyltrimethylammonium bromide in capillary zone electrophoresis. J High Resolut Chromatogr 10:622–624
20. Huang X, Luckey JA, Gordon MJ, Zare RN (1989) Quantitative analysis of low molecular weight carboxylic acids by capillary electrophoresis/conductivity detection. Anal Chem 61:766–770
21. Garner TW, Yeung ES (1993) Increased selectivity for electrochromatography by dynamic ion exchange. J Chromatogr A 640:397–402
22. Iskandarani Z, Pietrzyk J (1982) Ion interaction chromatography of organic anions on a poly(styrene-divinylbenzene) adsorbent in the presence of tetraalkylammonium salts. Anal Chem 54:1065–1071
23. Pfeffer WD, Yeung ES (1990) Open-tubular liquid chromatography with surfactant-enhanced electroosmotic flow. Anal Chem 62:2178–2182
24. Liu C, Ho Y, Pai Y (2000) Preparation and evaluation of an imidazole-coated capillary column for the electrophoretic separation of aromatic acids. J Chromatogr A 897:383–392
25. Qin W, Li SFY (2002) An ionic liquid coating for determination of sildenafil and UK-103,320 in human serum by capillary zone electrophoresis-ion trap mass spectrometry. Electrophoresis 23:4110–4116
26. Qin W, Wei H, Li SFY (2003) 1,3-Dialkylimidazolium-based room-temperature ionic liquids as background electrolyte and coating material in aqueous capillary electrophoresis. J Chromatogr A 985:447–454
27. Qin W, Li SFY (2003) Electrophoresis of DNA in ionic liquid coated capillary. Analyst 128:37–41
28. Yanes EG, Gratz SR, Baldwin MJ, Robison SE, Stalcup AM (2001) Capillary electrophoretic application of 1-alkyl-3-methylimidazolium-based ionic liquids. Anal Chem 73:3838–3844
29. Gao Y, Xu Y, Han B, Li J, Xiang Q (2009) Sensitive determination of verticine and verticinone in Bulbus Fritillariae by ionic liquid assisted capillary electrophoresis-electrochemiluminescence system. Talanta 80:448–453
30. Vaher M, Koel M, Kazarjan J, Kaljurand M (2011) Capillary electrophoretic analysis of neutral carbohydrates using ionic liquids as background electrolytes. Electrophoresis 32:1068–1073
31. Laamanen P, Busi S, Lahtinen M, Matilainen R (2005) A new ionic liquid dimethyldinonylammonium bromide as a flow modifier for the simultaneous determination of eight carboxylates by capillary electrophoresis. J Chromatogr A 1095:164–171
32. Marszall MP, Markuszewski MJ, Kaliszan R (2006) Separation of nicotinic acid and its structural isomers using 1-ethyl-3-methylimidazolium ionic liquid as a buffer additive by capillary electrophoresis. J Pharm Biomed Anal 41:329–332
33. Yu L, Qin W, Li SFY (2005) Ionic liquids as additives for separation of benzoic acid and chlorophenoxy acid herbicides by capillary electrophoresis. Anal Chim Acta 547:165–171
34. Mo H, Zhu L, Xu W (2008) Use of 1-alkyl-3-methylimidazolium-based ionic liquids as background electrolytes in capillary electrophoresis for the analysis of inorganic anions. J Sep Sci 31:2470–2475
35. Krizek T, Breitbach ZS, Armstrong DW, Tesarova E, Coufal P (2009) Separation of inorganic and small organic anions by CE using phosphonium-based mono- and dicationic reagents. Electrophoresis 30:3955–3963
36. Li J, Wang Q, Han H, Liu X, Jiang S (2010) Polymeric ionic liquid as additive for the high speed and efficient separation of aromatic acids by co-electroosmotic capillary electrophoresis. Talanta 82:56–60
37. Li J, Han H, Wang Q, Liu X, Jiang S (2011) Polymeric ionic liquid-coated capillary for capillary electrophoresis. J Sep Sci 34:1555–1560
38. Li J, Han H, Wang Q, Liu X, Jiang S (2010) Polymeric ionic liquid as a dynamic coating additive for separation of basic proteins by capillary electrophoresis. Anal Chim Acta 674:243–248
39. Yue M-E, Shi Y-P (2006) Application of 1-alkyl-3-methylimidazolium-based ionic liquids in separation of bioactive flavonoids by capillary zone electrophoresis. J Sep Sci 29:272–276
40. Jiang TF, Wang YH, Lv ZH (2006) Dynamic coating of a capillary with room-temperature ionic liquids for the separation of amino acids and acid drugs by capillary electrophoresis. J Anal Chem 61:1108–1112
41. Lu Y, Jia C, Yao Q, Zhong H, Breadmore MC (2013) Analysis of flavonoids by non-aqueous capillary electrophoresis with 1-ethyl-3-methylimidazolium ionic-liquids as background electrolytes. J Chromatogr A 1319:160–165

42. Cabovska B, Kreishman GP, Wassell DF, Stalcup AM (2003) Capillary electrophoretic and nuclear magnetic resonance studies of interactions between halophenols and ionic liquid or tetraalkylammonium cations. J Chromatogr A 1007:179–187
43. Borissova M, Gorbatsova J, Ebber A, Kaljurand M, Koel M, Vaher M (2007) Nonaqueous CE using contactless conductivity detection and ionic liquids as BGEs in ACN. Electrophoresis 28:3600–3605
44. Seiman A, Vaher M, Kaljurand M (2008) Monitoring of the electroosmotic flow of ionic liquid solutions in non-aqueous media using thermal marks. J Chromatogr A 1189:266–273
45. Bao Y, Yang F, Yang X (2011) CE-electrochemiluminescence with ionic liquid for the facile separation and determination of diester-diterpenoid aconitum alkaloids in traditional Chinese herbal medicine. Electrophoresis 32:1515–1521
46. Gao Y, Xiang Q, Xu Y, Tian Y, Wang E (2006) The use of CE-electrochemiluminescence with ionic liquid for the determination of bioactive constituents in Chinese traditional medicine. Electrophoresis 27:4842–4848
47. Jiang T-F, Gu Y-L, Liang B, Li J-B, Shi Y-P, Ou Q-Y (2003) Dynamically coating the capillary with 1-alkyl-3-methylimidazolium-based ionic liquids for separation of basic proteins by capillary electrophoresis. Anal Chim Acta 479:249–254
48. Corradini D, Nicoletti I, Bonn GK (2009) Co-electroosmotic capillary electrophoresis of basic proteins with 1-alkyl-3-methylimidazolium tetrafluoroborate ionic liquids as non-covalent coating agents of the fused-silica capillary and additives of the electrolyte solution. Electrophoresis 30:1869–1876
49. Mwongela SM, Numan A, Gill NL, Agbaria RA, Warner IM (2003) Separation of achiral and chiral analytes using polymeric surfactants with ionic liquids as modifiers in micellar electrokinetic chromatography. Anal Chem 75:6089–6096
50. Rizvi SAA, Shamsi SA (2006) Synthesis, characterization, and application of chiral ionic liquids and their polymers in micellar electrokinetic chromatography. Anal Chem 78:7061–7069
51. Wang B, He J, Bianchi V, Shamsi SA (2009) Combined use of chiral ionic liquid and cyclodextrin for MEKC: part I. Simultaneous enantioseparation of anionic profens. Electrophoresis 30:2812–2819
52. Tian K, Qi S, Cheng Y, Chen X, Hu Z (2005) Separation and determination of lignans from seeds of Schisandra species by micellar electrokinetic capillary chromatography using ionic liquid as modifier. J Chromatogr A 1078:181–187
53. Borissova M, Palk K, Koel M (2008) Micellar electrophoresis using ionic liquids. J Chromatogr A 1183:192–195
54. Cao J, Qu H, Cheng Y (2010) The use of novel ionic liquid-in-water microemulsion without the addition of organic solvents in a capillary electrophoretic system. Electrophoresis 31:3492–3498
55. Mwongela SM, Siminialayi N, Fletcher KA, Warner IM (2007) A comparison of ionic liquids to molecular organic solvents as additives for chiral separations in micellar electrokinetic chromatography. J Sep Sci 30:1334–1342
56. Francois Y, Varenne A, Juillerat E, Villemin D, Gareil P (2007) Evaluation of chiral ionic liquids as additives to cyclodextrins for enantiomeric separations by capillary electrophoresis. J Chromatogr A 1155:134–141
57. Mofaddel N, Krajian H, Villemin D, Desbene PL (2008) Enantioseparation of binaphthol and its mono derivatives by cyclodextrin-modified capillary zone electrophoresis. J Chromatogr A 1211:142–150
58. Tran CD, Mejac I (2008) Chiral ionic liquids for enantioseparation of pharmaceutical products by capillary electrophoresis. J Chromatogr A 1204:204–209
59. Huang L, Lin JM, Yu L, Xu L, Chen G (2009) Improved simultaneous enantioseparation of beta-agonists in CE using beta-CD and ionic liquids. Electrophoresis 30:1030–1036
60. Wang B, He J, Bianchi V, Shamsi SA (2009) Combined use of chiral ionic liquid and CD for MEKC: part II. Determination of binding constants. Electrophoresis 30:2820–2828
61. Zhao M, Cui Y, Yu J, Xu S, Guo X (2014) Combined use of hydroxypropyl-beta-cyclodextrin and ionic liquids for the simultaneous enantioseparation of four azole antifungals by CE and a study of the synergistic effect. J Sep Sci 37:151–157
62. Liu Q, Wu K, Tang F, Yao L, Yang F, Nie Z, Yao S (2009) Amino acid ionic liquids as chiral ligands in ligand-exchange chiral separations. Chemistry 15:9889–9896
63. Mu X, Qi L, Zhang H, Shen Y, Qiao J, Ma H (2012) Ionic liquids with amino acids as cations: novel chiral ligands in chiral ligand-exchange capillary electrophoresis. Talanta 97:349–354
64. Ma Z, Zhang L, Lin L, Ji P, Guo X (2010) Enantioseparation of rabeprazole and omeprazole by nonaqueous capillary electrophoresis with an ephedrine-based ionic liquid

as the chiral selector. Biomed Chromatogr 24:1332–1337

65. Stavrou IJ, Kapnissi-Christodoulou CP (2013) Use of chiral amino acid ester-based ionic liquids as chiral selectors in CE. Electrophoresis 34:524–530
66. Yu J, Zuo L, Liu H, Zhang L, Guo X (2013) Synthesis and application of a chiral ionic liquid functionalized beta-cyclodextrin as a chiral selector in capillary electrophoresis. Biomed Chromatogr 27:1027–1033
67. Zhang J, Du Y, Zhang Q, Lei Y (2014) Evaluation of vancomycin-based synergistic system with amino acid ester chiral ionic liquids as additives for enantioseparation of nonsteroidal anti-inflammatory drugs by capillary electrophoresis. Talanta 119:193–201
68. Zhang Q, Du Y (2013) Evaluation of the enantioselectivity of glycogen-based synergistic system with amino acid chiral ionic liquids as additives in capillary electrophoresis. J Chromatogr A 1306:97–103
69. Vaher M, Koel M, Kaljurand M (2001) Nonaqueous capillary electrophoresis in acetonitril using ionic-liquid buffer electrolytes. Chromatographia 53:302–306
70. Vaher M, Koel M, Kaljurand M (2002) Ionic liquids as electrolytes for nonaqueous capillary electrophoresis. Electrophoresis 23:426–430
71. Vaher M, Koel M, Kaljurand M (2002) Application of 1-alkyl-3-methylimidazloium-based ionic liquids in non-aqueous capillary electrophoresis. J Chromatogr A 979:27–32
72. Kuldvee R, Vaher M, Koel M, Kaljurand M (2003) Heteroconjugation-based capillary electrophoretic separation of phenolic compounds in acetonitrile and propylene carbonate. Electrophoresis 24:1627–1634
73. Francois Y, Varenne A, Juillerat E, Servais AC, Chiap P, Gareil P (2007) Nonaqueous capillary electrophoretic behavior of 2-aryl propionic acids in the presence of an achiral ionic liquid. A chemometric approach. J Chromatogr A 1138:268–275
74. Wedig M, Holzgrabe U (1999) Resolution of ephedrine derivatives by means of neutral and sulfated heptakis(2,3-di-O-acetyl)beta-cyclodextrins using capillary electrophoresis and nuclear magnetic resonance spectroscopy. Electrophoresis 20:2698–2704
75. Borst C, Holzgrabe U (2010) Comparison of chiral electrophoretic separation methods for phenethylamines and application on impurity analysis. J Pharm Biomed Anal 53:1201–1209

Chapter 9

CZE–CZE ESI–MS Coupling with a Fully Isolated Mechanical Valve

Felix J. Kohl and Christian Neusüß

Abstract

The hyphenation of capillary electrophoresis and electrospray ionization–mass spectrometry is a powerful tool for peptide and protein analysis. It provides high separation power in combination with sensitive and selective detection and the possibility of analyte identification. Unfortunately, many proven capillary electrophoresis methods are not compatible with electrospray-mass spectrometry since several compounds of best separating background electrolytes are interfering in the electrospray ionization. Here, we describe a two-dimensional capillary electrophoresis system using the second dimension as a cleanup stage in order to remove interfering compounds to enable electrospray–mass spectrometry coupling.

Key words 2D, Heart-cut, Capillary electrophoresis, Mass spectrometry, Electrospray ionization, Peptides, Proteins

1 Introduction

Capillary electrophoresis–mass spectrometry (CE–MS) gets more and more important, especially for the analysis of proteins [1] and peptides [2]. These compounds are easily charged and therefore ideal for CE separation using, e.g., an acidic background electrolyte. CE is providing higher peak capacity and different selectivity in comparison to liquid chromatography (LC). In addition, mass spectrometric (MS) detection provides high sensitivity, selectivity, and the possibility of analyte identification. Due to the ionic character of the analytes, coupling via electrospray ionization (ESI) is appropriate.

However, in many CZE applications with optical detection established in research and industry, background electrolytes (BGE) are used containing compounds which are not compatible with ESI–MS. Solvents or additives which are not volatile and get ionized by the ESI (e.g., gels, cyclodextrins, inorganic salts) will soil the ESI source and the MS instrument. Further, it leads to a

Philippe Schmitt-Kopplin (ed.), *Capillary Electrophoresis: Methods and Protocols*, Methods in Molecular Biology, vol. 1483,
DOI 10.1007/978-1-4939-6403-1_9,

high background signal and to massive quenching of the analyte ionization. For this reason, some strategy must be used in order to get rid of these interfering compounds before MS detection.

One strategy to prevent the compounds to reach the detector is the partial filling technique which was applied with ESI–MS hyphenation for, e.g., micellar electrokinetic chromatography (MEKC) [3] or chiral separation of dipeptides by crown ether containing electrolytes [4]. In this approach, the separation capillary is just partly filled by the MS interfering BGE. Thereby, a part of the capillary from the capillary outlet is filled with a volatile, noninterfering electrolyte working as a cleanup zone. By nature, applicability of this technique is limited due to disadvantages such as changes in selectivity, decreased resolution, and lower peak capacity. Further on, in MS coupling the electroosmotic flow must be suppressed in most applications. Otherwise, the EOF will either transport the interfering compounds to the detection or suck sheath liquid or air from the MS interface, respectively. Second, it must be ensured, that the nonvolatile additive is not migrating toward the detector by electromigration. Hence, it must be neutral or migrate toward the capillary inlet which restricts the number of possible additives.

Heart-cut two-dimensional (2D) systems are a good alternative to the partial filling strategy, since they are not restricted to suppressed EOF and selection of the additives. In this approach, analytes are separated by the first dimension, containing a non-ESI–MS compatible solvent or additive. Subsequently the portion of interest is subjected to the second dimension. Besides others, the second dimension can be used for a cleanup stage to remove the interfering compounds.

There is a large number of different interfaces which are used in CE-CE coupling like, e.g., tee-cross-unions [5, 6], dialysis interfaces [7, 8], or different gated interfaces [9–11]. Besides these, a mechanical valve with an integrated sample loop can be applied as an interface in 2D approaches. With the help of an additional detector, the portion of interest can be cut very precise and transferred to the second dimension. Further, nearly every method can be used in the first dimension, as the two dimensions are operated completely independent.

Here we describe how to use a fully isolated mechanical 4-port valve with a 20 nL internal sample loop in order to set up a heart-cut 2D system for 2D-CZE-ESI–MS coupling. In the following, the selection of the valve as well as the geometry is discussed in detail. It is shown, how to setup the hardware of a heart-cut 2D CE-ESI–MS system, including integration of additional external detectors, switching time calculation, and ESI–MS coupling. The feasibility of the system is demonstrated on the example of a 2D-CE–ESI–MS separation of a bovine serum albumin (BSA) tryptic digest. With the given instructions it is possible to setup a 2D system, which enables ESI–MS coupling of a large number of CE methods which are otherwise not compatible with ESI–MS detection.

2 Materials

2.1 Chemicals and Solutions

1. We recommend to use only solvents and chemicals of highest purity, preferably LC–MS grade for both dimensions, although only a small amount of the first dimensions BGE reaches the MS detector.
2. Ultrapure water was purchased by a SG Ultra Clear UV (SG Wasseraufbereitung und Regenerierstation GmbH, Hamburg, GER) ultra pure water system.
3. Isopropyl alcohol (Rotisolv, LC-MS) and acetic acid (Rotipuran) were purchased by Roth (Carl Roth GmbH & Co. KG, Karlsruhe, GER). Sodium hydroxide and phosphoric acid (p.a.) are purchased by Merck (Merck KGaA, Darmstadt, GER).
4. BSA tryptic digest samples are obtained from Bruker (Bruker Daltonics, Bremen, GER).
5. First dimension background electrolyte (BGE) depends on the application carried out. Second dimension BGE: 10% acetic acid in ultrapure water (*see* **Note 1**).
6. Sheath liquid: 1:1 (v/v) Isopropyl alcohol:ultrapure water (*see* **Note 2**).
7. Mix all solutions well and degas in an ultrasonic bath (*see* **Note 3**).

2.2 Instrumentation

2.2.1 Valve

1. A VICI C4N-4354-.02D four-port-valve with an internal 20 nL sample loop is used (VICI-Valco Instruments Co., Schenkon, CH). The rotor and the stator of the valve are both made from plastic material (Valcon E, PTFE/PEAK mixture) (*see* **Note 4**).
2. In addition to the 20 nL sample loop, the rotor has two shortcuts with a volume valued at 7 nL (roughly 1/3 of the loop).
3. Four capillaries can be installed at the valve by four connections. Connection S and W are used for the first and connections P and C for the second dimension. The valve can be switched in two positions, position A (load position) and position B (inject position) (*see* **Note 5**). Figure 1 illustrates the switching scheme of the valve.
4. In this valve design the two dimensions are never connected to each other. The loop is filled with the target analyte in the first (position A) and switched to the second dimension (position B). It is further possible to flush both dimensions separately and even simultaneously.
5. Capillaries are connected to the valve by four 1/32″ fingertight fittings in combination with appropriate 1/32″ sleeves for the use of capillaries with an o.d. of 325–375 μm. Attached well, the valve provides a negligible dead volume.
6. The valve is equipped with an electric valve actuator which allows switching the valve via two buttons in position A and B.

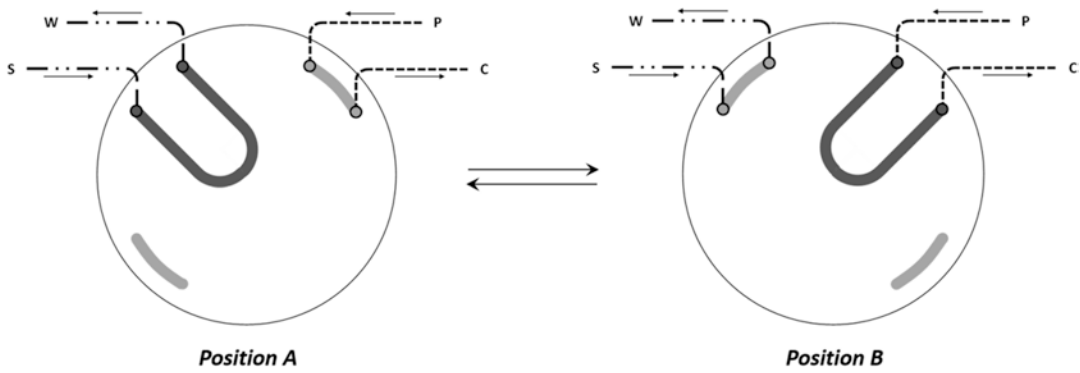

Fig. 1 Switching scheme of the 4-port valve. Position A load position; Position B inject position

2.2.2 CE

1. For 2D experiments, two high voltage (HV) sources and two grounded outlets are needed to have two independent dimensions. Using two CE instruments is ideal because this enables two pressurized inlets each equipped with an autosampler. Further, one of the two outlet vials is used for grounding of the first dimension. The second dimension electric circuit is enclosed by the ESI interface of the MS.
2. We are using a combination of a Beckman PA800+ (Beckman Coulter, Brea, USA) for the first (CE 1) and an Agilent G1600AX (Agilent Technologies, Waldbronn, GER) for the second dimension (CE 2) but any other combination of instruments, which are able to deliver 30 kV separation HV, may be sufficient as well (*see* **Note 6**).
3. Always make sure that all parts of the system are electrically shielded sufficiently in order to avoid accidents. This is especially important if you will use an external HV source and or grounding.
4. All instruments are controlled by the appropriate software. We are using Beckman 32 Karat V. 9.1 for control of the PA800+ and the Agilent 3D-CE ChemStation B.04.02 SP1 for the G1600AX. When possible, try to install the software on one computer.
5. Fused-silica capillaries with 365 μm o.d. and 50 μm i.d. are used in both dimensions (Polymicro Technologies, Phoenix, USA).
6. Four capillaries are needed in total. For first dimension: capillary 1A, from the inlet of CE 1 to connection S at the valve and capillary 1B, from connection W to the outlet of CE 1. For the second dimension: capillary 2A, from the inlet of CE 2 to connection P at the valve and capillary 2B from connection C to the ESI source. Capillary length depends on the assembly of the system and on the position of the valve. Typically capillary lengths are in the range of 50 cm for capillary 1A and 2A and 30 cm for capillary 1B and 2B leading to a total length of

80 cm. Keep the capillaries as short as possible to minimize total analysis time.

7. Cut the capillaries properly to achieve orthogonal and flat tips (*see* **Note 7**). In particular, the outlet of the second dimension which is inside the ESI source needs a well cut tip to enable a stable electrospray. Also the capillary tips which are connected to the valve should be as flat as possible to avoid damages while fixing.

2.2.3 MS Instrumentation

1. Here, we use a Bruker Esquire 6000 3D ion trap for MS detection (Bruker Daltonics, Bremen, GER). Other MS instruments may be sufficient as well (*see* **Notes 8** and **9**).
2. For the detection of the cationic peptides, ESI is used in positive ionization mode at a voltage of +4000 V. The ion trap operates in scan mode with a range of m/z 100–2500, a target of 2000 m/z, and an ICC of 20,000. Dry gas is delivered with a flow rate of 5 L/min at a temperature of 300 °C while nebulizer gas pressure is set to 10 psi.
3. The mass spectrometer is calibrated with sodium formate clusters. Clusters cover the used mass range with a higher number of mass points in comparison to the commercially available TuningMix which is used for higher m/z range (e.g. protein analysis).
4. ESI coupling is carried out by an Agilent coaxial sheath liquid CE ESI–MS sprayer kit (Agilent Technologies, Waldbronn, GER). Sheath liquid is delivered by a KD 78–9100 K syringe pump (KD Scientific, Holliston, USA) equipped with a 5 mL SGE 5MDR-GT gastight syringe (SGE analytical science, Melbourne, AUS) with a flow rate of 4 μL/min.

2.2.4 UV Detection

1. A TIDAS CCD UV/NIR external UV detector (J&M Analytik AG, Aalen, GER) is used for detection in the first dimension at a wavelength of 190 nm (*see* **Note 10**).
2. The detector is operated with the appropriate detection cell. The cell is mounted ≤4 cm before the valve by an in house constructed detection cell mount.
3. Control and data processing is carried out by the TIDASQ V. 2.39 (J&M Analytik AG, Aalen, GER) software.

3 Methods

3.1 Setting Up the 2D System

1. Place the two CE instruments as close to each other as possible and near to the MS interface (*see* **Notes 11** and **12**).
2. Mount the valve at an adequate position. Make sure that the capillary lengths fit to the positioning of the CE instruments, the ESI source, and the valve.

3. Prior to connecting to the valve, capillaries are conditioned separately in three flushing steps: (a) 5 min 1000 mbar H_2O, (b) 10 min 1000 mbar 1 M NaOH, (c) 5 min 1000 mbar H_2O. For preconditioning, install the capillary in one of the two CE instruments (*see* **Note 13**).
4. After the conditioning procedure, connect all capillaries to the valve and the two CE instruments (refer to Subheading 2.2.2, **item 6**) (*see* **Notes 14** and **15**).
5. Remove the polyimide coating at the outlet tip of capillary 2B by a pocket lighter and clean well with a towel wetted with isopropyl alcohol/ultrapure water 50:50. Install the capillary in the ESI sprayer. Check the proper positioning of the capillary by a loupe or a microscope. The capillary tip should slightly protrude the sprayer needle.
6. Install the ESI sprayer in the ESI source and connect nebulizer gas and sheath liquid. Start the syringe pump and flush the sheath liquid line by pressing fast forward.
7. Flush both dimensions with the respective BGE (about 10 min 1000 mbar). Switch the valve meanwhile to have every channel flushed.
8. For separation, both dimensions are operated at 30 kV in order to achieve a high separation efficiency. The appearing current is typically in the range of about 15 μA but is depending on the capillary lengths and on the used BGE (*see* **Note 16**).
9. A scheme of the complete two-dimensional setup is shown in Fig. 2.

3.2 Integration of a Detection Option in the First Dimension

1. The detection cell is placed at capillary 1A as near as possible to the valve and fixed by a mount (*see* **Note 17**).
2. Install the capillary and the detection cell and mark the position with a marker.
3. Remove the capillary to determine total length (l_{tot}) and effective length (l_{eff}).
4. A detection window must be manufactured at the capillary if optical detection should be used (*see* **Note 18**).
5. Reinstall the external detector at the capillary and connect the capillary again to the inlet of CE 1 and connection S at the valve.

3.3 Switching Time Calculation

1. Switching times are calculated "on the fly" by the UV detection signal in the first dimension.
2. Determine the migration time (t_m) at the middle of the target peak. The middle of the peak correlates to the middle of the sample plug.
3. Calculate the migration velocity (v_m) by:

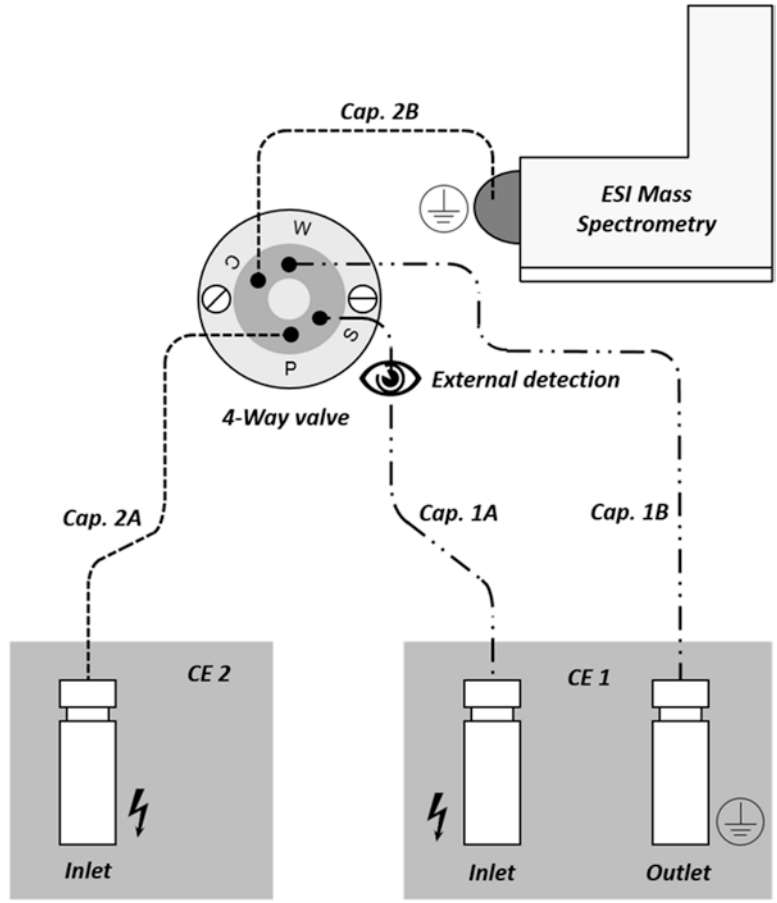

Fig. 2 Scheme of the 2D separation system

$$v_m = \frac{l_{eff}}{t_m}$$

4. With the help of v_m you can calculate the time the analyte needs to cover the distance from the external detection to the middle of the sample loop (t_d) (*see* **Note 19**) by:

$$t_d = \frac{l_{tot} - l_{eff} + 0.5\ \text{cm}}{v_m}$$

5. In order to cut the target peak, switch the valve (*see* **Note 20**) at t_s which is calculated by:

$$t_s = t_m + t_d$$

3.4 2D CZE–CZE–MS Separation

Figure 3 shows an exemplary 2D separation of a BSA tryptic digest. In order to demonstrate the feasibility of the 2D system, both dimensions were used with 10% acetic acid BGE (pH 2.2).

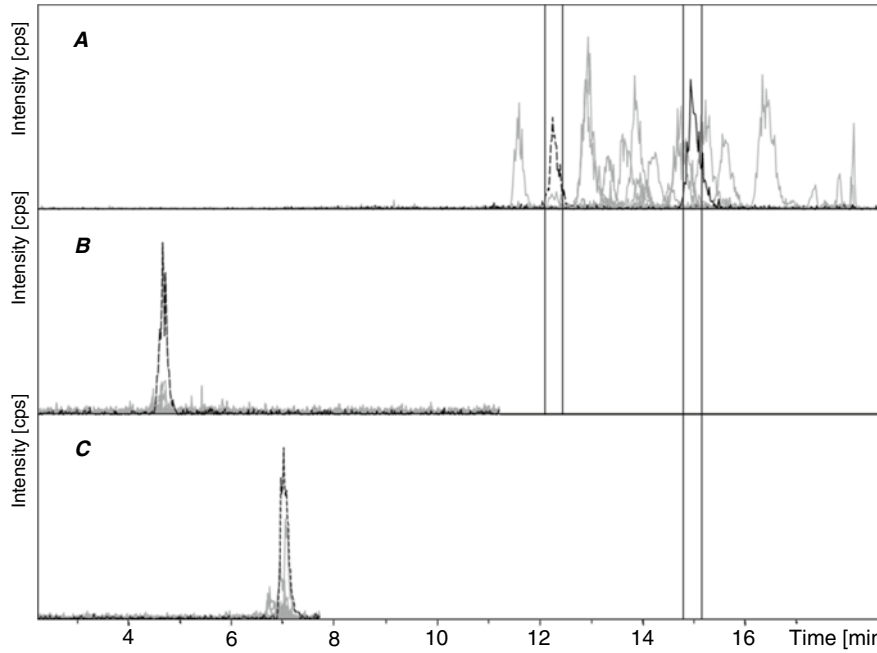

Fig. 3 CZE–CZE separation of a BSA tryptic digest; (**a**) 1D CZE–MS reference separation, EIC; (**b**, **c**) 2D CZE–CZE–MS separation

Figure 3a is a 1D CZE–MS separation of the sample. Here, the valve was used as injection valve: the loop was flushed with analyte solution from the first dimension and switched afterward. Subsequently, separation HV was applied to the second dimension. Figure 3b and 3c shows two different 2D CZE–CZE–MS experiments with two different switching times.

1. Prepare first dimension and second dimension BGE and degas both solutions. From each BGE, a vial is filled and positioned in the particular CE instrument.
2. Dissolve the sample, transfer to a sample vial with a µL-insert and position in CE1.
3. Switch the valve to position A.
4. Flush both dimensions with BGE for 5 min at 1000 mbar.
5. Inject the sample solution in the first dimension by hydrodynamic injection.
6. Apply first dimension separation HV (30 kV) and start external detector data acquisition simultaneously (*see* **Note 21**).
7. The current should be stable and in the range of some µA. When current breakdowns or a slow increasing of the current is observed, check solutions, capillaries, and valve (*see* **Notes 22** and **23**).

8. As the solutes reaches the detector in the first dimension, t_m of the target peak is determined and t_s is calculated by this value.
9. At a first dimension analysis time of t_s, shut off first dimension HV and switch the valve to position B.
10. Subsequently, apply second dimension separation HV (30 kV) Further ESI–HV as well as MS data acquisition is started simultaneously.

4 Notes

1. In protein analysis, 10% (v/v) acetic acid is mostly sufficient. In peptide analysis, often a formic acid buffer leads to a better separation. However, second dimension separation is not the issue in the system described.
2. If weak ionization efficiency is observed, ionization modifier may help. Add 0.1–1% (v/v) formic or acetic acid to the sheath liquid in case of positive ionization in peptide and protein analysis.
3. Degassing of all solutions is required in order to avoid gas bubble formation inside the CE capillary. Remaining gases in the solutions tend to form air bubbles especially in combination with joule heating while analysis. This bubbles cause very unstable currents and current breakdowns. If there are problems with the currents, check if all solutions are degased well.
4. Rotor and stator are produced from nonconductive material. Therefore, the valve itself is fully isolated and extra isolating from the two CE electric circuits is not necessary.
5. In position A, the two capillaries of the first dimension are connected by the loop and the two capillaries of the second dimension are connected by one of the shortcuts. The second shortcut is not used. Switching in position B, the two capillaries of the second dimension are connected by the loop and the first dimension by the second shortcut.
6. It is also possible to use an external HV source and an external BGE vial for grounding of the first dimension but this needs changes in the instrument hardware.
7. Usually, we cut the capillaries by a small ceramic cutting plate. Fix the capillary on a table and scratch the capillary orthogonal with a slight pressure. Break the capillary by pulling. Also diamond cutters are producing good results. Further on, ready cut and polished capillaries can be purchased by commercial retailers like Polymicro (Polymicro Technologies, Phoenix, USA).
8. In principle, MS instruments where ESI–HV is applied at the MS inlet and not at the ESI spray needle are preferred for CE hyphenation. In this instruments, fabricated by Bruker Daltonics and Agilent Technologies, the spray needle is grounded and

decouples the two HV circuits of CE and ESI. This is beneficial for method development and stable electrospray conditions.

9. TOF or Q-TOF mass spectrometers own a high mass range and mass accuracy which is important especially in protein analysis. These instruments perfectly measure the narrow peaks, typical in CE separations, due to the high acquisition speed. Quadrupole instruments and ion traps can be also appropriate for peptide analysis although, in particular quadrupole instruments are limited in CE coupling while they are comparably slow in scanning mode.
10. Depending on the application, external laser-induced fluorescence (LIF) or capacitively coupled conductivity detectors (C^4D) may be suitable as well. Make sure that you have the possibility to install cell/sensor of the external detection close to the valve (4 cm or less).
11. The valve needs to be firmly fixed. Otherwise it will move while switching and relocate the external detection. This leads to variations in the UV signal or the baseline, respectively. At best, use the provided valve mount and drill and tap two M3 threads on a stable surface, e.g., at one of the CE instruments, where you can fix the valve by two M3 flat head screws.
12. The valve should not be installed in an upright way. Otherwise, if the valve gets untight, the liquid will possibly enter and damage the valve electronics.
13. Especially in the analysis of proteins, often coating of the fused silica capillary is necessary to avoid attraction of the solutes to the capillary wall. Please check if a coating is needed and choose the type of coating according to your application.
14. The finger tight fittings should be tightened with care. If the fittings are attached with too high force, the capillary tip will possibly break and may damage or clog the connection in the rotor.
15. Make sure that the capillaries are connected in the correct direction. The inlet and outlet of the loop need to be the same in both dimensions.
16. The valve material tends to be damaged by high currents. Try to use BGEs with a comparable low ionic strength to avoid high currents. Otherwise, decrease separation HV.
17. The mount depends on the design of the sensor used and may be special constructed. Make sure that the cell/sensor is fixed well. The valve will move/vibrate while switching which may cause variations in the detector signal if the vibrations are transmitted in any way.
18. For the installation of the sensor when conductivity detection is applied, the same procedure as used for an optical detection cell (refer to Subheading 2.2, **items 1–5**) can be followed. Except **step 4** since a detection window is not needed.

19. The sample loop of the valve has a volume of 20 nL. This volume correlates to the volume of about 1 cm of a 50 μm i.d. capillary. Therefore, the distance from the detection window to the middle of the sample loop is $l_{tot} - l_{eff}$ + the length of a capillary correlating to half of the volume of the sample loop which is, in case of a 50 μm i.d. capillary, 0.5 cm.
20. Shutting off the separation HV while switching the valve leads to a more robust system. In principle it is possible to switch the valve while HV is applied but there is a risk of bubble formation or bubble entry by the switching process leading to current breakdowns in both dimensions. In order to avoid this, it is recommended to shut off HV at t_s and switch the valve subsequently. Migration of the analyte is stopped immediately when HV is turned to zero. Therefore, there is no issue with diffusion in switching the valve some seconds after t_s.
21. Triggering of the detector by the CE instrument is ideal when possible. Beckman CE instruments provide two relays which can be switched in the CE method at any point. Therefore, it is possible to trigger both, the detector of the first dimension and the MS. When there is only one possibility to trigger a detector, use it for the detection in the first dimension since a precise determination of the migration time is important in order to determine correct switching times.
22. When current is unstable, check if the capillaries are damaged (especially at the fragile detection window) or clogged and degas solutions. Further, the valve may be untight or clogged. Disassemble the valve and check the bores by a microscope. The bores can be cleaned with water pressed through by a pipet. Clean the valve carefully by a lint-free towel and reassemble.
23. When the current is slowly raising in one dimension, check the current in the other dimension. This current must always be zero. If it is not, the valve is untight and the current is able to flow between the dimensions. This is often due to damaging rotor or stator by the switching process. Disassemble the valve and check rotor and stator for scratches. If one of the parts is damaged, it will need to be replaced or polished, respectively.

References

1. Haselberg R, de Jong GJ, Somsen GW (2013) CE-MS for the analysis of intact proteins 2010–2012. Electrophoresis. doi:10.1002/elps.201200439
2. Herrero M, Ibañez E, Cifuentes A (2008) Capillary electrophoresis-electrospray-mass spectrometry in peptide analysis and peptidomics. Electrophoresis. doi:10.1002/elps.200700404
3. Wiedmer SK, Jussila M, Riekkola M-L (1998) On-line partial filling micellar electrokinetic capillary chromatography-electrospray ionization-mass spectrometry of corticosteroids. Electrophoresis. doi:10.1002/elps.1150191031
4. Xia S, Zhang L, Lu M et al (2009) Enantiomeric separation of chiral dipeptides by CE-ESI-MS

employing a partial filling technique with chiral crown ether. Electrophoresis. doi:10.1002/elps.200800799

5. Zhang Z-X, Zhang M-Z, Zhang S-S (2009) Online preconcentration and two-dimensional separation of cationic compounds via hyphenation of capillary zone electrophoresis with cyclodextrin-modified micellar electrokinetic capillary chromatography. Electrophoresis. doi:10.1002/elps.200800571
6. Zhang Z, Zhang X, Li F (2010) The multi-concentration and two-dimensional capillary electrophoresis method for the analysis of drugs in urine samples. Sci China Chem. doi:10.1007/s11426-010-0054-7
7. Yang C, Liu H, Yang Q et al (2002) On-line hyphenation of capillary isoelectric focusing and capillary gel electrophoresis by a dialysis interface. Anal Chem. doi:10.1021/ac026187p
8. Mohan D, Paša-Tolić L, Masselon CD et al (2003) Integration of electrokinetic-based multidimensional separation/concentration platform with electrospray ionization-fourier transform ion cyclotron resonance-mass spectrometry for proteome analysis of shewanella oneidensis. Anal Chem. doi:10.1021/ac0342572
9. Michels DA, Hu S, Dambrowitz KA et al (2004) Capillary sieving electrophoresis-micellar electrokinetic chromatography fully automated two-dimensional capillary electrophoresis analysis of Deinococcus radiodurans protein homogenate. Electrophoresis. doi:10.1002/elps.200405939
10. Hooker TF, Jorgenson JW (1997) A transparent flow gating interface for the coupling of microcolumn LC with CZE in a comprehensive two-dimensional system. Anal Chem. doi:10.1021/ac970342w
11. Michels DA, Hu S, Schoenherr RM et al (2002) Fully automated two-dimensional capillary electrophoresis for high sensitivity protein analysis. Mol Cell Proteomics. doi:10.1074/mcp.T100009-MCP200

Chapter 10

Capillary Electrophoresis-Inductively Coupled Plasma Mass Spectrometry

Bernhard Michalke

Abstract

During the recent years, capillary electrophoresis (CE) has been fully established as a powerful tool in separation sciences as well as in element speciation. This road of success is based on the rapid analysis time, low sample requirements, high separation efficiency, and low operating costs of CE. Inductively coupled plasma mass spectrometry (ICP-MS) is known for superior detection and multielement capability. Consequently, the combination of both instruments is approved for analysis of complex sample types at low element concentrations which require high detection power. Also the diversity of potential applications brings CE–ICP-MS coupling into central focus of element speciation. The key to successful combination of ICP-MS as an (multi-)element selective detector for CE is the availability of a suitable and effective interface.

Therefore, this chapter summarizes the most important and basic principles about coupling of capillary electrophoresis to ICP-MS. Specifically, the major requirements for interfacing are described and technical solutions are given. Such solutions include the closing of the electrical circuit from CE at the nebulization, the adoption of flow rates for efficient nebulization, the reduction of a suction flow through the capillary, caused by the nebulizer, and maintaining the high separation resolution from CE across the interface for ICP-MS detection. Additionally, detailed information is presented to determine and quantify the siphoning suction through the CE capillary by the nebulizer. Finally, two applications, namely, the manganese and selenium speciation in cerebrospinal fluid are shown as examples, providing the relevant operational parameter.

Key words Capillary electrophoresis, Inductively coupled plasma mass spectrometry, Interface, Problem solutions

Abbreviations

CE	Capillary electrophoresis
CZE	Free zone electrophoresis
ICP-MS	Inductively coupled plasma mass spectrometry
IEF	Isoelectric focusing
ITP	Isotachophoresis
LC	Liquid chromatography
LoD	Limit of detection
MEKC	Micellar electrokinetic chromatography
RF	Radiofrequency
USN	Ultrasonic nebulizer

Philippe Schmitt-Kopplin (ed.), *Capillary Electrophoresis: Methods and Protocols*, Methods in Molecular Biology, vol. 1483,
DOI 10.1007/978-1-4939-6403-1_10,

1 Introduction

Nowadays capillary electrophoresis (CE) is a useful tool with high reproducibility in separation sciences as well as in element speciation. CE provides rapid analysis time, low sample requirements, high separation efficiency, and low operating costs [1, 2]. Specifically the high separation potential of CE [3] combined with the superior multielement detection capability of ICP-MS must be considered as the outstanding potential of CE–ICP-MS. This together with the diversity of potential applications makes the coupling of CE to ICP-MS as a powerful technique for studies in the field of metallomics and element speciation, but also for quantitative proteomics based on elemental tagging. In each of these mentioned fields, the separation of metal-carrying- (organic-) molecules, so-called metal species, is followed by element selective detection resulting in paralleled element-selective electropherograms [1–3].

Consequently, this analytical approach is widely used for speciation analysis in various scientific fields, investigating topics such as lanthanides in humic substances [4] or As, Eu, Hg, Np, Se, U and organo-tins in environmental matrices [5–11], biomedical applications like manganese speciation in paired serum and cerebrospinal fluid samples, the determination of gadolinium-based MRI contrast agents or of phosphorus in DNA organotin compounds and the characterization of metal glycinate- and metal-phytosiderophores complexes [12–17], anticancer drug-related investigations [18–23], and elemental tagging for quantitative proteomics [24–30].

In all of those experiments, the key to a successful CE–ICP-MS hyphenation is an interface which is perfectly adapted to the specific requirements of both techniques. The analytical chemist should properly control the relevant variables for best overall performance [31].

Four major requirements for interfacing both instruments are known [3, 32, 33]: (1) The closing of electrical circuit from CE, (2) an optimized nebulization efficiency and mass transport into ICP-MS, (3) the reduction of suction flow through the capillary caused by the nebulizer, and (4) a low "dead volume."

Several successful approaches were described in literature for setting up such an interface, mostly working along similar technical solutions based on pneumatic nebulization systems [3, 31, 34–37]. Less applied attempts were using an USN device, a direct injection nebulizer with sheath flow or hydride generation.

This chapter summarizes basic principles for coupling CE to ICP-MS. Therefore, a special focus is drawn to interface developments and technical problems, i.e., requirements to the interface setup and respective solutions. Finally, two applications, namely, Mn- and Se-speciation in serum and/or cerebrospinal fluid, are described in detail to enable a simpler startup even for those operators who had not used such an instrumental combination in the past.

2 General Aspects: Limitation and Potential of CE–ICP-MS Coupling

Starting first with some limitations: The most important drawback of this hyphenation technique is the fact, that CE–ICP-MS has worse concentration detection limits than LC–ICP-MS. This is due to the low sample intake to be analyzed. Limits of detection (LoD) are often above environmental or biological relevant species concentrations in real samples. Consequently, many problems can be related to the attempt of decreasing concentration detection limits to real-world concentrations when using (partly inadequate) stacking and separation conditions. Difficulties are often related to chemical interactions of samples, electrolytes, and the capillary or detector interferences [38]. This is not surprising as species stability can be impaired by "wrong" CE conditions, predominantly complexing electrolytes, inadequate pH, etc. [39]. In protein-rich biological samples, a typical problem is a total or partial compound sticking to capillary. Such an outage appears more likely without temperature control of the CE capillary. Most CE systems nowadays provide such a temperature control, however, typically inside the instrument. Since the capillary is managed outside the instrument—at least its terminal part—for being interfaced to ICP-MS it may be advised to install an additional capillary cooling, e.g., in a tubing around the capillary where the coolant is driven by a peristaltic pump (*see* Fig. 1). In case protein sticking appears quantifications are usually wrong and "pseudo-species" may be detected. This is caused by accidentally redissolved protein particles from previously sticking ones. Such peaks may pretend species within a sample, but are only artifacts. If such artifacts appear at specific standard migration time they can be erroneously "identified" as a certain species. The well-known migration time variations caused by differences in ionic strength of buffers or samples are a further problem for species identification [40]. Standard additions help to overcome this uncertainty [41]. However, also the generation of new species during analysis must be considered. As ICP-MS is a sequential detection system, the monitoring of too many isotopes in parallel may result in missing fast migrating peaks of one isotope. Detection limits of the CE–ICP-MS system up to now are just suitable or still too high for several real-world samples. Thus, the demand for coupling to more sensitive detectors, e.g., ICP-sf-MS is recommended and is also realized in literature [17, 42].

Nevertheless, CE–ICP-MS is a powerful tool in metal speciation and elemental tagging approaches and the above-mentioned limitations mainly refer to the capillary electrophoresis side but less to the important interface between the two analytical systems.

It is of paramount importance for this hyphenation technique that the interface is working at its optimum. When the setup of an interface is successfully implementing the specific requirements

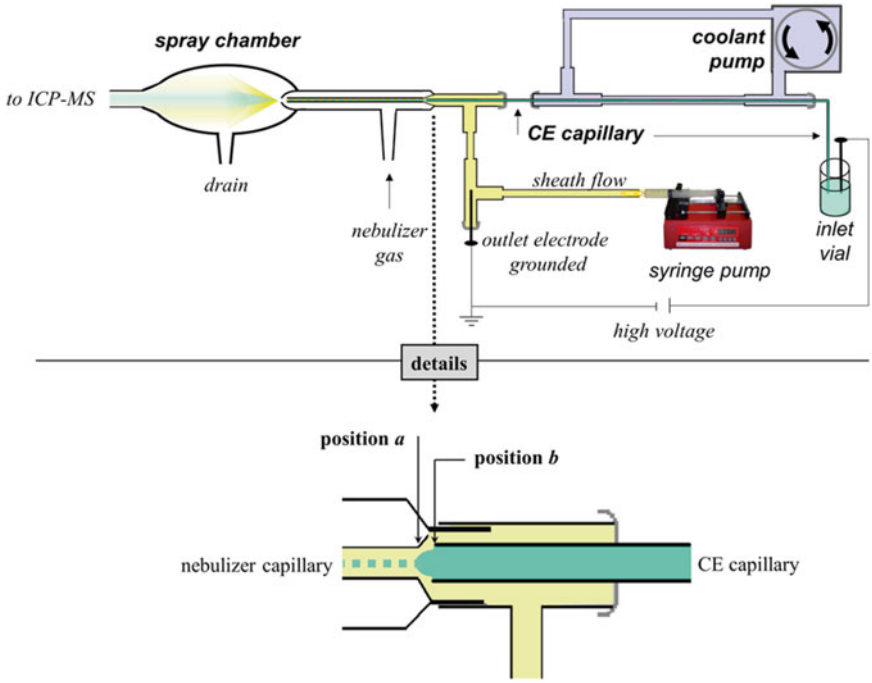

Fig. 1 The scheme shows an overview for mounting an interface between capillary electrophoresis and ICP-mass spectrometry. In the *upper part* the most important issues are demonstrated: Closing of electrical circuit for CE, feeding the sheath flow by a pulse-free syringe pump, temperature control of the capillary outside the CE instrument to ICP-MS, small volume spray chamber. The *lower part* shows the optimal positions of (**a**) the beginning of nebulizer capillary and (**b**) the end of CE capillary. The CE capillary should be moved close to the beginning of the nebulizer capillary, however, leaving sufficient space for the sheath liquid to flow around the capillary end

detailed in this chapter the interface is working reliable and no specific coupling problems occur. Investigations then can concentrate on the broad potential of this technique. The undisputed advantages and potential of CE–ICP-MS are its high separation capability, the short analysis time, and the high selectivity and sensitivity of detection. Since flow rates are low and volumes reaching the plasma are in the nL–μL range only [32] the ICP-MS accepts all buffers and modifiers without any problems. Plasma stability is not affected. Therefore, online preconcentration methods, such as isotachophoresis (ITP) combined with free zone electrophoresis (CZE) are easily possible, providing still acceptable species separation even when sample volumes are drastically increased for improvement of concentration-LoD. Buffer sandwiches or discontinuous buffer systems often result in improvements of separation. Even nearly non-aqueous buffer systems which maintain only little conductivity are accepted by the detector as the sheath flow (e.g., HNO_3) overcompensates the few nl coming from CE capillary. The different separation modes—CZE, ITP, isoelectric focusing (IEF), or micellar electrokinetic chromatography (MEKC)—allow separation solutions

for nearly all element species and stand for a wide characterization of the sample. The powerful ICP-MS detector provides element and isotope information, as well as multielement capability combined with low detection limits. Typical LoDs are in the 0.03–30 μg/l range, depending on species [39]. As with LC–ICP-MS species identification is realized by standard matching. Further, there are no stationary phases that can impair species stability [32]. Several authors already demonstrated applications to real-world samples of very different matrices and very low species concentrations.

3 Method: Important Details About Interfacing CE to ICP-MS

3.1 Requirements and Solutions

Much effort has been devoted (and still is) to interfacing CE with inductively coupled plasma (ICP) mass spectrometry (MS).

Designing an interface for the nebulization of micro-separation technique effluents into a fine aerosol and ensuring efficient transport into the plasma is not an easy task [43]. Thus, the most crucial point in hyphenating CE to ICP-MS first is the interface itself which must fulfill special requirements:

1. The closing of the electrical circuit from CE at the end of the capillary.
2. Adapting the flow rates best suited for CE and nebulization. The low flow rate from CE does not match the flow rate for an efficient nebulization.
3. Minimizing the siphoning suction flow through the capillary.
4. Preserving the high separation resolution from CE while transferring the analytes to ICP-MS.

The requirements 1–3 are solved principally in the same manner in (nearly) all described interfaces, independent on whether they are commercially available or laboratory constructed.

An electrolyte sheath flow, being in contact with the outlet electrode, is mixed with the capillary effluent at the end of the capillary, which is positioned as close as possible to the point of nebulization. When using commercial low-flow nebulizers the CE capillary can be positioned just before the nebulizer capillary (see position “a” and “b” in Fig. 1). Both capillaries should be positioned with minimal distance to each other for avoiding peak broadening, but there must be still a cleft to allow the sheath flow mixing with CE effluent. The task of this coaxial electrolyte flow around the CE capillary is multifacetted: First it must provide the electrical connection from the grounded outlet electrode to the end of the separation capillary. Usually, a current between 10 and 30 μA is determined. Second, the sheath flow is used to adapt the flow rate for suitable nebulization efficiency. It turned out that diluted nitric acid (ca. 0.1 %) was best suited for this task, although the sheath electrolyte also has the function of the outlet electrolyte with respect to suitable pH settings. Potential disadvantages of other

makeup solutions, such as plasma instability, poor precision, and degradation of ICP-MS performance, were avoided when using nitric acid. Further, the use of an inorganic acid instead of a salt solution provides the nebulizer from crusting and blocking.

In some applications pH stacking occurs resulting in peak sharpening. This is considered as a positive side effect. However, H^+ movement toward the inlet buffer (at −/+ polarity) can result in pH decrease in inlet electrolytes shifting separation conditions out of optimum. For keeping separation conditions defined at optimum, this buffer should be replaced regularly (in case even after each run) when HNO_3 is used as sheath electrolyte. For providing a sheath flow with lowest pulsation a syringe pump is preferred over peristaltic or HPLC pumps. Another task of the sheath flow is preserving an adequate flow rate for efficient nebulization (typically 10–100 μL, depending on the nebulizer used) which is in considerable excess compared to the analyte leaving CE capillary (typically < 2 μL/min). A careful optimization of the flow rate is crucial since a high flow rate often improves nebulization efficiency but contrary results in higher dilution of analytes coming from CE capillary. An additional positive effect of the sheath flow is the reduction of the suction force from nebulizer on the capillary lumen: The more this suction is fed from sheath flow the lower the suction affects the capillary lumen. Therefore, the suction flow usually gets controlled by capillaries with low inner diameter in commercial interfaces and/or by the dimensions of the separation capillary itself. Typically a suction flow is reduced by selection of appropriate column dimensions: a) using a long CE capillary (1.5 m) with a standard inner diameter of 50 μm [33], or b) by a short (2 cm) but narrow interface capillary (10 to ≤25 μm ID) set at the end of the CE capillary [44].

Both problem solutions are based on the law of Hagen–Poiseuille. Some approaches in literature apply a negative pressure at the inlet during separation. However, exactly meeting the point of equilibrium between nebulizer suction and counter suction at inlet is complicated to operate. Finally, self-aspiration of the sheath flow was suggested to overcome the suction flow. Before starting to analyze samples the suction flow should be checked and quantified. Two approaches are described in literature for checking the suction flow (e.g., by Michalke et al. [39, 45] or Schaumlöffel et al. [46, 47]), focusing on whether or not there is a suction flow or, more detailed, even quantifying the amount of the suction flow:

3.2 Method: Determining a Siphoning Suction Flow

The occurrence (yes/no) of the suction flow can be elucidated as described as follows:

The capillary gets first filled with buffer and the electrical current must be determined at high voltage, e.g., at 20 kV. Subsequently, the capillary's inlet should be kept into air while nebulization gas is turned on for 60 min. In case of a suction flow, air will intrude into the capillary. After 1 h the electrical circuit along the capillary must

be checked again when nebulization gas is turned off and the capillary's inlet is dipped again into the inlet electrolyte. In case a suction flow had occurred, an air bubble will now interrupt the electrical circuit and the measured current will be practically zero even at high voltage of 20 kV.

Quantifying a suction flow takes more than double the time compared to getting a simple yes/no answer:

The experiment starts as above with filling the capillary with electrolyte and measuring the current at 20 kV while the nebulizer gas is turned off. Subsequently, the capillary inlet is dipped into a standard solution at higher concentration (~200 μg/L) for 60 min. During this first step, the nebulizer gas remains "off." Therefore, the standard solution can enter the capillary only by diffusion. This "zero-flow–diffusion-value" will be needed later for correction. After 60 min the capillary inlet gets relocated into inlet electrolyte and the nebulizer gas gets turned on. In parallel ICP-MS detection is started while the capillary lumen is purged to ICP-MS. The monitored peak signal which is now detected corresponds to the standard amount which entered the capillary only by diffusion without suction forced flow.

In a second step, this experiment should be exactly repeated except that the nebulizer gas remains "on" during the 60 min period.

The peak signal monitored at the end of the second step corresponds to the standard amount entering the capillary by suction + diffusion.

The final experimental step for suction flow quantification aims for a peak area vs. capillary volume calibration: Therefore, the capillary must be filled completely with standard solution. Subsequently, the monitoring of the baseline by ICP-MS should be started. When now purging the capillary lumen with electrolyte to ICP-MS, the signal will first increase as long as standard from the previously filled capillary is reaching the detector. The signal falls back to baseline when the purging electrolyte has removed the standard solution from capillary lumen and reaches the detector. The area below the resulting broad hump corresponds to the capillary volume (in μL), which in turn is calculated by the equation $r^2 \times \pi \times L$ (r = radius, L = length, both in mm: volume results in (μL)).

The final equation $F\left[\frac{\mu L}{h}\right] = \frac{As - Ad}{Ac} \times Vc$ calculates the net suction flow (without diffusion) during 60 min (1 h), where As = peak area while nebulizer gas was turned on (suction + diffusion), Ad = peak area while nebulizer gas was turned off (diffusion), Ac = peak area while purging the filled capillary, and Vc = the calculated volume of the capillary.

Finally, requirement 4 (see earlier: preserving the separation of CE at the interface) is achieved by a low-volume spray chamber. An advantageous design for immediate peak response is given

when the chamber volume is minimal and spray direction is in direct line to the ICP entrance. Mostly such spray chamber designs are laboratory constructed.

Based on the earlier designs and rules for an interface the following two short sections give hints for Se and Mn speciation in biological samples.

4 Examples of Applications for CE Interfacing to ICP-MS

4.1 Selenium Speciation

4.1.1 Analytes

The chemical list consists of certified selenium stock standard (1000 mg/L, CPI, Santa Rosa, USA). Selenite, selenate, Selenomethionine, Selenocystine, Thioredoxinreductase (EC 1.8.1.9.), Glutathioneperoxidase (EC 232-749-6), human serum albumin (HSA), and TRIS buffer (Sigma-Aldrich, Deisenhofen, Germany). Ammonium acetate and acetic acid (Merck, Darmstadt, Germany). Ar_{liq} and methane (99.999% purity, Air Liquide, Gröbenzell, Germany).

4.1.2 Samples

Serum (and CSF if required) sample pairs should be drawn at a medical station or hospital. After ethical aspects are cleared and patients consented to the use of their samples for scientific investigations, the previously aliquoted, frozen-stored samples can be used for Se speciation. The samples should be thawed at 4 °C in the refrigerator, vortexed (and only for serum samples: diluted 1/5 with Milli-Q water), and subjected to sample vials of the CE device.

Working standards of Mnf species should be prepared daily from their stock standard solutions by appropriate dilution with Milli-Q water.

4.1.3 Capillary Electrophoresis (CE)-ICP-DRC-MS

"Biofocus 3000" (Bio-Rad, Munich, Germany) or PrinCe CEC 760 (Prince Technologies, Emmen, Netherlands) capillary electrophoresis system, equipped with an uncoated capillary (CS-Chromatographie Service GmbH, Langerwehe, Germany) 120 cm × 50 μm ID. Hyphenation is detailed earlier in this chapter. Analytical preparation: Before each run, purge the capillary with NH_4-acetate/acetic acid buffer, 10 mM, pH 3.0 (70 s, 8 bar).

Pressurized sample injection for 2 s, followed from 1 s buffer injection. The separation voltage is set to +25 kV. Sheath flow (diluted running buffer 1/25) around outlet electrode and capillary end: 80 μL/min

4.1.4 Parameter for Inductively Coupled Plasma Mass Spectrometry

Table 1 shows typical experimental settings chosen for ICP-DRC-MS after optimization.

4.1.5 Data Processing

Export Se data files from the NexIon software and process the files with a suitable chromatography software, e.g., "Clarity" from Data

Table 1

Typical experimental settings for ICP-DRC-MS regarding Se speciation

Instrument	Perkin Elmer Nexlon DRC
Plasma conditions	
RF power (W)	1250
Plasma gas flow (L/min)	15
Auxiliary gas flow (L/min)	1.05
Nebulizer gas flow (L/min)	0.98 Daily optimized
Nebulizer (optimal flow rate according to provider)	Meinhard low flow (100 μL/min)
Mass spectrometer settings	
Dwell time (ms)	100
Sweeps per reading	1
Readings per replicate	1600
Autolens	On
Ions monitored	^{78}Se, ^{80}Se
Reaction gas	CH_4
Reaction gas flow rate (mL/min)	0.6
Rejection parameter *q*	0.6
Rejection parameter *a*	0

Apex for peak area integration. Peak areas can be used for the calibration curve (standards) or for calculating the concentration according to the calibration curve (samples).

An example of separation is given in Fig. 2.

4.2 Manganese Speciation

4.2.1 Analytes

The chemical list consists of certified manganese stock standard (1000 mg/L, CPI, Santa Rosa, USA). $MnCl_2$, human serum albumin (HSA), transferrin, α2-macroglobuline, arginase, citrate, and TRIS buffer (Sigma-Aldrich, Deisenhofen, Germany). Ammonium acetate, sodium acetate, and acetic acid (Merck, Darmstadt, Germany). Ar_{liq} and methane (99.999% purity, Air Liquide, Gröbenzell, Germany).

Mn—citrate stock solution: mixing a solution of 1 g/L citrate with a $MnCl_2$ solution (5 mg/L) using a ratio of 4 + 1 (v:v), resulting in a Mn-citrate stock concentration of 1 mg Mn/L. Mn-albumin and Mn-transferrin stock solutions: in analogy by mixing 1 g/L protein solution with 5 mg/L $MnCl_2$ solution (4 + 1, each), resulting in 1 mg Mn/L for each compound. Working solutions should be prepared daily by appropriate dilution with Tris–HCl, 10 mM, pH 7.4.

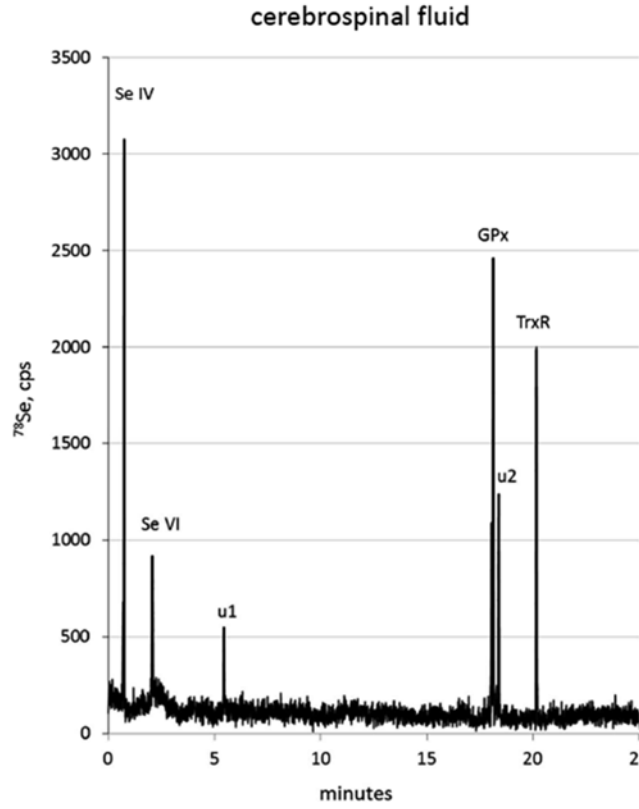

Fig. 2 This figure shows an electropherogram of Se species from a cerebrospinal fluid sample monitored at the isotope ^{78}Se. Se compounds u1 and u2 showed no standard match and were not identified. *GPx* glutathione peroxidase, *TrxR* thioredoxin reductase

4.2.2 Samples

Serum (and CSF if required) sample pairs, should be drawn at a medical station or hospital. After ethical aspects are cleared and patients consented to the use of their samples for scientific investigations, the previously aliquoted, frozen-stored samples can be used for Mn speciation. The samples should be thawed at 4 °C in the refrigerator, vortexed (and only for serum samples: diluted 1/5 with Milli-Q water), and subjected to sample vials of the CE device.

Working standards of Se species should be prepared daily from their stock standard solutions by appropriate dilution with Milli-Q water.

4.2.3 Capillary Electrophoresis (CE)–ICP-DRC-MS

"Biofocus 3000" (Bio-Rad, Munich, Germany) or PrinCe CEC 760 (Prince Technologies, Emmen, Netherlands) capillary electrophoresis system, equipped with an uncoated capillary (CS-Chromatographie Service GmbH, Langerwehe, Germany) 120 cm × 50 μm ID. Hyphenation is detailed earlier in this chapter. Analytical preparation: Before each run, the capillary should be

purged with Milli-Q H_2O (180 s, 8 bar) and TRIS (10 mM, adjusted to pH 8.0 with HAc) buffer = background electrolyte ("BE," 180 s, 8 bar).

For sample stacking a buffer sandwich gets injected consisting of 160 nL Na-acetate (200 mM, high conductivity), acting as leading electrolyte (LE), 60 nL sample, and 235 nL terminating electrolyte (TE), consisting of BE/H_2O (1:100; low conductivity). The inlet vial gets filled with BE adjusted to pH 6, the sheath flow at capillary end is BE/methanol (1:1). The applied voltage is set to +28 kV.

4.2.4 Parameter for Inductively Coupled Plasma Mass Spectrometry

Table 2 shows typical experimental settings chosen for ICP-DRC-MS after optimization.

4.2.5 Data Processing

Export Mn data files from the NexIon software and process the files with a suitable chromatography software, e.g., "Clarity" from

Table 2

Typical experimental settings for ICP-DRC-MS regarding Mn speciation

Instrument	Perkin Elmer NexIon DRC,
Plasma conditions	
RF power (W)	1250
Plasma gas flow (L/min)	15
Auxiliary gas flow (L/min)	1.05
Nebulizer gas flow (L/min)	1.02 Daily optimized
Nebulizer (optimal flow rate according to provider)	MicroMist low flow (50 μL/min)
Mass spectrometer settings	
Dwell time (ms)	100
Sweeps per reading	1
Readings per replicate	1000
Autolens	On
Ions monitored	^{55}Mn, ^{56}Fe
Reaction gas	NH_3
Reaction gas flow rate (mL/min)	0.58
Rejection parameter q	0.45
Rejection parameter a	0

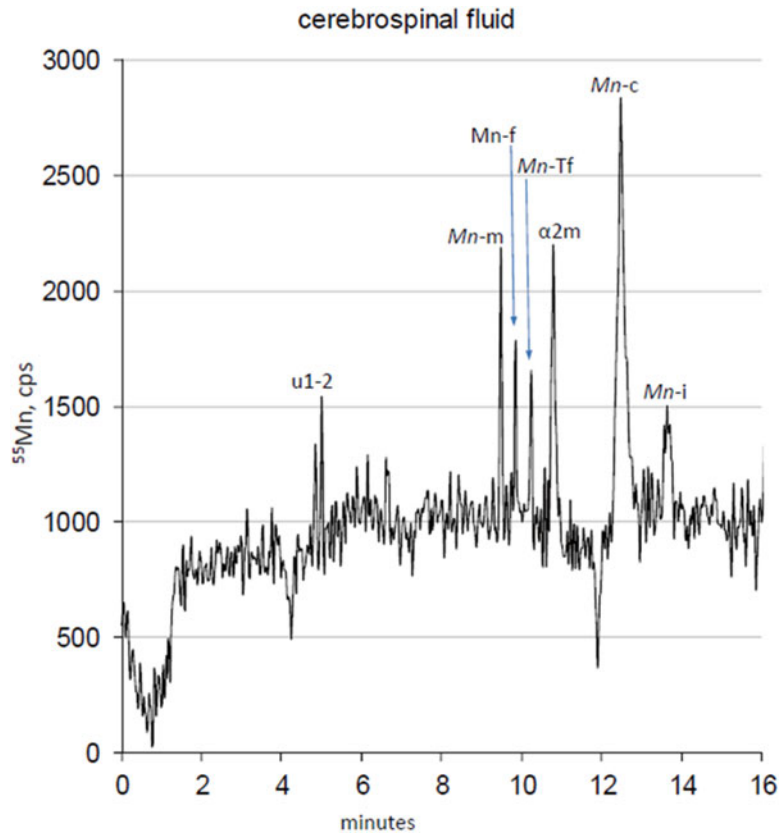

Fig. 3 This figure shows an electropherogram of Mn species from a cerebrospinal fluid sample monitored at the isotope ^{55}Mn. Mn species concentrations are rather low and noise of baseline is already clearly monitored. Mn compounds u1 and u2 showed no standard match and were not identified. Mn-m = Mn-malate, Mn-f = Mn-fumarate, Mn-Tf = Mn carrying transferrin, α2m = α-2-macroglobulin, Mn-c = Mn-citrate, Mn-i = inorganic Mn

Data Apex for peak area integration. Peak areas can be used for the calibration curve (standards) or for calculating the concentration according to the calibration curve (samples).

An example of separation is given in Fig. 3.

References

1. Barnes RM (1998) 1998 Winter Conference on Plasma Spectrochemistry Scottsdale, Arizona, January 5-10, 1998. Fresenius J Anal Chem 362(5):431–432
2. Kannamkumarath SS, Wrobel K, Wrobel K et al (2002) Capillary electrophoresis-inductively coupled plasma-mass spectrometry: an attractive complementary technique for elemental speciation analysis. J Chromatogr A 975(2):245–266
3. Sutton K, Sutton RMC, Caruso JA (1997) Inductively coupled plasma mass spectrometric detection for chromatography and capillary electrophoresis. J Chromatogr A 789(1–2):85–126
4. Kautenburger R, Hein C, Sander JM et al (2014) Influence of metal loading and humic acid functional groups on the complexation behavior of trivalent lanthanides analyzed by CE-ICP-MS. Anal Chim Acta 816:50–59

5. Han M, Zhao GX, Li SZ et al (2013) Speciation analysis of arsenic in groundwater by capillary electrophoresis-inductively coupled plasma mass spectrometry. Chin J Anal Chem 41(11):1780–1781
6. Stobener N, Amayri S, Gehl A et al (2012) Sensitive redox speciation of neptunium by CE-ICP-MS. Anal Bioanal Chem 404(8):2143–2150
7. Moser C, Kautenburger R, Philipp Beck H (2012) Complexation of europium and uranium by humic acids analyzed by capillary electrophoresis-inductively coupled plasma mass spectrometry. Electrophoresis 33(9-10):1482–1487
8. Li BH (2011) Rapid speciation analysis of mercury by short column capillary electrophoresis on-line coupled with inductively coupled plasma mass spectrometry. Anal Meth 3(1):116–121
9. Sun J, He B, Yin YG et al (2010) Speciation of organotin compounds in environmental samples with semi-permanent coated capillaries by capillary electrophoresis coupled with inductively coupled plasma mass spectrometry. Anal Meth 2(12):2025–2031
10. Hsieh MW, Liu CL, Chen JH et al (2010) Speciation analysis of arsenic and selenium compounds by CE-dynamic reaction cell-ICP-MS. Electrophoresis 31(13):2272–2278
11. Yang GD, Xua JH, Xu LJ et al (2010) Analysis of ultratrace triorganotin compounds in aquatic organisms by using capillary electrophoresis-inductively coupled plasma mass spectrometry. Talanta 80(5):1913–1918
12. Michalke B, Lucio M, Berthele A et al (2013) Manganese speciation in paired serum and CSF samples using SEC-DRC-ICP-MS and CE-ICP-DRC-MS. Anal Bioanal Chem 405(7):2301–2309
13. Telgmann L, Sperling M, Karst U (2013) Determination of gadolinium-based MRI contrast agents in biological and environmental samples: a review. Anal Chim Acta 764:1–16
14. Sun J, He B, Liu Q et al (2012) Characterization of interactions between organotin compounds and human serum albumin by capillary electrophoresis coupled with inductively coupled plasma mass spectrometry. Talanta 93:239–244
15. Fujii S, Inagaki K, Chiba K et al (2010) Quantification of phosphorus in DNA using capillary electrophoresis hyphenated with inductively coupled plasma mass spectrometry. J Chromatogr A 1217(50):7921–7925
16. Vacchina V, Oguey S, Ionescu C et al (2010) Characterization of metal glycinate complexes by electrospray Q-TOF-MS/MS and their determination by capillary electrophoresis-ICP-MS: application to premix samples. Anal Bioanal Chem 398(1):435–449
17. Dell'mour M, Koellensperger G, Quirino JP et al (2010) Complexation of metals by phytosiderophores revealed by CE-ESI-MS and CE-ICP-MS. Electrophoresis 31(7):1201–1207
18. Aleksenko SS, Matczuk M, Lu XF et al (2013) Metallomics for drug development: an integrated CE-ICP-MS and ICP-MS approach reveals the speciation changes for an investigational ruthenium(III) drug bound to holo-transferrin in simulated cancer cytosol. Metallomics 5(8):955–963
19. Nguyen TTTN, Ostergaard J, Sturup S et al (2013) Determination of platinum drug release and liposome stability in human plasma by CE-ICP-MS. Int J Pharm 449(1–2):95–102
20. Nguyen TTTN, Ostergaard J, Sturup S et al (2013) Metallomics in drug development: characterization of a liposomal cisplatin drug formulation in human plasma by CE-ICP-MS. Anal Bioanal Chem 405(6):1845–1854
21. Bytzek AK, Boeck K, Hermann G et al (2011) LC- and CZE-ICP-MS approaches for the in vivo analysis of the anticancer drug candidate sodium trans-[tetrachloridobis(1H-indazole)ruthenate(III)] (KP1339) in mouse plasma. Metallomics 3(10):1049–1055
22. Michalke B (2010) Platinum speciation used for elucidating activation or inhibition of Pt-containing anti-cancer drugs. J Trace Elem Med Biol 24(2):69–77
23. Abramski JK, Foteeva LS, Pawlak K et al (2009) A versatile approach for assaying in vitro metallodrug metabolism using CE hyphenated with ICP-MS. Analyst 134(10):1999–2002
24. Yang MW, Wu WH, Ruan YJ et al (2014) Ultra-sensitive quantification of lysozyme based on element chelate labeling and capillary electrophoresis inductively coupled plasma mass spectrometry. Anal Chim Acta 812:12–17
25. Sanz-Medel A, Montes-Bayon M, Bettmer J et al (2012) ICP-MS for absolute quantification of proteins for heteroatom-tagged, targeted proteomics. Trac-Trends Anal Chem 40:52–63
26. Meermann B, Sperling M (2012) Hyphenated techniques as tools for speciation analysis of metal-based pharmaceuticals: developments and applications. Anal Bioanal Chem 403(6):1501–1522

27. Yang MW, Wang ZW, Fang L et al (2012) Simultaneous and ultra-sensitive quantification of multiple peptides by using europium chelate labeling and capillary electrophoresis-inductively coupled plasma mass spectrometry. J Anal Atomic Spectrom 27(6):946–951
28. Li Y, Sun SK, Yang JL et al (2011) Label-free DNA hybridization detection and single base-mismatch discrimination using CE-ICP-MS assay. Analyst 136(23):5038–5045
29. Profrock D (2010) Progress and possible applications of miniaturised separation techniques and elemental mass spectrometry for quantitative, heteroatom-tagged proteomics. Anal Bioanal Chem 398(6):2383–2401
30. Liu JM, Li Y, Jiang Y et al (2010) Gold nanoparticles amplified ultrasensitive quantification of human urinary protein by capillary electrophoresis with on-line inductively coupled plasma mass spectroscopic detection. J Proteome Res 9(7):3545–3550
31. Olesik JW, Kinzer JA, Grunwald EJ et al (1998) The potential and challenges of elemental speciation by capillary electrophoresis inductively coupled plasma mass spectrometry and electrospray or ion spray mass spectrometry. Spectrochim Acta B Atom Spect 53(2):239–251
32. Tomlinson MJ, Lin L, Caruso JA (1995) Plasma mass spectrometry as a detector for chemical speciation studies. Analyst 120(3):583–589
33. Michalke B, Schramel P (1997) Coupling of capillary electrophoresis with ICP-MS for speciation investigations. Fresenius J Anal Chem 357(6):594–599
34. Tangen A, Trones R, Greibrokk T et al (1997) Microconcentric nebulizer for the coupling of micro liquid chromatography and capillary zone electrophoresis with inductively coupled plasma mass spectrometry. J Anal Atomic Spectrom 12(6):667–670
35. Michalke B, Schramel P (1996) Hyphenation of capillary electrophoresis to inductively coupled plasma mass spectrometry as an element-specific detection method for metal speciation. J Chromatogr A 750(1–2):51–62
36. Michalke B, Schramel P (1998) Capillary electrophoresis interfaced to inductively coupled plasma mass spectrometry for element selective detection in arsenic speciation. Electrophoresis 19(12):2220–2225
37. Michalke B, Schramel P (1998) Application of capillary zone electrophoresis-inductively coupled plasma mass spectrometry and capillary isoelectric focusing-inductively coupled plasma mass spectrometry for selenium speciation. J Chromatogr A 807(1):71–80
38. Michalke B (1999) Potential and limitations of capillary electrophoresis inductively coupled plasma mass spectrometry—invited lecture. J Anal Atomic Spectrom 14(9):1297–1302
39. Michalke B (2005) Capillary electrophoresis-inductively coupled plasma-mass spectrometry: a report on technical principles and problem solutions, potential, and limitations of this technology as well as on examples of application. Electrophoresis 26(7–8):1584–1597
40. Bondoux G, Jandik P, Jones WR (1992) New approach to the analysis of low levels of anions in water. J Chromatogr 602(1-2):79–88
41. Michalke B (1995) Capillary electrophoretic methods for a clear identification of selenoamino acids in complex matrices such as human milk. J Chromatogr A 716(1–2):323–329
42. Standler A, Koellensperger G, Buchberger W et al (2007) Determination of chloroplatinates by CE coupled to inductively coupled plasma sector field MS. Electrophoresis 28(19):3492–3499
43. Casiot C, Donard OFX, Potin-Gautier M (2002) Optimization of the hyphenation between capillary zone electrophoresis and inductively coupled plasma mass spectrometry for the measurement of As-, Sb-, Se- and Te-species, applicable to soil extracts. Spectrochim Acta B Atom Spect 57(1):173–187
44. Schaumlöffel D, Prange A (1999) A new interface for combining capillary electrophoresis with inductively coupled plasma-mass spectrometry. Fresenius J Anal Chem 364(5):452–456
45. Michalke B, Schramel P (1999) Iodine speciation in biological samples by capillary electrophoresis—inductively coupled plasma mass spectrometry. Electrophoresis 20(12):2547–2553
46. Prange A, Schaumloffel D (2002) Hyphenated techniques for the characterization and quantification of metallothionein isoforms. Anal Bioanal Chem 373(6):441–453
47. Prange A, Schaumloffel D, Bratter P et al (2001) Species analysis of metallothionein isoforms in human brain cytosols by use of capillary electrophoresis hyphenated to inductively coupled plasma-sector field mass spectrometry. Fresenius J Anal Chem 371(6):764–774

Chapter 11

Use of CE to Analyze Solutes in Pico- and Nano-Liter Samples from Plant Cells and Rhizosphere

A. Deri Tomos

Abstract

This chapter describes the use of capillary electrophoresis (CE) in the accurate quantitative mapping of small molecules and ions in intact function tissues between individual cells at single cell resolution. It can also be used for the analysis of the heterogeneity of soil surrounding roots at similar spatial resolution, providing a link between plant and environment. No pretreatment or genetic manipulation of the plant is required. The application is an extension of the Single Cell Sampling and Analysis technique (SiCSA), in which glass micromanipulation of microcapillaries allows samples in the pl and nl volume range to be obtained and manipulated under paraffin oil (to prevent evaporation) before being introduced to the CE column. An advantage of this approach is that the entire sample can be brought to the detector (without the loading losses associated with other techniques). The power of SiCSA-CE is that the results can be directly related to a range of other single-cell resolution parameters ranging from mechanical and hydraulic properties to gene expression. Several protocols and (contrasting) applications are provided.

Key words Capillary electrophoresis, Single cell sampling and analysis, Rhizosphere

1 Introduction

The functional heterogeneity of cells plays essential roles in all except the very simplest multicellular life forms. Analysis of averaged behavior from homogenized tissue cannot provide full mechanistic descriptions. In extreme cases, an "average" value for a parameter may not exist *anywhere* in the system. This chapter describes the use of Capillary Electrophoresis (CE) as part of an integrated suite of techniques based on the use of glass microcapillaries to sample the contents of individual living cells of plants growing under fully physiological conditions [1–4]. Crucially, no pretreatment or genetic manipulation of tissue is required. In addition, it permits cross correlation with mutually relevant information (such as cell mechanical and hydraulic properties, turgor pressure, osmotic pressure, individual solute concentrations, enzyme activity, and gene expression); thus opening the door for improved systems

Philippe Schmitt-Kopplin (ed.), *Capillary Electrophoresis: Methods and Protocols*, Methods in Molecular Biology, vol. 1483,
DOI 10.1007/978-1-4939-6403-1_11,

biology approaches. An example of this integration would be the quantitative correlation of turgor, osmotic pressure, and the sum of concentrations of the individual solutes. In this case biochemical processes that act essentially on the metabolism or transport of an individual solute can be correlated to the mechanical behavior of an organ at the level of its smallest functional unit (the cell). The overall suite of techniques has been called Single Cell Sampling and Analysis (SiCSA) [1, 2]. This has been applied to samples down to approximately 1pl volume [5]. Recently, it has also been extended to the analysis of functional heterogeneity in the rhizosphere—the soil–root interface important for the understanding of plant–soil interactions in agriculture and environmental services [6]. Due to the wide range of CE protocols illustrated by this volume and elsewhere [7, 8], the technique has the potential to replace several of the key SiCSA protocols, such as EDX and enzyme-linked fluorescent assays [4, 9] as well as opening up new approaches [10].

The challenges of single-cell analysis of small molecules are twofold. First, accessing an undisturbed sample. This is not an issue if individual cells are already available. This can be the case for bacteria and animal tissue cultures for which microfluidic and other techniques have been developed in recent years [11]. Disrupting integral tissues, however, is another matter. The redistribution of small molecules (including water) is very rapid when then microenvironment of cells is altered. This is exacerbated when tissues are damaged (such as occurs during cell separation and in all but the most sophisticated freezing procedures [12]). Techniques that minimize disturbance and the time for sample isolation are needed. Metabolic changes after sample isolation also must be avoided.

A disadvantage of the microcapillary sampling approach as described later is that it does not distinguish subcellular compartments. Although the sample will be dominated by the vacuole, cytosolic material must also be present since quantitative measurements of mRNA, not found in vacuoles, are possible [3]. However, chloroplasts do not enter the capillary tip and there is total exclusion of extracellular (apoplast) material.

Second, the volume of a single cell is usually small (pl to nl range). This demands very sensitive analytical techniques. However, to our advantage, often the solutes of interest are at relatively high concentrations (μM and mM) and being able to bring the entire sample to the detector of the analytical system minimizes this problem. Many plant cells have relatively high turgor pressures and volumetric elastic moduli [13]. This combination favors the use of glass microcapillaries to obtain samples from accessible cells within a fraction of a second. Rapid removal of the capillary from the cell then minimizes dilution due to osmotic flow of water [14]. Finally, solvent evaporation if the small sample volume exposed to air is avoided by performing all subsequent manipulations under water-saturated paraffin oil.

2 Materials and Equipment

2.1 Chemicals

1. All chemicals were obtained from Sigma-Aldrich UK, with the exception of low viscosity silicone oil AS4 (Wacker Chemie).
2. All solutions were made using purified water (18MΩ) (Elga UHQ), which was also used for all necessary washing procedures.

2.2 Equipment

2.2.1 Sampling

1. Stereo microscope (Leitz Wild M8).
2. Cold light source (Cole-Parmer 41723 series).
3. Micromanipulator (Leitz) fitted with clamp for microcapillary (Fig. 1b).
4. Pipette puller (Harvard Apparatus UK) (A current equivalent is the PC-10 Narishige).
5. Microforge (e.g., de Fonbrune). (A current equivalent is the MF-900 Narishige).
6. Borosilicate glass capillaries (1 mm o.d. Clarke Electromedical Instruments).
7. Appropriate sample holder (generally machined Perspex to suite subject) mounted on a standard mechanical micromanipulator (Harvard Apparatus UK). (*See* Fig. 1 for examples.)
8. A rigid metal base plate (e.g., Leitz or custom built) to which **items 1**, **3,** and 7 can be firmly bolted to avoid relative movement.

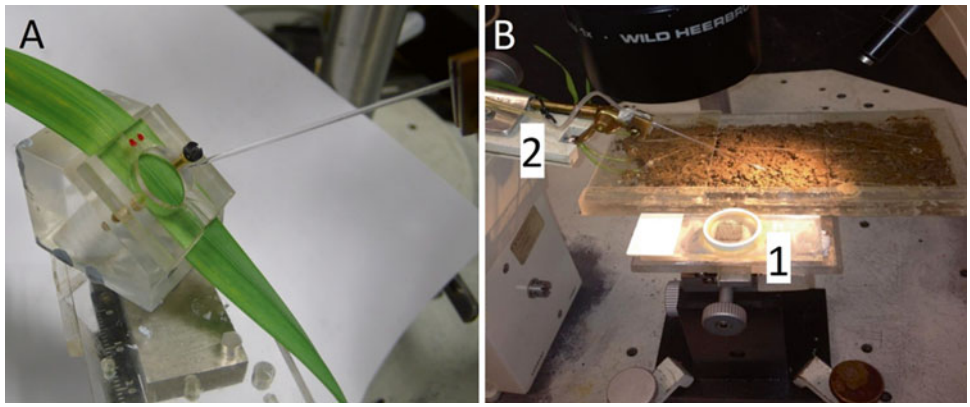

Fig. 1 Sampling and transfer of sample to CE analysis procedure. (**a**) Typical holder for a monocot leaf (hydroponic daffodil). (**b**) Wheat root microcosm (for rhizosphere) (for left-handed worker). The sample is transferred to the "oil well" (1) by raising the capillary, moving the well to the previous position of the soil or cell and lowering the capillary into the paraffin oil. The clamped capillary has been filled with silicone oil and attached to a plastic tube (2) leading to the branched pneumatic system described in Subheading 2.2.2, **item 2**. Scale: Glass capillary is 1 mm o.d.

9. Before mounting on the micromanipulator, the capillaries were filled with low viscosity silicone oil (water saturated) perfused into the microcapillary through a precision pipette needle (e.g., SGE type 100 replacement needle) mounted on a *glass* (*see* **Note 1**) syringe barrel (Hawksley, West Sussex, UK).
10. Watchmakers tweezers (Dumont Type 7. TAAB) for fine manual manipulation.
11. Glass cutting knife (Sigma Aldrich) to trim capillaries to appropriate length.

2.2.2 Sample Manipulation

1. The custom-built "oil well" (Figs. 1b and 4a) is the starting point of the CE analysis. A plastic or aluminum ring (a slice from a suitable tube) is attached with oil-resistant epoxy resin (Araldite) to a standard 76×26 mm microscope slide. A transparent reference grid (10 mm square) made by reduction photocopying of a suitable pattern onto overhead projector film (Lyreco) is attached with clear adhesive tape to the underside of the slide to enable identification of droplets (Figs. 4a and 5) (*see* **Note 1**).
2. A pneumatic manipulation system consisting of a 50 ml plastic syringe barrel attached to the open end of the glass capillary (or pipette) via a plastic tube (1 mm i.d.) (Fig. 1b). A side arm vent to the atmosphere was regulated using a solenoid "pinch valve" (constructed from a push 24VDC solenoid (part no 307-3405 RS Components Ltd, UK) pressing on a soft section of the side arm) activated by a foot pump (part no 316-901; RS). Pipette pressure is altered using the syringe and can be "instantly" returned to atmospheric by releasing the solenoid [9] (*see* **Note 2**).
3. Freshly pulled capillaries have a tip diameter of approximately 0.1 μm. For the SiCSA techniques, this needs to be widened to between 1 and 2 μm. To open the tip aperture, a new capillary is trimmed by gently lowering it onto the surface of the microforge heating element until a visible displacement (<5 μm) is seen (Fig. 2a) (*see* **Note 3**).
4. Constriction pipettes are constructed by brief melting of a side of a capillary at the required distance from the tip (Fig. 2b).

2.2.3 Capillary Electrophoresis Setup (Fig. 3)

1. *Safety note*. The CE apparatus is custom built and includes a very high voltage circuit. Ensure that it is regularly checked for Health & Safety requirements and serviced by the appropriate members of the Institution. Always adjust the current limiter setting on the power supply to a level just above the running current (*see* **Note 4**).
2. Earthed metal housing with door linked to power cut off on power supply (**item 4**). [A stripped-down microwave oven casing (Fig. 3) can play this role.]

Fig. 2 Preparing microcapillary tips and constriction pipettes. (**a**) To open the tip aperture, a new capillary is trimmed by gently lowering it onto the surface of the microforge heating element (1) until a visible displacement (<5 μm) is seen. (**b**) Forging the constriction. A large volume (nl range) pipette is shown. Scale: Heating element (**a**) approx 40 μm diameter

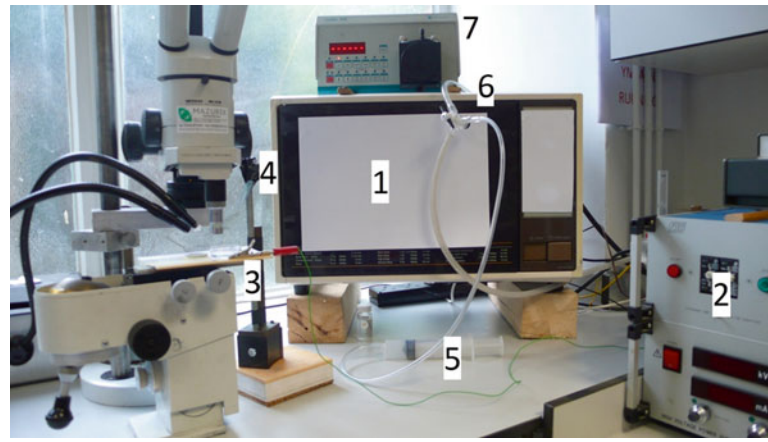

Fig. 3 A typical SiCSA-CE configuration. The high voltage electrode housing (detail Fig. 4b) is housed in an earthed metal box with a safety latch door (1) linked to the cutoff terminal on the high voltage power supply (2). The earth electrode and buffer (3; also detail in Fig. 4a) is mounted on a micromanipulator to allow smooth replacement of the "oil well" by the buffer. The CE column is moved up and down manually during this process through a plastic sleeve (4; a 1 ml Gilson tip is illustrated). Light pneumatic pressure and suction is applied to the column using a 50 ml syringe (5) attached to a three way tap (6), the other two exits of which are attached to the live electrode housing (Fig. 4b) and an air pump (suction) (not shown). The CE column passes through the CE cell of a spectrophotometer (7) where the polyamide coating (for 5 mm) has been removed to allow light transmittance

3. Earth electrode and buffer mounted alongside "oil well" storage system (Fig. 4a) on micromanipulator (Fig. 3).
4. "Live" platinum electrode and buffer (Fig. 4b) linked to air (suction) pump (KNF, Freiburg. N035AN.18 IP20) and to a manual pneumatic system (Fig. 3) (after [15]). (In the housing (**item 2**).)

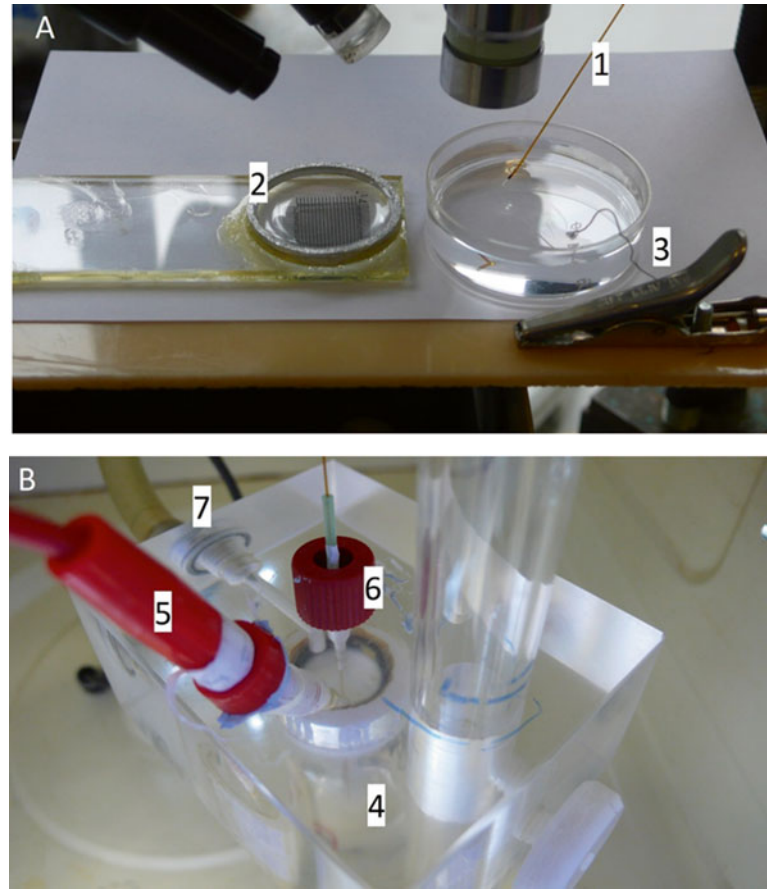

Fig. 4 A typical SiCSA-CE configuration (details). (**a**) Loading. The samples are drawn into the CE column (1; see detail Fig. 5) from the "oil well" (2), before raising the column, moving the buffer and earth electrode (3) into the previous position of the "oil well" and lowering the column. (This second position is shown.) (*See* **Note 5**). (**b**) Live electrode housing. The buffer (*see* **Note 6**) is contained in a 20 ml scintillation vial (4), screwed against an O-ring into a vial cap held firmly in a Perspex block using PTFE pipe-sealing tape (*see* **Note 7**). The center of the vial lid has been cut away to allow access for the live (platinum) electrode (5), the CE column (held in pace by a section of hplc tube in an hplc ferrule (6); air leakage is minimized by the use of PTFE tape) and the air exhaust to the pump or pneumatic syringe (7). The height of the housing can be adjusted to match that of the earth buffer to avoid siphoning artifacts. The Scale: Knurled hplc ferrule at (6) 12 mm o.d.

5. High voltage power supply (max 30 kV) FUG type HCN-6 M 30000 (Omiran Ltd, Suffolk).
6. UV-VIS spectrometer Lambda 1010 (Bischoff, Leonberg) fitted with a CE cell.
7. Polyimide-coated fused-silica capillaries; 50 μm id; 365 μm o.d. (Composite Metal Services Ltd, Shipley). Length 60–100 cm (cut with glass-cutting knife) from which the polyimide

coating had been burnt away (using a cigarette lighter) at the ends (5 mm; Figs. 4a and 5) and to make a "window" (5 mm) within the spectrometer. (The window was occasionally cleaned with isopropanol.)

8. Stereo microscope (Leitz Wild M8; or M3Z for higher magnification (Fig. 3)) equipped with an eye-piece graticule.
9. Data acquisition software; Clarity Lite by Data Apex (Spectro Service Ltd).
10. CE Buffers: For anions: 2.5 mM pyromellitic acid, 15 mM Tris, and 1 mM DoTAOH (prepared from DoTAB by ion exchange) pH 8.1 [15] [254 nm—indirect] Positive polarity. Internal standard Na Molybdate.

    For cations: 5 mM Imidazolesulfate, 2 mM 18-crown-6, pH 4.5 [15] [214 nm—indirect] Negative polarity. Internal standard CsCl.

    For sugars: 6 mM copper(II)sulfate; 500 mM ammonia at pH 11.6 [16] [245 nm—direct] Negative polarity. Various internal standards—e.g. glucose.

    For uranium (as UO_2^{2+}): 10 mM Citrate (pH 3.0) [17] [220 nm—direct] Negative polarity.

    For phenols: 43 mM NaTetraborate, 27 mM KH_2Phosphate, 8.5% acetonitrile (pH 9.15) [18] [240 nm—direct] Negative polarity. Internal standard L-DOPA.

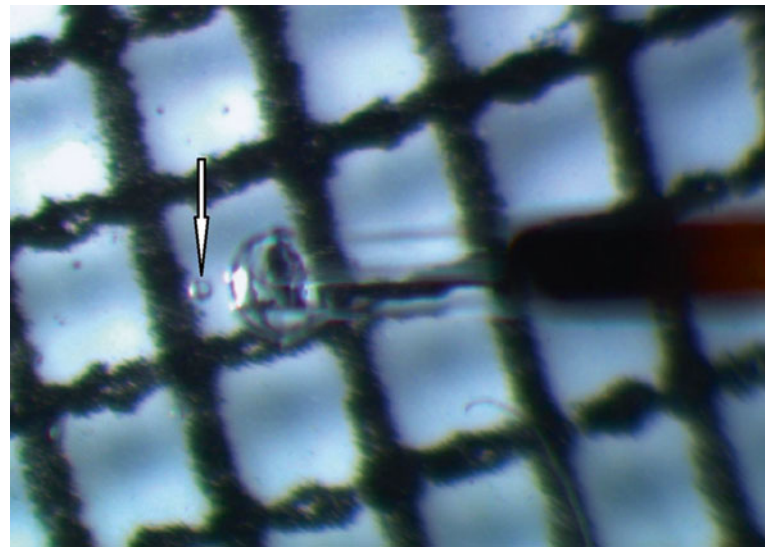

Fig. 5 Loading sample into CE column. The CE capillary (*right*) and sample (*arrowed*) are illustrated. Using the micromanipulator, the "oil well" is moved to bring the sample close to the CE column. The pneumatic syringe is used to extrude a small droplet of buffer (illustrated). The sample is then brought into contact with this "tongue," which is then withdrawn back into the column. Scale: CE column is 360 μm o.d. (without polyimide coat)

11. Each new capillary was conditioned by sucking (with the air pump; Fig. 3) 1 M NaOH, water and running buffer each for 20 min from the earth-buffer reservoir. This was also done if background noise became excessive. Columns were similarly washed with electrolyte for >3 min after every run (*see* **Note 8**).

3 Methods

Once set up, the apparatus can be used to sample a wide range of cells. (If given a self-contained power supply, this includes sampling in the field.) Unlike the cell pressure probe by Tomos et al. [1], it is not essential to prevent all vibration of the sample as leakage at the plasma membrane has little influence other than loss of sample volume. Although the tissue does need to be held sufficiently firmly to allow penetration of the cell wall rather than displacement by the capillary tip. The larger the cell, and the smaller the elastic modulus will result in the largest sample (*see* **Note 9**).

3.1 Plant Materials

The nature of the experimental system is very variable—but representative and contrasting examples of suitable subjects are as follows:

3.1.1 Leaves and Hydroponic Roots

Leaf growth can be typified by barley seedings grown (10–20 days) in potting compost (John Innes No 1) in 7 cm square pots. Using a soilless hydroponic system, however, allowed easy access to both leaf [19] and root [20] cells (*see* **Note 10**). These were incubated in a growth chamber (Sanyo Fitotron, SGC066.CPX). Typical conditions were 16 h light (20 °C), 8 h dark (16 °C), and 75% humidity. Light intensity was 480 μmol/m² s at leaf level. A typical leaf holder for sampling is shown in Fig. 1a.

3.1.2 Roots and Rhizosphere

Lupin albus (inoculated with Rhizobium) or wheat seeds were planted at the top of microcosms constructed from sheets of Perspex (of appropriate dimensions) covered with a series of microscope glass slides that could be removed individually to access the soil and roots. Perspex fillets on either side of the sheet maintained a 5 mm gap was filled with soil between the Perspex and glass. Figure 1b illustrates an example for 4–10 days wheat seedlings where the glass cover consisted of three 76×52 mm glass slides (Clarity). For older, larger, roots this setup was scaled up and Perspex sheets replaced the glass. These microcosms were maintained at approximately 20% moisture content by periodically opening and spraying deionized water. They were wrapped in black plastic film to avoid phototropic effects and algal growth. The entire package was held together with document clips and placed at a 30% angle from the vertical, glass side down, to increase the number of roots accessible for sampling. This was incubated in a growth chamber as in Subheading 3.1.1.

In the case of soil phenolic metabolism (Fig. 1b), the entire microcosm was sprayed with 5–20 mM phenolic solutions (e.g., syringic acid). Sampling at times intervals was then initiated within 1 mm of visible regions of roots (of known distances from the root tips.) In the case of uranium/organic acid interaction [6], small (1 mm) corroded fragments of depleted uranium shrapnel (collected from the QinetiQ, Eskmeals, UK site) were placed in the Lupin microcosm when cluster-root acid efflux was anticipated and sampling commenced.

3.2 Sampling of Single Cells and Microcosms

Sampling from cells of all types was driven by hydrostatic (turgor) pressure (generally in the 0.1–1 MPa range [1]) that forced vacuolar sap into the capillary as soon as the cell wall was punctured (Fig. 6a). The capillary was then removed immediately from the cell (*see* **Note 11**) and its contents expelled under the paraffin oil of the "oil well" to await analysis.

Sampling cells below the surface offers more of a challenge and individual cases require ingenuity. For example, leaf mesophyll and bundle sheath cells were accessed through the stomatal pore [3, 21]. Other cells can be reached by limited dissection [22] or careful penetration through overlying cells [20].

Sampling from soil was (generally) driven by the capillary force of the constriction pipette once the tip came into contact with a depot of soil moisture (Fig. 6b). (In the case of sandy soil these could be seen at the contact points between individual sand particles.) Occasionally, especially if μm-range soil particles are present, the pneumatic control can be used to apply a degree of suction (<0.1 MPa). By both approaches the capillary is filled up to the constriction.

3.3 Manipulation

The "oil well" is filled with water-saturated paraffin oil. Depot droplets of standards and water for rinsing capillary tips (typically approximately 200 nl) are deposited by hand at suitable positions on the grid, using a 2 μl automatic pipette (Gilson) fitted with a microloader tip.

Samples from the experimental systems (cells or soil) were loaded onto the grids as noted earlier. Subsequent manipulation was achieved by the use of appropriate size (10 pl to 5 nl) constriction pipettes (Fig. 6c) mounted on a micromanipulator and controlled using the syringe air pump described in Subheading 2.2.2, **item 2**. Preparation for quantification of the target solute was initiated by transferring an aliquot from the sample to another location on the grid using the constriction pipette. The pipette was then rinsed in a clean water droplet before being used to transfer an identical volume of internal standard, from a standard depot, to the aliquotted sample. The identical volumes allow subsequent quantification of the analytes from the known internal standard concentrations without having to measure the sample volumes [23, 24].

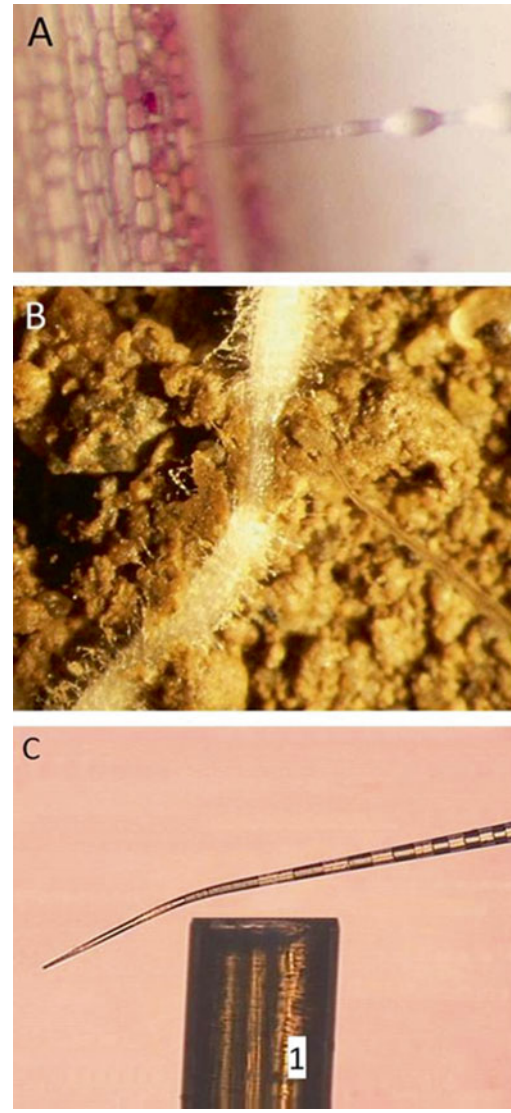

Fig. 6 Cell and soil sampling. (**a**) *Lolium temulentum* leaf sheath cells and approaching sampling capillary. (**b**) Rice root and rhizosphere with sampling constriction pipette. (**c**) Constriction pipette (containing multiple standard samples of identical volume) and CE column (1) compared. Scale: CE column (A) 365 μm o.d. (*see* **Note 17**). All three images close to identical magnification

3.4 CE Analysis of pl and nl Droplets

The combined sample/standard droplet was then drawn into the (to-be-earthed) end of the CE column. This was achieved by manipulating the "oil well" (rather than the column) until the sample was less than 100 μm from the column end (Fig. 5). By applying mild pressure to the (to-be-live) end of the CE column (via the pneumatic side arm; Figs. 3 and 4) a small droplet of CE buffer emerged from the end close to the sample (Fig. 5). Further manipulation of the "oil well" brought the sample into contact with this buffer—and the two mixed.

Application of mild suction to the CE column drew the projecting buffer/sample back into the column (*see* **Note 12**). The column was then rapidly and smoothly raised from the oil using a plastic sleeve (e.g., the 1 ml pipette tip in Fig. 3), and the earth electrode and buffer moved to its place. The CE column was immediately lowered into the buffer (Fig. 4a), the CE voltage switched on, and the recording software activated. Detection is by direct or indirect UV detection (*see* Subheading 2.2.3, **item 9**) with the signal processed using either chromatography or CE software (also *see* **Note 13**). It was important to ensure that as little oil as possible enters the CE column during loading as such contamination can cause artifacts as the droplets pass the detector—or even block the essential electrical electrophoretic circuit. By ensuring that the surface of the earth buffer and of the live buffer was at the same level (Fig. 4b), loss of sample and other artifacts due to siphoning was reduced to a minimum (*see* **Note 14**).

This entire process is made easier by ensuring *absolute* cleanliness of the floor of the oil well and of the oil, from which all traces of visible water and dust must be removed. "Oil wells" were cleaned after use by irrigation with ethanol followed by irrigation in UHQ water before drying (*see* **Note 15**). This resulted in spherical droplets resting on the well floor (*see* **Note 16**). Measurement of their diameters (*see* **Note 17**) allowed a calculation of approximate volume that could be used to confirm solute concentrations (but *see* **Note 18**).

4 Notes

1. Silicone oil will swell the rubber plunger of plastic syringes making them stiff. It also tends to dissolve the printing on the "oil well" reference grid, which will require regular replacement.
2. With practice, this enables volumes to be handled at pl precision.
3. As the tips block, they can be reopened by gentle abrasion against a suitable surface of Perspex. It is not recommended, however, to use tips larger than some 4 μm.
4. The FUG 30000 HCN-6M 30000 has a maximum output of 200 μA. At the initiation of a new buffer system (or if using a column of significantly different dimensions) set the current limiter to a position just above the expected current. Since the system described is not temperature controlled, the current may drift during a series of runs. The limiter should be set with this in mind. If the limiter current is exceeded during a run, the voltage will drop, resulting in a discontinuity of the electrophoresis.
5. It is essential to transfer the column to the buffer smoothly and quickly. The protocol described can be followed by viewing through the microscope, which will be focused on the original position of the sample—and at a suitable position for the earth end of the CE column.

6. Fresh buffer is required at least once a day. It is impractical to eliminate all air leakage around the column port as easy replacement of the column is required. Air drawn into the vial through the sleeve tends to lead to some evaporation of the buffer resulting in different buffer compositions on either end of the column. This is a cause of artifacts. Slight degassing of the buffer with minimum surface disturbance is an indication of sufficient vacuum.
7. PTFE tape, rather than adhesive as, with time the cap becomes worn and can be replaced without constructing the entire housing.
8. The lifetime of columns varies enormously. During training, several may be needed a day. With practice, a column may last for many weeks. Some buffer types can be readily replaced without changing the column. In practice, however, it is best to make a new column for each new buffer type.
9. Cells with a maximum dimension down to about 20 μm are accessible with practice. Note that the sample is generally dominated by vacuolar material and will only be a small proportion (ΔV) of the entire cell volume (V),

$$\frac{\Delta V}{V} \leq \frac{\text{Turgor}}{\epsilon}$$

where ε is the volumetric elastic modulus [25].
10. Soilless systems, although requiring a little more effort to set up, are very suited to traditional chemistry/biochemistry/molecular biology laboratories, for which procuring, handling, and disposing of soil can be a logistical problem. A simple hydroponic system only requires a beaker and an aquarium pump to oxygenate the nutrient solution.
11. This must be removed as quickly as possible (typically $< s$) after insertion of the capillary to avoid dilution as osmotic water enters the cell once water potential equilibrium across cell membranes is lost [14].
12. This is, in effect, a conventional hydrostatic loading. Bazzanella et al. [15] promoted this loading step by grinding the column end to a cone on a grinding wheel. This difficult procedure is not essential; although a simple ground bevel (as with a hypodermic needle) facing downwards was found to be a useful compromise in bringing the column bore closer to the floor of the "well." (Generally cutting the capillary with the glasscutter resulted in such a bevel. Rotating it to the correct orientation requires a bit of practice and was helped by the use of an adhesive paper label wrapped around a free section of the column to indicate its orientation without having to determine this under the microscope.)

13. A range of other detectors can be added to the custom-built CE system described here. We have had some initial success with the relatively inexpensive Argos 250B Mercury-Xenon-lamp-induced fluorescence detector (Flux Instruments).
14. Very occasionally, especially for larger (nl-scale) samples, bringing the bore of the CE column into contact with the sample droplet led to that droplet entering the column by capillary action, with no need for pressure manipulation.
15. Total dryness is essential as residual water droplets can mix with or be confused with samples and standards.
16. When droplets were released from the pipettes a little above the well floor, they will sediment downward to rest on it—displaying a small contact dimple. This is best achieved with the smallest pipette tip diameters (1 μm). Another "trick" is to use the manipulator to rapidly pull the pipette away from the droplet suspended (by surface tension) at its tip. This generally releases the droplet, but the resulting turbulence in the oil will result in the droplet sedimenting to the floor at an unpredictable point on the grid.
17. The very precise o.d. of the CE column is a useful standard against which to calibrate microscope eyepiece graticules (at different zoom values).
18. Each application raises new technical challenges. One of particular frustration is the difficulty caused by solutes of low polarity. The use of paraffin oil to prevent evaporation of the small samples is inappropriate for solutes such as chlorophenol (of interest to phytoremediation studies)—which rapidly dissolve out of the aqueous droplet. This also causes problems for another useful variant of CE—micellar electrokinetic separation [26]—that involves the use of detergents such as SDS. This material destabilizes the discrete aqueous droplets.

Acknowledgements

I gratefully thank Drs Alexis Bazzanella and Holger Lochmann (Arbeitsgruppe Bächmann, Darmstadt) and Prof Uli Schurr (now Jülich) for introducing me to the CE technique. Parts of the work were funded by DFG, BBSRC, NERC and the Governments of Wales, Libya and Saudi Arabia. I thank Ms Taghreed Alnusaire and Drs. Anthony Anisiobi and Naoki Morizuka for Figs. 1b, 5 and 6b.

References

1. Tomos AD, Leigh RA (1999) The pressure probe: a versatile tool in plant cell physiology. Annu Rev Plant Physiol Plant Mol Biol 50:447–472
2. Tomos AD, Sharrock RA (2001) Cell sampling and analysis (SiCSA). Metabolites measured at single cell resolution. J Exp Bot 52:623–630
3. Lu C, Koroleva OA, Farrar JF, Gallagher J, Pollock CJ, Tomos AD (2002) Measuring light-dependent gene expression in individual barley leaf cells using single-cell reverse transcription polymerase chain reaction (SC-RT-PCR). Plant Physiol 130:1335–1348
4. Fricke W (2013) Plant single cell sampling. Methods Mol Biol 953:209–231
5. Webster J, Davey RA, Smirnoff N, Fricke W, Hinde P, Tomos AD, Turner JCR (1995) Mannitol and hexoses are components of Buller's Drop. Mycol Res 99:833–838
6. Tandy S, Brittain SR, Grail BM, Mcleod CW, Paterson E, Tomos AD (2013) Fine scale measurement and mapping of uranium in soil solution in soil and plant-soil microcosms, with special reference to depleted uranium. Plant Soil 368:471–482
7. Camilleri P (ed) (1998) Capillary electrophoresis. Theory and practice, 2nd edn. CRC Press, Boca Raton, FL
8. Marina ML, Ríos A, Valcárcel M (eds) (2005) Analysis and detection by capillary electrophoresis. Comprehensive analytical chemistry. Vol 45. Elsevier
9. Tomos AD, Hinde P, Richardson P, Pritchard J, Fricke W (1994) Microsampling and measurements of solutes in single cells. In: Harris N, Oparka K (eds) Plant cell biology—a practical approach. IRL Press, Oxford, pp 297–314
10. Wieland K, Thiele B, Schurr U (2008) Analysis of alkaloids in single plant cells by capillary electrophoresis. Methods Mol Biol 384:771–782
11. Zenobi R (2013) Single-cell metabolomics: analytical and biological perspectives. Science 342:1201–1210
12. McCully ME, Canny MJ, Huang CX (2009) Cryo-scanning electron microscopy (CSEM) in the advancement of functional plant biology. Morphological and anatomical applications. Funct Plant Biol 36:97–124
13. Tomos AD (1988) Cellular water relations of plants. In Franks F (ed) Water science reviews Vol 3, Cambridge U.P., pp 186–277
14. Malone M, Tomos AD (1992) Measurement of gradients of water potential in elongating pea stem by pressure probe and picoliter osmometry. J Exp Bot 43:1325–1331
15. Bazzanella A, Lochmann H, Tomos AD, Bächmann K (1998) Determination of inorganic cations and anions in single plant cells by capillary zone electrophoresis. J Chromatogr A 809:231–239
16. Bazzanella A, Bächmann K (1998) Separation and direct UV detection of sugars by capillary electrophoresis using chelation of copper (II). J Chromatogr A 799:283–288
17. Al-Salih HS, Fathi RA, Godbold DL, Tomos AD (2014) Detection of uranium contamination in *Acacia* cell sap by capillary zone electrophoresis (CZE) technique. J Nat Sci Res 4:40–48
18. Lima DLD, Duarte AC, Esteves VI (2007) Optimization of phenolic compounds analysis by capillary electrophoresis. Talanta 72:1404–1409
19. Fricke W, Hinde PS, Leigh RA, Tomos AD (1995) Vacuolar solutes in the upper epidermis of barley leaves. Intercellular differences follow patterns. Planta 196:40–49
20. Pritchard J, Fricke W, Tomos AD (1996) Turgor-regulation during extension growth and osmotic stress of maize roots. An example of single—cell mapping. Plant Soil 187:11–21
21. Koroleva OA, Farrar JF, Tomos AD, Pollock CJ (1997) Solute patterns in individual mesophyll, bundle sheath and epidermal cells of barley leaves induced to accumulate carbohydrate. New Phytol 136:97–104
22. Knoblauch M, van Bel AJE (1998) Sieve tubes in action. Plant Cell 10:35–50
23. Malone M, Leigh RA, Tomos AD (1991) Concentrations of vacuolar inorganic ions in individual cells of intact wheat leaf epidermis. J Exp Bot 42:305–309
24. Beckers JL, Boček P (2004) Calibrationless quantitative analysis by indirect UV absorbance detection in capillary zone electrophoresis: the concept of the conversion factor. Electrophoresis 25:338–343
25. Dainty J (1963) Water relations of plant cells. Adv Botanical Res 1:279–326
26. Terabe S (2009) Capillary separation: Micellar electrokinetic chromatography. Ann Rev Anal Chem 2:99–120

Part II

Applications from Small to Macromolecules

Chapter 12

Analysis of Small Ions with Capillary Electrophoresis

Jatinder Singh Aulakh, Ramandeep Kaur, and Ashok Kumar Malik

Abstract

Small inorganic ions are easily separated through capillary electrophoresis because they have a high charge-to-mass ratio and suffer little from some of the undesired phenomenon affecting higher molecular weight species like adsorption to the capillary wall, decomposition, and precipitation. This chapter is focused on the analysis of small ions other than metal ions using capillary electrophoresis. Methods are described for the determination of ions of nitrogen, phosphorus, sulfur, fluorine, chlorine, bromine, and iodine.

Key words Capillary electrophoresis, Small ions, Nitrogen, Phosphorus, Sulfur, Fluorine, Chlorine, Bromine, Iodine

1 Introduction

Inorganic ions are important constituent of our nutrition and environment. As most of them are charged so the methods of choice in their analysis are capillary electrophoresis (CE). CE is a versatile technique and allows the analysis of a wide range of these analytes. It is very economical as it uses very low volumes of sample and electrolyte. This chapter is focused especially on small ions other than metal ions which include nitrates, phosphates, sulfides, halides, etc. Various review articles have been published focusing the presence of these ions in various environmental, food, and biological matrices [1–6].

Nitrogen containing ions include ammonium, nitrites, and nitrates. These are the major components of water entering from nitrogen-containing fertilizers from the fields, industrial waste, and products of feces. Nitrites are very harmful to human and animals as long exposure to them causes severe digestive and excretory system problems [7]. Nitrates and nitrites have been analyzed by capillary electrophoresis in seawater and natural water [8–10], vegetables and meat products [11], rat brain [12], and neuronal tissue [13].

Philippe Schmitt-Kopplin (ed.), *Capillary Electrophoresis: Methods and Protocols*, Methods in Molecular Biology, vol. 1483,
DOI 10.1007/978-1-4939-6403-1_12,

Phosphorus oxoacids and their salts have wide application in agriculture, industry, and biological processes. But excess of phosphate in water causes algal growth resulting in eutrophication. Phosphates are harmful to us as they cause kidney and bone diseases [14]. So their analysis in the environment is very important. Stover had reviewed CE methods for the analysis of phosphates with special emphasis on effect of electrolytes on separations and their applications to real samples [15]. Several excellent reviews have been published covering the analysis of small phosphorus-containing compounds in various matrices with CE employing different detection modes [15–18].

Sulfur and its compounds have remarkable use in agriculture and industries. They play an important role in the human metabolism and environmental cycles. These compounds are interlinked with oxidation and reduction processes. Some of the forms (e.g., H_2S) are quite toxic and they interfere with other ions such as metal ions [19]. So their analysis is very crucial for determining their potential impact on environment. Anions like sulfide and thiocyanate show UV absorbance and thus determined by direct UV detection [20]. Nonabsorbing anion like sulfates requires chromophoric compound in the background electrolyte and are detected with indirect UV detection [21]. Several buffers have been used for the determination of sulfur anions in various matrices including chromate [20, 22], phthalate [23], naphthalenesulphonates [24], pyromellitic acid [25, 26], and p-aminobenzoate [27].

Chlorine is the most widely used chemical for disinfection of water and wastes. It is also used as bleaching agent in paper and textile industry. It undergoes oxidation leading to the formation of anions with various oxidation states such as hypochlorite, chlorite, chlorate, and perchlorate [28]. These anions are very toxic even in low concentration so their determination is very important. For chlorine-containing anions indirect UV detection is the most popular detection mode. Jones and Jandik [29] have shown the CE separation of 36 different anions including several chlorine-containing anions using chromate electrolyte with indirect UV detection. Wu et al. [30] used 0.4 mM cetyltrimethylammonium bromide (CTAB) and Pirogov [31] used 2, 4-ionenes as capillary modifiers for the determination of chlorine-containing anions and several other anions. Electrochemical detection, i.e., amperometric, potentiometric, and conductometric detection is an alternative to optical detection for CE for these ions due to their excellent sensitivity as compared to the latter [32, 33].

Bromide ion is found in water and metabolic system along with chloride ion. It readily undergoes oxidation and forms oxidized products and even converted to acids. Bromate found in water is toxic due to its carcinogenic nature [34]. Bromide ions show high UV absorbance at 190–200 nm so can be determined with direct UV detection. Guan et al. [34] used bromide ions as

internal standard for the detection of nitrite and nitrate employing tetraborate as carrier electrolyte. This method could be used for the determination of bromide ions itself. Several anions including bromide ions have been determined by Song et al. [35] using NaCl buffer. Soga et al. [36] analyzed many UV absorbing anions with polyethyleneglycol-coated capillary which suppressed electroosmotic flow [EOF] using 20 mM phosphate buffer. A NaCl-based low pH buffer (10 mM sodium dithionate and 5 mM acetic acid) method has been developed by Rantakokko et al. for the determination of bromide ion in raw and drinking water [37].

Fluoride plays an important role in the prevention of cavities and hence a major component of toothpastes. The main source of fluoride emission in the environment is the various chemical processes such as metal smelting, aluminum reduction, and phosphate fertilization production. Excessive fluoride in the environment has bad effect not only on human health and livestock but also on agriculture and ecosystem [38]. Skocir et al. [39] and Shamsi et al. [40] have qualitatively determined fluoride in the toothpaste. CE method using CTAB as electroosmotic flow modifier and tungstate as internal indicator for the fluoride determination has been described by Wang et al. [41]. It is difficult to determine fluoride in natural waters due to complexation of fluoride with metal ions such as iron, calcium, etc., leading to poor detection. But this could be eliminated by addition of complexing agents like 1,2-cyclohexylenedinitrilotetraacetic acid (CDTA) [42], sodium 1,2-dihydroxybenzene-3,5-disulfonate (Tiron) [43], or citrate [44].

Iodine is one of the essential microelement needed for the appropriate functioning of thyroid gland [45]. Iodine nutrition has great impact on the neurological development. Therefore, determination of iodide and iodine species is very important in food, clinical, biological, environmental, and industrial samples [46]. Semenova et al. [47] described a CE-based method for the determination of iodide with UV detection at 230 nm in various matrices. Iodine in sea water has been qualitatively determined by Carou et al. [48] using mix of 50 mM borate and 1.5 mM sodium chloride as BGE while Mori et al. [49] used 0.3 M NaCl, 10 mM Zwittergent-3-14, 50 mM of nonionic surfactant Tween 20, and 5 mM phosphate (pH 7).

2 Material and Equipment

2.1 Analysis of Ammonium Ions and Metal Ions Using Ionic Liquid-Coated Capillary

The greatly improved resolution of the metal ions can be achieved by using the ionic-liquid coated capillary in which the EOF is reversed. The capillary zone electrophoresis (CZE) potential gradient detection (PGD) method coupled with field-amplified sample injection (FASI) can separate and detect the 11 ions with lower LOD than the conventional indirect optical detection method and

with acceptable reproducibility. A method giving comparison of normal and coated capillary for the analysis of ammonium ions is described here [50].

1. *Analytes*: Ammonium ions, nickel, lead, alkali, and alkaline metal ions.
2. *Stock solution preparation*: Prepare the stock solution by dissolving nitrates of ammonium, alkali and alkaline earth metals, nickel, and lead ions in distilled water with a concentration of 1 mg/ml. Filter all solutions with 0.20 μm filter and degas in an ultrasonic bath.
3. *CE instrumentation and capillary*: Prince CE system (Lauerlabs, The Netherlands) equipped UVIS 200 detector. For the CE–PGD (Post Gradient Detection) system use an IA-P1 (CE Resources, Singapore, Republic of Singapore) with CSW17 software (DataApex, Prague, Czech Republic) for recording electropherogram. Fused-silica capillaries of 50 μm I.D. × 360 μm O.D. (Polymicro Technologies, Phoenix, AZ, USA) used.
4. *CE Buffer*: 7.5 mM lactic acid, 0.6 mM 18-crown-6, 12 mM α-cyclodextrin (α-CD); adjust the pH to 4.0 by 1-hexyl-3-methylimidazolium hydroxide (HMIM hydroxide).

2.2 Analysis of Nitrite and Nitrate Ion [51]

Direct determination of nitrite and nitrate can be achieved by high performance capillary electrophoresis (HPCE). Nitrite, nitrate, and bromide (an internal standard) are well separated in the optimized buffer 20 mM of tetraborate plus 1.1 mM of cetyltrimethylammonium chloride (CTAC) as described in the method below.

1. *Analyte*: Nitrite, nitrate, and bromide.
2. *Stock solution*: Prepare stock solutions of sodium nitrite, sodium nitrate, sodium bromide (internal standard) in distilled water having concentration of 1.00 mg/ml.
3. *Sample*: River and tap water
4. *Sample preparation*: River and tap water spiked with nitrite and nitrate. No pretreatment is required other than filtration through 0.45 μm membrane.
5. *CE instrumentation and capillary*: CE system consists of BioFocus 3000 capillary electrophoresis system equipped with a high-voltage power supply (30 kV) and control software. A fused-silica capillary with 50 cm total length (45.5 cm to detector), 50 μm I.D., and 375 μm O.D.
6. *CE buffer*: 20 mM tetraborate (pH 8.94), 1.1 mM Cetyltrimethylammonium chloride (CTAC).

2.3 Analysis of Sulfur-Containing Anions in Complex Matrix

CE with conductivity detection and electrokinetic injection could be successfully applied for the determination of sulfur-containing anions as this injection mode is an excellent possibility to avoid contamination by the matrix and to preconcentrate the analytes via stacking processes [19].

1. *Analytes*: Sulfide, sulfate, thiocyanate, thiosulfate, sulfite.
2. *Stock Solutions*: Prepare standard solutions of sulfur containing anion from sodium sulfide, sulfate, sulfite, thiosulfate, and thiocyanate. All the standard solution prepared in triply distilled water.
3. *Sample*: Water samples of an open-pit mining lake from depth of 0.2 to 24 m.
4. *Sample preparation*: Collect the samples before and after precipitation of humic acid. Precipitation is done by addition of Fe (III) salts which lead to change in pH from 7.7 to 5.8. Samples containing humic substance are dark colored and have phenolic smell but samples after precipitation are light-brown colored with no significant smell. Filter the samples before analysis.
5. *CE instrumentation and Capillary*: For UV detection use CE with variable-wavelength UV detector, 900 series interface (270 A-HT system, PE applied Biosystems, Germany) and data acquisition with Turbochrom 4 software. A fused-silica capillary of 72 cm (50 cm to the detection window) × 75 μm I.D. For conductivity detection, use a Crystal CE system Model 310 by ATI Unicam (Boston, MA, USA) with Crystal 1000 conductivity detector and capillary (72 cm × 75 μm).
6. *CE Buffer*: Use two sets of buffer for UV detection (a) 1.5 mM pyromellitic acid (as a representative of buffer with low mobility 0.55 $cm^2/kV\ s$), 10 mM tris (hydroxymethyl) aminomethane (Tris), pH 9.15, (b) 5 mM sodium chromate (as a representative of buffer with high mobility 0.72 $cm^2/kV\ s$), 0.5 mM CTAB pH 8.0. For conductivity detection 50 mM cyclohexylaminoethanesulfonic acid (CHES), 35 mM LiOH, 0.03% Triton X-100 pH 9.2.

2.4 Analysis of Phosphorus Ions (In-Capillary Complexation)

CE method for the simultaneous determination of phosphonate, phosphate, and diphosphate is described below. In the presence of CH_3CN as an auxiliary solvent, the in-capillary complexation of phosphonate, phosphate, and diphosphate with Mo(VI) formed anionic polyoxomolybdate complexes: $[H_6(PHO_3)_2Mo_{15}O_{48}]^{4-}$, $[(PO_4)Mo_{12}O_{36}]^{3-}$, and $[(P_2O_7)Mo_{18}O_{54}]^{4-}$, respectively. The polyoxomolybdate anions, which were kinetically stable in the presence of an excess of Mo(VI), migrated toward the anode at different electrophoretic mobilities in the capillary [52].

1. *Analytes*: Phosphonate, phosphate, and diphosphate.

2. *Stock Solution*: Prepare standard solutions of phosphonate, phosphate, and diphosphate by the direct dissolution of H_2PHO_3, NaH_2PO_4, and $Na_4P_2O_7{\cdot}10H_2O$, respectively, in Millipore water. Prepare solutions of Mo (VI) by dissolving appropriate amounts of $Na_2MoO_4{\cdot}2H_2O$.
3. *Sample*: Tap water.
4. *Sample preparation*: Spike the tap water with these analytes.
5. *CE instrumentation and capillary*: CE system equipped with UV detector and Hitachi Model D-2500 chromato integrator. Capillary dimensions: 70 cm fused-silica capillary with 75 μm ID.
6. *CE buffer*: 3.0 mM Mo(VI), 45 % v/v CH_3CN, 0.05 M malonate buffer (pH 3.0).

2.5 Analysis of Bromide Ions

Presence of bromide ion influences the formation and disappearance of oxidants and formation of trihalomethanes (THMs) which have potential cancer risk. Sea water is rich in bromide ion concentration. Industries close to seawater uses seawater as coolant. Fukushi et al. developed CZE method using tenfold-diluted artificial seawater as the buffer solution for the determination of bromide ions in seawater. The method is simple, rapid, and possesses sufficient precision and freedom from the interference of chloride ion and from differences in salinity [53].

1. *Analyte*: Bromide ion.
2. *Stock Solution*: Prepare the standard solutions of bromide ion at a concentration of 100 mg/l from potassium bromide.
3. *Sample*: Water sample from sea.
4. *Sample preparation*: Filter the sea water samples with 0.45 μm pore size membrane and store in 500 ml polypropylene bottles in refrigerator.
5. *CE instrumentation and capillary*: Perkin-Elmer Model 270A Capillary electrophoretic analyzer used with a UV–Vis absorbance detector. A polyimide-coated fused-silica capillary column with 50 μm I.D. × 375 μm O.D. having total length 54 cm and the effective length 25 cm.
6. *CE Buffer*: Artificial seawater (tenfold diluted sea water, pH 7). Preparation is described in **Note 1**.

2.6 Analysis of Chlorine-Containing Anions

Chlorine is used as disinfectant in water and waste treatment and as bleaching agents in the paper industry. In these processes, numerous chlorine-containing anions are formed with different oxidation states, such as chloride, chlorite, chlorate, and perchlorate. This method describes the analysis of these ions using CE in the presence of nitrate and sulfate [54].

1. *Analyte*: Chloride, perchlorate, hypochlorite, chlorite, and chlorate anions.

2. *Stock Solution*: Prepare the stock solution from sodium perchlorate, sodium hypochlorite, sodium chlorite, chloride solution in deionized Milli-Q water with concentration 1000 mg/l and store in refrigerator.
3. *Sample*: Tap water, swimming pool water, bleaching preparation.
4. *Sample preparation*: Prepare the samples by spiking the fivefold diluted tap water, 50-fold diluted swimming pool water, and 200-fold diluted bleaching preparation with chlorine-containing anions.
5. *CE instrumentation and capillary*: Capillary Ion Analyzer from Waters equipped with a UV detector, autosampler, hydrostatic sample injection system, and data acquisition software Millenium 2010 Chromatography Manager. A fused-silica capillary Accusep 60 cm (52 cm effective length) × 75 μm I.D.
6. *CE buffer*: 4.6 mM sodium chromate (pH 8.0) containing 0.46 mM CIA-PAK OFM Anion BT (used as electroosmatic flow modifier from Waters).

2.7 Analysis of Monofluorophosphate and Fluoride in Toothpaste

Monofluorophosphate and fluoride in various brands of toothpaste can be determined by capillary electrophoresis (CE) with indirect UV detection as described in the method below [41].

1. *Analyte*: Fluoride, monofluorophosphate (MFP), nitrate, phosphate, sulfate.
2. *Stock solution*: Prepare the stock solution dissolving the appropriate amounts of the corresponding sodium salts in deionized water and making the concentration 1000 μg/ml. These solutions are diluted concentrations as required.
3. *Sample*: Toothpaste
4. *Sample preparation*: Weigh 1.50 g of toothpaste into a 100 ml beaker. Then add tungstate internal standard solution (4 ml) and deionized water (16 ml). Stir the solution and pass a portion of it through a Sep-Pak C_{18} cartridge in order to remove the organic contaminants and filter through 0.45 μm membrane filter.
5. *CE instrumentation and capillary*: Laboratory-built capillary electrophoresis system, equipped with a power supply, a UV detector (Lauerlabs, Netherlands), a fused-silica capillary (52 cm effective length × 75 μm I.D., total length 60 cm).
6. *CE buffer*: 10 mM sodium chromate and 0.1 mM CTAB, pH 9.3.

2.8 Analysis of Iodine Ions

CE technique for single-run determination of iodine and iodide is described. The method is based on the CE separation of iodine and iodide species followed by selective in-capillary derivatization of iodine to iodide with sulfite. The proposed method was applied to the rapid speciation of iodide and iodine in commercially available antiseptics such as povidone-iodine and ethanolic iodine solutions [46].

1. *Analyte*: Iodine and iodide.
2. *Stock Solution*: Prepare the iodide stock solution (0.01 M) from potassium iodide salt. Prepare the standard iodine stock solutions (about 0.005 M) daily by diluting iodine volumetric standard solution and standardize it by titration with 0.01 M sodium thiosulfate. Obtain the lower concentrations of standard iodine concentration by the appropriate dilution of this stock solution. For stock sulfite solutions (about 0.01 M) dissolve appropriate amount of Na_2SO_3 in water, and standardized by iodometric titration.
3. *Sample*: Commercially available antiseptics such as povidone-iodine and ethanolic iodine solutions.
4. *Sample preparation*: Dilute povidone-iodine and ethanolic iodine with deionized water.
5. *CE instrumentation and capillary*: CE 2100 apparatus equipped with a UV detector with wavelength filters (200, 214, 230 and 254 nm). Fused-silica capillary (Polymicro Technology, Phoenix, AZ, USA) of 75 μm i.d. and 57 cm total length (50 cm to the detector) used.
6. *CE buffer*: Tris(hydroxymethyl)aminomethane hydrochloride (Tris–HCl) pH 8.5.

3 Method

3.1 Analysis of Ammonium Ions

1. Dilute analytes in 50-fold diluted buffer before injection.
2. Filter solution with 0.20 μm filter and degas in ultrasonic bath.
3. Set the instrument at 8 kV.
4. For bare silica capillary perform hydrodynamic injection 50 mbar, 5 s and record the electropherogram (Fig. 1a).
5. For ionic liquid (IL) coated capillary coupled with PGT, treat the fresh capillary as reported in **Note 2**.
6. Rinse the pretreated capillary successively with toluene (10 min), methanol (10 min) and with deionized water for 30 min.
7. Dilute run buffer to 1/200 and inject into capillary at 50 mbar, 100 s as "water plug" which is removed by EOF during field amplified sample injection (FASI).
8. Then dip the injection end into the sample vial and apply voltage of 4 kV to inject sample electrokinetically into the capillary under positive electric field, injected plug will be pushed out from the capillary inlet by reversed EOF.
9. Record the signals by PGD detector. Signal increases with pushing out the plug of low conductivity and introduction of sample.
10. When the signals reach 90% of the maximum, increase the voltage to 8 kV till all the analytes are detected.

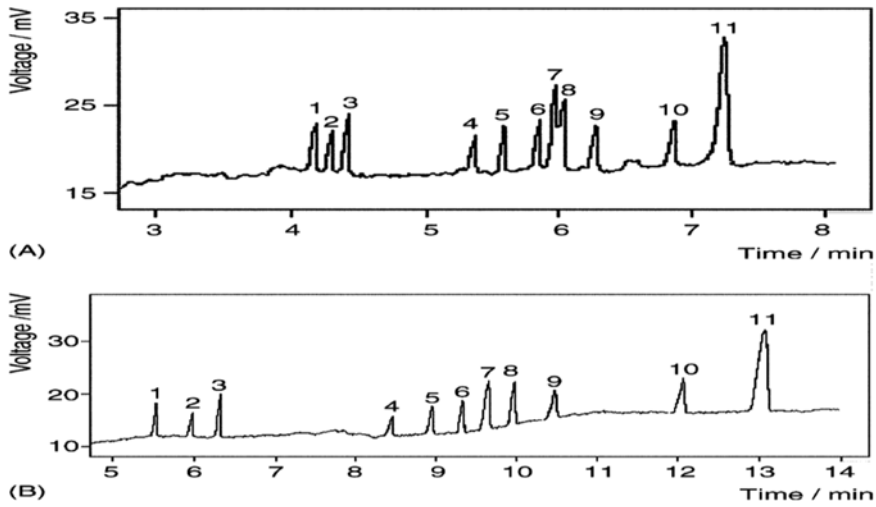

Fig. 1 Comparison of electropherograms of bare and IL-coated capillaries: (**a**) bare silica; (**b**) IL-coated capillary; buffer: 7.5 mM lactic acid, 0.6 mM 18-crown-6, 12 mM α-CD, adjusted to pH 4.0 by 100 mM HMIM hydroxide; peaks (concentrations in μg/ml): (1) Cs^+ (2.5); (2) NH_4^+ (0.1); (3) K^+ (0.5); (4) Ca^{2+} (0.5); (5) Sr^{2+} (1); (6) Na^+ (0.5); (7) Pb^{2+} (5); (8) Mg^{2+} (0.5); (9) Ba^{2+} (2.5); (10) Ni^{2+}(2.5); (11) Li^+ (0.5); capillary: 40 cm; applied voltage: 8 kV; injection: 50 mbar, 15 s; detection: PGD ref. [50]

11. Figure 1 shows the comparison of electropherogram for bare and ionic liquid (IL) coated capillaries.

3.2 Analysis of Nitrite and Nitrate Ions

1. Wash the capillary with 0.1 M NaOH for 5 min and then rinse with water.
2. Then equilibrate with the electrolyte for 10 min.
3. Set the polarity at the injection end of the capillary to negative.
4. Operate the CE system at 10 kV.
5. Inject the sample at high-pressure injection of 48.26 kPa s (7 psi. s) (which is related to sample volume in the range of 7–10 nl for a 50 cm × 50 μm capillary) or electrophoretic injection of 7.5 kV × 5 s.
6. Detect the analytes using UV detections at 191, 200, and 214 nm.
7. A standard capillary electropherogram for nitrate and nitrite is shown in Fig. 2
8. Apply the method for tap water and river water sample. Figure 3 shows the separation of nitrate and nitrite in tap water.

3.3 Analysis of Sulfur-Containing Anions

1. Rinse the capillary with 1 mM CTAB for 0.5 min before each analysis.
2. Operate the CE system at voltage of -20 kV for UV and -25 kV for conductivity detection.

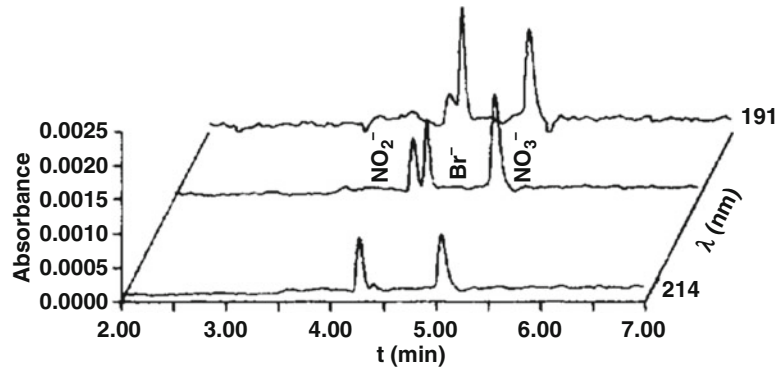

Fig. 2 Electropherogram of nitrite, bromide, and nitrate detected at 191, 200 and 214 nm. The concentrations of nitrite, bromide, and nitrate are 3.12, 4.66 and 3.30 μg/ml, respectively. Sample volumes are injected with 48.26 kPa s (7 p.s.i. s). The experiment done at 20 °C in a buffer of 20 mM tetraborate (pH 8.94) plus 1.1 mmol/l CTAC. Injection volume is −7.5 kV × 5 s and run voltage −10 kV ref. [51]

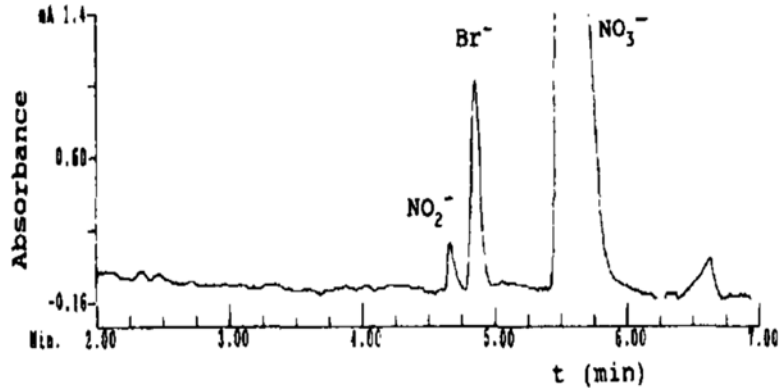

Fig. 3 Electropherogram of tap water spiked with nitrite. Nitrite, 0.78 μg/ml, and bromide, 4.66 μg/ml are spiked in tap water. Other conditions same as in Fig. 2 ref. [51]

3. Inject the sample hydrodynamically for 0.5 s (0.5 p.s.i) for UV detection and electrokinetic for 12 s 25 m bar for conductivity detection.
4. Detect the analyte using UV detection at 214 and 254 nm and conductivity detection at 1 μS/cm.
5. Prepare the calibration curves for the determination of sulfate and its anions in real samples.
6. Electropherograms showing a comparison of the separation of sulfur-containing anions and other anions in two different buffer system using UV detection is given in Fig. 4
7. Comparison of electropherograms using conductivity detection obtained at different concentrations of LiOH in the buffer is given in Fig. 5

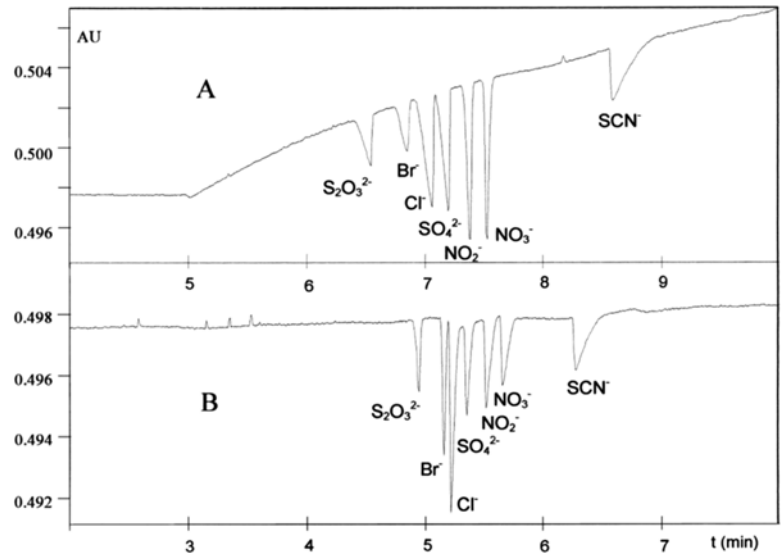

Fig. 4 Comparison of background electrolytes for the separation of anions. (**a**) 1.5 mM pyromellitic acid, 10 mM Tris, pH 9.15 (rinse capillary with 1 mM CTAB) and (**b**) 5 mM chromate, 0.5 mM CTAB, pH 8.0. Capillary: 72 cm (effective length 50 cm) × 75 μm, voltage: 220 kV, detection: UV 214 nm (**a**), 254 nm (**b**), injection: 5 s hydrodynamic 0.5 p.s.i., 10 mg/l standard mixture ref. [19]

8. Electropherogram for the sulfur-containing anions in water from an open pit mining lake by conductivity is given in Fig. 6.

3.4 Analysis of Phosphorus Ions

1. Fill the capillary with running electrolyte consisting of 3.0 mM Mo(VI), 45 % v/v CH_3CN, and 0.05 M malonate buffer (pH 3.0).
2. Set voltage at −12 kV and wavelength at 260 nm.
3. Inject sample into the capillary by vacuum injection for 4 s.
4. In capillary complexation converts anions into $[H_6(PHO_3)_2Mo_{15}O_{48}]^{4-}$, $[(PO_4)Mo_{12}O_{36}]^{3-}$, and $[(P_2O_7)Mo_{18}O_{54}]^{4-}$. Three peaks due the migration of these are obtained in electropherogram.
5. Figure 7 shows an electropherogram for mixture of phosphonate, phosphate, and diphosphate. Prepare the calibration curves for these anions.
6. Inject the spiked tap water samples and estimate their concentrations by comparison with the calibration graphs.

3.5 Analysis of Bromine Ions

1. Dilute 10 ml of sea water to 100 ml with distilled water.
2. Set wavelength at 200 nm, voltage at 11 kV.
3. Maintain thermostat at 30 °C.
4. Then wash capillary with 0.1 M NaOH and water for 3 min each.

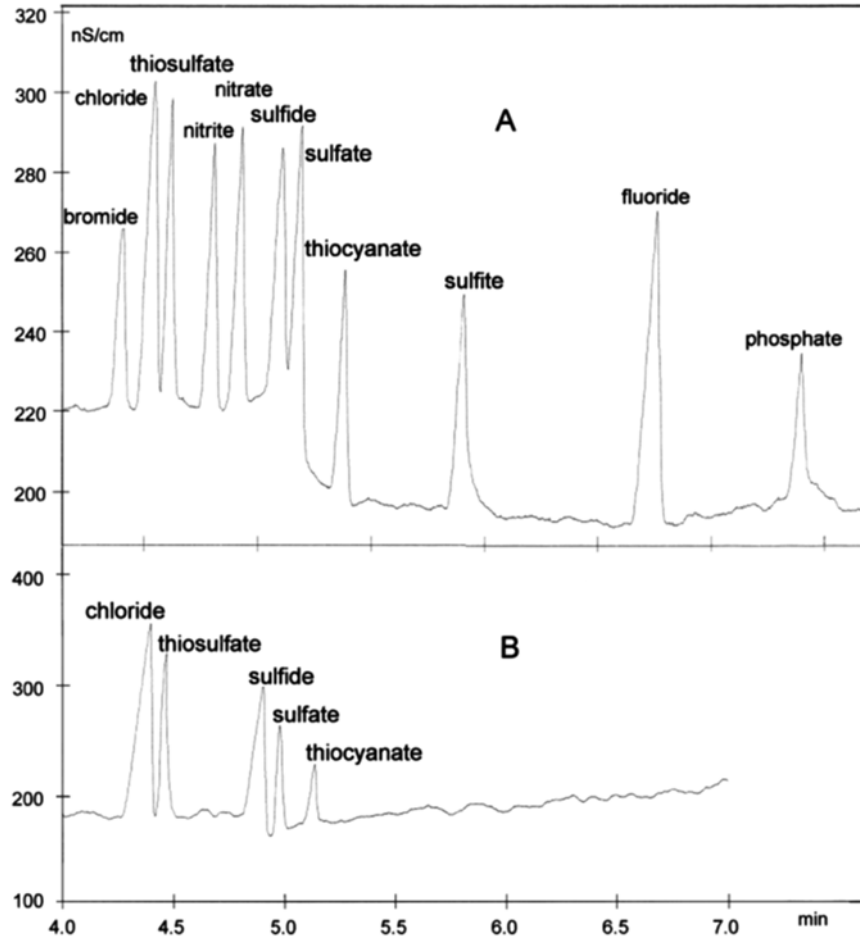

Fig. 5 Separation of anions using conductivity detection. (**a**) 50 mM CHES, 20 mM LiOH, 0.03 % Triton X-100, rinse with 1 mM CTAB. (**b**) Improved peak resolution by using 35 mM LiOH. Capillary: 72 cm 350 mm, voltage: 225 kV, detection: conductivity 1 μS/cm FS, injection: 12 s, 25 mbar, 10 mg/l anion standard mixture ref. [19]

5. Fill the capillary with buffer solution (tenfold diluted artificial sea water, pH 7) by vacuum for 3 min.
6. Inject 11 nl of diluted sample into the capillary for 2 s.
7. Run the sample at voltage of 11 kV with inlet as cathode.
8. Prepare the calibration graph using synthetic standard.
9. An electropherogram shown in Fig. 8 shows the analysis of bromide ion in real water sample.

3.6 Analysis of Chlorine Ions

1. Condition CE capillary overnight with water.
2. Operate CE system at 20 kV.
3. Inject sample hydrostatic 30 s with elevation of 10 cm.
4. Auto purge for 2 min and detect at wavelength 254 nm with UV detector.

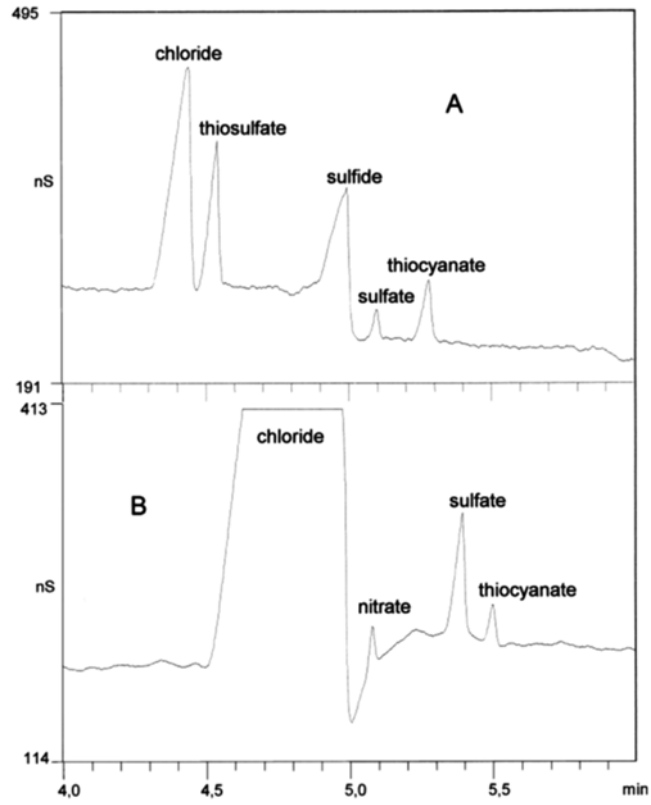

Fig. 6 Determination of sulfur-containing anions in water from an open-pit mining lake by CE conductivity detection (**a**) before, (**b**) after precipitation of humic substances. 50 mM CHES, 35 mM LiOH, 0.03 % Triton X-100, rinse with 1 mM CTAB. Capillary: 72 cm × 75 μm, voltage: 225 kV, detection: conductivity 1 μS/cm FS, injection: 6 s, 25 kV, water from 20 m depth ref. [19]

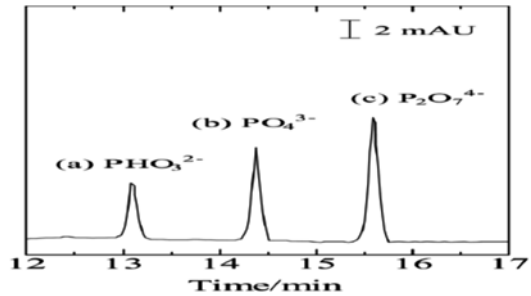

Fig. 7 An electropherogram containing a mixture of phosphonate, phosphate, and diphosphate at 5.0×10^{-5} M each in 0.01 M malonate buffer (pH 3.0). Running electrolyte: a 3.0 mM Mo(VI)-45 % v/v CH_3CN-0.05 M malonate buffer (pH 3.0) solution. (**a**) $[H_6(PHO_3)_2Mo_{15}O_{48}]^{4-}$; (**b**) $[(PO_4)Mo_{12}O_{36}]^{3-}$; (**c**) $[(P_2O_7)Mo_{18}O_{54}]^{4-}$, fused-silica capillary 70 cm with 75 μm I.D., 260 nm, –12 kV ref. [52]

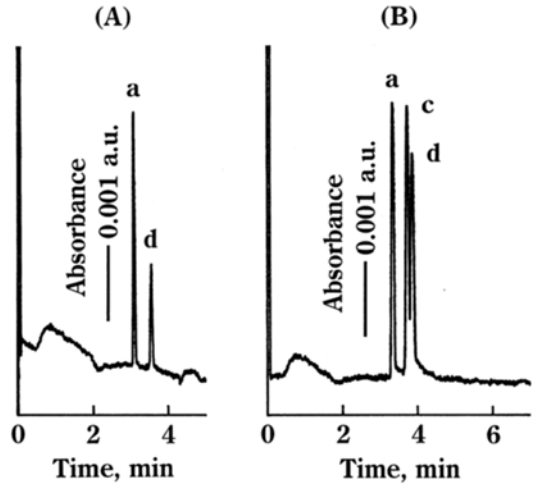

Fig. 8 Electropherograms for the separation of bromide, nitrite, and nitrate ions. (**a**) Sample, surface seawater from the Port of Amagasaki; (**b**) sample, tenfold-diluted artificial seawater containing 6.8 mg/l Br^-, 3.0 mg/l NO_2^-, and 1.0 mg/l NO_3^-. (**a**) Br^-; (**c**) NO_2^-; and (**d**) NO_3. Electrolyte: Artificial seawater (tenfold diluted sea water, pH 7), fused-silica capillary column with 50 μm I.D. × 375 μm O.D. having total length 54 cm and the effective length 25 cm, 200 nm, 30 °C, 11 kV ref. [53]

5. Prepare the calibration curves for the determination of chloride, chlorite, chlorate, hypochlorite, and perchlorate.
6. Apply the same procedure for analysis of chlorine-containing anions in bleaching powder, tap water, and swimming pool water.
7. Figure 9 shows an electropherogram obtained from tap water.

3.7 Analysis of Fluorine Ions

1. Before using the capillary pretreat with 0.2 M NaOH for about half an hour and then rinse with deionized water for 2 min and the electrolyte for 10 min (*see* **Note** 3).
2. To maintain reproducible migration times, flush the capillary with the running buffer for 2 min.
3. Operate CE at voltage of −15 kV.
4. Perform CE experiment at 20–22 °C and UV wavelength of 254 nm.
5. Inject sample hydrostatic for 25–30 s (10 cm).
6. Electropherogram obtained from standard solution is shown in Fig. 10. Prepare the calibration curve.
7. Electropherogram obtained from toothpaste under the optimized conditions is given in Fig. 11.

3.8 Analysis of Iodine Ions

1. Rinse the capillary with 1.0 mol/l sodium hydroxide and water for 10 min.
2. Then equilibrate the capillary with carrier electrolyte for 30 min at the beginning of each day.

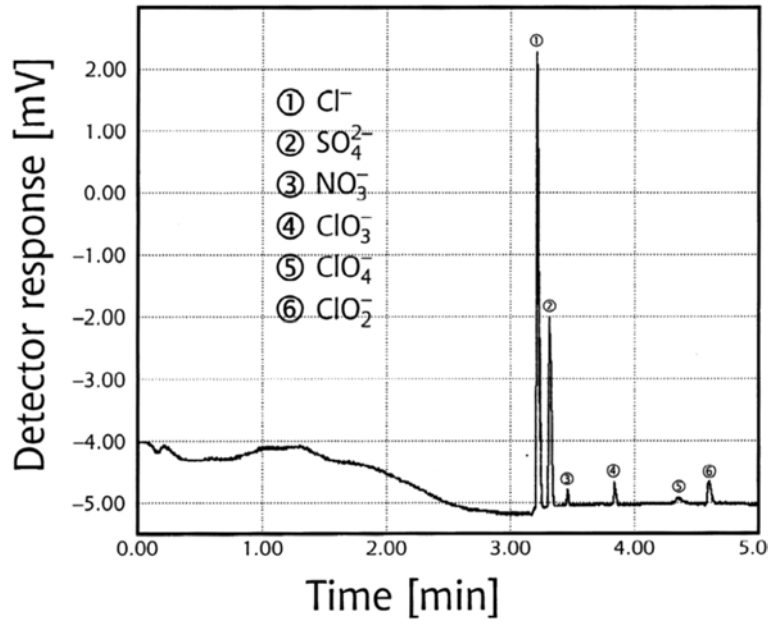

Fig. 9 Electropherogram of fivefold diluted tap water spiked with 2 mg/l of each chlorine containing anions using as electrolyte 4.6 mM sodium chromate of pH 8.0 containing 0.46 mM CIA-PAK OFM Anion BT. Applied voltage: 20 kV (negative polarity). Indirect detection at 254 nm ref. [54]

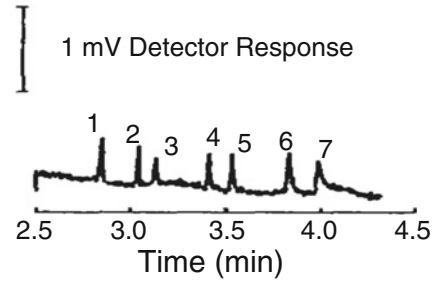

Fig. 10 Typical electropherogram of standard anions. Peaks: (1) chloride; (2) sulfate; (3) nitrate; (4) tungstate; (5) monofluoro-phosphate; (6) fluoride; (7) phosphate, a fused-silica capillary (52 cm effective length × 75 μm I.D., total length 60 cm), running electrolyte: 10 mM sodium chromate and 0.1 mM CTAB, pH 9.3. Applied voltage: –15 kV, 20–22 °C, 254 nm ref. [41]

3. Rinse the capillary for 2 min with carrier electrolyte between all electrophoretic separations.
4. Operate CE at 25 °C and wavelength 214 nm.
5. Inject the sample hydrodynamically for 6 s.
6. Push the sample zone toward the detector side by injection of large amount of the electrolyte solution 20–100 s.
7. Run CE at voltage of –30 kV.
8. Inject the reagent (sulfite) solution.

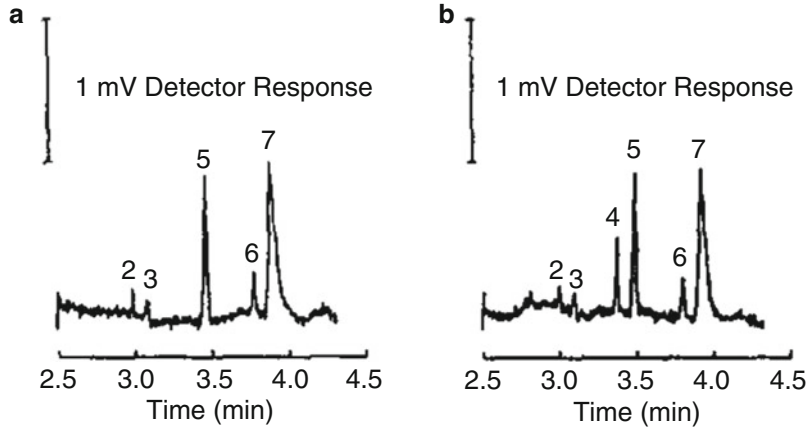

Fig. 11 (**a**) Electropherogram of toothpaste sample peaks: (2) sulfate; (3) nitrate; (5) monofluorophosphate; (6) fluoride; (7) phosphate (**b**) Electropherogram of toothpaste sample spiked with internal standard peaks: (2) sulfate; (3) nitrate; (4) tungstate; (5) monofluorophosphate; (6) fluoride; (7) phosphate. Other conditions same as Fig. 10 ref. [41]

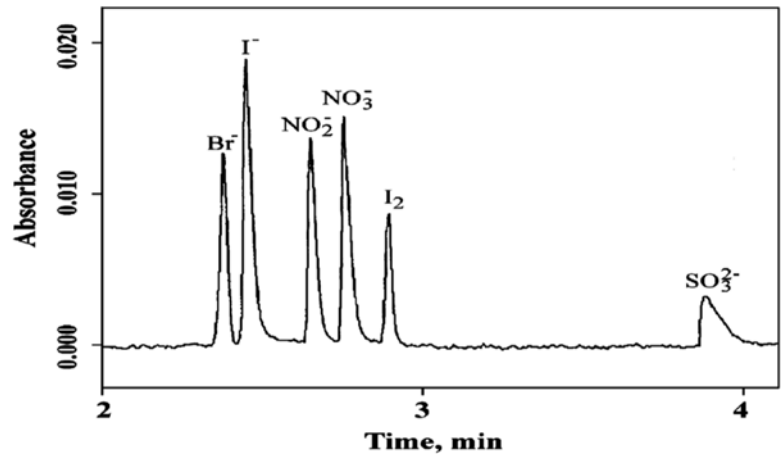

Fig. 12 Electropherogram obtained for a standard I^-/I_2 solution containing common UV absorbing anions. Injection, 6 s sample, 60 s electrolyte, and 6 s 2×10^{-3} M Na_2SO_3; Electrolyte: 0.02 M tris–HCl, pH 8.5; injection voltage, –30 kV; 214 nm ref. [46]

9. Record the signals.
10. A standard CE electropherogram is depicted in Fig. 12.
11. Apply the same method for the analysis of iodine and iodide in commercial antiseptic. Figure 13 shows electropherogram obtained from antiseptic povidone-iodine.

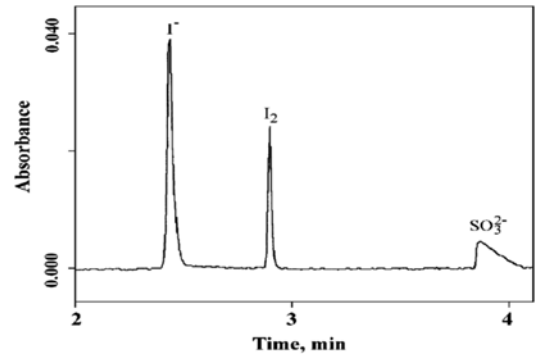

Fig. 13 Electropherogram of 1:200 diluted povidone-iodine sample. Other conditions same as stated in Fig. 12 ref. [46]

4 Notes

1. Preparation of artificial water: Prepare three groups of mixed solutions containing various salts. The first group is mixed solution of sodium chloride and sodium sulfate. The second group mixed solution of magnesium chloride, calcium chloride, and strontium chloride. The third group mixed solution of potassium chloride, sodium hygrogen carbonate, boric acid, and sodium fluoride. Then mix all the three solutions and filter through 0.45 μm membrane before use. Composition of seawater is given in Table 1.
2. Capillary coating: The fresh capillary flushed with 1 M NaOH for 2 h, followed by deionized water and 1 h of 1 M HCl. Then rinsed with deionized water and methanol for 10 min consecutively and then flushed with nitrogen gas and heated to 120 °C overnight. In a nitrogen-filled glove box, filter 3-chloropropyl-trimethoxysilane (CPTMS) and introduce into the capillary by positive pressure. Seal the capillary at both the ends and keep at 90 °C for 15 h. After that flush with nitrogen to drive out the CPTMS residue and then rinse with toluene. At room temperature, dissolve excess imidazole in toluene; filter the supernatant and introduce into the capillary. Then seal the capillary sealed and keep at 90 °C for 4 h, afterward rinse with toluene, dichloromethane progressively and consequently dry with nitrogen under 70 °C for 1 h. Rinse the capillary with 1-bromohexane for 10 min and then seal and heat under 80 °C for 10 h.
3. Fill the capillary with 0.2 M NaOH overnight in order to maintain the capillary wall in good condition.

Table 1

Composition of artificial seawater

Component	Concentration (g/1)
NaCl	24.54
$MgCl_2 \cdot 6H_2O$	11.10
Na_2SO_4	4.09
$CaCl_2$	1.16
KCl	0.69
$NaHCO_3$	0.20
H_3BO_3	0.03
$SrCl_2 \cdot 6H_2O$	0.04
NaF	0.003

References

1. Fritz JS (2000) Recent developments in the separation of inorganic and small organic ions by capillary electrophoresis. J Chromatogr A 884:261–275
2. Kaniansky D, Masar M, Marak J, Bodor R (1999) Capillary electrophoresis of inorganic anions. J Chromatogr A 834:133–178
3. Sadecka J, Polonsky J (1999) Determination of inorganic ions in food and beverages by capillary electrophoresis. J Chromatogr A 834:401–417
4. Polesello S, Valsecchi SM (1999) Electrochemical detection in the capillary electrophoresis analysis of inorganic compounds. J Chromatogr A 834:103–116
5. Timerbaev AR, Dabek-Zlotorzynskab E, Hoop AGT (1999) Inorganic environmental analysis by capillary electrophoresis. Analyst 124:811–826
6. Timerbaev AR, Buchberger W (1999) Prospects for detection and sensitivity enhancement of inorganic ions in capillary electrophoresis. J Chromatogr A 834:117–132
7. Martínková E, Křížek T, Coufal P (2014) Determination of nitrites and nitrates in drinking water using capillary electrophoresis. Chem Papers 68:1008–1014
8. Fukushi K, Tada K, Takeda S, Wakida S, Yamane M, Higashi K, Hiiro K (1999) Simultaneous determination of nitrate and nitrite ions in seawater by capillary zone electrophoresis using artificial seawater as the carrier solution. J Chromatogr A 838:303–311
9. Fukushi K, Nakayamaa Y, Tsujimoto J (2003) Highly sensitive capillary zone electrophoresis with artificial seawater as the background electrolyte and transient isotachophoresis as the online concentration procedure for simultaneous determination of nitrite and nitrate in seawater. J Chromatogr A 1005:197–205
10. Okemgbo AA, Hill HH, Siems WF, Metcalf SG (1999) Reverse polarity capillary zone electrophoretic analysis of nitrate and nitrite in natural water samples. Anal Chem 71:2725–2731
11. Oztekin N, Nutku MS, Erim FB (2002) Simultaneous determination of nitrite and nitrate in meat products and vegetables by capillary electrophoresis. Food Chem 76:103–106
12. Gao L, Barber-Singh J, Kottegoda S, Wirtshafter D, Shippy SA (2004) Determination of nitrate and nitrite in rat brain perfusates by capillary electrophoresis. Electrophoresis 25:1264–1269
13. Boudko DY, Cooper BY, Harvey WR, Moroz LL (2002) High-resolution microanalysis of nitrite and nitrate in neuronal tissues by capillary electrophoresis with conductivity detection. J Chromatogr B 774:97–104

14. Chang SY, Tseng WL, Mallipattu S, Chang HT (2005) Determination of small phosphorus-containing compounds by capillary electrophoresis. Talanta 66:411–421
15. Stover FS (1999) Capillary electrophoresis of phosphorus oxo anions. J Chromatogr A 834:243–256
16. Wang T, Li SFY (1999) Separation of inorganic phosphorus-containing anions by capillary electrophoresis. J Chromatogr A 834:233–241
17. Stalikas CD, Konidari CN (2001) Analytical methods to determine phosphonic and amino acid group-containing pesticides. J Chromatogr A 907:1–19
18. Hooijschuur EWJ, Kientz CE, Brinkman UA (2002) Analytical separation techniques for the determination of chemical warfare agents. J Chromatogr A 982:177–200
19. Hissner F, Mattusch J, Heinig K (1999) Quantitative determination of sulfur-containing anions in complex matrices with capillary electrophoresis and conductivity detection. J Chromatogr A 848:503–513
20. Bjergegaard C, Møller P, Sørensen H (1995) Determination of thiocyanate, iodide, nitrate and nitrite in biological samples by micellar electrokinetic capillary chromatography. J Chromatogr A 717:409–414
21. Masselter SM, Zemann AJ, Bonn GK (1996) Determination of inorganic anions in kraft pulping liquors by capillary electrophoresis. J High Resolut Chromatogr 19:131–136
22. Romano J, Jandik P, Jones WR, Jackson PE (1991) Optimization of inorganic capillary electrophoresis for the analysis of anionic solutes in real samples. J Chromatogr 546:411–421
23. Salimi-Moosavi H, Cassidy RM (1995) Capillary electrophoresis of inorganic anions in nonaqueous media with electrochemical and indirect UV detection. Anal Chem 67:1067–1073
24. Shamsi SA, Danielson ND (1994) Napthalenesulfonates as electrolytes for capillary electrophoresis of inorganic anions, organic-acids and surfactants with indirect photometric detection. Anal Chem 66:3757–3764
25. Rhemrev-Boom MM (1994) Determination of anions with capillary electrophoresis and indirect ultraviolet detection. J Chromatogr A 680:675–684
26. Motellier S, Gurdale K, Pitsch HJ (1997) Sulfur speciation by capillary electrophoresis with indirect spectrophotometric detection: in search of a suitable carrier electrolyte to maximize sensitivity. J Chromatogr A 770:311–319
27. Buchberger W, Haddad PR (1992) Effects of carrier electrolyte composition on selectivity in capillary zone electrophoresis of low-molecular mass anions. J Chromatogr 608:59–64
28. Li XA, Zhoub DM, Xua JJ, Chena HY (2008) Determination of chloride, chlorate and perchlorate by PDMS microchip electrophoresis with indirect amperometric detection. Talanta 75:157–162
29. Jones WR, Jandik P (1992) Various approaches to analysis of difficult sample matrices of anions using capillary ion electrophoresis. J Chromatogr 608:385
30. Wu MJ, Ren HX (1996) Capillary electrophoresis-indirect ultraviolet detection of anions of different morphotypes. Chin J Anal Chem 24:1178–1181
31. Pirogov AV, Yurev AV, Shpigun OA (2003) Use of ionenes as capillary modifiers in the simultaneous determination of azide, chlorate, and perchlorate ions by capillary electrophoresis. J Anal Chem 58:781
32. Wang J (2002) Electrochemical detection for microscale analytical systems: a review. Talanta 56:223–231
33. Wang J (2005) Electrochemical detection for capillary electrophoresis microchips: a review. Electrophoresis 17:1133–1140
34. Guan F, Wu H, Luo W (1996) Sensitive and selective method for direct determination of nitrite and nitrate by high-performance capillary electrophoresis . J Chromatogr A 719:427–433
35. Song L, Ou Q, Yu W, Xu G (1995) Effect of high concentrations of salts in samples on capillary electrophoresis of anions. J Chromatogr A 696:307–319
36. Soga T, Inoue Y, Ross G (1995) Analysis of halides, oxyhalides and metal oxoacids by capillary electrophoresis with suppressed electroosmotic flow. J Chromatogr A 718:421–428
37. Rantakokko P, Nissinen T, Vartiainen T (1999) Determination of bromide ion in raw and drinking waters by capillary zone electrophoresis. J Chromatogr A 839:217–225
38. Hoop MAG, Cleven RFM, Staden JJV, Neele J (1996) Analysis of fluoride in rain water comparison of capillary electrophoresis with ion chromatography and ion-selective electrode potentiometry. J Chromatogr A 739:241–248
39. Skocir E, Pecavar A, Krasnja A, Prosek M (1993) Quantitative determination of fluorine in toothpastes. J High Resolut Chrom 16:243–246

40. Shamsi SA, Danielson ND (1995) Ribonucleotide for capillary electrophoresis for phosphanates and polyphosphanates with adenosine monophosphate and indirect photometric detection. Anal Chem 67:1845–1852
41. Wang P, Li SFY, Lee HK (1997) Simultaneous determination of monofluorophosphate and fluoride in toothpaste by capillary electrophoresis. J Chromatogr A 765:353–359
42. Heidbuchel EW (1991) Fluor determination in toothpaste-extracts with fluoride-selected based on the kinetics of hydrolysis of sodiummonofluorophosphate. Pharm Acta Helv 66:290–297
43. Small H, Stevens TS, Bauman WC (1975) Novel ion exchange chromatographic method using conductimetric method. Anal Chem 47:1801–1809
44. Haddad RR, Jackson RE (1990) Ion chromatography—principles and applications Elsevier, Amsterdaml 4
45. Pantcková P, Urbánek M, Krivánkov L (2007) Determination of iodide in samples with complex matrices by hyphenation of capillary isotachophoresis and zone electrophoresis. Electrophoresis 28:3777–3785
46. Paliulionyte V, Padarauskas A (2002) Single-run capillary electrophoretic speciation of iodide and iodine. Anal Chim Acta 466:133–139
47. Semenova OP, Timerbaev AR, Gagstadter R, Bonn GK (1996) Speciation of chromium ions by capillary zone electrophoresis. J High Resolut Chromatogr 19:117–119
48. Carou MIT, Mahia PL, Lorenzo SM, Fernández EF, Rodriguez DP (2001) Direct analysis of inorganic anions in samples with high salt content by capillary zone electrophoresis. J Chromatogr Sci 39:397–401
49. Mori M, Hu W, Haddad PR, Fritz JS, Tanaka K, Tsue H, Tanaka S (2002) Capillary electrophoresis using high ionic strength background electrolytes containing zwitterionic and non-ionic surfactants. Anal Bioanal Chem 372:181–186
50. Qin W, Lia SFY (2004) Determination of ammonium and metal ions by capillary electrophoresis–potential gradient detection using ionic liquid as background electrolyte and covalent coating reagent. J Chromatogr A 1048:253–256
51. Guan F, Wu H, Luo Y (1996) Sensitive and selective method for direct determination of nitrite and nitrate by high-performance capillary electrophoresis. J Chromatogr A 719:427–433
52. Himeno S, Inazuma N, Kitano E (2007) Simultaneous determination of phosphonate, phosphate, and diphosphate by capillary electrophoresis using in-capillary complexation with Mo(VI). J Sep Sci 30:1077–1081
53. Fukushi K, Watanabea K, Takedab S, Wakidab S, Yamane M, Higashi K, Hiiro K (1998) Determination of bromide ions in seawater by capillary zone electrophoresis using diluted artificial seawater as the buffersolution. J Chromatogr A 802:211–217
54. Biesaga M, Kwiatkowska M, Trojanowicz M (1997) Separation of chlorine-containing anions by ion chromatography and capillary electrophoresis. J Chromatogr A 777: 375–381

Chapter 13

Metal Ions Analysis with Capillary Zone Electrophoresis

Ashok Kumar Malik, Jatinder Singh Aulakh, and Varinder Kaur

Abstract

Capillary electrophoresis has recently attracted considerable attention as a promising analytical technique for metal ion separations. Significant advances that open new application areas for capillary electrophoresis in the analysis of metal species occurred based on various auxiliary separation principles. These are mainly due to complexation, ion pairing, solvation, and micellization interactions between metal analytes and electrolyte additives, which alter the separation selectivity in a broad range. Likewise, many separation studies for metal ions have been concentrated on the use of preelectrophoresis derivatization methodology. Approaches suitable for manipulation of selectivity for different metal species including metal cations, metal complexes, metal oxoanions, and organometallic compounds, are discussed, with special attention paid to the related electrophoretic system variables using illustrative examples.

Key words Capillary zone electrophoresis, Metal ions, Complexing agents, Metal ligand interactions, Lanthanides, Actinides, Transition metal ions, Speciation

1 Introduction

Previously, most of the electrophoretic methods were applied in the fields of biochemistry and molecular biology for the separation and quantification of macromolecules of biological origin and few applications of electrophoretic techniques were reported for inorganic metal analysis [1–4]. Nowadays, CE is considered as a powerful method for inorganic ion separations due to extensive research in this field. Furthermore, in many cases the methods are known to be superior to the conventional HPLC methods for ionic multispecies analysis. Various advantages of using CE over HPLC include (a) high separation efficiency, (b) low material and sample consumption, (c) relatively short analysis, (d) low instrumental and operational cost, and (e) tolerance of complex matrices, as it can be processed without extensive pre-treatment. Various reviews are published in the literature to cover different aspects of the inorganic metal analysis [1–4]. The reports depicted that complete and optimized separation of rare earth elements (REEs) in geological

Philippe Schmitt-Kopplin (ed.), *Capillary Electrophoresis: Methods and Protocols*, Methods in Molecular Biology, vol. 1483,
DOI 10.1007/978-1-4939-6403-1_13,

samples (rock, mineral, or fluids) at trace levels (μg/g or ng/g) by CE techniques is a challenging analytical problem.

An up-to-date survey of the literature on the analysis of metal ion and organometallic species is given by Timerbaev and Boyce et al [1–4]. A large number of complexing agents have been employed in the past for the separation as well as to increase the selectivity and sensitivity for inorganic metal analysis. Among these, 4-(2-pyridylazo)resorcinol, 8-hydroxyquinoline-5-sulfonic acid, and various polyaminocarboxylic acids such as EDTA, CDTA, and others have already been examined as important reagents for the CE separation of metal cations [1–33]. Inorganic ligands like chloride and cyanide are less applicable as these require more rigid control on complexation conditions. A brief summary of various organic acids used as reagents is presented in Table 1. Different parameters affecting the separation of metal ions using CZE involve (a) nature of the complexing reagent, (b) the concentration of the free ligand, and (c) pH of the electrolyte.

2 Materials and Equipment

2.1 Main Group Elements

2.1.1 Analysis of Alkali and Alkaline Earth Metal Ion [17]

1. *Analytes*: K^+, Na^+, Ba^{2+}, Li^+, Sr^{2+}, Mg^{2+}, and Ca^{2+} 1000 μg/ml. Dilute these solutions as desired in the ppm range.
2. *Sample*: River water, urine, and a solid sample of calcium carbonate.
3. *Sample preparation*: Dilute the water and urine samples with deionized water and then mix with buffer to ensure that the differences in ionic strength, conductivity, and pH (between samples and running buffer) are negligible and peak heights are in the linear range of the calibration curve. Weigh 0.15 g calcium carbonate. Add a few drops of the deionized water to it. Add perchloric acid (60%) (*see* **Note 1**) until calcium carbonate is completely dissolved. Transfer the sample into a 10 ml volumetric flask and dilute with water as desired.
4. *CE instrument and capillary*: Capillary electrophoresis system equipped with a positive power supply (Spellman, Plainview, NY, USA). Linear UV–Vis 200 detector (linear Instruments Corp., Reno, NV, USA). Polyimide-coated fused-silica capillaries 39.5 cm long I.D. 75 μm (I.D.).
5. *CE buffer*: 0.8 mM Ethylenediamine-tetra acetic acid disodium salt (EDTA) as complexing agent, and 10 mM pyridine as carrier electrolyte and background absorber for indirect UV detection.

2.1.2 Determination of Na^+, K^+, Mg^{2+} , and Ca^{2+} by Indirect Detection [18]

1. *Analytes:* Prepare standard stock solution of Na^+, K^+, Mg^{2+}, and Ca^{2+} and further dilute as desired.
2. *Sample:* Sea water from Drøbak from a depth of 40 m and the formation water from a oil company. A certified reference material BCR CRM 399 (Brussels, Belgium).

Table 1
Separation parameters for some metal cations with organic acids as the complexing agents

Cations (number of cations)	Separation conditions	Separation time (min)	Reference
K^+, Na^+, Mg^{+2}, Li^+, lanthanides (18)	4 mM HIBA, 30 mM creatinine (pH 4.8)	5	[6]
Alkali, alkaline earth, transition metals, lanthanides (19)	5 mM HIBA, 6.5 mM Waters UVCat-1 (pH 4.4)	2	[7]
Alkali, alkaline earth, transition metals, lanthanides (26)	4.2 mM HIBA, 0.2 mM Triton X-100, 6 mM *N,N*-dimethylbenzylamine (pH 4.25)	10	[8]
Alkali, alkaline earth, transition metals, lanthanides, Pb^{2+} (27)	15 mm lactic acid, 5% methanol, 8 mm 4-methylbenzylamine (pH 4.25)	7	[9]
Alkali, alkaline earth, and transition metals (12)	2.5 mM tartaric acid, 20% methanol, 6 mM p-toluidine (pH 4.8)	9	[9]
Alkali, alkaline earth, and transition metals (14)	12 mM HIBA, 6 mM imidazole (pH 3.95)	<4	[10]
Alkali, alkaline earth, transition metals, Pb^{2+}, NH_4^+, (16)	11 mm lactic acid-2.6 mM 18-crown-6, 8% methanol, 7.5 mM 4-methylbenzyl amine (pH 4.3)	6	[11]
Alkali, alkaline earth, transition metals, Pb^{2+}(17)	13 mm glycolic acid, 10 mM imidazole (pH 4.0)	14	[12]
Alkali, alkaline earth, NH_4^+, Mn^{2+}, Cd^{2+} (12)	6 mm glycine-2 mM 18-crown-6, 2% methanol, 5 mM 1,1′-diphenylbipyridinium (pH 6.5)	5	[13]
Alkali, alkaline earth, transition metals, Pb^{2+}, NH_4^+ (17)	5 mM lactic acid-0.5 mM 18-crown-6, 10 mM imidazole (pH 6.5)	5	[14]
Alkali, alkaline earth, transition metals, Pb^{2+} (17)	1 mm oxalic acid—100 mM acetic acid (pH 2.84)	15	[15]

3. *Sample preparation:* Dilute the samples with 1:1000 with distilled water.
4. *CE instrument and capillary:* A Waters Quanta 4000 capillary electrophoresis system, equipped with a positive power supply and fused-silica capillary (60 cm total length, 75 μm I.D.; Waters AccuSep). The distance of 52 cm from the point of sample introduction to the detector window. Indirect UV detection at 185 and 254 nm with a mercury lamp and optical filters. Use polyethylene vials as containers for the carrier electrolyte and for all the standards and samples.
5. *CE buffer:* The running electrolyte consists of 6.5 mM HIBA (α-hydroxyisobutyric acid, Fluka, puriss), 5.0 mM UV CAT-1 (formethylbenzylamine), 6.2 mM 18-crown-6 (1,4,7,10,13,16-hexaoxacyclooctadecane, Merck, for synthesis), and 25% (v/v) methanol. Maintain the pH of the solution at 4.8.

2.1.3 Analysis of Alkali and Alkaline Earth Metals by Ionic Liquid [19]

1. *Analyte:* Li^+, K^+, Na^+, Cs^+, Mg^{2+}, Ba^{2+}, Ca^{2+}, and Sr^{2+}.
2. *Sample preparation*: Prepare samples by dissolving appropriate amounts of salts in deionized water and dilute as per the requirements.
3. *CE instrumentation and capillary:* A P/ACE system 5000 or 2100 (Beckman Coulter, Fullerton, CA, USA) fitted with a UV detector. A personal computer with the P/ACE 2000 series Control Program (version 2.64F) for data acquisition and handling. A bare fused silica or a neutral coated polyvinyl-alcohol capillary having 50 μm ID, and total and effective lengths of 47 and 40 cm (or 37 and 30 cm), respectively.
4. *CE buffer*: Adjust the pH of the electrolyte equal to 5.8 for hydroorganic and nonaqueous media. It may be adjusted by adding choline hydroxide if required.

2.2 Transition Metals

1. Analytes: Pd(II), Rh(III), Ru(III), Os(VI), and Ir(III).

2.2.1 Determination of Pd(II) as a Chloro Complex in the Presence of Rh(III), Ru(III), Os(VI), and Ir(III) [20]

2. Sample: *see* **Note 2**.
3. Sample preparation: (a) Pd(II) stock solution (1.0 mg/ml); (Dissolve 0.1 g of the Pd metal in aqua-regia, fume the solution to dryness with hydrochloric acid, and dilute to 100 ml with 1 M hydrochloric acid. Dilute the standard stock solution to 10.00 μg/ml with deionized water. Further, dilute the solution to have a 200-fold stoichiometric excess of Cl^- so that there is complete formation of Pd(II) choloro complex. (b) Prepare Rh(III), Ru(III), Os(III), and Ir(III) stock solution (100 μg/ml) by dissolving $(NH_4)_2{\cdot}Rh(H_2O)Cl_5$, $(NH_4)_2Ru(H_2O)Cl_5$, $(NH_4)_2{\cdot}OsCl_6$ in the presence of 5.0 g of ascorbic acid as reducing agent for dissolution, and $(NH_4)_3IrCl_6{\cdot}H_2O$ in 20 ml of 6 M HCl and finally diluting to 100 ml with deionized water.
4. CE instrument and capillary. Waters Quanta 4000 CE system (Millipore Waters, Milford, MA, USA) equipped with negative power supply. UV detector with Zn lamp and 214 nm optical filter. Waters AccSep fused-silica capillaries (52.2 cm×75 μm I.D.).
5. CE buffer: Prepare carrier electrolyte of 50 mM HCl–KCl (50 mM Cl^-; pH: 3.0) containing 0.2 mM cetyltrimethylammonium bromide (CTAB) by mixing 50 mM HCl containing 0.2 mM CTAB. Adjust the pH of the solution by adding KOH solution. Degas the electrolyte and filter through a 0.45 μm membrane prior to use.

2.2.2 Determination of Cr(III), Fe(III), Cu(II), and Pb(II) [21]

1. *Analytes:* Use 1000 mg/l $CrCl_3$, $FeCl_3$, $CuCl_2$ and $Pb(NO_3)_2$, $ZnCl_2$ and $AlCl_3$ and EDTA (solid) to prepare dilute metal-chelate solutions.
2. *Sample:* Waste water from tanning industry.

3. *Sample preparation:* Transfer a suitable volume of the unknown sample into a 100 ml Erlenmeyer flask and adjust the pH of the solution to 5.5 by adding 15 ml of 0.1 M acetate buffer and then add 0.2 g of EDTA and boil the mixture for 10 min. Violet colored $[Cr\text{-}EDTA]^-$ complex will form. Dilute this with 0.1 M acetate buffer. Filter the solution through a 0.45 μm filter. Degas and inject directly into the CZE system.
4. *CE instrument and capillary:* Analyte ISCO (Lincoln, NE, USA) Model 3850 integrated capillary electrophoresis system equipped with high voltage (up to 30 kV) and reversible polarity. Sample injection can be done by applying a 3.4 kPa vacuum at the detector end of the capillary. Perform the separation with unmodified fused-silica capillary column of length 46.5 cm (30.5 cm to the UV detector) and 80 cm (60 cm to the UV detector) with 50 μm I.D.
5. *CE buffer:* Prepare standard stock solution of 0.2 M sodium acetate and acetic acid and dilute it as desired with Millipore Milli-Q water (18 MΩ). Filter all the solutions through a 0.45 μm membrane filter and degas by ultrasound.

2.2.3 Determination of Cu(II), Fe(III), Zn(II), Co(II), and Ni(II) Using 4-(2-Pyridylazo)Resorcinol (PAR) [22]

1. *Analytes*: Prepare a stock solution of Co(II), Fe(III), Cu(II) from nitrates and Ni(II) and Zn(II) from sulfates with pH value 1. Prepare stock solution of PAR (Aldrich, USA) of pH 8.5.
2. *Sample*: Tea.
3. *Sample preparation*: Weigh 1.0 g of tea sample into a 200 ml beaker and add 50 ml HNO_3. After 10 min reaction, place the tea sample on hot plate and evaporate to dryness. Cool the tea sample, add 25 ml HNO_3 and 5 ml $HClO_4$ and heat again to dryness. Transfer the residue into a 100 ml calibrated flask and dilute with water. Prepare a blank, by following the same procedure as discussed earlier.
4. *CE instrument and capillary:* A CE-L1 capillary Electrophoresis system (CE Resources Pte Ltd., Singapore) with a SPD-10A UV–Vis detector of Shimadzu Co. (Kyoto, Japan) operating at 505 nm. Fused-silica capillaries (50 μm I.D.) of 80 cm length and effective length from the injection end to the detection window 66 cm (from Polymicro Technologies Phoenix, USA).
5. *CE buffer:* The separation electrolyte consists of *N*-tris[hydroxymethyl]methyl-3-aminopropanesulfonic acid (TAPS) (Sigma, USA) and mix it with PAR and ion additive to have a final concentration of 10 mM for TAPS, 0.1 mM for PAR. Adjust the pH value of 8.5 with NaOH.

2.2.4 Determination of Heavy Metal Ions Using Polyamidoamine Dendrimers [23]

1. *Analytes*: 2.5×10^{-3}–2.5 mg/l Pb(II), 1×10^{-3}–0.5 mg/l Cu(II), 5×10^{-3}–2.5 mg/l Hg(II), 5×10^{-4}–0.5 mg/l Zn(II), 2.5×10^{-4}–0.1 mg/l Co(II) ions.
2. *Sample*: Water sample, snow sample, and tap water.

3. *Sample preparation*: Collect snow sample from a roadside with moderate traffic volume and store in a clean screw-capped centrifuge tube at −15 °C. Weigh an aliquot of snow sample and keep it at room temperature. In the same way, collect rain water and tap water. Filter all the samples using 0.45 μm filter paper.
4. *CE instrument and capillary*: A DW-P303-1ACD8 high voltage supply (Dongwen High Tech., Tianjin, China), equipped with a homemade photometric detector. The light having maximum emission wavelength at 527 nm focused from the light-emitting diode (LED, Shifeng Corp., Shenzhen, China) by two plano-convex lenses on the detection window of the capillary. A capillary 45.0 cm long (effective length 38.0 cm) fused-silica capillary for preconcentration and separation.
5. *CE buffer*: Adjust the pH by L-Tryptophan and NaOH at a pH of 9.25.

2.2.5 Analysis of Cu^{2+} and Pb^{2+} as Aminobenzyl-EDTA (ABEDTA) Complexes [24]

1. *Analytes:* 5–60 μg/ml for Cu^{2+} and 5–25 μg/ml for Pb^{2+}.
2. *Sample:* R. Coptidis drug samples.
3. *Sample preparation:* Weigh 0.5 g R. Coptidis drug powder digested with 65 % HNO_3. Dissolve in water and centrifuge. Mix 0.5 ml of centrifuge with 20 μl of 1.0 mg/ml ABEDTA and then load into Al_2O_3 column. Wash with 10 ml water and elute with 10 ml of 5 % acetic acid–methanol solution. Vaporize the elute with water bath and dissolve residue in 0.2 ml water and keep for injection.
4. *CE instrument and capillary:* A Beckman P/ACETM MDQ HPCE setup equipped with a 2996 PDA detector. Electropherograms integrated with 32 Karat Software. Separations performed on a fused-silica capillary (57 cm × 75 mm i.d., an effective length of 50 cm).
5. *CE Buffer:* Prepare the running buffer composed of 0.05 mol/l acetate and 0.5 mmol/l CTAB solution (pH 5.5).

2.2.6 Analysis of Metal Ions as Their Phenanthroline Complexes [25]

1. *Analytes:* Fe(II), Zn(II), Cu(II), and Cd(II).
2. *Samples:* Wine samples.
3. *Sample preparation:* Filter the wine samples through filter papers to remove the suspended solids. Filter the samples through 0.45 μm membrane and inject directly without any other sample treatment. Dilute the sample as per the requirement of electrophoretic system.
4. *CE instrument and capillary:* A Beckman P/ACETM MDQ capillary electrophoresis system (Fullerton, USA) equipped with a photodiode array detection system. A 32 Karat software version 5.0 (Beckman) for instrument control, data acquisition, and data analyses. Uncoated fused-silica capillary (Restek,

USA) (40.0 cm length × 50 μm I.D.) and 30.0 cm effective length. Capillary detection at either selected wavelengths (200, 220, 225, and 254 nm) or in scanning mode (190–600 nm). The operating temperature should be 25 °C.

5. *CE Buffer:* Prepare the buffer of pH 6 by mixing acetic acid and acetate solutions in appropriate amount. Prepare 0.2 mol/l acetate buffer containing 20 % methanol with pH 5.5 as a running buffer.

2.2.7 Determination of Metal Ions by 2,6-Pyridinedicarboxylic Acid (PDC) [26]

1. *Analyte:* Ni (II), Cu(II), Zn(II), Fe(II), Fe(III), Co(II), Cd(II),V(IV), Pb(II), and Mn(II).
2. *Sample preparation:* Prepare stock solutions of metal ions of 1000 ppm of Ni(II), Cu(II), Zn(II), Fe(II), Fe(III), Co(II), Cd(II), V(IV), Pb(II), and Mn(II). Prepare nickel plating and copper plating solutions and dilute them to 1:20,000 and 1:10,000, respectively.
3. *CE instrument and capillary:* An HP3D CE (Agilent Technologies, Bracknell, UK), equipped with a negative power supply. A polyamide-coated, fused-silica capillary coated with 0.5 % 2,6-pyridinedicarboxylic acid, 70 cm length with 75 mm (I.D.) and a distance of 61.5 cm from the point of injection to the detection window.
4. *CE buffer: Prepare a* mixture of 5 mM PDC and 4 mM tetrabutylammonium hydroxide at pH 4.0.

2.2.8 Determination of Au(III), Cr(VI), Fe(III), UO_2(II), and Ni(II) Using Bis(salicylaldehyde) orthophenylenediamine [27]

1. *Analyte:* Au(III), Cr(VI), Fe(III), Fe(II), UO_2(II), and Ni(II).
2. *Sample:* The waste-water samples from the common tannery treatment plant of tannery complex and goldsmith factories.
3. *Sample preparation:* Prepare 1.37 mM of bis(salicylaldehyde) orthophenylenediamine solution in a known volume of double-distilled ethanol. Dissolve appropriate amounts of metal salts like gold chloride, potassium dichromate, ammonium ferrous sulfate hexahydrate, ammonium ferric sulfate dodecahydrate, uranium nitrate, and nickel chloride to make stock standard solution of 1000 μg/ml. Prepare a working solution of bis(salicylaldehyde) orthophenylenediamine solution (0.137–0.685 mM) from stock solution.
4. *CE instrument and capillary:* The CE system consists of Beckman–Coulter P/ACE MDQ, USA, equipped with photodiode array detector, and MDQ 32 Karat software. Uncoated fused-silica capillaries of 60 cm total length, 54 cm effective length, and 75 μm (I.D.) maintained at 25 °C.
5. *CE buffer:* Prepare buffer solutions of pH 1–10 at unit intervals by mixing hydrochloric acid (0.1 M) and potassium chloride (0.1 M) for pH 1–2; acetic acid (0.1 M) and sodium acetate (0.1 M) for pH 3–6; boric acid (0.1 M) and sodium

tetraborate (0.1 M) pH 8–9; sodium bicarbonate and sodium carbonate for pH 10; citric acid (0.1 M) and sodium oxalate (0.1 M) for pH 2–7; phosphoric acid (0.1 M) and sodium dihydrogen phosphate (0.1 M) for pH 2–7.

2.2.9 Determination of Heavy Metals by 2-(5-Nitro-2-pyridylazo)-5-(N-propyl-N-sulphopropyl-amino)phenol (Nitro-PAPS) [28]

1. *Analyte:* Co(II), Cu(II), Ni(II), Fe(II), and V(V).
2. *Sample:* Drinking water and wine.
3. *Sample preparation:* Use standard solutions (1000 mg/l) of metal ions and prepare their aqueous solutions with deionized water by stepwise dilution. Prepare 1.0×10^{-3} mol/l Nitro-PAPS solution by dissolving an accurate amount of Nitro-PAPS in water and store in a dark bottle. Prepare the working solutions by stepwise dilution.
4. *CE instrumentation and capillary*: A Beckman P/ACE TM MDQ capillary electrophoresis system (Beckman Instrument, Fullerton, USA) equipped with a photodiode array detector, a fused-silica capillary (Beckman) with a total length of 40.2 cm (30.0 cm effective length) × 50 μm I.D.
5. *CE buffer*: Prepare a mixture of acetate (25 mmol/l) of pH 5.0, phosphate (25 mmol/l) of pH 7.0, or borate (25 mmol/l) of pH 10.0.

2.3 Rare Earth Elements

2.3.1 Analysis of Rare Earth Elements (Lanthanides) [29]

1. *Analytes*: 1000 mg/l of all lanthanides (La–Lu).
2. *Sample*: Synthetic geochemical standards (SPV-1 and SPV-4).
3. *Sample preparation*: Prepare high purity oxides in deionized water by mixing the analytes as given in Table 2 and 3. Take 100 μl of each of these metal ions and evaporate and dilute to 500 μl and inject 20 μl of this solution to get the electropherogram.
4. *CE instrument and capillary*: A Quanta 4000 capillary electrophoresis instrument (Waters, Milford, MA, USA) equipped with positive power supply. Variable wavelength UV detection system Waters 820 Workstation for collecting electrographic data. Millennium 2000 software. Fused-silica capillary (36.5 cm length × 75 μm I.D.). The applied voltage was +30 kV. The UV detection was set at a wavelength of 214 nm using a zinc lamp. Hydrostatic injection mode is used for elevating the sample at a constant height of 10 cm for 20 s. A temperature control system was employed for fixing the working capillary column temperature.
5. *CE buffer*: Prepare 100 mM α-hydroxyisobutyric acid (HIBA) solution and further dilute to it to 4 mM. UV Cat-1 solution or electrolyte modifier (Waters) with a complexing agent solution of 4 mM HIBA. Adjust the pH of the solutions to pH 4.4 with dilute acetic acid and filter through a 0.22 μm membrane filter.

Table 2

Chemical composition pattern of the REE synthetic geochemical standards (SPV-1 and SPV-4)

REE	Chemical symbol	SPV-1 (mg/ml)	Quantity injected (ng)	SPV-4 (mg/ml)	Quantity injected (ng)
Lanthanum	La	34.627	138.508	78.525	314.100
Cerium	Ce	69.400	277.600	141.029	564.116
Praseodymium	Pr	10.784	43.136	14.531	58.124
Neodymium	Nd	42.334	169.336	69.945	279.780
Samarium	Sm	9.882	39.528	15.695	62.780
Europium	Eu	2.720	10.880	3.524	14.096
Gadolinium	Gd	10.251	41.004	11.144	44.576
Terbium	Tb	21.840	87.360	2.345	9.380
Dysprosium	Dy	10.669	42.676	7.267	29.068
Holmium	Ho	2.387	9.548	2.000	8.000
Erbium	Er	5.706	22.824	4.934	19.736
Thulium	Tm	1.084	4.336	0.756	3.024
Ytterbium	Yb	5.420	21.680	3.708	14.832
Lutetium	Lu	1.015	4.060	0.708	2.832

2.3.2 Determination of Uranium(VI) and Transition Metal Ions with 4-(2-thiazolylazo) resorcinol (TAR) [30]

1. *Analytes*: Prepare dilute solutions of cobalt, copper, cadmium, nickel, titanium, and uranium from their stock solutions in water. Prepare the metal complexes by reacting the appropriate metal ion with 1 mM TAR solution and use NaOH or HCl to adjust the pH to 8.3.
2. *Sample preparation:* Filter the solutions through a 2 μm membrane filter and keep them for 5 min before injection.
3. *CE instrument and capillary:* BioFocus 3000 CE system (Bio-Rad, Hercules, CA, USA) equipped with a 72 cm effective length × 50 μm I.D. fused-silica capillary (Alltech, Deerfield, IL, USA). Inject the samples hydrostatically into the capillary for 2 s and perform the separation in the normal polarity mode at +25 kV. Perform the detection at the cathodic end with a photodiode array detector functioning in either the single wavelength (530 nm) or scanning mode (370–600 nm).
4. *CE buffer:* The carrier electrolyte consists of 5×10^{-3} stock solution of TAR in 15 mM NaH_2PO_4–$Na_2B_4O_7$ buffer, pH 8.3.

2.3.3 Separation of Trivalent Lanthanides by Complexation with Humic Acid [31]

1. *Analyte:* Eu, Gd, La.
2. *Sample preparation:* Prepare samples of 100 μg/l (mixture of 3.29×10^{-7} mol/l Eu and 3.18×10^{-7} mol/l Gd) and 6000 μg/l

Table 3
Reproducibility tests based on six injections of standard solution SPV-1

REE	Chemical symbol	Quantity injected (ng)	Migration time[a] (%)	Peak area[a] (%)	Peak height[a] (%)
Lanthanum	La	138.508	0.12	0.30	0.18
Cerium	Ce	277.600	0.15	0.15	0.21
Praseodymium	Pr	43.136	0.12	0.88	0.93
Neodymium	Nd	169.336	0.10	0.17	0.74
Samarium	Sm	39.528	0.07	1.77	1.20
Europium	*Eu*	10.880	0.14	4.61	2.77
Gadolinium	*Gd*	41.004	0.06	2.63	2.81
Terbium	Tb	87.360	0.10	2.64	1.61
Dysprosium	Dy	42.676	0.11	1.54	0.48
Holmium	Ho	9.548	0.09	3.23	3.93
Erbium	Er	22.824	0.14	1.30	1.38
Thulium	Tm	4.336	0.18	9.30	5.36
Ytterbium	Yb	21.680	0.24	2.12	1.52
Lutetium	Lu	4.060	0.30	4.73	7.48

[a]The numbers refer to the relative standard deviation (RSD) values expressed in %

(mixture of 1.97×10^{-5} mol/l Eu and 1.91×10^{-5} mol/l Gd)) Ln(III), humic acid and 0.01 mol/l $NaClO_4$ in a final volume of 10 ml deionized water. Purify the humic acid from contaminants such as metal ions and then use it for the preparation of solution.

3. *CE instrument and capillary:* A P/ACE MDQ, Beckman Coulter Inc., Brea, CA, USA CE instrument hyphenated to inductively coupled plasma mass spectrometer (ICP-MS) using a homemade interface. Fused-silica (Polymicro Technologies) capillary with physical parameters 74 μm (I.D.), 362 mm (O.D.) and 80 cm (length).
4. *CE buffer:* Mix 0.1 mol/l acetic acid and 0.01 mol/l sodium acetate in appropriate volume to make pH 3.7.

2.4 Multielement Analysis

2.4.1 Multielement Analysis Using Precapillary Complexation [32]

1. *Analytes:* Ag(I), Al(III), Ba(II), Bi(III), Ca(II), Cd(II), Ce(II), Cu(II), Co(II), Cr(III), Fe(II), Fe(III), Hg(II), La(III), Mg(II), Mn(II), Mo(V), Ni(II), Pb(II), Pd(II), Sb(III), Sn(IV), Sr(II), Tl(I), U(VI), V(IV), V(V), W(VI), Zn(II), Zr(IV).
2. *Sample preparation:* 5×10^{-3} M solution of metals in 20 mM sodium borate.

3. *CE instrument and capillary:* Waters Quanta 4000 CE system (Millipore Waters, Milford, MA, USA) equipped with negative power supply. Polyimide coated fused-silica capillaries (Polymicro Technology, Phoenix, AZ, USA) 50 cm in length with and I.D. 75 μm UV–Vis detector. Condition the new capillaries by rinsing with 0.1 M NaOH for 1, followed by a 20 min rinse with water. Then rinse with 0.005 M NaOH and then with water to wash the capillary between runs with different electrolyte solutions. Also purge the capillary with electrolyte solution for 2 min before each run.
4. *CE buffer*: For the metal complexes add 5×10^{-3} M solution of reagent in 0.01 M sodium tetraborate to give 1×10^{-3} M CDTA solution to give a 2.5-fold molar excess in the final solution in 5 % ethylene glycol.

2.4.2 Separation of Metal Ions with EDTA [33]

1. *Analyte:* Metal atomic absorption standard solutions (1000 mg/l of cobalt(II) in 2 wt% nitric acid, 1028 mg/l of calcium(II) in 1.1 wt% HCl, 1017 mg/l of manganese(II) in 1.1 wt% HCl, and 999 mg/l of zinc(II) in 1 wt% HCl).
2. *Sample preparation:* EDTA stock solution: Dissolve 0.146 g of EDTA in 50 ml of purified water in a 100 ml volumetric flask by dropwise addition of ammonium hydroxide. After dissolution of solid, make the volume 100 ml with purified water. The pH of the resulting EDTA solution should be 9.4.
3. *CE capillary and instrumentation*: Agilent 3DCE system interfaced with an Agilent 6320 Ion Trap MS system using an Agilent G1607A ESI interface and controlled with Agilent Chemstation software. Sheath liquid flow supplied by an Agilent 1200 pump with a built-in 1:100 flow splitter with sheath liquid flow rate of 4.5 ml/min. Set nebulizer pressure to a minimum to provide stable electrospray operation (7.0 psi) and highest possible separation efficiency. Additional spray chamber parameters: dry gas flow rate 5.0 l/min, drying gas temperature 250 °C, electrospray voltage −3.0 kV (end plate voltage −3.0 kV). Fused-silica capillaries of 75 mm I.D. × 375 mm O.D. (from Polymicro Technologies, Phoenix, AZ, USA) and a length from the inlet to the ESI interface of 1 m. The temperature of capillary is maintained at 251 °C by a thermostat and the portion of the capillary that connects the CE to the ESIMS also at 251 °C. ESI–MS detection with an Agilent 6320 Ion Trap LC/MS, 6300 Ion Trap Control software, and Agilent Pump 1200 Series.
4. *CE Buffer:* Prepare electrolyte stock solutions of 1 M ammonium acetate (pH 7), 10 % ammonia, and 0.5 M ammonium hydrogen carbonate (pH 9.4). Adjust the pH of the ammonium hydrogen carbonate solution with ammonium hydroxide. Prepare these solutions every day by mixing appropriate

aliquots of the stock solutions of 0.5 M ammonium hydrogen carbonate and 5 mM EDTA, followed by dilution with purified water. Filter all the solutions with 0.45 m filters prior to use. It should be noted that white crystalline EDTA is only slightly soluble in water. A soluble sodium salt of EDTA is not an option because sodium ion is known to suppress ionization, as well as form adducts with charged ions in ESI–MS [20].

3 Methods

The methods described herein outline the methods for the analysis of lanthanides, alkali metal ions, and some transition metal ions using CE. The method involves the complexation with the carrier electrolytes HIBA, EDTA, and CDTA. The developed reported methods involve very good separation of all the elements with a wide range of applications. Any of the particular metal ions can be analyzed by these methods.

3.1 Main Group Elements

3.1.1 Analysis of Alkali and Alkaline Earth Metal Ion [17]

1. Place the sample solution in the sample vial.
2. Take 0.8 mM EDTA solution containing 10 mM pyridine solution as running electrolyte. Fig. 1 shows the effect of concentration of EDTA on the separation of metal ions.
3. Inject the sample solution by hydrostatic injection for 15 s with 4.0 cm height difference.
4. Repeat the injections and prepare the calibration curve up to 1.00 μg/ml. Figure 1 indicates the standard capillary electropherogram for the determination of alkali and alkaline earth metal ions.
5. Apply the method for the determination of magnesium in calcium carbonate sample, river water, and urine. Figure 2 shows the determination of magnesium in real samples.

3.1.2 Determination of Na^+, K^+, Mg^{2+}, and Ca^{2+} by Indirect Detection [18]

1. Rinse the capillary with 1 M NaOH for 15 min, followed by water for 15 min and finally with appropriate electrolyte solution for 15 min.
2. Filter the carrier electrolyte and sample with 0.45 μm filter prior to analysis.
3. Inject the samples into the capillary using 20 s hydrostatic injection from a height of 9.8 cm.
4. Apply a voltage of 20 kV and set the temperature at 13 °C.
5. Purge the capillary for 2.0 min between the runs.
6. Perform the indirect UV detection at 185 nm.
7. Figure 3 shows the standard capillary electropherogram of K^+, Ba^{+2}, Sr^{2+}, Ca^{2+}, Na^+, and Mg^{+2} and Figure 4 shows their separation in sea water.

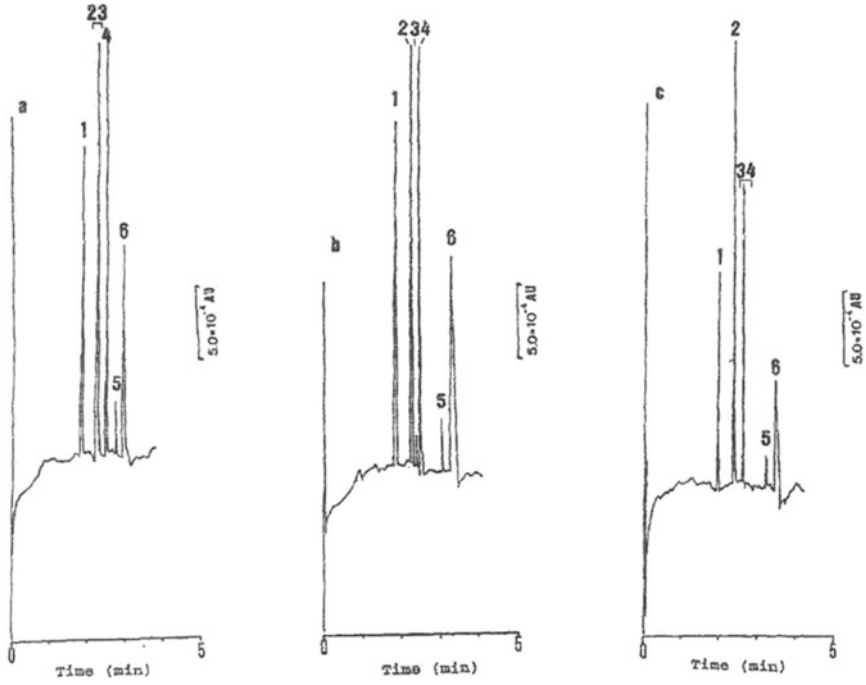

Fig. 1 Effect of concentration of EDTA on the separation of metal ions. Conditions: L_{total} = 395 cm, $L_{effective}$ = 300 cm pH = 50; 10 mM pyridine; hydrostatic injection for 15 s with 4.0 cm height difference (**a**) 0.6 mM EDTA; (**b**) 0.8 mM EDTA; (**c**) 1.0 mM EDTA. Peaks 1 = K^+, 2 = Na^+, 3 = Ba^{2+}, 4 = Li^+, 5 = Sr^{2+}, 6 = Mg^{2+} and 7 = Ca^{2+}. Sample concentration: K^+, Na^+, Ba^{2+}, Li^+, Sr^{2+}, Mg^{2+} and Ca^{2+} = 1 g/mL each in deionized water. (From ref. 17)

3.1.3 Analysis of Alkali and Alkaline Earth Metals by Ionic Liquid [19]

1. Perform the experiments in cathodic mode (injection at the anode and the detection near the cathode) with a constant voltage of 25 kV at 25 °C.
2. Inject the samples by applying a pressure injection of 0.5 psi (3447 Pa) for 10 s.
3. Rinse the PVA capillary with water and the running electrolyte for 10 min each.
4. Flush the capillary for 2 min with water followed by running electrolyte for 2 min after each analysis.
5. Rinse the fused-silica capillary with 1 M sodium hydroxide for 30 min followed by water for 15 min to activate the uncoated surface.
6. Condition with a concentrated solution of ionic liquid and the running electrolyte.
7. For nonaqueous capillary electrophoresis, rinse the activated capillary with methanol for 15 min and then with the separation medium for 10 min.

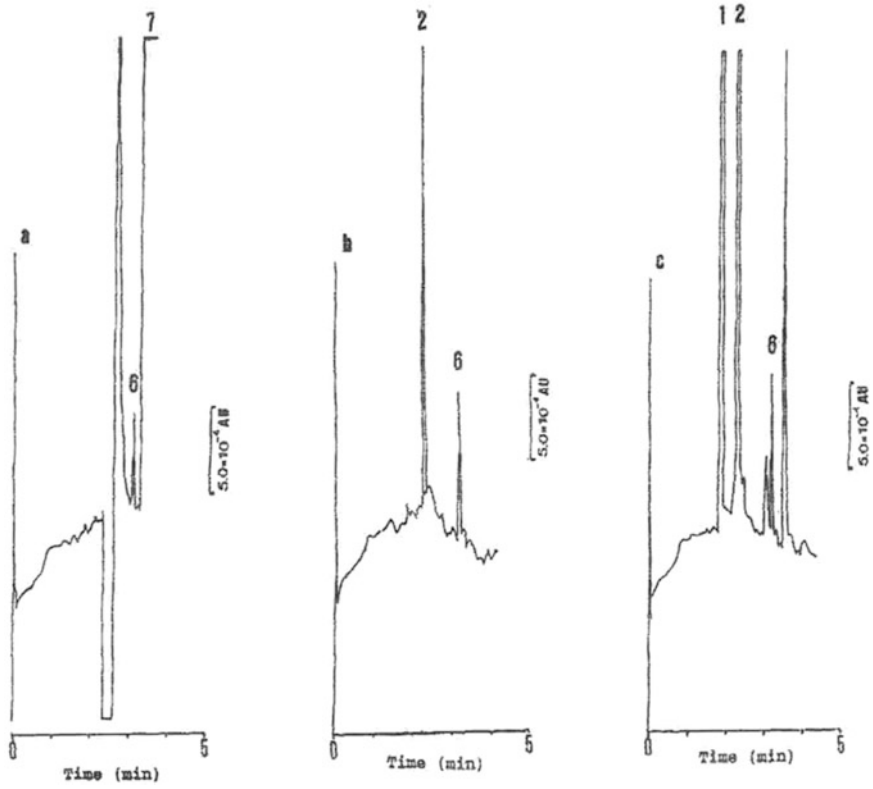

Fig. 2 Electropherograms obtained with some real samples. (**a**) Calcium carbonate sample, (**b**) river water, (**c**) urine. Conditions: L_{total} = 39.5 cm, $L_{effective}$ = 30.0 cm; pH 5.00; 10 mM pyridine; hydrostatic injection for 15 s with 4.0 cm height difference, 0.8 mM EDTA. Peaks: 1 = K^+, 2 = Na^+, 3 = Ba^{2+}, 4 = Li^+, 5 = Sr^{2+}, 6 = Mg^{2+}, and 7 = Ca^{2+} (1 μg/ml each in deionized water)

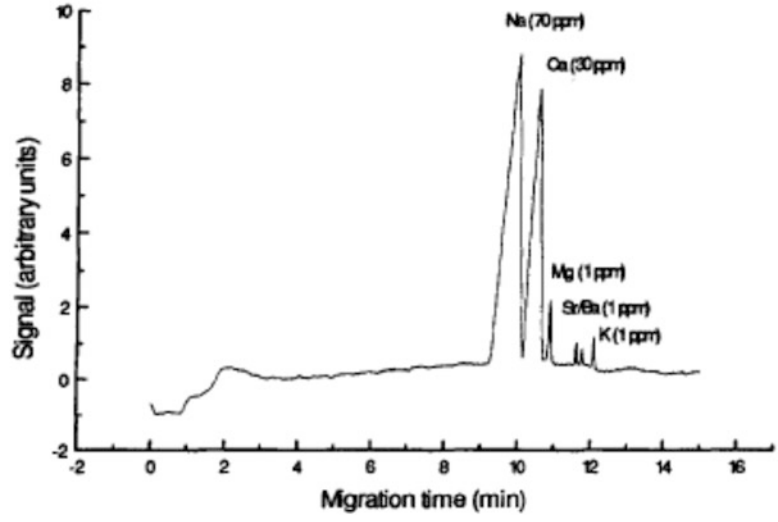

Fig. 3 Electropherogram of 70 ppm Na^+, 30 ppm Ca^{2+}, 1 ppm Mg^{2+}, Sr^{2+}, Ba^{2+}, and K^+. Electrolyte: 6.5 mM HIBA, 5.0 mM UVCAT-I,6.2 mM 18-crown-6 and 25.00 % (v/v) methanol (Ref. 18)

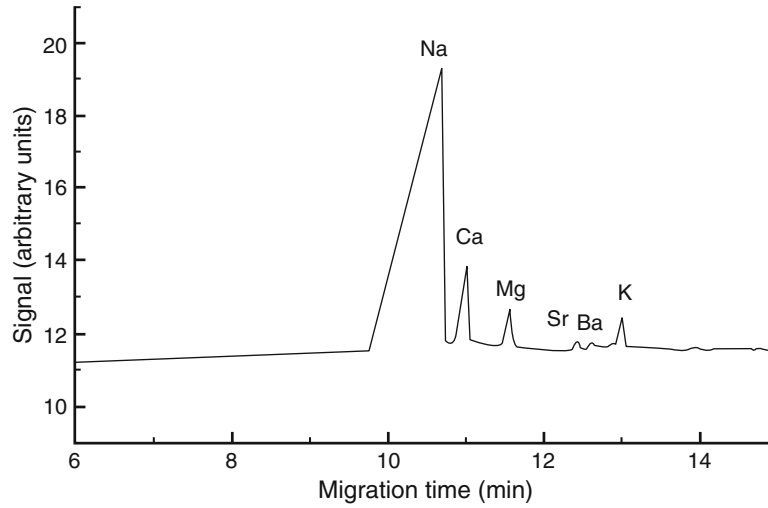

Fig. 4 Electropherogram of a mixture of seawater and formation water diluted by a factor of 125. Electrolyte: 6.5 mM HIBA, 5.0 mM UVCAT-I, 6.2 mM 18-crown-6, and 25.00 % (v/v) methanol (Ref. 18)

8. Inject the sample to get data and repeat the washing of capillary after each analysis.
9. Figure 5 represents separation of alkali and alkaline earth metals in aqueous samples.

3.2 Transition Metals

3.2.1 Determination of Pd(II) as a Chloro Complex in the Presence of Rh(III), Ru(III), Os(III), and Ir(III) [20]

1. Purge the electrolyte prior to injection of the samples for 3 min by employing a vacuum of 12–15 psi at the receiving electrolyte vial.
2. Inject the samples by gravity at the cathode.
3. Place the detector at 7.25 cm from the receiving electrolyte.
4. Determine the electroosmotic flow μ_{eo} from the migration time of formamide.
5. $PdCl_4^{2-}$ can be separated in the presence of 20 ppm of Ir(III), Os(III), Rh(III) and Ru(III), 100 ppm of Cu(II), Ni(II), Fe(II), and Co(II) and a large amount of Cl^-. The cations Cu(II), Ni(II), Fe(II), and Co(II) do not influence the determination of Pd since they travel in the opposite direction to the cathode and therefore the peaks due to Cu(II), Ni(II), Fe(II), and Co(II) do not appear in the chromatogram. An electropherogram for Pd(II) in the presence of other metal ions is shown in (Fig. 6).
6. The detection limit for $PdCl^{4-}$ is 20 ppb for 50 mM KCl–HCl carrier electrolyte containing 0.2 mM CTAB.

3.2.2 Analysis of Cr(III), Fe(III), Cu(II), and Pb(II) [21]

1. Rinse the capillary with de-ionized water for several hours.
2. Equilibrate the capillary with carrier solution for 40 min before the first run.

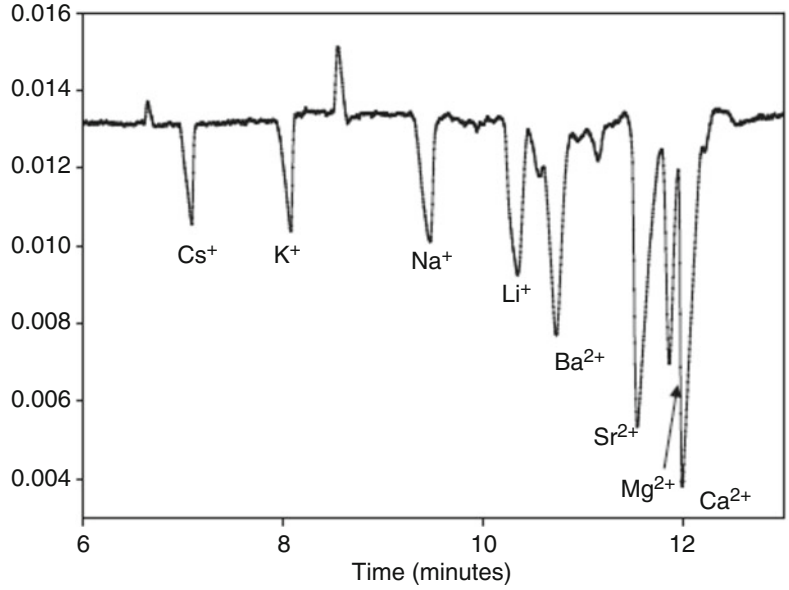

Fig. 5 Separation of alkali and alkaline earth metals in non-aqueous medium in the presence of phenylcholine NTf_2 and acetic acid (Ref. 19)

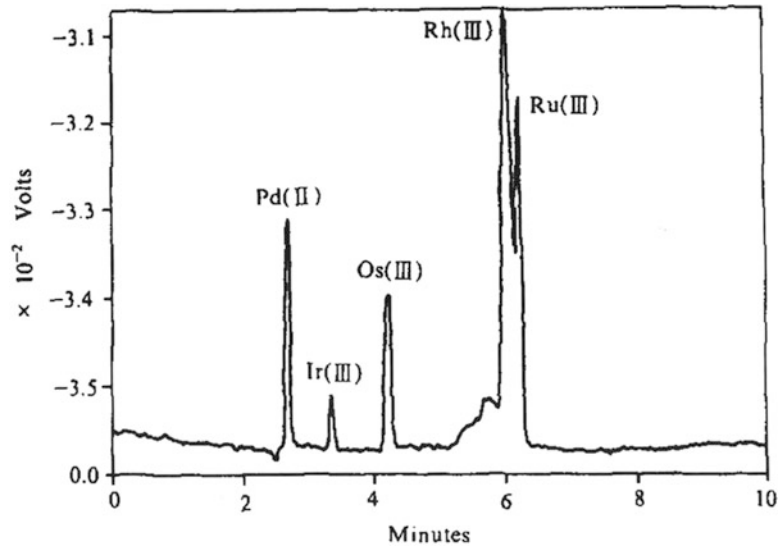

Fig. 6 Electropherogram for the determination of Pd(II) in the presence of 20 ppm each of Ir(III), Os(III), Rh(III), and Ru(III) chloride complexes and 100 ppm each of Cu(II), Ni(II), Fe(II), and Co(II). Carrier electrolyte, 50 mM HCl–KCl containing 0.2 mM CTAB at pH 3.0 applied voltage 17 kV, untreated fused-silica capillary, 52.2 cm × 75 μm I.D.; applied voltage, 15 kV (Ref. 20)

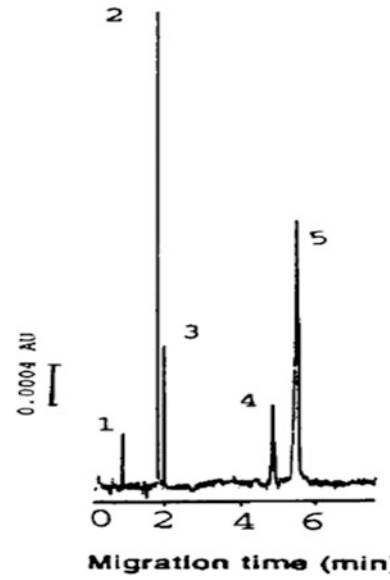

Fig. 7 Electropherogram for a standard metal solutions in excess of EDTA at –30 kV; 0.1 M acetate and 0.1 mM TTAB in carrier solution; 20 μg/ml of each metal ions. Peaks 1 = NO_3^-, 2 = EDTA; 3 = Cu-EDTA, Pb-EDTA, 4 = Cr-EDTA; 5 = Fe-EDTA (Ref. 21)

3. Fill the capillary with carrier solution using a syringe purge.
4. Dip both ends into two separate beakers filled with the same carrier solution.
5. Introduce the sample through cathodic or anodic end of the capillary by vacuum injection.
6. Apply a high voltage of –30 kV.
7. Figure 7 shows the separation of Cr(III), Fe(III), Cu(II), and Pb(II) as EDTA complexes.
8. Prepare the standard calibration curve for these ions and carry out the analysis.
9. The detection limit of the metal complexes is in the range of 6–27 μM.
10. Figure 8 indicates the capillary electropherogram of waste water from tannery effluent for the analysis of Cr(III).

3.2.3 Determination of Cu(II), Fe(III), Zn(II), Co(II) and Ni(II) Using 4-(2-Pyridylazo)Resorcinol (PAR) [22]

1. Rinse the capillary with 1 M NaOH for 15 min, followed by water for 15 min and a 15 min rinse with appropriate electrolyte solution.
2. Repeat the rinsing procedures after every ten runs.
3. Prepare the separation electrolytes daily.

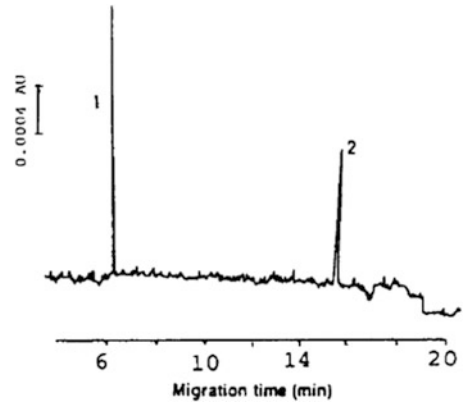

Fig. 8 Electropherogram of a tannery sample at −30 kV; 0.1 μ acetate and 0.1 mM TTAB in carrier solution (pH 5.5). Fused-silica capillary (80 cmx 50 μm I.D.). Sample preparation: diluted, pH 5.5 M-EDTA formed by boiling for 10 min in excess of EDTA, filtered, degassed, and injected. Peaks: 1 = EDTA; 2 = Cr-EDTA, 26.14 μg/ml Cr(III) (Ref. 21)

4. Prepare the PAR metal chelate complexes by mixing metal ion solution and 1 mM PAR reagent. Adjust the pH to 9.2 for the better stability of the complexes.
5. Introduce the samples into the capillary by applying the pressure.
6. Apply a voltage of 30 kV.
7. Prepare the standard calibration curve for the determination of these metal ions.
8. Figure 9 indicates the separation of Cu(II), Fe(III), Zn(II), Co(II) and Ni(II) under the optimum conditions. The detection limits calculated for Cu(II), Fe(III), Zn(II), Co(II) and Ni(II) are 17, 6, 30, 24, and 22 μg/l.
9. Figure 10 indicates the capillary electropherogram of Cui Ming green tea. The concentration of these metal ions reported for Cui Ming green tea is Cu(II), Fe(III), Zn(II), Co(II) and Ni(II) is 21.8, 74.0, 48.8, and 7.5 mg/kg, respectively.

3.2.4 Determination of Heavy Metal Ions Using Polyamidoamine (PAMAM) Dendrimers [23]

1. Fill the capillary with running buffer containing PAR. Then, load a plug of PAMAM solution by 22 cm, 20 s, corresponding to 21.52 mm in length.
2. Fill the anodic reservoir with sample solution and apply a positive voltage (+5 kV) across the capillary to electrokinetically inject the metal ions.
3. Apply backpressure (−0.6 kPa) at the injection end, generating a flow of 0.29 mm/s in order to avoid the solutes migrating far

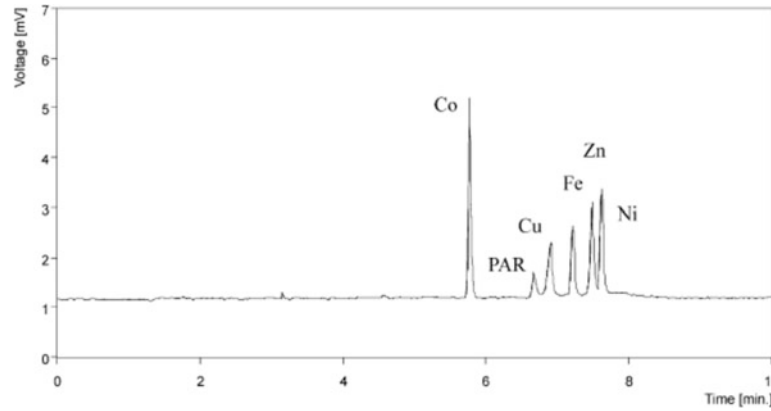

Fig. 9 Electropherogram of five metal ions under optimal conditions. The separation electrolyte, 10 mM TAPS, 0.1 mM PAR, 5 mM TBA, 5 mM TMA, pH value 8.75. Applied voltage, 30 kV. Sample introduction, pressure 10 s at 0.29 psi (Ref. 22)

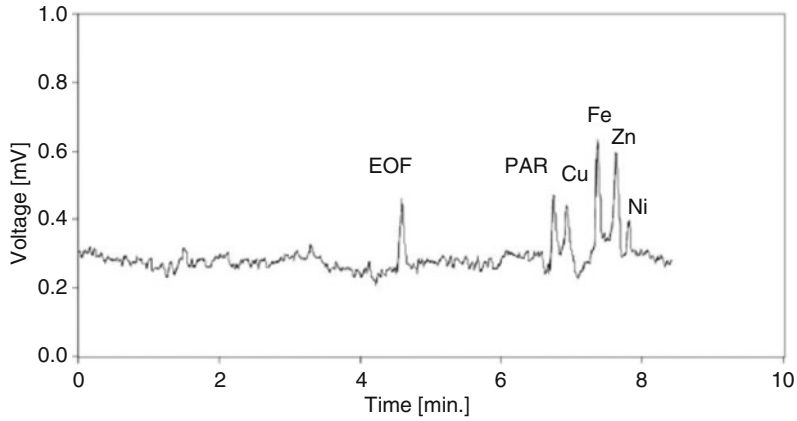

Fig. 10 Determination of metal ions in Cui Ming green tea. Running conditions were the same as Fig. 9 (Ref. 22)

away from the injection end by the cathodic electroosmotic flow (EOF,0.47 mm/s) while preventing PAR (moving at −0.25 mm/s) and the metal ion–PAR (M–PAR) complexes from moving out of the capillary.

4. At the beginning of the field amplified sampleinjection (FASI), the introduced metal ions are stacked by forming metal ion–PAMAM (M–PAMAM) complexes at the sample/PAMAM boundary. This procedure can be termed sweeping—by the partial-filling PAMAM.
5. It works until after 85 ± 3.4 s, when negatively charged PAR electrophoretically moving toward the injection end ultimately reaches the right edge of M-PAMAM zone.

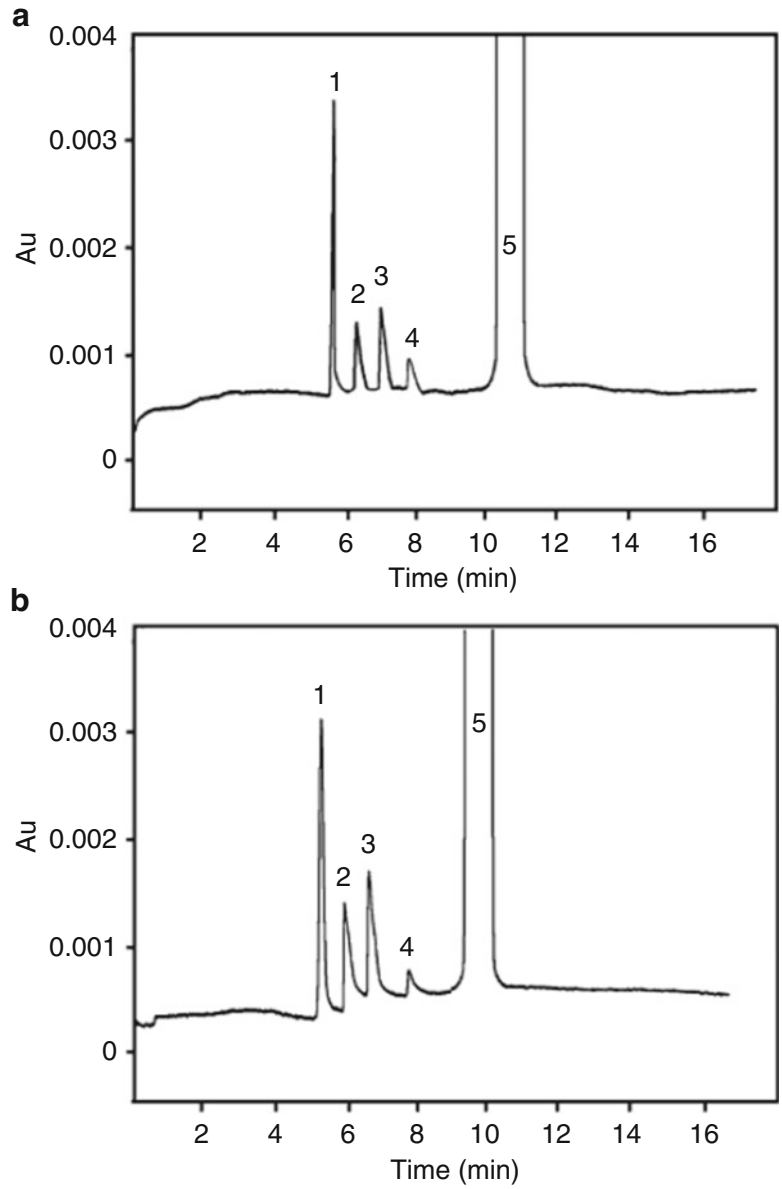

Fig. 11 Electropherograms of the studied metal ion standard solution (**a**) 10 mg/l standard solution without in-line preconcentration, (**b**) 1 mg/l solution with in-line preconcentration using optimum conditions (1 = Fe(II)-phen, 2 = Zn(II)-phen, 3 = Cu(II)-phen, 4 = Cd(II)-phen, 5 = Phen) (Ref. 25)

6. At this moment, another enrichment procedure takes place (Step c). The PAMAM-bound metal ions are released and simultaneously bound by PAR and stack at the metal ion/PAR boundary.

7. After injection, fill the anodic reservoir with running buffer, and apply a separation voltage (+10 kV) across the capillary.

3.2.5 Analysis of Cu and Pb as ABEDTA Complexes [24]

1. Add 1.0 ml water solution of Cu-ABEDTA containing 0.05 mg Cu^{2+} to neutral Al_2O_3 column conditioned with 2 ml methanol and water, respectively.
2. Wash column with 10 ml water and elute with 5 ml 5% acetic acid–methanol solution.
3. Collect the elute and perform detection at 254 nm.
4. Remove interfering components in sample by washing with 10 ml of water.

3.2.6 Analysis of Metal Ions as Their Phenanthroline Complexes [25]

1. Pre-treat all the new capillaries in five steps at 20 psi in the hydrodynamic mode with 0.1 mol/l HCl for 10 min followed by water for 5 min.
2. Then, treat the capillaries with 0.1 mol/l NaOH for 10 min under same conditions followed by water for 5 min.
3. Equilibrate the capillaries with the running buffer solution for 7 min.
4. Rinse the capillary each day with 0.1 mol/l NaOH for 10 min and then water for 7 min. Then, equilibrate the capillary with running buffer for 5 min.
5. Precondition the capillary with the running buffer solution for 5 min before each run.
6. For in-capillary derivatization, fill the capillary with the running buffer and then the solution of derivatizing agent (60 mmol/l of 1,10-phenanthroline) at 0.2 psi for 2 s.
7. Introduce the sample into the capillary with hydrodynamic injection at 0.5 psi for 60 s.
8. Apply the separation voltage of 16 kV through the capillary to carry out the reaction inside the capillary which moves the metal ions through 1,10-phenanthroline. Detect the separation at 225 nm by UV detector.
9. After completing the separation, flush capillary with 0.1 mol/l NaOH for 3 min and wash with water for 2 min.
10. Figure 11 shows electropherogram of the metals 1 = Fe(II)-phen, 2 = Zn(II)-phen, 3 = Cu(II)-phen, 4 = Cd(II)-phen, 5 = Phen) without in-line preconcentration and with in-line preconcentration.
11. Electropherograms of some wine samples are shown in Figure 12.

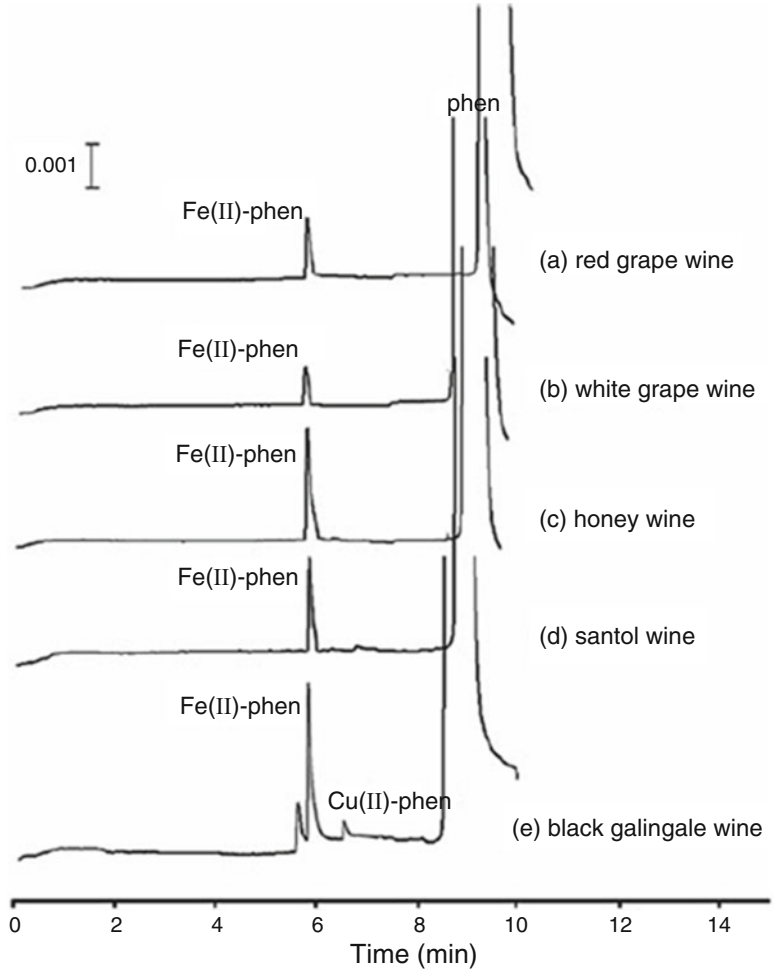

Fig. 12 Electropherograms of the studied wine samples under the optimum conditions (**a**) *red* grape wine, (**b**) *white* grape wine, (**c**) *honey* wine, (**d**) *santol* wine, and (**e**) *black* galingale wine (Ref. 25)

3.2.7 Determination of Metal Ions by 2,6-Pyridinedicarboxylic Acid (PDC) [26]

1. Apply separation voltage of −20 kV.
2. Maintain the temperature of the capillary tube during electrophoresis at 15 °C.
3. Before operation, pretreat the capillary by flushing with an electrolyte for 4 min.
4. Inject the analyte under a 50 mbar pressure and maintain injection time as 6 s.
5. Detect the electrophoretic zones at 214 nm with a photodiode array detector.

3.2.8 Determination of Au(III), Cr(VI), Fe(III), UO_2(II), and Ni(II) Using Bis(salicylaldehyde) [27]

1. Prior to the sample run, regenerate and condition the capillary with methanol for 1 min, followed by water for 0.5 min, HCl (0.1 M) for 2 min, water for 0.5 min, sodium hydroxide (1 M) for 2 min, water for 0.5 min, and finally, running buffer for 5 min.
2. Before each sample injection, wash the capillary with sodium hydroxide (0.1 M) for 10 min, water for 2 min, and then equilibrate with background electrolyte for 10 min to ensure the reproducibility of results.
3. Inject the sample by an autosampler with a pressure of 0.5 psi and record the results.

3.2.9 Determination of Heavy Metals by 2-(5-Nitro-2-Pyridylazo)-5-(N-Propyl-N-Sulphopropyl-Amino) Phenol (Nitro-PAPS) [28]

1. Prepare the metal-Nitro-PAPS chelates at the metal to ligand ratio (M:L) of 1:2 at pH 5.0.
2. Wash the capillary with methanol for 5 min, followed by water for 2 min, 0.1 mol/l HCl for 5 min, water for 2 min, 0.1 mol/l NaOH for 5 min, and water for 2 min.
3. At the beginning for each day, rinse the capillary with 0.1 mol/l NaOH and water for 5 min, equilibrate with electrolyte for 20 min.
4. In between all electrophoretic separations, automatically rinse the capillary with 0.1 mol/l NaOH for 3 min, water for 3 min, and the electrolyte for 5 min.
5. Apply the separation voltage of 15 kV, and maintain temperature of 25 °C for analyzing samples.

3.3 Rare Earth Elements (REEs)

3.3.1 Analysis of Rare Earth Elements Lanthanides [16]

1. Switch on the instrument and wait for 20 min.
2. Flush the capillary with deionized water and with working electrolyte for 10 min.
3. Use the hydrostatic mode for injecting the sample in to the capillary. Immerse the capillary in the sample at a height of 10 cm above the running electrolyte level for 20 s.
4. Lower the capillary into the electrolyte and apply the voltage of +30 kV.
5. Figure 13 presents an electropherogram showing partial separation of the REEs at 25 °C. These separations are possible in less than 2 min (~1.6) being a considerably reduced analysis time. La, Ce, Pr, Nd, Sm, Tb, Dy, and Er are base line separated. These elements can be easily detected as these easily show optimal peak shape. The following problems were observed: (a) the co-elution of Eu and Gd, (b) tailing problem in the Ho and Yb peaks, and (c) a poor sensitivity of the Tm and Lu peaks. The linearity response of the individual lanthanides is given in Table 4.
6. Figure 14 shows the separation of the lanthanides using lactic and 4-methylbenzylamine at pH 4.3. Europium is not resolved in the REEs standard mixture.

Table 4
Linearity of response for the individual REEs by CE (inferred from calibration curves with 4 data points)

REE	Chemical symbol	Quantity injected min.-max (ng)	Correlation coefficients
Lanthanum	La	0–415.5	0.9994
Cerium	Ce	0–832.8	0.9998
Praseodymium	Pr	0–129.4	0.9998
Neodymium	Nd	0–508.0	0.9998
Samarium	Sm	0–118.5	0.9972
Europium	*Eu*	0–32.6	0.9985
Gadolinium	*Gd*	0–123.0	0.9951
Terbium	Tb	0–262.1	0.9994
Dysprosium	Dy	0–128.0	0.9969
Holmium	Ho	0–28.6	0.9946
Erbium	Er	0–68.5	0.9996
Thulium	Tm	0–13.0	0.8840
Ytterbium	Yb	0–65.0	0.9971
Lutetium	Lu	0–12.2	0.6561

7. Temperature plays an important role in the separation of the lanthanides. For this study the separations at 35 and at 15 °C were performed. The separation at 35 °C did not involve the resolution of Eu and Gd whereas these are completely resolved at 15 °C (Fig. 15). A slightly longer time about ~1.6 min is required for the efficient separation of Eu and Gd at 15 °C.

3.3.2 Determination of Uranium(VI) and Transition Metal Ions with 4-(2-Thiazolylazo) Resorcinol (TAR) [30]

1. Rinse the capillary with 15 M $Na_2B_4O_7$ (pH 12) for 30 min, followed by a 30 min rinse with deionized water.
2. Perform all the experiments at 20 °C and make all the runs in triplicate. Before each run, rinse the capillary for 1 min with 15 M $Na_2B_4O_7$ (pH 12 buffer) followed by a 2 min rinse with deionized water and finally run buffer for 2 min.
3. Use Rhodamine B (Lambda Physik, Bedford, MA, USA) as the neutral marker to measure the electro-osmotic flow (EOF).
4. Inject the TAR–metal complexes into the capillary and carry out the separation.
5. Figure 16 indicates the separation of metal–TAR complexes.
6. The detection limits are found to be 88, 114, 59, 144, 733, and 1.7 ppm for cobalt, cadmium, nickel, copper, titanium, and uranium, respectively.

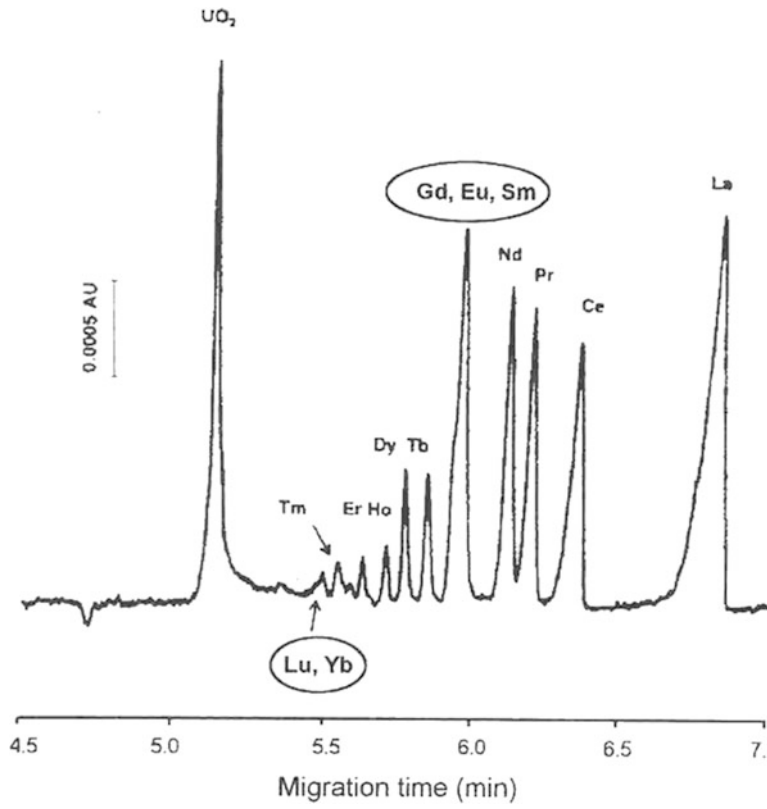

Fig. 13 Electropherogram of a typical separation pattern of 14 lanthanides. Background electrolyte 0.025 mM All in 15 MM citric acid and 20 mM Tris (pH 4.3); temperature 25 °C; separation voltage, –30 kV (30 μA); injection of a standard solution containing 10 μM of each metal [except 20 mM for Tm(III), Yb(III) and Lu(III)] in 10 mM HNO_3, for other operating details see Ref 29] (Ref. 16)

3.3.3 Separation of Trivalent Lanthanides by Complexation with Humic Acid [31]

1. Couple CE with ICP-MS by fitting a fused-silica CE-capillary into a MicroMist 50 μl nebulizer with a cinnabar cyclonic spray chamber in the external interface.
2. Adjust the gas flow of the nebulizer by the ICP-MS control.
3. Use a makeup (2% HNO_3, 24 nmol/l Ho, flow: 112 μl/min) fluid including 4 ng/l Ho as an internal standard within the interface.
4. Prior to sample injection perform washing and preconditioning of capillary with hydrochloric acid, sodium hydroxide, MilliQ-water, and apply CE buffer.
5. Inject the sample hydrodynamically at a pressure of 10 kPa for 20 s.
6. During the CE separation, apply a pressure of 20 kPa (to enforce a migration of the negatively charged species to the cathode) and a voltage of 30 kV.

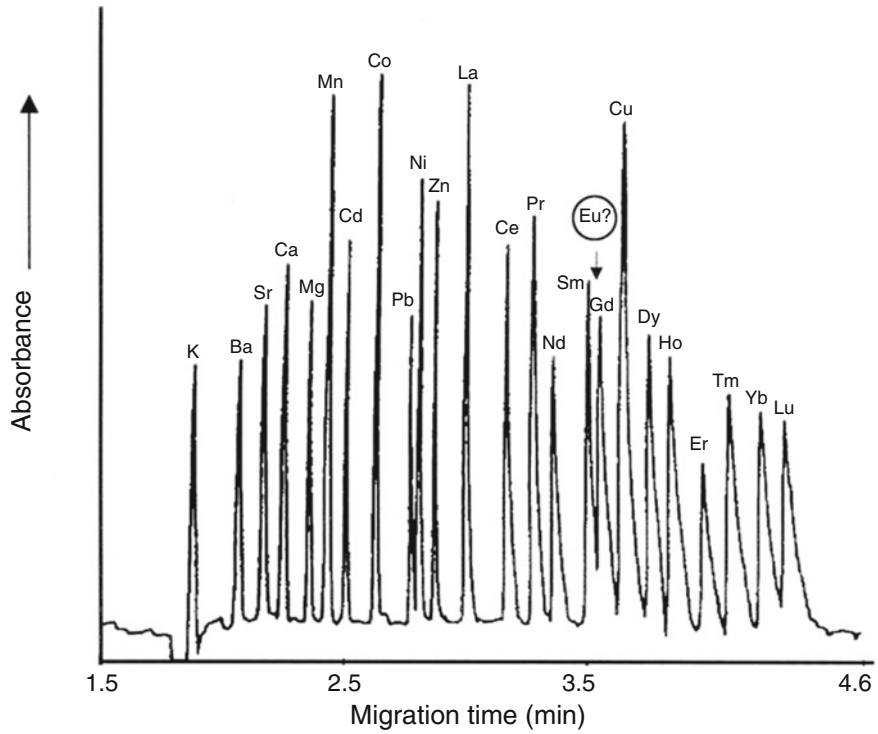

Fig. 14 Separation of some cations and lanthanide elements by co-EQF capillary electrophoresis with indirect Spectrophotometric detection. The electrolyte was 15 mM lactic acid and 10 mM 4-methylbenzylamine at pH 4.3. Europium was not included in the REE standard mixture (Ref. 16)

3.4 Multielement Analysis

3.4.1 Multielement Analysis Using Precapillary Complexation [32]

1. Prepare the electrolyte solution containing 20 mM sodium borate and 5% ethylene glycol.
2. Inject the solution of the metal ions in to the capillary by hydrostatic injection at 100 mm for 20 s.
3. Apply 12.5 kV and record the capillary electropherogram.
4. Separation of the metal complexes with non-modified borate electrolyte is shown in Figure 17. The carrier electrolyte consists of 10 mM sodium borate containing 1 mM CDTA (pH 9.0).
5. A standard capillary electropherogram is shown in Fig. 18. The separation of 23 cations is reported under these conditions.
6. The detection limits as reported (three times the signal to noise ratio) range from 1×10^{-7} M (Fe(III) to 4×10^{-6} M (Ca(II), Hg(II) and on average are 10^{-6} M.

3.4.2 Separation of Metal Ions with EDTA [33]

1. Precondition the capillary with 0.1 M sodium hydroxide for 10 min, followed by purified water for 10 min, methanol for 10 min, and finally flush purified water at about 950 mbar.
2. Flush the capillary with 10% ammonium hydroxide for 1 min followed by water for 2 min, and then the buffer solution for 5 min before each electrophoretic run.

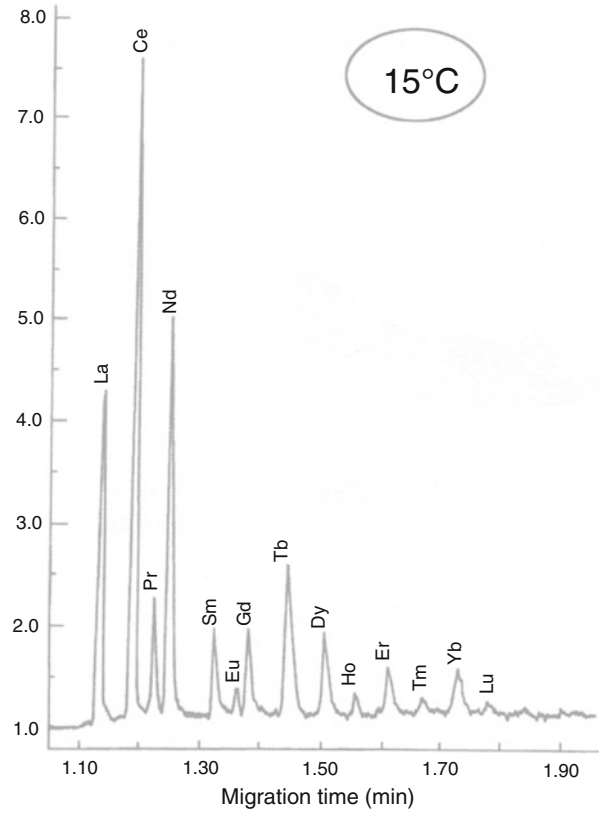

Fig. 15 Electropherogram of typical separation pattern of 14 lanthanides. Background electrolyte, 4 mM HIBA and 10 mM UV Cat-1 (pH 4.4 with acetic acid); temperature 15 °C; separation voltage +30 kV; injection of SPV-1 standard solution ref. [16]

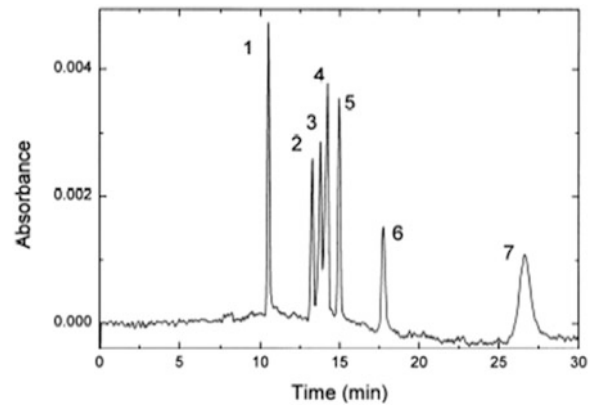

Fig. 16 Separation of TAR complexes in 15 mM NaH_2PO_4-$Na_2B_4O_7$, pH 8.3, 1×10^{-4} TAR (optimum conditions). 1 = Co(II) (5 ppm), 2 = free TAR, 3 = Cu(II) (5 ppm), 4 = Cd(II) (5 ppm), 5 = Ni(II) (2.5 ppm), 6 = Ti(II) (15 ppm), and 7 = U(VI) (30 ppm) (Ref. 30)

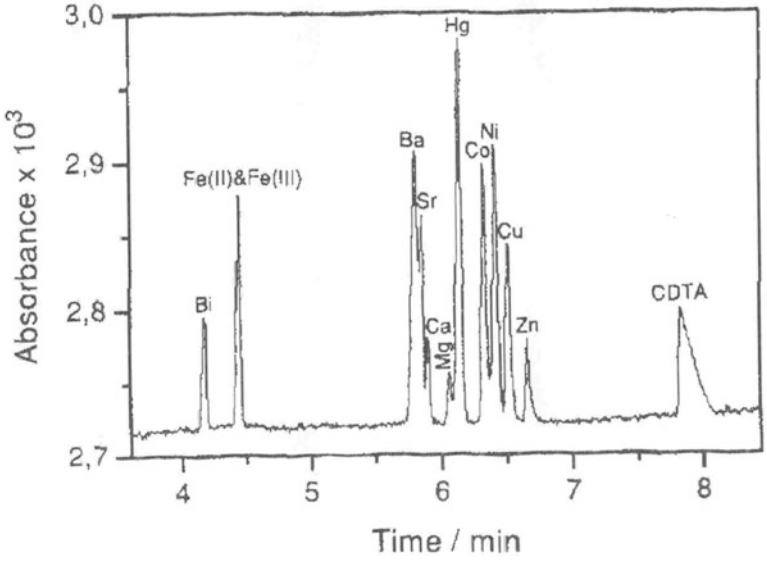

Fig. 17 Separation of metal complexes with non-modified borate electrolyte. Carrier electrolyte sodium borate: containing 1 mM CDTA (pH 9.0). Metal ion concentration: 5×10^{-5} M Fe(II), Fe(III) and 1.0×10^{-4} M other metals (Ref. 32)

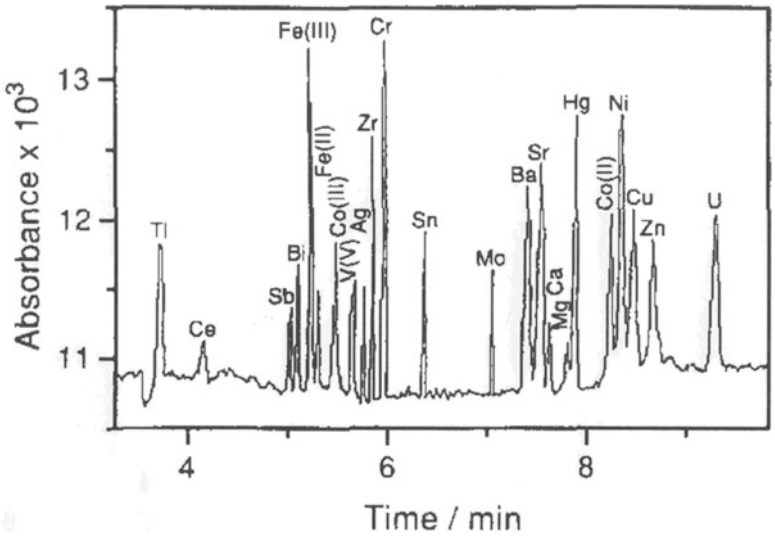

Fig. 18 Separation of metal–CDTA complexes using ethylene glycol as an electrolyte additive. Electrolyte: 20 mM sodium borate, 1 mM CDTA and 5 % ethylene glycol, voltage: 12.5 kV (Ref. 32)

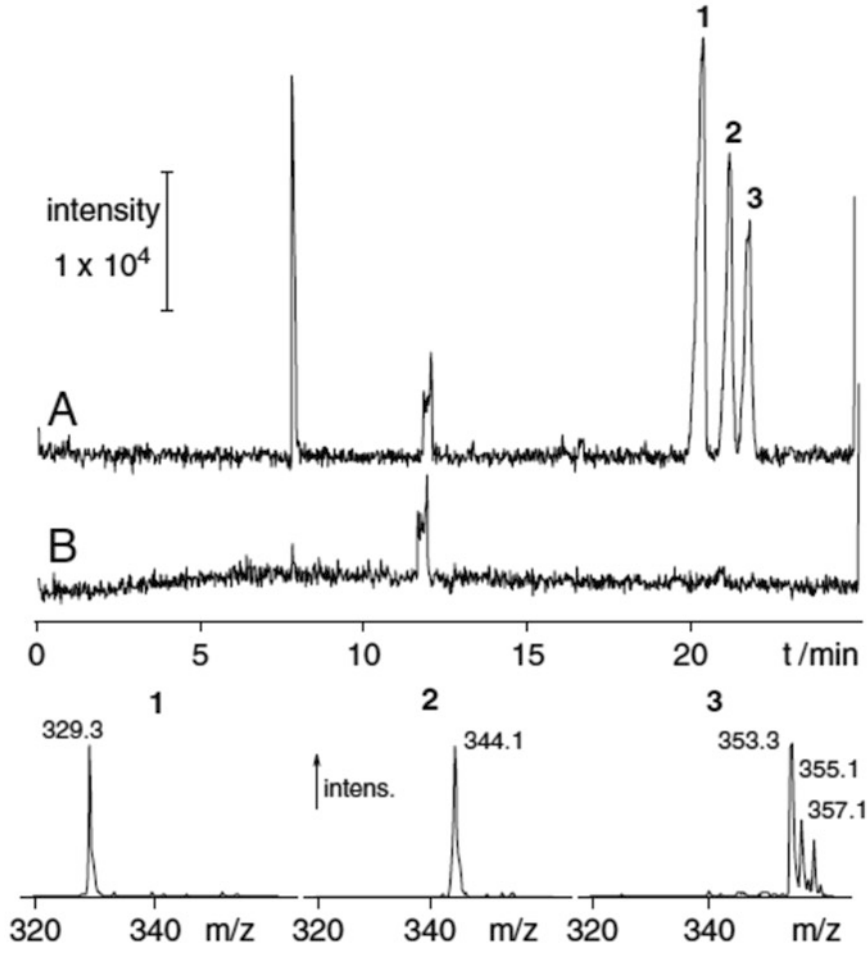

Fig. 19 A CZE–ESI–MS of (1) Ca^{2+}, (2) Mn^{2+}, and (3) Zn^{2+} with total ion count electropherograms: $m/z = 320–360$ and mass spectrum of the peaks [BGE: 20 mM ammonium hydrogen carbonate with 4 mM EDTA (pH 9.4); sample: 20 mg/l of each metal in water (**a**) and blank or water (**b**)] (Ref. 33)

3. Inject the sample at 50 mbar or 950 mbar at the inlet end of the capillary (farthest distance to the detector). For a typical injection, maintain the pressure at 50 mbar for 5 s and for sweeping, inject at 50 mbar or 950 mbar at appropriate time (i.e., up to 300 s).
4. Measure the lengths of samples injected inside the capillary using the Beckman CE Expert Software.
5. A CZE–ESI–MS of Ca^{2+}(1), Mn^{2+}(2), and Zn^{2+}(3) is shown in Fig. 19.

4 Notes

1. In order to avoid vigorous or explosive reactions first it must be ensured that there is no oxidizable matter in the samples before the addition of perchloric acid.
2. This method is recommended for the analysis of Pd(II) and Pt(II) as chloro complexes in the metal refining industry and in the control of waste water from synthetic rubber plants.

References

1. Timerbaev AR (1997) Strategies for selectivity control in capillary electrophoresis of metal species. J Chromatography A 792:495–518
2. Timerbaev AR (2002) Recent advances and tends in capillary electrophoresis of inorganic ions. Electrophoresis 23:3384–3906
3. Boyce MC, Haddad PR (2003) Tailoring the separation of metal complexes and organometallic compounds resolved by capillary electrophoresis using auxillary separation processes. Electrophoresis 24:2013–2022
4. Timerbaev AR (2004) Capillary electrophoresis of inorganic ions: an update. Electrophoresis 25:4008–4031
5. Shaw MJ, Haddad PR (2004) The determination of trace metal pollutants in environmental matrices using ion chromatography. Environ Int 30:403–431
6. Foret F, Fanali S, Nardi A, Bocek P (1990) Capillary zone electrophoresis of rare earth metals with indirect UV absorbance detection. Electrophoresis 11:780–783
7. Weston A, Brown PR, Jandik P, Jones WR, Heckenberg AL (1992) Optimization of detection sensitivity in the analysis of inorganic cations by capillary ion electrophoresis using indirect photometric detection. J Chromatogr 593:289
8. Chen M, Cassidy RM (1993) Separation of metal ions by capillary electrophoresis. J Chromatogr 640:425–431
9. Shi Y, Fritz JS (1993) Separation of metal ions by capillary electrophoresis with a complexing electrolyte. J Chromatogr 640:473–479
10. Quang C, Khaledi MG (1994) A prediction and optimization of the separation of metal cations by capillary electrophoresis with indirect UV detection. J Chromatogr 659:459–466
11. Shi Y, Fritz JS (1994) A new electrolyte systems for the determination of metal cations by capillary zone electrophoresis. J Chromatogr 671:429–435
12. Lee YH, Lin TI (1994) Determination of metal cations by capillary electrophoresis effect of background carrier and completing agents. J Chromatogr A 675:227–236
13. Dabek-Zlotorzynska E, Dlouhy JF (1995) Application of capillary electrophoresis in atmospheric aerosol analysis: determination of cations. J Chromatogr A 706:527–534
14. Francois C, Morin PH, Dreux M (1995) Separation of transition metal cations by capillary electrophoresis optimization of complexing agent concentrations (lactic acid and 18-crown-6). J Chromatogr A 717:393–408
15. Haber C, Jones WR, Soglia J, Surve MA, McGlynn MA, Caplan JR, Krstanovic RC (1996) Conductivity detection in capillary electrophoresis—a powerful tool in ion analysis. J Cap Electrophor 3:1–11
16. Verma SP, Roberto G, Santoyoa E, Apariciob A (2000) Improved capillary electrophoresis method for measuring rare-earth elements in synthetic geochemical standards. J Chromatogr A 884:317–328
17. Wang T, Li SFY (1995) Migration behaviour of alkali and alkaline-earth metal ion-EDTA complexes and quantitative analysis of magnesium in real samples by capillary electrophoresis with indirect ultraviolet detection. J Chromatogr A 707:343–353
18. Tangen A, Lund W, Frederiksen RB (1997) Determination of Na^+, K^+, Mg^{2+} and Ca^{2+} in mixtures of seawater and formation water by capillary electrophoresis. J Chromatogr A 767:311–317
19. Mofaddel N, Krajian H, Villemin D, Desbène PL (2009) New ionic liquid for inorganic cations analysis by capillary electrophoresis 2-hydroxy-N, N, N-trimethyl-1-phenylethanaminium bis (trifluoromethylsulfonyl)imide (phenylcholine NTf2). Anal Bioanal Chem 393:1545–1554
20. Zhang HW, Jia L, Hu ZD (1995) Determination of palladium(II) as a chloro complex by capillary zone electrophoresis. J Chromatogr A 704:242–246
21. Baraj B, Martinez M, Sastre A, Manuel A (1995) Simultaneous determination of Cr(III),

Fe(III), Cu(II) and Pb(II) as UV-absorbing EDTA complexes by capillary zone electrophoresis. J Chromatogr A 695:103–111

22. Feng H, Wang T, Fong S, Li Y (2003) Sensitive determination of trace-metal elements in tea with capillary electrophoresis by using chelating agent 4-(2-pyridylazo)resorcinol (PAR). Food Chem 81:607–611
23. Ge Y, Guo Y, Qin W (2014) Polyamidoamine dendrimers as sweeping agent and stationary phase for rapid and sensitive open-tubular capillary electrophoretic determination of heavy metal ions. Talanta 121:50–55
24. Men FY, Wei YQ, Lu H, Liu XX, Liu JX (2012) Simultaneous analysis of Cu and Pd as ABEDTA complexes in Rhizoma coptidis by capillary electrophoresis coupled with solid phase extraction. Chin Chem Lett 23:591–594
25. Boonchiangma S, Kukusamude C, Ngeontae W, Srijaranai S (2014) In-capillary derivatization and preconcentration for CE of metal ions as their phenanthroline complexes. Chromatographia 77:277–286
26. Vachirapatama N, Theerapittayatakul N (2012) Determination of transitions metal ions as complexes with 2, 6-pyridinedicarboxylic acid by capillary electrophoresis. Songklanakarin J Sci Technol 34:303–307
27. Soomro R, Memon SQ, Ahmed MJ, Memon N, Mallah A (2012) Bis(salicylaldehyde) orthophenylenediamine as complexing reagent in simultaneous determination of gold, chromium, iron, uranyl, and nickel using capillary zone electrophoresis. Acta Chromatographica 24:543–558
28. Pimrote W, Santaladchaiyakit Y, Kukusamude C, Sakai T, Srijaranai S (2012) Simultaneous determination of heavy metals in drinking waters and wines by methods: Ion pair-reversed phase high performance liquid chromatography and capillary zone electrophoresis. Int Food Res J 19:1079–1088
29. Macka M, Nesterenko P, Andersson P, Haddad P (1998) Separation of uranium(VI) and lanthanides by capillary electrophoresis using on-capillary complexation with arsenazo III. J Chromatogr A 803:279–290
30. Evans L, Collins GE (2001) Separation of uranium (VI) and transition metal ions with 4-(2-thiazolylazo)resorcinol by capillary electrophoresis. J Chromatogr A 911:127–133
31. Kautenburger R, Hein C, Sander JM, Beck HP (2014) Influence of metal loading and humic acid functional groups on the complexation behavior of trivalent lanthanides analyzed by CE-ICP-MS. Anal Chim Acta 816:50–59
32. Timerbaev AR, Semenova OE, Fritz JS (1996) Advanced possibilities on multi-element separation and detection of metal ions by capillary zone electrophoresis using precapillary complexation I. Separation aspects. J Chromatogr A 756:300–306
33. Quirino JP, Haddad PR (2011) Separation and sweeping of metal ions with EDTA in CZE-ESI-MS. J Sep Sci 34:2872–2878

Chapter 14

Bioanalytical Application of Amino Acid Detection by Capillary Electrophoresis

Daniela Fico, Antonio Pennetta, and Giuseppe E. De Benedetto

Abstract

This chapter illustrates the usefulness of capillary electrophoresis (CE) for the analysis of amino acids, and both normal and chiral separations are covered. In order to provide a general description of the main results and challenges in the biomedical field, some relevant applications and reviews on CE of amino acids are tabulated. Furthermore, some detailed experimental procedures are shown, regarding the CE analysis of amino acids in body fluids, in microdialysate, and released upon hydrolysis of proteins. In particular, the protocols will deal with the following compounds: (1) underivatized aminoacids in blood; (2) γ-Aminobutyric acid, glutamate, and L-Aspartate derivatized with Naphthalene-2,3-dicarboxaldehyde; (3) hydrolysate from bovine serum albumine derivatized with phenylisothiocyanate. By examining these applications on real matrices, the capillary electrophoresis efficiency as tool for Amino Acid analysis can be ascertained.

Key words Capillary zone electrophoresis, Micellar electrokinetic chromatography, Amino acids, Chiral separations, Bioanalytical applications

Abbreviations

ANDA	7-Amino-1,3-naphthalene disulfonic acid
APC	1-(9-Anthryl)-2-propyl chloroformate
BMIC	1-Butyl-3-methyl imidazolium chloride
BrBQCA	3-(4-Bromobenzoyl)-2-quinoline carboxaldehyde
C4D	Capacitively coupled contactless conductivity detection
CAPS	3-Cycloexylamino-1-propanesulfonic acid
CBQCA	3-(4-Carboxy benzoyl) quinoline-2-carboxaldehyde
CC	2,4,6-Trichloro-1,3,5-triazine
CFSE	5-Carboxy-fluorescein succinimidyl ester
ClBQCA	3-(4-Chlorobenzoyl)-2-quinoline carboxaldehyde
DMAB	4-(*N,N′*-dimethylamino)benzoic acid
Dns	5-(Dimethylamino) naphthelene-1-sulfonyl chloride
DTAF	5-(4 6-Dichloro-s-triazin-2-yl amino) fluorescein
FITC	Fluorescein isothiocyanate

Philippe Schmitt-Kopplin (ed.), *Capillary Electrophoresis: Methods and Protocols*, Methods in Molecular Biology, vol. 1483,
DOI 10.1007/978-1-4939-6403-1_14,

FMAC	*N*-fluorenylmethoxycarbonyl-l-alanyl *N*-carboxyanhydride
FNBDA	4-Fluoro-7-nitro-2,1,3-benzoxadiazole
GABA	γ-Amino-n-butyric acid
HM-β-CD	Heptakis(2,6-di-O-methyl)-β-CD
HP-β-CD	Hydroxypropyl-β-cyclodextrin
IAF	5-Iodoacetamidofluoresceine
MBA	4-Methylbenzylamine
MDMA-β-CD	3-Monodeoxy-3-monoamino-β-CD
MDP-β-CDCl	Mono-6-deoxy-6-(3R,4R-dihydroxypyrrolidine)-β-cyclodextrin chloride
MGA	*N*-methyl-d-glucamine
MHP-β-CD	Mono-6-deoxy-6-mono(3-hydroxy) propylamino-β-CD
MMI-β-CDCl	Mono-(3-methylimidazolium)-β-CD chloride
NBD-F	4-Fluoro-7-nitro-2,1,3-benzoxadiazole
NDA	Naphthalene-2,3-dicarboxaldehyde
OPA	*o*-Phthaldehyde
PITC	Phenyl isothiocyanate
SAMF	6-Oxy-(*N*-succinimidyl acetate)-9-(2′-methoxycarbonyl) fluorescein
THSBE	1,3,5,7-Tetramethyl-8-(*N*-hydroxy succinimidyl butyric ester) difluoro boradiaza-S-indacene

1 Introduction

One of the primary goals of biomedical research is the study of new methods for the early diagnosis of a disease, able to follow its progression and to evaluate the therapeutic efficacy of a treatment. Many diseases, however, have a complex and multifactorial behaviour and their diagnosis and understanding cannot be based only on the evaluation of a single molecular marker. Among the whole small molecules produced by metabolism encompassed in metabolomics, amino acids have a key role. The protein "building blocks" are also essential precursors of important biomolecules including nucleotides and nucleotide coenzymes such as heme, a variety of hormones and neurotransmitters; therefore, given the important role in metabolism, it is possible, by carrying out the analysis of the amino acid profile, to get useful indications on various metabolic processes and the functioning of liver, kidneys, heart, or immune system. Amino acids differing from basal levels, in fact, are often symptoms of diseases, as in phenylketonuria and cystinuria. As a result, amino acids are an important target for the "metabolic profiling," being frequently present in biological matrices and several methods have been developed to identify the presence and measure the concentration with the aim to perform screening of various diseases. From the analytic point of view, on considering that AAs have different behavior (acidic, neutral, or basic) and many of them lack of a strong chromophore, their determination is both interesting and intriguing and has been widely pursued by many authors with the issue of determining

more amino acids in a single run with lower detection limits. Another related boosting analytical field is the chiral separation of amino acids: the structure and symmetry of organic molecules plays a crucial role in different biochemical processes but many methods validated for the quantification of amino acids are not stereoselective. For some time the free amino acids in biological matrices were typically quantified as the sum of their enantiomers, because in terrestrial organisms they exist in the form of stereoisomers L. The amino acids of the series D had been identified only in few peptides, such as those of the cell wall of the bacteria. With the increased understanding of the biological significance of the D-amino acids, interest in enantioselective quantification is increased and more applications of chiral CE to real problems of biomedical importance find attention.

The wealth of papers continuously published on amino acids analysis is continuously reviewed and a review of the reviews could be useful to evidence the peculiar aspects each time tracked. Presently, it is important to mention the general reviews published every 2 years in Electrophoresis [1–3].

Aiming at having a general overview, few significant methods, mainly related to biomedical applications and set up to separate and detect AAs, have been collected together with the most relevant experimental information in two tables handling normal [4–66] and enantiomeric [67–94] separations, respectively. Within each table both capillary zone electrophoresis (CZE) and micellar electrokinetic chromatography (MEKC) have been described. All the referred methods also share the properties of being carried out on simple, commercial instruments, and, as a rule, they could be transferred on every CE system.

Different matrices, as far as the biomedical applications are concerned, have been analyzed: physiological fluids like urine, saliva, or plasma; cells like lymphocyte or erythrocyte; neurotransmitters and different hydrolysates (see column “Matrix” in Tables 1 and 2). Moreover, the hyphenation of microdialysis with the CE apparatus deserves attention as it allows both continuous and in vivo analysis: a fraction of the analytes can diffuse through the membrane dialysis and depending on them, temperature and probe characteristics, a definite recovery is attainable and quantitative measurements can be accomplished. Also fast monitoring of AAs is carried out by hyphenating microdialysis with CE: in particular if LIF is used as detector, thanks to the high separation efficiency and low volume sample requirement of CE and the very low detection limits of LIF detector, the sampling rate has been increased to levels not attainable by other analytical common techniques, like HPLC, and short-lasting changes in AAs concentration could be recorded. Moreover, to decrease the overall cost of the detector, the use of LED sources for fluorescence detectors is possible [24, 35, 90, 91].

Table 1
Selected applications of CZE and MEKC to biomedical applications

Analytes	Matrix	Labeling	BGE	Detection	Separation method	Capillary (i.d., effective/ total lenght)	Injection	Run time (min)	L.O.D.	Ref.
Lys, Arg, putrescine, cadaverine, spermidine, ornithine (Orn)	Saliva	FITC	12 g/l PSS, 3 mM CTAB, 80 mM borate buffer, pH 12.35	LIF, 483 nm	CZE, 22 kV, 25 °C	25 µm, 90 cm	Electrokinetic, 22 kV, 8 s	48	0.0072–0.26 nM	[4]
Creatinine, His	Urine	No	10 mM NaCl, 0.03% (w/v) HPMC, pH 2.5 with 1 M HCl	UV, 200 nm	CZE, 20 kV, 25 °C	50 µm, 50/52.4 cm	Electrokinetic, 10 kV, 100 s	10	4.8 nM (creatinine), 9.0 nM (His)	[5]
Gaba, Ala, Gln, Gly, Tau, Glu, Asp	Brain cortex or spinal cord tissue (mouse)	THSBE	5.5 mM CTAB, 70 mM PBS, pH 4/20% ACN	LIF, 488 nm	MEKC, –22.5 kV, 25 °C	75 µm, 50/60 cm	Hydrodynamic, 0.5 psi, 5 s	20	0.2–1.4 nM	[6]
Cys, Arg, Orn, Lys	Urine	No	1.0 M formic acid/10% MeOH	ESI-MS	CZE, 21 kV, 25 °C	50 µm, 70 cm	Hydrodynamic, 2 psi, 10 s	11	30.7–114.2 µM	[7]
Phe, Tyr	Blood	No	3 mM ammonium acetate buffer, pH 10.7	ESI-MS	CZE, 25 kV, 25 °C	50 µm, 40 cm	Electrokinetic, 25 kV, 3 s	3	0.03 mg/l (Phe), 0.07 mg/l (Tyr)	[8]
Ala, Glu, Asp, Ser, Tau, Gly	Serum	NDA/CN or OPA	50 mM borate buffer, pH 9.2	Amperometric, 0.75 V	CZE, 15 kV, 25 °C	25 µm, 65 cm	Electrokinetic, 10 s, 15 kV	30	0.55–2.8 µM	[9]
Asn, Ser, Thr, Tyr, Gly, Glu, Asp, Ala, Tau, GABA, NE, Val, DA, Ile, Leu, Phe, Arg, Lys	Cells	ClBQCA	38.5 mM SDS, 120 mM boric acid, pH 9.2/17% ACN	LIF, 488 nm	MEKC, 22.5 kV, 25 °C	75 µm, 50 cm	Hydrodynamic, 0.5 psi, 5 s	32	1.4–100 nM	[10]
28 Biogenic amino acids	Blood plasma, urine, saliva, and CSF	No	0.5–8 M acetic acid	C^4D	CZE, 20 kV, 25 °C	25 µm, 18/33 cm	Hydrodynamic, 50 mbar, 16 s	6	0.1–1.7 µM	[11]
Arg, Lys, Trp, Gaba, Ser, Ala, Tau, Gly, Glu and Asp	Brain microdialysate (rat)	FITC	70 mM SDS, 17.5 mM HP-β -CD, 5 mM DM-β-CD, 15 mM borate buffer, pH 10.2 /5% MeOH	LIF, 488 nm	MEKC, 22.5 kV, 25 °C	75 µm, 50/57 cm	Hydrodynamic, 0.5 psi, 5 s	20	0.10–1.00 nM	[12]

Asn, Ser, Thr, Tyr, Gly, Glu, Asp, Ala, Cys-Cys, Orn, Val, Gln, Phe, Arg, Lys, Cys, Pro	Urine	No	3.0% formic acid/5.0% MeOH	ESI-MS	CZE, 20 kV, 25 °C	50 μm, 60 cm	Hydrodynamic, 50 mbar, 40 s	11	0.0116–2.38 mg/l	[13]
Gly, Pro, Glu, and Ser	Saliva	No	50 mM $CuSO_4$, 0.05% acetic acid, pH 4.5	UV, 254 nm	CZE, 15 kV, 25 °C	50 μm, 57/65 cm	Gravity, 15 cm, 727 s	24	0.1–0.5 μM	[14]
Phe, Val, Gln, Pro, Gly, Ser, Ala	Urine	FITC	45 mM α-CD, 80 mM borate buffer, pH 9.2	LIF, 488 nm	CZE, –15 kV, 25 °C	50 μm, 50/60 cm	Gravity	15	160–330 nM	[15]
Trp, Tyr	CSF	No	LE: 250 mM acetate, pH 9.5 with ETA; TE: 0.1 M NaOH, 0.1% (v/v) ampholyte	UV, 280 nm	GEITP	30 μm, 6/15 cm	–	6	51 nM (Trp). 215 nM (Tyr)	[16]
21 Aas	Protein hydrolysate	No	0.8% formic acid/20% MeOH	ESI-MS (IT)	CZE, 30 kV, 25 °C	50 μm, 80 cm	Hydrodynamic, 1 psi, 10 s	13	15.9–172 μM	[17]
Adma, Sdma, Arg	Plasma	No	50 mM Tris/phosphate buffer, pH 2.30	UV, 190–200 nm	CZE,15 kV, 15 °C	75 μm, 50/60.2 cm	Hydrodynamic, 0.5 psi, 10 s	15	0.03 μM (ADMA, SDMA), 0.06 μM (Arg)	[18]
Arg, Glu	Gingival crevicular fluid	FITC	20 mM Carbonate buffer, pH 9.5	LIF, 488 nm	CZE, 21 kV, 25 °C	25 μm, 60 cm	Hydrodynamic, –19 psi, 0.2 s	–	–	[19]
Arg, Glu, Tau	Hemolymphe (Drosophila)	Fluorescamine	30 mM CsCl, 70 mM SDS, 20 mM borate buffer, pH 9.1	LIF, 405 nm	MEKC, 19 kV, 25 °C	50 μm, 36/50 cm,	Gravity, 15 cm, 15 s	10	–	[20]
Arg, Cit, and Argsuc	Neurons (Aplysia Californica)	Fluorescamine	30 mM borate buffer, pH 9.8	LIF, 350 nm	CZE, 20 kV, 20 °C	50 μm, 80 cm	Electrokinetic, 8 kV, 8 s	20	5.1 nM (Arg), 3.8 nM (Cit), 3.8 nM (ArgSuc)	[21]
Glu, Asp, Gaba, Gly, Tau, Gln	CSF, saliva	*N*-hydroxysuccinimidyl fluorescein-O-acetate	100 mM SDS, 100 mM borate buffer pH 9.6/8% MeOH	LIF, 488 nm	MEKC, 20 kV, 25 °C	75 μm, 50/60.2 cm	Hydrodynamic, 0.5 psi, 10 s	42	0.06–0.1 nM	[22]
Arg, Gln, Glu, Asp	Brain microdialysate (rat)	CBQCA	50 mM SDS, 55 mM β-CD, 20 mM borate buffer, pH 9.3	LIF, 488 nm	MEKC, 21.5 kV, 25 °C	50 μm, 30/38 cm	Gravity, 8 cm, 10 s	3	–	[23]
Gly, Leu, Glu, Asp	CSF microdialysate	In capillary, NDA/CN	75 mM borate buffer, pH 9.2	LED-IF, 410 nm	CZE, 25 kV, 30 °C	75 μm, 56/70 cm	Electrokinetic, 5 kV, 2.5 s	12	11–94 nM	[24]

(continued)

Table 1
(continued)

Analytes	Matrix	Labeling	BGE	Detection	Separation method	Capillary (i.d., effective/ total lenght)	Injection	Run time (min)	L.O.D.	Ref.
His, Hcyss, Trp, Phe, Tyr, Cyss, Gsh, Gssg	Blood	No	10 mM PBS, pH 2.9	UV, 200 nm	CZE, 15 kV, 18 °C	75 μm, 40/47 cm	Hydrodynamic, 0.5 psi, 10 s	30	0.9–36.6 μM	[25]
Trp and Trp Metabolites	CSF	No	5 mM ammonium acetate, pH 9.7/5% ACN	ESI-MS (TOF)	CZE, –30 kV, 25 °C	25 μm, 70 cm	Hydrodynamic, 50 mbar, 10–60 s	5	20 nM	[26]
Asn, Ser, Thr, Tyr, Gly, Glu, Asp, Ala, Ile, Leu, Val, Gln, Phe, Arg, Hlys, Lys, HPro, Pro	Tissue	No	1 M formic acid, pH 1.8	ESI-MS^2 (IT)	CZE, 25 kV, 20 °C	50 μm, 80 cm	Hydrodynamic, 0.8 psi, 60 s	20	0.05–2 mM (LLOQ)	[27]
Lys, Arg, Ala, Val, Met, Glu, Phe, Tyr	CSF	No	1 M formic acid, pH 1.8	ESI-MS (TOF)	CZE, 30 kV, 25 °C	PB-PVS coated, 50 μm, 130 cm	Hydrodynamic, 35 mbar, 10 s	13	85–225 nM	[28]
Lys, Arg, Ala, Val, Met, Glu, Phe, Tyr	Urine	No	1 M formic acid, pH 1.8	ESI-MS (TOF)	CZE, 30 kV, 25 °C	PB-PVS coated, 50 μm, 130 cm	Hydrodynamic, 90 mbar, 90 s	20	85–225 nM	[29]
His	Urine	No	Cathode: 1.0 mM NaCl, 50 mM PBS, pH 6.0; anode: 3 mM $NiCl_2$ 1.0 mM NaCl, 50 mM PBS, pH 6.0	UV, 208 nm	MAB-ACE, 25 °C, 30 kV	75 μm, 44/53 cm	Hydrodynamic, full of sample	8	43 ng/ml	[30]
Asn, Ser, Thr, Tyr, Gly, Glu, Asp, Ala, Tau, GABA, NE, Val, DA, Ile, Leu, Phe, Arg, Lys	Plasma and vitreous perfusate	BrBQCA	120 mM boric acid, pH 9.1, 38.5 mM SDS/19% ACN	LIF, 488 nm	MEKC, 22.5 kV, 25 °C	75 μm, 50/60.2 cm	Hydrodynamic, 0.5 psi, 5 s	33	0,65–5 nM (Aas), 58–73 nM (catecholamine)	[31]
Histidine, 1- and 3-methylhistidine	Urine	FITC	22 mM sodium tetraborate, pH 10.5/32% ACN	LIF, 488 nm	CZE, 25 kV, 25 °C	75 μm, 40/50.2 cm	Hydrodynamic, 0.5 psi, 3 s	30	0.023 ng/ml (His), 0.023 ng/ml (1-MH), 0.034 ng/ml (3-MH)	[32]

Pro, tetracaine, and enoxacin	Urine	No	70 mM phosphate, pH 8	ECL, 1.15 mV (5 mM $Ru(bpy)_3Cl_2$, 50 mM PBS, pH 9.6)	CZE, 15 kV, 25 °C	25 μm, 50 cm	Electrokinetic, 10 kV, 10 s	10	0.08 (Tetracaine), 0.06 (Pro), and 0.02(enoxacin) μg/ml	[33]
Ala, Glu, Asp, Ser, Tau, Gly	Cultured cells, CSF, saliva, vitreous humor	FITC	18 mM phosphate, pH 11.6	LIF, 488 nm	CZE, 28 kV, 23 °C	75 μm, 50/57 cm	Hydrodynamic, 0.5 psi, 3 s	12	0.075–0.2 μM	[34]
Tyr, Trp, DA, NE, 5-HT	Breast cancer cell lysate	NDA/CN	30 mM SDS, 0.1% PEO, 0.5 M Tris, pH 10.2	LED-IF 405 nm	MEKC, 15 kV, 25 °C	75 μm, 55 cm	Gravity, 31 cm, 10 s	16	2.06–19.17 nM	[35]
5-HTP, Trp, TA, 5-HT, and 5-HIAA	Urine and serum	No	2% Dextran sulfate, 100 mM Tris, pH 9.0	LIF, 266 nm	CZE, 15 kV, 25 °C	75 μm, 10 cm	Gravity, 20 cm, 20 s	20	4.1–366.0 pM	[36]
Trp, Phe, Tyr, tyramine, tryptamine	Mammalian decomposition fluids	No	70 mM boric acid, pH 9.5/32% MeOH	UV, 200 nm	CZE, 30 kV, 25 °C	75 μm, 56 cm	Hydrodynamic, 50 mbar, 2.5 s	12	5.8–8.6 mg/l	[37]
Phe, 4-hydroxyphenylacetic acid, phenylpyruvic acid, 2-hydroxyphenylacetic acid	Urine	No	35 mM SDS, 60 mM borate buffer, pH 8.2	C^4D and amperometric	MEKC, 16 kV, 25 °C	25 μm, 86.8 cm	Electrokinetic, 16 kV, 6 s	23	0.064–6.6 mg/l	[38]
Arg, monomethyl- and (symmetric and asymmetric) dimethylarginines	Plasma	No	1.5 M formic acid	ESI-MS^2 (IT)	CZE, 23 kV, 25 °C	50 μm, 79.5 cm	Hydrodynamic, 50 mbar, 10–20 s	12	20 nM (ADMA), 30 nM (MMA) and 10 nM (SDMA)	[39]
Gly, His, Ser, Ala, Glu, Trp, Asn, Tyr, Asp, Val, Pro, Orn, Ile, Phe, Gln, Lys, Leu, Met, Arg, Thr, and 4hyp	Latent fingerprints	No	1 M formic acid, pH 1.90 (by addition of ammonium formate) /5% ACN	ESI-MS	CZE, 28 kV, 23 °C	50 μm, 100 cm	Hydrodynamic, 50 mbar, 60 s	30	20–180 ng Deposited on the Mylar R substrate	[40]
Pro, pyroglutamic acid	Urine	No	25 mM TEA, pH 11.7/50% MeOH	ESI-MS	CZE, 30 kV, 20 °C	50 μm, 100 cm	Hydrodynamic, 0.5 psi, 30 s	20	2.6 μM (Pro); 3.6 μM (pyroglutamic acid)	[41]

(continued)

Table 1
(continued)

Analytes	Matrix	Labeling	BGE	Detection	Separation method	Capillary (i.d., effective/ total lenght)	Injection	Run time (min)	L.O.D.	Ref.
Ala, Phe, Pro, Tyr, Val	Serum	No	5 mM ammonium acetate, pH 10.8	ESI-MS	CZE, 25 kV, 25 °C	50 μm, 95 cm	Electrokinetic, 25 kV, 3 s	15	50–810 nM	[42]
Creatinine, Lys, Arg, His, Gly, Ala, Val, Ile, Leu, Thr, Asn, Met, Trp, Citruline, Phe, Pro, Tyr	Whole blood, serum, urine, plasma	No	2.5 M acetic acid, pH 2.0	C^4D	CZE, 30 kV, 25 °C	25 μm, 35/50 cm	Hydrodynamic, 50 mbar, 20 s	12	0.15–10 μM	[43]
Trp, Phe, Tyr, homophenylalanine	Urine	No	100 mM PBS, pH 2.0	UV, 200 nm	CZE, 20 kV, 25 °C	40 μm, 50/60 cm	Hydrodynamic, 0.5 psi, 10 s	14	70–500 nM	[44]
Ala, Asp, Gly, His, Leu, Lys, Phe, Ser, Tyr, Val	Brain (mouse)	No	1% formic acid	ESI-MS (TOF)	CZE, 20 kV, 25 °C	40 μm, 90 cm	Hydrodynamic	–	–	[45]
Trp, kynurenine	Plasma	No	100 mM Bis-Tris propane pH 2.15; 1 M phosphoric acid pH 2.15	UV, 226 nm	CZE, 12 kV, 20 °C	75 μm, 20/30 cm	Hydrodynamic, −0.5 psi, 10 s	9	400 nM (Trp), 150 nM (kynurenine)	[46]
Phe, Tyr	Urine	No	1 M formic acid, pH 1.8	UV, 200 nm	CZE, 30 kV, 25 °C	50 μm, 91/100 cm	Hydrodynamic, 50 mbar, 7 s (2.5% NH_3), 228 s (samples/ BGE, 1:1)	7.5	36 nM (Phe), 49 nM (Tyr)	[47]
Ala, Gly, Leu, D-L Orn, Val	Serum (rat)	No	1 M formic acid	ESI-MSMS	CZE, 25 kV, 25 °C	50 μm, 80 cm	Hydrodynamic, 0.8 psi, 60 s	–	0.5–10 μM	[48]
Orn, citrulline, alloleucine, β-alanine, GABA, pyroglutamic Acid	Serum (from patients with liver diseases)	No	0.1 μM formic acid, pH 2	ESI-MS	CZE, 25 kV, 25 °C	50 μm, 60 cm	–	–	0.04–0.19 mg/l	[49]
Ala, Asp, Gly, His, Leu, Lys, Phe, Ser, Tyr, Val, Trp, Cys, Thr, Arg, Gln, Pro, Met, Asn, Glu, Ile	Tissues (lung and prostate)	no	1 M formic acid, pH 2.2	ESI-MS (TOF)	CZE, 30 kV, 25 °C	50 μm, 80 cm	Hydrodynamic, 50 mbar, 10 s	–	–	[50]

Arg, Trp, Leu, Ile, Gln, Val, Thr, Pro, Ser, Ala, taurine, Gly, Tyr, His, Lys, Orn, Glu, Asp, Cys	Serum, urine, and saliva	CC, ANDA	20 mM borate buffer, pH 10.1	UV, 214 nm	CZE, 15 kV, 23 °C	50 μm, 40/47 cm	Hydrodynamic, 0.5 psi, 2 s	25	0.52–1.7 mg/l	[51]
Ala, Ser, Gly, taurine, Glu, Asp, homocysteic acid	Plasma, urine, blood	FITC	18 mM Na3PO4, pH 11.8	LIF, 488 nm	CZE, 28 kV, 25 °C	75 μm, 50/57 cm	Hydrodynamic, 0.5 psi, 5 s	12	–	[52]
Homocystein, Cys	Plasma	IAF	30 mM sodium phosphate, 33 mM boric acid, 75 mM *N*-methyl-d-glucamine, pH 11.3	LIF, 488 nm	CZE, 18 kV, 25 °C	75 μm, 50/57 cm	Hydrodynamic, 0.5 psi, 5 s	10	1.5 nM	[53]
Orn, His, Lys, Arg	Sweat	no	10 mM MBA, 3.5 mM citric acid, pH 4.05/25 % methanol	UV, 214 nm	CZE, 30 kV, 25 °C	75 μm, 100 cm	Hydrodynamic, 50 kPa, 3 s	13	0.27–0.79 μM	[54]
GABA, Gln, Ala, Gly, Tau, Glu, Asp	Lymphocytes	SAMF	40 mM sodium acetate, 2 mM Cu^{2+}, pH 6.0	LIF, 488 nm	CZE, 15 kV, 25 °C	75 μm, 50/57 cm	Hydrodynamic, 34.5 mbar, 5 s	35	0.1–0.2 nM	[55]
Glu, GABA, Gly, Tau, D-Ser	In vivo microdialysis (rat striatum)	NBD-F	100 mM borate, 20 mM HP-β-CD, pH 10.5	LIF, 488 nm	CZE, 22 kV, 25 °C	5 μm, 6.7 cm	Electrokinetic, −20 kV, 1 s	0.5	5.1–85 nM	[56]
Leu, Ile, Val	Ascites	NDA/CN	1.5 % m/v PEO, 10 mM borate buffer, pH 9.3	LED-IF	CZE, 20 kV, 25 °C	75 μm, 50/60 cm	Gravity, 30 cm, 5 s	7	10.6–10.9 nM	[57]
Glycine, taurine, D-serine, and glutamate	Astrocytes in vitro microdialysis	NBD-F	100 mM borate, 20 mM HP-β-CD, pH 10.5	LIF, 488 nm	CZE, 20 kV, 25 °C	40 μm, 50/60 cm	Electrokinetic, 18 kV, 0.7 s	0.5	100–250 nM	[58]
Tyr, Phe, Val, Pro, Gly, pyroglutamic acid, sarcosine	Urine	FITC	130 mM 18-crown-6, 80 mM borate buffer, pH 8.70	LIF, 488 nm	CZE, 24 kV, 25 °C	25 μm, 70/90 cm	Electrokinetic, 24 kV, 10 s	45	5–10 nM	[59]
Arg, Lys, Trp, Phe, Gln, Gaba, Asn, Pro, Ser, Ala, Tau, Gly, Glu, Asp	Dialysate of hypothalamus extracellular fluid (rats)	DTAF	5 mM HP-β-CD, 5 mM DM-β-CD, 100 mM SDS, 15 mM borate, pH 9.0/4 % isopropanol	LIF, 488 nm	MEKC, 17.5 kV, 25 °C	75 μm, 50/57 cm	Hydrodynamic, 0.5 psi, 5 s.	24	0.12–0.54 nM	[60]

(continued)

Table 1
(continued)

Analytes	Matrix	Labeling	BGE	Detection	Separation method	Capillary (i.d., effective/ total lenght)	Injection	Run time (min)	L.O.D.	Ref.
Arg, His, Lys, Met, Phe, Val, Ser, GABA, Tyr, Ala, Gly, Glu, Asp, taurine	Diabetic vitreous	CBQCA	0.6% PEO, 20 mM NaCl, 75 mM SDS, 55 mM β-CD, 20 mM borate buffer, pH 9.3	LIF, 488 nm	MEKC, 17 kV, 25 °C	50 µm, 30/40 cm	Gravity, 30 cm, 5 s	6	–	[61]
Ala, Pro, Gly, Val, Ile, Leu, Tyr, Gln, Trp, His, Met, Ser, Thr, Phe, Asn, Lys, Cys, Glu, Asp, Arg	Urine	No	150 mM ammonium perfluorooctanoate, pH 9.0	ESI-MS	MEKC, −22.5 kV, 25 °C	50 µm, 90 cm	Hydrodynamic, 30 mbar, 5 s	20	9–26 µg/l	[62]
Gly, Ser	Brain microdialysate (rat)	On-line, OPA	40 mM Borate, 0.9 mM HP-b-CD	LIF, 351 nm	CZE, 25 °C	–	–	15	–	[63]
Gly, Ala, Val, Leu, Ile, Met, Phe, Tyr, Trp, Ser, Pro, Thr, Cys, Asn, Gln, Lys, His, Arg, Asp, Glu	Blood	No	1 M formic acid	ESI-MS	CZE, 30 kV, 20 °C	20 µm, 115 cm	Hydrodynamic, 50 mbar, 6 s	35	1.0–14 fmol inj	[64]
Pro, Thr, Ser, Tyr, Ala, Val, Gly, Met, His, Ile, Leu, Phe, Glu, Lys, Asp, Arg	Protein hydrolysate	PITC	168.3 mM SDS, 29 mM PBS, pH 7.4	UV, 200 nm	MEKC, 25 kV, 26 °C	75 µm, 80/87 cm	Hydrodynamic, 0.6 psi, 10 s	30	100 fmol inj	[65]
Glu, Asp, GABA	Spinal dorsal horn microdialysate	NDA/CN	70 mM SDS, 10 mM HP-b-CD, 75 mM borate buffer, pH 9.2	LIF, 442 nm	MEKC, 25 kV, 25 °C	50 µm, 52/63 cm	Hydrodynamic, 0.6 psi, 10 s	10	1–3.7 nM	[66]

Table 2
Chiral separation of AAs enantiomers by CZE and MEKC

Analytes (D/L)	Matrix	Labeling	a. BGE b. Chiral selector	Detection	Separation method	Capillary (i.d., effective/total lenght)	Injection	Run time (min)	a. L.O.D. b. Resolution of AAs enantiomeric pairs	Ref.
Ser, Ile, Met	Standards	Dns-Cl	a. 5.0 mM NH_4Ac, 100.0 mM Tris/borate buffer, pH 8.2 b. 3 mM $ZnSO_4$, 6 mM L-Arg, 20 mM BMIC	UV, 254 nm	CLE-CE, −20 kV, 25 °C	50 μm, 50/65 cm	Gravity, 15 cm, 10 s	60	b. 4.18 (Ser), 6.44 (Ile), 4.18 (Met)	[67]
Trp, Tyr, Phe	Enzyme catalytic activity	No	a. 5.0 mM NH_4Ac, 100.0 mM boric acid, pH 8.2 b. 3 mM $ZnSO_4$, 6 mM L-Orn	UV, 254 nm	CLE-CE, −20 kV, 20 °C	50 μm, 50/57 cm	Gravity, 15 cm, 5 s	25	a. 6.5 μg/ml (D,L-Trp) b. 2.52 (Trp), 1.01 (Tyr), 3.62 (Phe)	[68]
Ala, Asn, Asp, Ile, Met, Ser, Phe, Thr, Tyr	Standards	Dns-Cl	a. 25 mM Cu(Ac)2, pH 4.0/20% Methanol b. 50 mM [L-Pro-CF3COO]	UV, 254 nm	CLE-CE, 20 kV, 25 °C	75 μm, 40/60 cm	Gravity, 15 cm, 8 s	60	b. 0.93 (Ser)—6.72 (Asp)	[69]
Ala, Asn, Asp, Cys, Glu, Ile, Leu, Lys, Met, Orn, Phe, Ser, Thr, Trp, Tyr, Val	Serum samples	Dns-Cl	a. 100 mM boric acid, 5 mM NH_4Ac, pH 8.4 b. 3 mM $ZnSO_4$, 6 mM L-Arg	UV, 214 nm	CLE-CE, −20 kV, 25 °C	50 μm, 50/57 cm	Hydrodynamic, 0.5 psi, 10 s	24	a. 9 μM b. 0.9 (Val)—5.1 (Cys)	[70]
Ala, Arg, Asn, Ile, Met, Ser, Phe, Thr, Tyr, Cys, Leu, Pro, Trp, Val	L-amino acid oxidase kinetic	No/Dns-Cl	a. 100 mM boric acid, 5 mM NH_4Ac, pH 8.1 b. 4 mM β-CD, 4 mM $ZnSO_4$, 8 mM L-valine	UV, 254 nm	CLE-CE, 21 kV, 20 °C	50 μm, 50/65 cm	Gravity, 15 cm, 5 s	70	a. 8 mg/l b. 1.05 (Tyr), 1.57 (Trp), 2.24 (Phe); 0.6 (Dns-Arg)—2.16 (Dns-Thr)	[71]
Asn, Ile, Met	L-amino acid oxidase kinetic	Dns-Cl	a. 100 mM boric acid, 5 mM NH_4Ac, pH 8.4 b. 6 mM [1-ethylpyridinium] [l-lysine], 3 mM $ZnSO_4$	UV, 254 nm	CLE-CE, −21 kV, 25 °C	75 μm, 50/65 cm	Gravity, 15 cm, 8 s	50	a. 13.40 μM (D,L-Met) b. 3.0 (D,L-Asn), 3.9 (D,L-Ile), 2.4 (D,L-Met)	[72]

(continued)

Table 2
(continued)

Analytes (D/L)	Matrix	Labeling	a. BGE b. Chiral selector	Detection	Separation method	Capillary (i.d., effective/total lenght)	Injection	Run time (min)	a. L.O.D. b. Resolution of AAs enantiomeric pairs	Ref.
Ser, Ile, Met, Asn	Standards	Dns-Cl	a. 5.0 mM NH_4Ac, 100.0 mM Tris/borate buffer, pH 8.2 b. 4 mM $ZnSO_4$, 8 mM L-phenylalaninamide	UV, 254 nm	CLE-CE, −23 kV, 25 °C	50 μm, 50/57 cm	Gravity, 15 cm, 10 s	50	b. 1.9 (Ile), 1.7 (Met), 2.3 (Ser), 1.1 (Asn)	[73]
His, Phe, Trp, and Tyr	Standards	No	a. 15 mM Cu(Ac)2, pH 4.0/30% MeOH b. 30 mM 1-hexyl-3-methylimidazolium L-proline, 15 mM Cu(Ac)2	UV, 200 nm	CLE-CE, 30 kV, 25 °C	50 μm, 40/50 cm	Hydrodynamic, 0.5 psi, 5 s	22	b. 1.34 (Hys)—4.27 (Tyr)	[74]
Ser, Ala, Ile, Leu, Glu, Asp	Cells (human and rat)	FITC	a. 80 mM Borate, pH 9.3 b. 0.5–1 mM HP-β-CD	LIF, 488 nm	CZE, 15 kV (0–44 min) then 22 kV	50 μm, 50/60.2 cm	Hydrodynamic, 0.5 psi, 10 s	76	a. 0.1 μM b. 1.03 (Ile)—1.85 (Ser)	[75]
AAs	Standards	FMOC	a. 50 mM Tris-H_3PO_4 buffer, pH 6.0 b. 2 mM vancomycin	UV, 214 or 254 nm.	CZE, 15 kV, 20 °C	PDMA-coated, 50 μm, 39.2 cm	Hydrodynamic, 0.2 psi, 5 s	4.2	b. 2 (Ser)—8 (Ala)	[76]
Ala, Aba, Nva, Val, Nle, Leu, Aca, Phe, Ser, Thr, Asp, Glu	Standards	Dns-Cl	a. 50 mM PBS, pH 8.0 b. 3 mM MMI-β-CDCl	UV, 214, 254, and 280 nm	CZE, 15 kV, 25 °C	50 μm, 59.2 cm	Hydrodynamic, 0.5 psi, 5 s	30	a. 0.8 mg/l (D-Ala), 1.5 mg/l (D-Ser) b. 0.82 (Ser)—3.02 (Phe)	[77]
D-Ser	Retinal ganglion cells (mouse)	FNBDA	a. 165 mM borate, pH 10.2 b. 34 mM HP-β-CD	LIF, 488 nm	CZE, −15 kV, 25 °C	50 μm, 30/40.2 cm	Hydrodynamic, 0.5 psi, 5 s	30		[78]
Ser, Thr, Met, Asp Val, Glu, norvaline	Standards	Dns-Cl	a. 50 mM PBS, pH 6.0 b. MDP-β-CDCl	UV, 214, 254 and 280 nm	CZE, 15 kV, 25 °C	50 μm, 40/50 cm	Hydrodynamic, 0.5 psi, 4 s	11	b. 1.85 (Thr), 1.30 (Met), 0.88 (Ser), 1.97 (Val), 2.69 (Asp), 1.00(Glu), 3.55 (norvaline)	[79]
Ala, Asn, Asp, Cit, Gln, Glu, Ile, Leu, Met, Phe, Pro, Ser, Thr, Trp, Tyr, Val	Standards	FMOC-Cl	a. 50 mM NH_4OOCH buffer, pH 7.0 b. 10 mM vancomycin	ESI-MS/MS2	CZE, −20 kV, 25 °C	HDB-coated, 50 μm, 100 cm;	Hydrodynamic, 50 mbar, 15 s	22	a. 0.1 μM (Trp)—3.1 μM (Tyr) b. 0.8 (Thr)—3.5 (Phe, Ala)	[80]

L-Pro, L-Phe, L-Leu, L-Ile, L/D-Orn, L-Gln, L-Ala, L-Thr, Gly, L/D-Ser, Tau and L-Glu	Plasma	NBD-F	a. 175 mM borate buffer, pH 10.25 b. 12.5 mM β-CD	LIF, 488 nm	CZE, 21 kV, 17 °C	75 μm, 60 cm	Hydrodynamic, 0.5 psi, 10 s	22	a. 69.5 nM (D-Ser), 38.3–433 nM (L- Aas)	[81]
Gly, L/D-Ser and taurine in urine. L-Gln,Gly, L-Glu and L-Asp in hippocampus tissue	Urine, hippocampus tissue	NBD-F	a. 90 mM borate buffer, pH 10.25 b. 12.5 mM β-CD	LIF, 488 nm	CZE, 21 kV, 25 °C	75 μm, 50/60 cm	Hydrodynamic, 0.5 psi, 10 s	20	a. 99–263 nM (human urine samples); 34.9–163 nM (hippocampus extracts)	[82]
L-Glu, L-Asp, D-Ser, L-Thr, L-Gln	Hippocampus slices (rats)	NDA/CN	a. 25 mM PBS, pH 2.15 b. 20 g/l sulfated β-CD	LIF, 420 nm	CZE, −21 kV, 25 °C	25 μm, 45/48 cm	Hydrodynamic, 380 mbar, 1 s	6	a. 14.7 nM (L-Glu), 16.0 nM (L-Asp), 19.3 nM (D-Ser), 26.2 nM (L-Thr), 12.5 nM (L-Gln)	[83]
Ser	Microdialysate (extract during ischemia/ reperfusion in rats)	FITC	a. 15 mM borate (pH 10.2) containing 5% (v/v) methanol, 70 mM SDS b. 17.5 mM HP-β-CD and 5 mM DM-β-CD	LIF, 488 nm	CZE, 22.5 kV, 25 °C	75 μm, 50/57 cm	Hydrodynamic, 0.5 psi, 5 s	20		[84]
Asp, Glu	Brain (chicken)	4-Fluoro-7-nitro-2,1,3-benzoxadiazole	a. 100 mM Borate, pH 8 b. 8 mM HDM-β-CD, 5 mM MHP-β-CD	LIF, 488 nm	CZE, −24 kV, 25 °C	Polyacrylamide coated, 75 μm, 50/60 cm	Hydrodynamic, 1 psi, 20 s	10	a. 17 nM (D-Asp), 9 nM (D-Glu)	[85]
Glu and Asp	Standards	5-(4,6-Dichloro-s-triazin-2--ylamino) fluorescein	a. 8 mM sodium borate, pH 8.9/10% methanol (Asp); 10 mM sodium borate, pH 9.1/5% methanol (Glu) b. 12 mM cholate, 0.8–1.6% human serum albumine	LIF, 488 nm	CZE, −25 kV, 25 °C	50 μm, 50/60.2 cm	Hydrodynamic, 0.5 psi, 5 s	10.5	a. 36 mg/l (D-Asp), 38 mg/l (L-Asp), 22 mg/l (D-Glu), 23 mg/l (L-Glu) b. 2.8 (Asp), 1.8 (Glu)	[86]

(continued)

Table 2
(continued)

Analytes (D/L)	Matrix	Labeling	a. BGE b. Chiral selector	Detection	Separation method	Capillary (i.d., effective/total lenght)	Injection	Run time (min)	a. L.O.D. b. Resolution of AAs enantiomeric pairs	Ref.
Ala, His, Leu, Trp, Tyr	Standards	FITC	a. 20 mM NH_4Ac, pH 6.4 b. 0.7 mM MDMA-β-CD	UV, 200 nm	CZE, 25 kV, 25 °C	75 µm, 50/60 cm	Hydrodynamic, 0.6 psi, 8 s	12	b. 5.00 (Ala), 2.07 (His), 3.06 (Leu), 2.69 (Trp), 3.28 (Tyr)	[87]
AAs	Standards	3,5-Dichloro-benzoyl chloride	a. 25 mM PBS, pH 7.0 b. 15 mM bromobalhimycin	UV, 214 nm	CZE, −25 kV, 25 °C	eCap capillary, 50 µm, 31.5/40 cm	Electrokinetic, −3 kV, 5 s	18	b. 5.37 (Ala), 2.35 (Leu), 4.13 (Met), 1.75 (Thr)	[88]
DOPA, Phe, Tyr	Nerve cells	No	a. 200 mM formic acid b. 5 mM Sulfated β-CD	ESI-MSMS	CZE, 30 kV, 20 °C	75 µm, 80 cm	Hydrodynamic, 50 mbar, 12 s	12	a. 510 nM (D-DOPA), 480 nM (L-DOPA)	[89]
Val, Leu, Ile	Urine, plasma	NDA/CN	a. 150 mM SDS, 0.5% PEO, 20 mM Tris-borate, pH 9.0; in capillary: 100 mM Tris-borate, 150 mM SDS b. 50 mM HP-β-CD	LED-IF, 410 nm	MEKC, 10 kV, 25 °C	50 µm, 40 cm	Gravity, 20 cm, 180 s	27	a. 0.18–0.22 nM b. 1.1 (Val), 1.3 (Leu), 3 (Ile)	[90]
Ile, Thr, Leu, His, Val, Asp	CSF	NDA/CN	a. 0.6% PEO, 150 mM SDS, 150 mM Tris/borate buffer, pH 9.0; in capillary: 150 mM SDS, 150 mM Tris/borate buffer, pH 9.0 b. 60 mM HP-β-CD	LED-IF, 410 nm	MEKC, 8 kV, 25 °C	75 µm, 50/60 cm	Gravity, 20 cm, 10 s	30	a. 24 nM (D-Asp), 25 nM (L-Asp)	[91]
Asp	Cerebral ganglia	NDA/CN	a. 50 mM SDS, 50 mM borate, pH 9.4 b. 20 mM β-CD	LIF, 457.9 nm	MEKC, 20 kV, 25 °C	50 µm, 50/86 cm	-	15		[92]
Arg, Ser, Leu, Ala, Gln, Glu, Lys, Asp	CSF	FITC	a. 100 mM sodium tetraborate, 80 mM SDS, pH 10 b. 20 mM β-CD	LIF, 488 nm	MEKC, 20 kV, 30 °C	50 µm, 50/57 cm	Hydrodynamic, 0.5 psi, 3 s	45	a. 0.7 nM (L-Leu), 16.5 nM (L-Asp) b. 2.6 (Arg)—9.5 (Glu)	[93]

As already pointed out, detection is a general concern, common to all the different separation schemes. Indeed, nonaromatic nonderivatized amino acids can only be efficiently detected by means of indirect methods; upon derivatization instead, the selected dye/tag determines the appropriate or most useful detector. Derivatization can be effectively employed to overcome both the lack of a chromophore on many AAs and the interferences caused by extraneous compounds in real samples: it results in both improved detection sensitivity and selectivity. Hence the choice of a derivatization reagent is of crucial importance and high demands are therefore put on its properties. Different approaches have been devised: precapillary and in-capillary. Precapillary derivatization is time consuming as it requires batch procedures but it is affordable and widely diffused (*see* tables). In-capillary (or on-column) derivatization [24, 63] is classified into either "on-site in-capillary derivatization" or "throughout in-capillary derivatization." In the former the inlet of a separation capillary is used as a reaction chamber and the reaction is performed by introducing an analyte into the capillary between two plugs of labeling reagent. In the latter, the separations and derivatizations of analytes are performed simultaneously during the electromigration of native analytes in a separation capillary tube filled with a run buffer containing a derivatization reagent.

In the last few years, however, two detection systems have been acknowledged as valuable: contactless conductivity and above all mass spectrometry detection. Both allow detection of free amino acids without derivatization, the former is universal and does not interact with the analytes or separation system, the latter is expensive but offer great selectivity. MS detection for CE is viewed, indeed, as more universal than UV or electrochemical detection. The selectivity and specificity of MS compensate for variations in migration times of the analytes, provides molecular weight and structural information. Most important, it adds a second dimension in separation selectivity for coeluting molecules having different fragmentation patterns. This is of great importance in chiral separation of AAs where this possibility greatly enhances the capability of the technique [80, 89].

As to the background electrolyte, an impressing variety respect to the pH (from about 2 up to 12) or the nature (from acetic or formic acid to borate or phosphate buffers) is found. The electrolyte modification with organic, which improves the separation possibly because of a decrease of EOF, lower solute adsorption to the capillary and Joule heating, or cyclodextrins is often reported and specific example can be found in the tables herein.

Chiral separations of amino acids are achieved by using mainly different and differently derivatizated cyclodextrins and selected antibiotics like vancomycin. Blends of chiral selector demonstrated useful in selected applications [84–86] as well. However, application

of ligand exchange CE, the separation of two enantiomer analytes due to the difference in complex stability constants of the two ternary diastereomeric mixed complexes formed by a metal ion (often Zinc or Copper), a chiral selector (one of the L-amino acids), and the analyte is increasing [67–74].

The protocols described in the following paragraphs represent different approaches to the AA analysis and all are related to possible application to biomedical problems.

2 Materials

2.1 Analysis of the Amino Acid Standards and the Blood Samples

1. 48% Hydrogen fluoride (Merck, Darmstadt, Germany).
2. Background electrolyte (BGE): 1 M formic acid solution: dilute 1.90 ml of 98–100% Suprapur formic acid (Merck) to 50 ml with water in a volumetric flask. Store at room temperature (*see* **Note 1**).
3. Sheath liquid: 5 mM ammonium acetate (Merck) in methanol/water (50:50, v/v).
4. Preparation of the blood sample: soak a 5 mm diameter blood spot on filter paper in 100 µl of water for 10 min. Then take a 20 µl aliquot of this solution and dilute to 200 µl with a solution of acetonitrile/water/formic acid (49.9/49.9/0.2; v/v).
5. High performance capillary electrophoresis/mass spectrometry system.
6. Uncoated 115 cm long, 20 µm i.d., 150 µm o.d. fused silica capillary (Polymicro Technologies, Inc., Phoenix, AZ).

2.2 Capillary Electrophoresis Combined with Microdialysis: Analysis of Trace Amino Acids Neurotransmitters

1. Ringer solution: 140.0 mM NaCl, 4.0 mM KCl, 1.2 mM $CaCl_2$, 1.0 mM $MgCl_2$, 10 mM $NaHCO_3$ at pH 7.4 (*see* **Note 1**).
2. Prepare the 1 mM γ-Aminobutyric acid (GABA), glutamate (Glu), and L-Aspartate (L-Asp) (all from Sigma-Aldrich) standard solutions in 0.1 M hydrogen chloride (prepared from 30% Suprapur hydrogen chloride, Merck) and store at 4 °C.
3. NDA solution: 3.0 mM Naphthalene-2,3-dicarboxaldehyde (NDA) (Buchs, Switzerland) in acetonitrile (hypergrade LiChrosolv, Merck)/water 50:50 v/v
4. Borate/NaCN solution: 0.5 M borate buffer pH 9.2/87 mM NaCN in water (100:20 v/v).
5. Internal standard: 0.1 mM cysteic acid in 0.1 M hydrogen chloride.
6. BGE: 75 mM sodium borate, 10 mM hydroxypropyl-β-cyclodextrin (HP-β-CD), 70 mM sodium dodecyl sulfate (SDS) buffer (pH 9.20). (Sigma-Aldrich) (*see* **Note 2**).

7. A microdialysis apparatus composed by a microinfusion pump and a microdialysis probe equipped with a polycarbonate ether dialysis membrane having a molecular weight cutoff of 20000 D.
8. High performance capillary electrophoresis equipped with a laser-induced fluorescence detector and Helium Cadmium laser (8 mW, 442 nm).
9. Uncoated 63 cm long, 50 μm i.d. fused silica capillary (Polymicro Technologies, Inc.). Effective length 52 cm.

2.3 Analysis of Protein Hydrolysates

1. Hydrochloric acid solution: 6 M HCl (Suprapur, Merck) containing 0.5% (w/v) phenol (Merck) (*see* **Note 1**).
2. Triethylamine solution: mix 2 ml of 99.5% ethanol, 2 ml of water, and 1 ml triethylamine.
3. PITC solution: mix 70 μl of 99.5% ethanol, 20 μl of triethylamine, and 10 μl of phenylisothiocyanate (Sigma-Aldrich).
4. Bovine serum albumin (BSA, 607 residues) was obtained from Sigma-Aldrich.
5. BGE: 29 mM phosphate buffer, pH 7.4, 168.3 mM SDS (Sigma-Aldrich) (*see* **Note 3**).
6. Glass tubes for hydrolysis and derivatization.
7. High performance capillary electrophoresis with UV–vis detection.
8. Uncoated 57 cm long, 50 μm i.d. fused silica (Polymicro Technologies). The length to the detector is 50 cm.

3 Methods

The methods described herein outline the use of different electrophoretic techniques to separate and detect AAs in biomedical applications. In the first example a CE–MS system is effectively used to detect phenylketonuria and tyrosinemia, two metabolic diseases, in blood samples. A sheath-flow interface is used due to its easy and reproducible setup. It also poses less constraints on buffer used in the separation. Pressure-assisted CE also minimizes loss of resolution due to the diffusion of counter ion from the sheath liquid back into the capillary. This hyphenation, as already observed, deserves great attention: the results are interesting and the methods can be further improved, for example, separating AAs after derivatization. MS, indeed, has a greater sensitivity when higher molecular weight compounds are detected, and a simpler tuning of the spectrometer is feasible if the tag represents the main part of the molecule.

CE–LIF demonstrated the method of choice for monitoring simultaneously neurotransmitters. Its sensitivity and the low

injected volume, typical of CE, make it an ideal technique for the analysis of biological samples, such as microdialysate from discrete brain areas, whose absolute amounts are very small. No cleanup procedures are required as the dialysis membrane is not crossed by high molecular weight substances like the proteins. By selecting the proper membrane cutoff, different real samples can be analyzed without time-consuming purification procedures. Also, if the perfusate is compatible with the derivatization mixture, the derivatized AAs can be collected and promptly analyzed avoiding batch operation.

The microdialysis-CE-LIF experiment, herein described, permitted to monitor the extracellular concentration of neurotransmitters which have a key role in the understanding of human chemical, physiological, and behavioral events.

The last protocol provides a rapid and sensitive tool for analysis of amino acids in polypeptide or protein hydrolysates, which can find application in different fields, from protein analysis to glue identification. The agreement with the conventional methods and the better sensitivity (the needed amounts are 100–1000 times lower than those used for the ninhydrin-based determinations) made the method valuable for real samples.

3.1 CE-ESI-MS

1. Electrophoresis sample to sample holder SI:A1. In some instruments for electrical reasons, the outlet terminal in normal mode becomes the inlet terminal with the external adapter.
2. BGE (2.0 ml) in sample holder position BI:A1.
3. 1 M NaOH solution (2.0 ml) in sample holder position B1:D1 and water (2.0 ml) in sample holder position BI:E1; place an empty vial in sample holders BI:C1.
4. Fill the syringe with the sheath liquid solution and place it in its holder on mass spectrometer.
5. Before the run, rinse at high forward pressure (20 psi) the capillary sequentially with NaOH (1 min), water (1 min), and electrophoresis buffer (4 min) (*see* **Note 4**)
6. CE programmed to inject electrophoresis sample for 5 s at low pressure (0.5 psi, 3.45 kPa).
7. The conditions used in the CE were as follows: voltage 30 kV, temperature 25 ± 0.5 °C, pneumatic assistance to classical electrophoretic driving force, 10 psi (*see* **Note 5**).
8. 1.5 kV were applied to the CE outlet/ESI electrode and the heated capillary used in these measurements is kept at 200 °C. The source temperature is maintained at 80 °C and nitrogen is used for both nebulizing (35 l/h) and drying (100 l/h). The sheath liquid flow at a flow rate of 5 μl/min is provided by the mass spectrometer controlled syringe pump (*see* **Note 6**).

9. Set up the mass spectrometer detector to scan the m/z range between 74 and 250 amu under positive ionization mode at unit mass resolution to monitor free AAs.
10. The UV detector, located 20 cm from the capillary injection end, can be operated continuously at 200 nm for coarse control of analyte migration.
11. Figure 1 shows the electropherograms of blood sample of both healthy and afflicted individuals.

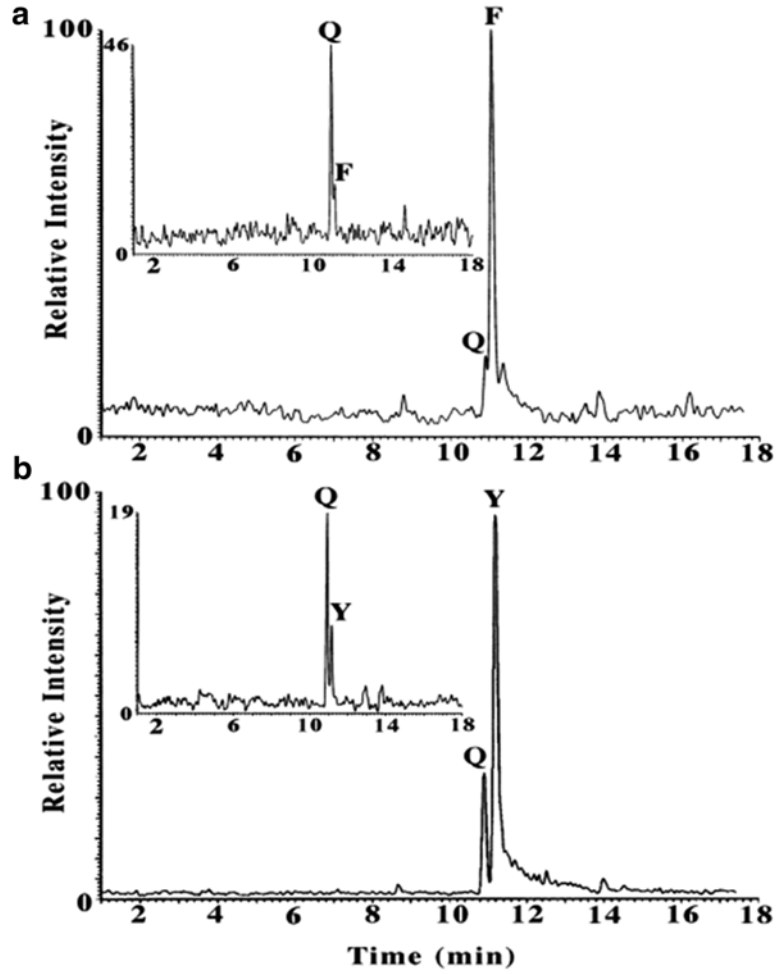

Fig. 1 Analysis by CE–MS. (**a**) Amino acid analysis of the blood of an individual afflicted with PKU and its comparison to that of a healthy one (inset). (**b**) Amino acid analysis of the blood of an infant afflicted with tyrosinemia. The *inset* contains the electropherogram of the blood of a healthy individual. Reprinted with permission from [64]. Copyright 2003 American Chemical Society

3.2 CE-LIF

1. Perfuse the microdialysis probe with the Ringer's solution at high flow rate (10 µl/min) for 1 h, then lower the flow rate to 2 µl/min and implant the probe. Monitor the basal level of the analytes for at least 30 min before stimulus.
2. Collect the perfusate fraction in microvials every 1 min (2 µl sample volume) and immediately store each of them at –40 °C before derivatization. Stop the fraction collection 30 min after the stimulus.
3. After recovery to room temperature, derivatize the microdialysate as follows: add 0.2 µl of the internal standard, 0.4 µl of the borate/NaCN, and 0.2 µl of the NDA solutions to the sample (2 µl). Let the mixture react for about 1 h (*see* **Note 7**).
4. Electrophoresis buffer (2 × 2.0 ml) in sample holder position BI:A1 and BO:A1. Electrophoresis sample in sample holder SI:A1. Standard solution in sample holder SI:B1.
5. 0.25 M NaOH solution (2.0 ml) in sample holder position B1:D1 and water (2.0 ml) in sample holder position BI:E1; place empty vials in sample holders BI:C1 and BO:B1.
6. CE programmed to inject electrophoresis sample for 10 s at 0.5 psi.
7. The conditions used in the CE were as follows: voltage, 25 kV, temperature 25 ± 0.5 °C. The excitation was performed with a Helium Cadmium laser (8 mW, 442 nm) whereas the fluorescence emission intensity was recorded at 490 nm.
8. Between runs, rinse at high pressure (20 psi) the capillary sequentially with 0.25 NaOH (30 s), water (1 min), and electrophoresis buffer (1 min).
9. Figure 2 shows the electropherograms relevant to the analysis of a microdialysate obtained from the spinal dorsal horn, a standard solution, and a brain dialysate from a rat striatum.

3.3 CE-UV

1. Hydrolysis of Proteins and Peptides: vacuum dry the solution of proteins or peptides in 5 × 35-mm glass tubes. Then add to each tube 40 µl of hydrochloric solution. Evacuate and flame seal the tubes. Put the tubes in an oven at 110 °C for 24 h. After opening of the tubes, dry with a gentle nitrogen flow (*see* **Note 8**).
2. Derivatization with phenylisothiocyanate: add to each tube 40 µl of triethylamine solution, vortex shortly and evaporate (*see* **Note 9**). Then add 3 µl 50% ethanol to each tube followed by subsequent addition of 7 µl of PITC solution. Vortex and incubate the samples for 30 min at room temperature. Dry the derivatized samples under vacuum overnight in a desiccator. Dissolve the PITC-AAs in water before CE analysis (*see* **Note 10**).

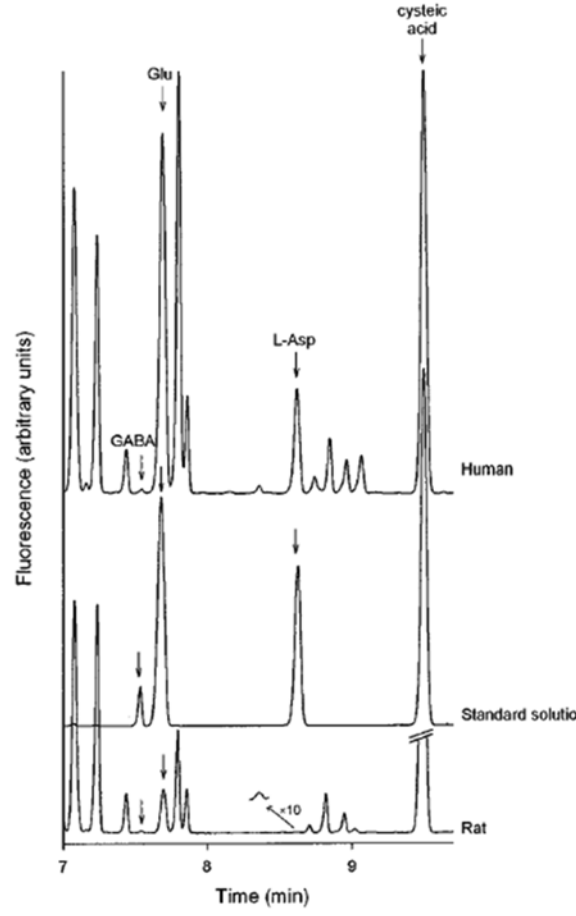

Fig. 2 Analysis by CE-LIF. Typical electropherograms of a microdialysate obtained from the spinal dorsal horn in a patient with chronic pain (*top*), a standard solution (*middle*) containing 5×10^{-7} mol/l GABA, 5×10^{-6} mol/l Glu/L-Asp compared to a brain dialysate obtained from rat striatum (*bottom*). Cysteic acid is the internal standard. Reprinted with permission from [66]. Copyright © 2004 WILEY-VCH Verlag GmbH & Co. KGaA, Weinheim

3. BGE (2×2.0 ml) in sample holder position BI:A1 and BO:A1. Electrophoresis sample to sample holder SI:A1.
4. CE programmed to inject electrophoresis sample for 5 s at 0.5 psi.
5. The conditions used in the CE were as follows: voltage, 27 kV, temperature 24 ± 0.5 °C. The online UV detector, located 7 cm from the capillary end, is operated continuously at 200 nm for control of analyte migration.
6. Change the BGE after each run and wash the capillary with the fresh electrolyte at least 5 min.
7. Figure 3 shows the electropherograms of a hydrolysate of BSA.

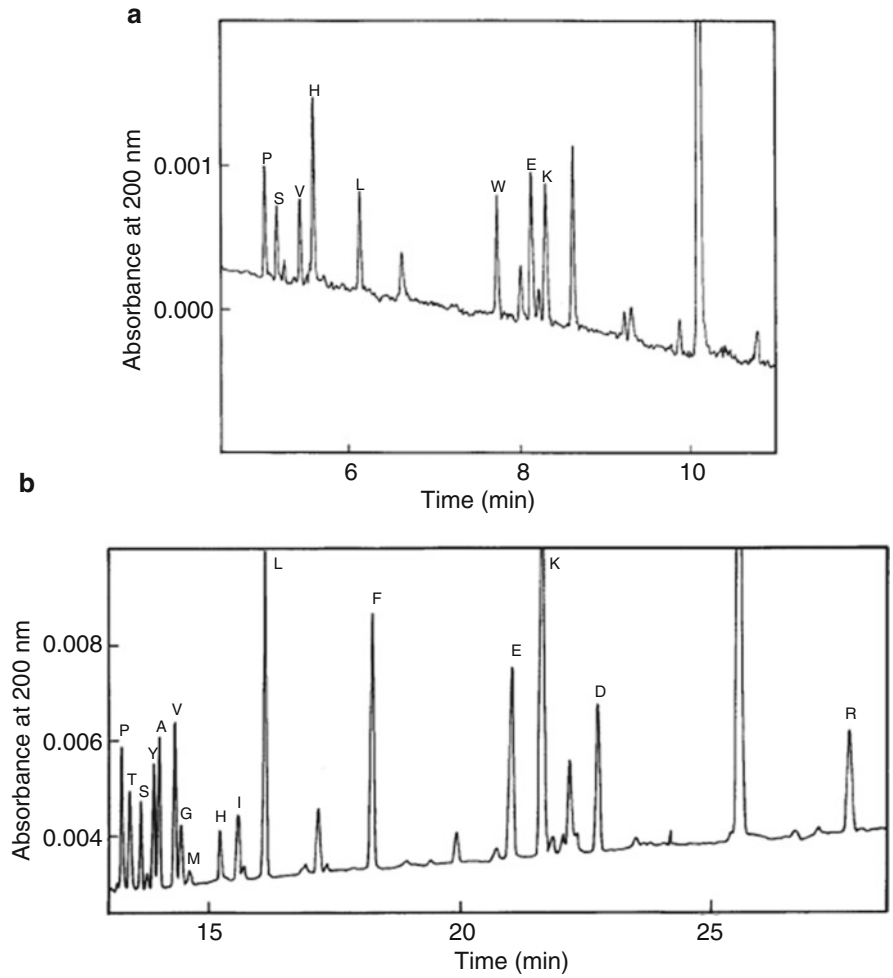

Fig. 3 Analysis by CE-UV. Capillary electrophoresis of PTC-derivatized hydrolysate amino acids. (**a**) 0.58 pmol of the 10-residue peptide SA-2, (**b**) 0.50 pmol of the 607-residue protein BSA. Reprinted from [65], Copyright 2000, with permission from Elsevier

4 Notes

1. All solutions were prepared in water that has a resistivity of 18.2 MΩ cm and total organic content of less than 5 ppb. An UltraClear system (SG Water, Hamburg, Germany) equipped with an UV lamp was used.
2. Filter the BGE through a 0.2 μm filter to prevent blockage of the CE capillary and for degassing.
3. The running buffer may conveniently be prepared by titration of phosphoric acid (Merck) with NaOH (Sigma-Aldrich).

Then dissolve the SDS and filter through 0.2-μm membranes before use. It could be stored at room temperature for at least 6 months.

4. Either a chemical or a mechanical method can be used to sharpen the outlet tip of a new capillary, before mounting it in the cartridge. If nitrile gloves and a fume hood are available, the chemical etching in 49 % hydrofluoric acid could be accomplished by soaking 2–4 mm of the capillary end for 5 min while passing nitrogen through the capillary to minimize the etching of the inner wall of the capillary. Otherwise the tip could also be sharpened mechanically with fine emery paper: in this case pay attention to the debris, not to clog the capillary. Moreover before use new capillaries should be eluted with 1 M NaOH for 2–4 h under constant pressure. At the beginning of each day the capillary should be conditioned by flushing with 1 M NaOH solution (5 min), followed by 5 min flush of water and 30 min of electrolyte solution.
5. If available use an HPLC pump as generally the baseline noise is halved.
6. With different CE equipment the pneumatic assistance, which is used to shorten analysis time, could be not available.
7. NDA is a fluorescent tag not fluorescent itself (in contrast with fluorescein isothiocyanate, for instance) and rapidly reacts to give stable fluorescent derivatives. However, since the internal standard cysteic acid reacts less quickly than Glu, L-Asp, and GABA, a reaction time of 1 h at room temperature is necessary to complete the derivatization reaction.
8. To get rid of the metal ions eventually present in the sample, it is possible to extract the proteic fraction in 6 N NH_3 first, then to dry the extract and hydrolyze it. For biomedical applications the glass tube should be pyrolyzed (400 °C, 3–4 h) before use.
9. This step is essential to remove residual hydrolysis acid.
10. Reagent mixtures were made fresh daily, stock PITC was stored at about 20 °C under nitrogen. Triethylamine and 50 % ethanol were stored at +4 °C. PTC–amino acids were stored at –20 °C.

Acknowledgement

This work was partly funded by Italian MIUR through the project PON 254/Ric./2011 (Cod. PONa3_00334). Francesca Liuzzi is gratefully acknowledged for compiling tables.

References

1. Poinsot V, Gavard P, Feurer B (2010) Recent advances in amino acid analysis by CE. Electrophoresis 31:105–121
2. Poinsot V, Carpene M-A, Bouajila J et al (2012) Recent advances in amino acid analysis by capillary electrophoresis. Electrophoresis 33:14–35
3. Poinsot V, Ong-Meang V, Gavard P et al (2014) Recent advances in amino acid analysis by capillary electromigration methods, 2011–2013. Electrophoresis 35:50–68
4. Li Z, Zhang Y, Tong F-H et al (2014) Capillary electrophoresis with laser-induced fluorescence detection of main polyamines and precursor amino acids in saliva. Chin Chem Lett 25:640–644
5. Hattori T, Fukushi K, Hirokawa T (2014) Role of counter-ions in background electrolyte for the analysis of cationgenic weak electrolytes and amino acids in neutral aqueous solutions by capillary electrophoresis with electrokinetic injection. J Chromatogr A 1326:130–133
6. Xiong X-J, Guo X-F, Ge X-X et al (2013) Determination of neurotransmitter amino acids in mouse central nervous system by CE-LIF. J Sep Sci 36:3264–3269
7. Barbosa CG, Goncalves NS, Bechara EJH et al (2013) Potential diagnostic assay for cystinuria by capillary electrophoresis coupled to mass spectrometry. J Braz Chem Soc 24:534–540
8. Jeong J-S, Kim S-K, Park S-R (2013) Amino acid analysis of dried blood spots for diagnosis of phenylketonuria using capillary electrophoresis-mass spectrometry equipped with a sheathless electrospray ionization interface. Anal Bioanal Chem 405:8063–8072
9. Ge S, Wang H, Wang Z et al (2013) Simultaneous determination of neuroactive amino acids in serum by CZE Coupled with amperometric detection. Chromatographia 76:149–155
10. Zhang N, Guo X-F, Wang H et al (2011) Determination of amino acids and catecholamines derivatized with 3-(4-chlorobenzoyl)-2-quinolinecarboxaldehyde in PC12 and HEK293 cells by capillary electrophoresis with laser-induced fluorescence detection. Anal Bioanal Chem 401:297–304
11. Tuma P, Malkova K, Samcova E et al (2010) Rapid monitoring of arrays of amino acids in clinical samples using capillary electrophoresis with contactless conductivity detection. J Sep Sci 33:2394–2401
12. Li H, Li C, Yan Z et al (2010) Simultaneous monitoring multiple neurotransmitters and neuromodulators during cerebral ischemia/reperfusion in rats by microdialysis and capillary electrophoresis. J Neurosci Meth 189:162–168
13. Wang S, Yang P, Zhao X (2009) Amino acid profile determination in the urine of bladder cancer patients by CE-MS with On-Line pH-mediated stacking and pattern recognition. Chromatographia 70:1479–1484
14. Jiang X, Xia Z, Wei W et al (2009) Direct UV detection of underivatized amino acids using capillary electrophoresis with online sweeping enrichment. J Sep Sci 32:1927–1933
15. Kaneta T, Maeda H, Miyazaki M et al (2008) Determination of amino acids in urine by cyclodextrin-modified capillary electrophoresis-laser-induced fluorescence detection. J Chromatogr Sci 46:712–716
16. Mamunooru M, Jenkins RJ, Davis NI et al (2008) Gradient elution isotachophoresis with direct ultraviolet absorption detection for sensitive amino acid analysis. J Chromatogr A 1202:203–211
17. Simionato AVC, Moraes EP, Carrilho E et al (2008) Determination of amino acids by capillary electrophoresis-electrospray ionization-mass spectrometry: an evaluation of different protein hydrolysis procedures. Electrophoresis 29:2051–2058
18. Zinellu A, Sotgia S, Zinellu E et al (2007) High-throughput CZE-UV determination of arginine and dimethylated arginines in human plasma. Electrophoresis 28:1942–1948
19. Tellez N, Aguilera N, Quinonez B et al (2008) Arginine and glutamate levels in the gingival crevicular fluid from patients with chronic periodontitis. Braz Dent J 19:318–322
20. Piyankarage SC, Augustin H, Grosjean Y et al (2010) Hemolymph amino acid variations following behavioral and genetic changes in individual Drosophila larvae. Amino Acids 38:779–788
21. Ye X, Kim WS, Rubakhin SS et al (2007) Ubiquitous presence of argininosuccinate at millimolar levels in the central nervous system of Aplysia californica. J Neurochem 101:632–640
22. Deng YH, Wang H, Zhang HS (2008) Determination of amino acid neurotransmitters in human cerebrospinal fluid and saliva by capillary electrophoresis with laser-induced fluorescence detection. J Sep Sci 31:3088–3097
23. Thongkhao-on K, Wirtshafter D, Shippy SA (2008) Feeding specific glutamate surge in the rat lateral hypothalamus revealed by low-flow push–pull perfusion. Pharmacol Biochem Behav 89:591–597

24. Denoroy L, Parrot S, Renaud L et al (2008) In-capillary derivatization and capillary electrophoresis separation of amino acid neurotransmitters from brain microdialysis samples. J Chromatogr A 1205:144–149
25. Zunic G, Spasic S (2008) Capillary electrophoresis method optimized with a factorial design for the determination of glutathione and amino acid status using human capillary blood. J Chromatogr B 873:70–76
26. Arvidsson B, Johannesson N, Citterio A et al (2007) High throughput analysis of tryptophan metabolites in a complex matrix using capillary electrophoresis coupled to time-of-flight mass spectrometry. J Chromatogr A 1159:154–158
27. Shama N, Bai SW, Chung BC et al (2008) Quantitative analysis of 17 amino acids in the connective tissue of patients with pelvic organ prolapse using capillary electrophoresis–tandem mass spectrometry. J Chromatogr B 865:18–24
28. Ramautar R, Mayboroda OA, Deelder AM et al (2008) Metabolic analysis of body fluids by capillary electrophoresis using noncovalently coated capillaries. J Chromatogr B 871:370–374
29. Ramautar R, Mayboroda OA, Derks RJ et al (2008) Capillary electrophoresis-time of flight-mass spectrometry using noncovalently bilayer-coated capillaries for the analysis of amino acids in human urine. Electrophoresis 29:2714–2722
30. Meng J, Zhang W, Cao CX et al (2010) Moving affinity boundary electrophoresis and its selective isolation of histidine in urine. Analyst 135:1592–1599
31. Zhang N, Zhang HS, Wang H (2009) Separation of free amino acids and catecholamines in human plasma and rabbit vitreous samples using a new fluorogenic reagent 3-(4-bromobenzoyl)-2-quinolinecarboxaldehyde with CE-LIF detection. Electrophoresis 30:2258–2265
32. Zhou L, Yan N, Zhang H et al (2010) Microwave-accelerated derivatization for capillary electrophoresis with laser-induced fluorescence detection: a case study for determination of histidine, 1- and 3-methylhistidine in human urine. Talanta 82:72–77
33. Sun H, Su M, Li L (2010) Simultaneous determination of tetracaine, proline, and enoxacin in human urine by CE with ECL detection. J Chromatogr Sci 48:49–54
34. Zinellu A, Sotgia S, Pisanu E et al (2010) Quantification of neurotransmitter amino acids by capillary electrophoresis laser-induced fluorescence detection in biological fluids. Anal Bioanal Chem 398:1973–1978
35. Kao YY, Liu KT, Huang MF et al (2010) Analysis of amino acids and biogenic amines in breast cancer cells by capillary electrophoresis using polymer solutions containing sodium dodecyl sulfate. J Chromatogr A 1217:582–587
36. Li MD, Tseng WL, Cheng TL (2009) Ultrasensitive detection of indoleamines by combination of nanoparticle-based extraction with capillary electrophoresis/laser-induced native fluorescence. J Chromatogr A 1216:6451–6458
37. Swann LM, Forbes SL, Lewis SW (2010) A capillary electrophoresis method for the determination of selected biogenic amines and amino acids in mammalian decomposition fluid. Talanta 81:1697–1702
38. Zhang DL, Li WL, Zhang JB et al (2010) Determination of unconjugated aromatic acids in urine by capillary electrophoresis with dual electrochemical detection – potential application in fast diagnosis of phenylketonuria. Electrophoresis 31:2989–2996
39. Desiderio C, Rossetti DV, Messana I et al (2010) Analysis of arginine and methylated metabolites in human plasma by field amplified sample injection capillary electrophoresis tandem mass spectrometry. Electrophoresis 31:1894–1902
40. Atherton T, Croxton R, Baron M et al (2012) Analysis of amino acids in latent fingerprint residue by capillary electrophoresis-mass spectrometry. J Sep Sci 35:2994–2999
41. Kok MGM, de Jong GJ, Somsen GW (2011) Sensitivity enhancement in capillary electrophoresis-mass spectrometry of anionic metabolites using a triethylamine-containing background electrolyte and sheath liquid. Electrophoresis 32:3016–3024
42. Jeong JS, Kim SK, Park SR (2012) Capillary electrophoresis mass spectrometry with sheathless electrospray ionization for high sensitivity analysis of underivatized amino acids. Electrophoresis 33:2112–2121
43. Strieglerová L, Kubáň P, Boček P (2011) Electromembrane extraction of amino acids from body fluids followed by capillary electrophoresis with capacitively coupled contactless conductivity detection. J Chromatogr A 1218: 6248–6255
44. Choi J, Choi K, Kim J et al (2011) Sensitive analysis of amino acids with carrier-mediated single drop microextraction in-line coupled with capillary electrophoresis. J Chromatogr A 1218:7227–7233
45. Knolhoff AM, Nautiyal KM, Nemes P et al (2013) Combining small-volume metabolomic and transcriptomic approaches for assessing brain chemistry. Anal Chem 85:3136–3143

46. Zinellu A, Sotgia S, Deiana L et al (2012) Simultaneous analysis of kynurenine and tryptophan in human plasma by capillary electrophoresis with UV detection. J Sep Sci 35:1146–1151
47. Tak YH, Somsen GW, de Jong GJ (2011) Optimization of dynamic pH junction for the sensitive determination of amino acids in urine by capillary electrophoresis. Anal Bioanal Chem 401:3275–3281
48. Bhowmik SK, Bong CC, Oh-Seung K et al (2012) Discovery of common urinary biomarkers for hepatotoxicity induced by carbon tetrachloride, acetaminophen and methotrexate by mass spectrometry-based metabolomics. J Appl Toxicol 32:505–520
49. Soga T, Sugimoto M, Honma M et al (2011) Serum metabolomics reveals γ-glutamyl dipeptides as biomarkers for discrimination among different forms of liver disease. J Hepatol 55:896–905
50. Kami K, Fujimori T, Sato H et al (2013) Metabolomic profiling of lung and prostate tumor tissues by capillary electrophoresis time-of-flight mass spectrometry. Metabolomics 9:444–453
51. Song L, Guo Z, Chen Y (2011) One-pot labeling-based capillary zone electrophoresis for separation of amino acid mixture and assay of biofluids. Anal Chim Acta 703:257–263
52. Zinellu A, Sotgia S, Deiana L (2013) Analysis of neurotransmitter amino acids by CE-LIF detection in biological fluids. Meth Mol Biol 919:35–42
53. Zinellu A, Sotgia S, Scanu B et al (2012) Low density lipoprotein S-homocysteinylation is increased in acute myocardial infarction patients. Clin Biochem 45:359–362
54. Hirokawa T, Okamoto H, Gosyo Y (2007) Simultaneous monitoring of inorganic cations, amines and amino acids in human sweat by capillary electrophoresis. Anal Chim Acta 581:83–88
55. Cao L, Zhang H, Hong W (2007) Analysis of amino acid neurotransmitters by capillary electrophoresis and laser-induced fluorescence using a new fluorescein-derived label. Microch Acta 158:361–368
56. Klinker CC, Bowser MT (2007) 4-Fluoro-7-nitro-2,1,3-benzoxadiazole as a fluorogenic labeling reagent for the in vivo analysis of amino acid neurotransmitters using online microdialysis-capillary electrophoresis. Anal Chem 79:8747–8754
57. Chang P-L, Chiu T-C, Wang T-E et al (2011) Quantitation of branched-chain amino acids in ascites by capillary electrophoresis with light-emitting diode-induced fluorescence detection. Electrophoresis 32:1080–1083
58. Hogerton AL, Bowser MT (2013) Monitoring neurochemical release from astrocytes using in vitro microdialysis coupled with high-speed capillary electrophoresis. Anal Chem 85:9070–9077
59. Zhang J-B, Li M-J, Li Z et al (2013) Study on urinary profile of inborn errors of metabolism by 18-crown-6 modified capillary electrophoresis with laser-induced fluorescence detection. J Chromatogr B 929:102–106
60. Li H, Yan Z-Y (2010) Analysis of amino acid neurotransmitters in hypothalamus of rats during cerebral ischemia-reperfusion by microdialysis and capillary electrophoresis. Biomed Chromatogr 24:1185–1192
61. Lu M-J, Pulido JS, McCannel CA et al (2007) Detection of elevated signaling amino acids in human diabetic vitreous by rapid capillary electrophoresis. Experim Diab Res ID 39765
62. Moreno-Gonzalez D, Sastre-Torano J, Gamiz-Garcia L et al (2013) Micellar electrokinetic chromatography–electrospray ionization mass spectrometry employing a volatile surfactant for the analysis of amino acids in human urine. Electrophoresis 34:2615–2622
63. Li Z, Zharikova A, Bastian J et al (2008) High temporal resolution of amino acid levels in rat nucleus accumbens during operant ethanol self-administration: involvement of elevated glycine in anticipation. J Neurochem 106:170–181
64. Schultz CL, Moini M (2003) Analysis of underivatized amino acids and their D/L--enantiomers by sheathless capillary electrophoresis/electrospray ionization mass spectrometry. Anal Chem 75:1508–1513
65. Zahou E, Jornvall H, Bergman T (2000) Amino acid analysis by capillary electrophoresis after phenylthiocarbamylation. Anal Biochem 281:115–122
66. Parrot S, Sauvinet V, Xavier J-M et al (2004) Capillary electrophoresis combined with microdialysis in the human spinal cord: a new tool for monitoring rapid peroperative changes in amino acid neurotransmitters within the dorsal horn. Electrophoresis 25:1511–1517
67. Wagner Z, Tábi T, Jakó T et al (2012) Chiral separation and determination of excitatory amino acids in brain samples by CE-LIF using dual cyclodextrin system. Anal Bioanal Chem 404:2363–2368
68. Scanlan C, Shi T, Hatcher NG et al (2010) Synthesis, accumulation, and release of d-aspartate in the Aplysia californica CNS. J Neurochem 115:1234–1244
69. Lin KC, Hsieh MM, Chang CW et al (2010) Stacking and separation of aspartic acid enantiomers under discontinuous system by capillary electrophoresis with light-emitting

diode-induced fluorescence detection. Talanta 82:1912–1918

70. Samakashvili S, Ibáñez C, Simó C et al (2011) Analysis of chiral amino acids in cerebrospinal fluid samples linked to different stages of Alzheimer disease. Electrophoresis 32:2757–2764
71. Sullivan SJ, Miller RF (2010) AMPA receptor mediated D-Ser release from retinal glial cells. J Neurochem 115:1681–1689
72. Kirschner DL, Wilson AL, Drew KL et al (2009) Simultaneous efflux of endogenous D-Ser and L-Glu from single acute hippocampus slices during oxygen glucose deprivation. J Neurosci Res 87:2812–2820
73. Lorenzo MP, Villasenor A, Ramamoorthy A et al (2013) Optimization and validation of a capillary electrophoresis laser-induced fluorescence method for amino acids determination in human plasma: application to bipolar disorder study. Electrophoresis 34:1701–1709
74. Huang Y, Shi M, Zhao S et al (2011) Trace analysis of d-tyrosine in biological samples by microchip electrophoresis with laser induced fluorescence detection. J Chromatogr B 879:3203–3207
75. Li C, Yan Z, Yang J et al (2010) Neuroprotective effects of resveratrol on ischemic injury mediated by modulating the release of neurotransmitter and neuromodulator in rats. Neurochem Int 56:495–500
76. Yuan B, Wu H, Sanders T et al (2011) Chiral capillary electrophoresis–mass spectrometry of 3,4-dihydroxyphenylalanine: evidence for its enantioselective metabolism in PC-12 nerve cells. Anal Biochem 416:191–195
77. Singh NS, Paul RK, Sichler M et al (2012) Capillary electrophoresis–laser-induced fluorescence (CE-LIF) assay for measurement of intracellular D-serine and serine racemase activity. Anal Biochem 421:460–466
78. Qi L, Yang G (2009) On-column labeling technique and chiral ligand-exchange CE with zinc(II)-L-arginine complex as a chiral selector for assay of dansylated D, L-amino acids. Electrophoresis 30:2882–2889
79. Lorenzo MP, Navarrete A, Balderas C et al (2013) Optimization and validation of a CE-LIF method for amino acid determination in biological samples. J Pharm Biomed Anal 73:116–124
80. Tseng WL, Hsu CY, Wu TH et al (2009) Highly sensitive detection of chiral amino acids by CE based on on-line stacking techniques. Electrophoresis 30:2558–2564
81. Qi L, Qiao J, Yang G et al (2009) Chiral ligand-exchange CE assays for separation of amino acid enantiomers and determination of enzyme kinetic constant. Electrophoresis 30:2266–2272
82. Liu Q, Wu K, Tang F et al (2009) Amino acid ionic liquids as chiral ligands in ligand-exchange chiral separations. Chemistry 15:9889–9896
83. Wang Z, Wang J, Hu Z et al (2007) Enantioseparation by CE with vancomycin as chiral selector: improving the separation performance by dynamic coating of the capillary with poly(dimethylacrylamide). Electrophoresis 28:938–943
84. Sanchez-Hernandez L, Dominguez-Vega E, Montealegre C et al (2014) Potential of vancomycin for the enantiomeric resolution of FMOC-amino acids by capillary electrophoresis-ion-trap-mass spectrometry. Electrophoresis 35:1244–1250
85. Peng Y, Zhang T, Wang T et al (2013) Use of neutral capillaries for the enantioseparation of N-benzoylated amino acids by capillary electrophoresis with bromobalhimycin as chiral selector. J Sep Sci 36:1568–1574
86. Zhang H, Qi L, Mu X et al (2013) Influence of ionic liquids as electrolyte additives on chiral separation of dansylated amino acids by using Zn(II) complex mediated chiral ligand exchange CE. J Sep Sci 36:886–891
87. Giuffrida A, Caruso R, Messina M et al (2012) Chiral separation of amino acids derivatised with fluorescein isothiocyanate by single isomer derivatives 3-monodeoxy-3-monoamino-β- and γ-cyclodextrins: the effect of the cavity size. J Chromatogr A 1269:360–365
88. Qi L, Yang G (2009) Enantioseparation of dansyl amino acids by ligand-exchange capillary electrophoresis with zinc(II)-L-phenylalaninamide complex. J Sep Sci 32:3209–3214
89. Xiao Y, Ong T-T, Tan TTY et al (2009) Synthesis and application of a novel single-isomer mono-6-deoxy-6-(3R,4R-dihydroxypyrrolidine)-β-cyclodextrin chloride as a chiral selector in capillary electrophoresis. J Chromatogr A 1216:994–999
90. Tang W, Ong TT, Ng S-C (2007) Chiral separation of dansyl amino acids in capillary electrophoresis using mono-(3-methyl-imidazolium) -β-cyclodextrin chloride as selector. J Sep Sci 30:1343–1349
91. Qi L, Yang G, Zhang H et al (2010) A chiral ligand exchange CE essay with zinc(II)–L-valine complex for determining enzyme kinetic constant of L-amino acid oxidase. Talanta 81:1554–1559
92. Wang S, Fan L, Cui S (2009) CE-LIF chiral separation of aspartic acid and glutamic acid enantiomers using human serum albumin and

sodium cholate as dual selectors. J Sep Sci 32:3184–3190

93. Mu X, Qi L, Zhang H et al (2012) Ionic liquids with amino acids as cations: novel chiral ligands in chiral ligand-exchange capillary electrophoresis. Talanta 97:349–354

94. Sun B, Mu X, Qi L (2014) Development of new chiral ligand exchange capillary electrophoresis system with amino acid ionic liquids ligands and its application in studying the kinetics of L-amino acid oxidase. Anal Chim Acta 821:97–102

Chapter 15

Enantiomer Separations by Capillary Electrophoresis

Gerhard K.E. Scriba, Henrik Harnisch, and Qingfu Zhu

Abstract

Capillary electrophoresis (CE) is a versatile and flexible technique for analytical enantioseparations. This is due to the large variety of chiral selectors as well as the different operation modes including electrokinetic chromatography, micellar electrokinetic chromatography, and microemulsion electrokinetic chromatography. The chiral selector, which is added to the background electrolyte, represents a pseudostationary phase with its own electrophoretic mobility allowing a variety of different separation protocols. The present chapter briefly addresses the basic fundamentals of CE enantioseparations as well as the most frequently applied chiral selectors and separation modes. The practical example illustrates the separation of the enantiomers of a positively charged analyte using native and charged cyclodextrin derivatives as chiral selectors.

Key words Capillary electrophoresis, Enantiomer separation, Chiral separation, Chiral selector, Migration mode

1 Introduction

In capillary electrophoresis (CE) separation techniques, the analyses are performed in narrow bore capillaries exploiting the electrophoretic mobilities of charged molecules upon the application of high electric field strength. In order to achieve the separation of enantiomers, a chiral selector is added to the background electrolyte. Thus, in CE the chiral selector represents a so-called pseudostationary phase that may possess its own electrophoretic mobility. In combination with the different modes of CE such as electrokinetic chromatography (EKC), micellar electrokinetic chromatography (MEKC) and microemulsion electrokinetic chromatography (MEEKC), a variety of separation modes can be realized contributing to the high flexibility of CE. The presence of the selector in the background electrolyte also allows rapid change of the experimental conditions enabling rapid method development. Moreover, the small amounts of samples and chemicals make CE an environmentally friendly and cost-effective technique. The advancement of CE enantioseparations is documented in many publications including recent reviews [1–6] and monographs [7, 8].

Philippe Schmitt-Kopplin (ed.), *Capillary Electrophoresis: Methods and Protocols*, Methods in Molecular Biology, vol. 1483,
DOI 10.1007/978-1-4939-6403-1_15,

The present chapter will briefly introduce the basic fundamentals of enantioseparations in CE and the most frequently used types of chiral selectors and separation modes. Capillary electrochromatography (CEC) which is often considered a hybrid technique between CE and HPLC will not be discussed. Practical examples of enantioseparations using cyclodextrins (CDs) as chiral selectors are presented.

1.1 Fundamentals of CE Enantioseparations

In CE, analyte separation is carried out in capillaries with an inner diameter of 20–100 μm so that dissipation of Joule heat is effective which allows the application of high voltages. The capillaries are manufactured from fused-silica so that detection modes such as UV- or laser-induced fluorescence detection are typically carried out by on-column detection but hyphenation to a mass spectrometer has become routine as well. Moreover, the output of commercial instruments resembles that of conventional chromatograms and can be integrated for quantitative analyses. Finally, CE allows the separation of small molecules including stereoisomers as well as the analysis of large molecules such as proteins or DNA and even whole cells.

The mobility of an analyte is determined by the electrophoretic mobility of a particle, μ_{ep}, as a function of charge, q, and size of the analyte represented by the radius, r, for a spherical particle according to:

$$\mu_{ep} = \frac{q}{6\pi\eta r} \tag{1}$$

η is the viscosity of the background electrolyte. In case of acidic or basic analytes, the charge is a function of the pH of the electrolyte solution. The charge-to-size ratio is also generally referred to as charge density.

In addition, the charged surface of the capillary leads to a general mass flow, the electroosmotic flow (EOF), which creates a plug-like flow profile as compared to the parabolic flow profile of pressure-driven chromatographic techniques making CE a high resolution technique. The mobility of the EOF is a function of the permittivity of the electrolyte solution, ε, and the zeta-potential, ζ, resulting from the negatively charged capillary surface due to pH-dependent dissociation of the silanol groups:

$$\mu_{EOF} = \frac{\varepsilon\zeta}{4\pi\eta} \tag{2}$$

Consequently, the effective mobility of a solute is the sum of both electrophoretic forces, μ_{ep} and μ_{EOF}, according to:

$$\mu_{eff} = \mu_{ep} + \mu_{EOF} \tag{3}$$

As in chromatography, CE enantioseparations can be grouped into indirect and direct methods. In the indirect approach the analyte enantiomers are derivatized with a single enantiomer reagent to form diastereomers via covalent bonds. These diastereomers can be separated, in principle, under achiral conditions. Direct methods refer to the separation of enantiomers in a chiral environment which requires the presence of a chiral selector in the background electrolyte. The separation is based on the formation of transient diastereomeric complexes in a thermodynamic equilibrium. This is identical to chromatographic techniques so that the stereospecific recognition of the analyte enantiomers by a chiral selector represents a chromatographic phenomenon. The fact that the selector is mobile in CE compared to chromatography (a so-called pseudostationary phase) is not a fundamental difference. Therefore, enantioseparations by CE are also referred to more correctly as electrokinetic chromatography (EKC). The transport of the analyte and/or the analyte–selector complex to the detector is accomplished by electrokinetic phenomena so that enantioseparations in CE are composed of a chromatographic and an electrophoretic mechanism.

Assuming the formation of analyte–selector complexes at a stoichiometric ratio of 1:1, the equilibria between the *S* and *R* enantiomers of the analyte and the chiral selector, *C*, are given by:

$$\begin{aligned} S + C &\rightarrow SC \quad K_S = \frac{[SC]}{[S][C]} \\ R + C &\rightarrow RC \quad K_R = \frac{[RC]}{[R][C]} \end{aligned} \tag{4}$$

In the presence of a complexation agent the analyte may exist in a complexed and a noncomplexed form so that the effective mobility can be described as a function of the mobilities of the free and complexed analytes resulting in the expression for the S-enantiomer:

$$\mu_{\text{eff}}^{S} = f\,\mu_f + (1-f)\mu_{\text{cplx}}^{S} \tag{5}$$

where μ_f is the mobility of the free enantiomer, μ^s_{eff} is the mobility of the analyte–selector complex, and *f* is the fraction of the noncomplexed species. Considering the complexation constant, *K*, and the concentration of the selector, [*C*], the effective mobility can be described by:

$$\mu_{\text{eff}}^{S} = \frac{\mu_f + \mu_{\text{cplx}}^{S} K_S[C]}{1 + K_S[C]} \tag{6}$$

Therefore, the effective mobility of an analyte interacting with a chiral selector is a function of the mobility of the free analyte, μ_f, the mobility of the analyte–selector complex, μ_{cplx}, the complexation constant, *K*, and the concentration of the chiral selector [9].

An enantioseparation is observed when the effective mobilities of the enantiomers differ:

$$\Delta\mu = \mu_{\text{eff}}^{S} - \mu_{\text{eff}}^{R} = \frac{\mu_{\text{f}} + \mu_{\text{cplx}}^{S} K_{\text{S}}[C]}{1 + K_{\text{S}}[C]} - \frac{\mu_{\text{f}} + \mu_{\text{cplx}}^{R} K_{\text{R}}[C]}{1 + K_{\text{R}}[C]} \quad (7)$$

The chromatographic enantioselective mechanism (also referred to as the thermodynamic mechanism) results from the different affinities of the enantiomers toward the chiral selector as reflected by differences in the complexation constants, i.e., $K_{\text{S}} \neq K_{\text{R}}$. The electrophoretic enantioselective mechanism is based on differences in the mobilities of the enantiomer–selector complexes, i.e., $\mu_{\text{eff}}^{S} \neq \mu_{\text{eff}}^{R}$, which may be caused by differences in the hydrodynamic radii of the complexes. Both mechanisms can contribute simultaneously but the chromatographic mechanism is typically the dominant mechanism because the hydrodynamic radii of the two enantiomer–selector complexes do not differ significantly and the effective charges of the two complexes are identical.

A striking difference between enantioseparations in pressure-driven chromatographic systems and systems based on electrophoretic phenomena is the fact that enantiomers can also be separated in the case of equal binding constants ($K_{\text{S}} = K_{\text{R}}$) solely based on differences in the electrophoretic mobilities of the diastereomeric complexes as discussed in [10]. This separation mechanism is not possible with the immobilized selectors in chromatography. Moreover, the designed combination of selectors with different mobilities is feasible in order to achieve an enantioseparation.

The simple mathematical model for CE enantioseparations described by Eq. 7 has several disadvantages such as the fact that it does not account for the protonation equilibria of the enantiomers in their free and complexed form. As a result, different charge densities of the diastereomeric complexes may exist at a given pH of the background electrolyte based on a complexation-induced pK_{a} shift leading to different mobilities of the diastereomeric selector–enantiomer complexes. Nonetheless the simple model provides a general understanding of the phenomena involved in CE enantioseparations. For a discussion of further complex models including the protonation equilibria or multiple equilibria see, for example, [4, 11–15].

1.2 Migration Modes

In CE, the analyte as well as the chiral selector may be neutral, anionic, cationic, or zwitterionic. Thus, in addition to buffer additives (other than the chiral selector) and the nature of the capillary wall, which may both affect the EOF, the charge of the solute and the chiral selector determine the mechanism and direction of the migration in CE. Therefore, the nature of the chiral additive contributes not only to the separation selectivity but in case of charged selectors

also to the migration direction and magnitude. As a consequence, various scenarios can be applied to affect the effective mobilities of the enantiomers in order to obtain a certain migration order. Considering the effect of the chromatographic principle reflected by the complexation of the solutes and the electrophoretic principle on the effective mobilities of the enantiomers, the following mechanisms may affect the enantiomer migration order [16, 17]:

- the strength of the complexation of the enantiomers by the selector
- the direction and magnitude of the electroosmotic flow (EOF)
- the direction and magnitude of the mobility of the free analyte
- the direction and magnitude of the mobility of the chiral selector
- the direction and magnitude of the mobility of the diastereomeric selector–enantiomer complexes.

Combinations of the mechanisms may apply. The various scenarios are also possible due to the fact that detection in CE can be performed at the cathodic end (normal polarity of the applied voltage) as well as the anodic end of the capillary (reversed polarity of the applied voltage) so that cathodic as well as anodic mobility of the analytes can be exploited. Selected migration modes considering charged or neutral analytes as well as neutral and charged chiral selectors are schematically shown in Fig. 1. Upon selection of appropriate experimental conditions, a reversal of the enantiomer migration order can be achieved. This may be important for the determination of the enantiomeric excess when the minor enantiomer has to be determined in the presence of a large excess of the major enantiomer. Because peak tailing and peak fronting can be observed in CE it may be desirable to determine the minor enantiomer in front of a large tailing peak or after a large fronting peak. Other experimental conditions resulting in a different enantiomer migration order can be envisioned, so that the scenarios shown in Fig. 1 cannot be comprehensive. For example, only single selector systems as well as neutral and negatively charged selectors have been considered here.

The enantiomers of basic compounds can be separated at low pH using uncharged selectors and detection is carried out at the cathode (Fig. 1a). Under these conditions the analyte is positively charged so that it migrates to the cathode. The weaker complexed enantiomer is detected first because it possesses the higher mobility. Negatively charged analytes can be separated using neutral selectors under high EOF (Fig. 1b) or low EOF conditions (Fig. 1c). The negatively charged enantiomers migrate to the anode. In the presence of a high EOF overall mobility is directed to the cathode so that the stronger complexed enantiomer will be

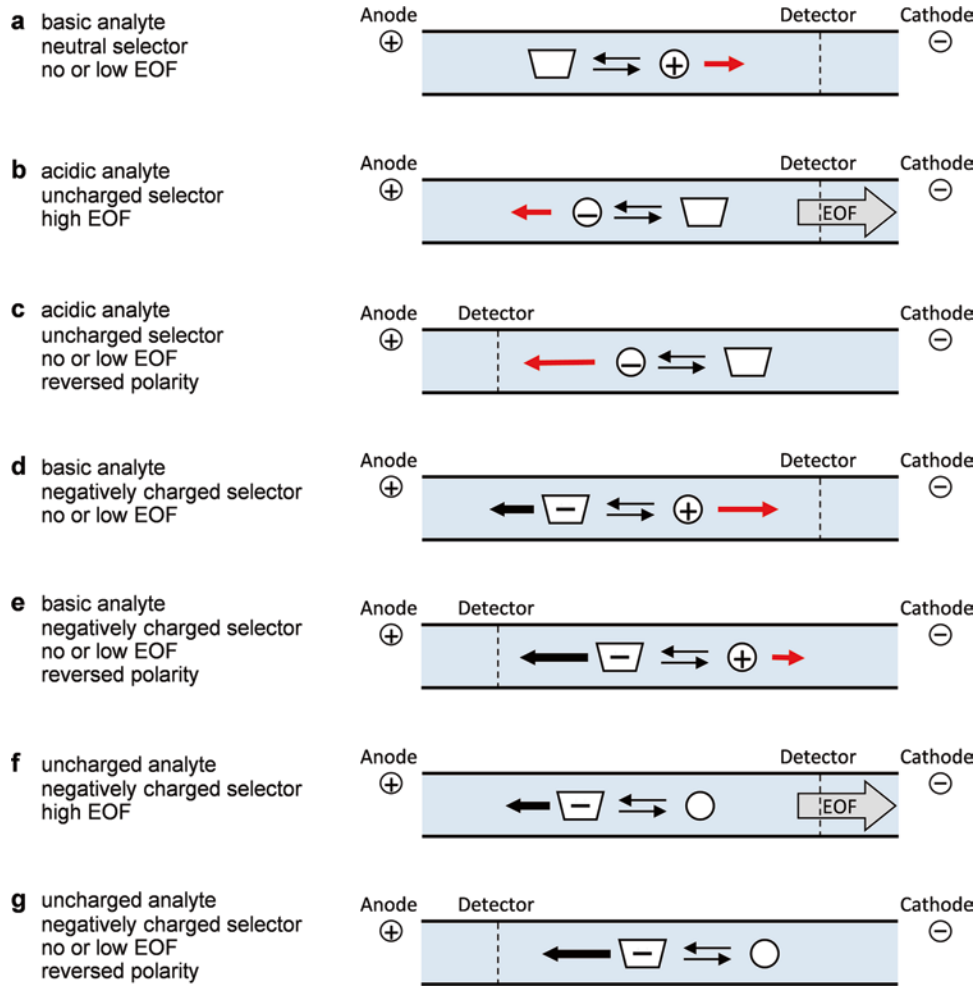

Fig. 1 Scheme of migration modes in CE. The circle represents the analyte while the trapezoid represents the chiral selector. The charge of analyte and selector is indicated by the plus or minus sign. The *red arrow* represents the electrophoretic mobility of analyte and the *black arrow* the mobility of the selector. The net mobility in the different modes is always directed toward the detector

detected first while it will be detected second under low EOF conditions and detection at the anode because the weaker complexed enantiomer possesses a relatively higher mobility toward the anode. Using a negatively charged complexation agent (possessing an electrophoretic anodic mobility) for the enantioseparation of a cationic compound, the weaker complexed enantiomer will be detected first at the cathodic end of the capillary at a low selector concentration (Fig. 1d). At a high concentration the carrier ability of the charged selector can be exploited detecting the analyte at the anode. Thus, upon reversal of the polarity of the applied voltage the stronger complexed analyte will be transported faster to the detector at the anodic end of the capillary (Fig. 1e). Due to

their electrophoretic mobility charged selectors can also be employed for the enantioseparation of neutral analytes as outlined for the combination of an uncharged analyte and a negatively charged selector in Fig. 1f, g. At low selector concentrations the weaker complexed enantiomer is detected first at the cathode in the presence of a sufficiently high EOF (Fig. 1f). In contrast, under reversed polarity of the applied voltage exploiting the carrier ability of the selector present at high concentrations in the background electrolyte, the stronger bound enantiomer will be detected first at the anodic end of the capillary (Fig. 1g).

It is obvious from these few examples that a designed migration order of the enantiomers can be achieved for a given compound by selection of the appropriate selector and conditions. Because each selector has its own enantioselective recognition toward analytes the migration order will be affected by the selector first. For example, it has been shown that the enantiomer migration order can depend on the size of the CD cavity so that different enantiomer migration orders were observed for α-, β-, and γ-CDs. Moreover, different derivatives of a CD may also display opposite migration order. Reversal of the enantiomer migration order may also be achieved by the selection of the appropriate experimental conditions. It is obvious that the situations schematically shown in Fig. 1b–e as well as Fig. 1f, g will lead to a different migration order of the enantiomers if the compound can be analyzed under the specific experimental conditions. Furthermore, if an amphoteric compound can be analyzed as protonated positively charged or as negatively charged species the migration order of the enantiomers may change as well provided that the chiral recognition of the selector toward the enantiomers does not change as a function of the charge of the analyte (Fig. 1a, c). For a more comprehensive discussion of the enantiomer migration order in CE, see also [15–17].

1.3 Chiral Selectors

A large number of structurally diverse chiral compounds have been investigated as chiral selectors in CE including cyclodextrins (CDs), cyclofructans, polysaccharides, macrocyclic glycopeptide antibiotics, proteins, crown ethers, aptamers, chiral ligand exchange, chiral ionic liquids, as well as chiral surfactants derived from steroids, amino acids, tartaric acid, or glycosides [7, 8, 18]. Depending on the chiral selector and the analyte enantiomers, formation of the diastereomeric selector-enantiomer complexes is driven by several types of interactions including ionic interactions, ion–dipole or dipole–dipole interactions, hydrogen bonds, van der Waals interactions, or π-π interactions. For a summary of the current understanding of the structures of the analyte–selector complexes see [19–21].

CDs are by far the most often applied chiral selectors owing to their commercial availability, UV transparency, and relatively low prices. CDs are cyclic oligosaccharides consisting of α(1, 4)-linked D-glucose units obtained by the digestion of starch by certain

Bacillus strains. The most important industrially produced CDs differ in the number of glucose units. α-CD contains 6 glucose molecules, β-CD 7 glucose molecules, and γ-CD 8 molecules (Table 1). CDs are shaped like a hollow torus with a lipophilic cavity and a hydrophilic outside. The narrow rim contains the primary 6-hydroxyl groups of the glucose molecules while the wider ring is formed by the secondary 2- and 3-hydroxyl groups. The hydroxyl groups can be derivatized resulting in a large variety of CD derivatives with uncharged or charged substituents. Complex formation is believed to occur via the inclusion of lipophilic moieties of the analytes in the hydrophobic cavity with secondary interactions including hydrogen bonding or dipole–dipole interactions with the hydroxyl groups or polar substituents. In the case of charged CDs, ionic interactions will contribute to the binding. CDs can be employed in aqueous as well as nonaqueous background electrolytes. Besides EKC, CDs have been used as chiral selectors in MEKC and MEEKC. The application of CDs in CE has been summarized [18, 22–27].

The most prominent representatives of the group of macrocyclic antibiotics also called macrocyclic glycopeptides are vancomycin, ristocetin A, teicoplanin, and teicoplanin aglycone (Fig. 2). The common structural feature of this class of compounds is a heptapeptide composed as interconnected macrocycles each containing two aromatic rings. Vancomycin contains three macrocycles, teicoplanin and ristocetin A are composed of four. The macrocycle forms a three-dimensional, C-shaped basket-like structure with the carbohydrate moieties positioned at the surface. Due to the presence of aromatic rings, polar groups as well as ionizable groups such as a carboxylic acid group or amino groups, a large number of interactions between analyte molecules and the glycopeptide antibiotics are possible including hydrogen bonds, π–π, dipole–dipole, and ionic interactions depending on the experimental conditions. Due to the stability in aqueous solutions, macrocyclic antibiotics are typically used in buffers within the pH range 4–8. Protonation at pH values below the pI of the glycopeptides may result in wall adsorption and, consequently, an irreproducible EOF. Moreover, the UV absorbance of the selectors has to be considered. For review articles on antibiotics as chiral selectors, see [28, 29].

The chiral crown ether (+)-(18-crown-6)-2,3,11,12-tetracarboxylic acid (Fig. 3) has been applied to the enantioseparation of primary amines. Complex formation occurs via hydrogen bonds between the protonated amino group and oxygen atoms of the crown ether. Consequently, enantioseparations are performed in acidic buffers as summarized in [30, 31]. Chiral ligand exchange is based on the reversible coordination of a chiral analyte into the sphere of a metal ion, which is complexed with a chelating selector, resulting in an analyte–metal ion–selector complex. Most frequently, amino acids derivatives including L-proline,

Table 1
Examples of commercially available CDs

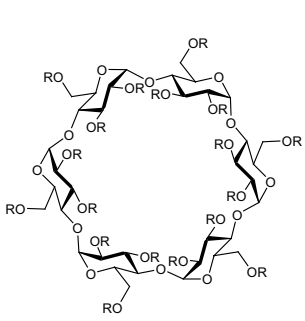
α-CD

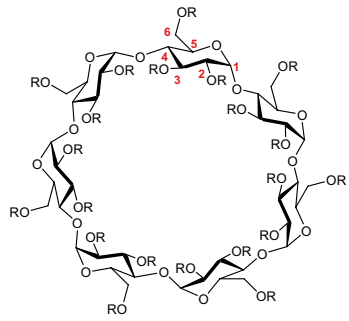
β-CD

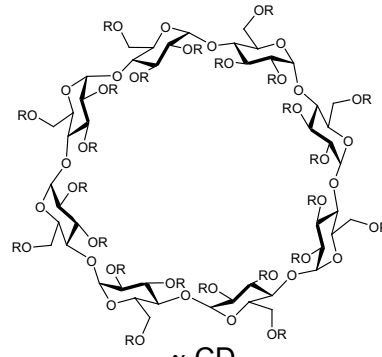
γ-CD

Derivative	Substituents
Native CDs	
α-CD	H
β-CD	H
γ-CD	H
Neutral CDs	
Methyl-α-CD	CH_3, randomly substituted
Methyl-β-CD	CH_3, randomly substituted
Heptakis-2,6-dimethyl-β-CD	CH_3 in positions 2 and 6
Heptakis-2,3,6-trimethyl-β-CD	CH_3 in positions 2, 3, and 6
Hydroxypropyl-α-CD	CH_2-CH_2-CH_2-OH, randomly substituted
Hydroxypropyl-β-CD	CH_2-CH_2-CH_2-OH, randomly substituted
Hydroxypropyl-γ-CD	CH_2-CH_2-CH_2-OH, randomly substituted
Negatively charged CDs	
Carboxymethyl-β-CD	CH_2-COONa, randomly substituted
Sulfated α-CD	SO_3Na, randomly substituted
Sulfated β-CD	SO_3Na, randomly substituted
Sulfated γ-CD	SO_3Na, randomly substituted
Sulfobutyl-β-CD	CH_2-CH_2-CH_2-CH_2-SO_3Na, randomly substituted
Heptakis-6-sulfo-β-CD	SO_3Na in position 6
Heptakis-(2,3-diacetyl-6-sulfo)-β-CD	CH_3CO in positions 2 and 3, SO_3Na in position 6
Heptakis-(2,3-dimethyl-6-sulfo)-β-CD	CH_3 in positions 2 and 3, SO_3Na in position 6

(continued)

Table 1
(continued)

Derivative	Substituents
Positively charged CDs	
2-Hydroxy-3-trimethylammoniopropyl-β-CD	CH_2-CH(OH)-CH_2-N(CH_3)$_3$Cl, randomly substituted
6-Monodeoxy-6-monoamino-β-CD	NH_2 instead of one 6-OH group

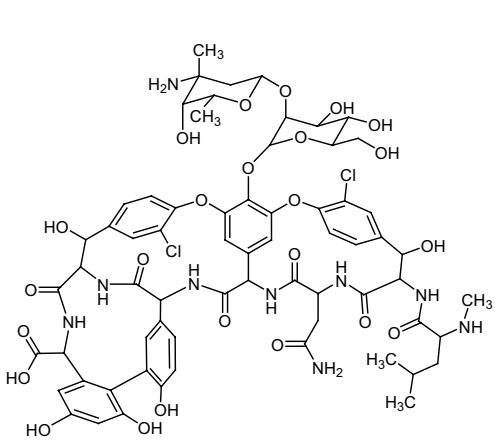

Vancomycin

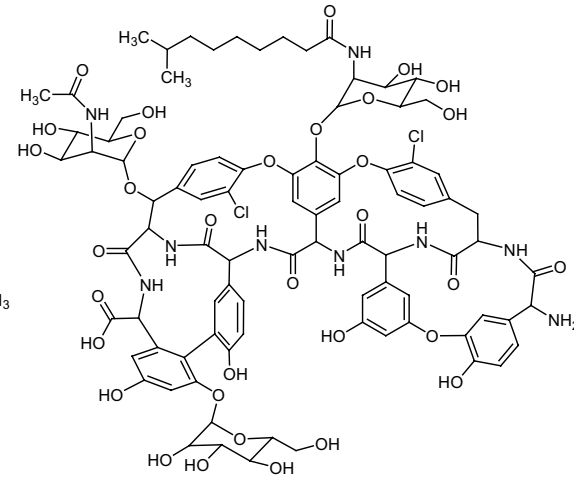

Teicoplanin $A_{2\text{-}2}$

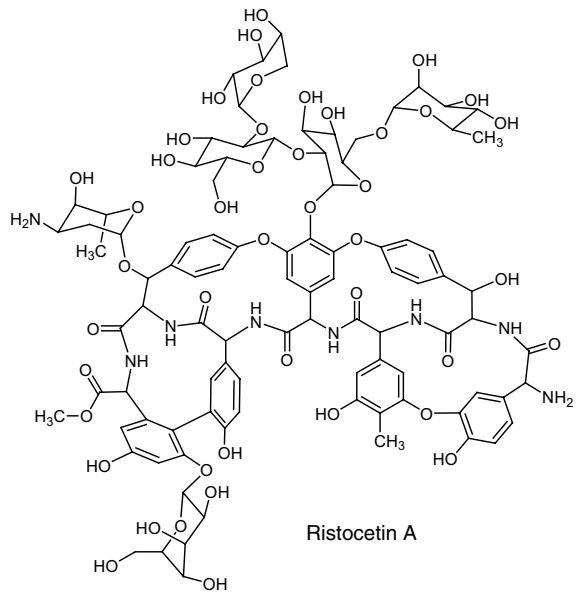

Ristocetin A

Fig. 2 Structures of the glycopeptide antibiotics vancomycin, teicoplanin $A_{2\text{-}2}$, and ristocetin A

L-hydroxyproline, L-proline amide, L-phenylalanine amide, or L-histidine have been employed as chelating agents but polyhydroxy acids such as D-quinic acid, D-gluconic acid, or L-threonic acid were also used. Typical metal ions include divalent metal ions such as Cu^{2+}, Zn^{2+}, or Ni^{2+}. Ligand exchange is restricted to analytes with 2 or 3 electron donating groups so that the method can be applied particularly to the enantioseparation of amino acids, α-hydroxy acids, or amino alcohols. The principles of chiral ligand exchange, selectors, and applications have been reviewed [32–34]. Chiral micelles are formed from monomeric chiral surfactants in aqueous solution at concentrations above the critical micelle concentration. Furthermore, polymeric micelles (also called molecular micelles) have been developed, which are obtained by polymerization of functionalized surfactants via the hydrophobic tails. The polymeric micelles overcome limitations caused by the dynamic nature of conventional micelles and instability upon addition of higher concentrations of organic solvents. Chiral surfactants with a large structural variety are available including bile acid derivatives or surfactants derived from amino acids or carbohydrates (Fig. 3). Molecular micelles are based on surfactants derived from amino acids or dipeptides. Reviews on the application of chiral micelles in enantioseparations can be found, for example, in [35, 36]. For a discussion of further chiral selectors applied in CE see [7, 8, 18].

1.4 CE Enantioseparation Modes

CE has been applied to enantioseparations in chemical, pharmaceutical, forensic, food, or environmental analysis as well as bioanalysis. The EKC mode is the most often applied technique for CE referring to a system with a chiral selector in a background electrolyte without the presence of a further pseudostationary phase such as micelles or a microemulsion. EKC is often (incorrectly) also referred to as chiral CE. The selector may be charged, thus, exhibiting an

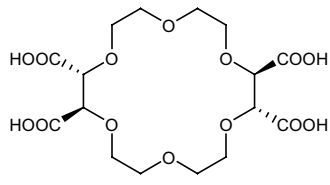

(+)-(18-crown-6)-2,3,11,12-tetracarboxylic

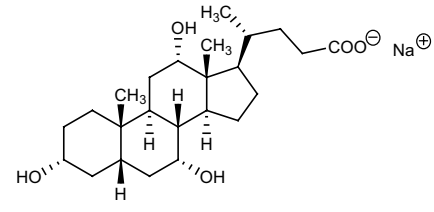

sodium cholate

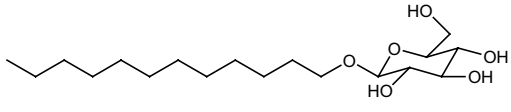

dodecyl-β-glucopyranoside

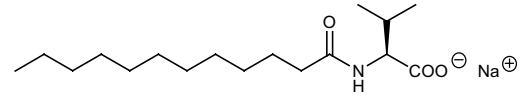

sodium *N*-dodecanoyl-L-valinate

Fig. 3 Structures of the chiral crown ether, (+)-(18-crown-6)-2,3,11,12-tetracarboxylic acid, and chiral surfactants

electrophoretic self-mobility allowing the enantioseparation of neutral analytes or uncharged so that it is transported with the EOF. Some separation scenarios are shown in Fig. 1. As discussed earlier, enantioseparations in EKC are based on different affinities of the enantiomers toward the chiral selector and/or differences in the mobilities of the diastereomeric analyte–selector complexes. Reviews on EKC enantioseparations can be found, for example, in [1–6]. Apart from aqueous buffers, nonaqueous background electrolytes may be applied in EKC enantioseparations [37, 38].

The fact that the chiral selector is dissolved in the background electrolyte in EKC is often considered an advantage in terms of the ease of changing the experimental conditions including the type of the chiral selector. However, this may become a disadvantage when CE is hyphenated to a mass spectrometer because the nonvolatile selectors contaminate the ion source when entering the mass spectrometer. Two strategies have been developed in order to avoid the entrance of significant amounts of the selector into the ion source. The first approach, the counter migration technique, exploits the self-mobility of a charged chiral selector migrating in the opposite direction of the mass spectrometer. Thus, the capillary is filled with the background electrolyte containing the chiral selector. Upon application of the separation voltage the analytes migrate toward the mass spectrometer while the selector migrates in the opposite direction. The second approach is the partial filling technique. In this case, only a part of the capillary is filled with the background electrolyte containing the selector while the remaining part contains a selector-free electrolyte. The experimental conditions have to be adjusted in such a way that the analytes migrating through the zone containing the chiral selector exhibit a higher velocity toward the mass spectrometer compared to the selector so that the analytes reach the mass spectrometer before the selector can enter the ion source. CE–MS enantioseparations have been summarized [39–41].

MEKC enantioseparations can be carried out by two basic approaches. The first mode employs a chiral surfactant used in concentrations above the critical micelle concentration. These surfactants comprise bile salts or charged or neutral compounds derived from glucopyranosides or N-acylamino acids surfactants [36]. Mixed micelles composed of chiral and achiral surfactants have also been used. Alternatively, polymeric micelles can be used [35]. In the second approach achiral micelles are combined with a chiral selector. A frequently employed combination is the use of SDS as surfactant with CDs. Also termed CD-modified MEKC, this system is based on several equilibria, i.e., the partitioning of the analyte between the (achiral) micelles and the aqueous phase as well as the stereoselective complexation of the enantiomers by the selector. Furthermore, distribution of the CD–analyte complexes into the micelles has to be considered as well as the binding of the enantiomers by CDs associated with the micelles, which may differ

from the complexation between CD and analyte in the aqueous phase. Both modes, MEKC using chiral micelles and CD-modified MEKC, have been successfully applied to the enantioseparations of many basic, acidic, or neutral compounds [36].

MEEKC can be regarded as analogous to MEKC using microemulsion droplets as pseudostationary phase as compared to micelles in MEKC. The microemulsion is formed by a water immiscible organic liquid stabilized by a surfactant and a cosurfactant. Thus, the general approaches for MEEKC enantioseparations resemble the approaches in MEKC. The first mode employs chiral components forming the microemulsion such as a chiral surfactant, chiral alkanols as cosurfactants, or chiral oil phases. The mechanism of the enantioseparations using a chiral oil droplet is based on the partitioning equilibria of the analyte enantiomers between the aqueous phase and the chiral oil phase. The second approach uses an achiral microemulsion in combination with a chiral selector such as a CD. Typically, the micelles are negatively charged due to the use of sodium dodecyl sulfate (SDS) as surfactant in combination with neutral or negatively charged CDs. In these systems two equilibria have to be considered, the partitioning of the analyte between the aqueous phase and the lipid phase as well as the stereospecific complexation of the enantiomers by the CDs. The partitioning of the diastereomeric enantiomer–CD complexes may, in principle, also take place.

For recent compilations of MEEKC enantioseparations see, for example [42, 43].

1.5 Method Development

Method development starts with the selection of the appropriate chiral selector and background electrolyte. Although some selectors are more or less limited to a certain group of analytes, for example, chiral crown ethers for enantioseparations of primary amines, there is no general rule for the use of certain selectors for a given analyte. Consequently, the choice of a certain selector currently depends on the experience and/or preferences of the analyst. Due to the large variety of derivatives as well as the commercial availability CDs are the most often applied chiral selectors in CE. Many analysts prefer charged selectors as they may be applied for charged and uncharged compounds. At low pH, basic analytes are protonated and migrate to the cathode while the negatively charged CDs migrate to the anode. Neutral compounds interacting with the negatively charged CDs are transported to the anode and can be detected upon reversing the polarity of the applied voltage. Most acidic analytes are protonated at low pH and behave as neutral compounds. General strategies for screening approaches utilizing CDs have been published in order to find generalized starting conditions without excessive testing of a large number of CDs, see for example [44, 45]. For basic analytes negatively charged CDs are often preferred due to the high success rate. Alternatively, MEKC or MEEKC may

be considered for charged as well as uncharged analytes. Following selection of the initial conditions, the concentration of the chiral selector, the pH and concentration of the background electrolyte, buffer additives, separation voltage, capillary temperature, etc., are further optimized in order to achieve the desired chiral resolution. In MEKC and MEEKC type and concentration of the surfactant and composition of the microemulsion, respectively, are optimized. In order to manipulate the EOF or to avoid analyte adsorption to the capillary wall, dynamic or permanent coating of the capillary wall may be considered [46, 47].

The aim of any method development of an analytical separation is to obtain a robust assay meeting the requirements of the intended use. Apart from the characteristics of the analytes, experimental factors such as type and concentration of the chiral selector, type, pH, and concentration of the background electrolyte as well as additives such as organic solvents or surfactants, the composition of a microemulsion, applied voltage, capillary temperature, etc., affect enantioseparations in CE. Optimizing one variable at a time while keeping all other variables constant, i.e., the univariate approach, results in a large number of experiments. Typically, this approach only leads to a local optimum of the conditions. Therefore, experimental design (chemometrics) methods may be used in order to find the global optimal conditions of the experimental variables [48, 49]. In such an approach, the variables which significantly affect a separation are first identified and subsequently optimized in a designed way. Testing of the robustness of the analytical method can also be addressed by experimental design.

2 Materials

2.1 CE Apparatus and Equipment

1. A commercial CE instrument with a high voltage source (up to 30 kV) and a photodiode array detector. A P/ACE MDQ CE System (Beckman Coulter, Fullerton, CA, USA) or a 7100 CE System (Agilent Technologies, Santa Clara, CA, USA) is suitable (*see* **Note 1**).
2. Uncoated fused-silica capillaries (e.g., from Polymicro Technologies, Phoenix, AZ, USA) with an internal diameter of 50 μm, an effective length of 30 cm, and a total length of 40.2 cm (*see* **Note 2**). Install the capillary into the capillary cartridge according to the manufacturer instructions (*see* **Note 3**).
3. A commercial pH meter for pH adjustment of the background electrolytes.
4. An ultrasonic bath for sample and CD dissolution as well as for degassing of the solutions.
5. Syringe filters containing polyester filter membranes with a pore size of 0.20 μm (e.g., from Macherey-Nagel, Düren, Germany). The use of 0.45 μm filters is also possible.

6. A Milli-Q water purification system for preparation of ultrapure water (e.g., a Milli-Q Direct 8 system, Millipore, Billerica, MA, USA).

2.2 Chemicals

1. β-CD (Sigma-Aldrich, St. Louis, MO, USA; or Cyclolab, Budapest, Hungary).
2. Sulfated β-CD, sodium salt (Sigma-Aldrich, St. Louis, MO, USA; or Cyclolab, Budapest, Hungary) (*see* **Notes 4** and **5**).
3. (*R*)-(−)-1,1′-binaphthyl-2,2′-diyl hydrogenphosphate and (*S*)-(+)-1,1′-binaphthyl-2,2′-diyl hydrogenphosphate (Sigma-Aldrich, St. Louis, MO, USA).
4. (1*S*,2*R*)-(+)-ephedrine hydrochloride and (1*R*,2*S*)-(−)-ephedrine hydrochloride (Sigma-Aldrich, St. Louis, MO, USA).

2.3 Background Electrolytes (See Notes 6 and 7)

1. BGE 1: 50 mM phosphate buffer, pH 3.0, 2.5 mg/mL of β-CD.

   Dissolve 340 μL of 85% H_3PO_4 in approx. 50 mL of Milli-Q water and adjust pH to 3.0 using 1 M NaOH. Adjust the volume of the solution to 100.0 mL with Milli-Q water. Dissolve 25 mg of β-CD in approx. 5 mL of the buffer (*see* **Note 8**) under sonication (5–10 min) and adjust the volume to 10.0 mL with buffer.
2. BGE 2: 50 mM phosphate buffer, pH 2.5, 2 mg/mL of sulfated β-CD.

   Dissolve 340 μL of 85% H_3PO_4 in approx. 50 mL of Milli-Q water and adjust pH to 2.5 using 1 M NaOH. Adjust the volume of the solution to 100.0 mL with Milli-Q water. Dissolve 20 mg of sulfated β-CD sodium salt (*see* **Notes 4** and **5**) in approx. 5 mL of the buffer and adjust the volume to 10.0 mL with buffer.
3. BGE 3: 50 mM phosphate buffer, pH 2.5, 30 mg/mL of sulfated β-CD.

   Dissolve 340 μL of 85% H_3PO_4 in approx. 50 mL of Milli-Q water and adjust pH to 2.5 using 1 M NaOH. Adjust the volume of the solution to 100.0 mL with Milli-Q water. Dissolve 300 mg of sulfated β-CD sodium salt (*see* **Notes 4** and **5**) in approx. 5 mL of the buffer and adjust the volume to 10.0 mL with buffer.

   Filter all buffer solutions through a 0.20 μm polyester membrane syringe filter into the buffer vials and degas by sonication for 5 min prior to use.

2.4 Sample Solutions

1. 1,1′-Binaphthyl-2,2′-diyl hydrogenphosphate solution (*see* **Note 9**):

   Prepare stock solutions (1 mg/mL) of each enantiomer of 1,1′-binaphthyl-2,2′-diyl hydrogenphosphate by dissolving 10 mg of each compound in approx. 5 mL of methanol and

adjust the volume to 10.0 mL with methanol. Mix 200 μL of (S)-(+)-1,1′-binaphthyl-2,2′-diyl hydrogenphosphate stock solution with 100 μL of (R)-(−)-1,1′-binaphthyl-2,2′-diyl hydrogenphosphate stock solution and adjust the volume to 10.0 mL with 10% aqueous methanol. Transfer solution to the sample vial.

2. Ephedrine solution (*see* **Note 9**).

   Prepare stock solutions (1 mg/mL) of each enantiomer of ephedrine by dissolving 10 mg of each compound in approx. 5 mL of 10% (v/v) 2-propanol and adjust the volume to 10.0 mL with 10% (v/v) 2-propanol. Mix 2.0 mL of (1*S*,2*R*)-(+)-ephedrine hydrochloride stock solution with 1.0 mL of (1*R*,2*S*)-(−)-ephedrine hydrochloride stock solution and adjust the volume to 10.0 mL with Milli-Q water. Transfer solution to the sample vial.

3 Methods

3.1 Conditioning and Rinsing Procedures for the Fused-Silica Capillary (See Note 10)

Filter all rinsing solutions through a 0.20 μm polyester membrane syringe filter. Rinse the new capillary at a pressure of 138 kPa (20 p.s.i.) subsequently with

3.1.1 Preconditioning of a New Capillary

1. 0.1 M phosphoric acid for 10 min.
2. 1 M sodium hydroxide for 20 min.
3. 0.1 M sodium hydroxide for 20 min.
4. Milli-Q water for 10 min.
5. The appropriate background electrolyte for 10 min.

3.1.2 Conditioning of the Capillary Between Analyses

Rinse subsequently with filtered (0.2 μm) solutions at a pressure of 138 kPa (20 p.s.i.) with

1. 0.1 M phosphoric acid for 2 min.
2. Milli-Q water for 2 min.
3. The appropriate background electrolyte for 4 min.

3.1.3 Rinsing of the Capillary for Storage

Rinse capillary subsequently at a pressure of 138 kPa (20 p.s.i.) with

1. 0.1 M phosphoric acid for 10 min.
2. 0.1 M sodium hydroxide for 10 min.
3. Milli-Q water for 10 min.

For short term (overnight) storage place capillary ends into vials containing Milli-Q water. For long-term storage dry capillary by purging with air at a pressure of 34.5 kPa (5 p.s.i.) for 5 min.

After the overnight storage of the capillary rinse it next day with **steps 1–3** as described in Subheading 3.1.3. Thereafter, rinse it at 138 kPa (20 p.s.i.) for 10 min with the appropriate background electrolyte. After the long-term storage condition the capillary as described in Subheading 3.1.1.

3.2 CE Analysis

After conditioning of the capillary (*see* **Note 10**), select the appropriate background electrolyte and fill into buffer vials (*see* **Note 11**). Set data sampling rate to 4 Hz and autozero time of the detector to 1.0 min. Set the temperature of the capillary to 20 °C. Place samples in sample vials (*see* **Note 12**). Carry out CE measurements at the specified parameters including UV detection wavelength and applied high voltage. Introduce sample solutions hydrodynamically at a pressure of 3.4 kPa (0.5 p.s.i.) for 6 s (*see* **Notes 13** and **14**).

Example 1

The example illustrates the separation of negatively charged analytes using a neutral CD in the absence of a significant EOF under reversed polarity of the applied voltage as illustrated schematically in Fig. 1c.

Use BGE 1 as run buffer and 1,1′-binaphthyl-2,2′-diyl hydrogenphosphate as analyte. Introduce the sample at the cathodic end of the capillary, carry out the detection at the anodic end.

Applied voltage: –30 kV (ramp time 0.17 min).

Detection wavelength: 210 nm (bandwidth 10 nm).

Detector reference wavelength: 340 nm (bandwidth 50 nm).

Generated current under the experimental conditions: approx. –50 μA.

A typical electropherogram is shown in Fig. 4. The weaker complexed enantiomer (*R*)-(–)-1,1′-binaphthyl-2,2′-diyl hydrogenphosphate is detected first.

Example 2

The example illustrates the separation of positively charged analytes using a negatively charged CD in the absence of a significant EOF under normal polarity conditions as illustrated schematically in Fig. 1d.

Use BGE 2 as run buffer and ephedrine as analyte. Introduce the sample at the cathodic end of the capillary, carry out the detection at the anodic end.

Applied voltage: +25 kV (ramp time 0.17 min).

Detection wavelength: 210 nm (bandwidth 10 nm).

Detector reference wavelength: 400 nm (bandwidth 10 nm).

Generated current under the experimental conditions: approx. +50 μA.

A typical electropherogram is shown in Fig. 5a. The weaker complexed (1*R*,2*S*)-enantiomer migrates first.

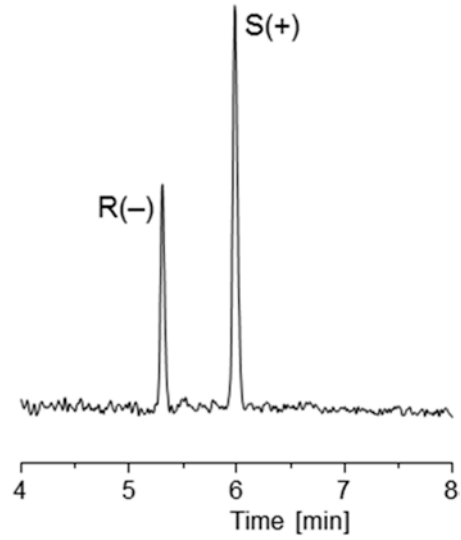

Fig. 4 Enantioseparation of 1,1′-binaphthyl-2,2′-diyl hydrogenphosphate using β-CD as chiral selector at pH 3.0

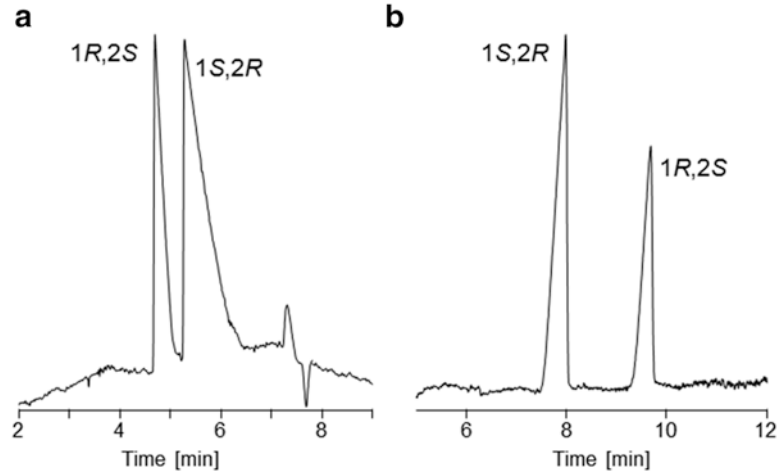

Fig. 5 Enantioseparation of ephedrine using sulfated β-CD as chiral selector at pH 2.5. (**a**) Low selector concentration (2 mg/mL) under normal polarity of the applied voltage and (**b**) exploiting the carrier ability of the selector at high concentrations (30 mg/mL) under reversed polarity of the applied voltage

Example 3

The example illustrates the separation of positively charged analytes using a negatively charged CD in the absence of a significant EOF exploiting the carrier ability of the selector under reversed polarity of the applied voltage as illustrated schematically in Fig. 1e.

Use BGE 3 as run buffer and ephedrine as analyte. Introduce the sample at the cathodic end of the capillary, carry out the detection at the anodic end.

Applied voltage: –20 kV (ramp time 0.17 min.)

Detection wavelength: 210 nm (bandwidth 10 nm).

Detector reference wavelength: 400 nm (bandwidth 10 nm).

Generated current under the experimental conditions: approx. –100 μA.

A typical electropherogram is shown in Fig. 5b. The stronger complexed (1*S*,2*R*)-enantiomer migrates first.

For additional practical examples of CD-mediated enantioseparations in CE see [50].

4 Notes

1. CE instruments from different companies as well as different instruments from the same supplier may yield slightly different results even when using identical experimental conditions. Thus, the variables may require slight changes when transferring a certain analytical method from one instrument to another so that slight adjustment of the parameters of a published method can be necessary.
2. Capillaries from different suppliers may lead to slightly different separation efficiencies. Even capillaries from the same supplier may vary to a certain extent. Thus, the purchase of larger quantities of capillaries is recommended especially if a method is intended for validated routine analysis in a regulated environment. One capillary should be used for only one application.
3. When cutting a capillary, it is important that the cut is straight and the ends are even. Uneven capillary ends will lead to peak tailing due to uneven injection plugs. The capillary ends should be checked under a magnifying glass or a microscope. Moreover, it may be advisable to burn off a few millimeters of the polyimide coating at the capillary ends. This will reduce carryover and give better precision. Burning off the coating is especially important especially when using organic solvents as buffer additives such as acetonitrile that make the polyimide swell. Removing the polyimide from the capillary ends is not advisable for coated capillaries as this will damage the inner coating.
4. Randomly substituted CDs are a mixture of isomers with varying degrees of substitution and substitution patterns (i.e., the number and positions of the substituents are different). Therefore, CDs from different sources and even different batches from the same supplier may vary in this respect which may lead to varying separation selectivity or resolution depending on the batch of selector used. In most cases the separation can be optimized by variation

of the concentration of the chiral selector. Chemically defined single isomer CDs are also available such as heptakis-6-sulfo-β-CD or heptakis-(2,3-dimethyl-6-sulfo)-β-CD.

5. While single isomer CDs may be preferable from the standpoint of reproducibility of a method, superior resolution of the enantiomers may also be observed using randomly substituted CDs as compared to single isomer chiral selectors. However, it cannot be predicted if a single isomer CD or a randomly substituted CD will result in superior resolution for a given racemate.
6. Preparation of buffers according to different procedures results in buffers differing in ionic strength which may affect the separation selectivity. For example, a 50 mM phosphate buffer, pH 2.5, may be prepared (1) by dissolving the appropriate amount of 85 % phosphoric acid in a certain amount of water and adjusting to pH 2.5 by addition of sodium hydroxide solution before making up the final volume by addition of water, (2) by adjusting 50 mM phosphoric acid to pH 2.5 by addition of a sodium hydroxide solution, and (3) by adjusting 50 mM sodium dihydrogen phosphate (monobasic sodium phosphate, NaH_2PO_4) to pH 2.5 by addition of diluted phosphoric acid. In the first case the buffer concentration is 50 mM with respect to phosphate, in case (2) the molarity of phosphate is below 50 mM and in case (3) phosphate molarity is higher than 50 mM. The deviation from the desired molarity will depend on the concentration of the sodium hydroxide solution and phosphoric acid used for pH adjustment. Phosphate buffers at higher pH (i.e., pH 6.2–8.2) may also be prepared by mixing 50 mM sodium dihydrogen phosphate (monobasic sodium phosphate, NaH_2PO_4) and 50 mM disodium hydrogen phosphate (dibasic sodium phosphate, Na_2HPO_4) in appropriate proportions to obtain the desired pH. Consequently, buffers differing in the ionic strength are obtained by the various procedures. This affects the magnitude of the EOF, the electric current, as well as Joule heating which, in turn, affect a given separation. Too high Joule heating may be derived from an Ohm plot.
   In addition, when using different salts, e.g., the potassium or lithium phosphate salts, or different bases, e.g., potassium hydroxide or lithium hydroxide, for the preparation, the resulting buffers differ in the counterions which may also affect a separation. Thus, careful characterization of the buffer is required for reproducible results. In addition, buffers can only be stored for a limited period of time even at low temperatures.
7. Due to the temperature dependence of dissociation equilibria, buffer pH should be adjusted at the temperature that is used during the electrophoretic run. Specifically, the change of the pK_a per Kelvin (or °C) of organic zwitterionic buffers is significant.

8. Due to the limited aqueous solubility of β-CD (approx. 18 mg/mL (16 mM) in water), urea at a concentration of 1–2 M is typically added when higher β-CD concentrations are required for an enantioseparation. It has been shown that urea can also affect separation selectivity.
9. Nonracemic mixtures can be used in order to determine the enantiomer migration order in a single experiment. Preparation of such solutions is only possible if at least one of the enantiomers is available in the pure form.
10. Conditioning of the capillary is important in order to obtain reproducible conditions of the inner wall of the capillary. Therefore, careful preconditioning of the capillary is required. Moreover, it is necessary to include all rinsing steps into validation procedures when developing CE procedures for quality control.
11. Different vials containing the background electrolyte should be used for rinsing of the capillary and for the analytical separation. Buffer levels should be the same in the analysis vials in order to avoid a hydrodynamic flow due to differences in hydrostatic pressure between the vials. The background electrolyte should be replaced after a number of injections (typically between 2 and 10 injections) because of buffer depletion. The frequency of buffer replacement depends on the buffer capacity of the background electrolyte and the volume of the vial. If a background electrolyte contains an organic solvent as modifier, evaporation of the solvent may also lead to irreproducible migration times.
12. When using microvials, air bubbles at the bottom of the vial should be avoided. During injection the outlet end of the capillary should be placed in a vial with a constant solvent level which is not the waste vial. A water (or buffer) plug may be injected after sample injection to prevent sample loss by thermal expansion when high voltage is switched on.
13. When applying hydrodynamic injection, the actually injected amount of the sample may vary depending on the temperature or the viscosity of the solution. Thus, adjustment of the injection time and/or pressure may be required. In the present examples the samples were injected at ambient temperature. Typical injection plug length in CE corresponds to approx. to 1–5 % of capillary length.
14. After injecting the sample, the end of the capillary should be dipped into a vial containing buffer solution or water in order to reduce carryover of the sample into the background electrolyte vial used for the separation.

References

1. Chankvetadze B (2007) Enantioseparations by using capillary electrophoretic techniques. The story of 20 and a few more years. J Chromatogr A 1168:45–70
2. Gübitz G, Schmid MG (2008) Chiral separations by capillary electrophoresis. J Chromatogr A 1204:140–156
3. Preinerstorfer B, Lämmerhofer M, Lindner W (2009) Advances in enantioselective separations using electromigration capillary techniques. Electrophoresis 30:100–132
4. Scriba GKE (2011) Fundamental aspects of chiral electromigration techniques and application in pharmaceutical and biomedical analysis. J Pharm Biomed Anal 55:688–701
5. Sanchez-Hernandez L, Castro-Puyana M, Marina ML et al (2012) Recent approaches in sensitive enantioseparations by CE. Electrophoresis 33:228–242
6. Jac P, Scriba GKE (2013) Recent advances in electrodriven enantioseparations. J Sep Sci 36:52–74
7. Chankvetadze B (1997) Capillary electrophoresis in chiral analysis. Wiley, Chichester
8. Van Eeekhaut A, Michotte Y (2009) Chiral separations by capillary electrophoresis. CRC Press, Boca Raton
9. Wren SAC, Rowe RC (1992) Theoretical aspects of chiral separation in capillary electrophoresis. I. Initial evaluation of a model. J Chromatogr A 603:235–241
10. Chankvetadze B, Lindner W, Scriba GKE (2004) Enantiomer separations in capillary electrophoresis in the case of equal binding constants of the enantiomer with a chiral selector: commentary on the feasibility of the concept. Anal Chem 76:4256–4260
11. Williams BA, Vigh G (1977) A dry look at CHARM (charged resolving agent migration) model of enantiomer separations by capillary electrophoresis. J Chromatogr A 777:295–309
12. Rizzi A (2001) Fundamental aspects of chiral separations by capillary electrophoresis. Electrophoresis 22:3079–3106
13. Dubsky P, Svobodova J, Gas B (2008) Model of CE enantioseparation systems with a mixture of chiral selectors. Part I. Theory of migration and interconversion. J Chromatogr B 875:30–34
14. Dubsky P, Svobodova J, Tesarova E et al (2010) Enhanced selectivity in CZE multi chiral selector enantioseparation systems: proposed separation mechanism. Electrophoresis 31:1435–1441
15. Scriba GKE (2013) Differentiation of enantiomers by capillary electrophoresis. Top Curr Chem 340:209–276
16. Chankvetadze B, Schulte G, Blaschke G (1997) Nature and design of enantiomer migration order in chiral capillary electrophoresis. Enantiomer 2:157–179
17. Chankvetadze B (2002) Enantiomer migration order in chiral capillary electrophoresis. Electrophoresis 23:4022–4035
18. Tsioupi DA, Stefan-Van Staden RI, Kapnissi-Christodoulou CP (2013) Chiral selectors in CE: recent developments and applications. Electrophoresis 34:178–204
19. Berthod A (2010) chiral recognition in separation methods. Springer, Heidelberg
20. Lämmerhofer M (2010) Chiral recognition by enantioselective liquid chromatography: mechanisms and modern chiral stationary phases. J Chromatogr A 1217:814–856
21. Scriba GKE (2012) Chiral recognition mechanisms in analytical separation sciences. Chromatographia 75:815–838
22. Juvancz Z, Kendrovics RB, Ivanyi R (2008) The role of cyclodextrins in chiral capillary electrophoresis. Electrophoresis 29:1701–1712
23. Fanali S (2009) Chiral separations by CE employing CDs. Electrophoresis 30:S203–S210
24. Chankvetadze B (2009) Separation of enantiomers with charged chiral selectors in CE. Electrophoresis 30:S211–S221
25. Scriba GKE (2008) Cyclodextrins in capillary electrophoresis—recent developments and applications. J Sep Sci 31:1991–2001
26. Cucinotta V, Contino A, Guiffrida A et al (2010) Application of single isomer derivatives of cyclodextrins in capillary electrophoresis for chiral analysis. J Chromatogr A 1217:953–967
27. Escuder-Gilabert L, Martin-Biosca Y, Medina-Hernandez MJ et al (2014) Cyclodextrins in capillary electrophoresis: Recent developments and trends. J Chromatogr A. 1357:2–23
28. Ward TJ, Farris AB (2001) Chiral separations using the macrocyclic antibiotics: a review. J Chromatogr A 906:73–89
29. Prokhorova AF, Shapovalova EN, Shpigun OA (2010) Chiral analysis of pharmaceuticals by capillary electrophoresis using antibiotics as chiral selectors. J Pharm Biomed Anal 53:1170–1179
30. Kuhn R (1999) Enantiomeric separations by capillary electrophoresis using a crown ether as chiral selector. Electrophoresis 20: 2605–2613

31. Elbashir AA, Aboul-Enein HY (2010) Application of crown ethers as buffer additives in capillary electrophoresis. Curr Pharm Anal 6:101–113
32. Schmid MG, Gübitz G (2011) Enantioseparation by chromatographic and electromigration techniques using ligand-exchange as chiral separation principle. Anal Bioanal Chem 400:2305–2316
33. Schmid MG (2012) Chiral metal-ion complexes for enantioseparation by capillary electrophoresis and capillary electrochromatography: a selective review. J Chromatogr A 1267:10–16
34. Zhang H, Qi L, Mao L et al (2012) Chiral separation using capillary electromigration techniques based on ligand exchange principle. J Sep Sci 35:1236–1248
35. Yarabe HH, Billot E, Warner IM (2000) Enantiomeric separations by use of polymeric surfactant electrokinetic chromatography. J Chromatogr A 875:179–206
36. Dey J, Ghosh A (2010) Chiral separations by micellar electrokinetic chromatography. In: Van Eeckhaut A, Michotte Y (eds) Chiral separations by capillary electrophoresis. CRC Press, Boca Raton, FL, USA, pp 195–234
37. Lämmerhofer M (2005) Chiral separations by capillary electromigration techniques in nonaqueous media. I. Enantioselective nonaqueous capillary electrophoresis. J Chromatogr A 1068:3–30
38. Hedeland Y, Pettersson C (2010) Chiral separations in nonaqueous media. In: Van Eeckhaut A, Michotte Y (eds) Chiral separations by capillary electrophoresis. CRC Press, Boca Raton, FL, USA, pp 271–312
39. Simo C, Garcia-Canas V, Cifuentes A (2010) Chiral CE-MS. Electrophoresis 31:1442–1456
40. Rudaz S, Veuthey J-L, Schappler J (2010) Chiral CE-MS. In: Van Eeckhaut A, Michotte Y (eds) Chiral separations by capillary electrophoresis. CRC Press, Boca Raton, FL, USA, pp 363–392
41. Somsen GW, Mol R, de Jong GJ (2010) On-line coupling of electrokinetic chromatography and mass spectrometry. J Chromatogr A 1217:3978–3991
42. Kahle KA, Foley JP (2010) Chiral microemulsion electrokinetic chromatography. In: Van Eeckhaut A, Michotte Y (eds) Chiral separations by capillary electrophoresis. CRC Press, Boca Raton, FL, USA, pp 235–269
43. Ryan R, Altria K, McEvoy E et al (2013) A review of developments in the methodology and application of microemulsion electrokinetic chromatography. Electrophoresis 34:159–177
44. Evans CE, Stalcup AM (2003) Comprehensive strategy for chiral separations using sulfated cyclodextrins in capillary electrophoresis. Chirality 15:709–723
45. Jimidar IM, van Ael W, van Nyen P et al (2004) A screening strategy for the development of enantiomeric separation method in capillary electrophoresis. Electrophoresis 25:2772–2785
46. Horvath J, Dolnik V (2001) Polymer wall coatings for capillary electrophoresis. Electrophoresis 22:644–655
47. Huhn C, Ramautar R, Wuhrer A et al (2010) Relevance and use of capillary coatings in capillary electrophoresis-mass spectrometry. Anal Bioanal Chem 396:297–314
48. Hanrahan G, Gomez FA (eds) (2010) Chemometric methods in capillary electrophoresis. Wiley, Hoboken, NJ
49. Orlandini S, Gotti R, Furlanetto S (2014) Multivariate optimization of capillary electrophoresis methods: a critical review. J Pharm Biomed Anal 87:290–307
50. Scriba GKE, Jac P (2013) Enantioseparations by capillary electrophoresis using cyclodextrins as chiral selectors. In: Scriba GKE (ed) Chiral separations: methods and protocols, methods in molecular biology, vol 970. Humana Press, New York, pp 271–287

Chapter 16

Capillary Electrophoresis of Mono- and Oligosaccharides

Mila Toppazzini, Anna Coslovi, Marco Rossi, Anna Flamigni, Edi Baiutti, and Cristiana Campa

Abstract

This chapter reports an overview of the recent advances in the analysis of mono- and oligosaccharides by capillary electrophoresis (CE); furthermore, relevant reviews and research articles recently published in the field are tabulated. Additionally, pretreatments and procedures applied to uncharged and acidic carbohydrates (i.e., monosaccharides and lower oligosaccharides carrying carboxylate, sulfate, or phosphate groups) are described.

Representative examples of such procedures are reported in detail, upon describing robust methodologies for the study of (1) neutral oligosaccharides derivatized by reductive amination and by formation of glycosylamines; (2) sialic acid derivatized with 2-aminoacridone, released from human serum immunoglobulin G; (3) anomeric couples of neutral glycosides separated using borate-based buffers; (4) unsaturated, underivatized oligosaccharides from lyase-treated alginate.

Key words Capillary electrophoresis, Neutral sugars, Glycosides, Monosaccharides, Oligosaccharides, Alditols, Reductive amination, Glycosylamines, Sugar acids, Sugar phosphates, Carboxylated sugars, Sulfated sugars, Glycosaminoglycans oligosaccharides, Uronic acids, Sialic acids

1 Introduction

Carbohydrates are the most abundant organic compounds in nature. According to the published IUPAC Recommendations [1], the term 'carbohydrate' includes monosaccharides, oligosaccharides, and polysaccharides, as well as substances derived from monosaccharides by reduction of the carbonyl group (alditols), by oxidation of one or more terminal groups to carboxylic acids, or by the replacement of one or more hydroxyl group(s) by a hydrogen atom, an amino group, a thiol group, or similar heteroatomic groups. Carbohydrates can also be linked to noncarbohydrate natural products (such as proteins or lipids) giving rise to the so-called glycoconjugates. The term 'sugar' is frequently applied to monosaccharides and lower oligosaccharides. This

Philippe Schmitt-Kopplin (ed.), *Capillary Electrophoresis: Methods and Protocols*, Methods in Molecular Biology, vol. 1483,
DOI 10.1007/978-1-4939-6403-1_16,

chapter will focus on the analysis of neutral and acidic sugars by capillary electrophoresis (CE), with special attention to mono-, oligo-saccharides, and glycosides.

Characterization of carbohydrates is a fundamental milestone for a full understanding of their numerous functions: besides their structural relevance in plants and invertebrates, they play a key role in molecular recognition events, and their structure elucidation has a high potential in the biomedical and pharmaceutical fields for the design of new and specific diagnostic and therapeutic tools. In particular, the biological relevance of sugar acids is increasingly being recognized [2–11]. Acidic sugars are monosaccharides and lower oligosaccharides carrying carboxylate, sulfate, or phosphate groups. For example, sialic acids are involved in cell–cell interactions [2–5]; the activation of antithrombin III depends on a specific sequence of heparin, having a characteristic sulfation pattern [6, 7]; sugar phosphates, are involved in cell signaling pathways [9]; an increase in sialylation is often manifested in tumors [10, 11], like in the case of α2-6-linked sialic acids attached to inner GalNAc-*O*-Ser/Thr units on *O*-glycans; Siaα2-6GalNAcα1-*O*-Ser/Thr (called sialyl-Tn) is currently a target for attempts in cancer immunotherapy [2]. Moreover, short fragments of acidic polysaccharides have great relevance in biotechnology: in alginate, for example, distribution of mannuronic and guluronic acid strongly influence the stability, strength, and porosity of the gels formed in the presence of calcium ions [12–15]; these properties are exploited for cell encapsulation, drug delivery, and tissue engineering.

Analysis of carbohydrates requires the use of highly sensitive and selective techniques, since these compounds often constitute highly complex mixtures, which can have a wide distribution of branching patterns, positions and substitutions of hydroxyl groups, and α- or β-anomericity of the glycosidic linkages: two identical monosaccharides can potentially give rise to eleven disaccharides, while two identical peptides can originate only one dipeptide.

Capillary electrophoresis (CE) [16–20] and chromatographic techniques [21–30] are widely used for separation of complex carbohydrates mixtures, providing complementary advantages, as demonstrated in various comparative studies [31–48].

Capillary electrophoresis (CE) provides several benefits which are partially counterbalanced by some drawbacks with respect to chromatographic techniques. The resolving power of CE is generally higher and analyses take place in a shorter time. It may be claimed that this is also a feature typical of micro-HPLC or UPLC; in CE, however, a less extensive cleanup of samples is required with respect to HPLC, since no column fouling can take place; moreover, postrun washes are much shorter, because not-relevant compounds from the matrix can be simply flushed out. Finally, CE has advantages in the automation of analysis, since it enables the

application of different methods simply replacing the running buffer: this feature allows, for example, the automated analysis of glycan mixtures in various modes [48]. A few milliliters of buffer are necessary to run a separation and no changes of columns are required for different categories of carbohydrates. Moreover, CE gives the possibility to analyze, together to carbohydrates, a wider range of nonsaccharidic compounds eventually present in the matrix [42–44, 49]: Soga and Imaizumi [42], for instance, reported the CE analysis of underivatized sugars, inorganic anions, organic acids, amino acids, nucleotides, in one run. Such versatility can be achieved upon using nonselective detection modes, like indirect UV (or indirect fluorescence) detection, which is successfully carried out without derivatization. Indirect UV detection methodology is based on the displacement of the chromophore (or fluorophore) in the background electrolyte by the analyte molecules [31, 42, 50–54], giving rise to negative peaks with limits of detection (LOD) in the 10^{-6} M range for negatively charged saccharides [44–50, 55–57]. This LOD value is higher by two orders of magnitude for acidic sugars with respect to that achieved for neutral sugars. On the other hand, UV detection sensitivity in on-capillary detection is limited by the small path length [56]. The use of electrochemical detection is advised in such cases, since it is independent of path lengths, allowing typical limits of detection equal to 10^{-8} M without derivatization [40, 58, 59]. Alternatively, the sensitivity drawback can be overcome upon using preconcentration techniques [60, 61] and/or upon suitable derivatization of the saccharidic compounds with chromophores or fluorophores. Commercially available detectors based on laser-induced fluorescence (LIF) allow narrow focusing of excitation light onto capillaries, leading to extremely low detection limits, typically equal to 10^{-11} M [56].

The use of CE for the analysis of acidic and neutral sugars and glycosides has been summarized in several books and reviews [5, 16–24, 31–42, 48, 62–73]. To date, the main applications of CE for mono- and oligosaccharides, glycosides, and alditols found in literature include:

1. CE method developments aimed to improve resolution/sensitivity for neutral [51, 74–100] and acidic sugars (including glyconic, glycaric, uronic, and sialic acids, as well as sulfated and phosphated sugars) [44–55, 57, 101–110];
2. Mono- and oligosaccharide composition in glycoproteins [44, 101, 111–123];
3. Analysis of sialic acids and sialylated oligosaccharides released from glycoconjugates using sialidases or mild acidic hydrolysis with [102, 103, 119, 124, 125] or without derivatization (UV wavelength 195–205 nm) [10, 126–128];
4. Food and beverage analysis [31, 40, 42, 43, 52, 53, 100, 106, 129–136];

5. Biopharmaceutical and clinical applications [46, 47, 137–150];
6. Plant extracts [54, 91, 151–165];
7. Neutral sugars from polysaccharide hydrolysis [76, 83, 99, 166–171] and acidic sugar released from chemical or enzymatic digestion of polysaccharides, like polyuronic acids, xylans, or glycosaminoglycans. This latter characterization is carried out following two main methodologies: hydrolysis of polysaccharides with enzymes called lyases, which give rise to unsaturated products, and subsequent CE analysis of the underivatized sugar acids with direct UV detection [8, 172–184]; other reported detection methodologies include electrospray mass spectrometry [185–188], indirect UV detection [55], or derivatization with a suitable chromophore or fluorophore [32, 35, 168, 184, 189–196].
8. Monitoring of reactions involving carbohydrates [197–202].

A selection of some relevant papers regarding these topics is reported in Table 1, where experimental details as well as specific applications are reported.

1.1 Derivatization of Sugars

Linkage of sugars with charged chromophoric or fluorophoric tags guarantees the lowest detection limits without renouncing to highly selective electrophoretic separations. Sugar derivatization is generally carried out before injection in the capillary and it is always preferred to exploit the reactivity of one only functional group, in order to minimize the presence of by-products. Furthermore, the yield of the reaction should be high and reproducible. The most widely used precolumn derivatization procedure is reductive amination, a one-pot reaction which is applicable both on neutral and on acidic sugars. It uses suitable chromophores or fluorophores carrying a primary amino group capable to react with the carbonyl group of reducing sugars, in the presence of sodium cyanoborohydride. In order to shift the initial equilibrium (Schiff base formation) into the direction of the condensation, at least a fivefold excess of the derivatizing agent is necessary [56].

Derivatization efficiency depends on the nature of the sugars as well as on the reaction conditions [94, 95, 117]. As an example, 2-aminopyridine (2-AP) is not suitable for derivatization of ketoses, while 4-aminobenzonitrile (4-ABN), 4-aminobenzoic acid (4-ABA) and its ethyl ester have been successfully used for the CE analysis of fructose and sorbose [91]; glycoprotein monosaccharides, like 2-deoxy-2-acetamido-sugars, are successfully derivatized with 2-aminobenzoic acid (2-ABA in literature reported also as 2-AA) [69, 94, 95, 148]. Concerning the reaction conditions, the yield is related to the nature of the organic acid used as the catalyst; while acetic acid (pK_a 4.75) is the most widely employed, it has been demonstrated that the highest yield for the reductive amination of

Table 1
Selected articles reporting CE analysis of neutral and acidic sugars

Ref.	Carbohydrate species	Matrix	Derivatizing agent	CE mode	Capillary; *T*	Buffer, Voltage	Detection mode	LOD
[42]	Inorganic anions, organic acids, amino acids, carbohydrates, nucleotides, aromatic acids, alcohols, phosphorylated saccharides, oxyhalides, metal oxoacids, metal–EDTA complexes, forensic anions, Good's buffers and herbicides	Std and sea urchin and sake	None	CZE	Fused silica (112.5/104 cm; ID = 50 μm) *T* = 15 °C	20 mM PDC, 0.5 mM CTAH pH 12.1;30 kV Outlet: anode	Indirect UV (350 nm)	Anions and amino acids (6–12 mg/L); Carbohydrates (23–37 mg/L)
[51]	Fuc, Gal, Glc, Ara, Tag, Xyl, Sor, Man, Fru, Rib, Lyx, Sucrose, Melibiose, Cell, Lac, Gentiobiose, Maltose, Meleziose, Raffinose, Stachyose, Galactonic acid, Gluconic acid, GalN, GlcN, mannitol, sorbitol	Std	None	CZE	Fused silica (56–57/32–35 cm; ID = 25 or 50 μm) RT	Phosphate buffer pH 12.1 or NaOH at various concentrations, with tryptophan or BCDC as markers; various voltages Outlet: cathode	Indirect UV (280 nm) with tryptophan as the marker. (290 nm) with a cationic marker: BCDC	fmol levels
[52]	Glc, Fru, Rha, Rib, maltose, Lac, sucrose, GlcA.	Std, beverages and drinks, serum	None	CZE	Fused silica (120/113 cm; ID = 50 μm) *T* = 25 °C	Investigated the suitability of six BGEs:NAA, 2-naphthalensulfonic acid, 1,3-dihydroxynaphthalene, phenylacetic acid, *p*-cresol and sorbic acid. Best composition: 2 mM NAA pH 12.2; 25 kV Outlet: cathode	Indirect UV (222 nm)	Rib: 0.2 mM GlcA: 0.01 mM Others: 0.1 mM
[53]	Sucralose, sucrose, Glc and Fru	Low-calorie soft drinks and std mixture	None	CZE	Fused silica (112.5 cm; ID = 50 μm) RT	3 mM 3,5-dinitrobenzoic acid (DNBA) pH 12.1; 20 kV Outlet: cathode	Indirect UV (238 nm)	Sucralose: 28 mg/L
[54]	Oligosaccharides (α-galactosides): sucrose, raffinose, stachyose, verbascose and ajugose Galactinol, Maltitol, and methyl-α-D-glucopyranoside as internal std	Std and samples of legum inous seed (Lupine)	None	CZE	Fused silica (80/70 cm; ID = 50 μm) *T* = 30 °C	Pyridine-2,6-dicarboxylic acid (BGE), 5–150 mM $Na_2B_4O_7 \times 10H_2O$, 0.5 mM hexadecyltrimethyl ammonium bromide pH 8.0–10.0; 10 kV Outlet: anode	Indirect UV (350 nm)	110 μg/mL for sucrose, raffinose and stachyose and 130 μg/mL for verbascose

(continued)

Table 1
(continued)

Ref.	Carbohydrate species	Matrix	Derivatizing agent	CE mode	Capillary; *T*	Buffer, Voltage	Detection mode	LOD
[75]	1. D-Xyl, D-Ara, D-Rib, D-Glc, D-Gal, L-Fuc, D-Man, D-Fru, D-GlcNAc, D-GalNAc, Gentiobiose, Lac, Maltose, Cell, Sucrose, Maltotriose, Raffinose, Stachyose, Maltotetraose, Trehalose, L-Sorbose, 2. Polyols: Myo-inositol, Sorbitol 3. Sialic acid, GlcA, GalA 4. Glycosylated hexapeptide	Std mixtures	None	CZE	Fused silica 1., 2., 3. (94/87 cm; ID = 75 μm) T comprised between 20 and 60 °C 4. (58/54 cm; ID: = 75 μm) *T* = 20 °C	1., 2., 3. 50–60 mM tetraborate, pH 9.3; 20 kV; 4. 50, 100, 150, 200 mM boric acid, pH 10.0; 20 kV Outlet: cathode	UV (195 nm)	n.a.
[85]	α-, β- and γ-cyclodextrins (CD)	1. Std 2. Components in 2,6–di-*O*-methyl-β-cyclo-dextrins	2,6-ANS (*Dynamic labeling*)	CZE	Fused silica (100 cm; ID = 50 μm)	1. 40 mM sodium phosphate pH 11.76 with 1.0 mM 2,6-ANS 2a. 30 mM benzoate pH 8.0 with 1.0 mM 2,6-ANS and 20% methanol; 30 kV 2b. 30 mM benzoate pH 4.0 with 40 μM TBAB and 1.0 mM 2,6-ANS; 30 kV.	LIF (λ_{EXC}: 363 nm, λ_{EM}: 424 nm)	62 μM for α-CD; 2.4 μM for β-CD; 24 μM for γ-CD
[91]	1. Gal, Fuc, Ara, Man, Fru, Glc, Lac, GlcNAc, Rib, Sorbose, Xyl, Melibiose, Cell, Lyx, Maltose, Rha, Maltotetraose, GalNAc, Gentiobiose, Maltotriose, 2-deoxy-Rib 2. GlcA, GalA, ManA 3. Sialic acid (Neu5Ac)	Std mixtures; plant hydro-lyzates	Ethyl 4-amino benzoate and 4-ABN	CZE	Fused silica (57.5/50 cm; or 66/58.5 cm)	100–500 mM tetraborate, 0.001% HDB *Ethyl 4-aminobenzoate*: pH 9.5–11.5, containing 0–20% of methanol, ethanol, n-propanol, i-propanol, acetonitrile, or ethyl-glycol *4-Aminobenzonitrile*: pH 9.75–10.5, containing 0–5% of methanol, ethanol, n-propanol, or acetonitrile Outlet: anode	UV (280 nm)	1 ppm, 50 fmol (ethyl 4-amino benzoate); 0.6 ppm, 30 fmol (4-amino benzonitrile)
[95]	1. GalNAc, GlcNAc, Rib, Fuc, Glc, Man, Gal 2. GlcA, GalA	Std mixtures	2-ABA	CZE	Fused silica (60/50 cm; ID = 75 μm) *T* = 25 °C	150 mM sodium borate—50 mM sodium phosphate, pH 7; 20 kV Outlet: cathode	UV (214 nm)	n.a.

[97]	12 disaccharides containing Glc, Man, and Gal	Std	4-ABA	CZE	Fused silica (92/84 cm; ID = 50 µm)	1. 10 mM borate pH 10.0; 20 kV 2. 50 mM ammonium acetate with 10 mM α-cyclodextrin pH 5.5; 20 kV Outlet: cathode	UV (254 nm) ESI-MS/MS (negative mode); electrospray voltage: -4.5 kV; sheath liquid: water-2-propanol (20:80) containing 0.5% NH_3	n.a.
[98]	Malto-oligosaccharides	Solution std	PMP (*On-capillary derivatization*)	ME KC	Fused silica (71 /49 cm; ID = 50 µm) T = 57 °C	200 mM borate, 200 mM SDS pH 8.2; 10 kV Outlet: cathode	UV (195 and 245 nm)	10^{-6} M
[100]	Fructose, Glc, Gal, Rib, sucrose, mannose, and lactose	Drinks and foodstuffs	None	CZE	Fused silica (32.6/18.3 cm; ID = 5 µm) T = 25 °C	75 mM NaOH; pH 12.81 15 kV Outlet: cathode	C^4D (sine-wave signal 1.25 MHz, effective voltage 50 V)	0.40-0.72 µM range
[102]	Neu5Ac, gluconic acid, GalA, glyceric acid	std	1. SA 1., 2., 3. ANDSA	CZE	Fused silica (80/50 cm; ID = 50 µm)	1. 100 mM phosphate, pH 2.0, 2.5, 3.0; 20 kV Outlet: anode 2.50 mM phosphate, pH 10.0; 20 kV Outlet: cathode 3. 100 mM borate, pH 10.0; 20 kV Outlet: cathode	1., 2. UV (247 nm); 3. Fluorescence (λ_{exc} = 315 nm)	1. 2. SA derivatives: 30 fmol; ANDSA derivatives: 15 fmol (10.5 and 5.3 fmol respectively with extended path) 3. ANDSA derivatives: 0.6 fmol
[107]	Poly(GalA), GalA, and tri(GalA)	std	1. APTS 2. *N*-(1-maltoheptaosamine)-3,6-diaminoacridine	1. CGE 2. ELFSE	Linear polyacrylamide (LPPA) coated (62/47 cm; ID = 50 µm)	1. 24 mM citric acid + 2 M urea + 4% LPAA, pH 3.0, pH 3.5, pH 4.2 (Trizma base); 2. 24 mM citric acid, pH = 5 (Trizma base) + metal chlorides (0–15 mM); 25 kV Outlet: cathode	LIF (λ_{exc} = 488 nm; λ_{em} = 514 nm)	n.a.

(continued)

Table 1
(continued)

Ref.	Carbohydrate species	Matrix	Derivatizing agent	CE mode	Capillary; *T*	Buffer, Voltage	Detection mode	LOD
[125]	Neu5Ac	std and released from human serum	BA	CZE	Fused silica (56 cm; ID = 50 μm) *T* = 25 °C	25 mM phosphate, pH 3.5, with 50% (v/v) CH_3CN; 30 kV Outlet: anode	UV (231 nm)	Neu5Ac: 2 μM; 5 pg (S/N = 3)
[127]	1. 3'-SL, 6'-SL, 3'-SLN, 6'-SLN, DST, 3'-S-3-FL, SLNT-a, SLNT-b, SLNT-c, DSLNT, DSFLNH 2. Sialylated oligosaccharides	1. Std 2. Human milk after acidic hydrolysis	None	MEKC	Fused silica (56 cm; ID = 50 μm) *T* = 25 °C	376 mM Trizma buffer,150 mM SDS, pH 7.9; 6% MeOH (v/v) 30 kV Outlet: cathode	UV (205 nm)	30–68 fmol
[128]	1., 2. Neu5Ac 3. Mix of 3' and 6' Neu5Ac-Lac	1. Std 2. From fetuins 3. after Treatment with sialidases	None	CZE	Coated with linear polyacrylamide (50 cm; ID = 50 μm) *T* = 37 °C	50 mM acetate buffer, pH 5.0; (+ sialidases, 250 mU/mL) 2. 5, 10,15 kV 1.2.3.: 5 or 20 kV Outlet: anode	UV (200 nm)	Neu5Ac: 25 μg/mL
[133]	Gal, Glc, Man, Fru, inositol, d-Rib, Xyl, raffinose, Ara, Fuc, mannitol, Rib, GlcN, sucrose, GalN, maltose, xylitol, and deoxyribose as internal std	Std and wine samples	None	CZE	Fused silica (70 cm; ID = 50 μm)	50–400 mM Diethylamine (DEA), pH 12.15–12.40 with methanol or acetonitrile (0–40%); 15–20 kV (voltage ramp 10 kV/s)	ESI-MS (negative mode) Sheath liquid: 80% 2-propanol and 20% water containing 0.25% DEA at 4 μL/min.	Range of 0.5 (raffinose)-3.0 (deoxyribose) mg/L
[134]	Glc, Gal, Lac, Fru, and sucrose	Soft drinks and fruit juice. Gal use as internal std	None	CZE	Fused silica 1. (68.5/60 cm; ID = 50 μm) 2. (44/35.5 cm; ID = 20 μm) *T* = 30 °C	1. 30 mM NaOH; 30 mM NaOH and 12% v/v CH_3OH; 30 mM NaOH with 15 mM Na_2HPO_4 (all contained 200 μM CTAB); 11 kV 2. 10 mM NaOH, 4.5 mM Na_2HPO_4, 200 μm CTAB; 25 kV Outlet: anode	CCD	Fru: 16 μM; Glc: 31 μM; Gal: 18 μM; sucrose: 13 μM
[140]	Fuc, Glc, Gal, and Ara	Human serum	BHZ	CZE	Fused silica (67/60 cm; ID = 50 μm) RT	100 mM boric acid pH 10.4; 23.1 kV Outlet: cathode	UV (200 nm)	15.6 μM for Gal; 31.2 μM for Glc

[148]	N-linked oligosaccharides from antibody	From monoclonal antibody treated with PNGase	2-ABA	CZE	DB-1 capillary (40/30 cm; ID = 100 μm) T = 25 °C	100 mM Tris-borate pH 8.3 with PEG35000; 25 kV Outlet: anode	LIF (λ_{exc} = 325 nm; λ_{em} = 405 nm)	n.a.
[165]	Rha, Cell, Xyl, Rib, Melibiose, Ara, Glc, Man, Fuc, Gal, GlcA, and D-thyminose (2-deoxy-D-ribose) as internal std	Std and plant extracts	Tryptamine	MEKC	Coated fused silica (76/53 cm; ID = 50 μm) T = 30 °C	35 mM cholic acid, 100 mM borate with 2% 1-propanol pH 9.7; 30 kV Outlet: cathode	UV (220 nm)	Picomole levels
[170]	Mannooligosaccharide caps from *Mycobacterium tuberculosis* H37rv mannosylated lipoarabinomannans (ManLAMs)	Acidic hydrolysis extracts and std	APTS	CZE	fused silica Analytical CE: (47/40 cm; ID = 50 μm) Micropreparative CE: (47/40 cm; ID = 75 μm) T = 25 °C	15 mM TEA in a 1% (w/v) solution of acetic acid in water, pH3.5 20 kV for analytical CE; 10 kV for micropreparative CE Outlet: anode	UV (254 nm) LIF (λ_{EXC}: 488 nm; λ_{EM}: 520 nm) MALDI-TOF (off-line) linear and reflectron modes in negative ion mode	50 fmol of std APTS-maltotriose; 100 fmol using a 200-ns extraction delay time
[189]	GalA oligomer mixture	Poly-(GalA) subjected to autoclave hydrolysis	CBQCA	CZE	Fused silica deactivated capillary filled with poly(acrylamide) gels at high concentrations (32/23 cm; ID = 50 μm)	0.1 M Tris, 0.25 M borate, 2 mM EDTA, pH 8.48; 234 V/cm Outlet: cathode	LIF (λ_{exc} = 457 nm)	amol range
[168]	1. Xyl, Glc, Man, Ara, Gal, ManA, GlcA, GalA; 2. Glc, Man, Ara; 3. Rha, Xyl, Glc, Ara, Man, Gal, 4-O-Me-GlcA, GlcA, GalA; 4. Xyl_n (n = 1–6), 4-O-MeGlcA, Aldobiuronic acid, aldotriuronic acid, aldotetrauronic acid 5. Xyl, Glc, Man, Ara, Aldobiuronic acid, Gal, 4-O-MeGlcA.	1., 2., 3., 4. Std 5. Hydrolyzed sample of spruce wood xylan (enzymatic or chemical hydrolysis)	6-AQ	CZE	Fused silica 1., 2. (61/56 cm; ID = 50 μm) 3., 4., 5.(43/3 cm; ID = 30 μm)	1. 220 mM borate, pH 9; 20 kV 2., 4., 5. 420 mM borate, pH 9; 20 kV 3. 420 mM borate, pH 9; 1200 mW Outlet: cathode	UV (245 nm)	1–5.6 μM
[194]	CS and DS disaccharides	Std and From human aortas after treatment with chondroitinases	AMAC	CZE	Fused silica (55/50 cm; ID = 75 μm) T = 20 °C	15 mM orthophosfate buffer, pH 3.0; 20 kV Outlet: anode	LIF (λ_{exc} = 488 nm) UV (254 nm).	LIF: 0.51 pM UV: 5–8 pM (S/N = 3)

(continued)

Table 1
(continued)

Ref.	Carbohydrate species	Matrix	Derivatizing agent	CE mode	Capillary; *T*	Buffer, Voltage	Detection mode	LOD
[203]	GAG-derived disaccharides	Enzymatic GAGs treatment	AMAC	CZE	Fused silica (85/70 cm; ID = 50 μm) *T* = 25 °C	50 mM phosphate buffer; 20 and 30 kV Outlet: anode	LIF (λ_{EXC}:488 nm)	fmol levels
[206]	Maltoheptaose and oligosaccharides (DP4-10) in corn syrup	Standard mixture	O-2-[amino ethyl] fluorescein	CZE	Fused silica (40/30 cm; ID = 50 μm) *T* = 30 °C	100 mM borate buffer titred to pH 8.65 with TRIS; 30 kV Outlet: anode	LIF (λ_{EXC}: 488 nm)	1 nM
[207]	Glc, Man, Gal, Rib, Xyl, Fuc, GalNAC, GlcNac and ManNac from ribonuclease B, fetuin, and erythropoietin	Std and glycoproteins digest	Rho110	CZE	fused silica (57/50 cm; ID = 75 μm) *T* = 25 °C	200 mM borate buffer, pH 10.5; 14 kV Outlet: cathode	LIF (λ_{EXC}: 488 nm; λ_{EM}: 530 nm)	36-70 amol
[209]	*N*-glycans	Standard mixture	Py-1	MEKC	Fused silica (85/60 cm; ID = 75 μm)	50 mM borate buffer, 150 mM SDS; pH 9.3; 25 kV; Outlet: cathode	LIF (λ_{EXC}: 546 nm; λ_{EM}: 570 nm) MALDI-ToF-MS positive reflectron mode	n.a.
[211]	Fucosylated and afucosylated *N*-glycans	Standard mixture	APTS	CZE	LPA coated capillary (50/40 cm; ID = 50 μm) *T* = 25 °C	25 mM boric acid pH 9.0 with 1,5 % LPA (Mw 10000); 600 V/cm	LIF (λ_{EXC}: 488 nm; λ_{EM}: 520 nm)	n.a.
[212]	Branched glycans	Glycans enzymetically released products from glycoproteins AGP and RNase B	APTS	CZE	Fused silica coated with 5 % phospholipids with a ratio [DMPC]/[DHPC] = 0.5 (60.2/50.0 cm; ID = 25 μm) *T* = 25 °C	100 mM MOPS pH 7.0 with10% phospholipids [DMPC]/[DHPC] = 2.5 incorporated with 1. neuroaminidase 2. ß1-4 galactosidase 3. ß-*N*-acetylglucosaminidase; 400 V/cm Outlet: anode	LIF (λ_{EXC}: 488 nm; λ_{EM}: 520 nm);	n.a.

[224]	Fructose, Glc, sucrose, and lactose	Forensic, pharmaceutical, and beverage samples	None	CZE	Fused silica modified with HDMB (60/50 cm; ID = 50 μm) T = 26.5 °C	98 mM NaOH; 120 mM NaCl; pH 13.0 14 kV Outlet: anode	UV (270 nm)	5–10 μM range

2-ABA 2-aminobenzoic acid, *3-ABA* 3-aminobenzoic acid, *4-ABA* 4-aminobenzoic acid, *4-ABN* 4-aminobenzonitrile, *6-AQ* 6-aminoquinoline, *All* allose, *Alt* altrose, *2,6-ANS* 2-anilinonaphtalene-6-sulfonic acid, *ANTS* 8-aminonaphtalene-1,3,6-trisulfonic acid, *APTS* 1-aminopyrene-3,6,8-trisulfonate, *Ara* arabinose, *BA* Benzoic anhydride, *BCDC* N-benzylcinchonidinium chloride, *BGE* background electrolyte, *BHZ* p-hydrazine-benzenesulfonic acid, *CBQCA* 3-(4-carboxybenzoyl)2-quinoline-carboxyaldehyde, *CCD* contactless conductivity detection, *Cell* cellobiose, *CGE* capillary gel electrophoresis, *CIEF* capillary isoelectric focusing, *CITP* capillary isotachophoresis, *CTAB* cetyltrimethylammonium bromide, *CTAH* cetyltrimethylammonium hydroxide, *CZE* capillary zone electrophoresis, *DEA* diethylamine, *DNBA* 3,5-dinitrobenzoic acid, *d-Rib* 2-Deoxyribose, *ED* electrochemical detection, *ESI-MS* electrospray ionization-mass spectrometry detector, *FACE* fluorophore-assisted carbohydrates electrophoresis, *Fru* fructose, *Fuc* fucose, *Gal* galactose, *GalA* galacturonic acid, *GalN* galactosamine, *GalNAc N*-Acetylgalactosamine, *Glc* glucose, *GlcA* glucuronic acid, *GlcN* glucosamine, *GlcNAc N*-Acetylglucosamine, *Gul* gulose, *HDB* hexadimethrine bromide, *HPAEC* high performance anion-exchange chromatography, *Ido* idose, *Lac* lactose, *LIF* laser-induced fluorescence, *LOD* limit of detection, *Lyx* lyxose, *MALDI-TOF* matrix-assisted laser desorption/ionization-time of flight-mass spectrometry detector, *Man* mannose, *MEKC* micellar electrokinetic capillary chromatography, *MS* mass spectrometry detector, *n.a.* not available, *NAA* 1-naphthylacetic acid, *NACE* non aqueous capillary electrophoresis, *Neu5Ac N*-Acetylneuraminic acid, *PAD* pulsed amperometric detection, *PAGE* polyacrylamide gel electrophoresis, *PDC* 2,6-pyridinedicarboxylic acid, *PEG* polyethylene glycol, *PF-MEKC* partial filling MEKC, PMP 1-phenyl-3-methyl-2-pyrazolin-5-one, *PNP* p-nitrophenol, *Rha* rhamnose, *RI* refractive index detector, *Rib* ribose, *RT* room temperature, *SA* sulfanilic acid,, *S/N* signal/noise ratio, *SDS* sodium dodecyl sulfate, *std* standard, *Tag* tagatose, *Tal* talose, *TBAB* tetra-butylammonium bromide, *TEA* triethylamine, *TFA* trifluoroacetic acid, *TOA* thermooptical absorbance, *UV* ultraviolet detector, *Xyl* xylose

N-linked oligosaccharides with 1-aminopyrene-3,6,8-trisulfonate (APTS) is obtained using citric acid (pK_a 3.13) or malic acid (pK_a 3.40) as catalysts [197]. This effect is much more relevant for sugars having *N*-acetylglucosamine at the reducing end. Among the chromophores, 4-ABN provides a relatively high sensitivity with respect to other chromophores [18, 56] and low values of detection limits (LODs) [18, 35, 56, 84]. Fluorophoric tags based on laser-induced fluorescence (LIF) detection used in reductive amination include 2-aminoacridone (AMAC) [194, 203, 204], which give rise to unprecedented sensitivity (LODs down to the pM range [194]) and APTS. The latter is one of the most preferred fluorescent tags in glycan profiling [46, 47, 144–147, 205] but in the last years the use of new fluorescent tags as O-2-[aminoethyl]fluorescein and rhodamine 110 (Rho110) [206–208] with high quantum yields (0.24 and 0.85, respectively) has been reported since this property allows in the case of Rho110 reaching LODs at subamol levels [207]. A fluorescent tag with peculiar behavior is pyrylium dye (Py-1), used for derivatization of oligosaccharides analyzed by CE and MALDI-ToF-MS; the introduction of a permanent positive charge upon pyridinium formation is particularly advantageous in this respect. Moreover, this tag eliminates the need to remove the excess dye used, since the free dye is nonfluorescent [209]. Recently, the 5-aminonaphtalene-2-sulfonic acid (ANSA) fluorophore has been suggested [210] to give better results for CE, high-performance liquid chromatography (HPLC), and MS applications in substitution of APTS since ANSA is compatible with all three techniques.

For neutral sugars the linkage with tags carrying ionizable groups guarantees highly selective electrophoretic separations: APTS and 8-aminonaphtalene-1,3,6-trisulfonic acid (ANTS) are extremely advantageous, since they introduce negative charges to the sugars for a wide pH range (i.e., pH ≥2), with consequent wide possibilities in the buffer composition optimization [83, 86, 87, 107, 117, 118, 192, 196, 211–213, 218]. They have been used not only as derivatizing agents for fluorescence detection, but also for online electrospray mass spectrometry detection and off-line matrix-assisted laser desorption ionization mass spectrometry [99, 170, 214]. Another efficient derivatization strategy which includes reductive amination is the conversion of reducing sugars in 1-amino-1-deoxyalditols and subsequent reaction with 3-(4-carboxybenzoyl)-2-quinolinecarboxyaldehyde (CBQCA) [5, 56, 101, 189] or with 5-carboxytetramethylrhodamine succinimidyl ester (TRSE) [198]. Finally, condensation between carbonyl group of reducing carbohydrates and the active hydrogens of 1-phenyl-3-methyl-5-pyrazolone (PMP) has been successfully employed [98, 190] for the characterization of various biological matrices [63, 73, 76] and in food analysis [215]. Table 2 reports the structures of the most widely used derivatizing agents, together with their main applications. Finally, selective methods are reported

for the labeling of carboxylated carbohydrates. The first is based on the formation of an amide bond between the carboxylate group of the sugar and the amino group of the tag in the presence of water-soluble carbodiimide; the amount of this catalyst has to be lower than that of the sugar acid, in order to avoid the formation of side products [56]. 7-aminonaphtalene-1,3-disulfonic acid (ANDSA) [102, 155, 193, 216] and sulfanilic acid (SA) [193, 216] have been successfully used for this approach.

In the choice of labeling procedure for glycan studies, particular care should be taken with sialoglycoconjugates since many methods used in the structural analysis of intact glycans cause disruption of sialic acid modifications [2]. As an example, during reductive amination of sialo-oligosaccharides, the use of catalysts having stronger acidity than acetic acid may lead to a loss of sialic acid. An interesting study on de-sialylation of sialyl-*N*-acetyllactosamine in different conditions of reductive amination with APTS has been reported by Evangelista et al. [117]. Other procedures for sialic acid derivatization include condensation with ANDSA and SA [102, 103] and perbenzoylation with benzoic anhydride (BA) [125], reaction with *ortho*-diamines [65] but the most popular agent is AMAC [119, 124, 203].

CE can be applied to monitor all the steps of manufacturing process for glycosylation profiling and for the identification of potentially immunogenic epitopes [139, 144, 146, 147]. N-glycosylation analysis of mAb therapeutics includes several steps: chemical or enzymatic digestion to release the N-glycans, fluorescence labeling, sample purification/desalting, and CE separation. For the N-glycan release, PNGase-F digestion is the most common approach, supported also by the use of a pressure-cycling technology to increase the speed of enzymatic glycans release [214]. Identification of glycan peaks is usually done on the basis of retention times of peaks in comparison with a maltose ladder used as reference (GU glucose units are used for this comparison). For the sequence elucidation the support provided by databases based on specific digestions with exoglycosidases aids in the CE–LIF data interpretation [145, 146] and the coupling to methods like MS completes the structural and compositional information [217]. An interesting application is the use of phospholipids as additives to obtain an in-capillary cleavage of terminal glycan residues with exoglycosidases reducing at the same time the enzyme consumption [212, 219]. Finally when the structures present in a mixture are known, CE can be used as a high-throughput profiling tool. Also in this case APTS is the tag the most used for N-glycan analysis but the use of other tags is increasing. Rho110 enables the separation of sialo-oligosaccharides and asialo-oligosaccharides with a simple running buffer change [208], 2-ABA revealed the presence of minor peaks not visible with APTS derivatization [148] and ANTS is viewing the development of a database for CGE-LED-induced fluorescence (CGE-LEDIF) based glycans profiling [146].

A disadvantage of all the previously mentioned derivatization strategies is that they are destructive. Nevertheless, some approaches have been proposed to minimize the sample consumption.

The first is on-capillary derivatization, which reduces the sample volume by two-three orders of magnitude [98, 140].

A second approach, the so-called dynamic labeling of carbohydrates, has been mainly used for cyclodextrins, which have the capacity to form inclusion complexes with charged fluorophores or chromophores added in the separation buffer increasing electrophoretic migration as well as the detection [85, 220].

A third interesting approach gives the possibility to reconvert the labeled products in the starting sugars and is based on the formation of chromophoric or fluorophoric glycosylamines; this strategy has been reported for both HPLC and CE analysis of reducing sugars: as an example, formation of N-(2-pyridinyl)-glycosylamines has been successfully used to label malto-oligosaccharides or pullulan oligomers prior to their HPLC analysis [200, 221]; glycosylamines originated from reaction with 4-aminobenzoic acid and various disaccharides have been analyzed with CE and negative-mode electrospray mass spectrometry: the glycosylamines approach turned out to provide more information on linkage and anomeric configuration than reductive amination [97, 222]. Another procedure based on the formation of glycosylamines consists in the preparation of 1-amino-1-deoxy-derivatives from the reducing sugars, which can then react with acylic groups of suitable tags like 9-fluorenyl-methyloxycarbonyl chloride (Fmoc) [199, 223]. In all the cases related to the glycosylamines-based strategies, the starting oligosaccharides can be recovered from glycosylamines upon weak acid hydrolysis [199, 200, 221, 223].

1.2 Underivatized Sugars

Direct UV detection can be typically carried out for acidic mono- and oligo-saccharides, especially when acetyl groups are present, or when unsaturated linkages are generated by some enzymatic treatment. Many buffer compositions can be chosen to separate such compounds [8, 127, 128, 172–184, 188], ranging from values close to pK_a to alkaline buffers, due to the presence of acidic groups; some examples are reported in Table 1.

Separation of neutral underivatized sugars is typically accomplished by the use of highly alkaline buffers. Highly alkaline buffers ($pH > 12$) are capable to induce acidic dissociation of underivatized sugars ($11.9 < pK_a < 12.8$) and of alditols ($pK_a \approx 13.5$) [65], which can migrate in the capillary through zone electrophoresis. This analysis mode is normally associated to electrochemical, mass spectrometry, or indirect ultraviolet/fluorescence detection [34, 72, 100, 106, 110, 133, 134, 224]. Electrochemical detection allows the highest sensitivity achievable for underivatized carbohydrates [56], contactless conductivity detection (C^4D) has also been used

as detection mode for the analysis of low-molecular saccharides with LODs lower than 1 μM [100]. Upon using volatile bases in the separation buffer, negative-mode electrospray mass spectrometry turns out to be a suitable detector for alditols, reducing and nonreducing neutral sugars [133]. When coupled with highly alkaline buffers, the most common UV or LIF detectors are successfully used in "indirect" mode, which is based on the displacement of the chromophores or fluorophores in the background electrolyte by any charged molecule in the sample, resulting in negative peaks [45, 56]. LODs in indirect UV (or fluorescence) depend on the nature of the chromophore (or fluorophore) in the background electrolyte as well as on the type of sugar: for instance, neutral carbohydrates analyzed with indirect UV detection show typical LODs equal to 10^{-4} M while, in the same analysis conditions, sugar acids have LOD values of 10^{-6} M [31, 55, 56]. The separation efficiency of CE using highly alkaline buffers shows a 10- to 20-fold increase with respect to HPAEC-PAD [34]. It should be mentioned that the use of highly alkaline buffers is advised not only for nonreducing sugars, but also for reducing sugars, when some relevant matrix components can be degraded under the typical derivatization conditions.

A direct UV method proposed by Rovio et al. for the separation under extremely high alkaline conditions permits the detection of neutral carbohydrates. In this approach neutral sugars are analyzed under their alcholate form and their direct UV detection which is claimed to be due to the absorption of the enediolate at 270 nm [49, 153, 224, 225]. Recently, the method proposed by Rovio et al. specific for neutral sugars has been implemented reversing the EOF through the addition of the CTAB surfactant allowing the simultaneous determination of uronics acids and neutral sugars [110].

1.3 Use of Borate-Based Separation Buffers for Derivatized and Underivatized Sugars

The use of borate-based buffers is widespread for the CE analysis of carbohydrates [18, 64, 68, 72, 74–76, 84, 90, 92, 95, 97, 102, 105, 140, 155, 200, 201, 207, 209, 211, 226]. Using such separation electrolyte, sugars can be converted in situ to anionic borate complexes. The stability of the mentioned complexes depends on the pH (typically, comprised between 7 and 10); moreover, it is related to the configuration of the hydroxyl groups involved in the interaction with boron: for cyclic carbohydrates, only vicinal hydroxyl groups with *cis* configuration can form stable complexes; for polyols, *cis*-1,2-diols are preferred in complexation over *trans*-1,2-diols; moreover, in general the stability of complexes increases with the number of hydroxyl groups [75, 105]. These features imply that borate-based buffers can exert a strong influence on the selectivity of the electrophoretic separation of carbohydrates, since the differential stability of in situ formed complexes contributes to the mobility of the analytes. Besides the introduction of the charge,

borate–carbohydrate complexes show an increase in UV response at 195 nm with respect to uncomplexed carbohydrates. As a consequence, borate-based buffers can make sugars suitable for CE analysis without the need of derivatization [75]. Indeed, the use of borate-based buffers is one of the methods of choice for capillary electrophoresis of glycosides, since they are not amenable to derivatization. The influence on separation selectivity and UV detection sensitivity explains why borate buffers are very often used for both derivatized and underivatized carbohydrates.

In the following sessions, some representative examples of CE analysis of neutral and acidic sugars will be shown, including experimental procedures.

Two different examples of reducing sugars derivatization will be illustrated: one for aldoses with ANTS, and another one reversible derivatization employing Fmoc with it subsequent removal.

Additionally, two representative examples of sugars analysis without derivatization will be shown: the first will be relative to CE analysis of allyl glycosides (usefulness of the borate complexation) while the second procedure will regard the study of unsaturated oligosaccharides arising from the treatment of an alginate sample with G-lyase [184]; this CE methodology can be extended to other relevant lyase-treated acidic polysaccharides, like glycosaminoglycans.

2 Materials

2.1 Derivatization of Reducing Sugars

2.1.1 Derivatization with ANTS (Dextrans)

1. *Samples*: Dextran 1000 standard (Fluka, Buchs, Switzerland).
2. *Reagents for derivatization*: sodium cyanoborohydride (Sigma, St. Louis, MO, USA), ANTS (Fluka, Buchs, Switzerland), dimethylsulfoxide, orthophosphoric acid 85%, glacial acetic acid (Merck, Darmstadt, Germany)
3. *CE buffer*: 50 mM sodium phosphate buffer pH 2.5.

2.1.2 Derivatization of Sugars by Conversion to Glycosylamines and Reaction with N-Fluorenyl-Methiloxycarbonyl (Fmoc) Chloride

1. *Samples:* D-galactose, D-glucose and lactose (Sigma, St. Louis, MO, USA).
2. *Reagents for derivatization*: ammonium hydrogen carbonate, concentrated ammonia, *N*-fluorenyl-methyloxycarbonyl (Fmoc) chloride, sodium hydrogen carbonate ($NaHCO_3$), dioxane and methanol (all reagents from Sigma, St. Louis, MO, USA); the structure of Fmoc is reported in Table 2.
3. *Reagent for Fmoc removal*: 15% aqueous ammonia solution (diluted from 28% ammonium hydroxide, Sigma, St. Louis, MO, USA).

Table 2
Main derivatizing tags suitable for CE analysis of neutral and acidic sugars

Derivatizing agent	Detection	Carbohydrates species	References
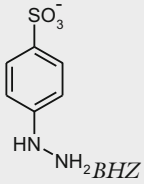 *p*-Hydrazine-benzenesulfonic acid *BHZ*	UV (200 nm)	Fuc, Glc, Gal, Ara	[140]
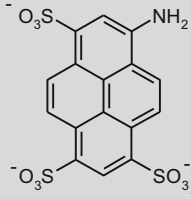 1-Aminopyrene-3,6,8-trisulfonic acid *APTS*	LIF (λ_{EXC}: 455 nm; λ_{EM}: 512 nm) UV (254 nm)	*N*-linked oligosaccharides GalNAc, GlcNAc, Rha, Man, Glc, Fru, Xyl, Fuc, Gal, Maltooligosaccharides (with up to 18 Glc residues) GalNAc, GlcNAc, Rha, Man, Glc, Xyl, Fuc, Gal, Ara, Rib, Gentibiose, maltose, Lac, Cell, Melibiose, Maltotetraose and its α-1-6 isomer, Sialyllactose PolyGalA, GalA, and triGalA GalNAc, GlcNAc, Man, Glc, Gal, Fuc, GlcNAc-Gal Mannooligosaccharide caps from *Mycobacterium tuberculosis* H37rv mannosylated lipoarabinomannans (ManLAMs) Gluco-oligosaccharide regioisomers with a degree of polymerization (DP) ranging from 2 to 9; several glucose disaccharide regioisomers Neu5Ac and neutral sugars. GlcA and neutral sugars	[46, 47, 117, 143–147, 205] [86] [87] [107] [119] [170] [202] [119] [196]
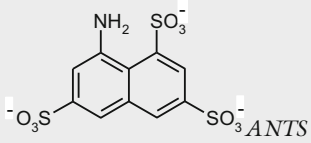 8-Aminonaphtalene-1,3,6-trisulfonic acid *ANTS*	LIF (λ_{EXC}: 370 nm; λ_{EM}: 520 nm) UV (214 e 223 nm)	Glc, Maltose and linear malto-oligosaccharides (with up to 40 Glc residues) Malto-oligosaccharides N-linked oligosaccharides GalA oligomer Dextran (Mw 1000 and 5000)	[83] [99] [146] [192] [213]
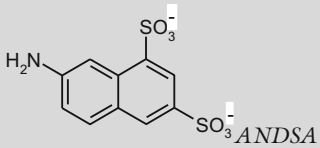 7-Aminonaphtalene-1,3-disulfonic acid *ANDSA*	LIF (λ_{EXC}: 315 nm; λ_{EM}: 420 nm) UV (247 nm)	Neu5Ac, gluconic acid, GalA, glyceric acid Sialooligosaccharides D,L-Ribose Chondroitin sulfates saccharides	[102] [103] [202] [193]

(continued)

Table 2
(continued)

Derivatizing agent	Detection	Carbohydrates species	References
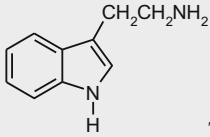 Tryptamine	UV (220 nm)	Rha, Cell, Xyl, Rib, Melibiose, Ara, Glc, Man, Fuc, Gal, GlcA, and D-thyminose	[165]
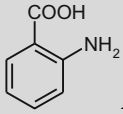 *2-ABA* 2-Aminobenzoic acid	UV (214 nm)	N-linked oligosaccharides GalNAc, GlcNAc, Rib, Fuc, Glc, Man, Gal GalNAc, GlcNAc, Rib, Fuc, Glc, Man, Gal, GlcA, GalA	[69, 148] [94] [95]
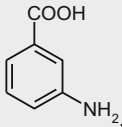 *3-ABA* 3-Aminobenzoic acid	LIF (λ_{EXC}: 325 nm; λ_{EM}: 405 nm)	*N*-linked oligosaccharides	[143]
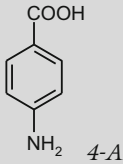 *4-ABA* 4-Aminobenzoic acid	UV (285 nm)	12 Disaccharides containing Glc, Man and Gal	[97]
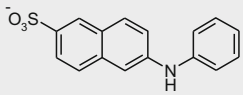 *2,6-ANS* 2-Anilinonaphtalene-6-sulfonic acid	LIF (λ_{EXC}: 363 nm; λ_{EM}: 424 nm)	α-, β- and γ-cyclodextrins	[85]
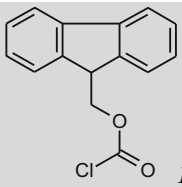 *Fmoc* *N*-fluorenyl-methyloxycarbonyl chloride	UV (260 nm)	Glc, Gal and Lac previously converted in the corresponding glycosylamines	[199]

(continued)

Table 2
(continued)

Derivatizing agent	Detection	Carbohydrates species	References
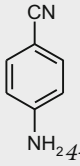 *4-ABN* 4-Aminobenzonitrile	UV (285 nm)	ManA oligomers Neutral mono-, di- and trisaccharides (Maltotriose, Maltose, Lac, L-Rha, D-Lyx, D-Xyl, Cell, Melibiose, L-Sorbose, D-Rib, D-Glc, D-Fru,D-Man, L-Ara, D-Fuc, D-Gal); sugar acids (D-GlcA, D-GalA) Gal, Fuc, Ara, Man, Fru, Glc, Lac, GlcNAc, Rib, Sorbose, Xyl, Melibiose, Cell, Lyx, Maltose, Rha, Maltotetraose, GalNAc, Gentiobiose, Maltotriose, 2-deoxy-Rib, GlcA, GalA, ManA, Sialic acid (Neu5Ac) Isomaltose, maltose, Glc, Glcα1 → 6Glcα1 → 6Glc, Glcα1 → 6Glcα1 → 4Glc GalA, GlcA	[35, 184] [84] [91] [200] [84]
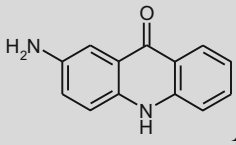 *AMAC* 2-Aminoacridone	LIF (λ_{EXC}: 425 nm; λ_{EM}: 520 nm)	Sialic acid (Neu5Ac) Neu5Ac, cinnamic acid, GlcA, GalA and neutral sugars Variously sulfated chondroitin/dermatan Δ-disaccharides GAG-derived disaccharides	[119] [119, 124] [194] [203]
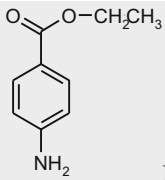 Ethyl 4-aminobenzoate	UV (305 nm)	Gal, Fuc, Ara, Man, Fru, Glc, Lac, GlcNAc, Rib, Sorbose, Xyl, Melibiose, Cell, Lyx, Maltose, Rha, Maltotetraose, GalNAc, Gentiobiose, Maltotriose, 2-deoxy-Rib, GlcA, GalA, ManA, Sialic acid (Neu5Ac)	[91]
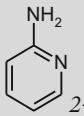 *2-AP* 2-aminopyridine	UV (240 nm)	GalA, GlcA, Gal, GalNAc, Ara, Fuc, Rha, Xyl, Lyx, GlcNAc, Glc, Rib	[74]
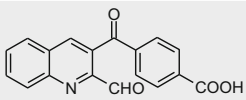 *CBQCA* 3-(4-Carboxybenzoyl)-2-quinolinecarboxyaldehyde	LIF (λ_{EXC}: 457 nm; λ_{EM}: 552 nm)	GlcN, GalN, 1-amino-1-deoxyglucosamine, 1-amino-1-galactosamine, 6-amino-6-deoxy-glucose, glucosaminic acid, galactosaminic acid, 1-amino-1-deoxyglucose, 1-amino-1-deoxygalactose, 2-amino-2-deoxyglucose, 2-amino-2-deoxygalactose glucosaminic acid, GlcA, Glc6P, and neutral sugars	[101] [101, 189]

(continued)

Table 2
(continued)

Derivatizing agent	Detection	Carbohydrates species	References
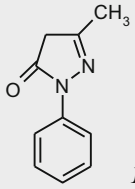 *PMP* 1-Phenyl-3-methyl-2-pyrazolin-5-one	UV (245 nm)	Xyl, Ara, Rib, Lyx, Glc, All, Alt, Man, Ido, Gul, Tal, Gal, Oligoglucans (up to 13 glucose residues Ara, Rib, Gal, Glc, Lyx, Xyl and Man, Fuc, GalNAc, GlcNAc Maltooligosaccharides Chondroitin sulfate disaccharides Lac, Mal, Gen, Mel, Cel, Gal, Man, Glc, GalNAc, GlcNAc, Rib, Lyx, Xyl, Ara.	[76] [77] [98] [190] [215]
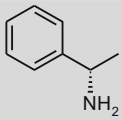 (S)-(−)-1-phenylethylamine	UV (200 nm)	D/L-Glc, D/L-All	[161]
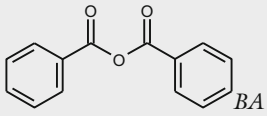 *BA* Benzoic anhydride	UV (231 nm)	Sialic acids	[125]
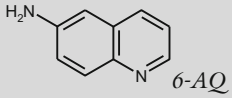 *6-AQ* 6-Aminoquinoline	UV (245 nm) LIF (λ_{exc} = 270 nm; λ_{em} > 495 nm)	Monosaccharides, uronic acids, xylooligosaccharides, xylan-derived acidic oligosaccharides	[168]
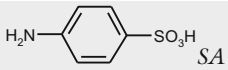 *SA* Sulfanilic acid	UV (247 nm)	Neu5Ac, gluconic acid, GalA, glyceric acid Xylonic acid, MeGlcA, aldobiuronic acid, aldotriuronic acid, aldotetrauronic acid	[102] [105]
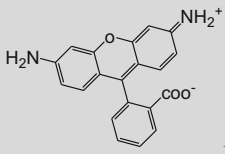 *Rho110* rhodamine 11	LIF (λ_{EXC}: 488 nm; λ_{EM}: 530 nm)	Glc, Man, Gal, Rib, Xyl, Fuc, GalNAC, GlcNac and ManNac from glycoproteins N-linked oligosaccharides	[207] [208]
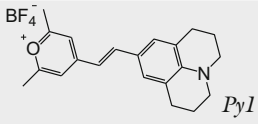 *Py1* Pyrylium dye	LIF (λ_{EXC}: 546 nm; λ_{EM}: 570 nm)	*N*-glycans	[209]

(continued)

Table 2
(continued)

Derivatizing agent	Detection	Carbohydrates species	References
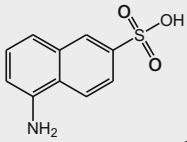 *ANSA* 5-Aminonaphtalene-2-sulfonic acid	LIF (λ_{EXC}:325 nm; λ_{EM}: 520 nm) HPLC (λ_{EXC}:325 nm; λ_{EM}: 475 nm) MALDI-ToF-MS linear negative ion mode	N-linked oligosaccharides mixture	[210]

2-ABA 2-aminobenzoic acid, *3-ABA* 3-aminobenzoic acid, *4-ABA* 4-aminobenzoic acid, *4-ABN* 4-aminobenzonitrile, *6-AQ* 6-aminoquinoline, *All* allose, *Alt* altrose, *2,6-ANS* 2-anilinonaphtalene-6-sulfonic acid, *ANTS* 8-aminonaphtalene -1,3,6-trisulfonic acid, *APTS* 1-aminopyrene-3,6,8-trisulfonate, *Ara* arabinose, *BA* Benzoic anhydride, *BCDC* N-benzylcinchonidinium chloride, *BGE* background electrolyte, *BHZ* p-hydrazine-benzenesulfonic acid, *CBQCA* 3-(4-carboxybenzoyl)2-quinoline-carboxyaldehyde, *CCD* contactless conductivity detection, *Cell* cellobiose, *CGE* capillary gel electrophoresis, *CIEF* capillary isoelectric focusing, *CITP* capillary isotachophoresis, *CTAB* cetyltrimethylammonium bromide, *CTAH* cetyltrimethylammonium hydroxide, *CZE* capillary zone electrophoresis, *DEA* diethylamine, *DNBA* 3,5-dinitrobenzoic acid, *d-Rib* 2-Deoxyribose, *ED* electrochemical detection, *ESI-MS* electrospray ionization-mass spectrometry detector, *FACE* fluorophore-assisted carbohydrates electrophoresis, *Fru* fructose, *Fuc* fucose, *Gal* galactose, *GalA* galacturonic acid, *GalN* galactosamine, *GalNAc* *N*-Acetylgalactosamine, *Glc* glucose, *GlcA* glucuronic acid, *GlcN* glucosamine, *GlcNAc* *N*-Acetylglucosamine, *Gul* gulose, *HDB* hexadimethrine bromide, *HPAEC* high performance anion-exchange chromatography, *Ido* idose, *Lac* lactose, *LIF* laser-induced fluorescence, *LOD* limit of detection, *Lyx* lyxose, *MALDI-TOF* matrix-assisted laser desorption/ionization-time of flight-mass spectrometry detector, *Man* mannose, *MEKC* micellar electrokinetic capillary chromatography, *MS* mass spectrometry detector, *n.a.* not available, *NAA* 1-naphthylacetic acid, *NACE* non aqueous capillary electrophoresis, *Neu5Ac* *N*-Acetylneuraminic acid, *PAD* pulsed amperometric detection, *PAGE* polyacrylamide gel electrophoresis, *PDC* 2,6-pyridinedicarboxylic acid, *PEG* polyethylene glycol, *PF-MEKC* partial filling MEKC, PMP 1-phenyl-3-methyl-2-pyrazolin-5-one, *PNP* p-nitrophenol, *Rha* rhamnose, *RI* refractive index detector, *Rib* ribose, *RT* room temperature, *SA* sulfanilic acid,, *S/N* signal/noise ratio, *SDS* sodium dodecyl sulfate, *std* standard, *Tag* tagatose, *Tal* talose, *TBAB* tetra-butylammonium bromide, *TEA* triethylamine, *TFA* trifluoroacetic acid, *TOA* thermooptical absorbance, *UV* ultraviolet detector, *Xyl* xylose

4. *Reagent for sugar regeneration*: 2% aqueous acetic acid solution (diluted from glacial acetic acid, Sigma, St. Louis, MO, USA).
5. *CE buffer*: 20 mM borax + 25 mM sodium dodecylsulfate (SDS) pH 9.2 (all reagents from Sigma, St. Louis, MO, USA).

2.2 Analysis of Underivatized Sugars

2.2.1 Use of Borate-Based Separation Buffers for Glycosides (Identification of Anomeric Forms of O-and C-Allyl Glycosides)

1. *Samples*: *O*-allyl-α-D-glucopyranoside, *O*-allyl-β-D-glucopyranoside, and *O*-allyl-α-D-galactopyranoside (from Glycon Biochemicals, Luckenwalde, GER); *O*-allyl-β-D-galactopyranoside previously synthesized according to the procedure reported in literature [201]. α- and β-*C*-allyl galactopyranosides and glucopyranosides were synthesized following the protocol reported in **Note 1**.
2. *CE buffer*: *C*-allyl-glycosides: 100 mM borax + 100 mM SDS (pH 9.2); *O*-allyl-glycosides: 25 mM borax + 250 mM SDS (pH 9.2) (all reagents from Sigma, St. Louis, MO, USA).

2.2.2 CZE-UV of Unsaturated, Underivatized Acidic Sugars Released from Alginates

1. *Samples*: unsaturated oligomers (2 mg/mL of freeze-dried mixture in water) released from alginate upon treatment with G-lyase (from *Klebsiella Pneumoniae;* from the University of Science and Technology NTNU, Trondheim, Norway) as previously described [184]. Alginate sample (containing 47% α-L-guluronic acid) was prepared treating poly-mannuronic acid with recombinant mannuronan C-5 epimerase [184], AlgE4, an enzyme which catalyzes the in-chain epimerization of β-D-mannuronic acid in α-L-guluronic residues in the last step of alginate biosynthesis.
2. *CE buffer*: 50 mM sodium tetraborate (pH 9.2) (from Sigma, St. Louis, MO, USA).

2.3 Equipment

1. High-performance capillary electrophoresis (CE) system (Applied Biosystems Model 270A-HT; Foster City, CA, USA), with Turbochrom Navigator (4.0) software. High-performance capillary electrophoresis system from Hewlett-Packard (Agilent, Waldbronn, Germany), Model HP^{3D}CE, with HP Chemstation software (Subheading 2.1.1).
2. Uncoated fused silica column (Supelco, St. Louis, MO, USA); inner diameter (ID): 50 μm; capillary length: 72 cm (50 cm to detector) (Subheadings 2.2.1 and 2.2.2). Fused silica column with extended light path (Agilent technologies, Waldbronn, Germany); ID: 50 μm; capillary length: 104 cm (95.5 cm to detector) (Subheading 2.1.1); Detection: UV on-column 220 nm (Subheading 2.1.1), 260 nm (Subheading 2.1.2); 195 nm (Subheading 2.2.1); 232 nm (Subheading 2.2.2).
3. C18 cartridge (Sep-Pak®, 10 g).
4. Nylaflo membrane filters 0.45 μm (Sigma, St. Louis, MO, USA).
5. Bio-Gel P2 (Bio-Rad, Hercules, CA, USA).
6. Filters: 0.45 μm pore size membrane (Millipore, Billerica, MA, USA).
7. Dry-bath heating block.

3 Methods

3.1 Derivatization of Neutral Reducing Sugars

3.1.1 Derivatization with ANTS

1. Conversion of dextran oligosaccharides in the corresponding ANTS derivatives: mix a solution containing 0.2 M ANTS (85% water, 15% glacial acetic acid) and dextran mixture (15 mg/mL) with a solution containing 1 M of sodium cyanoborohydride in DMSO. Leave the mixture for 12 h at 40 °C. Upon storage at +4 °C of the derivatized solution, no degradation was observed for 4 weeks (no further stability points collected) [213].

2. Rinse the capillary for 2 min with water (pressure 950 mbar).
3. Condition the capillary by flushing with separation buffer for 4 min (pressure 50 mbar)
4. Inject the sample at cathode for 12 s at 50 mbar
5. CE conditions: voltage: 25 kV (reversed polarity); detection: 195, 220 and 270 nm; temperature: 25 °C; buffer: 50 mM sodium phosphate buffer, pH 2.5.
6. Figure 1 shows the electropherograms relative to the analysis of dextran 1000 oligosaccharide derivatized with ANTS.

3.1.2 Derivatization of Sugars by Conversion to Glycosylamines and Reaction with N-Fluorenyl-Methiloxycarbonyl (Fmoc) Chloride

1. Conversion of glucose, galactose, and lactose in the corresponding glycosylamines: dissolve the reducing sugar (0.2 M) in an aqueous solution containing ammonia (16 M) and ammonium hydrogen carbonate (0.2 M). Leave the mixture for 36 h at 42 °C [199] (*see* **Note 2**).
2. Derivatization of glycosylamines with Fmoc: prepare 5 mL of a solution containing 0.1 mmol of glycosylamine in saturated aqueous sodium hydrogen carbonate; add this solution to 5 mL of Fmoc-Cl (0.4 mmol) in dioxane; stir the resulting

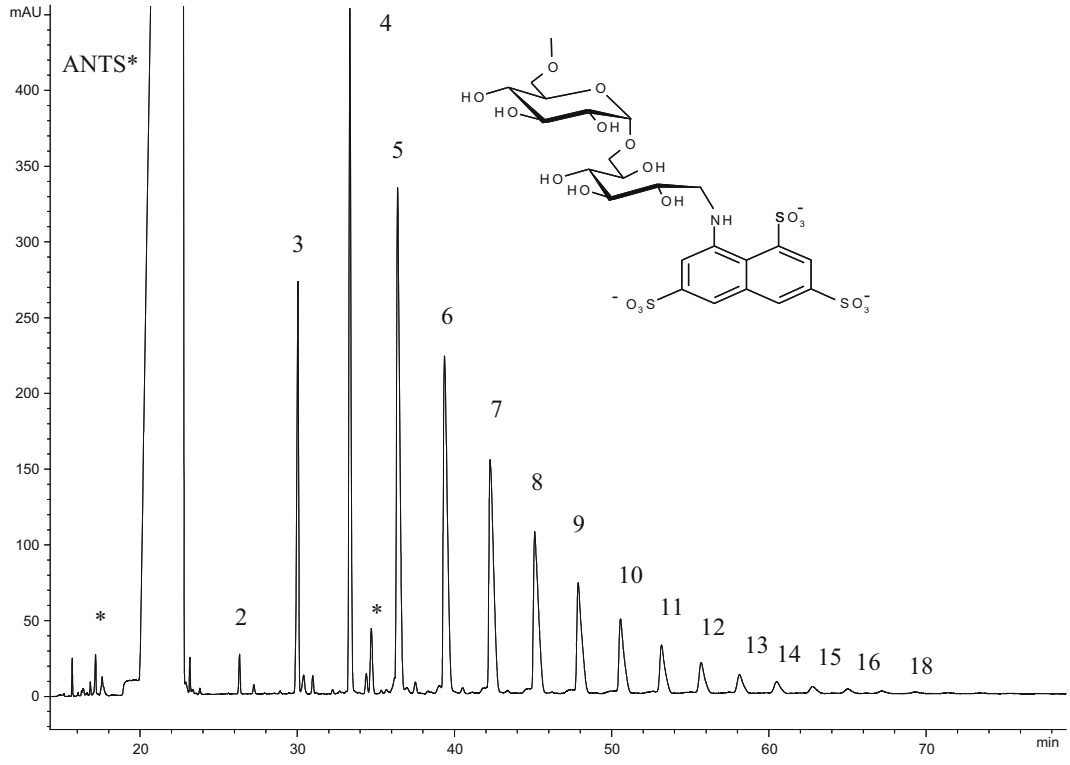

Fig. 1 CZE–UV analysis of dextran 1000 derivatized with ANTS (7.5 mg/mL); buffer: 50 mM phosphate pH 2.5; voltage: 25 kV (reversed polarity); wavelength: 220 nm (reprinted with permission from *J Chromatogr A* 1149, 38-45, Copyright Elsevier [213])

mixture overnight at ambient temperature. Load the sample on a C18 cartridge conditioned in water, wash it with water to remove salt and reducing carbohydrates, and then with methanol to recover the condensation product (*see* **Note 3**).

3. Rinse the capillary for 2 min with a 0.1 N NaOH solution at a vacuum pressure of 67.6 kPa.
4. Condition the capillary by flushing with separation buffer for 4 min at a vacuum pressure of 67.6 kPa.
5. Inject the sample under vacuum at a pressure of 16.9 kPa for 1.5 s.
6. CE conditions: voltage: 20 kV; detection: 260 nm at the cathode; temperature: 30 °C; buffer: 20 mM borax + 25 mM SDS, pH 9.2.
7. Figure 2 shows the electropherograms relative to the analysis of glucose, galactose, and lactose converted in the corresponding glycosylamines and derivatized with Fmoc (*see* **Note 4**).
8. Fmoc removal: keep the solution of glycosylamine-Fmoc (0.2 mmol, 20 mL) in 15% ammonia overnight at ambient temperature. Filter (Nylon, 0.45 μm), concentrate and freeze-dry the resulting mixture.
9. Recovery of the starting reducing sugar: glycosylamines are hydrolyzed with 2% aqueous acetic acid solution (2 mL) at 65 °C for 2 days.
10. An alternative nondestructive derivatization of carbohydrates based on the formation of glycosylamines is reported in **Note 5**.

3.2 Analysis of Underivatized Sugars

3.2.1 Use of Borate-Based Separation Buffers for Glycosides (Identification of Anomeric Forms of O-and C-Allyl Glycosides)

1. Wash for 2 min the capillary at a vacuum pressure of 67.6 kPa with NaOH 0.1 N.
2. Condition for 2 min the capillary by flushing the working buffer under a vacuum pressure of 67.6 kPa.
3. Load the samples under vacuum at a pressure of 16.9 kPa for 1.5 s.
4. CE conditions: voltage: 15 kV; detection: 195 nm at the cathode; temperature: 30 °C; buffer for *C*-allyl-glycosides: 100 mM borax + 100 mM SDS (pH 9.2); buffer for *O*-allyl-glycosides: 25 mM borax + 250 mM SDS (pH 9.2).
5. Figure 3 shows the electropherograms relative to a mixture of α-and β-*C*-allyl glucopyranosides (a) and galactopyranosides (b) (*see* **Note 6**) diluted 1:10 with water before injection in the CE system.
6. Figure 4 reports the results of the electrophoretic analysis of α- and β-*O*-allyl-galactopyranosides and α- and β-*O*-allyl-glucopyranosides (4.5–5 mM).
7. The presence of borate and SDS in the separation buffer improved both separation selectivity and detection sensitivity (*see* **Notes 7** and **8**).

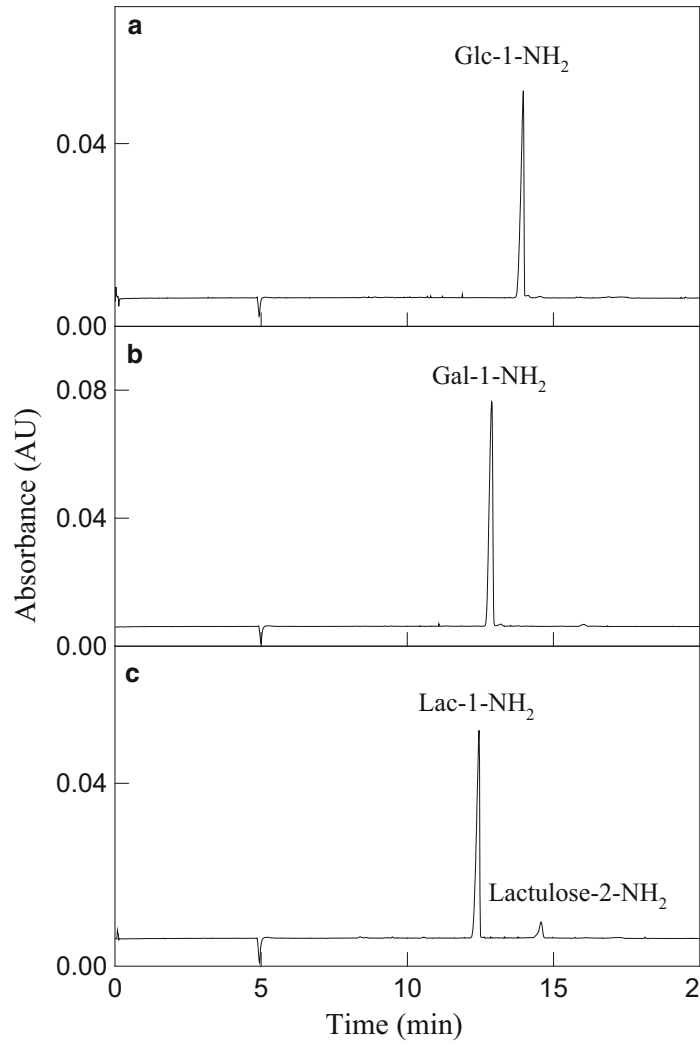

Fig. 2 MEKC-UV of: (**a**) glucose (0.8 mg/mL); (**b**) galactose (1.26 mg/mL); (**c**) lactose (1.0 mg/mL), all converted in glycosylamines and derivatized with Fmoc. Operative conditions: voltage: 20 kV; detection at 260 nm (cathode); temperature: 30 °C; buffer: 20 mM borax + 25 mM SDS, pH 9.2 (reprinted with permission from *J Carbohydr Chem* 20, 263-273, Copyright CRC Press [199])

3.3 CZE-UV of Unsaturated, Underivatized Acidic Sugars Released from Alginates

1. Wash the capillary for 2 min with 0.1 M NaOH and subsequently with buffer for 4 min (vacuum pressure, 67.6 kPa).
2. Load sample under vacuum at a pressure of 16.9 kPa (1.5 s).
3. CE conditions: voltage, 15 kV; detection, 232 nm (at cathode); temperature, 27 °C; buffer, 50 mM tetraborate (pH 9.2).
4. Figure 5 shows the CE analysis of underivatized alginate oligomers released from alginate, after G-lyase digestion. Unsaturated tetramer and dimer were the major constituents of the hydrolysis mixture; this result confirmed that AlgE4 works by a processive mode of action [184].

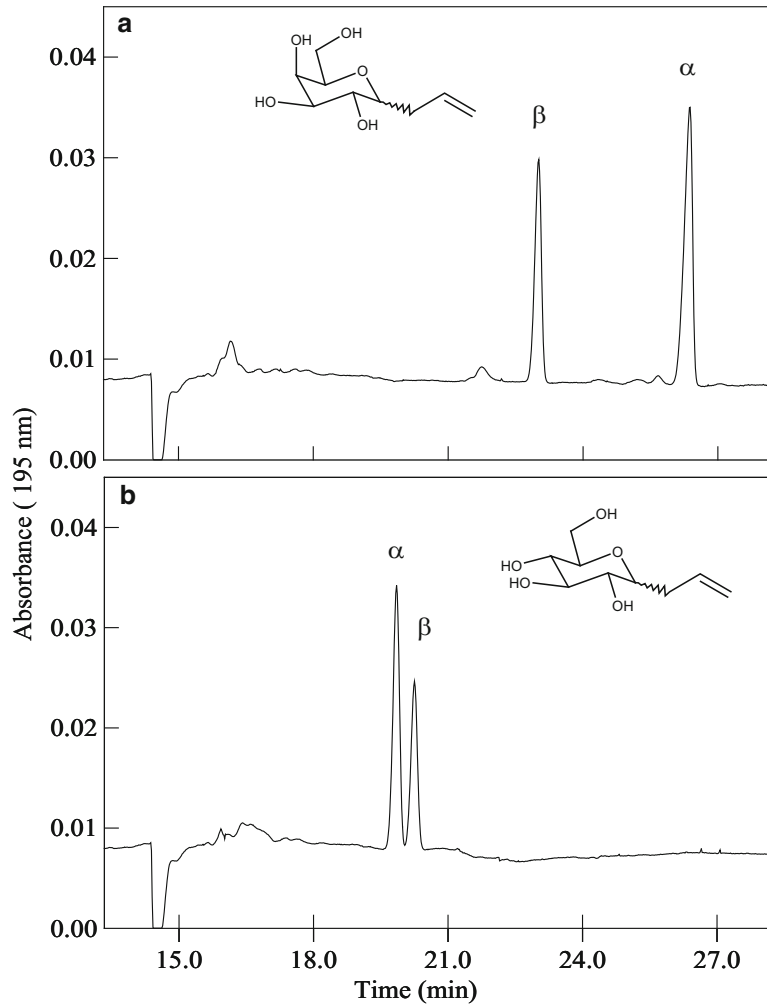

Fig. 3 MEKC-UV analysis of *C*-allyl-galactopyranosides (panel **a**) and *C*-allyl-glucopyranosides (panel **b**) anomeric mixtures from crude synthesis mixtures diluted 1:5 with water. Operative conditions: voltage: 15 kV; detection: 195 nm at the cathode; temperature: 30 °C; buffer: 100 mM borax + 100 mM SDS pH 9.2 (*see* **Note 6**) (Figure content selected with permission from Figs. 1 and 2 of the following article: Rossi M., Campa C., Gamini A. et al., (2006) *J Chromatogr A* 1110, 125–132, Copyrights Elsevier [226])

4 Notes

1. Procedure for the synthesis of *C*-allyl-galactospyranoside and *C*-allyl-glucopyranoside anomeric couples: glucose or galactose pentaacetate (1 mmol) in dichloroethane (2 mL) with allyl trimethylsilane (5 EQ) and boron trifluoride diethyl ether-

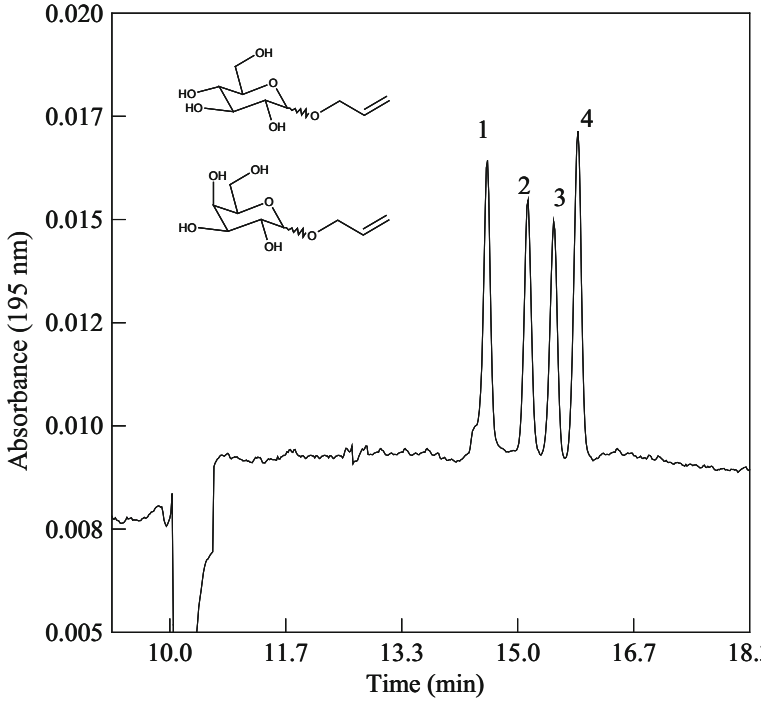

Fig. 4 MEKC-UV analysis of a mixture of 5 mM *O*-allyl-α-glucopyranoside (1), 4.5 mM *O*-allyl-β-glucopyranoside (2) 4.5 mM *O*-allyl-β-galactopyranoside (3) and 5 mM *O*-allyl-α-galactopyranoside (4). Operative conditions: voltage: 15 kV; detection: 195 nm at the cathode; temperature: 30 °C; buffer: 25 mM borax + 250 mM SDS, pH 9.2 (Figure content reproduced with permission from Fig. 6 of the following article: Rossi M., Campa C., Gamini A. et al., (2006) *J Chromatogr A* 1110, 125–132, Copyrights Elsevier [226])

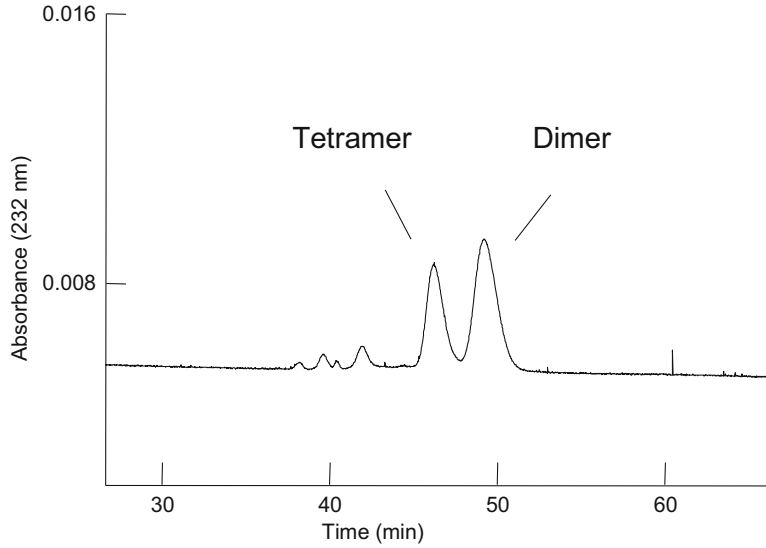

Fig. 5 CE analysis of underivatized, unsaturated alginate oligomers released from 47 % GulA alginate after G-lyase digestion. Operative conditions: buffer: 50 mM sodium tetraborate (pH 9.2); voltage: 15 kV; UV detection: 232 nm; temperature: 27 °C (reproduced with permission, from Campa, C., Holtan, S., Nilsen, et al. (2004), *Biochem J*, 381, 155–164. Copyrights The Biochemical Society) [184]

ate (5 EQ) were heated at 60 °C overnight. After extraction and purification with flash chromatography, the products were deacetylated in methanol solution (5 mL) with 2 mL of 0.5 M sodium methoxide overnight under reflux (all reagents from Sigma, St. Louis, MO, USA) [226].

2. Glycosylamines are readily hydrolyzed in neutral or weakly acidic solutions [199, 223]. The pH of the reactions in which glycosylamines are involved should not be comprised in this range, in order to avoid the formation of the starting reducing sugars.
3. Typically, the yield of the synthesis of glycosylamines is 75% [199]. Considering that subsequent reaction with Fmoc is quantitative, the value of the yield of the overall derivatization procedure is 75%. Careful calibration with standard amounts of sugars must be carried out for a reliable quantitative analysis.
4. The presence of lactulosylamine-Fmoc (Fig. 2, panel c) is originated by the isomerization of lactose in the highly alkaline conditions in which glycosylamines are synthesized [199].
5. Another convenient nondestructive derivatization of carbohydrates is formation of *N*-(2-pyridinyl)-glycosylamines with the use of 2-aminopyridine (2-AP, structure in Table 2) (λ_{max} = 240 nm). This reaction gives rise to UV-detectable glycosylamines: sugar (10 mg) is dissolved in 500 μL of aqueous 2-AP solution at pH 7 (prepared by dissolving 1 g of 2-AP in 0.8 mL 6 N HCl and 1.6 mL of water) at 65 °C for 10 h [200, 221]. The regeneration of the original sugars is an acidic hydrolysis with 2% aqueous acetic acid solution (2 mL) at 65 °C for 2 days.
6. The attribution of the peaks was possible by comparing the migration times obtained with the analysis of a solution containing 95% of α-anomer and 5% of β-anomer; this was achieved by simply performing the synthesis in acetonitrile instead of dichloroethane (*see* **Note 2**).
7. Comparison between the results obtained using borate-based buffers and acetate-based buffers (195 nm) demonstrated that complexation of glycosides with borate implies an increase in UV response of two times for glucosides and four times for galactosides. This different behavior reflects the different stabilities of the borate complexes for galactosides and glucosides [75].
8. The peculiar behavior of the galactoside and glucoside anomeric couples can be attributed to the various stabilities of borate–glycoside complexes as well as to the interaction with SDS micelles.

Acknowledgements

We wish to express our thanks to prof. Sergio Paoletti and his research group (Dipartimento di Scienze della Vita, University of Trieste) for introducing us to the wonders of glycobiology and we gratefully thank prof. Gudmund Skjåk Bræk and his research group (University of Science and Technology NTNU, Trondheim, Norway) for giving us the opportunity to discover the world of alginates.

References

1. McNaught AD (1997) Nomenclature of carbohydrates (recommendations 1996). Carbohydr Res 297:1–90
2. Varki A, Cummings R, Esko J et al (eds) (1999) Essentials of glycobiology, Cold Spring Laboratory Press, NY (available online in the Bookshelf of the PubMed site http://www.ncbi.nlm.nih.gov/entrez/query.fcgi)
3. Lindhorst TK (2000) Essentials of carbohydrate chemistry and biochemistry. Wiley-VCH, Wheinheim
4. Angata T, Varki A (2002) Chemical diversity in sialic acids and related α-keto acids: an evolutionary perspective. Chem Rev 102:439–469
5. Mechref Y, Novotny MV (2002) Structural investigations of glycoconjugates at high sensitivity. Chem Rev 102:321–369
6. Lindahl U, Lidholt K, Spillmann D et al (1994) More to "heparin" than anticoagulation. Thromb Res 75:1–32
7. Venkataraman G, Shriver Z, Raman R et al (1999) Sequencing complex polysaccharides. Science 286:537–542
8. Theocaris AD, Theocaris DA (2002) High-performance capillary electrophoretic analysis of hyaluronan and galactosaminoglycan-disaccharides in gastrointestinal carcinomas. Differential disaccharide composition as a possible tool-indicator for malignances. Biomed Chromatogr 16:157–161
9. Alberts B, Johnson A, Lewis J et al (2002) Molecular biology of the cell, 4th edn. Garland Publishing, New York (available online in the Bookshelf of the PubMed site http://www.ncbi.nlm.nih.gov/entrez/query.fcgi)
10. Dong X, Xi X, Han F et al (2001) Determination of sialic acids in the serum of cancer patients by capillary electrophoresis. Electrophoresis 22:2231–2235
11. Ciotczyk-Wierzbicka D, Gil D, Hoja-Lukowicz D et al (2002) Carbohydrate moieties of N-cadherin from human melanoma cell lines. Acta Biochim Polon 49:991–998
12. Giri TK, Thakur D, Alexander A et al (2012) Alginate based hydrogel as a potential biopolymeric carrier for drug delivery and cell delivery systems: present status and applications. Curr Drug Deliv 9:539–555
13. Draget KI, Strand B, Hartmann M et al (2000) Ionic and acid gel formation of epimerised alginates; the effect of AlgE4. Int J Biol Macromol 27:117–122
14. Donati I, Gamini A, Skjåk Bræk G et al (2003) Determination of the diadic composition of alginate by means of circular dichroism: a fast and accurate improved method. Carbohydr Res 338:1139–1142
15. Garate A, Murua A, Orive G et al (2012) Stem cells in alginate bioscaffolds. Ther Deliv 6:761–774
16. Linhardt RJ, Pervin A (1996) Separation of negatively charged carbohydrates by capillary electrophoresis. J Chromatogr A 720:323–335
17. Volpi N (ed) (2011) Capillary electrophoresis of carbohydrates: from monosaccharides to complex polysaccharides. Humana Press
18. Lamari F, Karamanos NK (1999) High performance capillary electrophoresis as a powerful analytical tool of glycoconjugates. J Liq Chrom & Rel Technol 22:1295–1317
19. Koketsu M, Linhardt RJ (2000) Electrophoresis for the analysis of acidic oligosaccharides. Anal Biochem 283:136–145
20. Mao W, Thanawiroon C, Linhardt RJ (2002) Capillary electrophoresis for the analysis of glycosaminoglycans and glycosaminoglycan-derived oligosaccharides. Biomed Chromatogr 16:77–94
21. El Rassi Z (ed) (2002) Carbohydrate analysis by modern chromatography and electrophoresis. Journal of Chromatography Library, vol 66, Elsevier, Amsterdam
22. Bleton J, Mejanelle P, Sansoulet J et al (1996) Characterization of neutral sugars and uronic acids after methanolysis and trimethylsi-

lylation for recognition of plant gums. J Chromatogr A 720:27–49
23. Heyraud A, Leonard C (1991) Analysis of oligouronates by reversed-phase ion-pair HPLC: role of the mobile phase. Carbohydr Res 215:105–115
24. Knutsen SH, Sletmoen M, Kristensen T et al (2001) A rapid method for the separation and analysis of carrageenan oligosaccharides released by iota- and kappa-carrageenase. Carbohydr Res 331:101–106
25. Cataldi TRI, Campa C, Margiotta G et al (1998) Role of barium ions in the anion-exchange chromatographic separation of carbohydrates with pulsed amperometric detection. Anal Chem 70:3940–3945
26. Cataldi TRI, Campa C, Angelotti M et al (1999) Isocratic separations of closely- related mono- and disaccharides by high- performance anion-exchange chromatography with pulsed amperometric detection using dilute alkaline spiked with barium acetate. J Chromatogr A 855:539–550
27. Okatch H, Torto N, Armateifio J (2003) Characterisation of legumes by enzymatic hydrolysis, microdialysis sampling, and micro-high-performance anion-exchange chromatography with electrospray ionisation mass spectrometry. J Chromatogr A 992:67–74
28. Karlsson NG, Schulz BL, Packer NH (2004) Structural determination of neutral O-linked oligosaccharide alditols by negative ion LC-Electrospray-MS^n. J Am Soc Mass Spectrom 15:659–672
29. Todoroki K, Hayama T, Ijiri S et al (2004) Rhodamine B amine as a highly sensitive fluorescence derivatization reagent for saccharides in reversed-phase liquid chromatography. J Chromatogr A 1038:113–120
30. Bhattacharyya L, Rohrer JS (eds) (2012) Applications of ion chromatography for pharmaceutical and biological products. Wiley, New York
31. Rizelio VM, Tenfen L, Silveira R et al (2012) Development of a fast capillary electrophoresis method for determination of carbohydrates in honey samples. Talanta 93:62–66
32. Kitagawa H, Kinoshita A, Sugahara K (1995) Microanalysis of glycosaminoglycan- derived disaccharides labelled with the fluorophore 2-aminoacridone by capillary electrophoresis and high- performance liquid chromatography. Anal Biochem 232:114–121
33. Ferro V, Li C, Fewings K et al (2002) Determination of the composition of the oligosaccharide phosphate fraction of *Pichia (Hansenula) holstii* NRRL Y-2448 phosphomannan by capillary electrophoresis and HPLC. Carbohydr Res 337:139–146
34. Soga T (2002) Analysis of carbohydrates in food and beverages by HPLC and CE. In: El Rassi Z (ed) Carbohydrate analysis by modern chromatography and electrophoresis. Journal of Chromatography Library, vol 66, Elsevier, Amsterdam, pp 483–502
35. Campa C, Oust A, Skjåk Bræk G et al (2004) Determination of average degree of polymerisation and distribution of oligosaccharides in a partially acid- hydrolysed homopolysaccharide: a comparison of four experimental methods applied to mannuronan. J Chromatogr A 1026:271–281
36. Smits HP, Cohen A, Buttler T et al (1998) Cleanup and analysis of sugar phosphates in biological extracts by using solid-phase extraction and anion- exchange chromatography with pulsed amperometric detection. Anal Biochem 261:36–42
37. Cataldi TRI, Campa C, Casella IG (1999) Study of sugar acids separation by high-performance anion- exchange chromatography- pulsed amperometric detection using alkaline eluents spiked with Ba^{2+}, Sr^{2+}, or Ca^{2+} as acetate or nitrate salts. J Chromatogr A 848:71–81
38. Cataldi TRI, Campa C, De Benedetto GE (2000) Carbohydrate analysis by high-performance anion-exchange chromatography with pulsed amperometric detection: the potential is still growing. Fresenius J Anal Chem 368:739–758
39. Roher JS (2000) Analyzing sialic acids using high- performance anion-exchange chromatography with pulsed amperometric detection. Anal Biochem 283:3–9
40. Yang Z, Li Z, Zhu J et al (2010) Use of different buffers for detection and separation in determination of physio-active components in oolong tea infusion cy CZE with amperometric detection. J Sep Sci 33:1312–1318
41. El Rassi Z (1997) Recent developments in capillary electrophoresis of carbohydrate species. Electrophoresis 18:2400–2407
42. Soga T, Imaizumi M (2001) Capillary electrophoresis method for the analysis of inorganic anions, organic acids, amino acids, nucleotides, carbohydrates and other anionic compounds. Electrophoresis 22:3418–3425
43. Cebolla-Cornejo J, Valcárcel M, Herrero-Martínez JM et al (2012) High efficiency joint CZE determination of sugars and acids in vegetables and fruits. Electrophoresis 33:2416–2423
44. Soga T, Heiger DN (1998) Simultaneous determination of monosaccharides in glycoproteins by capillary electrophoresis. Anal Biochem 261:73–78

45. Yeung ES, Kuhr WG (1991) Indirect detection methods for capillary separations. Anal Chem 63:275A–282A
46. Mittermayr S, Bones J, Doherty M et al (2011) Multiplexed analytical glycomics: rapid and confident IgG *N*-glycan structural elucidation. J Proteome Res 10:3820–3829
47. Adamczyk B, Tharmalingam-Jaikaran T, Schomberg M et al (2014) Comparison of separation techniques for the elucidation of IgG *N*-glycans pooled from healthy mammalian species. Carbohyd Res 389:174–185
48. Suzuki S (2013) Recent developments in liquid chromatography and capillary electrophoresis for the analysis of glycoprotein glycans. Anal Sci 29:1117–1128
49. Sarazin C, Delaunay N, Costanza C et al (2011) New avenue for mid-UV-range of underivatized carbohydrates and amino acids in capillary electrophoresis. Anal Chem 83:7381–7387
50. Bergholdt A, Overgaard J, Colding A (1993) Separation of D-galactonic and D-gluconic acids by capillary zone electrophoresis. J Chromatogr 644:412–415
51. Lu B, Westerlund D (1996) Indirect UV detection of carbohydrates in capillary zone electrophoresis by using tryptophan as a marker. Electrophoresis 17:325–332
52. Lee Y-H, Lin T-I (1996) Determination of carbohydrates by high-performance capillary electrophoresis with indirect absorbance detection. J Chromatogr B 681:87–97
53. Stroka J, Dossi N, Anklam E (2003) Determination of the artificial sweetener sucralose by capillary electrophoresis. Food Addit Contam 20:524–527
54. Andersen KE, Bjergegaard C, Møller P et al (2003) High-performance capillary electrophoresis with indirect UV detection for determination of alpha-galactosides in Leguminosae and Brassicaceae. J Agric Food Chem 51:6391–6397
55. Damm JB, Overklift GT (1994) Indirect UV detection as a non-selective detection method in the qualitative and quantitative analysis of heparin fragments by high-performance capillary electrophoresis. J Chromatogr A 678:151–165
56. Paulus A, Klockow A (1996) Detection of carbohydrates in capillary electrophoresis. J Chromatogr A 720:353–376
57. Buscher BAP, Tjaden UR, Irth H, Andersson EM et al (1995) Determination of 1,2,6-inositol triphosphate (derivatives) in plasma using iron(III)-loaded adsorbents and capillary zone electrophoresis-(indirect) UV detection. J Cromatogr A 718:413–419
58. Ye J, Baldwin RP (1993) Amperometric detection in capillary electrophoresis with normal size electrodes. Anal Chem 65:3525–3527
59. Baldwin R.P. (2002) Electrochemical detection of carbohydrates at constant potential after HPLC and CE separations, in *Carbohydrate analysis by modern chromatography and electrophoresis* (El Rassi, Z.,ed.), Journal of Chromatography Library, Vol. 66, Elsevier, Amsterdam, pp. 947-959.
60. Kitagawa F, Otsuka K (2014) Recent applications of on-line sample preconcentration techniques in capillary electrophoresis. J Chromatogr A 1335:43–60
61. Bahga SS, Santiago JG (2013) Coupling isotachophoresis and capillary electrophoresis: a review and comparison of methods. Analyst 138:735–754
62. Lamari FN, Kuhn R, Karamanos NK (2003) Derivatization of carbohydrates for chromatographic, electrophoretic and mass spectrometric structure analysis. J Chromatogr B 793:15–36
63. Thibault P, Honda S (eds) (2003) Capillary electrophoresis of carbohydrates, vol 213, Methods in molecular biology series. Humana Press, Totowa, NJ
64. El Rassi Z (1996) High performance capillary electrophoresis of carbohydrates. Beckman Instruments, Fullerton, CA
65. Novotny M, Sudor J (1993) High-performance capillary electrophoresis of glycoconjugates. Electrophoresis 14:373–389
66. Zhao J, Hu D, Lao K et al (2014) Advance of CE and CEC in phytochemical analysis (2012-2013). Electrophoresis 35:205–224
67. Ruhaak LR, Zauner G, Huhn C et al (2010) Glycan labeling strategies and their use in identification and quantification. Anal Bioanal Chem 397:3457–3481
68. Suzuki S, Honda S (1998) A tabulated review of capillary electrophoresis of carbohydrates. Electrophoresis 19:2539–2560
69. Volpi N, Maccari F (eds) (2013) Capillary electrophoresis of biomolecules: methods and protocols. Methods in Molecular Biology, vol 984, Humana Press
70. Baldwin RP (1999) Electrochemical determination of carbohydrates: enzyme electrodes and amperometric detection in liquid chromatography and capillary electrophoresis. J Pharm Biomed Anal 19:69–81
71. Raju TS (2000) Electrophoretic methods for the analysis of *N*-linked oligosaccharides. Anal Biochem 283:125–132
72. El Rassi Z (2002) Capillary electrophoresis and electrochromatography of carbohydrates. In El Rassi Z (ed) Carbohydrate analysis by

modern chromatography and electrophoresis. Journal of Chromatography Library, vol 66, Elsevier, Amsterdam, pp 597–676
73. Honda S, Suzuki S, Taga A (2003) Analysis of carbohydrates as 1-phenyl-3-methyl-5--pyrazolone derivatives by capillary/microchip electrophoresis and capillary electrochromatography. J Pharm Biomed Anal 30:1689–1714
74. Honda S, Iwase S, Makino A et al (1989) Simultaneous determination of reducing monosaccharides by capillary zone electrophoresis as the borate complexes of N-2-pyridylglycamines. Anal Biochem 176:72–77
75. Hoffstetter-Kuhn S, Paulus A, Gassmann E et al (1991) Influence of borate complexation on the electrophoretic behaviour of carbohydrates in capillary electrophoresis. Anal Chem 63:1541–1547
76. Honda S, Suzuki S, Nose A et al (1991) Capillary zone electrophoresis of reducing mono- and oligo-saccharides as the borate complexes of their 3-methyl-1-phenyl-2--pyrazolin-5-one derivatives. Carbohydr Res 215:193–198
77. Honda S, Yamamoto F, Suzuki S et al (1991) High-performance capillary zone electrophoresis of carbohydrates in the presence of alkaline earth metal ions. J Chromatogr 588:327–333
78. Oefner PJ, Vorndran AE, Grill E et al (1992) Capillary zone electrophoretic analysis of carbohydrates by direct and indirect UV detection. Chromatographia 34:308–316
79. Arentoft AM, Michaelsen S, Sørensen H (1993) Determination of oligosaccharides by capillary zone electrophoresis. J Chromatogr A 652:517–524
80. Stefansson M, Westerlund D (1993) Capillary electrophoresis of glycoconjugates in alkaline media. J Chromatogr 632:195–200
81. Morin P, Villard F, Dreux M (1993) Separation of flavonoid-7-O-glycosides differing in their flavonoid aglycone. J Chromatogr 628:153–160
82. Morin P, Villard F, Dreux M et al (1993) Separation of flavonoid-3-O-glycosides differing in their sugar moiety. J Chromatogr 628:161–169
83. Chiesa C, Horváth C (1993) Capillary zone electrophoresis of malto-oligosaccharides derivatized with 8-aminonaphtalene-1,3,6-trisulfonic acid. J Chromatogr 645:337–352
84. Schwaiger H, Oefner PJ, Huber C et al (1994) Capillary electrophoresis and micellar electrokinetic chromatography of 4-aminobenzonitrile carbohydrate derivatives. Electrophoresis 15:941–952
85. Penn SG, Chiu RW, Monnig CA (1994) Separation and analysis of cyclodextrins by capillary electrophoresis with dynamic fluorescence labelling and detection. J Chromatogr A 680:233–241
86. Evangelista RA, Liu M-S, Chen F-TA (1995) Characterization of 9-Aminopyrene-1,4,6-trisulfonate- derivatized sugars by capillary electrophoresis with laser-induced fluorescence detection. Anal Chem 67:2239–2245
87. Chen FA, Evangelista RA (1995) Analysis of mono- and oligosaccharide isomers derivatized with 9-aminopyrene-1,4,6-trisulfonate by capillary electrophoresis with laser-induced fluorescence. Anal Biochem 230:273–280
88. Noe CR, Freissmuth J (1995) Capillary zone electrophoresis of aldose enantiomers: separation after derivatization with S-(–)-1-phenylethylamine. J Chromatogr A 704:503–512
89. Xu X, Kok WT, Poppe H (1995) Sensitive determination of sugars by capillary zone electrophoresis with indirect UV detection under highly alkaline conditions. J Chromatogr A 716:231–240
90. Liu Y, Shu C, Lamb JD (1997) High-performance capillary electrophoretic separation of carbohydrates with indirect UV detection using diethylamine and borate as electrolyte additives. J Capillary Electrophor 4:97–103
91. Nguyen DT, Lerch H, Zemann A et al (1997) Separation of derivatized carbohydrates by co-electroosmotic capillary electrophoresis. Chromatographia 46:113–121
92. Plocek J, Chmelik J (1997) Separation of disaccharides as their borate complexes by capillary electrophoresis with indirect detection in visible range. Electrophoresis 18:1148–1152
93. Honda S, Taga A, Kotani M et al (1997) Separation of aldose enantiomers by capillary electrophoresis in the presence of optically active N-dodecoxycarbonylvalines. J Chromatogr A 792:385–391
94. Sato K, Sato K, Okubo A et al (1997) Determination of monosaccharides derivatized with 2-aminobenzoic acid by capillary electrophoresis. Anal Biochem 251:119–121
95. Sato K, Sato K, Okubo A et al (1998) Optimization of derivatization with 2-aminobenzoic acid for determination of monosaccharide composition by capillary electrophoresis. Anal Biochem 262:195–197
96. Akiyama T, Yamada T, Maitani T (2000) Analysis of enzymatically glucosylated flavonoids by capillary electrophoresis. J Chromatogr A 895:279–283

97. Li DT, Sheen JF, Her GR (2000) Structural analysis of chromophore-labeled disaccharides by capillary electrophoresis tandem mass spectrometry using ion trap mass spectrometry. J Am Soc Mass Spectrom 11:292–300
98. Taga A, Suzuki S, Honda S (2001) Capillary electrophoretic analysis of carbohydrates derivatized by in-capillary condensation with 1-phenyl-3-methyl-5-pyrazolone. J Chromatogr A 911:259–267
99. Larsson M, Sundberg R, Folestad S (2001) On-line capillary electrophoresis with mass spectrometry detection for the analysis of carbohydrates after derivatization with 8-aminonaphtalene-1,3,6- trisulfonic acid. J Chromatogr A 934:75–85
100. Tuma P, Málková K, Samcová E et al (2011) Rapid monitoring of mono- and disaccharides in drinks, foodstuffs and foodstuff additives by capillary electrophoresis with contactless conductivity detection. Anal Chim Acta 698:1–5
101. Liu J, Shirota O, Wiesler D et al (1991) Ultrasensitive fluorometric detection of carbohydrates as derivatives in mixtures separated by capillary electrophoresis. Proc Nat Acad Sci U S A 88:2302–2306
102. Mechref Y, El Rassi Z (1994) Capillary zone electrophoresis of derivatized acidic monosaccharides. Electrophoresis 15:627–634
103. Mechref Y, Ostrander GK, El Rassi Z (1997) Capillary electrophoresis of carboxylated carbohydrates IV. Adjusting the separation selectivity of derivatized carboxylated by controlling the electrolyte ionic strength at subambient temperature and in absence of electroosmotic flow. J Chromatogr A 792:75–82
104. Hauri DC, Shen P, Arkin AP et al (1997) Steady state measurements on the fructose 6-phosphate/fructose 1,6-bisphosphate interconversion cycle. J Phys Chem B 101:3872–3876
105. Schmitt-Kopplin P, Fischer K, Freitag D et al (1998) Capillary electrophoresis for the simultaneous separation of selected carboxylated carbohydrates and their related 1,4-lactones. J Chromatogr A 807:89–100
106. Soga T, Serwe M (2000) Determination of carbohydrates in food samples by capillary electrophoresis with indirect UV detection. Food Chem 69:339–344
107. Wiedmer SK, Cassely A, Hong M et al (2000) Electrophoretic studies of polygalacturonate oligomers and their interactions with metal ions. Electrophoresis 21:3212–3219
108. Soga T, Ueno Y, Naraoka H et al (2002) Simultaneous determination of anionic intermediates for *Bacillus subtilis* metabolic pathways by capillary electrophoresis electrospray ionization mass spectrometry. Anal Chem 74:2233–2239
109. Descroix S, Varenne A, Goasdou N et al (2003) Non-aqueous capillary electrophoresis of positional isomers of a sulphated monosaccharide. J Chromatogr A 987:467–476
110. Xia Y, Liang J, Yang B et al (2011) A new method for the quantitative determination of two uronic acids by CZE with direct UV detection. Biomed Chromatogr 25:1030–1037
111. Honda S, Makino A, Suzuki S et al (1990) Analysis of the oligosaccharides in ovalbumin by high-performance capillary electrophoresis. Anal Biochem 191:228–234
112. Liu J, Shirota O, Novotny M (1991) Capillary electrophoresis of amino sugars with laser-induced fluorescence detection. Anal Chem 63:413–417
113. Hermentin P, Doenges R, Witzel R et al (1994) A strategy for the mapping of N-glycans by high-performance capillary electrophoresis. Anal Biochem 221:29–41
114. Kakehi K, Susami A, Taga A et al (1994) High performance capillary electrophoresis of O-glycosidically linked sialic acid-containing oligosaccharides in glycoproteins as their alditol derivatives with low-wavelenght UV monitoring. J Chromatogr A 680:209–215
115. Camilleri P, Harland GB, Okafo G (1995) High resolution and rapid analysis of branched oligosaccharides by capillary electrophoresis. Anal Biochem 230:115–122
116. Weber PL, Lunte SM (1996) Capillary electrophoresis with pulsed amperometric detection of carbohydrates and glycopeptides. Electrophoresis 17:302–309
117. Evangelista RA, Chen FA, Guttman A (1996) Reductive amination of N-linked oligosaccharides using organic acid catalysis. J Chromatogr A 745:273–280
118. Guttman A, Chen FT, Evangelista RA et al (1996) High-resolution capillary gel electrophoresis of reducing oligosaccharides labelled with 1-aminopyrene-3,6,8-trisulfonate. Anal Biochem 233:234–242
119. Guttman A (1997) Analysis of monosaccharide composition by capillary electrophoresis. J Chromatogr A 763:271–277
120. Iwase H, Tanaka A, Hiky Y et al (1999) Mutual separation of hinge-glycopeptide isomers bearing five N-acetylgalactosamine residues from normal human serum immunoglobulin A1 by capillary electrophoresis. J Chromatogr B 728:175–183
121. Kakehi K, Funakubo T, Suzuki S et al (1999) 3-aminobenzamide and 3-aminobenzoic acid, tags for capillary electrophoresis of complex

carbohydrates with laser-induced fluorescent detection. J Chromatogr A 863:205–218
122. Huang Y, Mechref Y, Novotny M (2001) Microscale nonreductive release of O-linked glycans for subsequent analysis through MALDI mass spectrometry and capillary electrophoresis. Anal Chem 73:6063–6069
123. Gennaro LA, Delaney J, Vouros P et al (2002) Capillary electrophoresis/electrospray ion trap mass spectrometry for the analysis of negatively charged derivatized and underivatized glycans. Rapid Commun Mass Spectrom 16:192–200
124. Che F-Y, Shao X-X, Wang K-Y et al (1999) Characterization of derivatization of sialic acid with 2-aminoacridone and determination of sialic acid content in glycoproteins by capillary electrophoresis and high performance liquid chromatography- ion trap mass spectrometry. Electrophoresis 20:2930–2937
125. Strousopoulou K, Militsopoulou M, Stagiannis K et al (2002) A capillary zone electrophoresis method for determining N-acetylneuraminic acid in glycoproteins and blood sera. Biomed Chromatogr 16:146–150
126. Kakehi K, Kinoshita M, Hayase S et al (1999) Capillary electrophoresis of *N*-acetylneuraminic acid polymers and hyaluronic acid: correlation between migration order reversal and biological functions. Anal Chem 71:1592–1596
127. Shen Z, Warren CD, Newburg DS (2000) High-performance capillary electrophoresis of sialylated oligosaccharides of human milk. Anal Biochem 279:37–45
128. Taga A, Sugimura M, Suzuki S et al (2002) Estimation of sialic acid in a sialoglycan and a sialoglycoprotein by capillary electrophoresis with in-capillary sialidase digestion. J Chromatogr A 954:259–266
129. Cabálková J, Židková J, Přibyla L et al (2004) Determination of carbohydrates in juices by capillary electrophoresis, high-performance liquid chromatography, and matrix-assisted laser desorption/ionization-time of flight-mass spectrometry. Electrophoresis 25:487–493
130. Colón LA, Dadoo R, Zare RN (1993) Determination of carbohydrates by capillary zone electrophoresis with amperometric detection at a copper microelectrode. Anal Chem 65:476–481
131. Chen M-C, Huang H-J (1997) Application of a nickel-microelectrode-incorporated end-column detector for capillary electrophoretic determination of alditols and alcohols. Anal Chim Acta 341:83–90
132. Zemann A, Nguyen DT, Bonn G (1997) Fast separation of underivatized carbohydrates by coelectroosmotic capillary electrophoresis. Electrophoresis 18:1142–1147
133. Klampfl CW, Buchberger W (2001) Determination of carbohydrates by capillary electrophoresis with electrospray-mass spectrometric detection. Electrophoresis 22:2737–2742
134. Carvalho AZ, da Silva JA, do Lago CL (2003) Determination of mono- and disaccharides by capillary electrophoresis with contactless conductivity detection. Electrophoresis 24:2138–2143
135. Gel-Moreto N, Streich R, Galensa R (2003) Chiral separation of diastereomeric flavanone-7-O-glycosides in citrus by capillary electrophoresis. Electrophoresis 24:2716–2722
136. Simonet BM, Rios A, Grases F et al (2003) Determination of myo-inositol phosphates in food samples by flow injection-capillary zone electrophoresis. Electrophoresisis 24:2092–2098
137. Schmid D, Behnke B, Metzger J et al (2002) Nano-HPLC- mass spectrometry and MEKC for the analysis of oligosaccharides from human milk. Biomed Chromatogr 16:151–156
138. Zamfir A, Peter-Katalinic J (2004) Capillary electrophoresis-mass spectrometry for glycoscreening in biomedical research. Electrophoresis 25:1949–1963
139. Kamoda S, Kakehi K (2008) Evaluation of glycosylation for quality assurance of antibody pharmaceuticals by capillary electrophoresis. Electrophoresis 29:3595–3604
140. Wang XY, Chen Y, Li Z et al (2002) Analysis of carbohydrates by capillary zone electrophoresis with on-capillary derivatization. J Liq Chrom & Rel Technol 25:589–600
141. Song JF, Weng MQ, Wu SM et al (2002) Analysis of neutral saccharides in human milk derivatized with 2-aminoacridone by capillary electrophoresis with laser-induced fluorescence detection. Anal Biochem 304:126–129
142. Jamali B, Nielsen HM (2003) Development and validation of a capillary electrophoresis-indirect photometric detection method for the determination of the non-UV-absorbing 1,4-dideoxy-1,4-imino-D-arabinitol in active pharmaceutical ingredients, solutions and tablets using an internal standard. J Chromatogr A 996:213–223
143. Kamoda S, Nomura C, Kinoshita M et al (2004) Profiling analysis of oligosaccharides in antibody pharmaceuticals by capillary electrophoresis. J Chromatogr A 1050:211–216

144. Beck A (ed) (2013) Glycosylation engineering of biopharmaceuticals: methods and protocols. Springer Science, New York
145. Mittermayr S, Guttman A (2012) Influence of molecular configuration and conformation on the electromigration of oligosacchardies in narrow bore capillaries. Electrophoresis 33:1000–1007
146. Guttman A (2013) Capillary electrophoresis in the N-glycosilation analysis of biopharmaceuticals. Trend Anal Chem 48:132–142
147. Szabo Z, Guttman A, Bones J et al (2012) Ultrasensitive capillary electrophoretic analysis of potentially immunogenic carbohydrate residues in biologics: galactose-α-1,3-galactose containing oligosaccharides. Mol Pharmaceutics 9:1612–1619
148. Kamoda S, Ishikawa R, Kakehi K (2006) Capillary electrophoresis wit laser-induced fluorescence detection for detailed studies on *N*-linked oligosaccharide profile of therapeutic recombinant monoclonal antibodies. J Chromatogr A 1133:332–339
149. Kerékgyártó M, Guttman A (2014) Toward the generation of an aminonaphthalene trisulfonate labeled *N*-glycan database for capillary gel electrophoresis analysis of carbohydrates. Electrophoresis. 35:2222–2228
150. Szabo Z, Guttman A, Karger BL (2010) Rapid release of N-linked glycans form glycoproteins by pressure-cycling technology. Anal Chem 82:2588–2593
151. Kang SH, Jung H, Kim N et al (2000) Micellar electrokinetic chromatography for the analysis of D-amigdalin and its epimer in apricot kernel. J Chromatogr A 866:253–259
152. Kenndler E, Schwer C, Fritsche B et al (1990) Determination of arbutin in uvae-ursi folium (bearberry leaves) by capillary zone electrophoresis. J Chromatogr 514:383–388
153. Oliver JD, Gaborieau M, Hilder EF et al (2013) Simple and robust determination of monosaccharides in plant fibers in complex mixtures by capillary electrophoresis and high performance liquid chromatography. J Chromatogr A 1291:179–186
154. Morin P, Dreux M (1993) Factors influencing the separation of ionic and non-ionic chemical natural compounds in plant extract by capillary electrophoresis. J Liq Chrom 16:3735–3755
155. Frias J, Price KR, Fenwick GR et al (1996) Improved method for the analysis of alpha-galactosides in pea seeds by capillary zone electrophoresis. Comparison with high-performance liquid chromatography-triple-pulsed amperometric detection. J Chromatogr A 719:213–219
156. Campa C, Schmitt-Kopplin P, Cataldi TRI et al (2000) Analysis of cyanogenic glycosides by micellar capillary electrophoresis. J Chromatogr B 739:95–100
157. Suomi J, Sirén H, Hartonen K et al (2000) Extraction of iridoid glycosides and their determination by micellar electrokinetic capillary chromatography. J Chromatogr A 868:73–83
158. Warren CR, Adams MA (2000) Capillary electrophoresis for the determination of major amino acids and sugar in foliage: application to the nitrogen nutrition of sclerophyllus species. J Exp Bot 51:1147–1157
159. Bianco G, Schmitt-Kopplin P, De Benedetto G et al (2002) Determination of glycoalkaloids and relative aglycones by nonaqueous capillary electrophoresis coupled with electrospray ionization-ion trap mass spectrometry. Electrophoresis 23:2904–2912
160. Suomi J, Wiedmer SK, Jussila M et al (2002) Analysis of eleven iridoid glycosides by micellar electrokinetic capillary chromatography (MECC) and screening of plant samples by partial filling (MECC)-electrospray ionisation mass spectrometry. J Chromatogr A 970:287–296
161. Seigler DS, Pauli GF, Nahrstedt A et al (2002) Cyanogenic allosides and glucosides from Passiflora edulis and Carica papaya. Phytochemistry 60:873–882
162. Marchart E, Kopp B (2003) Capillary electrophoretic separation and quantification of flavone-*O*- and *C*-glycosides in *Achillea setacea* W. et K. J Chromatogr B 792:363–368
163. Marchart E, Krenn L, Kopp B (2003) Quantification of the flavonoid glycosides in Passiflora incarnata by capillary electrophoresis. Planta Med 69:452–456
164. Kang SH (2003) On-line micellar electrokinetic chromatography-electrospray ionization mass spectrometry for the direct analysis of amygdalin epimers. Bull Korean Chem Soc 24:144–146
165. Andersen KE, Bjergegaard C, Sørensen H (2003) Analysis of reducing carbohydrates by reductive tryptamine derivatization prior to micellar electrokinetic capillary chromatography. J Agric Food Chem 51:7234–7239
166. Stefannson M, Novotny M (1994) Resolution of the branched forms of oligosaccharides by high-performance capillary electrophoresis. Carbohydr Res 258:1–9
167. Stefannson M, Novotny M (1994) Separation of complex oligosaccharide mixtures by capillary electrophoresis in the open-tubular format. Anal Chem 66:1134–1140
168. Rydlund A, Dahlman O (1996) Efficient capillary zone electrophoretic separation of

wood-derived neutral acidic mono- and oligosaccharides. J Chromatogr A 738:129–140
169. Monsarrat B, Brando T, Condouret P et al (1999) Characterization of mannooligosaccharide caps in mybacterial lipoarabinomannan by capillary electrophoresis/electrospray mass spectrometry. Glycobiology 9:335–342
170. Ludwiczak P, Brando T, Monsarrat B et al (2001) Structural characterization of *Mycobacterium tuberculosis* lipoarabinomannans by the combination of capillary electrophoresis and matrix-assisted laser desorption/ionization time of flight mass spectrometry. Anal Chem 73:2323–2330
171. Cescutti P, Campa C, Delben F et al (2002) Structure of the oligomers obtained by enzymatic hydrolysis of the glucomannan produced by the plant Amorphophallus konjac. Carbohydr Res 337:2505–2511
172. Carney SL, Osborne DJ (1991) Separation of chondroitin sulphate disaccharides and hyaluronan oligosaccharides by capillary zone electrophoresis. Anal Biochem 195:132–140
173. Michaelsen S, Schrøder M, Sørensen H (1993) Separation and determination of glycosaminoglycans disaccharides by micellar electrokinetic capillary chromatography for studies of pelt glycosaminoglycans. J Chromatogr A 652:503–515
174. Pervin A, Al-Hakim A, Linhardt RJ (1994) Separation of glycosaminoglycans-derived oligosaccharides by capillary electrophoresis using reverse polarity. Anal Biochem 221:182–188
175. Karamanos NK, Axelsson S, Vanky P et al (1995) Determination of hyaluronan and galactosaminoglycan disaccharides by high-performance capillary electrophoresis at the attomole level. Applications to analyses of tissue and cell culture proteoglycans. J Chromatogr A 696:295–305
176. Scapol L, Marchi E, Viscomi GC (1996) Capillary electrophoresis of heparin and dermatan sulphate unsaturated disaccharides with triethylamine and acetonitrile as electrolyte additives. J Chromatogr A 735:367–374
177. Karamanos NK, Hjerpe A (1997) High- performance capillary electrophoretic analysis of hyaluronan in effusions from human malignant mesothelioma. J Chromatogr B 697:277–281
178. Rydlund A, Dahlman O (1997) Rapid analysis of unsatured acidic xylooligosaccharides from kraft pulps using capillary electrophoresis. J High Resol Chromatogr 20:72–76
179. Ruiz-Calero V, Puignou L, Galceran MT (1998) Use of reversed and pressure gradient in the analysis of disaccharide composition of heparin by capillary electrophoresis. J Chromatogr A 828:497–508
180. Payan E, Presle N, Lapicque F et al (1998) Separation and quantification by ion- association capillary zone electrophoresis of unsaturated disaccharide units of chondroitin sulfates and oligosaccharides derived from hyaluronan. Anal Chem 70:4780–4786
181. Gunay NS, Linhardt RJ (2003) Capillary electrophoretic separation of heparin oligosaccharides under conditions amenable to mass spectrometric detection. J Chromatogr A 1014:225–233
182. Militsopoulou M, Lamari F, Karamanos NK (2003) Capillary electrophoresis: a tool for studying interactions of glycans/proteoglycans with growth factors. J Pharm Biomed Anal 32:823–828
183. Stöm A, Williams MAK (2004) On the separation, detection and quantification of pectin derived oligosaccharides by capillary electrophoresis. Carbohydr Res 399:1711–1716
184. Campa C, Holtan S, Nilsen N et al (2004) Biochemical analysis of the processive mechanism for epimerisation of alginate by mannuronan C-5 epimerase AlgE4. Biochem J 381:155–164
185. Duteil S, Gareil P, Girault S et al (1999) Identification of heparin oligosaccharides by direct coupling of capillary electrophoresis/ionspray-mass spectrometry. Rapid Commun Mass Spectrom 13:1889–1898
186. Ruiz-Calero V, Moyano E, Puignou L et al (2001) Pressure-assisted capillary electrophoresis- ion trap mass spectrometry for the analysis of heparin depolymerised disaccharides. J Chromatogr A 914:277–291
187. Zamfir A, Seidler DG, Kresse H et al (2002) Structural characterization of chondroitin/dermatan sulfate oligosaccharides from bovine aorta by capillary electrophoresis and electrospray ionization quadrupole time-of-flight tandem mass spectrometry. Rapid Commun Mass Spectrom 16:2015–2024
188. Kühn AV, Rüttinger HH, Neubert RHH et al (2003) Identification of hyaluronic acid oligosaccharides by direct coupling of capillary electrophoresis with electrospray ion trap mass spectrometry. Rapid Commun Mass Spectrom 17:576–582
189. Liu J, Shirota O, Novotny MV (1992) Sensitive, laser-assisted determination of complex mixtures separated by capillary gel electrophoresis at high resolution. Anal Chem 64:973–975
190. Honda S, Ueno T, Kakehi K (1992) High-performance capillary electrophoresis of unsaturated oligosaccharides derived from glycosaminoglycans by digestion with chon-

droitinase ABC as 1-phenyl-3-methy-5--pyrazolone derivatives. J Chromatogr 608:289–295
191. Sudor J, Novotny MV (1995) End-label, free-solution capillary electrophoresis of highly charged oligosaccharides. Anal Chem 67:4205–4209
192. Mort AJ, Chen EMW (1996) Separation of 8-aminonaphtalene-1,3,6-trisulfaste (ANTS)-labeled oligomers containing galacturonic acid by capillary electrophoresis: application to determining the substrate specificity of endopolygalacturonases. Electrophoresis 17:379–383
193. El Rassi Z, Postlewait J, Mechref Y et al (1997) Capillary electrophoresis of carboxylated carbohydrates III. Selective precolumn derivatization of glycosaminoglycan disaccharides with 7-aminonaphthalene-1,3-disulfonic acid fluorescing tag for ultrasensitive laser-induced fluorescence detection. Anal Biochem 244:283–290
194. Lamari F, Theocaris A, Hjerpe A et al (1999) Ultrasensitive capillary electrophoresis of sulfated disaccharides in chondroitin/dermatan sulfates by laser-induced fluorescence after derivatization with 2-aminoacridone. J Chromatogr B 730:129–133
195. Ruiz-Calero V, Puignou L, Galceran MT (2003) Determination of glycosaminoglycan monosaccharides by capillary electrophoresis using laser- induced fluorescence detection. J Chromatogr B 791:193–2002
196. Khandurina J, Blum D, Stege J et al (2004) Automated carbohydrate profiling by capillary electrophoresis: a bioindustrial approach. Electrophoresis 25:2326–2331
197. Zhang Y, Le X, Dovichi NJ et al (1995) Monitoring biosynthetic transformations of N-acetyllactosamine using fluorescently labelled oligosaccharides and capillary electrophoretic separation. Anal Biochem 227:368–376
198. Le X, Scaman C, Zhang Y et al (1995) Analysis by capillary electrophoresis-laser-induced fluorescence detection of oligosaccharides produced from enzyme reactions. J Chromatogr A 716:215–220
199. Campa C, Donati I, Vetere A et al (2001) Synthesis of glycosylamines: identification and quantification of side-products. J Carbohydr Chem 20:263–273
200. Campa C, Vetere A, Gamini A et al (2002) Enzymatic synthesis and characterization of oligosaccharides structurally related to the repeating unit of pullulan. Biochem Biophys Res Commun 297:382–389
201. Vetere A, Medeot M, Campa C et al (2003) High-yield enzymatic synthesis of O-allyl-β-D-galactopyranoside. J Mol Catal B Enzymatic 21:153–156
202. Sun B, Miller G, Lee WY et al (2013) Analytical method development for directed enzyme evolution research: a high throughput high-performance liquid chromatography method for analysis of ribose and ribitol and a capillary electrophoresis method for the separation of ribose enantiomers. J Chromatogr A 1271:163–169
203. Chang Y, Yang B, Zhao X (2012) Analysis of glycosaminoglycan-derived disaccharides by capillary electrophoresis using laser-induced fluorescence detection. Anal Biochem 427:91–98
204. Zinellu A, Pisanu S, Zinellu E et al (2007) A novel LIF-CE method for the separation of hyaluronan- and chondroitin sulfate-derived disaccharides: application to structural and quantitative analyses of human plasma low- and high-charged chondroitin sulfate isomers. Electrophoresis 28:2439–2447
205. Jayo RG, Li J, Chen DDY (2012) Capillary electrophoresis mass spectrometry for the characterization of *O*-acetylated N-glycans form fish serum. Anal Chem 84:8756–8762
206. Kazarian A, Smith JA, Hilder EF et al (2010) Development of a novel fluorescent tag O-2-[aminoethyl]fluorescein for the electrophoretic separation of oligosaccharides. Anal Chim Acta 662:206–213
207. Ijiri S, Todoroki K, Yoshida H et al (2010) Sensitive determination of rhodamine 110-labeled monosaccharides in glycoprotein by capillary electrophoresis with laser-induced fluorescence detection. J Chromatogr A 1217:3161–3166
208. Ijiri S, Todoroki K, Yoshida H et al (2011) Highly sensitive capillary electrophoresis analysis of *N*-linked oligosaccharides in glycoproteins following fluorescence derivatization with rhodamine 110 and laser-induced fluorescence detection. Electrophoresis 32:3499–3509
209. Johannesen SA, Beeren SR, Blank D et al (2012) Glycan analysis via derivatization with a fluorogenic pyrylium dye. Carbohyd Res 352:94–100
210. Briggs JB, Keck RG, Ma S et al (2009) An analytical system for the characterization of highly heterogeneous mixtures of N-linked oligosaccharides. Anal Biochem 389:40–51
211. Szabo Z, Guttman A, Bones J et al (2011) Rapid high-resolution characterization of functionally important monoclonal antibody *N*-glycans by capillary electrophoresis. Anal Chem 83:5329–5336
212. Archer-Hartmann SA, Crihfield CL, Holland L (2011) Online enzymatic sequencing of glycans from Trastumab by phospholipid-assisted capillary electrophoresis. Electrophoresis 32:3491–3498

213. Abballe F, Toppazzini M, Campa C et al (2007) Study of molar response of dextrans in electrochemical detection. J Chromatogr A 1149:38–45
214. Che FY, Song JF, Zeng R et al (1999) Analysis of 8-aminonaphtalene-1,3,6-trisulfonate-derivatized oligosaccharides by capillary electrophoresis- electrospray ionization quadrupole ion trap mass spectrometry. J Chromatogr A 858:229–238
215. Taga A, Kodama S (2012) Analysis of reducing carbohydrates and fructosyl sacchardies in maple syrup and maple sugar by CE. Chromatographia 75:1009–1016
216. Lindquist A, Rydlund A, Dahlman O (1997) Selective determination of acidic carbohydrates using capillary electrophoresis. ISWPC 22/1-22/4
217. Mechref Y, Muzikar J, Novotny MV (2005) Comprehensive assessment of N-glycans derived from a murine monoclonal antibody: a case for multimethodological approach. Electrophoresis 26:2034–2046
218. Szabo Z, Guttman A, Rejtar T et al (2010) Improved sample preparation method for glycans analysis of glycoproteins by CE-LIF and CE-MS. Electrophoresis 31:1389–1395
219. Archer-Hartmann SA, Sargent LM, Lowry DT et al (2011) Microscale exoglycosidase processing and lectin capture o glycans with phospholipid assisted capillary electrophoresis separations. Anal Chem 83:2740–2747
220. Lee Y-H, Lin T-I (1996) Capillary electrophoretic analysis of cyclodextrins and determination of formation constants for inclusion complexes. Electrophoresis 17:333–340
221. Her GR, Santikarn S, Reinhold VN et al (1987) Simplified approach to HPLC precolumn fluorescent labeling of carbohydrates: N-(2-pyridinyl)-glycosylamines. J Carbohydr Chem 6:129–139
222. Li DT, Her GR (1993) Linkage analysis of chromophore-labeled disaccharides and linear oligosaccharides by negative ion fast atom bombardment ionization and collisional-induced dissociation with B/E scanning. Anal Biochem 211:250–257
223. Kallin E, Lönn H, Norberg T et al (1991) Derivatization procedures for reducing oligosaccharides. 4. Use of glycosylamines in a reversible derivatization of oligosaccharides with the 9-fluorenylmethoxycarbonyl group, and HPLC separations of the derivatives. J Carbohydr Chem 10:377–386
224. Sarazin C, Delaunay N, Costanza C et al (2012) Application of a new capillary electrophoretic method for the determination of carbohydrates in forensic, pharmaceutical, and beverage samples. Talanta 99:202–206
225. Rovio S, Yli Kauhaluoma J, Sirén H (2007) Determination of neutral carbohydrates by CZE with direct UV detection. Electrophoresis 28:3129–3135
226. Rossi M, Campa C, Gamini A et al (2006) Separation of O- and C-allyl glycoside anomeric mixtures by capillary electrophoresis and high-performance liquid chromatography. J Chromatogr A 1110:125–132

Chapter 17

Use of Capillary Electrophoresis for Polysaccharide Studies and Applications

Amelia Gamini, Anna Coslovi, Mila Toppazzini, Isabella Rustighi, Cristiana Campa, Amedeo Vetere, and Sergio Paoletti

Abstract

CE applications to charged polysaccharides are briefly reported. A simple procedure is presented to determine the esterification degree of a hyaluronan derivative. In this case the degree of substitution was as low as 14%.

The molecular weight distribution of mannuronic oligosaccharides mixture produced by hydrolysis of native polymannuronic is readily calculated from peak area of the species resolved by CE on the basis of a specific degree of polymerization.

The influence of the applied electric field strength on the free solution mobility of hyaluronan samples is briefly addressed for molar masses of the order of 10^5 and 10^6 g/mol. The data are compared with the results obtained for a 50% galactose substituted HA.

Mobility data obtained as a function of buffer pH for a native HA sample as well as for two galactosamide HA derivatives, having slightly different degrees of substitution, are presented and discussed in terms of the polymer charge density parameters ξ.

In most cases, more questions than answers arise from the application of CE to charged polysaccharides. However, perspectives are disclosed for a further understanding of the reliability of CE applied for the structural elucidation of such macromolecules.

Key words Charged polysaccharides, Hyaluronan, Capillary electrophoresis, Electrophoretic mobility, Charge density, Molar mass distribution, Random degradation, Glycoconjugates

1 Introduction

In the polysaccharide field capillary electrophoresis studies have followed two main streams: one is dealing mainly with identification and quantification of native biopolymers in pharmaceuticals, biological samples, and foods [1–26]. The other with the elucidation of chemical structure in terms of molar mass, polydispersity, and degree of substitution [27–43]. In this respect, Table 1 reports, more explicatively than exhaustively, the experimental details of the applied procedures. By inspection of Table 1 it turns out that the glycosaminoglycans are in general the most studied polysaccharides and important reviews have been also

Philippe Schmitt-Kopplin (ed.), *Capillary Electrophoresis: Methods and Protocols*, Methods in Molecular Biology, vol. 1483,
DOI 10.1007/978-1-4939-6403-1_17,

Table 1
CE technique(s) applied to polysaccharide investigations

Ref.	Carbohydrate species	Matrix	Derivatizing agent	CE mode	Capillary; *T*	Buffer, voltage	Detection mode	LOD
[1]	Heparin	1. Deproteinized plasma samples 2. Std	None	MEKC	Fused silica (*l* = 30 cm, ID = 50 μm); *T* = 20 °C	25 mM boric acid + 25 mM SDS (pH 8.5); 20 kV Outlet: cathode	UV (270 nm)	25 units/L
[2]	HA	Water-extracted fractions from pharmaceuticals	None	CZE	Fused silica (*L* = 64.5 cm, *l* = 56 cm, ID = 50 μm); *T* = 25 °C	20 mM phosphate (pH 7.4); 30 kV; Outlet: cathode	UV (195 nm, 200 nm)	10 μg/mL
[3]	HA	1. Std 2. From vitreous humor	None	MEKC	Fused silica (*l* = 50 cm, ID = 75 μm); *T* = 30 °C	50 mM disodium hydrogenphosphate, 40 mM SDS, 10 mM sodium tetraborate (pH 9); 15 kV; Outlet: cathode	UV (200 nm)	25 μg/mL
[4]	Chondroitin 4-sulfate, HA, heparan sulfate, heparin (LMW and HMW)	Intact and degraded GAGs	None	CZE	Fused silica (*L* = 68 cm, ID = 75 μm); RT	1. Intact GAGs: $CuSO_4$ 5 mM (pH 4.5); −20 kV 2. Enzymatically treated GAGs: sodium phosphate (pH 3.5); 20 kV Outlet: anode	UV (240 nm) UV (232 nm)	1. 10^{-9} g 2. n.a.
[5]	K4 and defructosylated K4 native polysaccharides	K4 anionic polysaccharide from *E.coli*	None	MEKC	Fused silica (*L* = 85 cm; *l* = 65 cm, ID = 50 μm); *T* = 25 °C	40 mM disodium hydrogen phosphate, 10 mM sodium tetraborate, 40 mM SDS (pH 9); 20 kV; Outlet: cathode	UV (200 nm)	less than 30 ng (0.5 μg/μL)
[7]	Starch	1. Glc (from starch depolymerisation) 2. Linear oligosaccharides (DP 3÷85) isoamylase treatment	APTS	CZE	Neutrally coated with eCAP™ buffer (Beckman), (*L* = 47 cm, ID =. 50 μm) *T* = 25 °C	eCAP™ buffer (Beckman); *V* = 23.5 kV; Outlet: cathode	LIF (λecc 488 nm)	n.a.

[8]	Derivatized HA mixtures	HA samples (from bovine trachea and S. zooepidemicus) also degraded by ultrasonication or enzyme treatment	APTS	CGE	Various lengths of coated (LPAA) (ID = 50 μm) 1. l = 50 cm 2. l = 45 cm 3. l = 45 cm) RT	1. Intact HA: 25 mM citric acid, 12.5 mM Tris buffer; 5% LPAA (pH 3.0); 430 V/cm 2. Enzymatic HA digests: 25 mM citric acid, 12.5 mM Tris buffer (pH 3.0), 4 M urea, 0.03% aminodextran, 3% LPAA; 416 V/cm 3. Ultrasonic degraded HA: as in 1. 416 V/cm; Outlet: anode	LIF (λexc 488 nm; λem 514 nm)	n.a.
[9]	k- ι- and λ-carrageenan	Stds and commercial food additives in water at RT and thermally treated (70°–90 °C)	APTS	CZE	1. Fused silica (l = 47 cm; ID 50 μm); T = 25, 37 and 50 °C; 2. For lower DP components: CHO-coated capillary (l = 47 cm; ID = 50 μm); T = 20 °C	1. 25 mM citrate (pH 3.0); 30 kV Outlet: anode; 2. Beckman gel buffer 30 kV; Outlet: anode	LIF (λexc 488 nm; λem 520 nm);	0.3 μg/mL
[10]	Chitosan	1. Stds 2. Chitosan in plasma and foods (acidified with 10%TFA acid)	None	CZE	Fused silica (L = 27 cm, l = 20 cm, ID = 50 μm); RT	100 mM triethylamine (TEA)-phosphate buffer (pH 2.0); 15 kV; Outlet: cathode	UV (195 nm)	0.25 mg/mL
[11]	Pectins	1. Stds 2. Enzymatically de-esterified pectins from lemon peel	None	CZE	Fused silica (L = 57 cm, l = 50 cm, ID = 100 μm); T = 30 °C	Phosphate (pH 7.0); 20 kV; Outlet: cathode	UV (192 nm)	0.5 mg/mL
[12]	Two starch hydrolyzed sample and four dextran samples	Stds	None	CZE	Coated (LPAA) (l = 80 cm, ID = 25 μm); RT	Aqueous NaOH (50–200 mM), eventually containing CTAB at a concentration between 0.25 mM and 10 mM; 20 kV; Outlet: cathode	ED. Working electrode: 127 μm Cu magnet wire whose side areas were covered with a nonconductive coating.	1.0×10^{-6}–1.0×10^{-7} M

(continued)

Table 1
(continued)

Ref.	Carbohydrate species	Matrix	Derivatizing agent	CE mode	Capillary; *T*	Buffer, voltage	Detection mode	LOD
[13]	Polygalacturonic acid	oligosaccharides mixture (wide DP range) from partially hydrolyzed polygalacturonic acid	CBQCA	CGE	Deactivated fused silica filled with LPAA gels at high concentration (L = 30 cm, l = 23 cm; ID = 50 μm); RT	0.1 M Tris, 0.25 M boric acid, 2 mM EDTA; (pH 8.48); 5 kV; Outlet: cathode	LIF (λ_{exc} 487 nm; λ_{em} 550 nm)	85 fM
[15]	Chitin and glucan hydrolysates	1. Stds of Glc and GlcNAc; 2. Total enzymatically digested chitin and glucan	6-AQ	CZE, CEC	Fused silica (L = 57 cm; l = 50 cm; ID = 50 μm); RT	1. 100 mM sodium phosphate monobasic, pH 5.0; V = 15 kV 2. Same V = 20 kV 3. Same containing 50 mM tetrabutylammonium bromide, pH 5.0; 15 kV; Outlet: cathode	UV (254 nm)	1.2×10^{-5} M
[19]	GAG	Mixture of heparin, chondroitin sulfate, and hyaluronic acid	None	CZE	Fused-silica (L = 60 cm, l = 50 cm, ID = 50 μm)	Various Tris buffer	UV (200 nm)	LOD: 0.91, 0.12 and 9.04 3 10^{23} mg/mL
[20]	Asparagus Polysaccharide	Mixture of hydolyzed monosaccharides	None	CZE	Fused-silica (L = 60 cm, ID = 25 μm)	120 mmol L-1 NaOH solution as separation electrolyte V = 12 kV	Amperometric detection	n/a
[21]	Polysaccharides from plant cell wall	Purified polysaccharides	APTS	DASH	Fused silica (L = 48.5 cm, l = 40 cm, ID = 50 μm) T = 25 °C	V = 20 kV	UV (254 nm)	
[23]	N. Meningitidis group C polysaccharide	Free oxidized polysaccharide in the presence of glycoconjugate	None	CZE	Fused silica capillary coated with polyimide (L = 112.5 cm, l = 104 cm, ID = 50 μm) T = 40 °C	50 mM TBNa buffer, pH 10 V = 30 kV	UV (200 nm)	LOD 0.0154 mg/mL

[26]	Gellan gum	Gellan gum intact polysaccharide or oligomers separated on the basis of degree of polymerization, degree of acylation, or conformation	None	CZE	Fused silica capillaries of various length ID = 50 μm T = 30÷55 °C	200 mM sodium borate buffer V = 20÷30,	UV (200 nm)	n.a.
[28]	Hydrolyzed fucoidan and heparin	Commercial samples	None	CZE	Fused silica (L = 34.5 cm, l = 26 cm, ID = 50 μm); T = 25 °C	Anisic acid, sulfosalicilic acid with Bis-Tris or Tris (various concentrations and pHs); 30 kV; Outlet: anode or cathode;	Indirect UV (450 nm)	n.a.
[29]	Derivatized polysaccharide samples	Alginate (200 kDa) HA (185, 750, 900, 1350, 3600, 9300 kDa)	APTS	CZE	Coated with LPAA and EHEC, (various lengths, ID = 50 μm) RT	50 mM phosphate, 55 mM Tris (pH 6.2); 5–300 V/cm; Outlet: cathode	LIF (λexc 488 nm; λem 515 nm)	n.a.
[30]	GAGs mimotope (chondroitin sulfate oligomer recognized by hydrolytic enzymes like chondroitinase and hyaluronidase)	Desulfated (by methanolysis or enzyme digestion) chondroitine sulphate	None	MEKC	Fused silica (L = 72 cm, l = 50 cm, ID = 50 μm); T = 40 °C	40 mM phosphate, 40 mM SDS, 10 mM borate (pH 9.0); 15 kV; Outlet: anode	UV (200 nm)	n.a.
[31]	1. Colominic acid or Neu5Ac polymers of different molecular weights (14,17,29,59,69 kDa) 2. HA	1. Neu5Ac polymers 2. Polysulfated hyaluronans (HAPS) from *Streptococcus zooepidemicus*	None	CZE	Coated (dimethylpolysiloxane) 1. (L = 27 cm, l = 20 cm, ID = 100 μm) 2. (L = 57 cm, l = 50 cm, ID = 100 μm)	1. 50 mM Tris-borate (pH 8.5) containing 10% PEG 70000; 6 kV 2. 50 mM Tris-borate (pH 8.5) containing 10% PEG 70000; 15 kV; Outlet: anode	UV (200 nm)	n.a.
[32]	1. Colominic acid 2. Polysialoglycoprotein (and other oligo/polySia acid chains with different interketosidic linkages) 3. Glycoprotein (KDN-gp)	Hydrolysates of different oligo/polySia chains	None	CZE	Fused silica (L = 108 cm, ID = 75 μm); T = 25 °C	100 mM SDS, 100 mM sodium bicarbonate (pH 8); 20 kV; Outlet: cathode	UV (200 nm)	n.a.

(continued)

Table 1
(continued)

Ref.	Carbohydrate species	Matrix	Derivatizing agent	CE mode	Capillary; *T*	Buffer, voltage	Detection mode	LOD
[33]	Dextrans (of various molecular weights) and carboxymethylcellulose Stds	Debranched polydextran (enzyme treatment) and cleaved carboxy-methyl cellulose (enzyme treatment)	CBQCA	MEKC	Fused silica (*L* = 15–60 cm, ID = 50 μm) uncoated or filled with different conc. of LPAA, Istacryl, Synergel; RT 1. *L* = 30 cm; 2. *L* = 55 cm; 3. *L* = 20 cm; 4. and 5. *L* = 15 cm	1. 25 mM boric acid, 25 mM sodium phosphate, 50 mM Tris (pH 9.1); 15 kV; 2. 50 mM boric acid, 50 mM sodium phosphate, 100 mM Tris (pH 8.81); 5–11 kV; 3. 50 mM boric acid, 50 mM sodium phosphate, 100 mM Tris (pH 8.81); 10 kV, 3 Hz; 4. 100 mM boric acid/ 100 mM Tris (pH 8.5); 10 kV; 5 Hz; 5. 50 mM Tris borate, 1 mM EDTA (pH 8.2); 10 kV; 3 Hz; Outlet: cathode or alternatively cathode/anode in pulse field conditions	LIF (λexc 457 nm; λem 555 nm)	n.a.
[35]	1. Oligomers of Neu5Ac 2. Oligomers of HA	1. Colominic acid (from partial hydrolysis) 2. HA oligomer mixture (hyaluronidase digestion)	None	CZE	Fused silica (*L* = 57 cm, *l* = 50 cm, ID = 100 μm) coated with dimethylpolysiloxane or (50% phenyl) methylpolysiloxane	0.1 M Tris-0.25 M borate (pH 8.5) containing PEG 70000 or HPC and HPHC having different viscosities as sieving material; 10 kV; Outlet: anode	UV (200 nm)	n.a.
[36]	1. Dextran 2. PU 3. HPG (modified guar gum where some hydroxyl groups are replaced by hydroxypropyl units)	Stds	APTS	MEKC	Various lengths of fused silica capillaries (ID = 50 μm) 1. LPAA 2. Uncoated RT	40 mM clorimipramine in citric acid-Tris (pH 3.95); Outlet: cathode	LIF (λexc 488 nm; λem 515 nm)	n.a.

[37]	Pectins of varying DE (side chains consisting in 200–1000 GalA units linked together by α-(1→4) glycosidic bonds	Stds Pectins from lemon peels, (different DE by using pectin esterase of Aspergillus)	None	CZE	Fused silica (L = 57 cm; l = 50 cm; ID = 100 μm); T = 30 °C	50 mM phosphate (pH7); 20 kV; Outlet: cathode	UV (192 nm)	n.a.
[38]	Cellulose and cellulose derivatized at a hydroxyl group with a hydrophilic substituent	Stds and enzymatically and chemically hydrolyzed	APTS	MECK	Various lengths of fused silica capillaries (ID = 50 μm) coated with a layer of linear polyacrylamide; RT	Various compositions of a citric acid/ tris buffer Further addictions of 1. SDS 2. Decylsulphate; Electric field strength = 350–500 V/cm; Outlet: anode	LIF (λexc 488 nm; λem 515 nm)	n.a.
[40]	Pectins	1. De-esterified pectins at different DE (pectin-esterase treatment) 2. Alkaline-de-esterified pectins	None	CZE	Fused silica (ID = 75 μm, l = 30 cm and l = 60 cm); T = 25 °C	50 mM phosphate (pH 6.5); V = 15 kV; Outlet: cathode	UV (192 nm)	n.a.
[41]	Chondroitin sulfate	Chondroitin disaccharides from articular cartilage	None	CZE	Fused silica (L = 46.5 cm, ID = 50 μm) T = 25 °C	Phosphate (15 mM) at pH 3.0 V = −20 kV	UV (232 nm)	n.a.
[54]	Sulfated Carbohydrate	Sulfate ion deriving from hydrolyzed polysaccharides	None	CZE	Fused silica (L = 66 cm, l = 56 cm, ID = 50 μm)	10 mM CrO3–2 mM hexamethonium bromide in 10% MeOH–water (pH 8.0) adjusted with triethanolamine V = −20 kV	Indirect detection at 254 nm	n.a.
[56]	GAGs	Mixture of GAGs analyzed in the presence of linear polyalkylamines	AMAC	CZE	Fused silica (L = 50 cm, l = 40 cm, ID = 75 μm) T = 15 °C	50 mM sodium phosphate, pH 2.3, containing 10% DMSO V = 10 kV	UV (254 nm)	n.a.

APTS 1-aminopyrene-3,6,8-trisulfonate, *6-AQ* 6-aminoquinoline, *CBQCA* 3-(4-carboxybenzoyl)2-quinoline-carboxyaldehyde, *CEC* capillary electrochromatography, *CGE* capillary gel electrophoresis, *CTAB* cetyltrimethylammonium bromide, *CZE* capillary zone electrophoresis, *DE* degree of esterification, *DP* degree of polymerization, *ED* electrochemical detection, *EHEC* ethyl(hydroxyethyl)cellulose, *ELFSE* end labeled free solution electrophoresis, *ESI-MS* electrospray ionization-mass spectrometry detector, *GAG* glycosaminoglycans, *GalA* galacturonic acid, *Glc* glucose, *GlcNAc N*-Acetylglucosamine, *Gul* gulose, *HA* hyaluronic acid, *HMW* high molecular weight, *HPCE* high performance capillary electrophoresis, *LIF* laser-induced fluorescence, *LMW* low molecular weight, *LOD* limit of detection, *LPAA* linear polyacrylamide, *MEKC* micellar electrokinetic capillary chromatography, *n.a.* not available, *Neu5Ac N*-Acetylneuraminic acid, *Neu5Gc N*-glycolylneuroaminic acid, *PAGE* polyacrilamide gel electrophoresis, *PEG* polyethylene glycol, *PU* pullulan, *RT* room temperature, *SD* standard deviation, *SDS* sodium dodecyl sulfate, *std* standard, *TEA* triethylamine, *TFA* trifluoroacetic acid, *UV* ultraviolet de

devoted to this subject (see, for instance ref. [44]). Besides, to overcome the experimental limit of mass separation when large biopolymers are studied, polysaccharides have also found wide application on CE techniques as sieving matrix [8, 27, 35, 45–55]. In this respect, however, much care should be taken on considering polysaccharide chains as inert sieving material, especially when the objective of their use is to separate structurally similar molecules. Certain cellulose derivatives, for instance, have peculiar features strictly related to their rather rigid backbone. As an example HPC (hydroxypropyl cellulose) [35, 47, 54] not only goes to phase separation in water at temperature slightly higher than 40 °C but is also known to aggregate in ordered structures leading, at sufficiently high concentration, to liotropic mesophases of cholesteric type [55]. Indeed, most polysaccharides easily form aggregated structures, in line with their more common, although less specialized, biological role. To mention only a few, viscoelastic, mechanical, protective, and gelling properties are indeed strictly related to polysaccharide secondary (if not tertiary) structures assumed in aqueous environment. These may range from coiled to worm-like type, the stiffness of which strongly depends on the chain molecularity (single-, double-, triple-, multi-chain) which itself may depend on the solution environment (temperature, salt concentration, and salt type).

1.1 Determination of the Degree of Substitution of Hyaluronic Acid Butyric Ester: CZE-UV of Released Butyric Acid

In recent years great attention has been directed towards synthetic glyco-polymers as well as naturally occurring glyco-polymers (i.e. polysaccharides) for their potential use as biomaterials. Polymer engineering is a term usually referred to a preexisting polymer chain ad hoc modified by introducing biologically active ligands developing third-generation biomaterials that are able to directly intervene in cell growth, differentiation, adhesion, and extracellular matrix production [56–61]. At the level of isolated molecules the ligand-receptor affinity is very low and can be dramatically increased by increasing the ligand density within the glyco-conjugate ("cluster" effect). A similar approach can be used by anchoring a biological and pharmacological active molecule, like butyric acid [62, 63] to a selective vehicle such as hyaluronan (HA) recognized by CD44 receptor overexpressed in stem and neoplastic cells [64, 65]. The CE as rapid and reliable technique to identify and quantify biologically active molecules anchored to polymer chains [61] is here applied to a HA butyric ester derivative (HA-but). The degree of substitution for the glycoconjugate is here determined by quantification of butyric acid released upon hydrolysis of the HA-but derivative.

1.2 MEKC-UV Determination of the Degree of Polymerization and Distribution of Oligosaccharides in a Partially Acid-Hydrolyzed Homopolysaccharide

Degradation studies are particularly useful for naturally occurring macromolecules the polymerization of which cannot be performed in laboratory. Although high molar mass polymers represent a challenge for CE characterization, macromolecular study in terms of de-polymerization mechanisms can be easily performed. As an example the molecular weight distribution of an oligo-mannuronic mixture resulted from acid hydrolysis of high molecular weight mannuronan turned out to be satisfactorily interpreted in terms of the most probable distribution for an early stage of polycondensation reaction [66]. Beside the definition of polysaccharides (and proteins) as condensation polymers, it is since long known that hydrolysis of cellulose occurs randomly for degree of polymerization x lower than 500 [67]. In this respect, if the polymer degradation consists of nonspecific (random) bond scission, a mixture from an extensively hydrolyzed polysaccharide solution might be considered as a snapshot of a polycondensation reaction taken at sufficiently low extent of condensation p (i.e. fraction of bond formed). Then, in the polymer mixture containing in total N_0 sugar residues there are $N_0 p$ intact linkages and $N_0(1-p)$ unbound residues, the latter corresponding also to the total number of chains N. The expected molecular weight distribution function (i.e. the frequency of occurrence of a given degree of polymerization x) expressed in terms of mole fraction $N_x, (= n_x / N,)$ and weight fraction $W_x (= xN_x / N_0)$ of the nx x-mers is then [67]:

$$N_x = (1-p)\,p^{(x-1)} \tag{1}$$

$$W_x = x(1-p)^2\,p^{(x-1)} \tag{2}$$

The number-average molecular weight $< M >_n$ and the weight-average molecular weight $< M >_w$ can as well be obtained by:

$$< M >_n = \mathrm{Mo} / (1-p)$$

and

$$< M >_w = \mathrm{Mo}(1+p) / (1-p)$$

1.3 Influence of Electric Field on the Electrophoretic Mobility of Polysaccharides: Application to Hyaluronic Acid

It is generally reported that application of capillary electrophoresis to large charged (bio)polymers in free solution cannot provide for their size separation when sharing the same mass to charge ratio (i.e.: for regular structures). Then, the general approach to achieve CE separation on molar mass basis is to let highly charged polymers of relatively big size migrate through and entangled polymer solution that is believed to act as an inert sieving matrix [31, 35, 45–54, 68]. Depending on the type,

dimensions and concentration of the host polymer different separation models have been developed and reported [51, 52]. The electrophoretic studies in free solutions dealing with charged (bio)polymers of relatively large sizes are in comparison sensibly fewer [69–74]. Before electrophoretic technique can be applied to macromolecular characterization beyond the qualitative size separation more systematic studies should be performed to asses and develop polyelectrolyte models that can better mimic electrophoretic behavior [73]. Discrepancies on experimental data as well as on theoretical predictions are such to render the assumption of a molar mass independent electrophoretic mobility in free solution somewhat doubtful [69, 70, 73]. Additional and systematic experimental data are needed especially to better understand when and how a dependence of electrophoretic mobility on macromolecular features such as chain conformation and chain stiffness may disclose and/or predicted. In this respect the wide spectrum of charge, chain conformation, and stiffness covered by native and modified charged polysaccharides might represent a resource for deeper studies on a wider range of polymer types. Beside the unsuccessful size separation in free solution, electrophoretic mobilities of charged polymers measured on increasing electric field strength generally showed a relatively steeper increase than the expected [52, 73]. A similar trend can be also observed when naturally occurring or synthetic polyelectrolytes migrate through entangled polymer solutions [52, 53, 68]. A phenomenon the origin of which, generally ascribed either to chain distorsion or to a viscosity drop by Joule heating, would likely deserve for deeper investigations. As an example, the electrophoretic mobility of five hyaluronan samples of different molar mass is here reported as a function of the applied voltage. The data obtained for molar masses of the order 10^5–10^6 g/mol are also compared with the electric field dependence of electrophoretic mobility observed when 50% of the charged groups of one of those HA sample are substituted by an amide- linked galactose residue.

The dependence of the intrinsic mobility on electric fields strength, here only shortly addressed, shows interesting features. In line with elsewhere reported findings [52, 73] an increase of the mobility is observed on increasing the applied voltage value in the entire investigate field strength range (i.e. $124 \div 420$ V/cm). Heating effects are reported to occur at field strength higher than 250 V/cm (i.e.: $\geq$16 kV in our case) [53, 73]. Although their presence cannot be excluded, the much smoother increase of the mobility presently observed with respect to steeper variations elsewhere reported [52, 53, 73] should more likely come from field induced perturbation of the ion cloud.

1.4 Influence of pH on the Electrophoretic Mobility of Polysaccharide: Application to Hyaluronic Acid and Related Glyco conjugates

Electrokinetics models have been generally applied more successful to electrophoretic migration of colloidal particles [75–77]. Indeed, accurate models as those elaborated by Booth and Overbeek that take into account polarization and relaxation of the ion cloud induced by the flow/electric field well represent the electrophoretic behavior of spherical charged particles [78–80]. However a solid nonconducting spherical model hardly applies to real macroions. Even if their shape can approximately be spherical their charge distribution is not expected to be spherically symmetrical.

However, to have simple estimation of approximate values of the electrophoretic mobility of spherical macroions with low potential surface the Henry's equation is often used [81]:

$$\mu = \frac{Ze}{6\pi\eta R} \times \frac{f(kR)}{1+kR} \tag{3}$$

where Z is the number of charge units, e is the elementary charge, R is the radius, k is the Debye-Hückel parameter. $f(kR)$ is a complicated function which, however, lies between 1 and 1.5 in the $0.1 \div 10^3$ kR range and departs very little from unit for $kR \leq 1$. Equation 1 coincides with the first term of the more elaborate Booth equation [76].

Hyaluronan is a low charged polymer, its chain, when fully ionized, has approximately one fixed charge per nm length. The charge state being generally represented by the charge density parameter ξ defined as the ratio between the Bjerrum length l_b and the average distance b separating two consecutive charged sites on the polymer backbone: $\xi = l_b / b = \left(e^2 / 4pDk_BTb\right)$. Where e is the elementary charge, D is the dielectric permittivity of the medium, k_B the Boltzmann's constant and T the absolute temperature (i.e. $l_b = 0.714\,\text{nm}$ in water at 25 °C). The mobility of the unsubstituted HA4 hyaluronan and of the HA7 and HA8 galactose substituted hyaluronans, all having an identical molar mass, measured as a function of pH and at constant ionic strength is here reported. The fully ionized state is characterized by a linear charge density parameter ξ of 0.72, 0.55, and 0.48 for HA4, HA7, and HA8, respectively. In this case, for which potentiometric data are also available, the mobility dependence on the ionization degree α_{ion} can then be resorted by using:

$$\alpha_{ion} = \alpha_N + 10^{-pH} / C_p \tag{4}$$

where αN is given by the added base to total carboxyl equivalent ratio and C_p is expressed in equivalent of repeating units/L. Furthermore, the very same data can be plotted as well as a function of the linear charge density varying with α_{ion} (i.e.: $\xi' = \xi\alpha_{ion}$).

It has been reported that the electrophoretic mobility of hyaluronan can be reproduced rather well by the so-called "frozen-wormlike model" [74, 81]. In the present case, a very simple approach is used: Eq. 3 is taken as a reference point to compare the electrophoretic mobilities of hyaluronan samples on a qualitative basis. Indeed, beside the above mention restrictions for Eq. 3 to apply an additional one is given by the "conducting" surface of a weak polyacid, as hyaluronan, with carboxyl groups rapidly exchanging protons. What we will use are the two statements implied in Eq. 3: one that the electrophoretic mobility is directly proportional to the charge Z of the polyion and the other that is inversely proportional to the frictional coefficient under the assumption of a spherical macroion shape.

2 Materials

2.1 Determination of the Degree of Substitution of Hyaluronic Acid Butyric Ester: CZE-UV of Released Butyric Acid

1. *Samples*: hyaluronic acid (85 kDa) (from Bioibérica, Barcelona, Spain).
2. *Reagents for linkage of butyric acid to HA*: butyric anhydride, tertrabutylammonium (TBA) (from Sigma St Louis, MO, USA). The derivatization procedure was previously described [64].
3. *Reagents for basic hydrolysis*: sodium hydroxide (from Sigma St Louis, MO, USA).
4. *CE buffer*: 50 mM sodium tetraborate (borax), pH 9.2 (from Sigma St Louis, MO, USA).

2.2 MEKC-UV Determination of the Degree of Polymerization and Distribution of Oligosaccharides in a Partially Acid-Hydrolyzed Homopolysaccharide

1. *Samples*: mannuronan oligomers released upon hydrolysis from high molecular weight mannuronan (from fermentation broth of a mannuronan C-5 epimerase negative strain of *Pseudomonas fluorescens*) [66].
2. *Reagents for oligosaccharides derivatization*:4-aminobenzonitrile (ABN) (Aldrich, St. Louis, MO, USA), sodium cianoborohydride, glacial acetic acid, and methanol (Merck, Darmstadt, Germany).
3. *CE buffer*: boric acid 660 mM (pH 8) containing 100 mM SDS.

2.3 Influence of Electric Field on the Electrophoretic Mobility of Polysaccharides: Application to Hyaluronic Acid

1. *Samples*: sodium hyaluronate (rooster comb) samples were kindly provided from FIDIA S.p.A (Abano Terme, Padova, Italy). The details of the different hyaluronic acid samples are summarized in Table 2.
2. Samples were prepared dissolving 1 mg of intact or galactose-modified sodium hyaluronate in 1 mL of bi-distilled water and analyzed without further dilution.
3. *Reagents for linkage of galactose to HA*: 1-amino-1-deoxy-β-d-galactose (galactosylamine) was prepared as reported in literature [82], 2-[N-morpholino]ethanesulfonic acid (MES),

Table 2
HA samples analyzed by CE-UV

HA samples	MW (kDa)	DS
HA1	120	(–)
HA2	160	(–)
HA3	160	0.5
HA4	210	(–)
HA5	850	(–)
HA6	1050	(–)
HA7	210	0.2
HA8	210	0.3

N-hydroxysuccinimide (NHS), and 1-Ethyl-3-[3-(dimethtlamino)-propyl]carbodiimide hydrochloride (EDC). All reagents were from Sigma, St. Louis, MO, USA.

4. *CE buffer*: 50 mM sodium tetraborate (borax), pH 9.2 (from Sigma St Louis, MO, USA).

2.4 Influence of pH on the Electrophoretic Mobility of Polysaccharide: Application to Hyaluronic Acid

1. *Samples: see* Subheading 2.3.
2. *Reagents for linkage of galactose on HA*: *see* Subheading 2.3.
3. *CE-buffer*: a series of potassium phosphate buffers (KH_2PO_4/K_2HPO_4 from Merck, Darmstadt, Germany) at constant ionic strength (0.05 M) and at different pH values (pH range between 3 and 9).

2.5 Equipment

For Subheadings 2.1, 2.2, 2.4. High-performance capillary electrophoresis (CE) system (Applied Biosystems HPCE Model 270A-HT; Foster City, CA, USA) with Turbochrom Navigator (4.0) software.

For Subheading 2.3 High-performance capillary electrophoresis (HP3D CE system; Waldbronn, Germany), with HP Chemstation software.

For Subheadings 2.1 and 2.2: uncoated fused silica column (Supelco, St. Louis,MO, USA) with an inner and outer diameter of 50 and 375 μm respectively; capillary length: 92 cm (70.0 cm to detector);

For Subheading 2.3: uncoated fused silica column (Agilent technologies, Germany) with internal diameter of 50 μm; capillary length: cm 64.2 (56.0 cm to detector) extended light path.

For Subheading 2.4: linear polyacrilamide (LPA) coated capillary (Bio-Rad Laboratories, Hercules, CA, U.S.A.) with an inner

and outer diameter of 50 and 375 μm, respectively; capillary length: 80 cm (62 cm to detector) (*see* **Note 1**).

Detection: UV on column 195 nm for all samples but oligomannuronic acids (285 nm).

3 Methods

3.1 Determination of the Degree of Substitution of Hyaluronic Acid Butyric Ester: CZE-UV of Released Butyric Acid

Beside the low sample consuming, CE is shown to be an easy and rapid technique to accurately quantify pendent species, chemically introduced onto polymer chain [58], in amounts that are in the detection limit range of the important and widespread NMR technique.

1. Rinse the capillary for 2 min with a 0.1 N NaOH solution at a pressure equal to 67.6 kPa.
2. Condition the silica capillary with electrophoresis buffer (pressure 67.6 kPa) for 4 min.
3. Program the instrument to load the sample under vacuum at a pressure of 16.9 kPa for 1.5 s.
4. Operative conditions: voltage: 20 kV; detection: 195 nm at the cathode; temperature: 27 °C; buffer: borax 50 mM (pH 9.2).
5. Hydrolysis procedure:

   Dissolve 4 mg of the substituted polymer in 1 mL of 0.1 N NaOH solution. Incubate the mixture at RT and after 2 h neutralize it with 1 mL HCl 0.1 N.
6. Figure 1 shows the electropherogram of: (A) intact HA derivative; hydrolyzed mixture (B) before and (C) after co-injection of a standard butyric acid solution. A degree of substitution as low as 0.14 was determined. The calibration curve from peak area to migration time ratio (A/t) vs. solute concentration $\left(A/t = 15.151x + 2.558, r^2 = 0.999\right)$ was linear in the investigated 1 mM÷4.5 mM butyric acid concentration range [64].

3.2 MEKC-UV Determination of the Degree of Polymerization and Distribution of Oligosaccharides in a Partially Acid-Hydrolyzed Homopolysaccharide

As far as the CE is concerned, the relatively short mannuronic chains are singularly tagged so that the peak area to retention time ratios for the CE resolved x values (i.e.: $1 \div 18$ monomeric units) are proportional to the number (moles) of chains containing x-monomers (i.e.: nx). Both number (moles) and weight fractions as a function of x can then be obtained and compared with the theoretically expected distribution functions.

Operatively:

$$n_x = \left(A/t\right)_x$$

$$N_0 = \Sigma_x x\left(A/t\right)_x$$

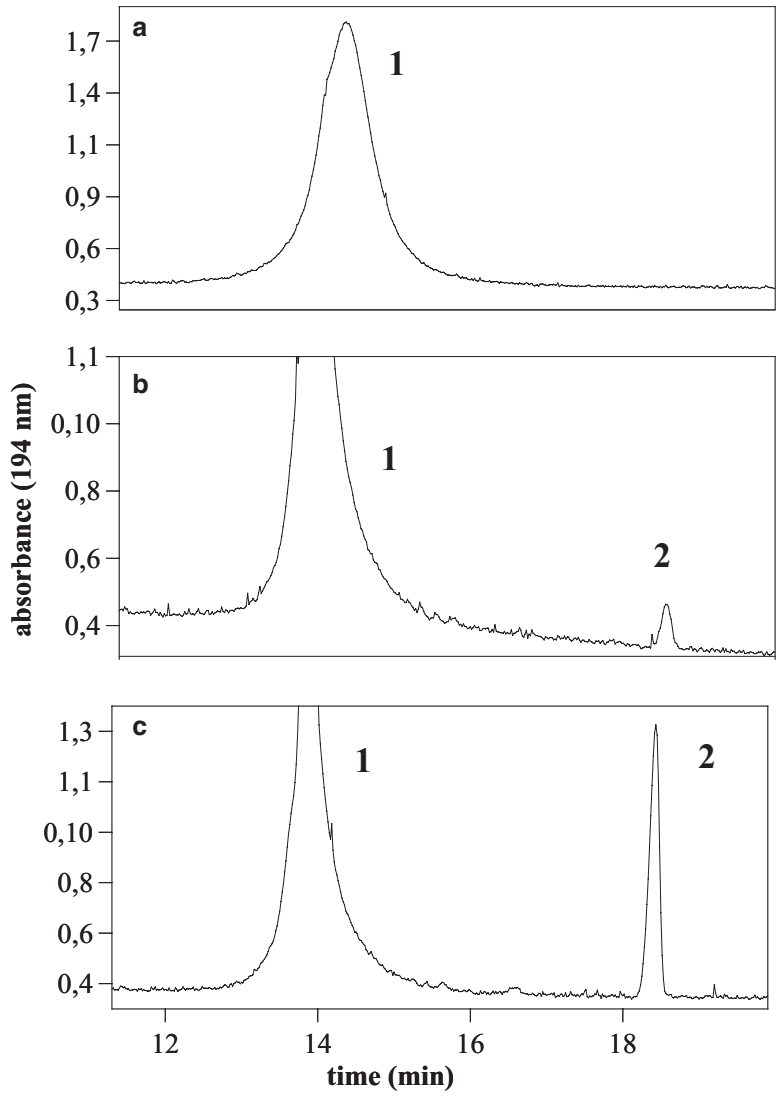

Fig. 1 Electropherogram of: intact HA butyric ester (**a**); Hydrolyzed mixture before (**b**) and after (**c**) co-injection of butyric acid solution

$$N = \Sigma_x \left(A / t \right)_x$$

1. Rinse the capillary for 2 min with a 0.1 N NaOH solution at a pressure of 67.6 kPa.
2. Condition the silica capillary with electrophoresis buffer.
3. Program the instrument to load the sample under vacuum at a pressure of 16.9 kPa for 1.5 s.
4. Operative conditions: voltage: 18 kV; detection: 285 nm at the cathode; temperature: 30 °C; buffer: H_3BO_3 660 mM (pH 8) containing 100 mM SDS.

5. Derivatizing procedure:Derivatize standards (1 mg/mL) or hydrolysis mixture (4 mg/mL) with 0.5 M ABN in the presence of 0.16 M $NaCNBH_3$ in 1 mL MeOH/AcOH (95/5) for 15 min at 90 °C. For CE analysis dilute the samples five times with H_{2O} or buffer.
6. Figure 2a Weight, *Wx*, and number (mole), *Nx*, fractions, Fig. 2b, of mannuronic oligomers obtained from *A/t* of resolved *x* species in the electropherogram of the hydrolyzed

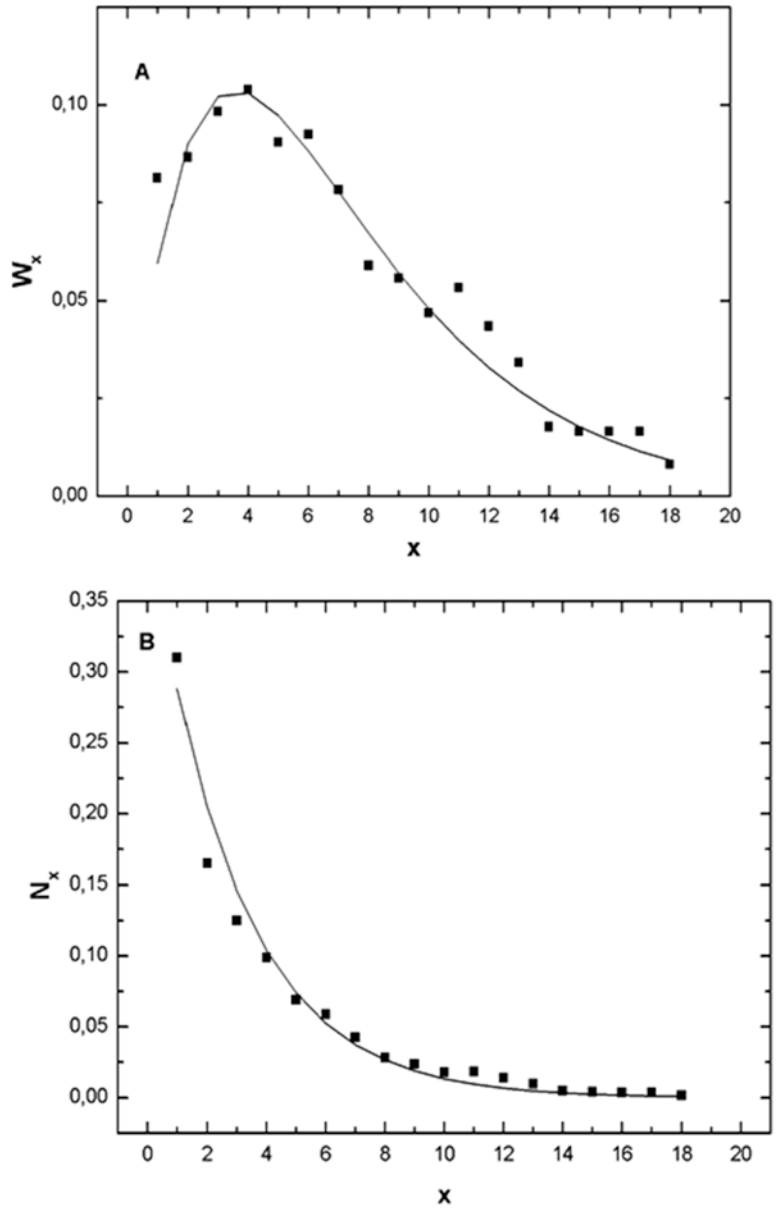

Fig. 2 (**a**) Weight fraction of mannuronic oligomers as a function of the degree of polymerization *x*. (**b**) Mole fraction. Solid curves are calculated from Eqs. 1 and 2 with *p* equal to 0.75 and 0.72 for weight and number fractions, respectively

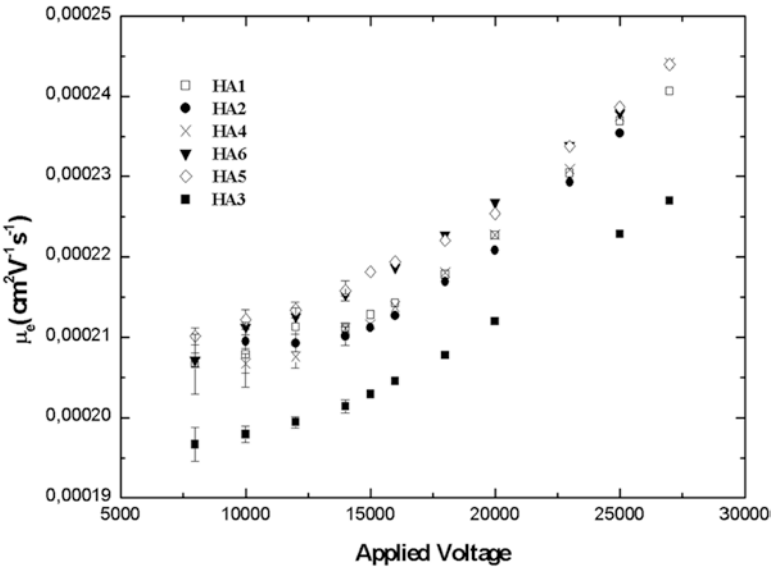

Fig. 3 Electrophoretic mobility as a function of the applied voltage (*V*) for HA1, HA2, HA4, HA5, and HA6 samples

mannuronic mixture. Solid curves are best fitting curves obtained from Eqs. 1 and 2 at values of 0.72 and 0.75 for the fraction of unbroken linkages *p*, respectively.

3.3 Influence of Electric Field on the Electrophoretic Mobility of Polysaccharides: Application to Hyaluronic Acid

Field dependence of the free solution mobility of HA samples having different molar masses is here reported together with mobility data observed for HA having lower charge density .

1. Rinse the capillary for 2 min with a 0.1 N NaOH solution at a pressure of 960 mbar.
2. Condition the silica capillary with electrophoresis buffer (pressure 960 bar) for 4 min.
3. Program the instrument to load the sample under vacuum at a pressure of 25 mbar for 3 s.
4. Operative conditions: different values of voltage, ranging from 8 to 27 kV (*see* Fig. 3); detection: 195 nm at the cathode; temperature: 25 °C; buffer: 50 mM borax (pH 9.2).
5. Galactose-substituted hyaluronan synthesis procedure: *see* **Note 2**.
6. Figure 3 shows that the mobilities measured for the HA samples increase smoothly from approximately a common low field asymptotic value to merge to an overlapping value at high fields. Just above the asymptotic low field behavior a window in the range of applied field values exists where the mobility of the larger molecules is slightly but distinctively higher than that measured for shorter HA chains. Albeit small the measured dif-

ferences are above the standard errors. Any mobility difference can instead be deduced neither between HA5 and HA6 nor between HA1, HA2, and HA4. From the linear increase of the current in the 8-20 kV voltage range and from the relatively low conductivity of the used buffer [70] the presence of heat artifacts below 16 kV (i.e.: E=250 V/cm) should be safely excluded. Additional measurements are needed to clarify the role that borax may as well play in the electrolyte-polymer system [70]. As an example, at low field strength (i.e. 50–150 V/cm) free solution mobility of DNA molecules has been reported to increase with molar mass in a very limited range of chain length (i.e. 20–400 bp) and to attain molecular mass independent values beyond that upper limit [70], the rise being ascribed to electrolyte drag forces the effects of which are vanishing with chain dimensions. Such an increase, although over estimated by 10–15%, has as well been predicted by molecular modeling of short DNA fragments (20–60 bp), in the rod limit diffusion behavior, that included ion relaxation. In our case, if retardation effects of deformed ion clouds are responsible for the distinct migration behavior reported in Fig. 3, they appear to be either weaker for, or better recovered by, expanded coiled shapes of large sizes. The HA samples here investigated not only have larger sizes than the above reported DNA molecules but also are less charged and, perhaps more important, are much more flexible. A worm-like chain model with a persistence length of roughly 10 nm applies reasonably well in the entire range of chain lengths here investigated [83]. As indicated by the expected low electrophoretic mobility disclosed by the low charge bearing galactose substituted hyaluronan, HA3 (M_w=1.6×105), the charge-to-size value that contribute to the electrophoretic mobility of HA5 and HA6 measured in the 13 kV – 18 kV range must apparently be higher than that of the low molecular weight hyaluronans. Only for comparison purposes we may try to treat the polymer samples simply as charged bodies and to compute the charge Q by which they contribute to the electrophoretic mobility measured at 15 kV ($\mu = Q / f$), assuming the frictional coefficient being described by Stokes law, $f = 6\pi\eta R$, and taking R equal to the measured average-root-mean-square radius of gyration [69]. It can then be shown that low molar mass hyaluronans (HA1, HA2, and HA4) contribute to the electrophoretic mobility with ≈18 – 19% of the total charge actually carried by the chains whereas the charge contribution to the mobility of the higher HA5 and HA6 is roughly 10% of the charge they actually have; this suggests, as expected, that much higher electrostatic and hydrodynamic screening effects are characterizing the expanded larger sized coils. The electrophoretic mobility of the low charged HA3 sample is compatible with that observed for the parent HA2 polymer if a degree of substitution of 0.6 is consid-

ered (to be compared with $\text{D.S.} = 0.5$ independently measured by traditional methods, *see* **Note 3**) assuming a charge contribution of 18% and, moreover, disregarding R_g variations that likely occur with substitution, assuming that both HA2 and HA3 share an identical average size. In this specific case, the CE technique although sensitive, cannot substitute the more assessed methodologies for the determination of chemical structural parameters like the degree of substitution.

Unfortunately, disclosure of differences in migration behavior eventually present at low fields is precluded by the large standard errors affecting the experimental data. Unclear as well are the reasons for the high field behavior where the overlapping mobility value is apparently more rapidly reached by HA1 and HA2 (low molar mass samples) than by HA5 and HA6 samples. Long flexible chains can be oriented by an electric/flow field and even deformed at high flow field strengths as resulted, for instance, from viscoelastic and flow/electric birefrangence measurements. Besides the need to ascertain the influence of heat artifacts, deeper investigations of the field dependence migration on well characterized and differently charged macromolecules, in general, and on charged polysaccharides, in particular, should be addressed to gain better insights on the several and not too well understood mutual influences of dynamic, conformation, and electrostatic features that actually contribute to the electrophoretic behavior of wormlike chains.

3.4 Influence of pH on the Electrophoretic Mobility of Polysaccharides: Application to Hyaluronic Acid

1. Rinse the capillary for 2 min with bidistilled water at a pressure of 67.6 kPa.
2. Condition the silica capillary with electrophoresis buffer (pressure 67.6 kPa) for 4 min.
3. Program the instrument to load the sample under vacuum at a pressure of 16.9 kPa for 3 s.
4. Operative conditions: voltage 20 kV; detection: 190 nm at the anode; temperature: 30 °C; buffer: potassium phosphate solutions in a pH range between 3 and 9 and constant ionic strength (0.05 M).
5. Figure 4 shows the electrophoretic migration measured as a function of pH for native hyaluronan $\left(\text{HA4}, Mw = 2.1 \times 10^5 \text{ g / mol}\right)$ and for the galactose substituted HA7 (D.S. 0.24) and HA8 (D.S. 0.34) samples. The higher charge density of HA4 accounts for the higher mobility measured with respect to the less charged HA7 and HA8 (and, even more, for HA3 sample, *see* Table 2).

Figure 5 reports the mobility values as a function of the degree of ionization measured for HA4, HA7, and HA8, for which poten-

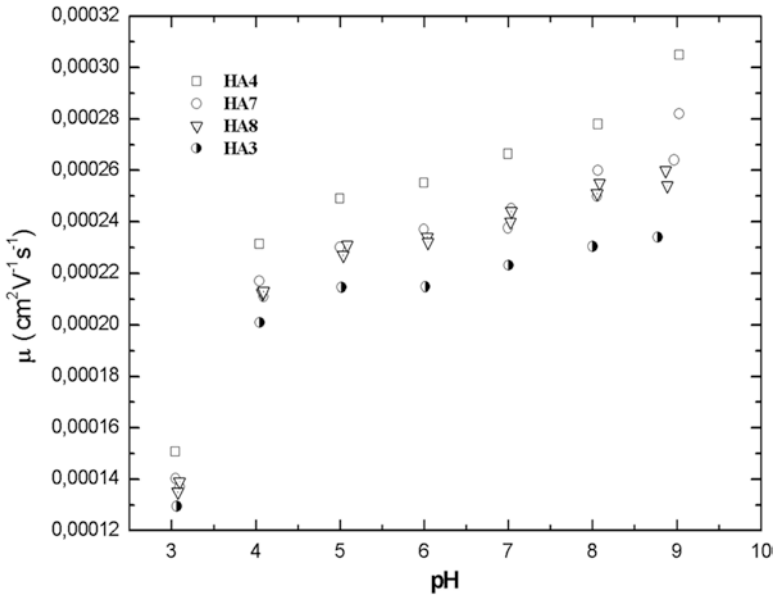

Fig. 4 Electrophoretic mobility as a function of pH for native (HA4) and galactose substituted HA7 and HA8 samples. For comparison purposes mobility measured for the higher substituted HA3 sample are also reported

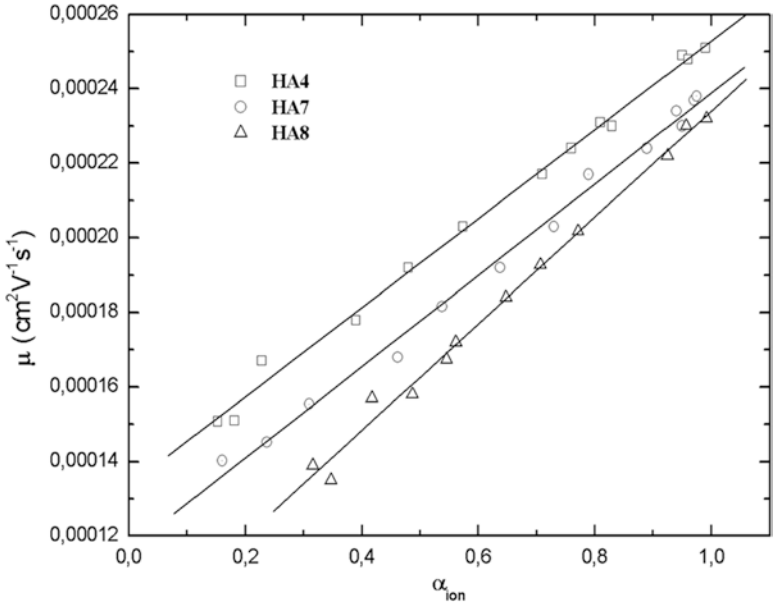

Fig. 5 Data of Fig. 4 are plotted as a function of the degree of ionization α_{ion} (Eq. 4). Solid lines are least-square fits of the experimental points

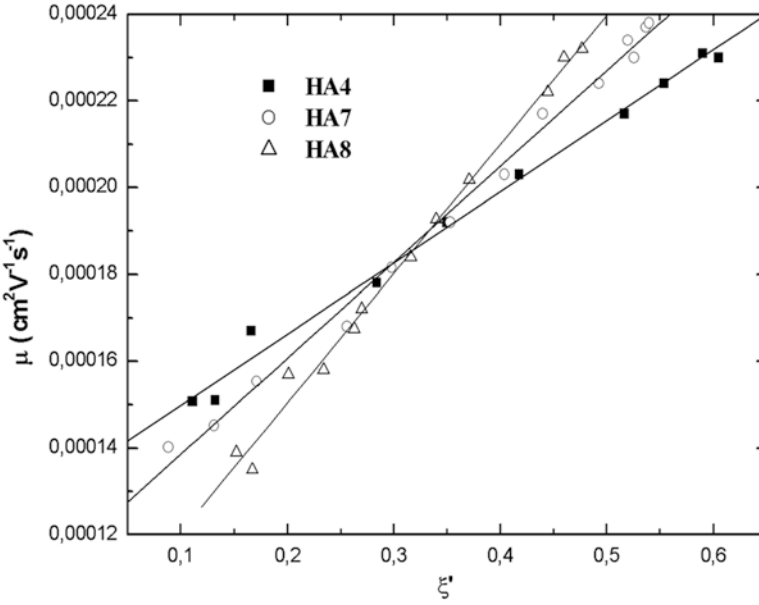

Fig. 6 Mobility data are here reported as a function of the charge density parameter $\xi' = \xi\alpha_{ion}$. Solid lines are least-square fits of the experimental points

tiometric data were available. There, the pH values were transformed into α_{ion} by applying Eq. 4.

Figure 6: more interesting features are disclosed by analyzing the mobility data in terms of the linear charge density that depends on the degree of ionization, $\xi' = \xi\alpha_{ion}$.

In all cases, as expected, an approximately linear dependence of the mobility is observed as a function of the charge density parameter. Different instead is the rate by which the mobility changes on charging the polymer chains. On the basis of the simple statements made in the introduction, data of Fig. 6 show that the potential surface of HA7 and HA8 increases with chain charging more rapidly than that of HA4. In turn, on increasing the degree of substitution a decrease of the chain frictional coefficient is suggested for the galactose substituted hyaluronans in comparison with a more "unperturbed" behavior of HA4.

4 Notes

1. Differently from what recommended for PVA coated capillary, LPA coated one is a general-purpose capillary which is suitable to be used in a wide pH range (typically, from 2 to 9).
2. Add galactosylamine (2.70 mg, 1.35 mg or 0.95 mg to yield respectively substitution degrees (DS) of 0.5, 0.3, and 0.2) to a stirred solution of hyaluronan sodium salt (1.5 g) in 0.2 M

MES buffer (pH 4.5, 400 mL) containing NHS and EDC ([EDC]/[HA repeating unit] = 1.5; [NHS]/[EDC] = 1). Stir the solution for 24 h at RT, dialyze the polymer at 4 °C against $NaHCO_3$ 0.05 M for 1 day and then exhaustively against mQ water. Adjust, if necessary, the pH to 6.5, filter the polymer solution and freeze-dry it to obtain the modified hyaluronans.

3. The determination of the degree of substitution was made by potentiometric titration and elemental analysis.

References

1. Zhou X-M, Liu J-W, Zhang M-E et al (1998) Determination of plasma heparin by micellar electrokinetic capillary chromatography. Talanta 46:757–760
2. Plätzer M, Ozegowski JH, Neubert RHH (1999) Quantification of hyaluronan in pharmaceutical formulations using high performance capillary electrophoresis and the modified uronic acid carbazole reaction. J Pharm Biomed Anal 21:491–496
3. Grimshaw J et al (1996) Quantitative analysis of hyaluronan in vitreous humor using capillary electrophoresis. Electrophoresis 15:936–940
4. Toida T, Linhardt RJ (1996) Detection of glycosaminoglycans as a copper (II) complex in capillary electrophoresis. Electrophoresis 17:341–346
5. Volpi N (2004) Separation of capsular polysaccharide K4 and defructosylated K4 by high-performance capillary electrophoresis. Electrophoresis 25(4–5):692–696
6. Damm JBL, Overclift GT, Vermeulen BWM (1992) Separation of natural and synthetic heparin fragments by high-performance capillary electrophoresis. J Chromatogr 608:297–309
7. Morell MK, Samuel MS, O'Shea MG (1998) Analysis of starch structure using fluorophore-assisted carbohydrate electrophoresis. Electrophoresis 19:2603–2611
8. Hong M, Sudor J, Stefansson M, Novotny M (1998) High-resolution studies of hyaluronic acid mixtures through capillary electrophoresis. Anal Chem 70(3):568–573
9. Roberts MA, Zhong H-J, Prodolliet J, Goodall DM (1998) Separation of high-molecular-mass carrageenan polysaccharides by capillary electrophoresis with laser-induced fluorescence detection. J Chromatogr A 817:353–366
10. Ban E, Choi O-K et al (2001) Capillary electrophoresis of high-molecular chitosan: the natural carbohydrate polymer. Electrophoresis 22:2217–2221
11. Zhong H-J, Williams MAK, Keenan RD, Goodall DM, Rolin C (1997) Separation and quantification of pectins using capillary electrophoresis: a preliminary study. Carbohydr Polym 32:27–32
12. Zhou W, Baldwin RP (1996) Capillary electrophoresis and electrochemical detection of underivatized oligo- and polysaccharides with surfactant-controlled electroosmotic flow. Electrophoresis 17:319–324
13. Liu J, Shirota O, Novotny MV (1992) Sensitive, laser-assisted determination of complex oligosaccharide mixtures separated by capillary gel electrophoresis at high resolution. Anal Chem 64:973–975
14. Wiedmer SK, Cassely A, Hong M et al (2000) Electrophoretic studies of polygalacturonate oligomers and their interactions with metal ions. Electrophoresis 21:3212–3219
15. Zhang M, Melouk HA, Chenault K et al (2001) Determination of cellular carbohydrates in peanut fungal pathogenesis and Baker's yeast by capillary electrophoresis and electrochromatography. J Agric Food Chem 49(11):5265–5269
16. Teodor ED, Truică G, Radu GL (2012) Hyaluronic acid detection from natural extract by diode array-capillary electrophoresis methods. Rev Roum Chim 57(3):223–227
17. Matysiak J, Dereziński P, Urbaniak B et al (2013) A new method for determination of hyaluronidase activity in biological samples using capillary zone electrophoresis. Biomed Chromatogr 17:1070–1078
18. Gao Q, Araia M, Leck C et al (2010) Characterization of exopolysaccharides in marine colloids by capillary electrophoresis with indirect UV detection. Anal Chim Acta 662:193–199
19. Liu X, Sun C, Zang H (2012) Capillary electrophoresis for simultaneous analysis of heparin, chondroitin sulfate and hyaluronic acid and its application in preparations and synovial fluid. J Chromatogr Sci 50:373–379
20. Yang Z, Wang H, Zhang W (2012) Analysis of neutral sugars of Asparagus officinalis Linn. Polysaccharide by CZE with amperometric detection. Chromatographia 75:297–304

21. Li X, Jackson P, Rubtsov DV et al (2013) Development and application of a high throughput carbohydrate profiling technique for analyzing plant cell wall polysaccharides and carbohydrate active enzymes. Biotechnol Biofuels 6:94–105
22. Albrecht S, Schols HA, Klarenbeek B (2010) Introducing capillary electrophoresis with Laser-Induced Fluorescence (CE – LIF) as a potential analysis and quantification tool for galactooligosaccharides extracted from complex food matrices. J Agric Food Chem 58:2787–2794
23. Medeiros de Souza I, Neto da Silva M, Scott Figueira E et al (2013) Single validation of CE method for determining free polysaccharide content in a Brazilian meningococcal C conjugate vaccine. Electrophoresis 34:3221–3226
24. Zhang Q, Chen X, Zhu Z et al (2013) Structural analysis of low molecular weight heparin by ultraperformance size exclusion chromatography/time of flight mass spectrometry and capillary zone electrophoresis. Anal Chem 85:1819–1827
25. Volpi N, Maccari F, Suwan J (2012) Electrophoresis for the analysis of heparin purity and quality. Electrophoresis 33:1531–1537
26. Taylor DL, Ferris CJ, Maniego AR (2012) Characterization of gellan gum by capillary electrophoresis. Aust J Chem 65:1156–1164
27. Hayase S, Oda Y, Honda S et al (1997) High-performance capillary electrophoresis of hyaluronic acid: determination of its amount and molecular mass. J Chromatogr A 768:295–307
28. Kim MY, Varenne A, Daniel R et al (2003) Capillary electrophoresis profiles of fucoidan and heparin fractions: significance of mobility dispersity for their characterisation. J Sep Sci 26:1154–1162
29. Stefansson M (1999) Electrohydrodynamic instabilities and segregation of polysaccharides in capillary polymer solution electrophoresis. Biopolymers 49(6):515–524
30. Carney SL, Caterson B, Penticost HR (1996) The investigation of glycosaminoglycan mimotope structure using capillary electrophoresis and other complementary electrophoretic techniques. Electrophoresis 17:384–390
31. Kinoshita M, Shiraishi H (2002) Determination of molecular mass of acidic polysaccharides by capillary electrophoresis. Biomed Chromatogr 16:141–145
32. Cheng M-C, Lin S-L, Wu S-H et al (1998) High-performance capillary electrophoresis characterization of different types of oligo- and polysialic acid chains. Anal Biochem 260:154–159
33. Sudor J, Novotny M (1993) Electromigration behaviour of polysaccharides in capillary electrophoresis under pulsed-field conditions. Proc Natl Acad Sci U S A 90:9451–9455
34. Stefansson M, Novotny M (1994) Modification of the electrophoretic mobility of neutral and charged polysaccharides. Anal Chem 66:3466–3471
35. Kakehi K, Kinoshita M, Hayase S et al (1999) Capillary electrophoresis of N-acetylneuraminic acid polymers and hyaluronic acid: correlation between migration order reversal and biological functions. Anal Chem 71:1592–1596
36. Tokarz M, Gustavsson P, Stefansson M (2002) Employment of detergent-tag/solute interactions in capillary electrophoresis of neutral polysaccharide. Biomed Chromatogr 16:134–140
37. Zhong H-J, Williams MAK, Goodall DM et al (1998) Capillary electrophoresis studies of pectins. Carbohydr Res 308:1–8
38. Stefansson M (1998) Characterization of cellulose derivatives and their migration behaviour in capillary electrophoresis. Carbohydr Res 312:45–52
39. Williams MAK, Foster TJ, Schols HA (2003) Elucidation of pectin methylester distributions by capillary electrophoresis. J Agric Food Chem 51(7):1777–1781
40. Jiang C-M, Wu M-C, Chang Chang H-M (2001) Determination of random- and blockwise-type de-esterified pectins by capillary zone electrophoresis. J Agric Food Chem 49(11):5584–5588
41. Piripi SA, Williams MAK, Thompson KG (2010) On the sulfation pattern of polysaccharides in the extracellular matrix of sheep with chondrodysplasia. Cartilage 21:36–39
42. Kinoshita M, Kakoi N, Matsuno Y-K (2010) Determination of sulfate ester content insulfated oligo- and poly-saccharides by capillary electrophoresis with indirect UV detection. Biomed Chromatogr 25:588–593
43. King JT, Desai UR (2011) Linear polyalkylamines as fingerprinting agents in capillary electrophoresis of low-molecular-weight heparins and glycosaminoglycans. Electrophoresis 32:3070–3077
44. Karamanos NK, Hjerpe A (2002) Capillary electrophoresis of intact and depolymerized glycosaminoglycans and proteoglycans. In: El Rassi Z (ed) Carbohydrate analysis by modern chromatography and electrophoresis. J Crom Libr, vol 22, Elsevier Sci
45. Kakehi K, Kinoshita M, Yasueda S-i (2003) Hyaluronic acid: separation and biological implications. J Chromatogr 797:347–353
46. Kakehi K, Kinoshita M, Nakano M (2002) Analysis of glycoproteins and the oligosaccharides thereof by high performance capillary electrophoresis-significance in regulatory stud-

ies on biopharmaceutical products. Biomed Chromatogr 16:103–115
47. Magnusdottir S, Isambert H, Heller C, Viovy J-L (1999) Electrodynamically induced aggregation during constant and pulsed field capillary electrophoresis of DNA. Biopolymers 49:385–401
48. Quesada MA (1997) Replaceable polymers in DNA sequencing by capillary electrophoresis. Curr Opin Biotechnol 8:82–93
49. Welch CF, Hoagland DA (2001) Molecular weight analysis of polycations by capillary electrophoresis in a solution of neutral polymer. Polymer 42:5915–5920
50. Bohrisch J, Grosche O, Wendler U, Jaeger W, Engelhard H (2000) Electroosmotic mobility and aggregation phenomena of model polymers with permanent cationic groups. Macromol Chem Phys 201:447–452
51. Clos HN, Engelhard H (1998) Separation of ionic and cationic synthetic polyelectrolytes by capillare gel electrophoresis. J Chromatogr A 802:149–157
52. Cottet H, Gareil P (1997) Electrophoretic behaviour of fully sulfonated polystyrenes in capillary filled with entangled polymer solutions. J Chromatogr A 772:369–384
53. Starkweather EM, Hoagland DA, Muthukumar M (2000) Polyelectrolyte electrophoresis in a dilute solution of neutral polymer: model studies. Macromolecules 33:1245–1253
54. Heller C (1995) Capillary electrophoresis of proteins and nucleic acids in gels and entangled polymer solutions. J Chromatogr A 698:19–31
55. Guido S (1995) Cholesteric textures of aqueous hydroxypropylcellulose solutions. Mol Cryst Liq Crist 266:111–119
56. Kobayashi A, Akaike H (1986) Enhanced adhesion and survival efficiency of liver cell in culture disches coated with a lactose carrying styrene homopolymer. Makromol Chem Rapid Commun 7:645–650
57. Maeda H, Ueda M, Morinaga T, Matsumoto T (1985) Conjugation of poly(styrene-*co*-maleic acid) derivatives to the antitumor protein neocarzinostatin: pronounced improvements in pharmacological properties. J Med Chem 28:455
58. Donati I, Gamini A, Vetere A, Campa C, Paoletti S (2002) Synthesis, characterization and preliminary biological study of glycoconjugates of poly(styrene-*co*-maleic acid). Biomacromolecules 3:805–812
59. Hubbel JA (1999) Bioactive biomaterials. Curr Opin Biotechnol 10:123–129
60. Henc L, Polak GM (2002) Third generation biomedical materials. Science 5557:1014–1017
61. Donati I, Stredanska S, Silvestrini G, Vetere A, Marcon P, Marsich E, Mozetic P, Gamini A, Paoletti S, Vittur F (2005) The aggregation of pig articular chondrocyte and synthesis of extracellular matrix by lactose modified chitosan. Biomaterials 26:987–998
62. Pellizzaro C, Coradini D, Abolafio G, Daidone MG (2001) Modulation of cell cycle-related proteins but not of p53 expression by sodium butyrate in a human non-small cell lung cancer cell line. Int J Cancer 91:658–664
63. Yamamoto H, Fujimoto J, Okamoto E, Furujama J, Tamaoki T, Hashimoto-Tamaoki T (1998) Suppression of growth of hepatocellular carcinoma by sodium butyrate in vitro and in vivo. Int J Cancer 76:897–902
64. Coradini D, Pellizzaro C, Abolafio G, Bosco M, Scarlata I, Cantoni S, Stucchi L, Zorzet S, Turrin C, Sava G, Perbellini A, Daidone MG (2004) Hyaluronic-acid butyric esters as promising antineoplastic agents in human lung cancer carcinoma: a preclinical study. Invest New Drugs 22:207–217
65. Ventura C, Maioli M, Asara Y, Santoni D, Scarlata I, Cantoni S, Perbellini A (2004) Butyric and retinoic mixed ester of hyaluronan. A novel differenting glycoconjugate affording a high throughput of cardiogenesis in embryonic stem cells. J Biol Chem 279:23574–23579
66. Campa C, Oust A, Skjåk-Bræk G, Paulsen BS, Paoletti S, Christensen BE, Ballance S (2004) Determination of average degree of polymerization and distribution of oligosaccahrides in partially acid hydrolyssed homopolysaccharide: a comparison of four experimental method applied to mannuronan. J Chromogr 1026:271–281
67. Flory PJ (1953) Principles of polymer chemistry. Cornell University Press, Ithaca, NY
68. Cottet A, Gareil P (2001) On the use of the activation energy concept to investigate analyte and network deformations in entangled polymer solution capillary electrophoresis of synthetic polyelectrolytes. Electrophoresis 22:684–691
69. Allison A, Mazur S (1998) Modeling free solution electrophoretic mobility of short DNA fragments. Biopolymers 46:359–373
70. Stellwagen NC, Gelfi C, Righetti PG (1997) The free solution mobility of DNA. Biopolymers 42:687–703
71. Gao JY, Dubin P, Sato T, Morishima Y (1997) Separation of polyelectrolytes of variable composition by free-zone capillary electrophoresis. J Chromogr 766:233–236
72. Popov A, Hoagland DA (2004) Electrophoresis evidence for a new type of counterion conden-

sation. J Polym Sci B Polym Phys 42:3616–3627
73. Hoagland DA, Arvanitidou E, Welch C (1999) Capillary electrophoresis measurements of free solution mobility for seversal model polyelectrolyte systems. Macromolecules 32(19):6180–6190
74. Cleland RL (1991) Electrophoretic mobility of wormlike chains.1. Experiment: hyaluronate and chondroitin-4-sulfate. Macromolecules 24(15):4386–4390
75. Overbeek JTG (1943) Theorie der elektrophorese. Kolloid-Beih 54:287–364
76. Booth F (1950) The cataphoresis of spherical, solid non conducting particles in a symmetrical electrolyte. Proc R Soc Lond 203:533–551
77. Saville DA (1994) Dielectric behavior of colloidal dispersions. Colloids Surf A 92:29–40
78. Ohshima H (2002) Modified Henry function for the electrophoretic mobility of a charged spherical colloid particle covered with an ion-penetrable uncharged polymer layer. J Colloid Interface Sci 252:119–125
79. Cohen JA, Korosheva VA (2001) Electrokinetic measurement of hydrodynamic properties of grafted polymer layers on liposome surfaces. Colloids Surf A Physicochem Eng Aspects 195:113–127
80. Tanford C (1965) Physical chemistry of macromolecules. Wiley, New York
81. Cleland RL (1991) Electrophoretic mobility of wormlike chains 2. Theory Macromol 24(15):4391–4402
82. Campa C, Donati I, Vetere A, Gamini A, Paoletti S (2001) Synthesis of glycosylamines: identification and quantification of side products. J Carbohydr Chem 20(3&4):263–273
83. Gamini A, Paoletti S, Zanetti F (1992) Chain rigidity of polyuronates: static light scattering of aqueous solutions of hyaluronate and alginate. In: Harding SE, Sattelle DB, Bloomfield VA (eds) Laser light scattering in biochemistry. Royal Society of Chemistry, London, UK

Chapter 18

Separation of Peptides by Capillary Electrophoresis

Gerhard K.E. Scriba

Abstract

Peptides are an important class of analytes in chemistry, biochemistry, food chemistry, as well as medical and pharmaceutical sciences including biomarker analysis in peptidomics and proteomics. As a high-resolution technique, capillary electrophoresis (CE) is well suited for the analysis of polar compounds such as peptides. In addition, CE is orthogonal to high-performance liquid chromatography (HPLC) as both techniques are based on different physicochemical separation principles. For the successful development of peptide separations by CE, operational parameters including puffer pH, buffer concentration and buffer type, applied voltage, capillary dimensions, as well as background electrolyte additives such as detergents, ion-pairing reagents, cyclodextrins, (poly)amines, and soluble polymers have to be considered and optimized.

Key words Capillary electrophoresis, Electromigration techniques, Peptides, Peptide analysis, Method development

1 Introduction

Peptides represent an important class of biologically active compounds acting as hormones, neurotransmitters, immunomodulators, coenzymes, enzyme inhibitors, toxins, or antibiotics. In addition, peptides can serve as biomarkers in clinical analysis. Finally, peptides and peptidomimetics comprise an important class of approved drugs and drug candidates under development. While high-performance liquid chromatography (HPLC) has been traditionally the method of choice for the separation and analysis of peptides, capillary electrophoresis (CE) has emerged as a very useful technique for peptide analysis in recent years. CE is complementary to HPLC as the selectivities of both techniques are based on different physicochemical principles. While HPLC separations are primarily based on the lipophilicity/hydrophobicity of the analytes, separations in CE are accomplished due to differences in the charge density (charge-to-mass ratio) of compounds. Thus, separations that are difficult to achieve with one technique may be easily performed by the other method. In addition, CE offers rapid

Philippe Schmitt-Kopplin (ed.), *Capillary Electrophoresis: Methods and Protocols*, Methods in Molecular Biology, vol. 1483,
DOI 10.1007/978-1-4939-6403-1_18,

method development and is an extremely flexible technique that offers high peak resolution. CE is very economic since only low amounts of chemicals and sample are required and no or little organic solvent is used.

Natural peptides of eukaryotic cells are primarily composed of the 21 so-called proteinogenic L-configured amino acids but D-amino acids as well as unusual amino acids can also be found. Depending on the composition and number of amino acid residues, peptides may differ in charge, size, shape, hydrophobicity, and binding capabilities. These physicochemical properties allow their separation by the various capillary electromigration techniques, i.e., capillary zone electrophoresis (CZE), micellar electrokinetic chromatography (MEKC), capillary isoelectric focusing (CIEF), or capillary electrochromatography (CEC). This chapter focuses on the analysis of peptides by CZE. Following a short general overview in peptide CE separations, important considerations for method development are discussed and a practical example is presented. For further details including specifics of the other electromigration techniques in peptide analysis the reader is referred to recent reviews [1–11], book chapters [12, 13], and a monograph [14]. The specifics of the migration behavior of peptides and proteins in CEC as a combination of analyte migration and retention by the stationary phase have been elaborated [15, 16].

1.1 Overview

1.1.1 Analyte Separation

In CE, analytes are separated on the basis of the applied field as a function of the physicochemical properties such as its charge density (charge-to-mass ratio) depending on the background electrolyte. The overall charge of the peptide is the sum of the charges of the deprotonated (negative) groups and protonated (positive) groups. Negatively charged groups can arise from the carboxyl acid terminus as well as the side-chain groups of Asp, Glu, Cys, and Tyr. Groups that can be positively charged are the terminal amino function and the lateral groups of Lys, Arg, and His. The charge of a peptide at a certain pH value can be calculated provided that the exact pK_a values of the ionizable groups of a given peptide are known. However, the pK_a values of peptides are a complex function not only of the amino acid sequence but also of the whole structure (i.e., the secondary and tertiary structure) of the peptides. For theoretical considerations approximations of the pK_a values can be used [1, 12].

The electrophoretic mobility, μ, of a particle in electrophoresis is described by the electrophoretic equation

$$\mu = \frac{Q}{6\pi\eta r}$$

where q is the charge and r the Stokes radius of the particle. η is the viscosity of the electrolyte solution and 6π a factor for spherical particles. In order to predict the mobility of a peptide, the Stokes

radius, r, must be known. As this information cannot be obtained from the amino acid sequence, different approaches have been taken in order to predict the mobility of peptide analytes [8, 9, 17]. The first approaches correlated the size (expressed as molecular mass or number of amino acids) and charge (derived from the pK_a values of functional groups) as variables with the observed electrophoretic mobility. In several studies good correlations between the electrophoretic mobility, μ_{eff}, and the ratio q/M_r^x were observed with the parameter x with values between 1/3 and 2/3. However, these two-variable models were mostly applicable only to a relatively narrow set of peptides differing not too much with respect to size, charge, and charge distribution. Subsequently, multi-variable models including further parameters such as length and width of the peptide chain, a steric substitution constant, or molar refractivity (related to the volume of the molecules) were developed in order to achieve a better fit between the mobility and the variables. Artificial neuronal network approaches have also been undertaken [17]. Nonetheless, the exact prediction of the mobilities of peptides as a function of their charge and size remains a challenging task.

Background electrolyte pH is the most important factor in CE as it regulates the charge of the peptides. Theoretical considerations [12] suggest that the best resolution between peptides occurs at a pH value where the peptide mobility is not very high. However, since short analysis time is often required separations are often performed at a lower pH value where resolution is still good and peptide charge is high. Other requirements such as stability or suppression of wall interactions may also apply. Overall, good separations are often achieved at a buffer pH close to the pK_a values of the terminal carboxyl group or side-chain carboxyl groups when Asp or Glu is present. Further variables influencing the electrophoretic analyte mobility may have to be optimized if buffer pH modulation cannot achieve sufficient resolution. These factors include the ionic strength (concentration) of the buffer, capillary temperature, applied voltage, or the use of buffer additives such as organic solvents, surfactants, ion pair reagents, metal ions, or chiral selectors (see method development).

Different separation modes are available in CE. Capillary zone electrophoresis (CZE, often simply also referred to as CE) is the most universal, most powerful, and most frequently used separation mode for peptide analysis. The peptides are resolved based on charge and size, i.e., differences in the electrophoretic mobility due to different charge densities. In micellar electrokinetic chromatography (MEKC) a detergent is added at concentrations above the critical micelle concentration resulting in the formation of micelles as a pseudostationary phase. In this mode analytes are separated based on the partition coefficients between the aqueous and the micellar phase in addition to electrophoretic mobility. Thus, MEKC can be applied to the analysis of electroneutral (uncharged) peptides but it

can also be utilized for charged compounds when sufficient resolution by CZE cannot be obtained. Microemulsion electrokinetic chromatography (MEEKC) utilizes an optically transparent microemulsion as pseudostationary phase. The separation mechanism and analytical applications of MEEKC are comparable to MEKC. Analyte separation in capillary isotachophoresis (CITP) is based on the mobilities of the compounds between a leading electrolyte and a terminating electrolyte leading to distinct zone of the individual analytes immediately following each other. CITP as such has not been widely applied to peptide separations but isotachophoretic principles are used in preconcentration stacking procedures. In capillary isoelectric focusing (CIEF) peptides are separated in a pH gradient based on their isoelectric point. However, because the effective charge of small peptides similar to amino acid approaches zero over a rather broad pH range, the application of CIEF to oligopeptide analysis is rather limited. It is used for the characterization of large polypeptides as well as for the determination of microheterogeneity of polypeptides. Capillary gel electrophoresis (CGE) utilizing separations based on molecular size in sieving media (gels) is primarily used for the analysis of oligonucleotides and macromolecules such as DNA or proteins. Capillary electrochromatography (CEC) is considered a hybrid technique between HPLC and CE combining the high peak efficiency of CE with the separation selectivity of a stationary phase. The driving force in CEC is the electroosmotic flow generated upon application of the electric field along the capillary as a consequence of the charged surface of the capillary or the packing material. Although currently not considered a mature technique CEC has been also applied to peptide analysis. For a discussion of the migration behavior of peptides in CEC *see* ref. [16].

1.1.2 Detection

As for other analytes the detection of peptides in CE can be a challenging task due to the microscale capillary dimensions and the small amount of injected sample. UV detection in the short wavelength region at 200–220 nm is the most commonly used method of detection of peptides in CE. The absorbance in this UV region is due to the absorbance of the peptide amide bonds. Some structural information such as the presence of aromatic amino acids such as Phe, Tyr, or Trp can be obtained by scanning the UV spectrum when using a diode array detector (DAD). UV detection limits are typically not better than the low micromolar range (10^{-5}–10^{-6} M). Lower detection limits may be achieved by increasing the optical pathlength by applying different capillary detection cell geometries such as bubble cells or Z-cells. Another approach to increase the sensitivity is the derivatization of the peptides yielding derivatives with higher molar absorptivities [18, 19].

Fluorescence as a more sensitive detection method of native peptides is only possible when the aromatic amino acids Tyr or Trp are present but both amino acids are poor fluorophores and require

excitation in the 210–290 nm wavelength range. Detection limits may be improved by a factor of 10–100. More commonly, laser-induced fluorescence (LIF) detection of peptides in CE is based on labeling the peptides with a fluorescent tag that can be excited at the wavelength of the commercially available He-Cd laser (325 nm) or argon-ion laser (488 nm). Several chemistries have been developed mostly derivatizing the amine residues in peptides [18–23]. Examples include o-phthalaldehyde, naphthalene-2,3-dicarboxaldehyde, fluorescamine, or 3-(4-carboxybenzyl)-2-quinoline carboxaldehyde as reagents for primary amino groups. 9-Fluorenylmethyl chloroformate and fluorescein isothiocyanate label primary and secondary amino groups. When multiple reactive sites are available the chemistry has to be optimized to yield a single product. Derivatization is performed either after the CE separation (post-column) or more frequently before injecting the samples into the system (pre-column). Typically the detection limit of LIF is in the 10^{-9} M range, corresponding to an increase in sensitivity of 1000 compared to UV detection.

Mass spectrometry (MS) is an ideal detection technique in peptide CE analysis especially for complex mixtures of biomolecules [24–26] including biomarker peptidomics/proteomics analysis [27–30]. CE-MS not only allows high-accuracy determination of the relative molecular masses of the separated peptides but also provides important structural data on the amino acid sequence or sites of post-translational modifications via tandem MS (MS/MS). Electrospray ionization (ESI) MS is the preferred mode for online coupling of CE with MS. Typical mass analyzers comprise triple-quadrupole, time-of-flight (TOF), quadrupole-TOF, as well as ion-trap instruments. Unfortunately, CE-ESI-MS is not extremely sensitive due to the necessity of a sheath liquid flow in most applications in order to obtain a stable electrospray. This results in a dilution of the sample with concomitant loss of sensitivity. Nevertheless, very sensitive applications have also been developed. Matrix-assisted laser desorption ionization (MALDI) is applied primarily in the off-line mode. Furthermore, CE coupled to Fourier-transform ion cyclotron resonance (FT-ICR) MS has been applied in peptide analysis [31, 32].

Further detection modes applied in CE include refractive index, electrochemical (potentiometric, amperometric, capacitively coupled contactless conductivity), chemiluminescence, and mid-infrared detectors.

1.1.3 Suppression of Wall Adsorption

The suppression of the adsorption of peptides to the inner surface of unmodified fused silica capillaries may be required for larger peptides while small peptides normally do not trend to adsorb to the capillary wall. Wall adsorption is believed to be based primarily on ionic interactions between the ionized silanol groups of the fused silica wall and the peptides, especially basic peptides. Subsequently, several strategies for a suppression of wall adsorption may be

employed. The analysis can be performed at extreme pH values of the background electrolyte where either the silanol groups are not dissociated (low pH) or the peptide is negatively charged (high pH) leading to electrostatic repulsion. High-ionic-strength buffers also reduce analyte-wall interactions due to competition of the buffer ions with the binding sites on the capillary wall. However, their use is limited due to the high electrical current generated leading to excessive Joule heating and subsequent loss in separation efficiency. More appropriate and effective suppression of wall adsorption can be achieved by dynamic or permanent coating of the capillary surface blocking the silanol interaction sites for the analytes. Dynamic (reversible) coating can be performed by the addition of (oligo) amines or quaternary ammonium compounds, neutral polymers, or neutral and zwitterionic surfactants to the background electrolyte [33–35]. Positively charged coatings based on polybrene, multilayer coatings such as polybrene-dextran sulfate-polybrene, polyethyleneimine, or *N,N*-dimethylacrylamide-ethylpyrrolidine methacrylate in combination with low-pH-background electrolytes can be employed because under these conditions both peptides and capillary wall are positively charged avoiding peptide-wall interactions.

Permanent coatings require the formation of a chemical bond between the silanol groups of the fused silica capillary and the coating material, usually a polymer. The reactions typically involve the formation of a covalent bond with a reagent containing a double bond and subsequent binding of a polymer to this intermediate layer. Several chemistries have been developed for the reproducible formation of hydrolytically stable, covalently bound polymers including poly(acrylamide) derivatives, polyvinyl alcohol, polyethylene glycol, and cellulose derivatives [34–37].

Both dynamic and permanent coatings are also used for efficient control of the EOF [35]. Coated capillaries as well as kits for dynamic coatings are commercially available. Strategies in peptide analysis can also be found in refs. [2, 3, 6–11].

1.1.4 Sample Concentration

The concentration of peptides in synthetic samples usually does not represent a problem. However, for the analysis of compounds in biological samples preconcentration may be required in order to achieve the appropriate sensitivity. Generally, the same principles are applied in peptide CE analysis as for nonpeptide analytes. Sample concentration can be either performed off-line by solid-phase or liquid-liquid extraction or online by chromatographic or more frequently by electrophoretic stacking techniques. CE with online enrichment for the analysis of biological samples by chromatographic and electrophoretic preconcentration [38] as well as general sample stacking strategies [39–42] have been summarized. Further specific examples in peptide analysis can be found in references [2, 3, 6–11].

1.1.5 Applications

The separation of peptides by CE has been described in numerous publications. Especially the increasing number of recombinant DNA technology products has expedited the use of CE in peptide analysis as the major technique for peptide characterization as well as a complementary method to HPLC in quality control of synthetic and fermentation products. Any reaction resulting in a change of the charge and/or size of a peptide can be monitored by CE. These include degradation reactions such as hydrolysis, oxidation, or deamidation as well as posttranslational modifications such as glycosylation or phosphorylation. In addition, sample microheterogeneity resulting from multiple modification sites may be analyzed.

Analytical CE of peptides can be divided into the following categories: (1) the use of peptides as model compounds to study fundamental aspects of CE or to demonstrate the feasibility of a certain concept or technique; (2) the analysis of synthetic peptides for purity control; (3) the analysis of bioactive peptides in biological samples; and (4) the analysis of peptide maps following tryptic digestion of proteins. The latter is also used to study posttranslational modifications. Applications of CE to peptide analysis have been summarized in Table 1. Further examples

Table 1

Examples of the application of CE to the analysis of peptides

Type of analysis	Examples
Peptide mapping	Growth hormones, erythropoietin, granulocyte-stimulating factor, ovalbumin, human tissue plasminogen activator, somatotropin, interleukins, α-casein, β-casein, β-lactoglobulin
Peptide identification/separation of closely related peptides	Natural and synthetic peptides including enkephalins, insulins, dynorphin analogs
Purity of peptides	Adrenocorticotropic hormone, endorphins, cholecystokinin, insulin, neuropeptide Y, hirudin, insulin-like growth factor, bradykinin, ginseng polypeptide, protergin IB-367, somatostatin, vasopressin, tetracosactide, cyclosporine A, dalargin, lecirelin, IgG1 fragment
Peptide degradation/stability	Insulin, goserelin, Asp tripeptides, Asp hexapeptide, neuropeptide Y, LHRH analogs, cyclosporin A
Stereoisomer analysis	Di-, tri-, and tetrapeptides, N-derivatized peptides, peptide-derived drugs, neuropeptide Y
Bioanalysis of physiological peptides	Enkephalins, vasoactive intestinal peptide, cytokines, gonadorelin, angiotensin II, glutathione, neurotensin, vasopressin, somatostatin, thyreotropin-releasing hormone, amyloid peptides, glutathione, neuropeptides
Determination of reaction kinetics	Peptide oxidation, kinase and phosphatase activity, angiotensin-converting enzyme activity
Determination of pK_a	Di-, tri-, and tetrapeptides, enkephalins, phosphinic pseudopeptides

include monitoring reactions such as homo- and heterodimer formation, cis/trans interconversion of Pro-peptides, and peptide folding and unfolding as well as the complexation between peptides and natural or synthetic polymers (*see* also refs. [1–13]). CE can be used for the determination of physicochemical constants such as pK_a and pI values or lipophilicity (log *D*).

CE-MS has also been established as a powerful analytical tool in biomarker discovery and peptidomics/proteomics [27, 28, 43]. Peptidomics comprise the qualitative and quantitative analysis of physiologically active peptides within an organelle, a cell, a tissue, or an organism under a certain condition or at a given point of time [44]. The term typically refers to polypeptides in the range of about 500–20,000 Da, bridging the gap between proteomics and metabolomics. The polypeptides may be intact small molecules such as hormones, cytokines, and growth factors released by the action of proteolytic enzymes from large protein precursors or they may be protein degradation products. Therefore, peptides in biological fluids reflect protein synthesis, processing, and degradation which may be different in health and disease states of individuals. Serum and urine have been primary physiological fluids analyzed in peptidomics with thousands of polypeptides identified in these matrices [29, 30, 43, 45–47]. Analyzing serum, it should be kept in mind that some of the high-abundance peptides originate from coagulation and complement cascades that occur ex vivo after obtaining the sample. Databases as well as standards have been established for the peptidome in human urine for clinical diagnosis [48–50].

A specific application of CE is the separation of peptide stereoisomers. Such analyses are important to monitor stereoisomer purity of synthetic peptides in quality control. Peptide diastereomers can often be separated in CE without chiral background electrolyte additives as diastereomers differ in their physicochemical properties. Thus, careful manipulation of the buffer pH can exploit the small differences in the pK_a values. Most peptide diastereomer separations reported so far have been achieved in the acidic pH region. The resolution of peptide enantiomers can be performed by the indirect or direct method. The indirect method involves the derivatization with a stereochemically pure agent to form diastereomers, which can be subsequently separated in an achiral system [51–55]. The direct enantioseparation is based on the formation of transient diastereomeric complexes between the analyte enantiomers and a stereochemically pure chiral selector. Native and derivatized cyclodextrins, the chiral crown ether (+)-(18-crown-6)-2,3,11,12-tetracarboxylic acid, the macrocyclic antibiotics vancomycin and teicoplanin, chiral ligand exchange complexation, and chiral ion-pair formation have been applied for peptide enantioseparations [51–55].

1.2 Method Development

Generally, method development in CE analysis of peptides follows the principal considerations for method development of non-peptide

analytes. The effect of important variables on peptide analysis will be briefly discussed here; a more general and detailed discussion of the various parameters can be found in the literature [56, 57].

1.2.1 Separation Capillary

In CE, the resolution and efficiency are proportional to the length of the capillary under a constant electric field. Efficiency and migration times increase linearly while resolution depends on the square root of length. Therefore, improving efficiency and resolution by increasing the length of the capillary occurs at the expense of increased analysis time. Generally, longer capillaries may be required for the analysis of complex mixtures while short capillaries are preferred for less complex mixtures or in the case of very long analysis times.

With respect to the inner diameter (ID) of the capillary, some loss of efficiency and resolution is observed when increasing the capillary diameter. Small ID capillaries allow the use of higher ionic strength buffers and higher applied voltages because less Joule heat is generated. The capillary diameter has only little effect on the electroosmotic flow. On the other hand, the sensitivity increases with diameter because the optical path is increased. Moreover, large-bore capillaries allow higher mass loading.

In CE peptide separations, unmodified fused-silica capillaries are often used. If surface interaction of the analytes is observed, intermediate rinses with sodium hydroxide solutions may be required. Alternatively, coated capillaries can be used to suppress wall interactions. Hydrophilicity and hydrophobicity of the inner wall can be manipulated. In addition, coated or surface-modified capillaries modify, stabilize, eliminate, or reverse the electroosmotic flow by producing a stable, reproducible surface. Surface coating may also alter the separation selectivity. For the various chemistries for dynamic and permanent surface modifications *see* refs. [33–37]. Low-pH background electrolytes are often combined with either positively charged dynamic coatings or neutral permanent coatings.

1.2.2 Separation Buffer

In CE, solute migration velocity, separation efficiency, and peak shape are sensitive to characteristics of the buffer (background electrolyte). The buffer controls not only the ionization and migration of the analytes but also the magnitude of the electroosmotic flow (EOF) which is driven by the residual charges of the inner wall of the separation capillary. Moreover, the buffer capacity has to be high enough to ensure that the local pH and conductivity will not change as the result of the introduction and migration of the sample across the capillary. Additional factors that should be considered when selecting an appropriate buffer in CE are the compatibility of the background electrolyte with the stability of the analytes and other additives, running current (see applied voltage above), or UV absorbance. A detailed discussion can be found in ref. [58].

The pH of the separation buffer is the most important parameter for optimizing the separation selectivity. Although CE peptide

analysis has been reported over a wide range of pH, two pH regions appear to be especially useful. At low pH, i.e., pH 2–4, the basic groups of the peptides are protonated and the peptides migrate as cations. Selectivity (differences in the electrophoretic mobilities) can be achieved by exploiting small differences in the dissociation equilibria of the acidic groups. The pK_a of the C-terminal carboxyl groups is around 3, and the pK_a of side-chain carboxyl groups of Asp and Glu ranges between 3.5 and 4.5. The exact pK_a depends not only on the individual amino acid but also on the amino acid sequence and the microenvironment within the peptide resulting in small pK_a differences even of closely related peptides, which can be exploited for their CE separation. In addition, at pH < 3 the dissociation of the silanol groups of the capillary wall is negligible so that wall adsorption of analytes onto the surface is suppressed. Figure 1 illustrates the effect of pH between 2.5 and 3.5 for a set of nine peptides. At pH 2.5 two peptides comigrate (bradykinin and angiotensin I). Increasing the pH results in a separation of these two peptides but interference between other peptides is observed. In addition, the migration order of peptides 5–8 changes. For example, the dipeptide L-Ala-D-Phe (peptide 5) migrates faster than the tripeptide Gly-Leu-Tyr (peptide 6) below pH 3 while the migration order is reversed at pH values of 3.0 and above. Apparently the carboxylic acid group of L-Ala-D-Phe is more acidic resulting in a lower overall positive charge of the smaller peptide which translates into slower electrophoretic migration at pH 3 and above.

An example for a separation of closely related peptides based on differences in the pK_a values is shown in Fig. 2. The peptides differ only in the position of the amide bond with respect to Asp. In one peptide Asp is connected to the following amino acid via the α-carboxyl group, while the amide bond is formed with the β-carboxyl group of the side chain of Asp in the case of the other peptide (so-called β-Asp or *iso*-Asp linkage). Moreover, peptide diastereomers can also be separated at acidic pH due to small differences in the dissociation equilibria of the diastereomers. This is illustrated by the separation of L-Ala-L-Phe and L-Ala-D-Phe in Fig. 1 as well as by the examples of the pair of isomeric tripeptides Phe-Asp-GlyNH_2 and Phe-β-Asp-GlyNH_2 in Fig. 3. The latter example shows the simultaneous separation of isomeric α-Asp and β-Asp peptides and their diastereomers.

Phosphate buffers are often used at acidic pH values. Substituting the buffer cation by organic amines such as triethylamine or triethanolamine may be beneficial for peptide separations. The amines are positively charged at low pH covering residual charges on the capillary wall and, thus, suppressing analyte wall interactions. In addition, an anodic EOF is generated by adsorption of the amines to the capillary wall often resulting in increased efficiency. Figure 4 compares the effect for a mixture of peptides at pH 2.7 using sodium phosphate buffer and triethanolamine-phosphate buffer obtained by titration of phosphoric acid with triethanolamine to pH 2.7.

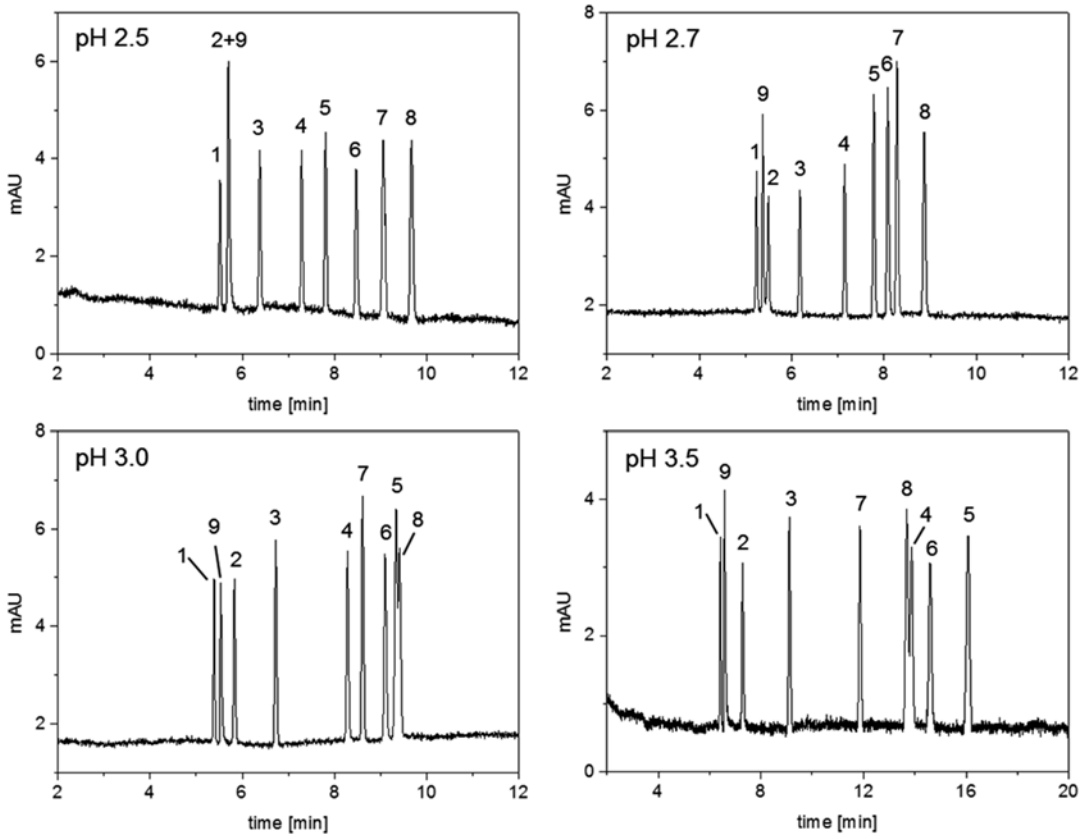

Fig. 1 Separation of model peptides at different buffer pH values. Experimental conditions: fused-silica capillary, 50 cm effective length, 57 cm total length, 50 μm ID; 50 mM sodium phosphate buffer; 25 kV, 20 °C; detection wavelength 215 nm. For peptide identification *see* Table 2

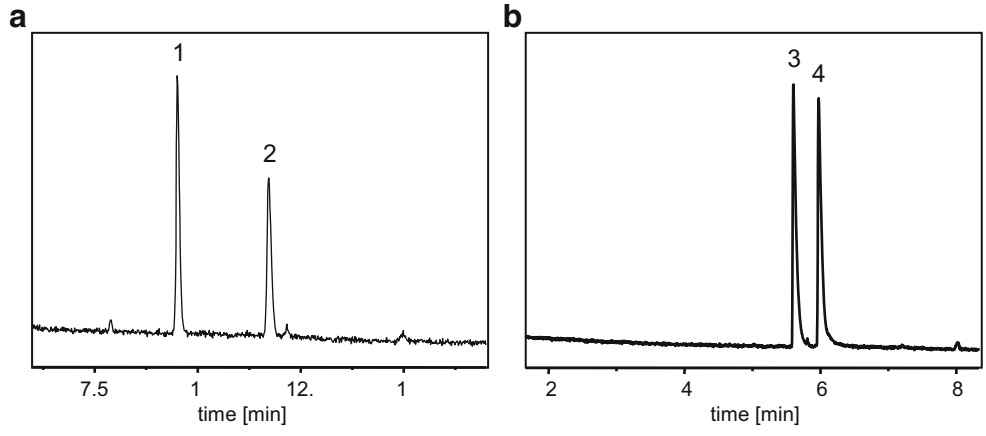

Fig. 2 Separation of α-Asp and β-Asp peptides. (**a**) Isomeric angiotensin II peptides Asp-Arg-Val-Tyr-Ile-His-Pro-Phe (1) and β-Asp-Arg-Val-Tyr-Ile-His-Pro-Phe (2); (**b**) isomeric β-amyloid peptide fragment (4) Phe-Arg-His-Asp-Ser-Gly (3) and Phe-Arg-His-β-Asp-Ser-Gly. Experimental conditions: fused-silica capillary, 40 cm effective length, 47 cm total length, 50 μm ID; 50 mM sodium phosphate buffer, pH 2.5 (**a**) or pH 3.0 (**b**); 20 kV, 20 °C; detection wavelength 215 nm

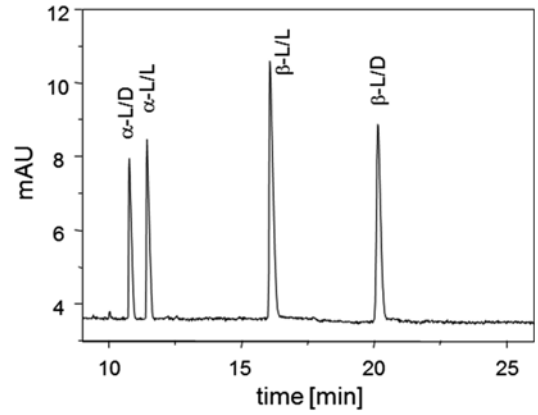

Fig. 3 Simultaneous separation of the diastereomers of the isomeric tripeptides Phe-α-Asp-GlyNH$_2$ and Phe-β-Asp-GlyNH$_2$. Experimental conditions: fused-silica capillary, 40 cm effective length, 47 cm total length, 50 μm ID; 50 mM sodium phosphate buffer, pH 3.0; 23 kV, 20 °C; detection wavelength 215 nm

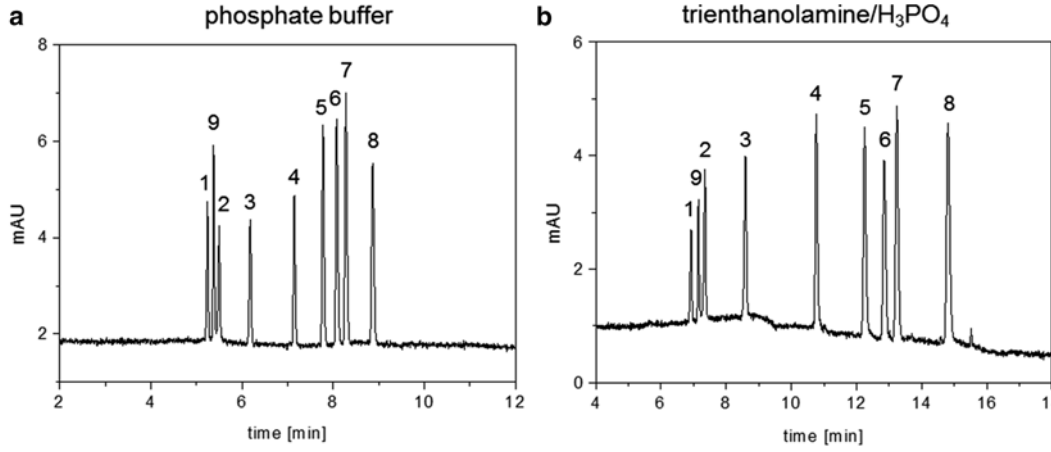

Fig. 4 Influence of the buffer type on the separation of model peptides. (**a**) 50 mM Sodium phosphate buffer, pH 2.7; (**b**) 50 mM phosphoric acid titrated to pH 2.7 with triethanolamine. Experimental conditions: fused-silica capillary, 50 cm effective length, 57 cm total length, 50 μm ID; 25 kV, 20 °C; detection wavelength 215 nm. For peptide identification *see* Table 2

A further useful pH range especially for basic peptides is pH 8–10. At this pH the peptides bear negative charges and migrate as anions. The dissociation equilibria of basic groups can be targeted to achieve selectivity. The pK_a values of peptide N-termini range between 7.5 and 9 depending on the amino acid while pK_a values of His and Lys are about 6 and 10, respectively. The pK_a of Arg is too high to be useful. At high pH the fused-silica silanol groups are also deprotonated so that the adsorption of peptides onto the capillary wall is minimized due to electrostatic repulsion.

Table 2

Peptides and amino acid sequence

No.	Amino acid sequence	Peptide
1	Arg-Val-Tyr-Ile-His-Pro-Phe	Angiotensin III
2	Asp-Arg-Val-Tyr-Ile-His-Pro-Phe-His-Leu	Angiotensin I
3	Asp-Arg-Val-Tyr-Ile-His-Pro-Phe	Angiotensin II
4	L-Ala-L-Phe	
5	L-Ala-D-Phe	
6	Gly-Leu-Tyr	
7	Trp-Met-Asp-PheNH_2	Tetragastrin
8	Tyr-Gla-Gly-Phe-Leu	Leu-enkephalin
9	Arg-Pro-Pro-Gly-Phe-Ser-Pro-Phe-Arg	Bradykinin

Buffer capacity has to be high enough to provide a stable pH throughout the separation. The capacity is directly proportional to the overall concentration of the buffer as well as the concentration ratio of the acidic and basic buffer species. A buffer is most effective at pH values close to the pK_a of the buffer acid. Generally, a buffer should only be applied in the pH range within ±1 units of the pK_a. High buffer concentrations (ionic strength) reduce analyte wall interactions, EOF, and electrophoretic analyte mobility resulting in an increase in resolution and efficiency (Fig. 5). In addition, analyte stacking effects can be achieved using high concentrations of separation buffers. On the other hand, the concentration of the electrolytes influences the electrical current and Joule heating, thus limiting the buffer concentration. Buffer anions as well as buffer cations can influence the EOF, analyte mobility, selectivity, and resolution so that careful adjustment of the buffer can improve a separation. A special class of buffers are the so-called isoelectric buffers. These buffers consisting of amphoteric compounds such as cysteic acid, iminodiacetic acid, aspartic acid, or glutamic acid possess a much lower conductivity compared to ionic salt buffers so that high operating voltages can be applied. For a detailed discussion of the theory and application of these buffers *see* ref. [59].

1.2.3 *Buffer Additives*

If pH optimization does not result in a sufficient resolution, buffer additives can be applied in order to maximize differences between the analytes and/or suppress undesired interactions. The most important classes of additives will be briefly addressed. Additives may be combined.

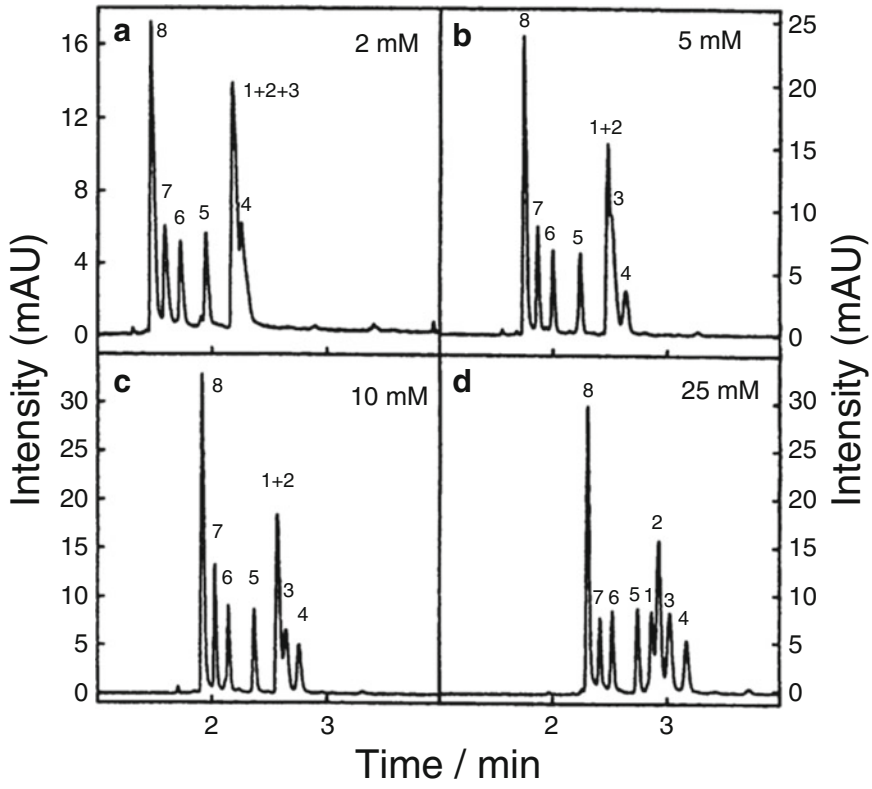

Fig. 5 Influence of buffer concentration on the separation of a mixture of synthetic peptides. Experimental conditions: fused-silica capillary, 8.5 cm effective length, 37 cm total length, 100 μm ID; sodium phosphate buffer, pH 2.0; –6.8 kV, 22 °C; detection wavelength 214 nm. Peptides: 1, Asp-His-Asp-Ile-Asn-Arg; 2, Trp-Asp-His-Asp-Ile-Asn-Arg; 3, Ser-Trp-Asp-His-Asp-Ile-Asn-Arg; 4, Asn-Ser-Trp-Asp-His-Asp-Ile-Asn-Arg; 5, His-Asn-Ser-Trp-Asp-His-Asp-Ile-Asn-Arg; 6, His-His-Asn-Ser-Trp-Asp-His-Asp-Ile-Asn-Arg; 7, His-His-His-Asn-Ser-Trp-Asp-His-Asp-Ile-Asn-Arg; 8, his-His-His-Asn-Ser-Trp (reprinted with permission by Elsevier from ref. [66] © 2003)

Organic solvents such as methanol, ethanol, 1-propanol, 2-propanol, or acetonitrile modify buffer viscosity, separation selectivity, and EOF. The electrical current decreases as the concentration of the organic solvent is increased. The effect of the organic solvents on a separation is difficult to predict. Acetonitrile typically leads to an increase of the EOF and a reduction of the analysis time while methanol increases the migration time of the analytes. Trifluoroethanol has also been successfully applied to peptide separations [60]. Organic solvents also affect the dissociation equilibria of solutes resulting in a change of the electrophoretic mobility compared to pure aqueous buffers. Thus, resolution and separation efficiency can change.

The addition of detergents above the critical micelle concentration (cmc) yields micelles as pseudostationary phase. This separation mode, also called micellar electrokinetic chromatography

(MEKC), was developed for the separation of neutral (uncharged) analytes. A separation is based on the partitioning of the analytes between the micelles and the buffer according to the lipophilicity of the compounds. With respect to peptide analysis, MEKC is suitable for the separation of hydrophobic peptides and peptides derivatized at the N- or C-terminus. But the method can also be employed to modulate the selectivity in the separation of closely related charged peptides by introducing lipophilicity as an additional differentiating parameter. Sodium dodecyl sulfate (SDS) is probably the most frequently used surfactant in MEKC working well in alkaline to neutral pH buffers but separations in low pH buffers have also been reported. Cationic surfactants, for example, cetyltrimethylammonium bromide (CTAB) or dodecyltrimethylammonium bromide (DTAB), reverse the EOF due to the formation of a layer producing a positively charged capillary surface. Zwitterionic surfactants such as 3-[(3-cholamidopropyl) dimethylammonio]-1-propanesulfonate (CHAPS), neutral detergents, for example, derivatives of the Tween or Brij series, as well as combinations of detergents have also been used. Altering the nature of the surfactant greatly affects the analyte interactions with the micelles and, therefore, separation selectivity and analyte migration order. Detergents are often combined with organic solvents or cyclodextrins. For a detailed discussion on theoretical considerations and surfactant selection in MEKC of peptides *see* ref. [61]. Figure 6 illustrates the effect of MEKC in the separation of a set of dynorphin analogs obtained by an Ala scan using the zwitterionic detergent CHAPS as additive.

Addition of ion-pair reagents, for example trifluoroacetic acid or the sodium salts of alkylsulfonic acids such as hexanesulfonic acid or heptanesulfonic acid, has been especially useful for the separation of smaller hydrophilic peptides. The ion-pair reagent neutralizes ionic groups of opposite charge and increases the hydrodynamic radius of the analytes. In addition, the ionic strength of the background electrolyte is increased and the EOF is reduced. The combined effects may or may not improve the resolution depending on the nature of the analytes. In addition, selectivity changes may be observed. An example comparing the separation of dynorphin analogs using "plain" buffer and upon addition of the ion-pair reagent hexanesulfonic acid sodium salt is illustrated in Fig. 6.

Cyclodextrins (CDs) are typically employed as chiral selectors for enantioseparations. CDs are cyclic oligosaccharides. The most commonly used compounds are α-CD, β-CD, and γ-CD consisting of 6, 7, and 8 α-(1,4)-linked glucopyranose units, respectively. Many neutral and charged derivatives especially of β-CD are commercially available. CDs have the shape of a truncated cone with a hydrophobic cavity and a hydrophilic outer side. They form complexes with a variety of solutes by inclusion of lipophilic moieties of these molecules into the cavity. CDs have been effectively used for

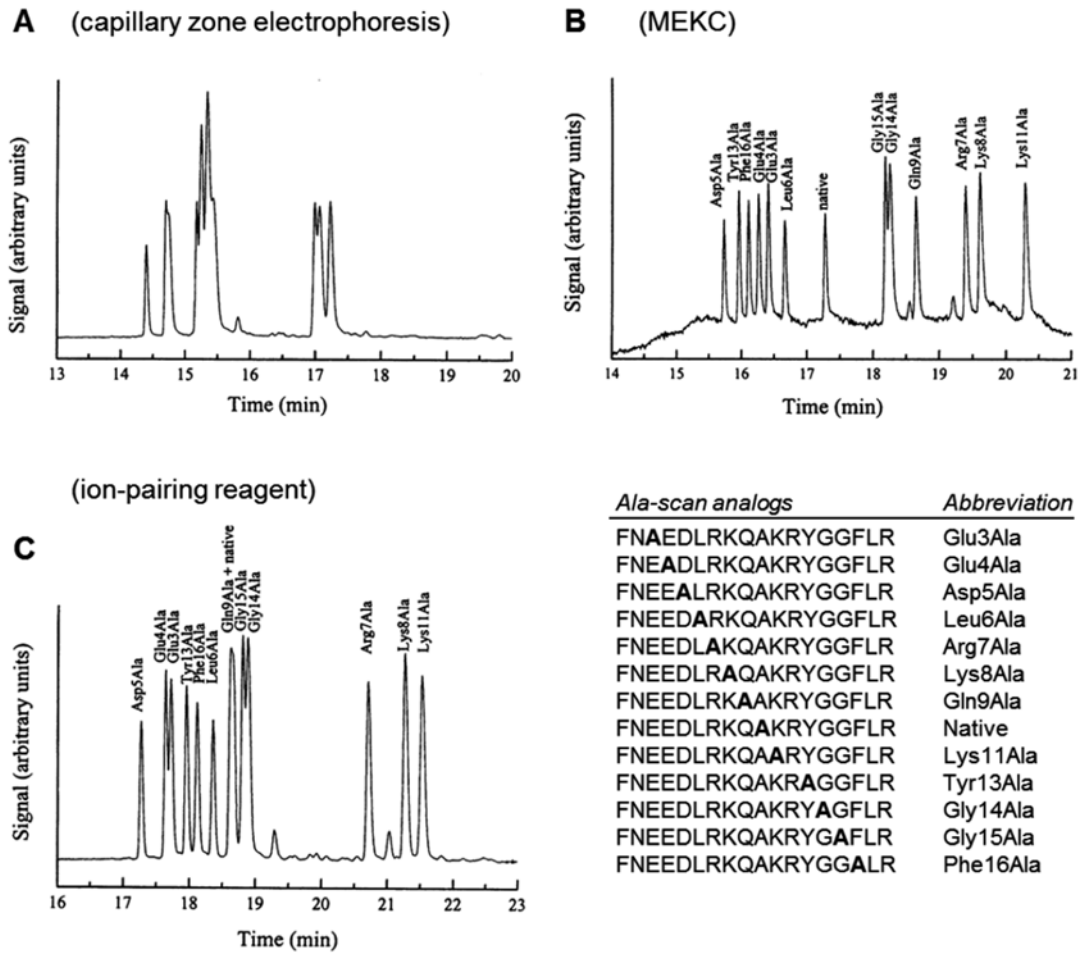

Ala-scan analogs	*Abbreviation*
FN**A**EDLRKQAKRYGGFLR	Glu3Ala
FNE**A**DLRKQAKRYGGFLR	Glu4Ala
FNEE**A**LRKQAKRYGGFLR	Asp5Ala
FNEED**A**RKQAKRYGGFLR	Leu6Ala
FNEEDL**A**KQAKRYGGFLR	Arg7Ala
FNEEDLR**A**QAKRYGGFLR	Lys8Ala
FNEEDLRK**A**AKRYGGFLR	Gln9Ala
FNEEDLRKQ**A**KRYGGFLR	Native
FNEEDLRKQA**A**RYGGFLR	Lys11Ala
FNEEDLRKQAK**A**GGFLR	Tyr13Ala
FNEEDLRKQAKRY**A**GFLR	Gly14Ala
FNEEDLRKQAKRYG**A**FLR	Gly15Ala
FNEEDLRKQAKRYGG**A**LR	Phe16Ala

Fig. 6 Comparison of the separation of peptides in (**a**) CZE mode, (**b**) MEKC mode, and (**c**) addition of an ion-pair reagent. Experimental conditions: fused-silica capillary 61.2 cm effective length, 69.7 cm total length, 50 mm ID; (**a**) 100 mM sodium phosphate buffer, pH 3.5, (**b**) 100 mM sodium phosphate buffer, pH 3.5, containing 35 mM 3-[(3-cholamidopropyl)dimethylammonio]-1-propanesulfonate (CHAPS), and (**c**) 100 mM sodium phosphate buffer, pH 3.5, containing 100 mM 1-hexanesulfonic acid sodium salt; 25 kV, 17 °C; detection wavelength 200 nm (adapted with permission by WILEY-VCH from ref. [67] © 2000)

the separation of the enantiomers of small peptides (for reviews also on the use of other chiral selectors for peptide enantioseparations *see* refs. [51–55]). However, the compounds can also be used to alter resolution and selectivity of peptide separations when chiral resolution of analytes is not an issue. Complexation results in an altered hydrodynamic radius and, subsequently, in a different electrophoretic mobility of the solutes.

Further additives include amines, zwitterions, urea, soluble polymers, water-miscible solvents with high viscosity, and metal ions. (Poly)amines are modifiers of the EOF and suppress analyte-wall interactions as do soluble polymers. Metal ions such as Zn^{2+} can be useful for the analysis of His-containing peptides.

1.2.4 Applied Voltage

The applied voltage affects efficiency, resolution, and migration time (Fig. 7). Efficiency and resolution increase with increasing voltage while migration time decreases. However, high voltage produces high Joule heat. The optimum applied voltage can be derived from an Ohm's plot depicting the current as a function of the applied

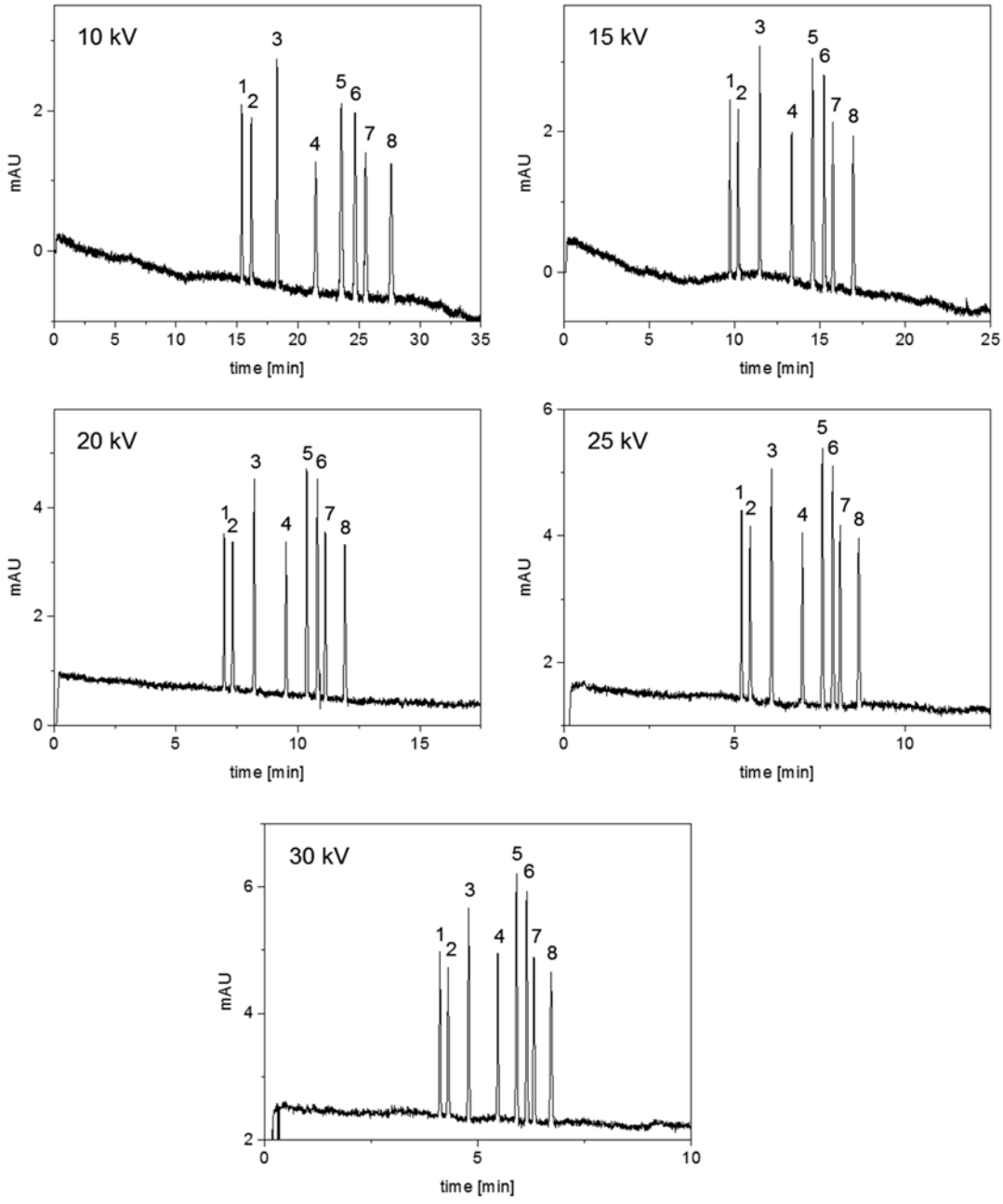

Fig. 7 Separation of model peptides at different applied voltages. Experimental conditions: fused-silica capillary, 50 cm effective length, 57 cm total length, 50 μm ID; 50 mM sodium phosphate buffer; 20 °C; detection wavelength 215 nm. For peptide identification *see* Table 2

voltage. Deviation of current from the linear relationship signals the generation of Joule heat. Certain buffers such as the so-called Good buffers produce only relatively low currents even at high concentrations. It has also been shown that it may be feasible to use a voltage gradient during the electrophoretic run instead of a constant applied voltage in order to increase the separation efficiency [62].

1.2.5 Capillary Temperature

The temperature of the capillary has significant effects on the viscosity of the background electrolyte, electric current, and migration time. Therefore, efficient capillary temperature control is required for reproducible analyses. Increasing the temperature results in a lower viscosity of the separation buffer and a higher electrophoretic mobility of the analytes (Fig. 8). Both are inversely proportional to temperature. High temperatures also result in high currents. In addition, temperature can affect analyte solubility and buffer pH, resolution, and efficiency. High temperatures should be avoided when organic solvents are used as buffer additives.

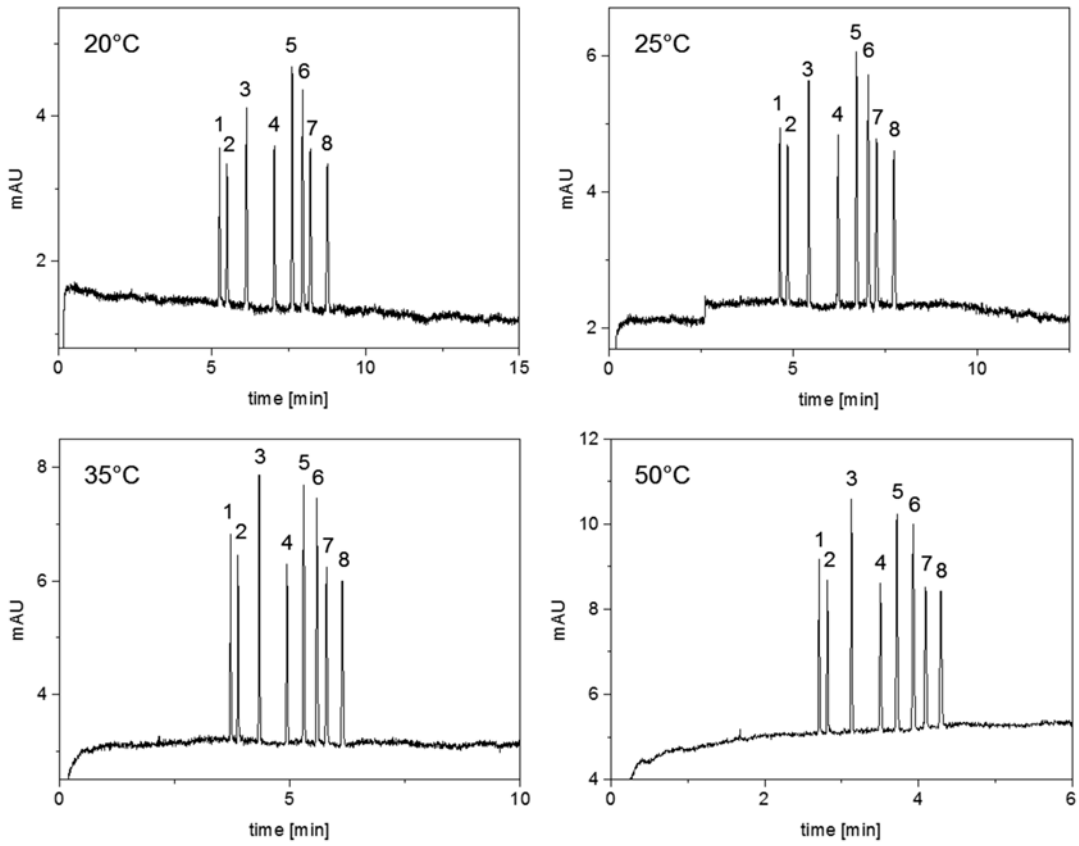

Fig. 8 Separation of model peptides at different temperatures. Experimental conditions: fused-silica capillary, 50 cm effective length, 57 cm total length, 50 μm ID; 50 mM sodium phosphate buffer, pH 2.7; 25 kV; detection wavelength 215 nm. For peptide identification *see* Table 2

1.2.6 Sample Matrix and Injection

The type of sample matrix can range from a (simple) aqueous solution to a complex biological sample such as plasma. Interactions of matrix components with analytes or the capillary wall may be the reason for reduced efficiency and reproducibility. Ideally, the sample has a lower conductivity than the run buffer allowing online focusing (stacking) of the components. High salt content of the sample results in peak broadening. In addition, the injected amount of the sample should be considered. The injected amount can be increased either by increasing the sample concentration or by applying longer injection times. While sufficiently high concentrations are needed to achieve the desired sensitivity, too high concentrations lead to mass overload. A long injection plug, i.e., using long injection times, results in reduced resolution. Stacking techniques should be considered when high sensitivity is required [39–42].

1.2.7 Method Development Strategy

According to the points outlined above a successful method development strategy includes evaluation of the parameters listed below. The listing is not comprehensive; further parameters may apply. For rational method development multivariate optimization of the experimental parameters using chemometric approaches (experimental design) is preferable as compared to univariate method optimization [63–65].

1. *Peptide solubility*: Ensure that the analytes are soluble and stable in all separation solutions. If large amounts of organic solvents are necessary, evaluate the application of MEKC for peptide analysis.
2. *Capillary dimensions*: A fused-silica capillary with an effective length of 40–50 cm and an inner diameter of 50 µm is a good first choice with respect to resolution, effective heat dissipation, and detection sensitivity. For increased detection sensitivity or increased mass loading capacity capillaries with larger inner diameters (100–200 µm) may be required.
3. *Capillary coating*: Coated capillaries can be used for specific applications and modification of the EOF as well as suppression of analyte adsorption to the capillary wall. Dynamic as well as permanent coatings may be applied. Low-pH-background electrolytes are often combined with either positively charged dynamic coatings or neutral permanent coatings. Permanently coated capillaries as well as kits for dynamic coatings are commercially available.
4. *Capillary temperature*: 20–25 °C is a good starting point. For fast separations use 30–60 °C; for high-concentration buffers or difficult separations 15–20 °C may apply. For optimization vary the temperature in 5 K increments.
5. *Optimization of buffer pH*: pH 2.5–4.0 (pK_a of acidic groups) and pH 8.0–10.0 (pK_a of basic groups) can be used for most

peptides. In the pH range 4–7 the EOF will vary significantly with small changes of the buffer pH which can lead to poor repeatability of the migration times. The buffer should be selected to provide good pH control of the specific pH (pK_a of buffer acid close to pH). Optimization of the pH should be performed in 0.1–0.5 pH increments.

6. *Optimization of buffer concentration*: Start with 50–100 mM buffers for 50 μm ID capillaries. Use higher ionic strength buffers for the separations of closely related peptides or if a large number of peptides has to be analyzed simultaneously.
7. Optimization of separation voltage: Construction of an Ohm's plot (observed current versus applied voltage) for a given separation buffer indicates the voltage that will give the best resolution and efficiency within the shortest analysis time. Use 2.5–5 kV increments for the construction of Ohm's plots.
8. Selection of buffer additives: The use of buffer additives may be required in order to maximize selectivity and/or to mask interactions. Organic solvents (1–50%) increase the solubility of lipophilic peptides and modify the EOF. Ionic surfactants (5–200 mM depending on the surfactant) can be applied in the case of hydrophobic and neutral peptides; the additional use of nonionic surfactants (5–50 mM) or organic solvents (1–20%) can modify analyte partitioning. Ion-pair reagents (10–100 mM) are effective for the separation of small hydrophilic peptides. CDs (10–50 mM) may also be used for selectivity enhancement for separations of smaller peptides. (Poly)amines and soluble polymers suppress hydrophobic interactions between peptides and the capillary wall.

2 Materials

2.1 CE Instrument and Equipment

1. A commercial CE instrument with a high voltage source (up to 30 kV) and a photodiode array detector. A P/ACE MDQ CE System (Beckman Coulter, Fullerton, CA, USA) is suitable (*see* **Note 1**).
2. Uncoated fused silica capillaries (e.g., from Polymicro Technologies, Phoenix, AZ, USA) with an internal diameter of 50 μm, an effective length of 30 cm, and a total length of 40.2 cm (*see* **Note 2**). Install the capillary into the capillary cartridge according to the manufacturer's instructions (*see* **Note 3**).
3. A commercial pH meter for pH adjustment of the background electrolytes.
4. An ultrasonic bath for sample and CD dissolution as well as for degassing of the solutions.
5. Syringe filters containing polyester filter membranes with a pore size of 0.20 μm (e.g., from Macherey-Nagel, Düren, Germany). The use of 0.45 μm filters is also possible.

6. A Milli-Q water purification system for preparation of ultrapure water (e.g., a Milli-Q Direct 8 system, Millipore, Billerica, MA, USA).

2.2 Chemicals

Buffer salts, acids, and bases are obtained from commercial sources at the highest purity available.

1. L-Ala-L-Phe (Bachem AG, Bubendorf, Switzerland).
2. L-Ala-D-Phe (Bachem AG, Bubendorf, Switzerland).
3. Gly-Leu-Tyr (Bachem AG, Bubendorf, Switzerland).
4. Angiotensin I trifluoroacetate (Bachem AG, Bubendorf, Switzerland).
5. Angiotensin II acetate (Bachem AG, Bubendorf, Switzerland).
6. Angiotensin III (Bachem AG, Bubendorf, Switzerland).
7. Bradykinin acetate (Bachem AG, Bubendorf, Switzerland, or Sigma-Aldrich, St. Louis, MO, USA).
8. Leu-enkephalin (Bachem AG, Bubendorf, Switzerland, or Sigma-Aldrich, St. Louis, MO, USA).
9. Tetragastrin (Bachem AG, Bubendorf, Switzerland, or Sigma-Aldrich, St. Louis, MO, USA).

For the amino acid sequence of the peptides *see* Table 2.

2.3 Background Electrolytes (See Notes 4 and 5)

50 mM sodium phosphate buffer (pH 2.5–3.5): Dissolve 780 mg sodium dihydrogen phosphate monohydrate ($NaH_2PO_4 \times H_2O$) in approximately 50 mL Milli-Q water and adjust to the desired pH using either 0.1 M H_3PO_4 or 1 M NaOH. Adjust the volume of the solution to 100.0 mL with Milli-Q water. The buffer solution is filtered through a 0.2 or 0.45 μm membrane filter and degassed by sonication before use.

2.4 Sample Solutions

Stock solutions of the peptides at a concentration of 500 μg/mL are prepared by dissolution of the peptides in Milli-Q water. In some cases the addition of 0.2% phosphoric acid is required for complete dissolution of the peptide. Before injection the stock solution is diluted 1:10 with Milli-Q water. Mixtures of the peptides are prepared accordingly.

3 Methods

3.1 Conditioning and Rinsing Procedures for the Fused Silica Capillary (See Note 6)

3.1.1 Preconditioning of a New Capillary

Filter all rinsing solutions through a 0.20 or 0.45 μm polyester membrane syringe filter. Rinse the new capillary at a pressure of 138 kPa (20 psi) subsequently with

1. 0.1 M phosphoric acid for 10 min.
2. 1 M sodium hydroxide for 20 min.
3. 0.1 M sodium hydroxide for 20 min.

4. Milli-Q water for 10 min.
5. The appropriate background electrolyte for 10 min.

3.1.2 Conditioning of the Capillary Between Analyses

Rinse subsequently with filtered (0.2 or 0.45 μm) solutions at a pressure of 138 kPa (20 psi) with

1. 0.1 M phosphoric acid for 2 min.
2. 0.1 M sodium hydroxide for 2 min.
3. Milli-Q water for 2 min.
4. The appropriate background electrolyte for 4 min.

3.1.3 Rinsing of the Capillary for Storage

Rinse capillary subsequently with filtered (0.2 or 0.45 μm) solutions at a pressure of 138 kPa (20 p.s.i.) with

1. 0.1 M phosphoric acid for 10 min.
2. 0.1 M sodium hydroxide for 10 min.
3. Milli-Q water for 10 min.

For short-term (overnight) storage place capillary ends into vials containing Milli-Q water. For long-term storage dry capillary by purging with air at a pressure of 34.5 kPa (5 psi) for 5 min.

After the overnight storage of the capillary rinse it next day with **steps 1–3** as described in Subheading 3.1.3. Thereafter rinse it at 138 kPa (20 psi) for 10 min with the appropriate background electrolyte. After the long-term storage condition the capillary as described in Subheading 3.1.1.

3.2 CE Analysis

After conditioning of the capillary (*see* **Note 6**) select the appropriate background electrolyte and fill into buffer vials (*see* **Note 7**). Set data sampling rate to 4 Hz and autozero time of the detector to 1.0 min. Place samples in sample vials (*see* **Note 8**) and introduce the sample solutions hydrodynamically at a pressure of 3.4 kPa (0.5 psi) for 3 s (*see* **Notes 9** and **10**) at the anodic end of the capillary, carry out the detection at the cathodic end.

Capillary temperature: 20 °C.

Applied voltage: +25 kV (ramp time 0.17 min).

Detection wavelength: 215 nm (bandwidth 10 nm).

Detector reference wavelength 340 nm (bandwidth 50 nm).

Typical electropherograms of the separation of the model peptides in the pH range 2.5–3.5 are shown in Fig. 1 (*see* **Note 11**).

4 Notes

1. Different CE instruments from the same supplier as well as instruments from different companies may yield slightly different results even when using identical experimental conditions.

Thus, the experimental variables may require slight changes when transferring a given analytical method from one instrument to another. Therefore, fine-tuning of the parameters of a published method may be necessary.

2. Capillaries from different suppliers may lead to slightly different separation efficiencies. Even capillaries from the same supplier may vary to a certain extent. Thus, the purchase of larger quantities of capillaries is recommended especially if a method is intended for validated routine analysis in an industrial environment. One capillary should be used for only one application.
3. When cutting a capillary, it is important that the cut is straight and the ends are even. Uneven capillary ends will lead to peak tailing due to uneven injection plugs. The capillary ends should be checked under a magnifying glass or a microscope. Moreover, it may be advisable to burn off a few millimeters of the polyimide coating at the capillary ends. This will reduce carryover and give better precision. Burning off the coating is especially important especially when using organic solvents as buffer additives such as acetonitrile that make the polyimide swell. Removing the polyimide from the capillary ends is not advisable for coated capillaries as this will damage the inner coating.
4. Preparation of buffers according to different procedures results in buffers differing in ionic strength which may affect the separation selectivity. For example, a 50 mM phosphate buffer, pH 2.5, may be prepared (1) by dissolving the appropriate amount of 85% phosphoric acid in a certain amount of water and adjusting to pH 2.5 by addition of sodium hydroxide solution before making up the final volume by addition of water, (2) by adjusting 50 mM phosphoric acid to pH 2.5 by addition of a sodium hydroxide solution, and (3) by adjusting 50 mM sodium dihydrogen phosphate (monobasic sodium phosphate, NaH2PO4) to pH 2.5 by addition of diluted phosphoric acid. In the first case the buffer concentration is 50 mM with respect to phosphate; in case (2) the molarity of phosphate is below 50 mM; and in case (3) phosphate molarity is higher than 50 mM. The deviation from the desired molarity will depend on the concentration of the sodium hydroxide solution and phosphoric acid used for pH adjustment. Phosphate buffers at higher pH (i.e., pH 6.2–8.2) may also be prepared by mixing 50 mM sodium dihydrogen phosphate (monobasic sodium phosphate, NaH_2PO_4) and 50 mM disodium hydrogen phosphate (dibasic sodium phosphate, Na_2HPO_4) in appropriate proportions to obtain the desired pH. Consequently, buffers differing in the ionic strength are obtained by the various procedures. This affects the magnitude of the EOF, the electric current, as well as Joule heating which, in turn, affect a given separation. Too high Joule heating may be derived from an

Ohm's plot. In addition, when using different salts, e.g., the potassium or lithium phosphate salts, or different bases, e.g., potassium hydroxide or lithium hydroxide, for the preparation, the resulting buffers differ in the counterions which may also affect a separation. Thus, careful characterization of the buffer is required for reproducible results. In addition, buffers can only be stored for a limited period of time even at low temperatures.

5. Due to the temperature dependence of dissociation equilibria, buffer pH should be adjusted at the temperature that is used during the electrophoretic run. Specifically, the change of the pK_a per Kelvin (or degree Celsius) of organic zwitterionic buffers is significant. Ideally the buffer is prepared at the same temperature as described in the analytical conditions.
6. Conditioning of the capillary is important in order to obtain reproducible conditions of the inner wall of the capillary. Therefore, careful preconditioning of the capillary is required. Moreover, it is necessary to include all rinsing steps into validation procedures when developing CE procedures for quality control.
7. Different vials containing the background electrolyte should be used for rinsing of the capillary and for the analytical separation. Buffer levels should be the same in the analysis vials in order to avoid a hydrodynamic flow due to differences in hydrostatic pressure between the vials. Buffer should be replaced after a number of injections (typically between two and ten injections) because of buffer depletion.
8. When using microvials, air bubbles at the bottom of the vial should be avoided. During injection the outlet end of the capillary should be placed in a vial with a constant solvent level which is not the waste vial. A water (or buffer) plug may be injected after sample injection to prevent sample loss by thermal expansion when high voltage is switched on.
9. When applying hydrodynamic injection, the actually injected amount of the sample may vary depending on the temperature or the viscosity of the solution. Thus, adjustment of the injection time and/or pressure may be required. In the present example the samples were injected at ambient temperature. Typical injection plug lengths in CE correspond to approx. 1–5 % of capillary length.
10. After injecting the sample, the end of the capillary should be dipped into a vial containing buffer solution or water in order to reduce carryover of the sample into the background electrolyte vial used for the separation.
11. The separation between bradykinin (peptide 9) and angiotensin I (peptide 2) at pH 2.7 may not always be achieved depending on the commercial source and separation "history" of the

capillary. If baseline resolution cannot be achieved with the present capillary, a longer separation capillary or increased buffer concentration may fix the problem. If the buffer pH is raised to 2.8 comigration of Gly-Leu-Try (peptide 6) and tetragastrin (peptide 7) is observed.

References

1. Messana I, Rossetti DV, Cassiano L et al (1997) Peptide analysis by capillary (zone) electrophoresis. J Chromatogr B 699:149–171
2. Kasicka V (1999) Capillary electrophoresis of peptides. Electrophoresis 20:3084–3105
3. Kasicka V (2001) Recent advances in capillary electrophoresis of peptides. Electrophoresis 22:4139–4162
4. Hearn MTW (2001) Peptide analysis by rapid, orthogonal technologies with high separation selectivities and sensitivities. Biologicals 29:159–178
5. Hu S, Dovichi NJ (2002) Capillary electrophoresis for the analysis of biopolymers. Anal Chem 74:2833–2850
6. Kasicka V (2003) Recent advances in capillary electrophoresis and capillary electrochromatography of peptides. Electrophoresis 24:4013–4046
7. Kasicka V (2006) Recent developments in capillary electrophoresis and capillary electrochromatography of peptides. Electrophoresis 27:142–175
8. Kasicka V (2008) Recent developments in CE and CEC of peptides. Electrophoresis 29:179–206
9. Kasicka V (2010) Recent advances in CE and CEC of peptides. Electrophoresis 31:122–146
10. Kasicka V (2012) Recent developments in CE and CEC of peptides. Electrophoresis 33:48–73
11. Kasicka V (2014) Recent developments in capillary and microchip electroseparations of peptides. Electrophoresis 35:69–95
12. Castagnola M, Messana I, Rossetti DV (1996) Capillary zone electrophoresis for the analysis of peptides. In: Hancock WS (ed) Capillary electrophoresis in analytical biotechnology. CRC Press, Boca Raton, FL, pp 239–275
13. Van de Goor T, Apffel A, Chakel J et al (1997) Capillary electrophoresis of peptides. In: Landers JP (ed) Handbook of capillary electrophoresis, 2nd edn. CRC Press, Boca Raton, FL, pp 213–258
14. Strege MA, Lagu AL (eds) Capillary electrophoresis of proteins and peptides. Methods in molecular biology, vol 276, Totowa, NJ
15. Bandilla D, Skinner CD (2004) Capillary electrochromatography of peptides and proteins. J Chromatogr A 1044:113–129
16. Freitag R, Hilbrig F (2007) Theory and practical understanding of the migration behavior of proteins and peptides in CE and related techniques. Electrophoresis 28:2125–2144
17. Mittermayr S, Olajos M, Chovan T et al (2008) Mobility modeling of peptides in capillary electrophoresis. Trends Anal Chem 27:407–417
18. Underberg WJM, Waterval JCM (2002) Derivatization trends in capillary electrophoresis: an update. Electrophoresis 23:3922–3933
19. Bardelmeijer HA, Waterval JCM, Lingeman H et al (1997) Pre-, on-, and post-column derivatization in capillary electrophoresis. Electrophoresis 18:2214–2227
20. Szökö E, Tabi T (2010) Analysis of biological samples by capillary electrophoresis with laser induced fluorescence detection. J Pharm Biomed Anal 53:1180–1192
21. Rosenfeld JM (2003) Derivatization in the current practice of analytical chemistry. Trends Anal Chem 22:785–798
22. Garcia-Campana AM, Taverna M, Fabre H (2007) LIF detection of peptides and proteins in CE. Electrophoresis 28:208–232
23. Lacroix M, Poinsot V, Fournier C et al (2005) Laser-induced fluorescence detection schemes for the analysis of proteins and peptides using capillary electrophoresis. Electrophoresis 26:2608–2621
24. Hernandez-Borges J, Neusuess C, Cifuentes A et al (2004) On-line capillary electrophoresis-mass spectrometry for the analysis of biomolecules. Electrophoresis 25:2257–2281
25. Moini M (2004) Capillary electrophoresis-electrospray ionization mass spectrometry of amino acids, peptides and proteins. In: Strege MA, Lagu AL (eds) Capillary electrophoresis of proteins and peptides. Methods in molecular biology, vol 276, Totowa, NJ, pp 253–290
26. Pantickova P, Gebauer P, Bocek P et al (2011) Recent advances in CE-MS: synergy of wet chemistry and instrumentation innovations. Electrophoresis 32:43–51

27. Herrero M, Ibanez E, Cifuentes A (2008) Capillary electrophoresis-electrospray-mass spectrometry in peptide analysis and peptidomics. Electrophoresis 29:2148–2160
28. Kolch W, Neusüß C, Pelzing W et al (2005) Capillary electrophoresis-mass spectrometry as a powerful tool in clinical diagnosis and biomarker discovery. Mass Spectrom Rev 24:959–977
29. Mischak H, Schanstra JP (2011) CE-MS in biomarker discovery, validation, and clinical application. Proteomics Clin Appl 5:9–23
30. Stalmach A, Aibalat A, Mullen W et al (2013) Recent advances in capillary electrophoresis coupled to mass spectrometry for clinical proteomic applications. Electrophoresis 34:1452–1464
31. Tsybin YO, Ramstroem M, Witt M et al (2004) Peptide and protein characterization by high-rate electron capture dissociation Fourier transform ion cyclotron resonance mass spectrometry. J Mass Spectrom 39:719–729
32. Hofstadler SA, Wahl JH, Bakhtiar R et al (1996) Capillary electrophoresis/Fourier-transform ion-cyclotron-resonance mass spectrometry with sustained off-resonance irradiation fot he characterization of protein and peptide mixtures. J Am Soc Mass Spectrom 5:894–899
33. Righetti PG, Gelfi C, Verzola B et al (2001) The state of the art of dynamic coatings. Electrophoresis 22:603–611
34. Rodriguez I, Si SFY (1999) Surface deactivation in protein and peptide analysis by capillary electrophoresis. Anal Chim Acta 383:1–26
35. Huhn C, Ramautar R, Wuhrer A et al (2010) Relevance and use of capillary coatings in capillary electrophoresis-mass spectrometry. Anal Bioanal Chem 396:297–314
36. Horvath J, Dolnik V (2001) Polymer wall coatings for capillary electrophoresis. Electrophoresis 22:644–655
37. Doherty EAS, Meagher RJ, Albarghouthi MN et al (2003) Microchannel wall coatings for protein separation by capillary and chip electrophoresis. Electrophoresis 24:34–54
38. Sentellas S, Puigno L, Galceran MT (2002) Capillary electrophoresis with on-line enrichment for the analysis of biological samples. J Sep Sci 25:975–987
39. Urbanek M, Krivankova L, Bocek P (2003) Stacking phenomena in electromigration: from basic principles to practical procedures. Electrophoresis 24:466–485
40. Kitagawa F, Otsuka K (2014) Recent applications of on-line sample preconcentration techniques in capillary electrophoresis. J Chromatogr A 1335:43–60
41. Slampova A, Zdena P, Pantuckova P et al (2013) Contemporary sample stacking in analytical electrophoresis. Electrophoresis 34:3–18
42. Wen Y, Li J, Ma J et al (2012) Recent advances in enrichment techniques for trace analysis in capillary electrophoresis. Electrophoresis 33:2933–2952
43. Kaiser T, Wittke S, Just I et al (2004) Capillary electrophoresis coupled to mass spectrometer for automated and robust polypeptide determination in body fluids for clinical use. Electrophoresis 25:2044–2055
44. Schulz-Knappe P, Schrader M, Zucht H-D (2005) The peptidome concept. Comb Chem High Throughput Screen 8:697–704
45. Schiffer E, Mischak H, Novak J (2006) High resolution proteome/peptidome analysis of body fluids by capillary electrophoresis coupled with MS. Proteomics 6:5615–5627
46. Albalat A, Mischak H, Mullen W (2011) Clinical application of urinary proteomics/peptidomics. Expert Rev Proteomics 8:615–629
47. Mischak H, Vlahou A, Ioannidis JPA (2013) Technical aspects and inter-laboratory variability in native peptide profiling: the CE-MS experience. Clin Biochem 46:432–443
48. Coon JJ, Zürbig P, Dakna M et al (2008) CE-MS analysis of the human urinary proteome for biomarker discovery and disease diagnostics. Proteomics Clin Appl 2:964–973
49. Siwy J, Mullen W, Golovko I et al (2011) Human urinary peptide database for multiple disease biomarker discovery. Proteomics Clin Appl 5:367–374
50. Mischak H, Kolch W, Aivaliotis M et al (2010) Comprehensive human urine standards for comparability and standardization in clinical proteome analysis. Proteomics Clin Appl 4:464–478
51. Wan H, Blomberg LG (2000) Chiral separation of amino acids and peptides by capillary electrophoresis. J Chromatogr A 875:43–88
52. Scriba GKE (2003) Recent advances in enantioseparations of peptides by capillary electrophoresis. Electrophoresis 24:4063–4077
53. Czerwenka C, Lindner W (2005) Stereoselective peptide analysis. Anal Bioanal Chem 382:599–638
54. Scriba GKE (2006) Recent advances in peptide and peptidomimetic stereoisomer separations by capillary electromigration techniques. Electrophoresis 27:222–230

55. Scriba GKE (2009) Recent developments in peptide stereoisomer separations by capillary electromigration techniques. Electrophoresis 30:S222–S228
56. Wätzig H, Degenhardt M, Kunkel A (1998) Strategies for capillary electrophoresis: method development and validation for pharmaceutical and biomedical applications. Electrophoresis 19:2695–2752
57. McLaughlin GM, Anderson KW, Hauffe DK (1998) Peptide analysis by capillary electrophoresis: method development and optimization, sensitivity enhancement strategies, and applications. In: Khaledi MG (ed) High performance capillary electrophoresis. Wiley, New York, NY, pp 637–681
58. Janini GM, Issaq HJ (2001) Selection of buffers in capillary zone electrophoresis: application to peptide and protein analysis. Chromatographia 53:S18–S26
59. Righetti PG, Gelfi C, Perego M et al (1997) Capillary zone electrophoresis of oligonucleotides and peptides in isoelectric buffers. Theory and methodology. Electrophoresis 18:2145–2153
60. Castagnola M, Cassiano L, Messana I et al (1996) Effect of 2,2,2-trifluoroethanol on capillary zone electrophoretic peptide separations. J Chromatogr A 735:271–281
61. Matsubara N, Terabe S (1996) Micellar electrokinetic chromatography in the analysis of amino acids and peptides. In: Hancock WS (ed) Capillary electrophoresis in analytical biotechnology. CRC Press, Boca Raton, FL, pp 155–182
62. Yang Y, Boysen RI, Hearn MTW (2004) Analysis of synthetic peptides by capillary electrophoresis. Effect of organic solvent modifiers and variable electrical potentials on separation efficiencies. J Chromatogr A 1043:91–97
63. Sentellas S, Saurina J (2003) Chemometrics in capillary electrophoresis. Par A: methods for optimization. J Sep Sci 26:875–885
64. Orlandini S, Gotti R, Furlanetto S (2014) Multivariate optimization of capillary electrophoresis methods: a critical review. J Pharm Biomed Anal 87:290–307
65. Hanrahan G, Gomez FA (eds) (2010) Chemometric methods in capillary electrophoresis. Wiley, Hoboken, NJ
66. Yang Y, Boysen RI, Chen JC et al (2003) Separation of structurally related synthetic peptides by capillary zone electrophoresis. J Chromatogr A 1009:3–14
67. Fürtös-Matei A, Day R, St-Pierre SA et al (2000) Micellar electrokinetic chromatography separations of dynorphin peptide analogs. Electrophoresis 21:715–723

Chapter 19

Microbial Analysis of *Escherichia coli* ATCC, *Lactobacteria* and *Saccharomyces cerevisiae* Using Capillary Electrophoresis Approach

Paweł Pomastowski, Viorica Railean-Plugaru, and Bogusław Buszewski

Abstract

Rapid detection and identification of microorganisms is a challenging and important aspect in many areas of our life, beginning with medicine, ending with industry. Unfortunately, classical methods of microorganisms identification are based on time-consuming and labor-intensive approaches. Screening techniques require rapid and cheap grouping of bacterial isolates; however, modern bioanalytics demands comprehensive bacterial studies on molecular level. The new approach to the rapid identification of bacteria is to use the electromigration techniques, especially capillary zone electrophoresis (CZE). CZE is an important technique used in the analysis of microorganisms. However, the analysis of microbial complexes using this technology still encounters several problems—uncontrolled aggregation and/or adhesion to the capillary surface. One way to resolve this issue is the CZE analysis of microbial cell with surface charge modification by bivalent metal ions (e.g., Ca^{2+}_{aq}, Zn_{aq}). Under the above conditions, bacterial cells create compact aggregates, and fewer high-intensity signals are observed in electropherograms. The chapter presents the capillary electrophoresis of microbial aggregates approach with UV and one-dimensional intact cell matrix-assisted laser desorption/ionization time-of-flight mass spectrometry (ICM MS) detection.

Key words Bacterial aggregation, Capillary electrophoresis, Matrix-assisted laser desorption/ionization mass spectrometry, Intact cell analysis

1 Introduction

One of the fundamental stages of microbial analysis is the identification of microorganisms. In modern medicine early detection of pathogens provides an opportunity to determine the risk of neoplastic process in the infected organs, and to implement appropriate preventive and screening actions, which would minimize the risk of developing the disease. In the case of food (e.g., dairy) and pharmaceutical industry, identification of microorganisms is an essential step of a technological process, which determines the quality of the manufactured product [1]. Furthermore, in medicine—detection of a disease in an early stage of development would

Philippe Schmitt-Kopplin (ed.), *Capillary Electrophoresis: Methods and Protocols*, Methods in Molecular Biology, vol. 1483,
DOI 10.1007/978-1-4939-6403-1_19,

allow to achieve better results of a treatment, in industry—identification of pathogens in early stages of technological process saves money, production time, and influences improvements in the decision-making processes. Classical methods for identification of microorganisms commonly used in routine microbiological laboratories are based on a set of tests and analyses of biochemical properties of microorganisms, as well as on methods utilizing antigen–antibody reactions [2]. Recent years have brought increasing interest in automation of identification methods based on a study of biochemical characteristics of microorganisms, along with improvement of serological methods, causing a significant increase in the diversity of rapid identification tests. Nevertheless, waiting for the result of identification is still long enough, and depending on the method and the analytical system, it ranges from 4 to 8 h for automated methods to about 24 h for semiautomatic ones. Therefore, emphasis has been put on the search for new, precise, and rapid methods of identification of microorganisms. One of them is the use of capillary electrophoresis approaches for analysis of bacterial and yeast cells [1, 2]. Available literature sources confirm the widespread interest of electromigration techniques in the identification and separation of microorganisms (Table 1) [3–17]. Despite its popularity, the method has certain limitations, such as the aggregation and/or adhesion of bacteria to capillary surface.

1.1 Historical Aspects

The charge on the surface, determined by the characteristic properties of functional groups of membranes and/or cell wall, affects the behavior of the microorganisms (biocolloids) in the electric field. This phenomenon determines its own electrophoretic mobility and enables the separation of biocolloids. The first report using the electromigration techniques of microorganisms separation comes from 1987. Hjertèn performing electrophoretic separation, the tobacco mosaic virus and *Lactobacillus cesei*, observed their migration from the electroosmotic flow. Applied analysis conditions did not allow for effective separation of the examined microorganisms. In 1993, it was performed electrophoretic separation of *Escherichia coli*. It was observed, the bacteria formed aggregates, which resulted in uniqueness analysis and bordering of the band [18]. In subsequent years, it was determined the electrophoretic mobility of various microorganisms (e.g., *Saccharomyces cerevisiae*). It has been observed that with increasing ionic strength occurs a narrowing of the band. Moreover, it has been observed a relationship between a charge surface of microorganism and the surrounding environment. At the end of the nineties of the twentieth century, Armstrong et al. introduced the innovation resulting in an improved selectivity and resolution of electrophoretic separation. The use of the additive poly(ethylene oxide) (PEO, polyethylene glycol) in the buffer led to a reduction of the electroosmotic flow (EOF), increased buffer viscosity, and likely to reduce the electrostatic interaction between the capillary wall and the

Table 1

Capillary zone electrophoresis of Escherichia coli ATCC, Lactobacillus spp. and *Saccharomyces spp.*

Nr.	Microorganisms	Detection method	Separation conditions/technique used	Supporting electrolyte (BGE)	Ref.
1.	*Escherichia coli*	UV	27 cm × 100 μm, U = 10 kV (CZE)[a]	TBE(4.5 mmol/L Tris/4.5 mmol/L H_3BO_3/0.1 mmol/L EDTA); pH 8.4; 0.00125 % PEO	[3]
			33.5 cm × 75 μm, U = 20 kV (CZE)[b]	5 mmol/L phosphate buffer Tris (pH 8.5)	[4]
			80 cm × 50 μm, U = 10 kV (CZE)[a]	10 mmol/L phosphate buffer (pH 7.0,7.8) with addition NaCl C = (0.019–0.227) mol/L	[5]
			47 cm × 75 μm, U = 15 kV (CZE)[a]	25 mmol/L phosphate buffer (pH 7.0); 25 μmol/L CaCl2; 35 μmol/L myo-inositol hexaphosphate	[6]
			33.5 cm × 75 μm, U = −15 kV (CZE)[c]	TBE(4.5 mmol/L Tris/4.5 mmol/L H_3BO_3/0.1 mmol/L EDTA); pH 8.53; 0.00125 % PEO	[7]
			27 cm × 100 μm, U = (−) 20 kV (CIEF)[a]	20 mmol/LNaOH; 100 mmol/L H_3PO_4; PB-PEG	[8]
			33.5 cm × 50 μm, U = 20 kV (CZE)[a]	TBE(4.5 mmol/L Tris/4.5 mmol/L H_3BO_3/0.1 mmol/L EDTA); pH 8.53; 5 mmol/LMES (pH 6.1); 0.00125 % PEO	[9]
		UV/LIF	27 cm × 100 μm U = −15 kV (CZE)[b]	TBE(4.5 mmol/L Tris/4.5 mmol/L H_3BO_3/0.1 mmol/L EDTA); pH 8.5; 0.00125 % PEO	[10]
			30 cm × 100 μm, U = −2 kV (CZE)[a]	1 mmol/L Tris 0.33 mmol/L citric acid (pH 7.0); CTAB	[11]
			35 cm × 100 μm, U = (−)20 kV (CIEF)[a]	60 mmol/L NaOH; 100 mmol/L H_3PO_4; C_2H_5OH; PEG	[12]
		LIF	32 cm × 100 μm, U = (−) 20 kV (CIEF)[a]	20 mmol/LNaOH; 100 mmol/L H_3PO_4; C_2H_5OH; PB-PEG	[13]

(continued)

Table 1
(continued)

Nr.	Microorganisms	Detection method	Separation conditions/technique used	Supporting electrolyte (BGE)	Ref.
2.	*Saccharomyces cerevisiae*	UV	U = 20 kV (CZE)[d]	20 mmol/L NaOH; 20 mmol/L H_3PO_4	[3]
			80 cm × 50 μm, U = 10 kV (CZE)[a]	10 mmol/L phosphate buffer (pH 7.0,7.8) with addition NaCl (I = 0.019 mol/L –0.227 mol/L)	[5]
			27 cm × 100 μm, U = (–) 20 kV (CIEF)[a]	20 mmol/L NaOH; 100 mmol/L H_3PO_4; PB-PEG	[8]
3.	*Lactobacillus acidophilus; Saccharomyces cerevisiae*	LIF	30 cm × 100 μm, U = 15 kV (CZE)[a]	TBE (4.5 mmol/L Tris/4.5 mmol/L H_3BO_3/0.1 mmol/L EDTA); pH 8.4; 0.00125 % PEO	[14]
			58 cm × 100 μm, U = 15 kV (CZE)[a]	TBE (0.5 mmol/L–9.0 mmol/L Tris/(0.5–9.0) mmol/L H_3BO_3/(0.011–0.2) mmol/L EDTA); pH 8.4; PAA; PAcA; PEO; PVP	[15]
4.	*Lactobacillus delbrueckii*	UV	56 cm × 100 μm, U = 20 kV (CZE)[a]	TBE (4.5 mmol/L Tris/4.5 mmol/L H_3BO_3/0.1 mmol/L EDTA); pH 8.4; 0.00125 % PEO	[16]
5.	*Lactobacillus plantarum*		47 cm × 75 μm, U = 15 kV (CZE)[a]	25 mmol/L phosphate buffer (pH 7.0); 25 μmol/L CaCl2; 35 μmol/L myo-inositol hexaphosphate	[6]
6.	*Lactobacillus delbrueckii Saccharomyces cerevisiae*	LIF	Microchip type D, type T 110 cm × 50 μm (CE)	TBE (4.5 mmol/L Tris/4.5 mmol/L H_3BO_3/0.1 mmol/L EDTA); pH 8.4; 0.00125 % PEO	[17]

Saccharomyces cerevisiae
[a]Quartz capillary
[b]Quartz capillary modified acrylamide
[c]Quartz capillary modified DVB, trimethylchlorosilane
[d]Quartz capillary modified methylcellulose

microorganisms [18]. PEO contributes to the aggregation of bacterial cells. EOF was decreased, but reproducible analyses were not achieved, probably due to the system instability. Casual interactions between PEO and bacterial cells, and the inner surface of the capillary (different film thickness) further deepened the system instability. The use of charge-coupled devices (CCD) and fluorescence microscope to observe the electrophoretic migration of microorganisms in

the capillary greatly expanded knowledge about the phenomenon of aggregation (adhesion). It was noted that with the increase of cluster size, increasing the speed of aggregation and the size of the forming unit depends on the difference in zeta potential (ζ). It was also shown that increasing the ionic strength of the buffer increases the rate of formation of aggregates. Further ways of improving selectivity and resolution electrophoretic analysis of microorganisms was the introduction of modifications to the inner surface of the capillary (e.g., acrylamide). The introduction of these modifications results in increased hydrophobicity of the surface and the probable occurrence of micro-organism interactions—ligand (such as π–π) contributing to the improvement of selectivity.

Another solution for improving the selectivity of the electrophoretic separation was carried out by the modification of the inner surface of the capillary by cationic surfactants and carry out the separation of bacteria with reversed electroosmotic flow. Oukacine et al. [19] performed electrophoretic analysis of bacterial cells using the mechanism of transient isotachophoresis (ITP). According to the investigators, this method has a high selectivity and reproducibility. Furthermore, it was demonstrated that with increasing numbers of microbial cells, there is a linear relationship as to the height of peaks on the electropherogram. It was proposed an innovative solution for the separation of microorganisms by introducing a negatively ionized polymer–antibody system. These complexes interact selectively with the cell resulting in improved separation selectivity. At present another aspect of the upgrades is miniaturization. It is getting more popular because of the unique benefits, i.e., a short time and low cost. Optimizing connection-on-chip electrophoresis for separation of microorganisms gives a new look for the identification of pathogenic cells in physiological fluids for the early detection of the disease [20]. Buszewski et al. [21] carried out optimization of electrophoretic conditions for separation of microorganisms in biological matrices (e.g., urine). These studies have shown that capillary zone electrophoresis, can become widely used, as sensitive tool in medical diagnostics.

An interesting proposal was presented by Horka et al. [22, 23] using electromigration technique in the identification, characterization, and quantification, e.g., *Lactobacteri*a isolated from cow's milk. It has been shown the combination of capillary isoelectric focusing (CIEF) with matrix-assisted laser desorption/ionization time-of-flight mass spectrometry (MALDI-TOF MS). On the other hand, Buszewski et al. [24] have been shown that cell of bacteria can be rapidly analyzed by CE with modified bivalent metal ions. The modification of surface bacterial groups with calcium ions decreased the number of undesired signals in the electropherograms and increased the reproducibly of analysis. Moreover, it resulted in the creation of controlled aggregates and signal amplification. Therefore, it was possible to collect focused cell aggregates and to detect their MALDI spectra.

1.2 Outline of Method

Every bacterial species has a complex and characteristic composition of the cell wall. Macromolecules that are present in the cell wall and bacterial membranes, including proteins, phospholipids, teichoic acid, teichuronic acid, and lipopolysaccharides, produce unique biochemical fingerprints. Those macromolecules also contribute to the surface charge of bacterial cells through the ionization of proton active functional groups, such as carboxyl, phosphate, amino, and hydroxyl groups, and the adsorption of ions from the solution. On the other hand, the presence of electric charge and consequently electrical double layer at the interface solution/capillary wall is a cause of EOF. During the electrophoretic analysis of microorganisms, it was observed unfavorable effect of adhesion [20–24]. In some cases, adverse phenomenon of adhesion is eliminated by coating of capillary (e.g., polyacrylamide). Then, the electroosmotic flow is eliminated and the migration of cells based on their electrophoretic mobility. However, research studies have demonstrated that the discussed mostly macromolecules play a significant role in bacterial aggregation and adhesion to solid and contribute to microbial differentiation [24].

Buszewski et al. [24] demonstrate that microbial analysis performed by Fourier transform infrared (FTIR), X-ray photoelectron (XPS), and nuclear magnetic resonance (NMR) spectroscopy yields valuable information and indicate relationship between surface heterogeneity of microorganism and its electrophoretic mobility. Furthermore, it has been demonstrated their complementary to other biochemical and physical cell surface methods, such as zeta potential and potentiometric titration [24].

Bacterial adhesion was first explained by the DLVO (Derjaguin, Landau, Verwey, Overbeek) theory. Bacterial adhesions mediated by interplay between Lifshitz–van der Waals forces and electrostatic interactions originating from the overlap of electrical double layers and the solid surface. This theory has been extended to acid–base interactions [25]. Another problem is the detection of microbes in CE mode. Common UV and DAD system do not allow for obtaining specific spectra that would enable a satisfactory identification of separated bacterial cells. The obtained spectra do not provide sufficient information about the aggregation of microorganisms. Moreover, the conventional linear buffer system (e.g., phosphoric buffers) is not effective in this case.

The problem of uncontrolled aggregation was resolved due to the modification of the bacterial surface by bivalent metal ions (Fig. 1). Modified surface charge of microbial cells facilitates cell aggregation and improves the selectivity of electrophoretic analysis. According to DLVO theory, attractive electrostatic forces have to dominate repulsive forces for bacterial cells to aggregate [25]. Deprotonated functional groups on the surface of bacterial cells support the formation of cationic bridges. Calcium ions bound to the surface of cells improve their hydrophobicity, and they evoke

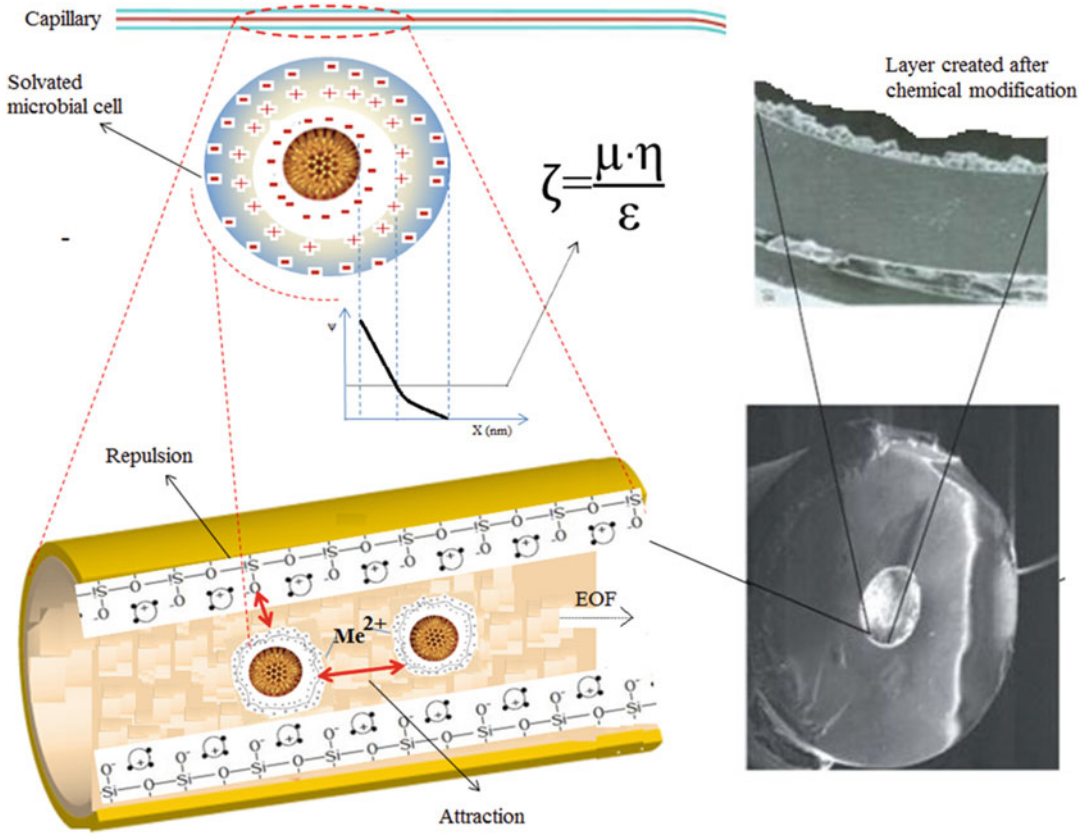

Fig. 1 Capillary electrophoresis of microbial aggregation

the participation of attractive acid–base forces. Calcium ions facilitate overcoming of the electrostatic energy barrier between cells, which in turn facilitates cell aggregation. Extracellular structures, including fimbriae, which bind metal ions at terminal sites, also overcome repulsive force. Furthermore, modification of bacteria with calcium ions determines the change in their electrophoretic mobility and reduces repulsive forces. This results in the creation of controlled aggregates and signal amplification [26]. The use of buffers with different ions mobility allows on creation of focusing zones. Therefore, it was possible to collect focused cell aggregates and carried out precise one-dimensional intact cell MALDI TOF (ICM) detection. Spectrometric analysis of a sample with this method provides comprehensive information within a couple of minutes. In addition, one of the advantages of IC MS method is the fact that only single colony is needed for microbiological analysis. This procedure is based on analysis of the unique protein profile of a microorganism, known as molecular fingerprint (MF) and comparison of characteristic peak patterns and markers peaks with references spectra [27].

2 Materials and Equipment

2.1 Microbial Culture

The strains of *Escherichia coli* ATCC 25922, ATCC 10536, ATCC 10536 *Lactococcus lactis subsp. lactis* ATCC 11454 and ATCC 19435, *Lactobacillus casei* ATCC 334 and ATCC 393, *Lactobacillus acidophilus* ATCC 314, *Lactobacillus paracasei* ATCC BAA-52, *Saccharomyces cerevisiae* ATCC 18824 were obtained from Pol-Aura (Dywity, Poland).

Agar plates (Pol-Aura, Dywity, Poland) for growth of *Escherichia coli* ATCC were Tryptone Soya Agar (TSA), Mueller Hinton (MH2). Tryptic Soy Broth (TSB, Difco) was used for cultivation of *E. coli*. *Lactobacteria* were cultivated on Schaedler Broth (SB), Schaedler agar (SCHE) with 5% sheep blood (bioMérieux, Warsaw, Poland) and Milk agar (MA) with 10% (v/v) lactose (Pol-Aura, Dywity, Poland). The yeast was cultivated on YPD agar plates (Sigma Aldrich, Steinheim, Germany) (*see* **Note 1**).

2.2 Electrophoretic Analysis of Microbial Aggregates

Hydrochloric acid, sodium hydroxide solution, potassium chloride, TRIS (tris(hydroxymethyl)aminomethane), boric acid (B), and calcium nitrate were purchased from Sigma Aldrich (Steinheim, Germany). Ultra-pure water from a Milli-Q water system (Millipore, Bedford, MS, USA) was used throughout the work. Capillary electrophoresis (CE) experiments were performed with an HP3DCE system (Agilent Technologies, Waldbronn, Germany) equipped with DAD and fused silica capillaries (id = 75 μm, 100 μm; L_{tot} = 33.5 cm; L_{eff} = 25 cm). Isopropanol was used for the cleaning the detection window.

Fused silica capillaries (id = 75 μm, 100 μm) were purchased from Polymicro Technologies (Phoenix, AZ, USA).

For coating procedure were used γ-methacryloxypropyltrimet hoxysilane (γ-MAPS), toluene, acrylamide, ammonium persulfate, TEMED (*N,N,N′,N′*-tetramethylethylenediamine). All of them were purchased from Sigma Aldrich (Steinheim, Germany).

2.3 Spectrometric Analysis of Bacteria

All chemicals (acetonitrile (ACN), methanol, trifluoroacetic acid (TFA)) for MALDI-MS analyses were supplied at the highest commercially available purity from Fluka Feinchemikalien GmbH (part of Sigma Aldrich, Steinheim, Germany). Ground steel targets (Bruker Daltonik, Bremen, Germany) were used for sample deposition. α-cyano-4-hydroxycinnamic acid (HCCA) and 2,5-dihydroxybenzoic acid (DHB) were employed as matrices for MALDI analysis of intact bacterial cells (dried droplet method). Bruker Bacterial Test Standard (BTS) were used for external calibration.

Intact cell mass spectrometric analysis conducted with the use of mass spectrometer, e.g., ultrafleXtreme MALDI-TOF/TOF (Bruker Daltonik, Bremen, Germany) equipped with a modified Nd:YAG laser (smartbeam II™) operating at the wavelength of 355 nm and the frequency of 2 kHz.

3 Methods

3.1 Preparation of Microbial Suspension

3.1.1 Microbial Culture

1. Bacterial cells of *E. coli* culture on TSA, MH2 agar plate, *Lactobacteria* on MA with 10% (v/v) of lactose and SCHE agar. Yeast culture on YPD agar. Incubate them in aerobic condition for 24 h at 37 °C. In the case of liquid media culture, microbial cells in 3 mL of TSB or SB with 0.5% yeast extract for 24 h at 37 °C. Then, bacterial cultures in the amount of 3 mL transfer to flask with 1 L of the same liquid medium and grown in a shaking incubator for another 24 h at 37 °C.
2. In the case of liquid cultivation, bacterial cells separate from the medium by centrifugation (14,000 rpm, 10 min). The pellet with bacterial cells rinse twice with 0.09% (m/v) KCl, to remove the growth medium from bacterial surfaces [26]. In the case of agar plate cultivation, transfer microbial colony to sterile Eppendorf tube (1.5 mL), add 1 mL of 0.09% (m/v) KCl, vortex (2 min) and centrifuge (14,000 rpm, 10 min) (*see* **Note 2**).

3.1.2 Sample Preparation for CZE Analysis

1. Obtained microbial pellets rinse with deionized water twice (1 mL), vortex (1 min) and centrifuge (14,000 rpm, 10 min) and finally, remove supernatant (*see* **Note 3**). Then, add 1 mL of 0.005 M $Ca(NO_3)_2$ solution in order to modify the surface charges, vortex mixture 10 min at room temperature.
2. After 1 h the pellet with bacterial cells wash again to remove free Ca^{2+}_{aq} ions, with deionized water twice (1 mL), vortex (1 min) and centrifuge (14,000 rpm,10 min) and finally, remove supernatant.
3. Final pellet of washed bacteria and yeast suspend in 0.5 mL of TB buffer (5 mM TRIS (T), 50 mM boric acid (B); pH 8.20–8.60), vortex (2 min) (*see* **Note 3**).

3.2 Electrophoretic Analysis of Microbial Aggregates [24]

3.2.1 Uncoated Mode

1. New, uncoated capillaries rinse hydrodynamic, before use with 1.0 M NaOH (5 min), 0.1 M HCl (2 min), deionized water (3 min), and BGE (background electrophoretic buffer, outlet buffer) for 2 min.
2. The electrophoretic analysis perform in a nonlinear system, namely: outlet buffer: TB (C_{TRIS} = 5 mM, C_B = 50 mM, pH 8.20–8.60), inlet buffer: TB-HCl (C_{TRIS} = 5 mM, C_B = 50 mM, C_{HCl} = 4.4 mM, pH 7.10–7.30), I_{max} = 100 μA, U = 15 kV, t = 23 °C, λ = 214 nm, and injection in the pressure mode at 50 mbar for 25 s. Between runs, the capillaries wash hydrodynamic with 0.1 M NaOH, deionized water—for 2 min each, and a BGE for 4 min (*see* **Note 4**).
3. A total volume of 0.5 mL stock bacterial (and yeast) suspension is used for electrophoretic measurements (*see* **Note 2**).

4. The focused fractions of bacterial aggregates collect manually in CE–MS (L_{tot} = 80 cm, L_{eff} = 26 cm) mode to sterile Eppendorf tube, centrifuge (4 °C, 14,000 rpm, 5 min) and remove supernatant. Then, pellet of microbial cell resuspend in 50 μL of deionized water and transferred to a MALDI target according to the below-mentioned procedure (*see* **Note 5**, *see* Subheading 3.3).

3.2.2 Noncross Linked Polyacrylamide Coating (See Note 6) [27]

1. Firstly, a 3 mm detection window form on the capillary by burning off the polyimide coating, approximately 8 cm from one end of the capillary (*see* **Note 7**). Wipe detection window by isopropanol. Then in the pretreatment step the capillary wash with methanol for 3 min, 1 M NaOH for 3 min, 1 M HCl for 3 min and finally deionized water for 5 min, dried by flushing with N_2 for 20 min in order to obtain a fresh and clean inner capillary surface structure and thus the reproducibility of the coating and consequently of the runs (*see* **Note 8**).
2. The capillary fill with a 50% solution of γ-MAPS in toluene, left for 24 h (while both ends of the capillaries were immersed in the same solution) and then rinse with toluene for 30 s.
3. The polymerization carry out with 150 μL of deaerated acrylamide (4%, m/v) (remove oxygen) containing 3 μL of ammonium persulfate (10%, m/v) as the initiator and 3 μL of TEMED as the catalyzer. After 90 min, the excess of (not attached) polyacrylamide was removed simply by rinsing with deionized water delivered by an HPLC pump.
4. New coated capillaries, rinse before use with deionized water (3 min), and BGE (background electrophoretic buffer, outlet buffer) for 2 min. The next steps are performed analogously to the above-mentioned procedure **(**Subheading 3.2.1**)**.

3.3 MALDI TOF MS Analysis of Micro organism

3.3.1 Sample Preparation

1. References strain. Microbial samples (one colony) transfer from agar plate (or on loop of microbial pellets from liquid culture) to a 50 μL solvent mixture EtOH/ACN/H_2O/TFA, 1:1:1:0.001 (v/v/v/v), that OD_{600} of the final bacterial suspension ranged between 0.04 and 0.6 (10^9–10^{12} cells per mL). In order to evaluate how this change affects the amount of cells per spot, the bacterial suspension dilute with the solvent mixture at 1:1, 1:10, 1:100, 1:1000, and 1:10 000.
2. Microbial cells after electrophoretic analysis. Obtained microbial pellets resuspend in 10 μL solvent mixture EtOH/ACN/H_2O/TFA, 1:1:1:0.001 (v/v/v/v), and follow the earlier procedure (*see* Subheading 3.3.1, **step 1**). Then, 3 μL of microbial suspension transfer to sterile Eppendorf tube and add already made matrix solution: DHB (50 mg/mL), HCCA (10 mg/mL) in 1:1 ratio (*see* **Note 9**). Mix carefully using pipette and spot 1 μL of mixture onto MALDI target and left to dry at room temperature.

3.3.2 Intact Cell MALDI TOF MS Analysis of Bacteria and Yeast

1. ICM MS spectra of record in linear positive mode within *m/z* range of 3000–30,000 and applying the acceleration voltage of 25 kV. Turn on the suppression mode at 2900 Da (*see* **Note 10**)
2. All mass spectra were acquired and processed with the dedicated software: e.g., flexControl and flexAnalysis, respectively (both from Bruker). For identification of microbial strains, it is possible to use the dedicated software or perform home-made analysis (*see* **Note 11**).
3. In case of home-made analysis, first record the ICM spectra of references species and next spectra of microorganisms cell after CE analysis. For identification use markers peaks and/or match molecular fingerprint of references spectra with analyzed sample spectra (Fig. 2)

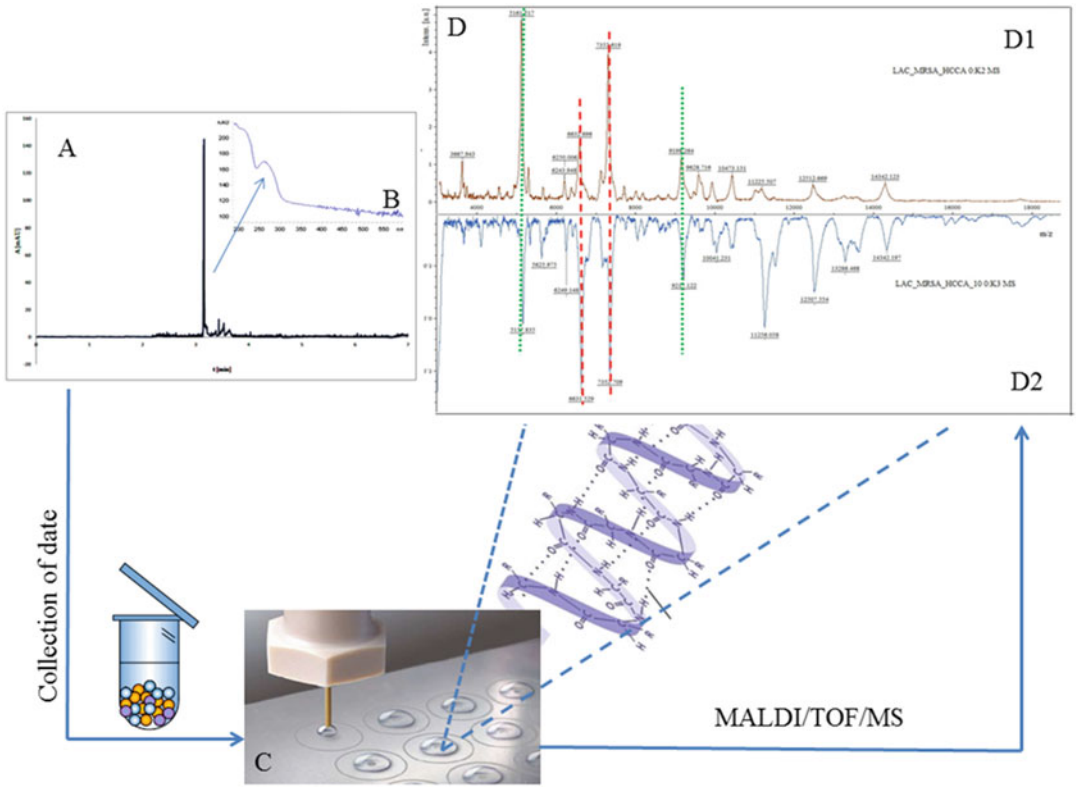

Fig. 2 Connection of CE-DAD with MALDI/TOF/MS detection in analysis of microbial aggregation (**a**) Electrophorogram of *L. lactis*, $\lambda = 214$ nm; (**b**) UV spectra of *L. lactis*; (**c**) Spotting of MALDI target; (**d**) Intact cell MALDI/TOF spectra of reference bacteria (**D1**) and (**D2**) its spectra obtained after CE analysis (*dashed line*—peak marker; *dotted line*—unspecified peak, e.g., ribosomal protein)

4 Notes

1. The cultivation of bacterial strains on agar plates was carried out on disposable, sterile Petri dishes (with appropriate media culture) using disposable loops. In a case of media culture sterilization and preparation for *Lactobacteria*, solution of lactose sterilizes using the 0.1 μm filter (e.g., Millipore). After the inoculation procedure the plates were placed medium up in an incubator with convection (10–30%) (*see* Subheading 3.1.1). Cultivate the *S. cerevisiae* on YPD solid medium for the propagation of yeast, prepare immediately before inoculation procedure.
2. Use the sterile loop. OD_{600} of the final bacterial suspension ranged between 0.04 and 0.6 (10^9–10^{12} cells per mL). The spectrophotometric measurements were carried out by one-drop method using NanoDrop (Thermo Scientific, Wilmington, USA).
3. After vortex, sonicate optionally cells of yeast for 3 min. In the case of bacteria, 1 min of sonication on ultrabath (in middle range, e.g., $t = 25$ °C, 35 kHz) immediately before electrophoretic measurement. Performing this procedure prevents cells agglomeration, but unfortunately too long sonication can result in lysis of cells.
4. Analyze the bacteria cells (*E. coli* ATCC, *Lactobacteria*) in 75 μm (ID), analyze the cells of yeast in 100 μm capillary.
5. First, microbial cells analyzed in CE mode. When the system will be stable (focused zone, sharpening of the peaks, straight baseline) the runs will be reproducible (e.g., RSD < 2%, $n = 10$), then change the mode to CE–MS and collect the fractions.
6. This method is based on a bifunctional compound in which one group reacted specifically with the glass wall and the other with a monomer taking part in a polymerization process. γ-MAPS (γ-methacryloxypropyltrimethoxysilane) was used as bifunctional compound and acrylamide as monomer. The methoxy groups in γ-MAPS react with silanol groups in the capillary, whereas the acryl groups with the acryl monomers to form non-cross-linked polyacrylamide. Noncovalently attached polymer was then removed and thin, well-defined monomolecular layer of polyacrylamide remained covalently bound to the fused silica wall.
7. For total length of the capillary 33.5 cm. The formation of window procedure can be omitted at this stage. Performing the next steps with already make detection window is difficult (huge possibility breaking the capillary). Therefore, it is recomended to make the detection window on the capillary at the end of coating procedure, before electrophoretic measurement using the scalpel.

8. Technically, when washing the capillary one end was immersed in the washing solution and the order end connected to vacuum simply by pressing together the vacuum tube around capillary.
9. Prepare matrix solution immediately before spectrometric analysis. For suspension use solvent mixture (EtOH/ACN/H_2O/TFA, 1:1:1:0.001 (v/v/v/v) for appropriate concentration: DHB (50 mg/mL), HCCA (10 mg/mL). Then, sonicate (room temperature–RT, 5 min) and centrifuge (RT, 14,000 rpm, 3 min) the obtained mixture of matrix vortex (2 min).
10. Check the optimal value of laser power before recording the spectra. The optimal value is dependent on the attenuation, power, and type of laser. In the case of ultrafleXtreme MALDI-TOF/TOF check optimal smartbeam parameter and select the best of them. In our experiment, global attenuator offset was 25 %, attenuator range 40 %, and laser power 85 %.
11. Commercial systems are mainly used in routine identification of microorganism, namely: BioTyper, SARAMIS, VITEK MS and Andromas, provided by Bruker, Shimadzu, bioMérieux and Andromas SAS, respectively. Homemade database (repository) can be developed and applied to targeted identification of microorganisms and as a complementary method to classical molecular or biochemical techniques. Moreover, a local repository of reference bacterial strains can also be used for statistic evaluation of one-dimensional ICM MS spectra (using, e.g., Statistica, StatSoft) or in a detection approach for separation analysis of microorganisms.

Acknowledgements

We gratefully acknowledge to Dr. Anikó Kilár (The Department of Analytical and Environmental Chemistry, Faculty of Sciences, University of Pécs, Hungary) for valuable advice and procedure of capillary coating.

References

1. Petr J, Maier V (2012) Analysis of microorganism by capillary electrophoresis. Trends Anal Chem 31:9–22
2. Desai M, Armstrong D (2003) Separation, identification and characterization of microorganisms by capillary electrophoresis. Microbiol Mol Biol Rev 67:38–51
3. Armstrong DW, Schulte G, Schneiderheinze JM et al (1999) Separating microbes in the manner of molecules. Capillary electrokinetic approaches. Anal Chem 71:5465–5469
4. Buszewski B, Szumski M, Klodzinska E et al (2003) Separation of bacteria by capillary electrophoresis. J Sep Sci 26:1045–1049
5. Torimura M, Ito S, Kano K et al (1999) Surface characterization and on-line activity measurements of microorganisms by capillary zone electrophoresis. J Chromatogr B 721:31–37
6. Palenzuela B, Simonet BM, Garcia RM et al (2004) Monitoring of bacterial contamination in food samples using capillary zone electrophoresis. Anal Chem 76:3012–3017

7. Szumski M, Kłodzińska E, Buszewski B (2005) Separation of microorganisms using electromigration techniques. J Chromatogr A 1084:186–193
8. Horka M, Ruzicka F, Horky J et al (2006) Capillary isoelectric focusing of proteins and microorganisms in dynamically modified fused silica with UV detection. J Chromatogr B 841:152–159
9. Kłodzińska E, Dahm H, Rozycki H et al (2006) Rapid identification of Escherichia coli and Helicobacter pylori in biological samples by capillary zone electrophoresis. J Sep Sci 29:1180–1187
10. Gao P, Xu G, Shi X et al (2006) Rapid detection of Staphylococcus aureus by a combination of monoclonal antibody-coated latex and capillary electrophoresis. Electrophoresis 27:1784–1789
11. Rodriguez MA, Lantz AW, Armstrong DW (2006) Capillary electrophoretic method for the detection of bacterial contamination. Anal Chem 78:4759–4767
12. Horka M, Kubicek O, Ruzicka F et al (2007) Capillary isoelectric focusing of native and inactivated microorganisms. J Chromatogr A 1155:164–171
13. Horka M, Ruzicka F, Horky J et al (2006) Capillary isoelectric focusing and fluorometric detection of proteins and microorganisms dynamically modified by poly (ethylene glycol) pyrenebutanoate. Anal Chem 78:8438–8444
14. Armstrong DW, He L (2001) Determination of cell viability in single or mixed samples using capillary electrophoresis laser-induced fluorescence microfluidic systems. Anal Chem 73:4551–4557
15. Girod M, Armstrong DW (2002) Monitoring the migration behavior of living microorganisms in capillary electrophoresis using laser-induced fluorescence detection with a charge-coupled device imaging system. Electrophoresis 23:2048–2056
16. Armstrong DW, Schneiderheinze JM (2000) Rapid indentification of the bacterial pathogens responsible for urinary tract infections using direct injection. Anal Chem 72:4474–4476
17. Shintani T, Torimura M, Sato H et al (2005) Rapid separation of microorganisms by quartz microchip capillary electrophoresis. Anal Sci 21:57–60
18. Armstrong D, Schneiderheinze J, Kullman J (2001) Rapid CE microbial assays for consumer products that contain active bacteria. FEMS Microbiol Lett 194:33–37
19. Oukacine F, Garrelly L, Romestand B (2011) Focusing and mobilization of bacteria in capillary electrophoresis. Anal Chem 83:1571–1578
20. Eboigbodin K, Ojeda J, Biggs C (2007) Investigating the surface properties of Escherichia coli under glucose controlled conditions and its effect on aggregation. Langmuir 23:6691–6697
21. Kłodzińska E, Szumski M, Dziubakiewicz E (2010) Effect of zeta potential value on bacterial behavior during electrophoteric separation. Electrophoresis 31:1590–1596
22. Horká M, Karásek P, Salplachta J (2013) Capillary isoelectric focusing of probiotic bacteria from cow's milk in tapered fused silica capillary with off-line matrix-assisted laser desorption/ionization time-of-flight mass spectrometry identification. Anal Chim Acta 25:193–199
23. Salplachta J, Kubesová A, Moravcová D (2013) Use of electrophoretic techniques and MALDI-TOF MS for rapid and reliable characterization of bacteria: analysis of intact cells, cell lysates, and "washed pellets". Anal Bioanal Chem 405:3165–3175
24. Dziubakiewicz E, Buszewski B (2014) Capillary electrophoresis of microbial aggregates. Electrophoresis 35:1160–1164
25. Hermansson M (1999) The DLVO theory in microbial adhesion. Coll Surf B 14:105–119
26. Dziubakiewicz E, Hrynkiewicz K, Walczyk M (2013) Study of charge distribution on the surface of biocolloids. Coll Surf B 104:122–127
27. Pomastowski P, Szultka-Młyńska M, Kupczyk W, Jackowski M, Buszewski B (2015) Evaluation of intact cell matrix-assisted laser desorption/ionization time of-flight mass spectrometry for capillary electrophoresis detection of controlled bacterial clumping. J Anal Bioanal Tech. doi:10.4172/2155-9872.S13-008

Chapter 20

Capillary Electrophoretic Analysis of Classical Organic Pollutants

Ashok Kumar Malik, Jatinder Singh Aulakh, and Varinder Kaur

Abstract

The synthesis and usage of a wide range of organic compounds have shown a considerable increase in the past few decades. Many of these compounds are potential pollutants for the environment. They differ from each other in their chemical structure and properties. Correspondingly different separation strategies are required for their separation. There is need to assess the human exposure to these chemicals and to identify and develop analytical methods for their identification. In this chapter we have presented some methods for the separation and the analysis of the organic pollutants like dyes, phenolic pollutants, phthalates, endocrine disrupting chemicals, polycyclic aromatic hydrocarbon, explosives, agricultural pesticides, and toxins.

Key words Capillary electrophoresis, UV detection, Environmental organic pollutants, Phenoxy acids, Dithiocarbamates, Paraquat and diquat, Polycyclic aromatic hydrocarbons, Endocrine disruptors, Toxins, Explosives, Phthalates, Phenolic pollutants, Dyes

1 Introduction

Synthetic organic compounds have been used in a wide range of agricultural, domestic, and industrial commodities; many of these are potential pollutants and result in vigorous deterioration of environment and human health [1–3]. Analytical studies have confirmed the presence of these pollutants in various environmental and biological matrices. As the pollutant range is continuously becoming more and more complex, their monitoring is coming up as a major challenge faced by environmental analytical chemists. Many of these compounds can enter the environment via surface and groundwater [4]. To prevent pollution, analytical chemists need to develop such systems, which can give fast and reliable information on the identity and quantity of suspected pollutants. Capillary electrophoresis (CE) has an unrealized potential for analytes of environmental concern, particularly those that are more polar and ionic.

Philippe Schmitt-Kopplin (ed.), *Capillary Electrophoresis: Methods and Protocols*, Methods in Molecular Biology, vol. 1483,
DOI 10.1007/978-1-4939-6403-1_20,

Several research articles have cited the importance of capillary electrophoresis as an analytical tool for the qualitative and quantitative analysis of organic pollutants [4] like polycyclic aromatic hydrocarbons [1, 5–8], parabens [9], azarenes [10], agrochemical [11–17], endocrine disrupting agents [18], warfare agents [19, 20], phenolic pollutants [21, 22], phthalates [23], and dyes [24, 25] in environmental and biological matrices. Sovocool et al. [26] have reviewed analysis of various organic and inorganic pollutants using CE. Various aspects for the analysis of agrochemicals (pesticides) are reviewed by Malik et al. [16] and Kettrup et al. [11].

UV-Vis detection is the most widely used detection method in commercial capillary electrophoresis (CE) instruments [27] (*see* **Note 1**). The majority of the work [28] with UV-Vis detection is focused on the methods that improve the analysis precision, detection limits, and system miniaturization. Such methods include the use of capillaries with widened inner diameter at the position of detection and compact light sources such as light-emitting diodes (LEDs). In normal detection systems, the maximum optical path length corresponds to the inner diameter of the separation capillary (usually in the range of 30–100 μm), which limits optical detector sensitivity due to small detection volume.

Photodiode array detector has also been used for the detection and separation of explosives [29]. The use of LEDs as light source relies on the formation of a colored derivative between analytes and additives, which shifts the monitoring wavelength towards red (e.g., >500 nm). LED's light source is particularly attractive in UV-Vis detection due to its excellent output stability, low power requirements, and low cost. Most importantly, LED could be easily implemented into an electrophoresis microchip owing to its small size.

Generally, the main steps [30] involved in the environmental analysis are (1) sampling and sample preparation (2) cleanup and/or extraction, (3) preconcentration, and (4) final separation with qualitative and quantitative determination. Since the analytes can be contained in a wide variety of matrices (i.e., aqueous samples including water from rain, tap, river, marine ground and industrial wastes, solid samples including soils and sediments, and other type of solid waste; and air samples). Zhou et al. have developed N-doped TiO_2 nanotube-based solid-phase extraction cartridge for the preconcentration of paraquat and diquat prior to capillary electrophoresis [31]. Sagrado et al. have reviewed applications of cyclodextrins in capillary electrophoresis [32]. Xie et al. have developed method for the separation and preconcentration of persistent organic pollutants by cloud point extraction [33].

This chapter exemplifies some methods taken from literature for the separation and analysis of the organic pollutants like phthalates, dyes, polycyclic aromatic hydrocarbon, phenoxy acids, dithiocarbamates, paraquat and diquat, endocrine disruptors, toxins, phenolic pollutants, and explosives using UV detection.

2 Materials and Equipment

2.1 Analysis of the Derivatives and Isomers of Benzoate and Phthalate

Phthalates or phthalate esters are esters of phthalic acid and are mainly used as plasticizers (substances added to plastics to increase their flexibility, transparency, durability, and longevity). They are used primarily to soften polyvinyl chloride (PVC). Method for their separation as described by Chien-Hao et al. [23] is given below.

1. *Analytes:* Monomethyl terephthalate, isophthalic acid (*m*-phthalic acid), *o*-phthalic acid, terephthalic acid (*p*-phthalic acid, TPA), 4-carboxybenzaldehyde, *p*-toluic acid, benzoic acid, salicylic acid, aspirin (acetylsalicylic acid), *p*-hydroxybenzoic acid, 2-carboxybenzaldehyde, p-acetamidobenzoic acid. Mesityl oxide is added to the samples as a neutral marker for the electrophoretic mobility determination.
2. *Sample:* Prepare a mixture of 10 mM standard solution of each of these analytes. Dilute to final concentration of 0.1 mM for each analyte prior to injection.
3. *CE instrument and capillary:* Automated PrinCE-C455 system (Prince Technologies, Emmen, The Netherlands), equipped with a Varian ProStar 340 UV-Vis detector (Palo Alto, CA, USA). The data is collected and processed by a DaX data system (Prince Technologies). The separation capillaries (bare fused silica), 68 cm (61 cm to the detector), 75 μm I.D., 365 μm O.D.
4. *Background electrolyte:* (a) Adjust the pH of 10 mM phosphate buffer to 7.0 using 1 M or 0.1 M NaOH. (b) 10 mM Phosphate buffer with 4 mM α-CD, 8 mM β-CD, and 4% poly(ethylene glycol) PEG 600, pH of the buffer adjusted to 11.0 using NaOH.

2.2 Analysis of Sudan Dyes in Chilli Powder

Azo dyes are important organic colorant and are used for many industrial applications. The main reason for their widespread usage is their color fastness and low price. These dyes are biologically active through their metabolites. Due to their potential carcinogenicity it has been banned for human consumption in many countries. Method for the separation of Sudan dyes as described by Garcia et al. [24] is given below (structures are given in Fig. 1).

1. *Analytes:* Sudan I (1-(phenylazo)-2-naphthalenol), Sudan II (1-[(2,4-dimethylphenyl)azo]-2-naphthalenol), Sudan III (1-(4-phenylazophenylazo)-2-naphthalenol), and Sudan IV (*o*-tolylazo-otolylazo-betanaphthalenol).
2. *Stock solution:* Prepare a stock solution of Sudan (I, II = 0.5 mg/mL; III, IV = 1.0 mg/mL) in acetone and store at room temperature.
3. *Sample preparation:* Take 50 mg of chilli powder in 1 mL acetone in a centrifuge tube to perform extraction. Vortex the sam-

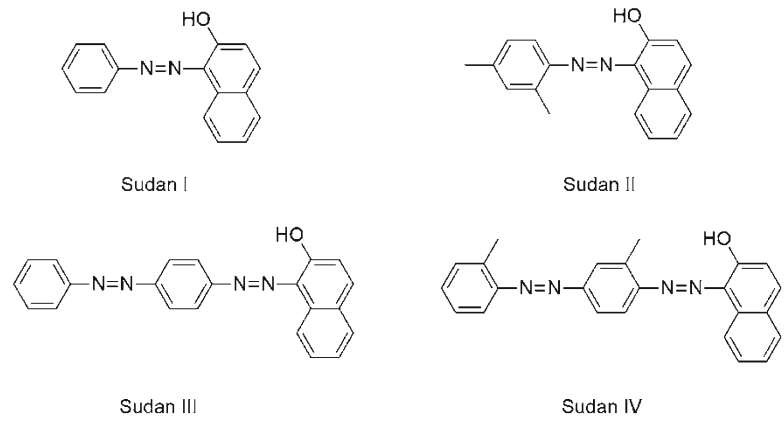

Fig. 1 Molecular structures of the selected Sudan dyes

ple for 2 min and centrifuge for 5 min at 13,500 rpm to precipitate the solids. Dilute the supernatant ten times with the BGE and analyze as described. Spike the samples by adding 50 μL of a stock Sudan solution (I, II = 0.5 mg/mL; III, IV = 1.0 mg/mL) to a dry powder sample before performing the extraction.

4. *CE instrument and capillary*: Use Beckman-Coulter P/ACE MDQ (Fullerton, CA) capillary electrophoresis system (AZ). Adjust the anode and cathode positioned at the inlet and outlet ends of the capillary, respectively. Use Karat 32 software (Beckman-Coulter, Fullerton, CA) for data acquisition. Use polyimide-coated capillaries (50 μm ID,· 375 μm OD,·57 cm long; Polymicro Technologies, Phoenix).
5. *CE buffer:* 5 mM borate (pH 9.3), 20 mM SDS, and 20% acetonitrile.

2.3 Analysis of Phenoxy Acids

Phenoxy acids are important class of pesticides, which have a high toxicity even at low concentration. Various methods are available for the analysis of phenoxy acids [12] and their enantiomers [12]. Here we have presented a simple method for the analysis of the phenoxy acids.

1. *Analyte*: (a) 2-(2,4,5-trichlorophenoxy)propionic acid (fenoprop), (b) 2-(4-chloro-2-methyl-phenoxy)propionic acid (Mecoprop), (c) 2-(2,4-dichlorophenoxy)propionic acid (dichloroprop), (d) 4-(4-Chloro-2-methylphenoxy)butanoic acid (MCPB), (e) (4-Chloro-2-methylphenoxy)acetic acid (MCPA). Structure of phenoxy acids is shown in Fig. 2.
2. *Stock solution*: Dissolve 40 mg of each analyte in 100 mL of pesticide-grade methanol and dilute 1:100 to prepare 4 μg/mL of each analyte.
3. *CE instrument and capillary*: Beckman P/ACE 2100 series HPCE with Beckman system Gold chromatography software. The fused silica CE column [65 cm (50 cm to the detec-

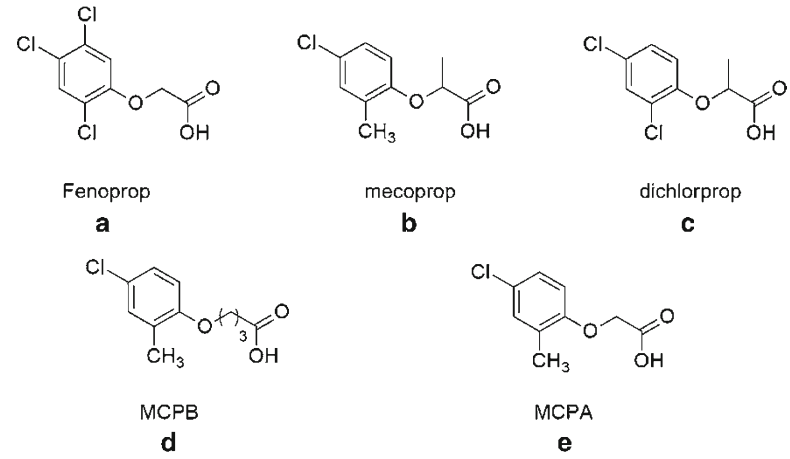

Fig. 2 Structures of phenoxy acids (**a**) 2-(2,4,5-trichlorophenoxy)propionic acid (fenoprop), (**b**) 2-(4-chloro-2-methyl-phenoxy)propionicacid (Mecoprop), (**c**) 2-(2,4-dichlorophenoxy)propionic acid (dichloroprop), (**d**) 4-(4-Chloro-2- methyl-phenoxy)butanoic acid (MCPB), (**e**) (4-Chloro-2-methylphenoxy)acetic acid (MCPA)

tor) × 300 μm O.D. × 75 μm I.D.] fitted in a 100 × 200 μm aperture cartridge.

4. *CE buffer*: 25 mM Acetate buffer (0.05 M glacial acetic acid and 0.05 M sodium acetate (1:1, v/v)) of pH 4.45.

2.4 Analysis of the Dithiocarbamate Pesticides [13, 14]

Dithiocarbamates are an important class of compounds which find application in the rubber industry as vulcanization accelerators and in agriculture as fungicides. Here, a method for the analysis of these compounds is described which is applicable for their analysis in grains and in commercial samples.

1. *Analytes*: Maneb, metham, sodium diethyldithiocarbamate trihydrate, and potassium *o*-ethylxanthate.
2. *Stock solutions:* Prepare 200 mg/L solution of each pesticide by dissolving 20 mg each of metham, sodium diethyl dithiocarbamate trihydrate, and potassium *o*-ethylxanthate in doubly distilled water and dilute to 100 mL in a calibrated flask. Prepare stock solution of maneb by dissolving maneb in 0.1 M NaOH and dilute further with distilled water. Prepare working solutions of lower concentrations by appropriate dilutions with water.
3. *Sample:* Grains and commercial samples "Dithane M 45."
   (a) *Extraction from grains:* Weigh about 10 g of grain sample accurately and spray with 5 mL of aqueous dispersions of maneb containing different amounts of 0.1% solution. Dry the samples in the sun for 1 h and thereafter in the shade for 24 h to remove excess moisture. Prepare a blank assay by spraying the same amount of grain with 5 mL of water. Treat the grounded samples with 50 mL of 0.1 M

NaOH for 10 min and centrifuge at 2000 rpm for 5 min. Filter the aliquots of the resulting solutions through 45 μm filter and analyze by the general procedure.

(b) *Commercial sample*: Apply the method to the determination of maneb in a commercial sample of "Dithane M 45." Dissolve it in 0.1 M NaOH and further dilute with distilled water.

4. *CE instrument and capillary*: CE system equipped with TSP 1000, software for data acquisition. Fused silica capillaries (100 μm i.d. 75 cm long and 45 cm to the detector).
5. *CE buffer*: 20 mM Sodium tetraborate buffer solution of pH 9.0.

2.5 Analysis of Paraquat and Diquat [15, 16]

Paraquat and diquat belong to quaternary class of herbicides. These are quick-acting herbicides that are absorbed by the plants and translocated, which results in desiccation of the foliage. These are strongly adsorbed by the soil and thus get deactivated at a fast rate. A representative method for the analysis of paraquat and diquat is given below:

1. *Analytes*: Paraquat and diquat (structures of paraquat and diquat are shown in Fig. 3). 2-Amino pyridine can be used as the internal standard and phenol as the tracer to measure the electroosmotic flow.
2. *Stock solution:* Use doubly distilled water for the preparation of solutions of paraquat and diquat. Dilute paraquat and diquat solutions in running electrolyte 0.1 M sodium phosphate (pH 3.5). Filter the solutions with 0.2 μm filter to avoid capillary plugging.
3. *Sample*: Wastewater sample.
4. *Sample preparation*: Filter the water sample through a 0.2 μm filter.
5. *CE instrument and capillary*: The CE system consists of 30 kV DC power supply of positive polarity and system equipped with an UV absorbance detector. Fused silica capillaries (50 μm I.D. 80 cm long and 50 cm to the detector).
6. *CE buffer:* 0.10 M Sodium phosphate, pH 3.5.

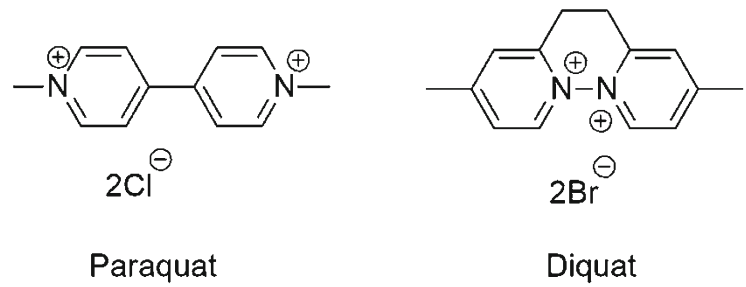

Fig. 3 Structures of paraquat and diquat

2.6 Analysis of Endocrine Disruptors [18]

Nowadays, various chemicals are found to have endocrine disrupting effects. For the assessment of human exposure to these chemicals analytical methods for their identification are required. In this section a method developed by Regan et al. [18] as a representative of endocrine disruptors is described.

1. *Analytes*: (a) Pentachlorophenol (PCP); (b) trichlorophenol (TCP); (c) 17β-estradiol; (d) dichlorophenol (DCP); (e) estrone; (f) estriol; (g) diethylstilbestrol (DES); (h) ethynyloestradiol (EO); (i) lindane; (j) dieldrin; (k) octylphenol (OP); (l) nonylphenol (NP); (m) bisphenol-A (BPA). Structure of endocrine disruptors is shown in Fig. 4.
2. *Stock solutions:* Prepare the stock solutions endocrine disrupting compounds (EDCs) in 100% acetonitrile (ACN) with the exception to estriol and estrone (prepare in 100% methanol). Store the stock solutions at 4 °C in the refrigerator to minimize evaporative loss and cover in the foil to minimize photodegradation of the analytes.
3. *Sample:* River water.
4. *Sample preparation:* Spike the river water sample with six test analytes (NP, OP, EO, DES, 17β-oestradiol, and BPA) of the analysis using cyclodextrin-modified micellar electrokinetic chromatography. In order to minimize differences between the sample zone and surrounding buffer zone, add some of the key buffer components directly to the river water sample prior to analysis, which include cyclodextrin, surfactant, and buffer. Due to the limited solubility of analytes in aqueous samples at high concentrations, add 10 mL of acetonitrile to aid analyte solubility. Analyze an un-spiked sample in order to identify possible matrix effects.
5. *CE instrument and capillary:* Use Beckman P/ACE 5500 system (Beckman Coulter, Fullerton, CA, USA), equipped with a photo-diode array detection (DAD) system and Windows P/ACE Station Software version 1.21. Integration data is calculated by P/ACE Station using the USP (United States Pharmacopoeia) method. The 57 cm long fused silica capillaries (Beckman) with an internal diameter of 50 μm.
6. Background electrolytes:
   (a) 100 mM Cyclohexylamino-1-propane sulfonic acid (CAPS) at pH 11.5 with 20% methanol.
   (b) 20 mM Cyclohexylamino-1-propane sulfonic acid (CAPS) pH 11.5 with 15% ACN and 25 mM sodium dodecylsulfate (SDS). Adjust pH with 0.1 M HCl and 0.1 M NaOH.
   (c) 100 mM Sodium phosphate pH 1.8, 25 mM SDS, 12.5% ACN, 1 mM HP-β-CD.

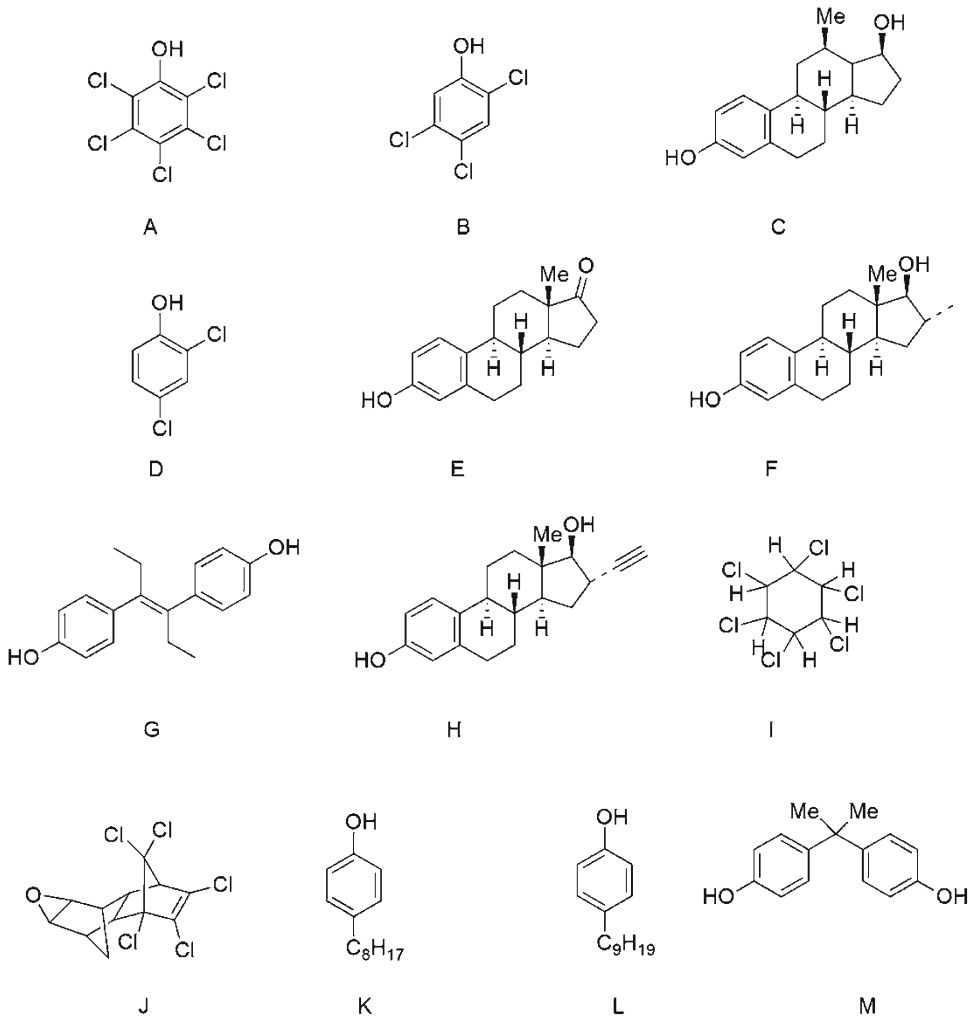

Fig. 4 Structures of some typical EDCs used in this study. (**a**) Pentachlorophenol (PCP); (**b**) trichlorophenol (TCP); (**c**) 17β-estradiol; (**d**) dichlorophenol (DCP); (**e**) estrone; (**f**) estriol; (**g**) diethylstilbestrol (DES); (**h**) ethynyloestradiol (EO); (**i**) lindane; (**j**) dieldrin; (**k**) octylphenol (OP); (**l**) nonylphenol (NP); (**m**) bisphenol-A (BPA) [18]

2.7 Analysis of Toxins

The analysis of toxins is very important due to their food-poisoning effect. A routinely and practicable method for the analysis of toxins is given below which is exemplified with the analysis of domoic acid (DA) from mussel tissue as described by Pineiro et al. [34].

1. *Analytes*: Domoic acid and paralytic shell fish-poisoning (PSP) toxins. Domoic acid calibration solution (DACS-1B) and mussel tissue reference material (MUS-1) containing 100 mg DA/mL and 100 mg DA/g, respectively, can be obtained from the Marine Analytical Chemistry standards program, National Research Council of Canada. Acetic acid solutions (0.03 M) of saxitoxin (STX) and decarbamoyl saxitoxin (dcSTX) (20 mg/mL) are provided by RIVM hoven, the Netherlands. For

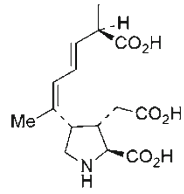

A

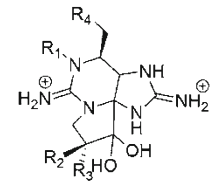

B

			R_4		
R_1	R_2	R_3	Carbamoyl toxins	N-sulfocarbamoyl toxins	Decarbamoyl toxins
H	H	H	STX	GTXS	deSTX
H	H	OSO_3	GTX_2	epi GTXS	dE GTX_2
H	OSO_3	H	GTX_3	GTX8	de GTX_3
OH	H	H	neo STX	GTX6	deneo STX
OH	H	OSO_3	GTX_1	C_3	de GTX_1
OH	OSO3	H	GTX_4	C_4	de GTX_4

Fig. 5 Chemical structure of (**a**) domoic acid and (**b**) PSP toxins [34]

breakpoint cluster region (BCR), standard measurements and testing program certification study can be used. The chemical structure of domoic acid and PSP toxins is shown in Fig. 5.

2. *Sample*: Amnesic shellfish poisoning (ASP)-contaminated samples of razor clams and mussels from Rıa de Vivero (Lugo) can be obtained from Delegacion "Provincial de Pesca de Lugo, Conselleria de Pesca, Xunta de Galicia." PSP-contaminated mussel samples from Rıa de Vigo can be obtained from Conselleria de Sanidade, Xunta de Galicia. Freeze the samples at (−18 °C) until analysis.
3. *Sample preparation*:
   (a) *Extraction of domoic acid:*

   To 4 g homogenized tissue, add 16.0 mL methanol–water (1:1, v/v). Homogenize the mixture for 3 min and then centrifuge at 4500 rpm for 10 min. Filter the supernatant through a 0.45 mm filter (Millex-HV) and keep in the fridge until analysis.

   (b) *Cleanup for ASP toxins:*

   The conditions required for this cleanup are as described below.

Step 1: Pass 5.0 mL of extract through a strong anion-exchange (SAX) cartridge (part No. 1210-2044, lot No. 182639, 3 mL of capacity, 500 mg, Varian), previously conditioned with methanol, water, and methanol–water (1:1, v/v). Wash the extract with methanol–water (1:1) and elute with 5 mL 0.1 M formic acid.
Step 2: Load through a strong cation-exchange (SCX) cartridge (part No. 1211-3039, 10 mL/500 mg of size, lot No. 171069) preconditioned with methanol, water, 0.1 M formic acid, and 5 mL of SAX. Wash the cartridge with 5 mL of 0.01 M formic acid. Elute with 0.5 mL of 25 mM sodium tetraborate (pH 9.2)–acetonitrile (9:1, v/v). Elute with six portions of 2 mL of 25 mM sodium tetraborate (pH 9.2)–acetonitrile (9:1) and domoic acid starts to appear in the third eluate.

(c) *Extraction and cleanup of PSP toxins.*
Extract the paralytic shellfish-poisoning toxins from mussel samples for the analysis of PSP toxin in food. Pass 3.0 mL volume of supernatant obtained in the extraction procedure through a C_{18} cartridge and collect 1.5–2.0 mL of eluate for the analysis. Condition the cartridge with methanol and water under the conditions. After purification on a C_{18} cartridge, ultrafilter the extracts in a 0.45–18 μm membrane (Ultrafree-MC, Millipore) and analyze by CE–UV.

4. *CE instrument and capillary*: HP-3D CE (Hewlett-Packard) system equipped with diode array detection system. Different capillaries and conditions are required for the ASP and PSP toxin analysis:
   (a) For analysis of ASP toxins fused silica capillaries 66 cm × 363 μm O.D., 50 μm I.D. with a UV window located 15 cm from the exit end of the capillary at room temperature and perform detection at 242 nm. Inject the sample at 50 mbar for 12 s and apply a voltage of 30 kV.
   (b) For PSP toxins perform the CE separations in a polyvinyl alcohol (PVA)-coated capillary (104 cm × 75 μm I.D.) under a constant voltage of 20 kV at the injector end of the capillary. Apply the sample under constant pressure (50 mbar) to introduce 20% volume of the capillary. Perform the UV detection at 200 nm.
5. *CE buffer.*
   (a) *For ASP toxins*: 25 mM Borate buffer.
   (b) *For PSP toxins*: Capillary iso-tachophoretic (cITP) electrolyte is 10 mM formic acid. cITP preconcentration is performed with 50 mM morpholine in water adjusted to pH 5 with formic acid.

2.8 Analysis of Explosives

Explosives and their degradation products are the important environmental contaminants. Standard methods for their analysis due to sea remediation efforts, forensic analysis after the terrorist, or other criminal activity are required. Herein the analysis of nitramine and nitro aromatic explosives [20] as their representative is described.

1. *Analytes*: Explosives as given in Table 1.
2. *Sample*: Extract the small piece of explosive in less than 3–4 mL of acetonitrile.
3. *Sample preparation*: Dilute the extracts with the running electrolyte in a ratio of 1:5.
4. *CE instrument and capillary*: Capillary electrophoresis system. Detection at 185, 214, 229 and 254 nm. AccuSep polyimide fused silica capillaries (Waters, Milford, MA, USA) of dimension 60 cm × 50 μm I.D. Computer control and data acquisition with a Waters Millennium 2010 Chromatography Manager.
5. *CE buffer*: 25 mM Mono- and dibasic phosphate (dilute the contents of packet to 200 mL) as electrolyte solution. 50 mM Sodium dodecyl sulfate (SDS) (electrophoresis grade, Millipore).

Table 1

Names and abbreviations of explosives analyzed by MECC

Name	Abbreviation
1,3,5,7-Tetranitro-*N*-methylaniline	HMX
1,3,5-Trinitro-1,3,5-triazacyclohexane	RDX
1,3,5-Trinitrobenzene	TNB
Trinitrotoluene	TNT
2,4-Dinitrotoluene	2,4-DNT
2,6-Dinitrotoluene	2,6-DNT
1,2,3-Propanetriol trinitrate (nitroglycerin)	NG
Pentaerythritol tetranitrate	PETN
2,4,6-*N*-tetranitro-*N*-methylaniline	Teryl
2-Nitrotoluene	2-NT
3-Nitrotoluene	3-NT
4-Nitrotoluene	4-NT
Nitrobenzene	NB
1,3-Dinitrobenzene	DNB

2.9 Separation of Bisphenol A and Three Alkylphenols by MEKC

Bisphenol A and alkylphenols are consumed in large volumes for industrial use. Bisphenol A is used for the production of polycarbonate or epoxy resin. These have endocrine disrupting effects. A method for the determination as described by Wakida et al. [22] is described here.

1. *Analytes:* Bisphenol A (BPA), 4-tert-butylphenol (4-tBP), 4-(1,1,3,3-tetramethylbutyl)phenol (TMBP), nonylphenol (4-NP).
2. *Samples:* Prepare the samples by diluting the stock solution with the running buffer and make the final concentration of each solute to 50 mg/L.
3. *Instrumentation and capillary:* P/ACE 5010 CE system (Beckman, CA, USA). The instrument control, data collections, and analysis are performed with Compaq Deskpro personal computer (Compaq, TX, USA). A 50 μm I.D. fused silica capillary of 57 cm total length and the effective length of 50 cm to the detector and 50 μm I.D.
4. *Running buffer:* 20 mM Borate-phosphate (pH 8.0); concentration of surfactant (sodium dodecyl sulfate) 20 mM; acetonitrile 5 %.
5. *CE conditions:* Applied voltage, 20 kV; detection wavelength, 214 nm; temperature 25 °C.

2.10 Analysis of Polycyclic Aromatic Hydrocarbons

The PAHs are very important environmental pollutants. Their analysis is very important because of toxicity, mutagenicity, and carcinogenicity to animals. A method described by Freitag et al. [6] is given as an example.

1. *Analytes*: Anthracene, benzo[a]pyrene, chrysene, fluorene, phenanthrene, pyrene, fluoranthene.
2. *Stock solution*: Prepare 1 mg/mL concentration of each in acetonitrile.
3. *Samples*: Soil sand, soil sample contaminated with machine oil.
4. *Sample preparation*: (a) For soil sample, spike 10 g of sand (heath) with 0.5 mL of a solution containing seven standard PAHs, each at a concentration of 1 mg/mL. (b) Prepare second sample by contaminating 30 g of sand (heath) with 1 mL of spent machine oil from garage. Extract after 2 h with acetonitrile.
5. *Sample extraction:* (a) Extract the PAHs from 0.5 g of soil sample with the help of 6 mL cyclohexane with vigorous shaking (15 min). Wash with an additional 4 mL of cyclohexane and evaporate to dryness. Dissolve the residue in 0.5 mL of acetonitrile. (b) Extract the PAHs from the 10 g machine oil-contaminated soil with 10 mL of cyclohexane (10 mL for washing) and evaporate to dryness and dissolve in 2.5 mL of acetonitrile.

6. *CE instrument and capillary:* Hewlett-Packard 3D-CE instrument equipped with HP 3D-CE (Rev. A. 01.02.) software for data collection, data analysis, spectral identification, and system control. Perform detection using UV-Vis absorbance with a photodiode-array detector (total range, 190–690 nm; range used, 190–350 nm). The fused silica capillaries 28 cm (length from inlet to detector), 50 μm internal diameter.
7. *CE buffer*: Borate buffer 8.5 mM (pH 9.9) containing 85 mM SDS and 50% (v/v) acetonitrile as the electrophoresis buffer.

3 Methods

3.1 Analysis of the Derivatives and Isomers of Benzoate and Phthalate

1. Rinse the capillary consecutively with 0.1 M NaOH and water for 2 min, and equilibrate with the carrier electrolyte for 2 min before each run.
2. Filter the buffer and sample through 0.2 μm membrane.
3. Set the instrument conditions at +25 kV and 25 °C.
4. Introduce the sample using controlled pressure of 50 mbar for 0.5 min.
5. Perform the detection at two fixed wavelengths 215 and 240 nm.
6. Prepare the calibration graphs by injecting mixed sample of standard solution using electrolyte (A) that is phosphate buffer 10 mM, pH 7.0 (Fig. 6).
7. Perform the same separation using the electrolyte (B) that is phosphate buffer 10 mM with 4 mM α-CD, 8 mM β-CD, and 4% PEG 600 at pH 11.0. Electropherogram obtained under these conditions is given in Fig. 7.
8. Method can be applied to check the purity of terephthalic acid which is important for polyester production.

3.2 Analysis of Sudan Dyes in Chilli Powder

1. Before starting the separation rinse the capillary sequentially with 0.1 M NaOH (5 min/20 psi), deionized water (5 min/20 psi), methanol (5 min/10 psi), deionized water (5 min/20 psi), and BGE (10 min/10 psi).
2. Rinse the capillary between consecutive analyses with BGE for 5 min at 20 psi. At the end of the day, rinse the capillary sequentially with 0.1 M sodium hydroxide (2 min/20 psi), deionized water (10 min/20 psi), methanol (2 min/20 psi), deionized water (5 min/20 psi), and then finally air-dry (10 min/20 psi).
3. Degas the BGE using ultrasonication and filter through 0.45 μm membrane filter.
4. Operate CE system at 20 kV and 25 °C.

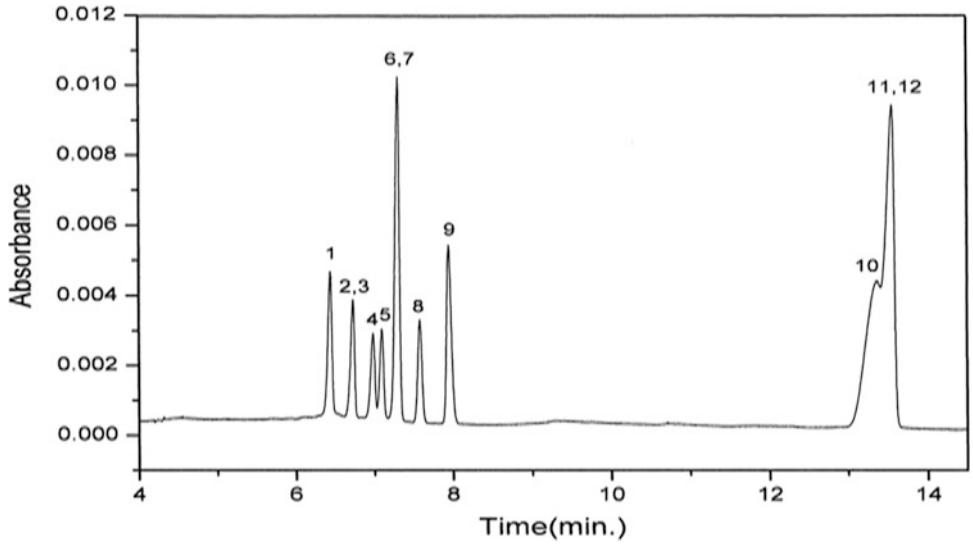

Fig. 6 Electropherogram of benzoic acid and 11 of its derivatives (0.1 mM each) run in 10 mM phosphate buffer (pH 7.0). Peaks (1) *p*-acetamidobenzoic acid; (2) monomethyl terephthalate; (3) aspirin; (4) *p*-hydroxybenzoic acid; (5) *p*-toluic acid; (6) 2-carboxybenzaldehyde; (7) 4-carboxybenzaldehyde; (8) benzoic acid; (9) salicylic acid; (10) *o*-phthalic acid; (11) terephthalic acid; (12) isophthalic acid. Absorbance measured at 215 nm, +25 kV, and 25 °C. The separation capillaries (bare fused silica), 68 cm (61 cm to the detector), 75 μm I.D., 365 μm O.D. [23]

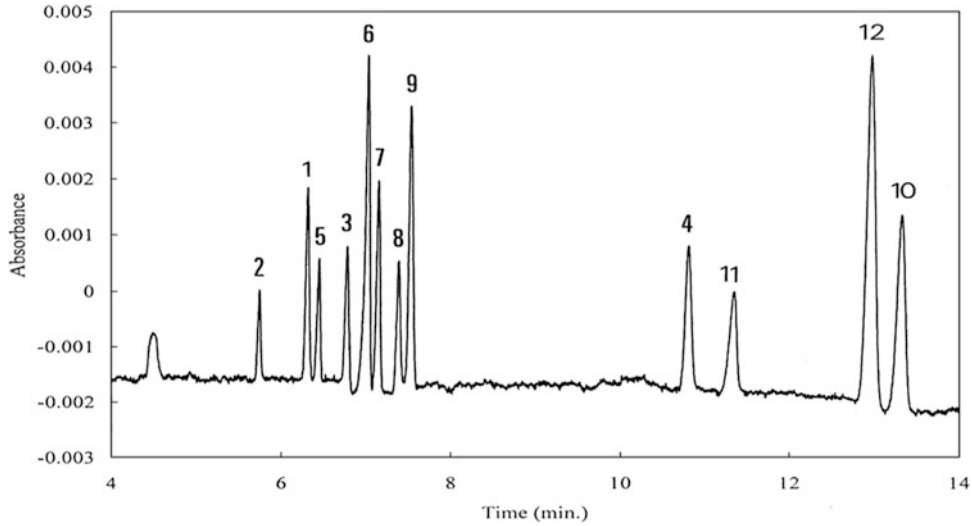

Fig. 7 Electropherogram of mixture of standards (0.1 mM each) run in phosphate buffer 10 mM with 4 mM α-CD, 8 mM β-CD, and 4 % PEG 600 at pH 11.0. Peaks (1) *p*-acetamidobenzoic acid; (2) monomethyl terephthalate; (3) aspirin; (4) *p*-hydroxybenzoic acid; (5) *p*-toluic acid; (6) 2-carboxybenzaldehyde; (7) 4-carboxybenzaldehyde; (8) benzoic acid; (9) salicylic acid; (10) *o*-phthalic acid; (11) terephthalic acid; (12) isophthalic acid. Absorbance measured at 215 nm, +25 kV, and 25 °C. The separation capillaries (bare fused silica), 68 cm (61 cm to the detector), 75 μm I.D., 365 μm O.D. [23]

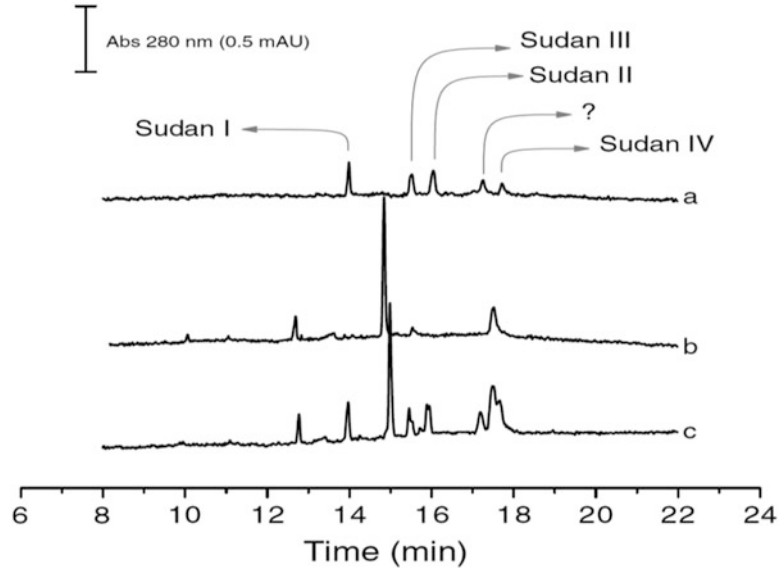

Fig. 8 Electropherograms corresponding to (**a**) a mixture of standards, (**b**) chilli powder sample, (**c**) chilli powder sample spiked with three Sudan dyes. Conditions: 5 mM borate (pH 9.3), 20 mM SDS, and 20 % acetonitrile, 20 kV, injection = 5 s, 0.5 psi, temperature = 25 °C. UV = 214 nm [24]

5. Inject the mixture of standard solutions of dyes and prepare the calibration curves for the determination of Sudan I, Sudan II, Sudan III, and Sudan IV.
6. Apply the method on the chilli powder samples and spiked chilli powder samples. A typical electropherogram for the separation of these dyes at 214 nm is given in Fig. 8.

3.3 Analysis of Phenoxy Acids

1. Maintain the capillary at the constant temperature of 30 °C.
2. Rinse the capillary with 0.1 M NaOH, and the separation buffer before each run.
3. Operate the CE system at a 20 kV and 30 °C.
4. Set the detector wavelength to 230 nm.
5. Inject the sample hydrodynamically at 5 s.
6. Electropherogram showing separation of the phenoxy acids is given in Fig. 9.

3.4 Analysis of Dithiocarbamate Pesticides

1. Rinse the capillary consecutively with 1 M NaOH, 0.1 M NaOH, and water for 2 min, and equilibrate with the carrier electrolyte for 2 min.
2. Between the electrophoretic separations, use equilibrium step with carrier electrolyte. Filter all electrolyte solutions through a 0.45 μm membrane filter.

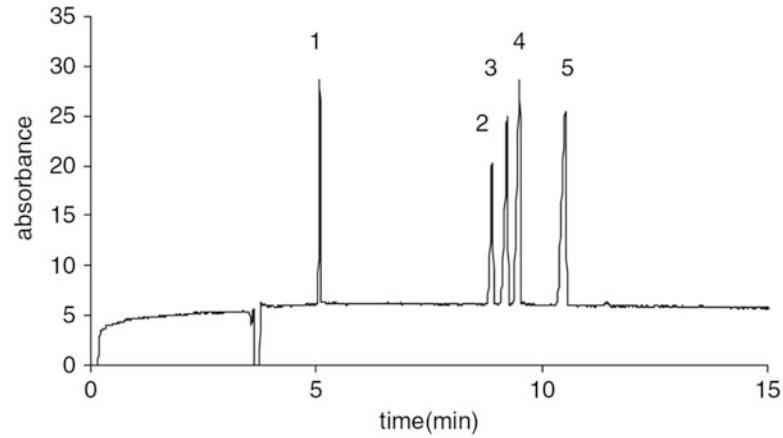

Fig. 9 Electropherogram of the phenoxy acid herbicides (1) MCPB, (2) fenoprop, (3) mecoprop, (4) dichloroprop, (5) MCPA, each at concentration 20 ppm. Background electrolyte: 25 mmol acetate buffer, 4.5 pH, separation voltage 30 kV, capillary dimensions: 57 total length 50 cm to detector, 75 μm (i.d.), 5-s injection, temperature 30 °C, and wavelength 215 nm

3. Inject the solutes for 2 s (injection volume 13.1 nL) in the hydrodynamic mode by vacuum.
4. Perform detection by direct UV absorbance at 254 nm.
5. Operate the instrument at 30 kV.
6. Prepare the calibration graphs by injecting a series of solutions with thio compounds into the capillary. Figure 10 and Fig 11 shows the separation of a mixture of dithiocarbamates using CE.
7. A typical capillary electropherogram of the commercial sample of maneb is shown in Fig. 11 (*see* **Note 2**).
8. Carry out the electrophoretic separation according to the general procedure for grain sample. Take untreated samples of wheat grains as reference.

3.5 Analysis of Paraquat and Diquat

1. Rinse the capillary with 0.1 M NaOH, and the separation buffer before each run.
2. Operate the CE system at a voltage of 15 kV.
3. Inject paraquat and diquat for 2 s (injection volume 13.1 nL) in the hydrodynamic mode by vacuum and record the electropherogram with a UV-Visible spectrophotometer.
4. A typical electropherogram is shown in Fig. 12 for the determination of paraquat and diquat at 254 nm.
5. The λ_{max} for paraquat and diquat are 258 nm and 308 nm, respectively.

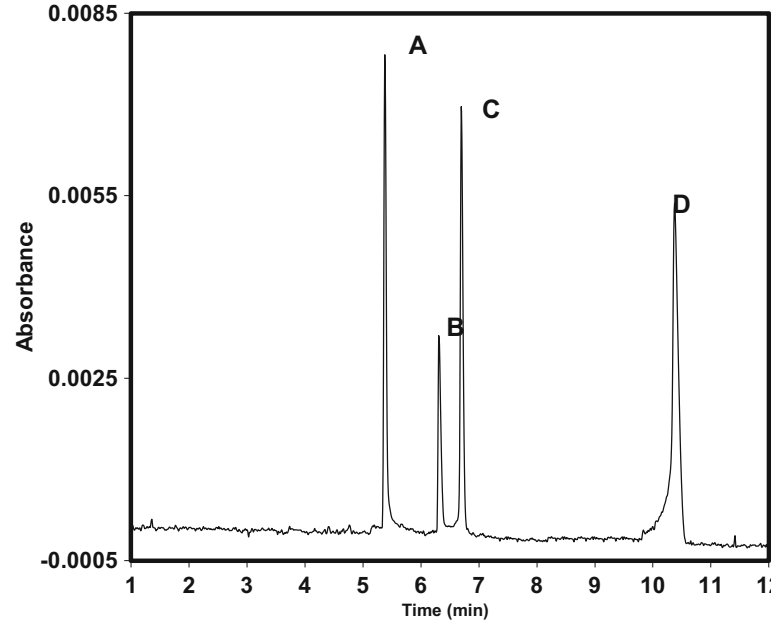

Fig. 10 Capillary electropherogram of sodium diethyldithiocarbamate (0.083 mM) (**a**), potassium *o*-ethylxanthate (0.017 mM) (**b**); metham (0.018 mM) (**c**), and (0.04 mM) maneb (**d**), using 20 mM boric acid buffer (pH 9.0) as the carrier electrolyte, voltage applied ~+ 25 kV, detection at $\lambda = 254$ nm [14]

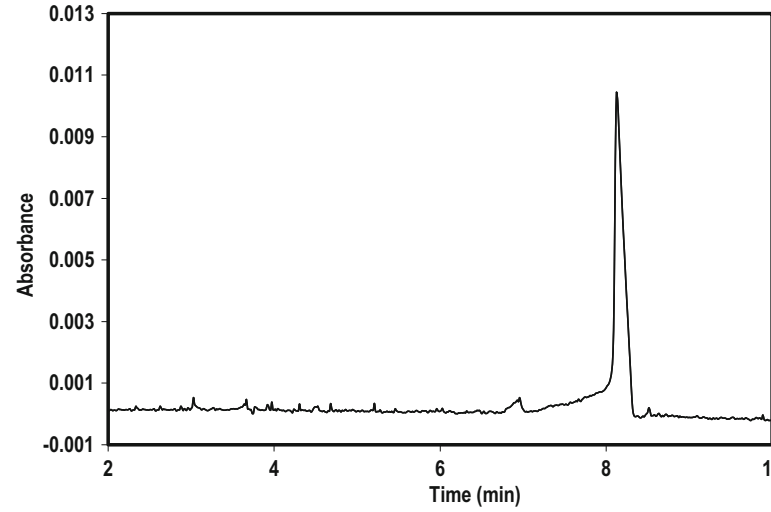

Fig. 11 Capillary electropherogram of a commercial sample of "Dithane M 45" Maneb 0.074 mM, same conditions as in Fig. 10 [14]

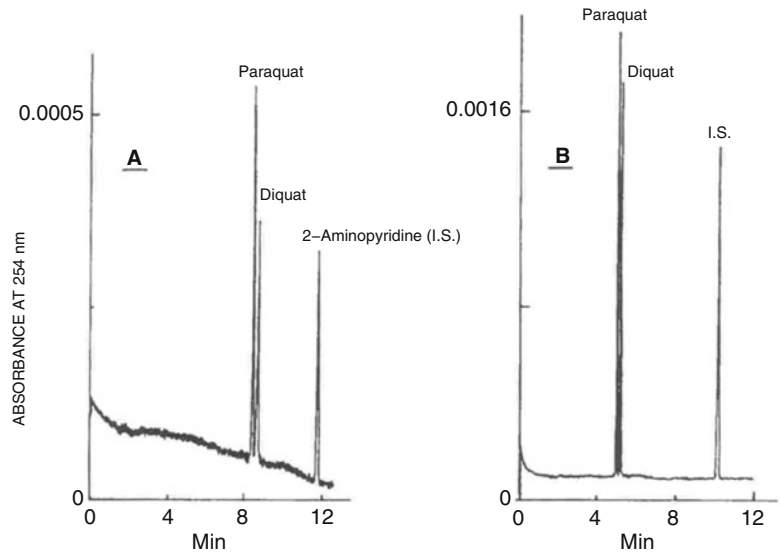

Fig. 12 A typical electropherogram illustrating the rapid separation of herbicides by CZE. Separation capillary, untreated fused silica capillary 50 cm (to the detection point), 80 cm total length 50 cm I.D.; running electrolyte, 0.10 M sodium phosphate, pH 3.5 in A, pH 7.0 in B, sample injection electromigration, 5-s, running voltage, 15 kV, internal standard 2-aminopyridine, detection 254 nm [16]

3.6 Analysis of Endocrine Disruptors

1. Rinse the capillary with 0.1 M NaOH followed by buffer for 10 min before the first use every day.
2. Rinse for 3 min with 0.1 M NaOH, deionized water, and buffer before each separation.
3. Filter the buffer through a 0.2 μm filter.
4. Select the DAD detector in the range of 190–300 nm.
5. Perform the hydrodynamic injection for 5 s at high pressure.
6. For three natural estrogens that is estriol, 17-estradiol, and estrone use 100 mM CAPS buffer (pH 11.5) and 20% methanol. Electropherogram obtained at 210 nm and 30 kV is given in Fig. 13.
7. For the separation of 19 EDCs use 20 mM CAPS (pH 11.5) with 15% ACN and 25 mM SDS. Electropherogram obtained at 200 nm with 20 kV is given in Fig. 14.
8. Analyze the spiked river water sample using 100 mM sodium phosphate (pH 1.8), 25 mM SDS, 12.5% ACN, and 1 mM (2-hydroxypropyl)-β-cyclodextrin (HP-β-CD). Electropherogram obtained at 214 nm with CE operating at 20 kV and 25 °C is given in Fig. 15.

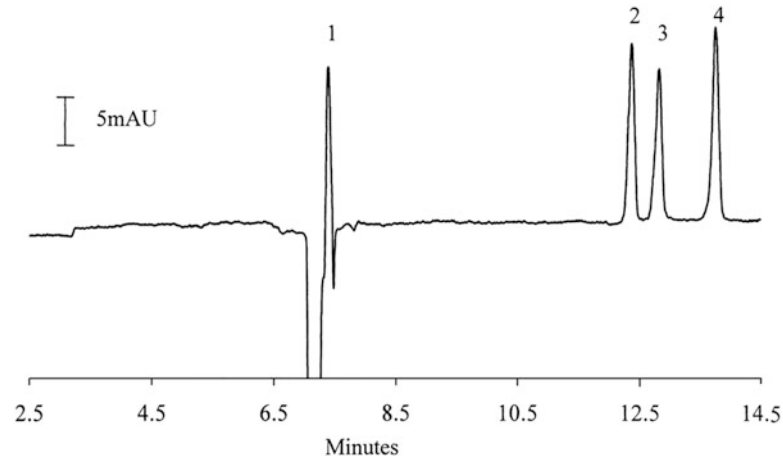

Fig. 13 Separation of three natural estrogens. Separation conditions: 100 mM CAPS buffer pH 11.5 and 20 % MeOH. Applied voltage 30 kV; detection UV 210 nm. Analytes dissolved in 100 % MeOH. Peak identification (1) MeOH, (2) 0.5 mM estriol, (3) 1 mM 17β-estradiol, (4) 0.5 mM estrone [18]

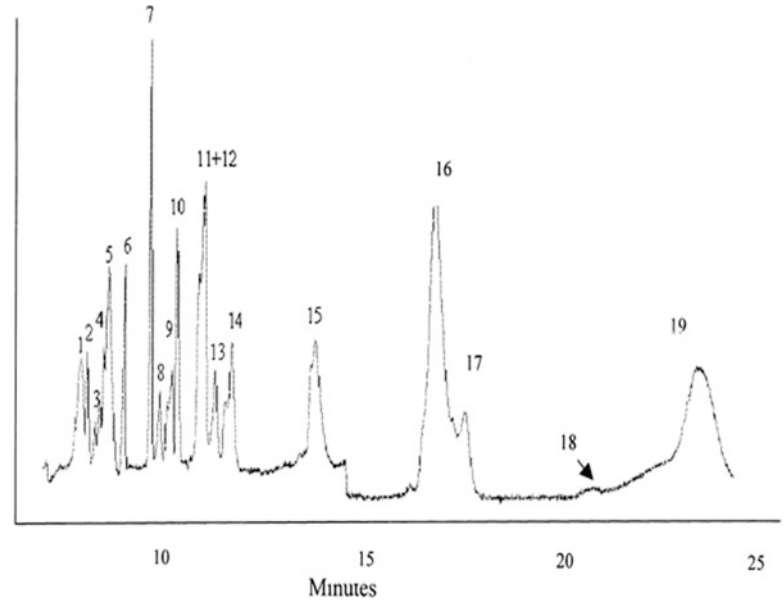

Fig. 14 Separation of 19 target EDCs using MEKC. Separation conditions: 20 mM CAPS pH 11.5 with 15 % ACN and 25 mM SDS; voltage 20 kV; detection at 200 nm; injection sample MeOH–buffer (50:50, v/v). Peak identification: 1 = ethylphenol, 2 = estriol, 3 = methylparaben, 4 = phenol, 5 = propylphenol, 6 = lindane, 7 = trichlorophenol, 8 = bisphenol-A, 9 = pentachlorophenol, 10 = butylphenol, 11 = estrone, 12 = 17 β-estradiol, 13 = DES, 14 = hexylphenol, 15 = dieldrin, 16 = ethynyloestradiol, 17 = NP12, 18 = NP2EO, 19 = nonylphenol [18]

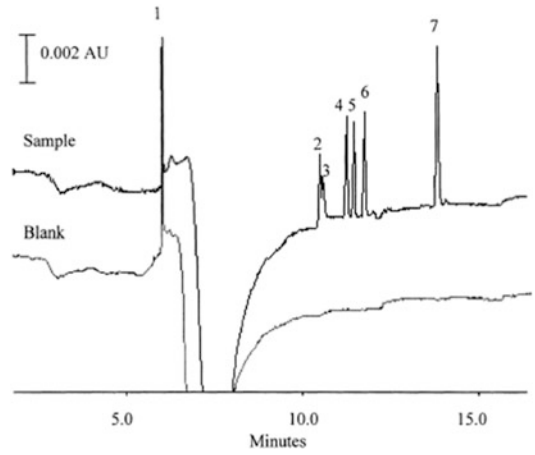

Fig. 15 Analysis of spiked river water sample. Separation conditions: 100 mM phosphate pH 1.8, 25 mM SDS, 12.5 % ACN, 1 mM HP-β-CD (M.S. 0.8). +ve polarity, capillary 57 cm × 50 μm I.D.; 25 °C. Applied voltage +20 kV; 214 nm. Analytes dissolved in 10 % ACN, 90 % run buffer. Analyte concentration 20 mg/L. Peak identification: 1 = sample matrix, 2 = OP, 3 = NP, 4 = DES, 5 = EO, 6 = 17 β-estradiol, 7 = BPA [18]

3.7 Analysis of Toxins

3.7.1 CE–UV Analysis of ASP Toxins

1. Perform CE analysis of ASP toxins using UV detection at a wavelength of 242 nm.
2. Inject the sample at 50 mbar pressure for 12 s and set the voltage for the separation at 30 kV. Use different buffer electrolyte concentrations in a range of 10, 25, and 50 mM in borate buffer.
3. Figure 16 shows CE-UV/DAD analysis of domoic acid and MUS-1 reference material.

3.7.2 CE–UV Analysis of PSP Toxins

1. Perform CE separation in a polyvinylalcohol (PVA)-coated capillary (104 cm × 375 μm I.D.) under a constant voltage of 20 kV at the injector end of the capillary.
2. Apply the sample under constant pressure (50 mbar) and introduce 20 % volume of the capillary.
3. Record the electropherogram at 200 nm.
4. Figure 17 shows CE-UV/DAD analysis of PSP toxins.

3.8 Analysis of Explosives

1. Rinse the capillary with 1 M NaOH and water for 2 min, and equilibrate with the carrier electrolyte for 2 min.
2. Prepare solutions of the various explosives at a concentration of 5.0 mg/L.
3. Take 3–4 mL of extract of the explosives in acetonitrile.
4. Dilute the extracts with the running electrolyte in a ratio of 1:5.

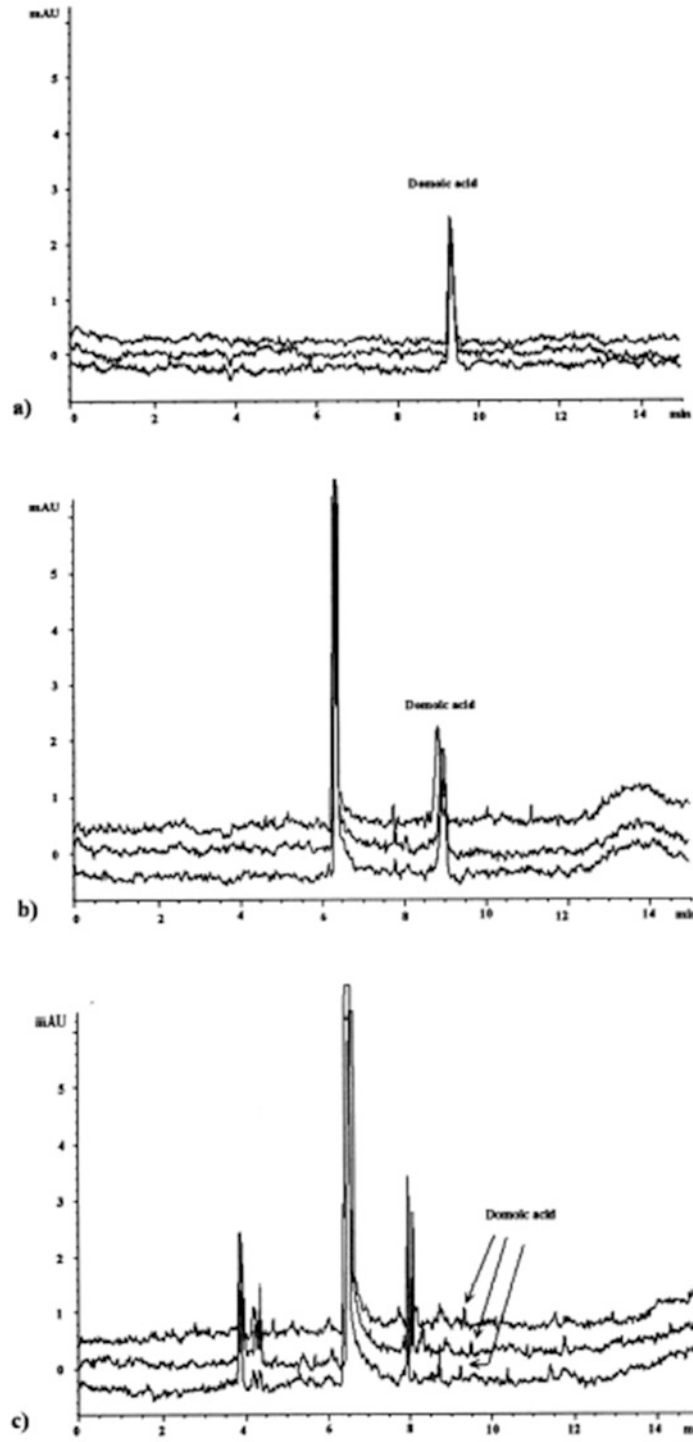

Fig. 16 CE–UV/DAD analysis of (**a**) domoic acid standard, (**b**) MUS-1 reference material after SAX-SCX cleanup, and (**c**) Galician razor clam sample after SAX-SCX cleanup [34]

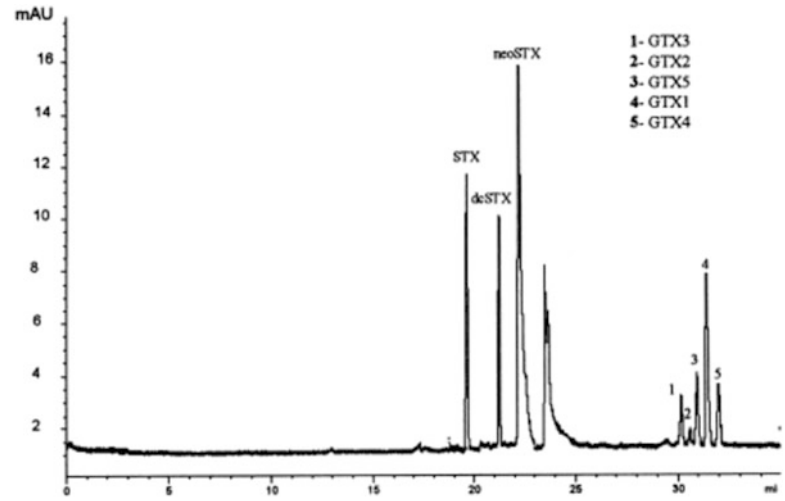

Fig. 17 Standard of PSP toxins, 20 kV, 50 mM morpholine, pH 5 [34]

5. Inject the standard samples into the capillary and prepare the standard calibration curve.
6. Figure 18 shows the separation of a mixture of the explosives.
7. Figures 19, 20, and 21 show the capillary electropherogram for the determination of explosives from different acetonitrile extracts.

3.9 Separation of Bisphenol A and Three Alkylphenols by MEKC

1. Filter the running electrolyte using 0.45 μm pore size membrane filter prior to use.
2. Rinse the capillary with 1 M NaOH for 2 min, followed by subsequent washings with water for 2 min and running solution for 2 min.
3. Operate the CE system at a voltage of 20 kV and 25 °C.
4. Inject the samples using pressure (0.5 p.s.i., 5 s).
5. Prepare the standard calibration curves for bisphenol A and alkylphenols.
6. A typical electropherogram is shown in Fig. 22.

3.10 Analysis of PAHs

1. Regenerate the capillaries with 0.1 M NaOH for 1 min and buffer for 2 min.
2. Degas the mobile phase by ultrasonication.
3. Operate the instrument at 30 kV and 20 °C.
4. Set detection in range of 190–350 nm using PDA detector.
5. Inject the standard mixture of PAHs solution by applying a vacuum of 30 mbar for 5 s and record the capillary electrophe-

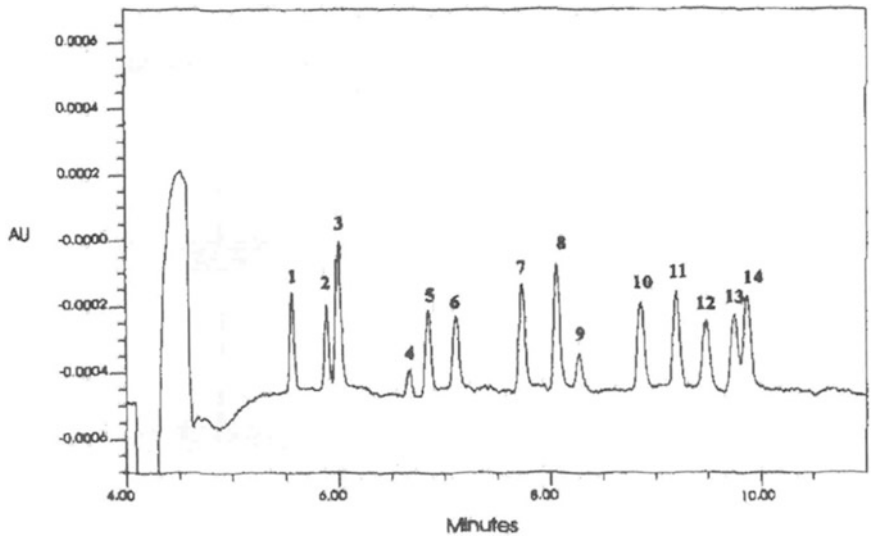

Fig. 18 Electropherogram of a 5 mg/L explosives standard. CE Conditions: fused silica 60 cm × 50 μm I.D. capillary, voltage: 20 kV (positive); electrolyte: 25 mM phosphate-50 mM SDS; direct UV detection at 214 nm; hydrostatic injection (10 cm for 20 s). Solutes:1 = HMX; 2 = RDX; 3 = TNB; 4 = NG; 5 = DNB; 6 = NB; 7 = TNT; 8 = tetryl; 9 = PETN; 10-2,4-DNT; I I = 2,6-DNT; 12-2-NT; 13 = 3-NT; 14 = 4-NT. Refer to Table 1 for full names of solutes [20]

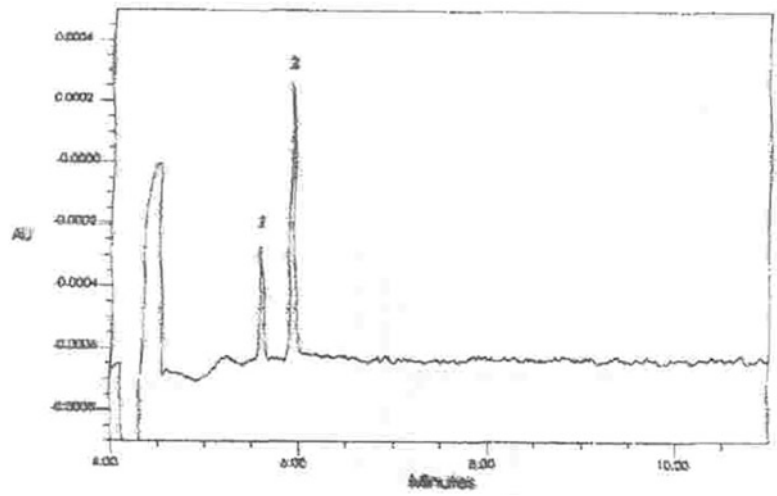

Fig. 19 Electropherogram of composition C-4 extract. Conditions as stated in Fig. 18. Solutes:1 =HMX; 2 = RDX. Refer to Table for full names of solutes [20]

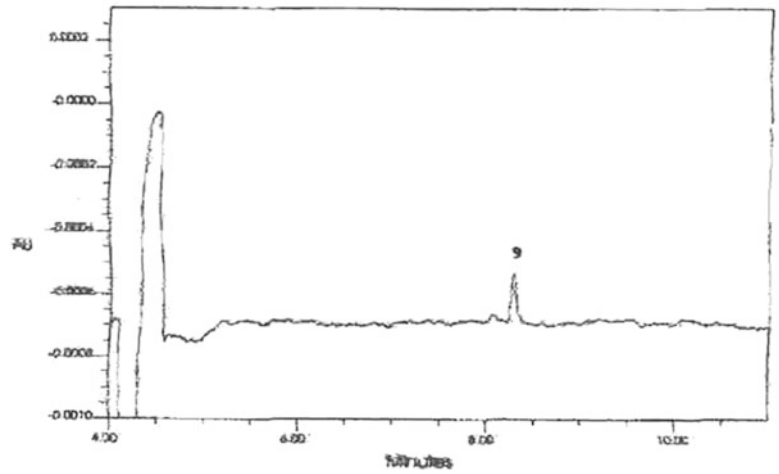

Fig. 20 Eleetropherogram of detonating cord extract. Conditions as stated in Fig. 18. Solutes: 9 = PETN. Refer to Table 1 for full names of solutes [20]

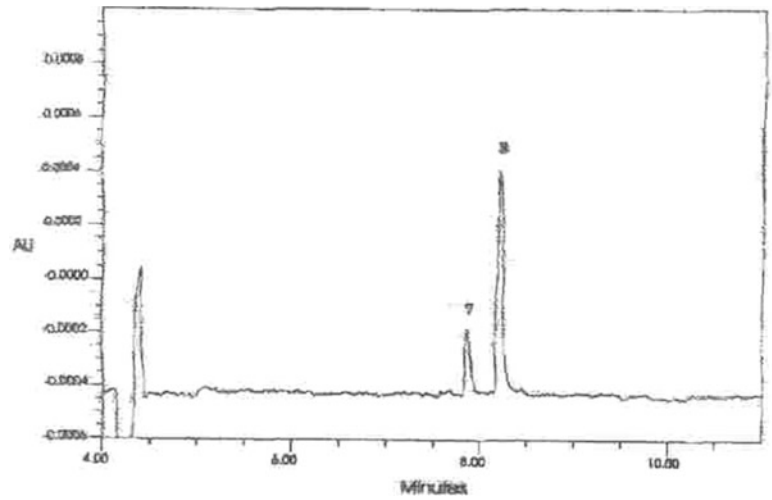

Fig. 21 Electropherogram of tetrytol extract. Conditions as stated in Fig. 18. Solutes: 7 = TNT; 8 = Tetryl. Refer to Table **1** for full names of solutes ref. [20]

rogram (Fig. 23). Prepare the standard calibration curve for the analysis of the PAHs and find out the concentration of the unknown samples (*see* **Note 3**).

6. Inject the spiked soil sample, record the electropherogram (Fig. 24), and find the recoveries.
7. Inject soil sample contaminated with machine oil and record the electropherogram (Fig. 25) depicting the absence of PAH.

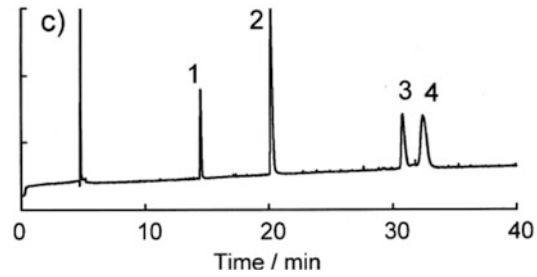

Fig. 22 Electropherogram for bisphenol A and alkyl phenols (1) 4-*tert*-butylphenol (4-tBP), (2) bisphenol A (BPA), (3) 4-(1,1,3,3-tetramethylbutyl)phenol (TMBP), (4) nonylphenol (4-NP). Running electrolyte: 20 mM borate-phosphate (pH 8.0), 20 mM SDS, 5 % ACN, CE conditions: Applied voltage, 20 kV; detection wavelength, 214 nm; temperature 25 °C [22]

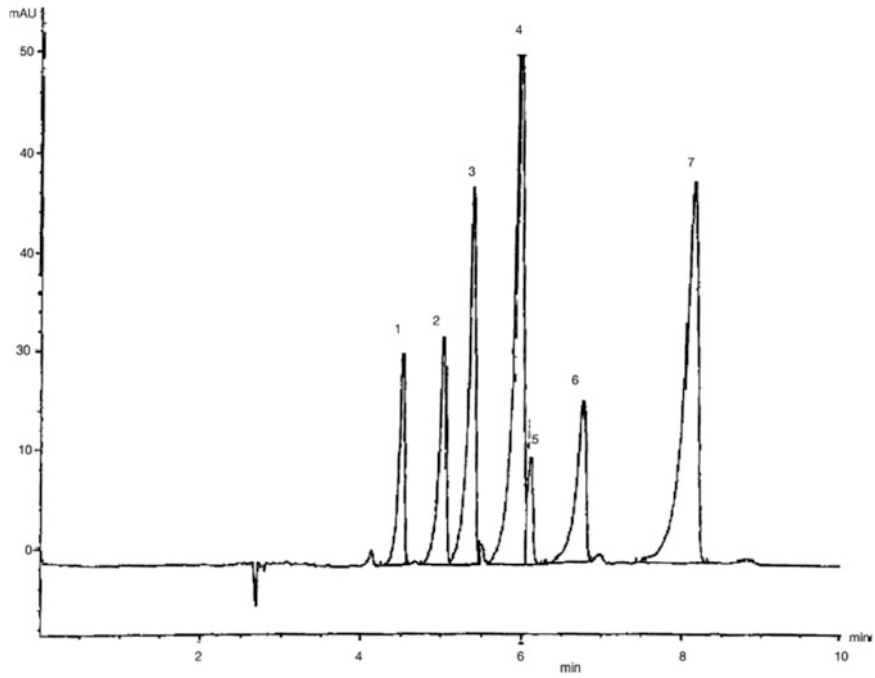

Fig. 23 Separation mix of standard PAHs: (1) Anthracene, (2) fluorene, (3) phenanthrene, (4) fluoranthene, (5) pyrene, (6) chrysene, (7) benzo[a]pyrene. Background electrolyte: Borate buffer 8.5 mM (pH 9.9) containing 85 m*M* SDS and 50 % (v/v) acetonitrile as the electrophoresis buffer (SDS method). The fused silica capillaries 28 cm (length from inlet to detector), 50 μm internal diameter, 30 kV, and 20 °C [6]

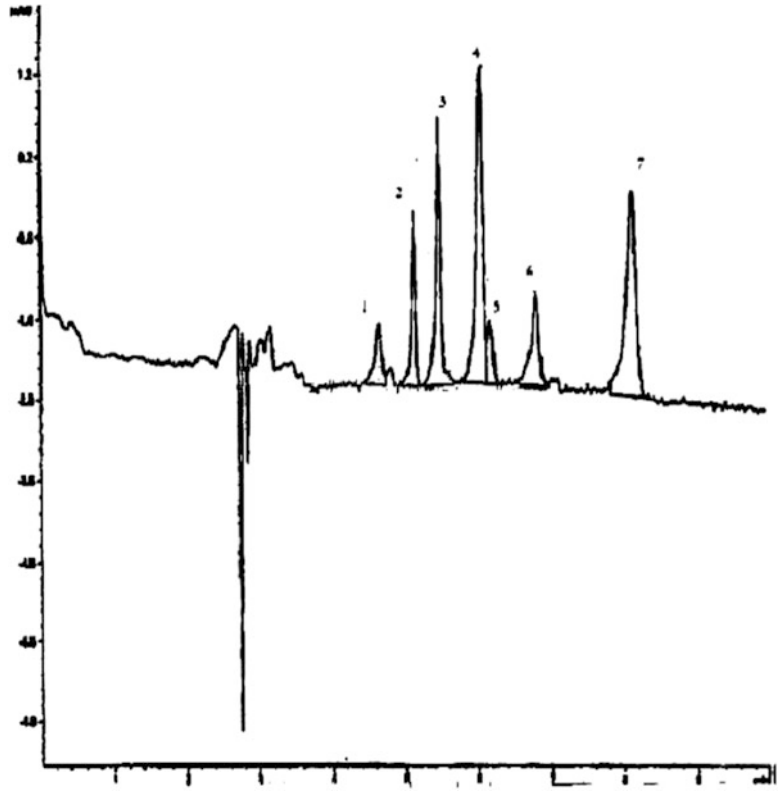

Fig. 24 Separation mix of standard PAHs from spiked soil sample: (1) Anthracene, (2) fluorene, (3) phenanthrene, (4) fluoranthene, (5) pyrene, (6) chrysene, (7) benzo[a]pyrene. Background electrolyte: Borate buffer 8.5 mM (pH 9.9) containing 85 mM SDS and 50 % (v/v) acetonitrile as the electrophoresis buffer (SDS method). The fused silica capillaries 28 cm (length from inlet to detector), 50 μm internal diameter, 30 kV, and 20 °C [6]

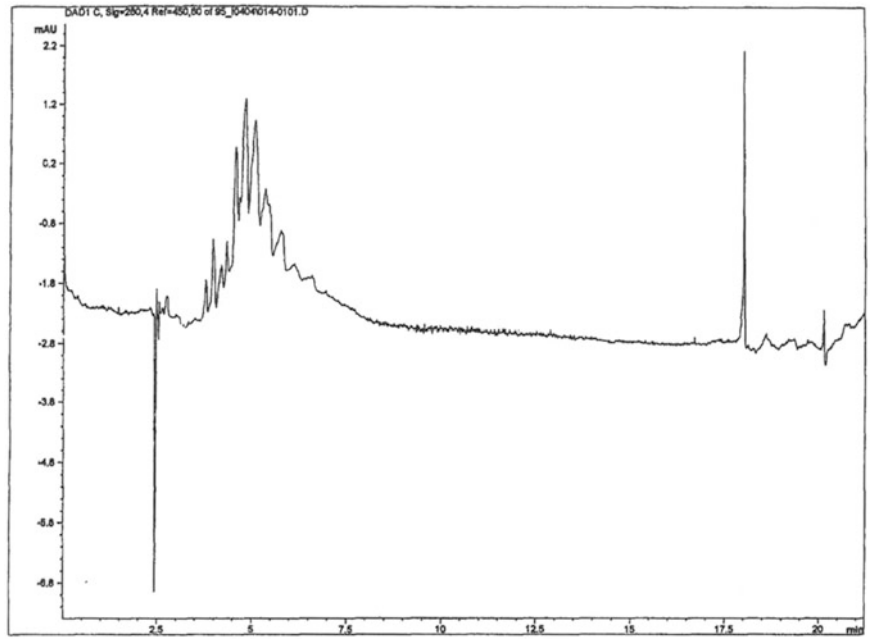

Fig. 25 Analysis of a soil sample contaminated with machine oil. Background electrolyte: Borate buffer 8.5 mM (pH 9.9) containing 85 mM SDS and 50 % (v/v) acetonitrile as the electrophoresis buffer (SDS method). The fused silica capillaries 28 cm (length from inlet to detector), 50 μm I.D., 30 kV, and 20 °C [6]

4 Notes

1. A comparison of various detectors is given in Table 2.
2. It was observed that the peak due to maneb appears earlier as compared to pure sample of maneb in the presence of other dithiocarbamates. The migration time of maneb is different in commercial sample analysis as there is decrease in electroosmotic flow due to the presence of other compounds in the test mixture. This observation is similar to the observation that the

Table 2

Comparison of the detection limits for different spectroscopic detectors used for capillary electrophoresis

Detection mode	Approx. linear range (M) (S/N = 2 or 3)	Approx. mass LOD (M)	Applications	Advantages	Disadvantages	References
UV-V is absorbance	10^{-6}–10^{-3}	10^{-15}	Pesticides, aromatic amines, etc.	Easy to use	Not so sensitive	[4, 26]
Indirect UV-V is absorbance	10^{-5}–10^{-3}	10^{-14}	Aliphatic compounds	Selective and sensitive	Imposes limits on choices of buffer	[4, 26]
Optical absorbance (LED)	10^{-6}–10^{-3}	10^{-15}	Aliphatic and aromatic amines, etc.	Selective and sensitive	Selective in detection	[4, 26]
Laser-induced fluorescence	10^{-18}–10^{-12}	10^{-21}	Formaldehyde acetaldehyde, etc.	Highly sensitive	Selective and expensive	[35, 36]
Mass spectrometry	10^{-12}–10^{-9}	10^{-15}	Phenols, PAHs, etc.	Highly sensitive	Selective and expensive	[35, 37]
ICP-MS	10^{-12}–10^{-9}	10^{-21}	Organophosphorus pesticides, etc.	Highly sensitive	Selective and expensive	[38]
Nuclear magnetic resonance (NMR)	10^{-6}–10^{-3}	10^{-15}	Aromatic sulfonates, etc.	Highly sensitive	Low selectivity and expensive	[39]
Photothermal (thermal lensing)	10^{-18}–10^{-12}	10^{-21}	Pesticides, PAHs, etc.	Highly sensitive, short analysis time	Expensive and difficult to handle	[27]

migration time increases with the buffer concentration. The experiments with pure maneb sample and the corresponding peak appear at the same time as commercial samples. Therefore, it is concluded that the presence of other analytes is affecting the migration time.

3. The buffer in the outlet vial is to be exchanged after each run to improve the reproducibility. After each injection dip the capillary in a second buffer vial to remove all traces of the sample from the outer capillary wall.

References

1. Keyte IJ, Harrison RM, Lammel G (2013) Chemical reactivity and long-range transport potential of polycyclic aromatic hydrocarbons—a review. Chem Soc Rev 42:9333–9391
2. Wang H, Yan H, Wang C, Chen C, Mac M, Wang W, Wang X (2012) Analysis of phenolic pollutants in human samples by high performance capillary electrophoresis based on pretreatment of ultrasound-assisted emulsification microextraction and solidification of floating organic droplet. J Chromatogr A 1253:16–21
3. Tang HP (2013) Recent development in analysis of persistent organic pollutants under the Stockholm Convention. Trends Anal Chem 45:48–66
4. Slobodn J, Louter AJH, Vreuls JJ, Lika I, Brinkman UAT (1997) Monitoring of micropollutant in surface water by automated on-line trace enrichment liquid and gas chromatographic systems with ultraviolet diode-array and mass spectrometric detection. J Chromatogr A 768:239–258
5. Delaunay et al (2014) Optimizing separation conditions of 19 polycyclic aromatic hydrocarbons by cyclodextrin-modified capillary electrophoresis and applications to edible oils. Talanta 119:572–581
6. Brfiggemann O, Freitag R (1995) Determination of polycyclic aromatic hydrocarbons in soil samples by micellar electrokinetic capillary chromatography with photodiode-array detection. J Chromatogr A 717:309–324
7. Yan C, Dadoo R, Zhao H, Zare RN (1995) Capillary electrochromatography: analysis of polycyclic aromatic hydrocarbons. Anal Chem 67:2026–2029
8. Grimmer G, Jacob J, Naujack KW, Dettbarn GF (1981) Inventory and biological impact of polycyclic carcinogens in the environment. Part 13. Profile of the polycyclic aromatic hydrocarbons from used engine oil-inventory GCGC/MS-PAH in environmental materials. Part 2 Fresen *Z.* Anal Chem 309:13–19
9. Dolzan MD, Spudeit DA, Azevedo MS, Costa ACO, Oliveira MAL, Micke GA (2013) A fast method for simultaneous analysis of methyl, ethyl, propyl and butylparaben in cosmetics and pharmaceutical formulations using capillary zone electrophoresis with UV detection. Anal Methods 5:6023–6029
10. Ricardo et al (2014) Capillary zone electrophoresis separation of azaarenes with sensitive UV absorption photometric detection after cationic solid phase extraction and field amplified sample stacking. Fuel 129:20–26
11. Menzinger F, Schmitt-Kopplin P, Freitag D, Kettrup A (2000) Analysis of agrochemicals by capillary electrophoresis. J Chromatogr A 891:45–67
12. Garisson AW, Schmitt P, Kettrup A (1994) Separation of phenoxy acid herbicides and their enantiomers by high-performance capillary electrophoresis. J Chromatogr A 688:317–327
13. Malik AK, Faubel W (1999) Review methods of analysis of dithiocarbamate pesticides. Pesticide Sci 55:1–6
14. Malik AK, Faubel W (2000) Capillary electrophoretic determination of dithiocarbamates and ethyl xanthate. Fresenius J Anal Chem 367:211–214
15. Pico Y, Font G, Molto JC, Manes J (2000) Solid-phase extraction of quaternary ammonium herbicides. J Chromatogr A 885:251–271
16. Cai J, EL Rassi Z (1992) Capillary electrophoresis of two cationic herbicides paraquat and diquat. J Liquid Chromatogr 15:1193–1200
17. Malik AK, Faubel W (2001) A review of analysis of pesticides using capillary electrophoretsis. Crit Rev Anal Chem 31:223–279
18. Regan F, Moran A, Fogarty B, Dempsey E (2003) Novel modes of capillary electrophore-

sis for the determination of endocrine disrupting chemicals. J Chromatogr 1014:141–152

19. Aleksenko SS, Gareil P, Timerbaev AR (2011) Analysis of degradation products of chemical warfare agents using capillary electrophoresis. Analyst 136:4103–4118
20. Stuart AO (1996) Analysis of nitramine and nitroaromatic explosives by capillary electrophoresis. J Chromatogr A 745:233–237
21. Zhonga S, Tanb SN, Geb L, Wanga W, Chena J (2011) Determination of bisphenol A and naphthols in river water samples by capillary zone electrophoresis after cloud point extraction. Talanta 85:488–492
22. Takeda S, Iida S, Chayama K, Tsuji H, Fukushi K, Wakida S (2000) Separation of bisphenol A and three alkylphenols by micellar electrokinetic chromatography. J Chromatr A 895:213–218
23. Wua CH, Lob YS, Niana HC, Lina YY (2003) Capillary electrophoretic analysis of the derivatives and isomers of benzoate and phthalate. J Chromatogr A 1003:179–187
24. Mejia E, Ding Y, Mora MF, Garcia CD (2007) Determination of banned sudan dyes in chili powder by capillary electrophoresis. Food Chem 102:1027–1033
25. Rebane R, Leito I, Yurchenko S, Herodes K (2010) A review of analytical techniques for determination of Sudan I–IV dyes in food matrixes. J Chromatogr A 1217:2747–2757
26. Sovocool GW, Brumley WC, Donelli JR (1999) Capillary electrophoresis and capillary electrochromatography of organic pollutants. Electrophoresis 20:3297–3310
27. Malik AK, Faubel W (2000) Photothermal and light emitting diodes as detector for trace detection in capillary electrophoresis. Chem Soc Rev 29:275–282
28. Zlotorzynska D, Chen H, Ding L (2003) Recent advances in capillary electrophoresis and capillary electrochromatography of pollutants. Electrophoresis 24:4128–4149
29. Lu Q, Collins GE, Smith M, Wang J (2002) Sensitive capillary electrophoresis microchip determination of trinitroaromatic explosives in nonaqueous electrolyte following solid phase extraction. Anal Chim Acta 469:253–260
30. Martynez D, Cugat MJ, Borrull F, Calull M (2000) Solid-phase extraction coupling to capillary electrophoresis with emphasis on environmental analysis. J Chromatogr A 902:65–89
31. Zhou Q, Mao J, Xiao J, Xie G (2010) Determination of paraquat and diquat preconcentrated with N doped TiO_2 nanotubes solid phase extraction cartridge prior to capillary electrophoresis. Anal Methods 2:1063–1068
32. Escuder-Gilabert L, Martín-Biosca Y, Medina-Hernández MJ, Sagrado S (2014) Cyclodextrins in capillary electrophoresis: Recent developments and new trends. J Chromatogr A 1357:2–23
33. Xie S, Paau MC, Li CF, Xiao D, Choi MMF (2010) Separation and preconcentration of persistent organic pollutants by cloud point extraction. J Chromatogr A 1217:2306–2317
34. Pineiro N, Leao JM, Gago Martýnez A, Rodrýguez Vazquez JA (1999) Capillary electrophoresis with diode array detection as an alternative analytical method for paralytic and amnesic shellfish toxins. J Chromatogr A 847:223–232
35. Reemtsma T (2003) Liquid chromatography–mass spectrometry and strategies for trace-level analysis of polar organic pollutants. J Chromatogr A 1000:477–501
36. Pereira EA, Carrilho E, Tavaresa MFM (2002) Laser-induced fluorescence and UV detection of derivatized aldehydes in air samples using capillary electrophoresis. J Chromatogr A 979:409–416
37. Riu J, Eichhorn P, Guerrero JA, Knepper TP, Barcelo D (2000) Determination of linear alkylbenzenesulfonates in waste water treatment plants and coastal waters by automated solid-phase extraction followed by capillary electrophoresis–UV detection and confirmation by capillary electrophoresis–mass spectrometry. J Chromatogr A 889:221–229
38. Wuiloud RG, Shah M, Kannamkumarath SS, Altamirano JC (2005) The potential of inductively coupled plasma-mass spectrometric detection for capillary electrophoretic analysis of pesticides. Electrophoresis 26:1598–1605
39. Malik AK, Faubel W (1999) A review on capillary electrophoretic separations and their studies by nuclear magnetic resonance. J Capillary Electrophor 6:97–108

Chapter 21

Capillary Electrophoresis in Metabolomics

Tanja Verena Maier and Philippe Schmitt-Kopplin

Abstract

Metabolomics is an analytical toolbox to describe (all) low-molecular-weight compounds in a biological system, as cells, tissues, urine, and feces, as well as in serum and plasma. To analyze such complex biological samples, high requirements on the analytical technique are needed due to the high variation in compound physico-chemistry (cholesterol derivatives, amino acids, fatty acids as SCFA, MCFA, or LCFA, or pathway-related metabolites belonging to each individual organism) and concentration dynamic range. All main separation techniques (LC-MS, GC-MS) are applied in routine to metabolomics hyphenated or not to mass spectrometry, and capillary electrophoresis is a powerful high-resolving technique but still underused in this field of complex samples. Metabolomics can be performed in the non-targeted way to gain an overview on metabolite profiles in biological samples. Targeted metabolomics is applied to analyze quantitatively pre-selected metabolites. This chapter reviews the use of capillary electrophoresis in the field of metabolomics and exemplifies solutions in metabolite profiling and analysis in urine and plasma.

Key words Capillary electrophoresis, Metabolomics, Mass spectrometry, Fatty acids, Targeted, Non-targeted

1 Application Review of Metabolomics Using Capillary Electrophoresis

Several studies using capillary electrophoresis in the field of metabolomics have been shown during the last few years. Therefore, various reviews were published dealing especially with CE and metabolomics in general [1–7] between 2008 and 2014. Furthermore, reviews being about special topics as Foodomics [8], single-cell [9–11] diseases (e.g., cancer) [12–14] in toxicology [15], human blood [16], host-gut microbiota metabolic interactions [17], as well as non-targeted fingerprinting [18, 19] and biomarker discovery [20–25]. More reviews involving CE have been published, which are shown in Table 1.

In addition, Tables 2, 3, 4, 5, 6, 7, 8, 9, and 10 present several applications dealing with CE and metabolomics classified on the analyzed matrix (e.g. urine, plasma).

Philippe Schmitt-Kopplin (ed.), *Capillary Electrophoresis: Methods and Protocols*, Methods in Molecular Biology, vol. 1483,
DOI 10.1007/978-1-4939-6403-1_21,

Table 1
List of review articles dealing with metabolomics and capillary electrophoresis on special topics

	Title	Reference
1	Recent advances of chromatography and mass spectrometry in lipidomics	[26]
2	Metabolome analysis by capillary electrophoresis-mass spectrometry	[27]
3	Analysis of carboxylic acids in biological fluids by capillary electrophoresis	[28]
4	Advances in analytical methodology for bioinorganic speciation analysis: metallomics, metalloproteomics, and heteroatom-tagged proteomics and metabolomics	[29]
5	Review: microfluidic applications in metabolomics and metabolic profiling	[30]
6	Separation and mass spectrometry in microbial metabolomics	[31]
7	Advances in separation science applied to metabonomics	[32]
8	Profiling of primary metabolite by means of capillary electrophoresis-mass spectrometry and its application for plant science	[33]
9	Capillary electrophoresis-mass spectrometry: 15 years of developments and applications	[34]
10	Capillary electrophoresis-mass spectrometry for analysis of complex samples	[35]
11	Recent advances in amino acid analysis by capillary electromigration methods, 2011–2013	[36]
12	New advances in separation science for metabolomics: resolving chemical diversity in a post-genomic era	[37]
13	The use of metabolomics to dissect plant responses to abiotic stresses	[38]
14	Growing trend of CE at the omics level: the frontier of systems biology—an update	[39]
15	Capillary electrophoresis at the omics level: towards systems biology	[40]
16	MS-based analytical methodologies to characterize genetically modified crops	[41]
17	Applications of mass spectrometry to metabolomics and metabonomics: detection of biomarkers of aging and of age-related diseases	[42]
18	Multidimensional separations in the pharmaceutical arena	[43]
19	Metabolomics as a tool for the comprehensive understanding of fermented and functional foods with lactic acid bacteria	[44]
20	Metabolomics in cancer biomarker discovery: current trends and future perspectives	[45]
21	Determination of organic acids by CE and CEC methods	[46]

Table 2
Urine

Individual	Targeted/ non-targeted	Analytes	BGE	Capillary	Detection	Ionization	Reference
Rat	Targeted	Anionic metabolites	25 mM TEA (pH 11.7)	Fused silica [100 cm length × i.d. 50 μm]	micrOTOF		[47]
Rat	Targeted	Urinary amino acids	1 M Formic acid	Untreated silica [80 cm length × 50 μm i.d. × 52 μm o.d.]	Ion Trap	ESI (+)	[48]
Rat	Targeted	Amino acids	1 M Formic acid	Untreated silica [80 cm length × 50 μm i.d. × 52 μm o.d.]	IonTrap	ESI (+)	[49]
Rat	Targeted	BAMP and HAMP derivatives of carboxylic acids	1 M Formic acid	Bare fused silica [100 cm length × 50 μm i.d. × 365 μm o.d.]	QqTOF	ESI (+)	[50]
Rat	Non-targeted	–		Fused silica [100 cm length × 50 m i.d.]	TOF		[51]
Rat	Non-targeted	-	Cationic: 1 M Formic acid; anionic: 50 mM ammonium acetate (pH 8.5)	Fused silica [80 cm length × 50 μm i.d.]	TOF		[52]
Rat	Non-targeted	Urine fingerprinting	CD-MEKC: 25 mM Sodium tretraborate decahydrate, 75 mM SDS, and 6.25 mM sulfated β-CD (pH 9.0) CZE: 0.2 M phosphoric acid, adjusted to pH 6.10 with NaOH, and 10% (v/v) methanol	CD-MEKC: fused silica [60 cm length × 75 μm i.d.] CZE: polyacrylamide (PAG)-coated capillary [60 cm length × 50 μm i.d.]	DAD (200 nm)		[53]
Rat	Non-targeted	-	CD-MEKC: 25 mM Sodium tretraborate decahydrate, 75 mM SDS, and 6.25 mM sulfated β-CD (pH 9.0) CZE: 0.2 M phosphoric acid, adjusted to pH 6.10 with NaOH, and 10% methanol	CD-MEKC: fused silica [60 cm length × 75 μm i.d.] CZE: polyacrylamide (PAG)-coated capillary [57 cm length × 50 μm i.d.]	UV	-	[54]
Rat	Targeted and non-targeted	Non-targeted and targeted glutathione as well as four short chain organic acids	CD-MEKC: 25 mM Sodium tretraborate decahydrate, 75 mM SDS, and 6.25 mM sulfated β-CD (pH 9.0) CZE: 0.2 M phosphoric acid, adjusted to pH 6.10 with NaOH, and 10% (v/v) methanol	CD-MEKC: fused silica [60 cm length × 75 μm i.d.] CZE: polyacrylamide (PAG)-coated capillary [57 cm length × 50 μm i.d.]	DAD (200 nm)	-	[55]
Mice	Non-targeted	Metabolic profiling	20% MeOH with 2 M formic acid	Fused silica [100 cm length × 50 μm i.d.)	micrOTOF	ESI (+)	[56]

(continued)

Table 2
(continued)

Individual	Targeted/ non-targeted	Analytes	BGE	Capillary	Detection	Ionisation	Reference
Mice	Non-targeted	Metabolic fingerprinting	CD-MEKC: 25 mM sodium tretraborate decahydrate, 75 mM SDS, and 6.25 mM sulfated β-CD (pH 9.0) CZE: 0.2 M phosphoric acid, adjusted to pH 6.10 with NaOH, and 10% (v/v) methanol	CD-MEKC: fused silica [50 cm length × 50 μm i.d.] CZE: polyacrylamide (PAG)-coated capillary [60 cm length × 50 μm i.d.]	UV		[57]
Mice	Non-targeted		CD-MEKC: 25 mM Sodium tretraborate decahydrate, 75 mM SDS, and 6.25 mM sulfated β-CD (pH 9.0) CZE: 0.2 M phosphoric acid, adjusted to pH 6.10 with NaOH, and 10% (v/v) methanol	CD-MEKC: fused silica [47 cm length × 50 μm i.d.] CZE: polyacrylamide (PAG)-coated capillary [57 cm length × 50 μm i.d.]	DAD		[58]
Mice	Non-targeted		CD-MEKC: 25 mM Sodium tretraborate decahydrate, 75 mM SDS, and 6.25 mM sulfated β-CD (pH 9.0) CZE: 0.2 M phosphoric acid, adjusted to pH 6.10 with NaOH, and 10% methanol	CD-MEKC: fused silica [47 cm length × 50 μm i.d.] CZE: polyacrylamide (PAG)-coated capillary [57 cm length × 50 μm i.d.]	DAD		[59]
Human	Targeted	Short-chain organic acids	pH 6 sodium phosphate buffer (200 mmol/L) with 100 mL/L methanol	Neutral coated capillary [37 cm length × 0.75 μm i.d.]	UV		[60]
Human	Targeted	Organic acids, AA	1.2 M Formic acid (pH 1.8)	Uncoated fused silica [90 cm length × 50 μm i.d.]	MSD TRAP	ESI (+)	[61]
Human	Targeted	AA	1 M (formic acid)	Uncoated fused silica capillaries [90 cm length × 50 μm i.d.]	MSD TRAP		[62]
Human	Targeted	Nucleosides	100 mM borate, 72.5 mM phosphate, 160 mM SDS, pH 6.7	Untreated fused silica [70 cm length × 50 μm i.d.	DAD		[63]
Human	Targeted	Amino acids	1 M Formic acid	Fused silica [100 cm length × 50 μm i.d.	Triple-quadrupole		[64]

Human	Non-targeted		0.8 mL/L Formic acid (pH 1.9) and 10% methanol (v/v)	Fused silica [100 cm length × 50 μm i.d.]	TOF		[65]
Human	Non-targeted	Cationic metabolites	Sheathless: Aqueous acetic acid (10% v/v, pH 2.2) Sheath flow: filled with either 1 mol/L formic acid or 10% (v/v) aqueous acetic acid (pH 2.2)	Sheathless: Fused silica [90 cm length × 30 μm i.d. × 150 μm o.d] Sheath flow: fused silica [100 cm length × 50 μm i.d. × 360 μm o.d.]	TOF		[66]
Human	Non-targeted	Metabolic fingerprinting	50 mM ionic strength ammonia/ammonium acetate (pH 9)	Fused silica [50 cm length × 50 μm i.d. × 365 μm o.d.]	TOF	ESI (+), ESI(-)	[67]
Human	Non-targeted	Metabolic profiling	10% Acetic acid (pH 2.2)	Sheathless: Fused silica [100 cm length × 30 μm i.d. × 150 μm o.d.] Sheath flow: fused silica [100 cm length × 50 μm i.d.]	microTOF	ESI (+), ESI(-)	[68]
Human	Non-targeted	Anionic metabolites	25 mM TEA (pH 11.7)	Fused-silica [100 cm length × 50 μm i.d.]	micrOTOF-QII	ESI(-)	[69]
Human	Non-targeted	Urine fingerprinting	0.8 mol/L formic acid prepared in 10% methanol with no pH adjustment	Fused silica [100 cm length × 50 μm i.d.]	TOF-MS	ESI (+)	[70]
Human	Non-targeted		CD-MEKC: 25 mM Sodium tretraborate decahydrate, 75 mM SDS, and 1.43% (p/v) β-CD sulfated (pH 9.5) CZE: 0.2 M ortho-phosphoric acid, adjusted to pH 6.10 with NaOH, and 10% (v/v) methanol	CD-MEKC: fused silica [60 cm length × 75 μm i.d.] CZE: polyacrylamide (PAG)-coated capillary [60 cm length × 50 μm i.d.]	DAD		[71]
Human	Targeted/ non-targeted	MEKC for 3-methylhistidine and non-targeted	1 M Formic acid (pH 1.8)	Fused silica [130 cm length × 50 μm i.d.)	ToF UV (3-methyl-histidine		[72]

Table 3
Blood/blood cells, plasma, and serum

Individual	Targeted/ non-targeted	Matrix	Analytes	BGE	Capillary	Detection	Ionization	Reference
Rat	Non-targeted	Plasma	Cationic and anionic metabolites	Cationic: 1 M formic acid Anionic: 50 mM ammonium acetate solution (pH 8.5)	Cationic: fused silica [104 cm length × 50 μm i.d. anionic: COSMO(+) capillary	TOF	ESI (+), ESI (-)	[73]
Rat	Non-targeted	Plasma	Cationic, anionic metabolites	Cationic: 1 M formic acid Anionic: 50 mM ammonium acetate solution (pH 8.5)	Cationic: fused silica [100 cm length × 50 μm i.d.] anionic: COSMO(+) capillary [100 cm length × 50 μm i.d.]	TOF	ESI(+), ESI(-)	[74]
Rat	Non-targeted	Plasma	Non-targeted	Cationic: 1 M formic acid Anionic: 50 mM ammonium acetate solution (pH 8.5)	Cationic: fused silica [100 cm length × 50 μm i.d.] anionic: COSMO(+), chemically coated with a cationic polymer [100 cm length × 50 μm i.d.]	TOF	ESI(+), ESI(-)	[75]
Human	Non-targeted	Plasma	Metabolite profiling	Cationic: 1 M formic acid Anionic: 50 mM ammonium acetate pH 7.5	Fused silica [100 cm length × i.d. 50 μm]	TOF		[76]
Human	Targeted/ non-targeted	Plasma	Targeted (free thiols) / non-targeted (thiol metabolism-related metabolites)	1 M Formic acid, pH 1.8	Uncoated fused silica [80 cm length × 50 μm i.d.]	XCT 3D ion trap		[77]
Rat	Non-targeted	Serum	Cationic metabolites and anionic metabolites	Cationic: 1 M Formic acid Anionic: 50 mM ammonium acetate solution (pH 8.5)	Cationic: fused silica [100 cm length × 50 μm i.d.] anionic: COSMO(+), chemically coated with a cationic polymer [100 cm length × 50 μm i.d.]	LC–MSD TOFMS system	ESI (+), ESI(-)	[78]
Rat	Non-targeted	Serum	Cationic and anionic metabolites	Cationic: 1 M Formic acid Anionic: 50 mM ammonium acetate solution (pH 8.5)	Cationic: fused silica [100 cm length × 50 μm i.d.] anionic: COSMO(+), chemically coated with a cationic polymer [111 cm length × 50 μm i.d.]	TOFMS	ESI (+), ESI(-)	[79]

Rat	Non-targeted	Serum	Non-targeted	0.8 mol/L Formic acid in 10% methanol	Fused silica [96 cm length × 50 μm i.d]	TOF	ESI (+)	[80]
Human	Targeted	Serum	Bile acids	10 mM Sodium borate–10 mM sodium dihydrogen phosphate, pH 7.0, SDS (5 mM), β-CD (5 mM); HP-β-CD (5 mM), and 10% (v/v) ACN	Uncoated fused silica [60 cm length × 75 μm i.d.]	UV (185 nm)		[81]
Human	Targeted	Serum	Bile acids	10 mM Sodium borate–10 mM sodium dihydrogen phosphate, pH 7.0, SDS (5 mM), β-CD (5 mM), HP-β-CD (5 mM), and 10% (v/v) ACN	Uncoated fused silica [60 cm length × 75 μm i.d.]	UV		[82] [81]
Human	Targeted	Serum	c-Glutamyl dipeptides, AA	1 M Formic acid	Fused silica capillary [100 cm length × 50 μm i.d.]	TOF	ESI(+)	[83]
Human	Non-targeted	Serum		1 mol/L Formic acid	Fused silica capillary [100 cm length × 50 μm i.d.]	LC/MSD TOF system	ESI(+)	[84]
Human	Non-targeted	Serum	Cationic and anionic metabolites	Cationic: 1 mol/l Formic acid anionic: 50 mmol/L ammonium acetate solution (pH 8.5)	Cationic: fused silica capillary [100 cm total length × 50 μm i.d.] Anionic: COSMO(+) capillary, chemically coated with a cationic polymer	LC/MSD TOF	ESI(+), ESI(-)	[85]
Human	Non-targeted	WBC lysate		Acidic BGE: 1 M formic acid, pH 1.8 Alkaline BGE: 50 mM ammonium acetate, pH 8.5	Uncoated fused silica [80 cm length × 50-μm i.d.]	ion trap mass	ESI(+), ESI(-)	[86]
Human	Non-targeted	Blood		Cationic: 1 M Formic acid, pH 1.8, anionic: 50 mM ammonium acetate, pH 8.5	Uncoated fused silica [80 cm length × 50-μm i.d.]	XCT 3D ion trap	ESI (+), ESI(-)	[87]
Human	Targeted	RBC	Metabolites of glycolysis and the pentose phosphate cycle	1 M Formic acid	Fused silica capillary [100 cm length × 50 μm i.d.]	TOF-MS	ESI(+)	[88] [89]

Table 4
Tissue

Individual	Targeted/ non-targeted	Analytes	BGE	Capillary	Detection	Ionization	Reference
Mice	Non-targeted	Cationic and anionic metabolites	Cationic: 1 M formic acid Anionic: 50 mM ammonium acetate solution (pH 8.5)	Cationic: fused silica [100 cm × 50 μm] Anionic: cationic polymer-coated SMILE (+) capillary [100 cm length × 50 mm i.d. [90]	TOF	ESI (+), ESI(-)	[89]
Mice	Non-targeted	Cationic and anionic metabolites	N.A.	Cationic: Fused silica capillary [80 cm length × 50 μm i.d.] Anionic: Fused silica [80 cm length × 50 μm i.d.]	TOF	ESI(+), ESI(-)	[91]
Mice	Non-targeted	Cationic and anionic metabolites	N.A.	Cationic: Fused silica [80 cm length × 50 μm i.d.] Anionic: Fused silica [80 cm length × 50 μm i.d.]	TOF and DAD	ESI(+), ESI(-)	[92]
Mice	Non-targeted	Anionic (components of glycolysis, pentose phosphate, and the TCA pathways)	Anionic: 50 mM Ammonium acetate (pH 8.5)	Anionic: COSMO(+), chemically coated with a cationic polymer [110 cm length × 50 μm i.d.]	LC/MSD TOF system	ESI (-)	[93]
Mice	Non-targeted	-	0.8 mol/L Formic acid in 10% MeOH	Fused silica [96 cm length × 50 μm]	TOF		[94] [80]
Mice	Non-targeted	-	Cationic: 1 M Formic acid Anionic: 50 mM Ammonium acetate solution (pH 8.5)	Cationic: Fused silica (100 cm length × 50 μm] Anionic: Cationic polymer-coated SMILE (+) capillary [100 cm length × 50 mm i.d. [90]	TOF	ESI (+), ESI(-)	[95] [89]
Hamster	Targeted	Charged and lipid metabolites	Cationic: 1 M Formic acid Anionic: 50 mM Ammonium acetate solution (pH 8.5)	Cationic: Fused silica [100 cm length × 50 μm i.d.] Anionic: COSMO(+), chemically coated with a cationic polymer [110 cm length × 50 μm i.d.]	ToFMS	ESI (+), ESI (-)	[96] [89]
Human	Targeted	Bile acids	10 mM Sodium borate, 10 mM sodium dihydrogen phosphate (pH 7) + 50 mM SDS, 5 mM β-CD, and 5 mM HP-β-CD	Fused silica capillary [60 cm length × 75 μm i.d.]	DAD (200 nm)		[97]
Human	Non-targeted	Cationic metabolites, anionic metabolites, and nucleotide-related metabolites	Cationic: 1 mol/L Formic acid Anionic: 50 mmol/L Ammonium acetate (pH 8.5) Nucleotide related: 50 mmol/l Ammonium acetate (pH 7.5)	Cationic: Fused silica (100 cm length × 50 μm i.d.] Anionic: cationic-polymer–coated SMILE(+) capillary [100 cm length × 50 mm i.d.] [90] Nucleotide related: Fused silica [100 cm length × 50 μm]	TOF	ESI(+), ESI(-)	[98]
Human	Non-targeted	Cationic and anionic metabolites (overall metabolomic profile)	Cationic: 1 M Formic acid Anionic: 50 mM Ammonium acetate solution (pH 8.5)	Cationic and anionic: Fused silica capillary [80 cm length × 50 μm i.d.]	TOFMS	ESI (+), ESI(-)	[99]

Table 5
CSF, salvia, and feces

Individual	Targeted/ non-targeted	Matrix	Analytes	BGE	Capillary	Detection	Ionization	Reference
Human	Non-targeted	CSF	-	0.5 M Formic acid at pH 1.8	PVA-coated [125 cm length × 50 μm i.d.] and uncoated fused silica capillary [87 cm length × 50 μm i.d.]	micrOTOF	ESI(+)	[100]
Mice	Non-targeted	CSF	Metabolic profiling	10% Acetic acid (pH 2.2)	Bare fused silica (etched with a porous tip)	UHR-TOF-MS	ESI(+)	[101]
Mice	Non-targeted	Feces	Cationic, anionic metabolites and nucleotides	Cationic: 1 M Formic acid Anionic: 50 mM Ammonium acetate (pH 8.5) Nucleotides: 50 mM Ammonium acetate (pH 7.5)	Cationic: Fused silica capillary [100 cm × 50 μm i.d.] Anionic: Polymer-coated SMILE(+) capillary [100 cm length × 50 mm i.d. [90] Nucleotides: Fused silica [100 cm length × 50 μm i.d]	TOF	ESI(+) ESI(-)	[102], [103], [104], [105], [106], [90]
Human	Non-targeted	Salvia	-	1 M Formic acid	Fused silica [100 cm length × 50 μm i.d.]	TOF	ESI (+)	[107]
Human	Non-targeted	Salvia	-	Cationic: 1 Mol/L formic acid Anionic: 50 mMol/L ammonium acetate solution (pH 8.5)	Cationic: Fused silica [100 cm length × 50 μm i.d.] Anionic: COSMO(+) capillary [110 cm length × 50 μm i.d.]	TOFMS	ESI (+) ESI (-)	[108]

Table 6
Microorganism

Individual	Targeted/ non-targeted	Analytes	BGE	Capillary	Detection	Ionization	Reference
Synechocystis sp. PCC 6803	Targeted		Cationic: 1 M Formic acid	Fused silica capillary [100 cm length × 50 μm i.d.]	TOF		[109]
E.coli	Targeted	Nucleotides	50 mM Ammonium acetate solution (pH 7.5)	Fused silica capillary [100 cm length × 50 μm i.d.]	Quadrupole	ESI (-)	[105]
E.coli	Targeted	Coenzyme, nucleotide, sugar phosphates, metabolites of TCA	20 mM Ammonium acetate (pH 9.5)	Capillary with integrated interface and porous junction [70 cm length × 50 μm i.d. × 360 μm o.d.] [110]		ESI (-)	[111]
D. vulgaris	Targeted	Cationic metabolites (amino acids, polyamines, purines, and pyrimidines)	1.6 M Formic acid in methanol and water (20:80, v/v)	Untreated, fused silica capillary [100 cm length × 50 μm i.d. × 365 μm o.d.]	Single-quadrupole/micrOTOF/ Apex Qe FT-ICR MS	ESI (+)	[112]
C. jejuni	Targeted	Sugar nucleotides	Morpholine/formate (35 mM; pH 9.0) + 5 % methanol	Bare, fused silica capillaries [90 cm length × 50 μm i.d.]	Triple-quadrupole or a Q-Star mass spectrometer	ESI (+), ESI(-)	[113]
C. jejuni	Targeted	Sugar nucleotides	Morpholine formate (30 mM; pH 9.0)	Fused silica capillaries [100 cm × 50 μm i.d.]	QTRAP	ESI (-)	[114]
E. coli	Targeted	Sugar phosphates	30 mm Morpholine/ formate pH 9.0	Bare, fused silica capillaries [100 cm length × 50 μm i.d.)	4000 Q TRAP mass spectrometer		[115]
C. jejuni and *E. coli*	Targeted	Lipid-linked oligosaccharides	10 mM Ammonium actetate	Bare fused-silica capillary [90 cm length × 365 μm o.d. × 50 μm i.d.]	4000 QTrap mass spectrometer	ESI	[116]
Anaerobic bacteria	Targeted	SCFA	Benzoic acid and histidine (each 10 mM) pH 6.0	Fused silica capillary [75 cm length × 375 μm i.d.]	UV (220 nm)		[117]
C. roseus	Targeted	Nucleotides, coenzymes, organic acids	50 mM Ammonium acetate (pH 9.0)	FunCap-CE type S [80 cm in length × 50 μm i.d.]	4000 QTRAP hybrid triple-quadrupole linear ion trap	ESI(-)	[118]

	Targeted	Nucleotides	150 mM Glycine buffer (pH 9.5)	[95 cm Total length × 75 μm i.d. × 375 μm o.d.]	UV/Vis diode array detector		[119]
E. coli and *pseudomonas*	Targeted	TCA cycle	0.4 M NaH_2PO_4, 0.1 M Na_2HPO_4, and 6% (v/v) methanol (pH 5.65)	Fused silica [75 cm length × 50 μm i.d.]	DAD detector	200 nm	[120]
	Non-targeted	Charged metabolites (TCA, glycolysis, nucleotides, CoA)	Cationic: 1 M Formic acid Anionic: 50 mM Ammonium acetate (pH 8.5)	Cationic: Fused silica capillary [100 cm length × 50 μm i.d.] Anionic: Cationic polymer-coated SMILE (+) capillary [100 cm length × 50 μm i.d.]	Quadrupole	ESI (+), ESI(-)	[121]
	Non-targeted	Negatively charged metabolites	50 mM Ammonium acetate (pH 8.7) in 5% v/v methanol in water	Fused silica [100 cm length × 50 μm i.d.] coated with PolyE-323 for 20 min [122]	TOF		[123]
JHH7 and Hc cells	Non-targeted	Non-targeted	Cationic: 1 M Formic acid; anionic: 50 mM ammonium acetate (pH 8.5) Nucleotides: 50 mM Ammonium acetate (pH 7.5)	Cationic: Fused silica [100 cm length × 50 μm i.d.]; anionic: SMILE(+)-coated capillary [100 cm length × 50 m i.d.] Nucleotides: Fused silica [100 cm length × 50 μm i.d.]	TOF		[124], [103]
E. coli	Non-targeted	Cationic metabolites, anionic metabolites and nucleotides	Cationic: 1 M Formic acid Anionic: 50 mM Ammonium acetate solution (pH 8.5) Nucleotides: 50 mM Ammonium acetate (pH 7.5)	Cationic: Fused silica capillary [100 cm length × 50 μm] Anionic: Cationic polymer-coated SMILE (+) capillary Nucleotides: A fused silica capillary	TOF	ESI (+), ESI(-)	[125]

(continued)

Table 6
(continued)

Individual	Targeted/ non-targeted	Analytes	BGE	Capillary	Detection	Ionization	Reference
E.coli	Non-targeted	Cationic metabolites, anionic metabolites, and nucleotides	Cationic: 1 M Formic acid Anionic: 50 mM Ammonium acetate (pH 8.5) Nucleotides: 50 mM Ammonium acetate (pH 7.5)	Cationic: Fused silica capillary [100 cm length × 50 μm i.d.] Anionic: Polymer-coated SMILE(+) capillary [100 cm length × 50 μm i.d.] Nucleotides: Fused silica capillary [100 cm length × 50 μm i.d.]	TOF	ESI (+), ESI(-)	[103]
A. thiooxidans and A. ferrooxidans	Non-targeted	Cationic and anionic metabolites (aa, nucleotides, coenzymes, metabolites TCA)	Cationic: 1 mol/L Formic acid Anionic: 50 mmol/L Ammonium acetate (pH 8.5)	Cationic: Fused silica capillary [100 cm length × 50 μm i.d.] Anionic: Cationic polymer-coated SMILE(+) capillary	TOFMS	ESI (+), ESI (-)	[126]
P. gingivalis; *S. gordonii*	Non-targeted	Cationic/anionic metabolites	Cationic: H3301-1001, anionic: H3302-1021	Fused silica capillary [80 cm length × 50 μm i.d.]	TOF	ESI (+), ESI (-)	[127]
E. coli	Non-targeted	Cationic metabolites	Cationic: 1 M Formic acid	Cationic: Fused silica [100 cm length × 50 μm i.d.]	TOF	ESI(+)	[128], [89]
Leishmania infantum	Non-targeted	Non-targeted	10% (v/v) Formic acid	Fused silica capillaries [100 cm length × 50 μm i.d. × 150 μm o.d.]	TOF	ESI(+)	[129]
Yeast	Non-targeted	Metabolites central metabolic pathway	20 mM CH3COONH4 (pH 8.0)	Fused silica [75/50 cm length × 50 μm i.d. × 363 μm o.d.]	UV/MALDI		[130]

Yeast	Non-targeted	Anionic metabolites	50 mM NH4HCO3 buffer (pH 8.5) 150 mM NH4HCO3-formate buffer (pH 6.0) 150 mM NH4HCO3-formate buffer (pH 5.0)	SMILE(+)-coated fused silica capillaries [100 cm length × 50 μm i.d. × 375 μm o.d.] PEEK [100 cm length × 50 μm i.d. × 356 μm o.d.] PTFE [100 cm length × 50 μm i.d. × 356 μm o.d]	IonTrap		[131]
Yeast	Non-targeted	Cationic metabolites, anionic metabolites	Cationic: 1 M Formic acid Anionic: 50 mM Ammonium acetate (pH 8.5)	Cationic: Fused silica [100 cm length × 50 μm i.d.] Anionic: Cationic polymer-coated SMILE (+) capillary	TOF	ESI (+), ESI(-)	[132]
Yeast	Non-targeted	Cationic and anionic metabolites	Cationic: 1 M Formic acid Anionic: 50 mM Ammonium acetate (pH 8.5)	Cationic: Fused silica [100 cm length × 50 μm i.d.] Anionic: Cationic polymer-coated COSMO(+) capillary [110 cm length × 50 μm i.d.]	TOF	ESI(+), ESI(-)	[133]
Yeast	Non-targeted		N.A.	Cationic and anionic: Fused silica [80 cm length × 50 μm i.d.]	TOF-MS	ESI(+), ESI(-) ESI(+), ESI(-)	[134]
Yeast	Targeted	Sulfur-related metabolites	1 M Formic acid solution (pH 1.8)	Untreated fused silica capillary [100 cm length × 50 μm i.d × 375 μm o.d.]	Ion trap	ESI(+)	[135]

Table 7
Plants, insects, and single cell

Individual	Targeted/ non-targeted	Matrix	Analytes	BGE	Capillary	Detection	Ionization	Reference
Plants	Targeted		Organic acids and phosphorylated compounds; amino acids	20 mM Ammonium acetate (pH 8.5) Anionic; 1 M formic acid (pH 1.9)	PEG-coated capillary (anionic) Uncoated fused silica (cationic)			[136]
Plants	Targeted		88 Metabolites (glycolysis, TCA cycle, pentose phosphate pathway, photorespiration, and amino acid biosynthesis)	Cationic: 1 M Formic acid (pH 1.8) anionic: 50 mM ammonium acetate (pH 8.5) Group C (nucleotides and coenzymes): 50 mM Ammonium acetate (pH 7.5) Group D (sugars): 2,6-Pyridinedi-carboxylic acid; 0.5 mM acetyltrimethyl -ammonium hydroxide (pH 12.1)	Cationic: Fused silica Anionic: SMILE(+) cationic polymer-coated capillary Group C (): non-charged polymer-coated capillary Group D: CZE with UV	TOF/DAD	ESI (+), ESI(-)	[137]
Plants	Targeted	Rice	A: Cationic metabolites: AA, amines B: Anionic metabolites: organic acids, sugar phosphates C: Nucleotides, coenzymes; D: sugars	A: 1 M Formic acid B: 50 mM Ammonium acetate solution (pH 8.5) C: 50 mM Ammonium acetate solution (pH 7.5) D: Basic anion buffer for CE	A: Fused silica capillary [100 cm length × 50 μm i.d.] B: Cationic polymer-coated SMILE(+) capillary C: Uncharged polymer-coated gas chromatograph capillary, polydimethyl-siloxane (DB-1) D: Fused silica capillary [112.5 cm length×50 μm i.d.]	1100 Series MSD mass spectro meter/DAD (350 nm)	ESI(-), ESI (+)	[138]
Plants	Targeted	Maize	Genetically modified organism metabolomics	5% Formic acid in water (pH 1.90)	Uncoated fused silica capillary [80 cm length × 50 μm i.d. × 375 μm o.d]	Time-of-flight micrOTOF	ESI (+)	[139]
Plants	Targeted	Gentian	A: Organic acids, phosphates, and nucleotides B: Amino acids and polyamines	A: 20 mM Ammonium acetate (pH 9.0) B: 1 M Formic acid (pH 1.9)	A: Polyethylene glycol-coated capillary B: Uncoated fused silica capillary			[140]
Plants	Targeted		Phosphorylated disaccharide isomers	50 mM Ammonium acetate (pH 9.0)	Fused silica [132 cm length × 50-μm i.d × 365 μm, o.d.]	MicroTOF-QII	ESI (-)	[141]

Plants	Targeted		Inorganic anions and cations	Cations: 10 mM Imidazole, 2 mM 18-crown-6 at (pH 4.2) Anions: 20 mM 2,6-Pyridine-dicarboxylic acid, 0.5 mM cetyltrimethylammonium bromide (pH 5.6)	Bare fused silica [50 cm length × 50 μm i.d]	UV		[142]
Plants	Non-targeted	Maize	-	5% Formic acid (pH 1.90)	Uncoated fused silica capillary with [80 cm length × 50 μm i.d. × 375 μm o.d]	microTOF		[143]
Plants	Non-targeted	Rice	-		Untreated fused silica capillary [100 cm length × 50 μm i.d. × 375 μm o.d]]	Esquire 3000 plus ion trap	ESI (+)	[144]
Plants	Non-targeted	Herbal medicines	-	1 M Formic acid (pH 1.8)	Fused silica capillaries [100 cm length × 50 μm i.d.]	TOF	ESI (+)	[145]
Plants	Non-targeted	R. officinale and *R. tangu ticum*	-	15 mM Sodium tetraborate, 15 mM sodium dihydrogen phosphate monohydrate, 30 mM sodium deoxycholate, and 30% ACN v/v (pH 8.3)	Fused silica capillary [70 cm length × 50 μm i.d.]	UV-C		[146]
Plants	Non-targeted/ targeted		-	Cationic: 1 M Formic acid Anionic: 50 mM Ammonium acetate (pH 8.5)	Cationic: Fused silica capillary [100 cm length × 50 μm i.d.] Anionic: Cationic polymer-coated SMILE (+) capillary [100 cm length × 50 μm i.d.]	Quadrupole	ESI (+), ESI(-)	[147] [121]
Plants	Targeted	*Medicago truncatula*	Amino acids	1 M Formic acid	Fused silica [70 cm length × 50 μm i.d.]	Single quadrupole	ESI (+)	[148]
Plants/insect	Non-targeted		-	Cationic: 1 mol/L Formic acid Anionic: 50 mmol/L Ammonium acetate solution (pH 8.5)	Cationic: Fused silica capillaries [100 cm length × 50 μm i.d.] Anionic: COSMO(+) capillary [110 cm length × 50 μm i.d.]	TOF	ESI (+), ESI(-)	[149]
Single cell		*A. californica*	Metabolomic profiling	1% Formic acid in water	Fused silica [100 cm length × 40 μm i.d. × 105 μm o.d.]	QToF, TOF		[150]

Table 8
Food and environmental

Individual	Targeted/non-targeted	Matrix	Analytes	BGE	Capillary	Detection	Ionization	Reference
Food	Non-targeted	Soybean (CGJ)	Metabolite profiling	Cationic: 1 M formic acid Anionic: 20 mM ammonium formate (pH 10.0)	Fused silica capillary [100 cm length × 50 μm i.d.]	TOF	ESI(+), ESI(-)	[151]
Food	Non-targeted	Rice wine	Metabolite profiling	Cationic: 1 mol/L Formic acid Anionic: 50 mmol/L Ammonium acetate solution (pH 8.5)	Cationic: Fused silica capillary [100 cm length × 50 μm i.d.] Anionic: COSMO(+) capillary [110 cm length × 50 μm i.d.]	TOF	ESI(+), ESI(-)	[152]
Environmental	Non-targeted	Atmospheric aerosols	-	Ammonium acetate (pH 4.7) Ammonium formate (pH 2.5)	Fused silica capillary [70 cm length × 75 μm i.d. × 365 μm o.d.]	DAD/single quadrupole	ESI(-)	[153]

2 Application Examples for Targeted Fatty Acid Analysis and Non-targeted Metabolomics

2.1 Plasma and Urine Metabolic Fingerprinting of Type 1 Diabetic Children[70]

2.1.1 Materials, Equipment, and Conditions

In this study, a non-targeted approach for urine fingerprinting by CE-MS and plasma fingerprinting by LC-MS is described. Therefore, 24-h urine samples from diabetic children (in total, 49 children took part at the study and were under metabolic control through insulin treatment; urine samples for CE-MS metabolic fingerprinting only were available from 31 diabetic children [15] control and 16 diabetic samples). Samples were stored at −80 °C until analysis. This study was part of a previous implemented study (Balderas [71]).

Analytes and Sample Preparation

0.5 mL of urine was first vortex-mixed for 1 min and then centrifuged—in order to remove the pellet—for 20 min (16,000 × *g*, 4 °C). 50 μL of the supernatant was taken and mixed with 200 μL of water (MilliQ) and centrifuged again (16,000 × *g*, 4 °C) for 20 min. 200 μL out of this was used for analysis by CE-MS.

CE and MS Instrument and Capillary, CE Buffer

The CE instrument was a 7100 Agilent Technologies capillary electrophoresis system coupled to a TOF-MS (6224) from the same company. The capillary which was used for separation was a

Table 9
Cell culture

Individual	Targeted/ non-targeted	Matrix	Analytes	BGE	Capillary	Detection	Ionization	Reference
Human	Non-targeted	OSCC cells	-	Cationic: 1 mol/L formic acid Anionic: 50 mmol/L Ammonium acetate solution (pH 8.5)	Cationic: Fused silica capillary [100 cm length × 50 μm i.d.] Anionic: COSMO(+) capillary [102 cm length × 50 μm i.d.]	TOF	ESI(+), ESI(-)	[154]
Mice	Non-targeted	ATDC5 cell line	Cationic and anionic metabolites, nucleotides	Cationic: 1 M Formic acid Anionic: 50 mM ammonium acetate (pH 8.5)	For all analyses: Fused silica capillary [80 cm length × 50 μm i.d.]	TOF	ESI(+), ESI(-)	[155]
Mice	Non-targeted	Macrophage-like RAW264.7 cells	Metabolite profiling	Cationic: 1 mol/L Formic acid Anionic: 50 mmol/L Ammonium acetate solution (pH 8.5)	Cationic: Fused silica capillary [100 cm length × 50 μm i.d.] Anionic: COSMO(+) capillary [110 cm length × 50 μm i.d.]	TOF	ESI(+), ESI(-)	[156]

Table 10
Multiple sample analysis

Individual	Targeted/ non-targeted	Matrix	Analytes	BGE	Capillary	Detection	Ionization	Reference
Human	Non-targeted	Urine, serum	Cationic and anionic metabolites, nucleotide-related metabolites	Cationic: 1 mol/L Formic acid Anionic: 50 mM Ammonium acetate solution (pH 8.5) Nucleotide related: 50 mM Ammonium acetate (pH 7.5)	Cationic: Fused silica capillary [100 cm length × 50 μm i.d.] Anionic: COSMO (+) [110 cm length × 50 μm i.d.] Nucleotide related: Fused silica capillary	TOF	ESI(+), ESI(-)	[157], [89], [93]
Rat	Targeted	Urine, plasma	Nucleotides (sugars), coenzymes, sugar phosphates	50 mM Ammonium acetate (pH 9.0)	FunCap-CE type S [80 cm length × 50 μm i.d.]	QTRAP	ESI(-)	[158]

100 cm long fused-silica capillary (Agilent Technologies) with an inner diameter of 50 µm. As CE buffer 0.8 mol/L formic acid in 10% methanol was used. No pH adjustment was done.

2.1.2 Methods

1. First, the new capillary was pretreated with 1 mol/L NaOH for 40 min and deionized water for 30 min.
2. For analysis, samples were injected hydrodynamically at 50 mbar for 17 s.
3. Separation voltage was 30 kV with 25 mbar of internal pressure.
4. As sheath liquid a mixture of methanol and water (1:1, v/v) containing 1 mmol/L formic acid was used. The flow rate of the sheath liquid was 0.4 mL/min, split 1:100.
5. The capillary was conditioned between runs with the CE buffer for 5 min at 950 mbar.
6. The MS was operated in the positive ESI mode. Data were obtained in the full scan mode (mass range from 80 to 1000 *m/z*). Nebulizer pressure: 22.0 psi; dry gas temperature: 200 °C (flow rate: 12.0 L/min); capillary voltage: 3500 V (scan rate: 1.02 scans/s). For the purpose of mass correction and to ensure high accurate mass, two compounds (121.0509 [$C_5H_4N_4$] and 922.0098 [$C_{18}H_{18}O_6N_3P_3F_{24}$]) were spiked into analyses.
7. Quality control (QC) samples (pooled urine samples) were also measured to control instrument stability and performance. QCs were run every five samples.

2.1.3 Data Analysis

First, background noise and regardless ions were removed from the obtained data set by CE-MS analysis (by Molecular Feature Extraction Tool in the MassHunter Qualitative Analysis B.05.00 [Agilent Technologies]). 5841 features could be detected by CE-MS analysis. After some filtering steps and alignment (by Mass Profiler Professional Version B.02.02 [Agilent Technologies]) a data matrix with possible features was created.

Statistical analyses were done by *t*-test for some metabolites and determined by Microsoft Excel 2010® (Redmon, WA, USA). Furthermore, multivariate data analysis was done by SIMCA-P+ 12.0.1.0 (Umëa, Sweden), which reveals a separation in the scores plot by OPLS-DA comparing healthy and diabetic children (Fig. 1). In order to assign features, they were searched against several online available databases as HMDB (http://hmdb.ca), METLIN (http://metlin.scrips.edu), and LIPID MAPS (http://www.lipidmaps.com). To confirm matching results of the mentioned databases and the analyzed features, standards were also measured by CE-MS. Metabolites which could be assigned to compounds or molecular formulas and could be associated with either healthy or diabetic children are shown in Table 11.

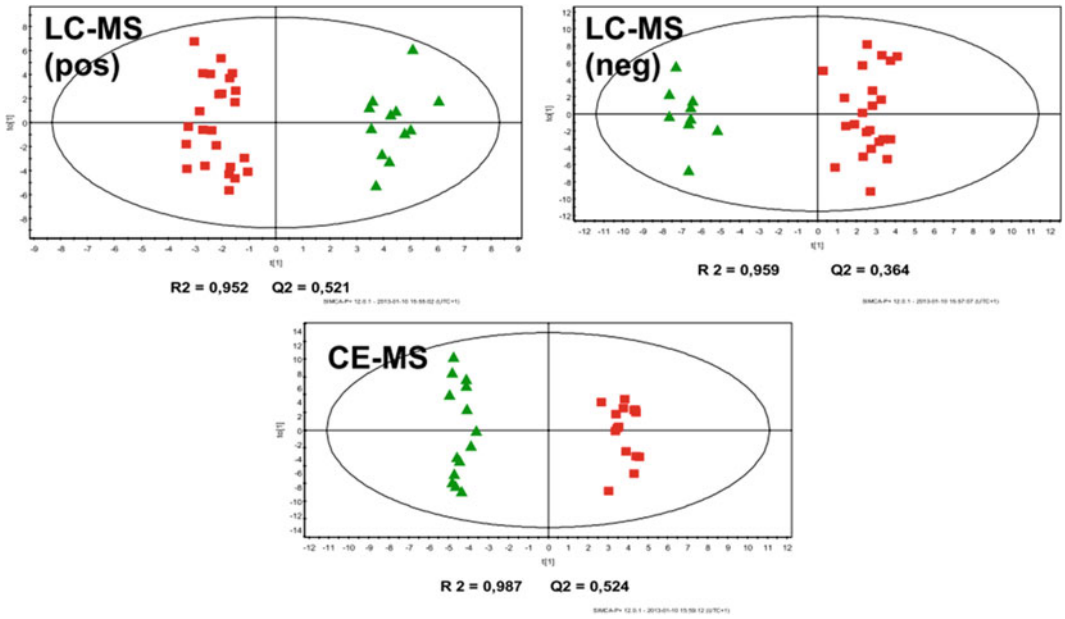

Fig. 1 OPLS-DA score plot comparing healthy and diabetic children due to LC-MS (positive and negative ionisation mode) and CE-MS (positive ionization mode) results. Presented with permission of John Wiley and Sons

2.2 Comparative Metabolite Profiling of Carboxylic Acids in Rate Urine by CE-ESI -MS/MS Through Positively Pre-charged and H^2-Coded Derivatization [50]

2.2.1 Materials and Equipment

Analytes and Sample

BAMP (*N*-butyl-4-aminomethyl-pyridinium iodide) and HAMP (*N*-hexyl-4-aminomethylpyridinium iodide) derivatives of carboxylic acids (*see* Table 12 below).

For the study, urine samples from Sprague-Dawley female rats (7–8 weeks old) were collected and stored at −80 °C. Rats were fed ad libitum with a commercial standard rodent diet from Harlan.

Sample Preparation

(a) Preparation of derivatization reagents.
Synthesis of BAMP and HAMP was done based on Bardsley et al. [159]. 15 g of phthalic anhydride (100 mmol) and 10 mL of 4-aminomethylpyridine (100 mmol) were mixed and afterwards incubated at 170 °C for 30 min. Crude phthalimido was synthesized, which then was recrystallized using methanol. To prepare BAMP, 5 g of the recrystallized product was 1:1 dissolved in 20 mL methanol and iodobutane (88 mmol) or iodohexane (67 mmol) to synthesize HAMP. Afterwards, both reactions were refluxed for 48 h (BAMP) and 72 h (HAMP). Further preparation steps were done including cooling down the mixture to room temperature, removing the solvent

Table 11
Results of CE-MS analyses; identified and unknown urine metabolites (a = confirmed by CE-MS analysis of the standard solution), which revealed differences due to multivariate data analysis comparing healthy and diabetic children

Name	Compound	MW(DB)	RT (min)	Mass (EXP)	Error (ppm)	CV for QC (%)	Change (%)	*p*-Value
Serine[a]	$C_3H_7NO_3$	105.04260	16.4	105.0430	3.9	8.0	25.2	0.286
Asparagine[a]	$C_4H_3N_2O_3$	132.05349	17.1	132.0524	–8.3	4.5		0.142
Lysine[a]	$C_5H_{18}N_2O_2$	174.13583	11.9	174.1349	–11.1	10.2	89.8	0.039
Valine[a]	$C_5H_{11}NO_2$	117.07897	18.7	117.0791	1.2	5.0	143.4	0.002
Leucine/isoleucine[a]	$C_6H_{13}NO_2$	131.09463	16.8	131.0946	–0.2	29.7	63.1	0.043
Phenylalanine[a]	$C_9H_{11}NO_2$	165.07898	17.9	165.0792	1.3	13.0	35.6	0.130
Phenylacetamide	C_8H_9NO	135.06842	18.3	135.0684	–0.1	4.5	14.0	0.530
Guanidinoacetic acid[a]	$C_3H_7N_3O_2$	117.05383	13.7	117.0539	0.6	6.3	37.6	0.179
L-kynurenine/ formyl-5-hydroxykynurenamine	$C_{10}H_{12}N_2O_3$	208.08479	16.7	208.0851	1.5	5.5	38.1	0.218
Guanidinosuccinic acid	$C_5H_9N_3O_4$	175.05931	16.5	175.0595	1.1	5.5	38.7	0.067
Acetylarginine	$C_8H_{16}N_4O_3$	216.12224	16.1	216.1236	6.3	21.3	100.8	0.001
Hydroxytrimethyllysine	$C_9H_{20}N_2O_3$	204.14739	12.8	204.1471	–1.4	16.0	48.1	0.098
Trimethyllysine	$C_9H_{20}N_2O_2$	188.15248	12.2	188.1522	–1.5	7.8	78.5	0.098
6-Methyltetrahydropterin	$C_7H_{11}N_5O$	181.09636	19.4	181.0952	–6.4	14.0	32.2	0.053
Choline[a]	$C_5H_{13}NO$	103.09971	11.4	103.1000	2.8	9.1	10.8	0.549
Carboxyethylarginine	$C_9H_{18}N_4O_4$	246.13281	14.6	246.1327	–0.4	8.3	23.5	0.345
Fructosamine (hexosamine)	$C_6H_{13}NO_5$	179.07937	15.3	179.0797	1.8	10.70	117.6	0.051

6-Hydroxyl-1,6-dihydropurine ribonucleoside	$C_{10}H_{14}N_4O_5$	270.09642	14.5	270.0964	–0.1	8.6	92.0	0.115
Dihydrothymine	$C_5H_8N_2O_2$	128.05858	14.5	128.0586	0.2	6.4	14.3	0.471
Galactosylglycerol	$C_9H_{18}O_8$	254.10017	15.5	254.0914	–34.5	6.3	7.3	0.697
Asp Asp	$C_8H_{12}N_2O_7$	248.06445	20.6	248.0662	7.0	8.3	–13.3	0.466
Pro Ile Lys	$C_{17}H_{32}N_4O_4$	356.23270	12.7	356.2409	23.0	9.3	38.8	0.083
His Phe Asn	$C_{19}H_{24}N_6O_5$	416.18082	13.8	416.1903	22.8	8.9	95.1	0.004
Cystine[a]	$C_6H_{12}N_2O_4S_2$	240.02385	18.1	240.0239	0.2	7.1	51.8	0.040
Unknown	$C_6H_4Cl_2O_5$	225.94358	8.9	225.9447	5.0	2.0	–4.7	0.738
Unknown	$C_{19}H_{20}N_2O_2$	308.15248	14.5	308.1583	18.9	6.6	72.5	0.024
Unknown	$C_{11}H_9NO_2$	187.05931	17.8	187.0634	21.9	7.1	34.0	0.185
Unknown	$C_{22}H_{22}O_7$	398.13655	12.1	398.1364	–0.4	9.4	21.2	0.379
Unknown	$C_{31}H_{24}O_{12}$	588.12678	21.7	588.1400	22.5	7.3	79.2	0.057
Unknown	$C_4H_9NO_2$	103.06332	13.0	103.0638	4.7	3.7	322.9	0.126

List includes name of the compound, molecular formula, molecular weight (MW, database), retention time (RT in minutes), molecular weight (MW, experimental after alignment), error MW_{DB} and $MASS_{EXP}$ (ppm), *p*-value, CV for QC (%), and its CHANGE (changes in the abundances of diabetic-control/control) (%). Presented with permission of John Wiley and Sons

Table 12
List of carboxylic acids derivatized with BAMP and HAMP, including information on *m/z*, concentrations (μg), mass (pg), and RSD of the migration time (%)

		BAMP			HAMP			
		Detection limit[a]				Detection limit		
Peak	Carboxylic acid	*m/z*	Conc. (μM)	Mass (pg)	*m/z*	Cone. (μM)	Mass (pg)	Migration time RSD (%, $n=5$)[b]
1	Oxaloacetic acid, di-	213.37 (+ 2)	20.0	26.0	241.38 (+ 2)	5.0	6.0	1.20
2	Oxalic acid, di-	192.35 (+ 2)	20.0	18.0	220.40 (+ 2)	5.0	4.0	1.11
3	Malonic acid, di-	199.33 (+ 2)	10.0	10.0	227.36 (+ 2)	2.0	2.0	0.92
4	Fumaric acid, di-	205.37 (+ 2)	5.0	5.0	233.35 (+ 2)	1.0	1.0	1.16
5	Succinic acid di-	206.36 (+ 2)	2.0	2.0	234.37 (+ 2)	0.5	0.6	0.99
6	Maleic acid, di-	205.37 (+ 2)	5.0	5.0	233.35 (+ 2)	1.0	1.0	1.29
7	Maleic acid, di-	214.37 (+ 2)	2.0	2.0	242.39 (+ 2)	0.5	0.6	1.18
7	Citric acid, di-, $-H_2O$	234.33 (+ 2)	5.0	9.0	262.36 (+ 2)	1.0	2.0	1.18
7	Ketoglutaric acid, di-	220.38 (+ 2)	10.0	14.0	248.38 (+ 2)	2.0	3.0	1.18
8	Isocitric acid, di-, $-H_2O$	234.33 (+ 2)	10.0	19.0	262.36 (+ 2)	2.0	4.0	1.23
9	Tartaric acid, di-	222.36 (+ 2)	5.0	7.0	250.37 (+ 2)	1.0	1.0	1.26
10	Adipic acid, di-	220.57 (+ 2)	2.0	2.0	248.38 (+ 2)	0.5	0.7	1.32
11	Citric acid, di-	243.33 (+ 2)	5.0	9.0	271.33 (+ 2)	1.0	2.0	1.01
12	Isocitric acid, di-	243.33 (+ 2)	5.0	9.0	271.03 (+ 2)	1.0	2.0	1.00
12	Formic acid	193.33 (+ 1)	5.0	2.0	221.32 (+ 1)	1.0	0.5	1.00
13	Acetic acid	207.34 (+ 1)	10.0	6.0	235.33 (+ 1)	5.0	3.0	1.06

(continued)

Table 12
(continued)

		BAMP			HAMP			
		Detection limit[a]			Detection limit			Migration time
Peak	Carboxylic acid	*m/z*	Conc. (μM)	Mass (pg)	*m/z*	Cone. (μM)	Mass (pg)	RSD (%, *n*=5)[b]
14	Propionic acid	221.37 (+1)	2.0	1.0	249.14 (+1)	1.0	0.7	1.08
15	Pyruvic acid	235.37 (+1)	10.0	8.0	263.37 (+l)	2.0	1.0	1.14
15	Lactic acid	237.34 (+1)	10.0	9.0	265.37 (+1)	2.0	2.0	1.14
16	Butyric + isobutyric acid[c]	235.32 (+1)	2.0	1.0	263.37 (+1)	1.0	0.8	1.20
17	Benzanic acid	269.33 (+1)	2.0	2.0	297.32 (+1)	0.5	0.6	1.28
18	Shikimic acid	321.36 (+1)	10.0	17.0	349.34 (+1)	2.0	3.0	1.24
19	Quinic acid	339.35 (+1)	100.0	192.0	367.36 (+1)	20.0	38.0	1.27

Presented with permission of John Wiley and Sons
[a] Injection volume 10 nL, Mean of 3 injections of 5 different levels (concentration range: 100–1 mM).
[b] Successive injections (n=5) of standard mixture at the concentration of 100 mM.
[c] Not separated by CE/MS.

(by evaporation under vacuum), and at least recrystallization by acetone. To continue the synthesis of both derivatization reagents, crystals were again refluxed by HBr (20 mL, 86% v/v) for 6 h and 10 mL of water was added. In order to remove the phthalic acid, reagents were filtered. Filtrates were afterwards extracted with ether (2×10 mL) and evaporated under vacuum. To complete the synthesis of BAMP and HAMP another recrystallization step from acetone was implemented. Additionally, the same procedure as described before was applied to synthesize the deuterated product of BAMP (d9-BAMP), substituting iodobutane to d9-iodobutane. This book chapter will not go into detail on the results of d9-BAMP derivatives.

(b) Derivatization.
First, both derivatization reagents and EDC were dissolved in water (0.1 M). Twenty-four carboxylic acids were pooled and dissolved in water. Each carboxylic acid was concentrated at 0.45 mM (divergent concentrations are listed in Table 1). For the derivatization reaction 50 μL of standard mix and 100 μL

of the derivatizing reagent were mixed and incubated for 2 h at 50 °C.

(c) Preparation of urine samples with derivatization reagents.
In order to compare CE-MS results of standards and the real sample, derivatization of urine samples was done under similar conditions as standard derivatization. Therefore, urine samples were centrifuged for 10 min (3000 × *g*, 4 °C). 500 µL of the supernatant was mixed with 200 µL of the derivatization reagent and 15 mg of EDC. Due to titration with 2 M HCl or 2 M NaOH the pH of the mixture was adjusted to a range of 4–6. Afterwards, the samples (urine + derivatization reagent + EDC) were finally incubated at 50 °C for 2 h.

(d) SPE.

Purification of the derivatized carboxylic acids was done by SPE using Oasis® WCX cartridges (Waters, Milford, MA, USA). Therefore, a 1 mL cartridge was conditioned with 1 mL methanol, followed by 1 mL water. Derivatized samples and 300 µL of 5 % ammonium hydroxide were mixed and loaded onto the cartridge. Afterwards, 1 mL of 5 % ammonium hydroxide and 1 mL methanol were loaded on the cartridge. Elution of the derivatives was done using 1 mL of 2 % formic acid in methanol. At last, they were vacuum dried and diluted with CE running buffer to the original volume, before CE-MS analysis.

CE and MS Instrument and Capillary, CE Buffer

CE measurements were performed by a Beckman-Coulter PA800 CE System (Beckman-Coulter, Fullerton, CA, USA) coupled to a QStar mass spectrometer from Applied Biosystems (Foster City, CA, USA). A CE-MS Upgrad Kit from Applied Biosystems/MSD SCIEX (Concord, Ont., Canada) was used as interface. Separations were done on a 100 cm long bare fused-silica capillary (Polymicro Technologies, Phoenix, AZ, USA) with an inner diameter (id) of 50 µm and 365 µm outer diameters (od). 1 M formic acid was chosen as background electrolyte (BGE).

2.2.2 Methods

1. Capillary (before connecting to the MS) was flushed with 0.1 M NaOH overnight, in order to gain high EOF to optimize separations. Additionally, the capillary was also flushed overnight with water and BGE, for 10 min each.
2. Due to preconditioning, 30 V/cm were off-line applied on the column for 30 min.
3. Samples were injected by pressure injection (5 s, 2 psi).
4. Chosen voltage to perform separations was 30 V/cm.
5. 50 % v/v methanol with 0.1 % v/v formic acid I water was used as sheath liquid, with a flow rate of 1 µL/min performed by the syringe pump.

6. The capillary was flushed with 0.1 M NaOH and BGE for 2 min (50 psi) between each run.
7. MS conditions are as follows: positive ionization mode (ESI+); scan range 190–500 *m/z* (BAMP) and 200–500 *m/z* (HAMP) with 1 scan/s.
8. Parameters of the ion source, as well as parameters as sheath flow rate, ESI sensitivity, and stability, were optimized using electrokinetic pumping (potential of 300 V/cm, 2 psi).
9. Optimized parameters are as follows: ion spray voltage 4800 V; curtain gas 30; ion source gas 1, 40; ion source 2, 0; declustering potential 50 V; focusing potential 220 V; declustering potential 2, 10 V.
10. MS/MS experiments were done by CID; collision energy was 40 eV and collision gas was 5.
11. Data acquisition and processing were performed using Analyst software (Applied Biosystems/MSD SCIEX).

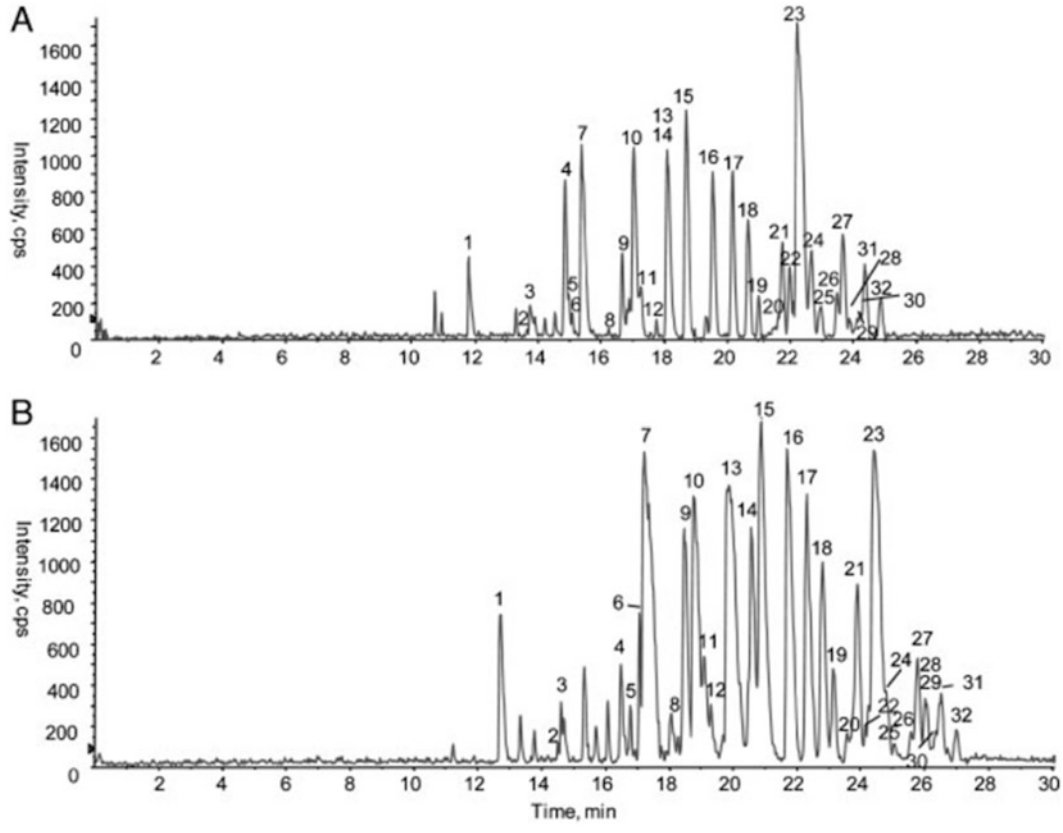

Fig. 2 Basepeak chromatogram of CE-ESI-MS analysis of BAMP (**a**) and HAMP (**b**) derivatives of carboxylic acids in the pooled rat urine sample. Peak numbers are listed in Table 13. Presented with permission of John Wiley and Sons

Table 13
Identified peaks of the base peak chromatogram in Fig. 2

	BAMP			HAMP			Identification[b]	
Peak	Tr (min)	*m/z*	Int.[a] (%)	Tr (min)	*m/z*	Int.[a] (%)	*Mr*	Compound
1	11.81	235.19(+ 1)	1.11	12.7	264.21(+ 1)	0.78	88.21	U
1	11.81	320.46(+ 1)	0.71	12.7	348.47(+ 1)	0.5	173.17	*N*-Acetylleucine (R)
2	13.67	299.37(+ 1)	0.49	14.52	327.42(+ 1)	0.35	152.12	**U**
3	13.76	313.35(+ 1)	0.88	14.72	341.39(+ 1)	0.63	166.09	**U**
4	14.99	204.78(+ 3)	0.88	16.5	232.79(+ 3)	0.63	172.47	**U**
4	14.99	254.35(+ 1)	0.88	16.5	282.36(+ 1)	0.63	107.06	**U**
4	14.99	303.30(+ 1)	1.28	16.5	331.33(+ 1)	0.91	156.03	Furan-2,5-dicarboxylic acid, mono- (**R**)
4	14.99	278.40(+2)	3.99	16.5	306.87(+ 2)	2.83	263.14	**U**
5	15.08	270.33(+ 1)	0.88	16.8	298.33(+ 1)	0.63	123.03	Nicotinic acid (**S**)
6	15.2	213.37(+ 2)	0.8	17	241.38(+ 2)	0.56	132.16	Oxaloacetic acid, di- (**S**)
6	15.22	211.35(+ 1)	0.26	17.08	239.37(+ 1)	0.18	64.07	**U**
7	15.38	191.31(+ 1)	3.98	17.22	219.35(+ 1)	2.82	44.05	**U**
7	15.38	299.37(+ 1)	4.86	17.23	327.32(+ 1)	3.45	152.02	**U**
7	15.45	274.32(+ 1)	1.46	17.4	302 40(+ 1)	1.03	127.1	δ-Piperideine-6-L-carboxylate δ-piperideine-2-carboxylate (**L**)
8	16.25	192.36(+ 2)	0.32	18.08	220.40(+ 2)	0.66	90.2	Oxalic acid (**S**)
8	16.27	203.84(+ 2)	0.48	18.08	231.87(+ 2)	0.34	113.14	**U**
9	16.68	206.36(+ 2)	2.37	18.48	234.37(+ 2)	1.68	118.14	Succinic acid, di- (**S**)
10	17.05	234.34(+ 2)	4.87	18.82	262.34(+ 2)	3.45	174.08	Citric acid, di-, -H_2O (**S**)
10	17.04	214.37(+ 2)	0.38	18.92	242.39(+ 2)	0.27	134.18	Maleic acid, di- (**S**)
11	17.27	220.38(+ 2)	0.27	19.09	248.38(+ 2)	0.19	146.16	α-Ketoglutaric acid, di- (**S**)
11	17.27	234.34(+ 2)	1.6	19.14	262.36(+ 2)	1.01	174.12	Isocitric acid, di-, -H_2O (**S**)
11	17.27	225.37(+ 2)	1.33	19.17	253.35(+ 2)	0.94	156.1	Furan-2,5-dicarboxylic acid, di- (**R**)
11	17.3	255.25(+ 2)	1.16	19.34	283.25(+ 2)	0.82	215.9	5-Oxopent-3-ene-1,2,5-tricarboxylate 5-Carboxymethyl-2-hydroxymuconate H_2O **L**)
12	17.75	269.85(+ 2)	0.76	19.45	297.86(+ 2)	0.54	245.12	**U**
13	18.05	250.84(+ 2)	1.59	19.76	278.88(+ 2)	1.12	207.16	Methylcitric acid, di- (**S**)
13	18.07	220.57(+ 2)	0.44	19.8	248.38(+ 2)	0.31	146.16	Adipic acid, di- (**S**)
13	18.1	207,38(+ 1)	1.11	19.84	235.31(+ 1)	0.78	60.01	**U**
13	18.1	243.33(+ 2)	5.13	19.92	271.32(+ 2)	3.64	192.08	Citric acid, di- (**S**)
14	18.28	234.33(+ 2)	0.8	20.23	262.36(+ 2)	0.57	174.12	Subehc acid, di- (**S**)
14	18.3	257.39(+ 2)	0.35	20.52	285 40(+ 2)	0.25	220.02	3-Hydroxy-3-(carboxymethyl)-adipic acid, di- (**R**)

(continued)

Table 13
(continued)

	BAMP			HAMP			Identification[b]	
Peak	Tr (min)	*m/z*	Int.[a] (%)	Tr (min)	*m/z*	Int.[a] (%)	*Mr*	Compound
14	18.32	243.35(+ 2)	0.71	20.58	271.34(+ 2)	0.5	192.08	Isocitric acid, di- (**S**)
14	18.37	220.39(+ 2)	0.42	20.59	248.37(+ 2)	0.29	146.16	3-Methylglutaric acid, di- (**S**)
15	18.7	193.31(+ 1)	5.77	20.88	221.32(+ 1)	4.09	46.02	Formic acid (`)
16	19.55	208.31(+ 1)	4.32	21.72	236.32(+ 1)	3.06	61.02	Carbonic acid (**S**)
17	20.27	221.37(+ 1)	0.27	22.3	249.37(+ 1)	0.19	74.07	Glyoxylic acid (**S**)
17	20.18	207.31(+ 1)	4.43	22.33	235.33(+ 1)	3.14	60.03	Acetic acid (**S**)
18	20.45	247.32(+ 1)	3.07	22.83	275.33(+ 1)	2.17		Artifact[c]
19	21	221.37(+ 1)	1.26	23.15	249.38(+ 1)	0.89	74.08	Propionic acid, (**S**)
20	21.5	261.33(+ 1)	0.46	23.64	289.36(+ 1)	0.32	114.06	2-Hydroxy-2,4-pentadienoate cis-2-hydroxypenta-2,4-dienoate cis-acetylacrylate (**L**)
20	21.53	235.37(+ 1)	0.57	23.64	263.37(+ 1)	0.4	88.07	Pyruvic acid (**S**)
21	21.65	236.36(+ 1)	0.46	23.81	264.38(+ 1)	0.33	89.08	Oxamic acid, (**S**)
21	21.75	235.37(+ 1)	1.77	23.9	263.37(+ 1)	1.25	88.07	Butyric acid, isobutyric acid (**S**)
21	21.75	237.34(+ 1)	2.78	23.92	265.35(+ 1)	1.97	90.05	Lactic acid (**S**)
22	21.98	295.30(+ 1)	2.18	24.17	323.34(+ 1)	1.54	148.04	O-Methylmalic acid, mono- (**R**)
22	22.1	264.33(+ 1)	1.22	24.26	292.36(+ 1)	0.86	117.06	3-Nitroacrylate (**L**)
23	22.23	269.34(+ 1)	7.97	24.4	297.32(+ 1)	5.65	122.02	Benzoic acid (**S**)
23	22.55	273.36(+ 1)	1.14	24.47	301.36(+ 1)	0.81	126.06	5-Methylfuran-2-carboxylic acid (**R**)
23	22.58	287.36(+ 1)	1.06	24.79	315.34(+ 1)	0.75	140.04	2-Hydroxy-2-ethylsuccinic acid, mono- (**R**)
24	22.68	283.31(+ 1)	2.37	24.82	311.39(+ 1)	1.68	136.09	Phenylacetic acid (**S**)
25	22.98	263.39(+ 1)	0.9	25.07	291.41(+ 1)	0.63	116.01	3-Methy1-2-oxobutanoic acid Hexylic acid 3-Oxopentanoic acid 2-Oxopentanoic acid (**L**)
25	22.98	297.36(+ 1)	1.01	25.08	325.41(+ 1)	0.72	150.11	3-Phenyl-propionic acid (**S**)
26	23.48	322.35(+ 1)	1.34	25.6	350.39(+ 1)	0.95	175.09	3-lndoleacetic acid (**S**)
26	23.57	299.35(+ 1)	0.6	25.68	327.40(+ 1)	0.43	152.1	α-Hydroxyphenylacetic acid (**S**)
27	23.67	313.35(+ 1)	2.89	25.78	341.38(+ 1)	2.04	166.08	4-Hydroxyphenylhydracrylic acid (**R**)
28	23.88	323.36(+ 1)	0.73	26.1	351.38(+ 1)	0.52	176.08	5,6,7,8-Tetrahydro-2-naphthoic acid (**L**)
29	24.05	321.32(+ 1)	0.44	26.2	349.34(+ 1)	0.31	174.04	Suberic acid, mono- (**S**)

(continued)

Table 13
(continued)

	BAMP			HAMP			Identification[b]	
Peak	Tr (min)	*m/z*	Int.[a] (%)	Tr (min)	*m/z*	Int.[a] (%)	*Mr*	Compound
30	24.19	348 36(+ 1)	0.53	26.31	376.38(+ 1)	0.37	201.08	**U**
30	24.22	326.37(+ 1)	0.84	26.38	354.37(+ 1)	0.59	179.07	Hippuric acid, (**S**)
31	24.37	340.37(+ 1)	2.17	26.53	368.37(+ 1)	1.54	193.07	5,6-Dihydroxyindole-2-carboxylate Phenylacetylglycine D-Dopachrome (**L**)
32	24.87	379.36(+ 1)	1.23	27	407.38(+ 1)	0.87	232.08	Nalidixic acid (**S**)

Table contains retention time (Tr/min), *m/z* and intensity (%) of each BAMP and HAMP derivatives of signals including identification of carboxylic acids. (S) = confirmation of identification by standards, (L) = molecular mass matching from http://www.genome.ad.jp/kegg/ligand.html; release date: June 12, 2006 by Kyoto University, Japan); (U) = not identified carboxylic acids; (R) = found in literature. Presented with permission of John Wiley and Sons

[a] Normalization was performed by normalizing the individual peak intensity to the highest peak intensity of all peaks shown in the table.

[b] Molecular weight was calculated from the m/z of a derivative and the mass of the tag. U = unidentified carboxylic acid; L = identification based on molecular mass matching from the ligand database; R = compound was also found in the literature; S = Confirmation by standard identification.

[c] This ion was found in the standard chromatogram, but it was not represented in any carboxylic acid standard.Therrfore, it was treated as artifact.

2.2.3 *Data Analysis*

The developed CE-MS method was first tested on a standard solution of 24 carboxylic acids derivatives of BAMP and HAMP. To investigate the applicability of the developed method on biological samples, the pooled rat urine samples were measured also by CE-MS as described in Subheading 2.2.2. The resulting base peak chromatogram is presented in Fig. 2.

Most of the peaks in the base peak chromatogram could be assigned to either BAMP and HAMP derivatives of carboxylic acids (Table 13). For the identification of carboxylic acids, it was assumed that compounds are double charged (double-derivatized molecules) or triple charged (triple-derivatized molecules). Molecular mass of the derivatizing reagent was subtracted from ions found in the spectra to calculate the original molecular mass and was afterwards searched against the LIGAND database (http://www.genome.ad.jp/kegg/ligand.html). Compounds without a carboxylic function were excluded. At the end 59 compounds were selected as potential derivative candidates; 32 out of them could be assigned to standards (S in Table 13) which were used in the standard solution. To conclude this developed method is highly suitable for carboxylic acid analysis in biological samples due to derivatization by BAMP and HAMP.

References

1. Ramautar R et al (2011) CE-MS for metabolomics: developments and applications in the period 2008-2010. Electrophoresis 32(1):52–65
2. Ramautar R, Somsen GW, de Jong GJ (2009) CE-MS in metabolomics. Electrophoresis 30(1):276–291
3. Schmitt-Kopplin P, Englmann M (2005) Capillary electrophoresis—mass spectrometry: survey on developments and applications 2003-2004. Electrophoresis 26(7–8):1209–1220
4. Ramautar R, Somsen GW, de Jong GJ (2013) CE-MS for metabolomics: developments and applications in the period 2010-2012. Electrophoresis 34(1):86–98
5. Ramautar R, Demirci A, Jong GJD (2006) Capillary electrophoresis in metabolomics. TrAC Trends Anal Chem 25(5):455–466
6. Hirayama A, Wakayama M, Soga T (2014) Metabolome analysis based on capillary electrophoresis-mass spectrometry. TrAC Trends Anal Chem 61:215–222
7. Kok MGM, Somsen GW, de Jong GJ (2014) The role of capillary electrophoresis in metabolic profiling studies employing multiple analytical techniques. TrAC Trends Anal Chem 61:223–235
8. Ibanez C et al (2013) Metabolomics, peptidomics and proteomics applications of capillary electrophoresis-mass spectrometry in foodomics: a review. Anal Chim Acta 802:1–13
9. Zenobi R (2013) Single-cell metabolomics: analytical and biological perspectives. Science 342(6163):1243259
10. Kleparnik K (2013) Recent advances in the combination of capillary electrophoresis with mass spectrometry: from element to single-cell analysis. Electrophoresis 34(1):70–85
11. Amantonico A, Urban PL, Zenobi R (2010) Analytical techniques for single-cell metabolomics: state of the art and trends. Anal Bioanal Chem 398(6):2493–2504
12. Williams MD et al (2013) Metabolomics of colorectal cancer: past and current analytical platforms. Anal Bioanal Chem 405(15):5013–5030
13. Koslinski P et al (2011) Metabolic profiling of pteridines for determination of potential biomarkers in cancer diseases. Electrophoresis 32(15):2044–2054
14. Zhao YY (2013) Metabolomics in chronic kidney disease. Clin Chim Acta 422:59–69
15. Robertson DG (2005) Metabonomics in toxicology: a review. Toxicol Sci 85(2):809–822
16. Trifonova OP, Lokhov PG, Archakov AI (2013) Metabolic profiling of human blood. Biochem (Moscow) Suppl Series B Biomed Chem 7(3):179–186
17. Nicholson JK et al (2012) Host-gut microbiota metabolic interactions. Science 336(6086):1262–1267
18. Barbas C, Moraes EP, Villasenor A (2011) Capillary electrophoresis as a metabolomics tool for non-targeted fingerprinting of biological samples. J Pharm Biomed Anal 55(4):823–831
19. Garcia-Perez I et al (2008) Metabolic fingerprinting with capillary electrophoresis. J Chromatogr A 1204(2):130–139
20. Mischak H et al (2009) Capillary electrophoresis-mass spectrometry as a powerful tool in biomarker discovery and clinical diagnosis: an update of recent developments. Mass Spectrom Rev 28(5):703–724
21. Huck CW, Bakry R, Bonn GK (2006) Progress in capillary electrophoresis of biomarkers and metabolites between 2002 and 2005. Electrophoresis 27(1):111–125
22. Xu XH et al (2012) Metabolomics: a novel approach to identify potential diagnostic biomarkers and pathogenesis in Alzheimer's disease. Neurosci Bull 28(5):641–648
23. Bonne NJ, Wong DTW (2012) Salivary biomarker development using genomic, proteomic and metabolomic approaches. Genome Med 4(10):82
24. Buzatto AZ et al (2013) Metabolomic investigation of human diseases biomarkers by CE and LC coupled to MS. Electrophoresis 35(9):1285–1307
25. Mikus P, Marakova K (2009) Advanced CE for chiral analysis of drugs, metabolites, and biomarkers in biological samples. Electrophoresis 30(16):2773–2802
26. Li M et al (2011) Recent advances of chromatography and mass spectrometry in lipidomics. Anal Bioanal Chem 399(1):243–249
27. Monton MR, Soga T (2007) Metabolome analysis by capillary electrophoresis-mass spectrometry. J Chromatogr A 1168(1–2):237–246, discussion 236
28. Baena B, Cifuentes A, Barbas C (2005) Analysis of carboxylic acids in biological fluids by capillary electrophoresis. Electrophoresis 26(13):2622–2636
29. Szpunar J (2005) Advances in analytical methodology for bioinorganic speciation analysis: metallomics, metalloproteomics and heteroatom-tagged proteomics and metabolomics. Analyst 130(4):442–465
30. Kraly JR et al (2009) Review: microfluidic applications in metabolomics and metabolic profiling. Anal Chim Acta 653(1):23–35

31. Garcia DE et al (2008) Separation and mass spectrometry in microbial metabolomics. Curr Opin Microbiol 11(3):233–239
32. Xiayan L, Legido-Quigley C (2008) Advances in separation science applied to metabonomics. Electrophoresis 29(18):3724–3736
33. Harada K, Fukusaki E (2009) Profiling of primary metabolite by means of capillary electrophoresis-mass spectrometry and its application for plant science. Plant Biotechnol 26(1):47–52
34. Schmitt-Kopplin P, Frommberger M (2003) Capillary electrophoresis-mass spectrometry: 15 years of developments and applications. Electrophoresis 24(22–23):3837–3867
35. Zhao SS et al (2012) Capillary electrophoresis-mass spectrometry for analysis of complex samples. Proteomics 12(19–20):2991–3012
36. Poinsot V et al (2014) Recent advances in amino acid analysis by capillary electromigration methods, 2011-2013. Electrophoresis 35(1):50–68
37. Kuehnbaum NL, Britz-McKibbin P (2013) New advances in separation science for metabolomics: resolving chemical diversity in a post-genomic era. Chem Rev 113(4): 2437–2468
38. Obata T, Fernie AR (2012) The use of metabolomics to dissect plant responses to abiotic stresses. Cell Mol Life Sci 69(19): 3225–3243
39. Ban E et al (2012) Growing trend of CE at the omics level: the frontier of systems biology—an update. Electrophoresis 33(1):2–13
40. Babu S et al (2006) Capillary electrophoresis at the omics level: towards systems biology. Electrophoresis 27(1):97–110
41. Garcia-Canas V et al (2011) MS-based analytical methodologies to characterize genetically modified crops. Mass Spectrom Rev 30(3):396–416
42. Mishur RJ, Rea SL (2012) Applications of mass spectrometry to metabolomics and metabonomics: detection of biomarkers of aging and of age-related diseases. Mass Spectrom Rev 31(1):70–95
43. Guttman A, Varoglu M, Khandurina J (2004) Multidimensional separations in the pharmaceutical arena. Drug Discov Today 9(3): 136–144
44. Mozzi F et al (2013) Metabolomics as a tool for the comprehensive understanding of fermented and functional foods with lactic acid bacteria. Food Res Int 54(1):1152–1161
45. Armitage EG, Barbas C (2014) Metabolomics in cancer biomarker discovery: current trends and future perspectives. J Pharm Biomed Anal 87:1–11
46. Klampfl CW (2007) Determination of organic acids by CE and CEC methods. Electrophoresis 28(19):3362–3378
47. Kok MG et al (2013) Anionic metabolic profiling of urine from antibiotic-treated rats by capillary electrophoresis-mass spectrometry. Anal Bioanal Chem 405(8):2585–2594
48. Kumar BS et al (2012) Discovery of common urinary biomarkers for hepatotoxicity induced by carbon tetrachloride, acetaminophen and methotrexate by mass spectrometry-based metabolomics. J Appl Toxicol 32(7): 505–520
49. Kumar BS et al (2010) Discovery of safety biomarkers for atorvastatin in rat urine using mass spectrometry based metabolomics combined with global and targeted approach. Anal Chim Acta 661(1):47–59
50. Yang WC, Regnier FE, Adamec J (2008) Comparative metabolite profiling of carboxylic acids in rat urine by CE-ESI MS/MS through positively pre-charged and H-2-coded derivatization. Electrophoresis 29(22): 4549–4560
51. Godzien J et al (2011) Effect of a nutraceutical treatment on diabetic rats with targeted and CE-MS non-targeted approaches. Metabolomics 9(S1):188–202
52. Zeng J et al (2013) Effect of bisphenol A on rat metabolic profiling studied by using capillary electrophoresis time-of-flight mass spectrometry. Environ Sci Technol 47(13): 7457–7465
53. Vallejo M et al (2008) New perspective of diabetes response to an antioxidant treatment through metabolic fingerprinting of urine by capillary electrophoresis. J Chromatogr A 1187(1–2):267–274
54. Barbas C et al (2008) Capillary electrophoresis as a metabolomic tool in antioxidant therapy studies. J Pharm Biomed Anal 47(2): 388–398
55. Ruperez FJ et al (2009) Dunaliella salina extract effect on diabetic rats: metabolic fingerprinting and target metabolite analysis. J Pharm Biomed Anal 49(3):786–792
56. Nevedomskaya E et al (2010) CE-MS for metabolic profiling of volume-limited urine samples: application to accelerated aging TTD mice. J Proteome Res 9(9):4869–4874
57. Garcia-Perez I et al (2012) Urinary metabolic phenotyping the slc26a6 (chloride-oxalate exchanger) null mouse model. J Proteome Res 11(9):4425–4435
58. Angulo S et al (2009) The autocorrelation matrix probing biochemical relationships after metabolic fingerprinting with CE. Electrophoresis 30(7):1221–1227

59. Garcia-Perez I et al (2008) Metabolic fingerprinting of Schistosoma mansoni infection in mice urine with capillary electrophoresis. Electrophoresis 29(15):3201–3206
60. Barbas C et al (1998) Quantitative determination of short-chain organic acids in urine by capillary electrophoresis. Clin Chem 44(6 Pt 1):1340–1342
61. Chen JL et al (2012) Urine metabolite profiling of human colorectal cancer by capillary electrophoresis mass spectrometry based on MRB. Gastroenterol Res Pract 2012:125890
62. Chen JL, Fan J, Lu XJ (2013) CE-MS based on moving reaction boundary method for urinary metabolomic analysis of gastric cancer patients. Electrophoresis 35(7):1032–1039
63. Szymanska E et al (2010) Altered levels of nucleoside metabolite profiles in urogenital tract cancer measured by capillary electrophoresis. J Pharm Biomed Anal 53(5): 1305–1312
64. Soga T et al (2004) Qualitative and quantitative analysis of amino acids by capillary electrophoresis-electrospray ionization-tandem mass spectrometry. Electrophoresis 25(13):1964–1972
65. Alberice JV et al (2013) Searching for urine biomarkers of bladder cancer recurrence using a liquid chromatography-mass spectrometry and capillary electrophoresis-mass spectrometry metabolomics approach. J Chromatogr A 1318:163–170
66. Hirayama A, Tomita M, Soga T (2012) Sheathless capillary electrophoresis-mass spectrometry with a high-sensitivity porous sprayer for cationic metabolome analysis. Analyst 137(21):5026–5033
67. Allard E et al (2008) Comparing capillary electrophoresis-mass spectrometry fingerprints of urine samples obtained after intake of coffee, tea, or water. Anal Chem 80(23):8946–8955
68. Ramautar R et al (2012) Enhancing the coverage of the urinary metabolome by sheathless capillary electrophoresis-mass spectrometry. Anal Chem 84(2):885–892
69. Kok MG, de Jong GJ, Somsen GW (2011) Sensitivity enhancement in capillary electrophoresis-mass spectrometry of anionic metabolites using a triethylamine-containing background electrolyte and sheath liquid. Electrophoresis 32(21):3016–3024
70. Balderas C et al (2013) Plasma and urine metabolic fingerprinting of type 1 diabetic children. Electrophoresis 34(19):2882–2890
71. Balderas C et al (2010) Metabolomic approach to the nutraceutical effect of rosemary extract plus Omega-3 PUFAs in diabetic children with capillary electrophoresis. J Pharm Biomed Anal 53(5):1298–1304
72. Ramautar R et al (2009) Explorative analysis of urine by capillary electrophoresis-mass spectrometry in chronic patients with complex regional pain syndrome. J Proteome Res 8(12):5559–5567
73. Uehara T et al (2013) Identification of metabolomic biomarkers for drug-induced acute kidney injury in rats. J Appl Toxicol 34(10):1087–1095
74. Akiyama Y et al (2012) A metabolomic approach to clarifying the effect of AST-120 on 5/6 nephrectomized rats by capillary electrophoresis with mass spectrometry (CE-MS). Toxins (Basel) 4(11):1309–1322
75. Toyohara T et al (2011) Metabolomic profiling of the autosomal dominant polycystic kidney disease rat model. Clin Exp Nephrol 15(5):676–687
76. Kuwabara H et al (2013) Altered metabolites in the plasma of autism spectrum disorder: a capillary electrophoresis time-of-flight mass spectroscopy study. PLoS One 8(9), e73814
77. D'Agostino LA et al (2011) Comprehensive plasma thiol redox status determination for metabolomics. J Proteome Res 10(2): 592–603
78. Takeuchi K et al (2013) Metabolic profiling to identify potential serum biomarkers for gastric ulceration induced by nonsteroid anti-inflammatory drugs. J Proteome Res 12(3): 1399–1407
79. Takeuchi K et al (2014) Metabolomic analysis of the effects of omeprazole and famotidine on aspirin-induced gastric injury. Metabolomics 10:995–1004
80. Naz S et al (2013) Method development and validation for rat serum fingerprinting with CE-MS: application to ventilator-induced-lung-injury study. Anal Bioanal Chem 405(14):4849–4858
81. Tripodi VP et al (2003) Simultaneous determination of free and conjugated bile acids in serum by cyclodextrin-modified micellar electrokinetic chromatography. J Chromatogr B Analyt Technol Biomed Life Sci 785(1): 147–155
82. Castano G et al (2006) Bile acid profiles by capillary electrophoresis in intrahepatic cholestasis of pregnancy. Clin Sci (Lond) 110(4): 459–465
83. Soga T et al (2011) Serum metabolomics reveals gamma-glutamyl dipeptides as biomarkers for discrimination among different forms of liver disease. J Hepatol 55(4): 896–905
84. Saito T et al (2013) Dynamics of serum metabolites in patients with chronic hepatitis C receiving pegylated interferon plus ribavirin: a metabolomics analysis. Metabolism 62(11):1577–1586

85. Hirayama A et al (2012) Metabolic profiling reveals new serum biomarkers for differentiating diabetic nephropathy. Anal Bioanal Chem 404(10):3101–3109
86. Lee R, Britz-McKibbin P (2010) Metabolomic studies of radiation-induced apoptosis of human leukocytes by capillary electrophoresis-mass spectrometry and flow cytometry: adaptive cellular responses to ionizing radiation. Electrophoresis 31(14):2328–2337
87. Lee R et al (2010) Differential metabolomics for quantitative assessment of oxidative stress with strenuous exercise and nutritional intervention: thiol-specific regulation of cellular metabolism with N-acetyl-L-cysteine pretreatment. Anal Chem 82(7):2959–2968
88. Karasawa T et al (2013) Metabolome analysis of erythrocytes from patients with chronic hepatitis C reveals the etiology of ribavirin-induced hemolysis. Int J Med Sci 10(11): 1575–1577
89. Soga T et al (2006) Differential metabolomics reveals ophthalmic acid as an oxidative stress biomarker indicating hepatic glutathione consumption. J Biol Chem 281(24): 16768–16776
90. Soga T et al (2002) Simultaneous determination of anionic intermediates for Bacillus subtilis metabolic pathways by capillary electrophoresis electrospray ionization mass spectrometry. Anal Chem 74(10): 2233–2239
91. Fustin JM et al (2012) Rhythmic nucleotide synthesis in the liver: temporal segregation of metabolites. Cell Rep 1(4):341–349
92. Sugiura Y, Taguchi R, Setou M (2011) Visualization of spatiotemporal energy dynamics of hippocampal neurons by mass spectrometry during a kainate-induced seizure. PLoS One 6(3):e17952
93. Soga T et al (2009) Metabolomic profiling of anionic metabolites by capillary electrophoresis mass spectrometry. Anal Chem 81(15): 6165–6174
94. Naz S, Garcia A, Barbas C (2013) Multiplatform analytical methodology for metabolic fingerprinting of lung tissue. Anal Chem 85(22):10941–10948
95. Saheki T et al (2011) Metabolomic analysis reveals hepatic metabolite perturbations in citrin/mitochondrial glycerol-3-phosphate dehydrogenase double-knockout mice, a model of human citrin deficiency. Mol Genet Metab 104(4):492–500
96. Maekawa K et al (2013) Global metabolomic analysis of heart tissue in a hamster model for dilated cardiomyopathy. J Mol Cell Cardiol 59:76–85
97. Papaspyridonos K et al (2008) Fingerprinting of human bile during liver transplantation by capillary electrophoresis. J Sep Sci 31(16–17): 3058–3064
98. Hirayama A et al (2009) Quantitative metabolome profiling of colon and stomach cancer microenvironment by capillary electrophoresis time-of-flight mass spectrometry. Cancer Res 69(11):4918–4925
99. Kami K et al (2013) Metabolomic profiling of lung and prostate tumor tissues by capillary electrophoresis time-of-flight mass spectrometry. Metabolomics 9(2):444–453
100. Ibanez C et al (2012) Toward a predictive model of Alzheimer's disease progression using capillary electrophoresis-mass spectrometry metabolomics. Anal Chem 84(20): 8532–8540
101. Ramautar R et al (2012) Metabolic profiling of mouse cerebrospinal fluid by sheathless CE-MS. Anal Bioanal Chem 404(10): 2895–2900
102. Matsumoto M et al (2012) Impact of intestinal microbiota on intestinal luminal metabolome. Sci Rep 2:233
103. Ohashi Y et al (2008) Depiction of metabolome changes in histidine-starved Escherichia coli by CE-TOFMS. Mol Biosyst 4(2): 135–147
104. Ooga T et al (2011) Metabolomic anatomy of an animal model revealing homeostatic imbalances in dyslipidaemia. Mol Biosyst 7(4): 1217–1223
105. Soga T et al (2007) Analysis of nucleotides by pressure-assisted capillary electrophoresis-mass spectrometry using silanol mask technique. J Chromatogr A 1159(1–2):125–133
106. Soga T, Heiger DN (2000) Amino acid analysis by capillary electrophoresis electrospray ionization mass spectrometry. Anal Chem 72(6):1236–1241
107. Sugimoto M et al (2010) Capillary electrophoresis mass spectrometry-based saliva metabolomics identified oral, breast and pancreatic cancer-specific profiles. Metabolomics 6(1):78–95
108. Sugimoto M et al (2013) Physiological and environmental parameters associated with mass spectrometry-based salivary metabolomic profiles. Metabolomics 9(2):454–463
109. Osanai T et al (2014) Capillary electrophoresis-mass spectrometry reveals the distribution of carbon metabolites during nitrogen starvation in Synechocystis sp. PCC 6803. Environ Microbiol 16(2):512–524
110. Janini GM et al (2003) A sheathless nanoflow electrospray interface for on-line capillary electrophoresis mass spectrometry. Anal Chem 75(7):1615–1619
111. Edwards JL et al (2006) Negative mode sheathless capillary electrophoresis electrospray ionization-mass spectrometry for

metabolite analysis of prokaryotes. J Chromatogr A 1106(1–2):80–88
112. Baidoo EE et al (2008) Capillary electrophoresis-fourier transform ion cyclotron resonance mass spectrometry for the identification of cationic metabolites via a pH-mediated stacking-transient isotachophoretic method. Anal Chem 80(9):3112–3122
113. Soo EC et al (2004) Selective detection and identification of sugar nucleotides by CE-electrospray-MS and its application to bacterial metabolomics. Anal Chem 76(3): 619–626
114. McNally DJ et al (2006) Functional characterization of the flagellar glycosylation locus in Campylobacter jejuni 81-176 using a focused metabolomics approach. J Biol Chem 281(27):18489–18498
115. Hui JP et al (2007) Selective detection of sugar phosphates by capillary electrophoresis/mass spectrometry and its application to an engineered E. coli host. Chembiochem 8(10):1180–1188
116. Reid CW et al (2008) Affinity-capture tandem mass spectrometric characterization of polyprenyl-linked oligosaccharides: tool to study protein N-glycosylation pathways. Anal Chem 80(14):5468–5475
117. Arellano M et al (2000) Routine analysis of short-chain fatty acids for anaerobic bacteria identification using capillary electrophoresis and indirect ultraviolet detection. J Chromatogr B 741(1):89–100
118. Harada K et al (2008) Quantitative analysis of anionic metabolites for Catharanthus roseus by capillary electrophoresis using sulfonated capillary coupled with electrospray ionization-tandem mass spectrometry. J Biosci Bioeng 105(3):249–260
119. Musilova J, Klejdus B, Glatz Z (2013) Simultaneous quantification of energetically important metabolites in various cell types by CZE. J Sep Sci 36(23):3807–3812
120. Gao P et al (2007) Investigation on response of the metabolites in tricarboxylic acid cycle of Escherichi coli and Pseudomonas aeruginosa to antibiotic perturbation by capillary electrophoresis. J Pharm Biomed Anal 44(1): 180–187
121. Soga T et al (2003) Quantitative metabolome analysis using capillary electrophoresis mass spectrometry. J Proteome Res 2(5):488–494
122. Hardenborg E et al (2003) Novel polyamine coating providing non-covalent deactivation and reversed electroosmotic flow of fused-silica capillaries for capillary electrophoresis. J Chromatogr A 1003(1–2):217–221
123. Timischl B et al (2008) Development of a quantitative, validated capillary electrophoresis-time of flight-mass spectrometry method with integrated high-confidence analyte identification for metabolomics. Electrophoresis 29(10):2203–2214
124. Qin XY et al (2013) The effect of acyclic retinoid on the metabolomic profiles of hepatocytes and hepatocellular carcinoma cells. PLoS One 8(12):e82860
125. Saito N et al (2009) Metabolite profiling reveals YihU as a novel hydroxybutyrate dehydrogenase for alternative succinic semialdehyde metabolism in Escherichia coli. J Biol Chem 284(24):16442–16451
126. Martinez P et al (2013) Metabolomic study of Chilean biomining bacteria Acidithiobacillus ferrooxidans strain Wenelen and Acidithiobacillus thiooxidans strain Licanantay. Metabolomics 9(1):247–257
127. Hashino E et al (2013) Erythritol alters microstructure and metabolomic profiles of biofilm composed of Streptococcus gordonii and Porphyromonas gingivalis. Mol Oral Microbiol 28(6):435–451
128. Robert M et al (2012) Extracellular metabolite dynamics and temporal organization of metabolic function in E. coli. Proceedings of IEEE/ICME International Conference on Complex Medical Engineering (CME 2012). 197–202
129. Canuto GA et al (2012) CE-ESI-MS metabolic fingerprinting of Leishmania resistance to antimony treatment. Electrophoresis 33(12):1901–1910
130. Amantonico A, Urban PL, Zenobi R (2009) Facile analysis of metabolites by capillary electrophoresis coupled to matrix-assisted laser desorption/ionization mass spectrometry using target plates with polysilazane nanocoating and grooves. Analyst 134(8):1536–1540
131. Tanaka Y et al (2008) Development of a capillary electrophoresis-mass spectrometry method using polymer capillaries for metabolomic analysis of yeast. Electrophoresis 29(10):2016–2023
132. Buscher JM et al (2009) Cross-platform comparison of methods for quantitative metabolomics of primary metabolism. Anal Chem 81(6):2135–2143
133. Sasidharan K et al (2012) A yeast metabolite extraction protocol optimised for time-series analyses. PLoS One 7(8):e44283
134. Matsushika A et al (2013) Fermentation of xylose causes inefficient metabolic state due to carbon/energy starvation and reduced glycolytic flux in recombinant industrial Saccharomyces cerevisiae. PLoS One 8(7):e69005
135. Tanaka Y et al (2007) Quantitative analysis of sulfur-related metabolites during cadmium

stress response in yeast by capillary electrophoresis-mass spectrometry. J Pharm Biomed Anal 44(2):608–613
136. Miyagi A et al (2013) Metabolome analysis of food-chain between plants and insects. Metabolomics 9(6):1254–1261
137. Sato S et al (2004) Simultaneous determination of the main metabolites in rice leaves using capillary electrophoresis mass spectrometry and capillary electrophoresis diode array detection. Plant J 40(1):151–163
138. Sato S et al (2008) Time-resolved metabolomics reveals metabolic modulation in rice foliage. BMC Syst Biol 2:51
139. Leon C et al (2009) Metabolomics of transgenic maize combining Fourier transform-ion cyclotron resonance-mass spectrometry, capillary electrophoresis-mass spectrometry and pressurized liquid extraction. J Chromatogr A 1216(43):7314–7323
140. Takahashi H et al (2011) Comparative metabolomics of developmental alterations caused by mineral deficiency during in vitro culture of Gentiana triflora. Metabolomics 8(1):154–163
141. Delatte TL et al (2011) Capillary electrophoresis-mass spectrometry analysis of trehalose-6-phosphate in Arabidopsis thaliana seedlings. Anal Bioanal Chem 400(4): 1137–1144
142. Warren CR, Aranda I, Cano FJ (2011) Metabolomics demonstrates divergent responses of two Eucalyptus species to water stress. Metabolomics 8(2):186–200
143. Levandi T et al (2008) Capillary electrophoresis time-of-flight mass spectrometry for comparative metabolomics of transgenic versus conventional maize. Anal Chem 80(16):6329–6335
144. Cho K et al (2008) Integrated transcriptomics, proteomics, and metabolomics analyses to survey ozone responses in the leaves of rice seedling. J Proteome Res 7(7): 2980–2998
145. Iino K et al (2011) Profiling of the charged metabolites of traditional herbal medicines using capillary electrophoresis time-of-flight mass spectrometry. Metabolomics 8(1): 99–108
146. Tseng YJ et al (2013) Metabolomic characterization of rhubarb species by capillary electrophoresis and ultra-high-pressure liquid chromatography. Electrophoresis 34(19): 2918–2927
147. Urano K et al (2009) Characterization of the ABA-regulated global responses to dehydration in Arabidopsis by metabolomics. Plant J 57(6):1065–1078
148. Williams BJ et al (2007) Amino acid profiling in plant cell cultures: an inter-laboratory comparison of CE-MS and GC-MS. Electrophoresis 28(9):1371–1379
149. Sato D et al (2013) Metabolomic profiling of the response of susceptible and resistant soybean strains to foxglove aphid, Aulacorthum solani Kaltenbach. J Chromatogr B Analyt Technol Biomed Life Sci 925:95–103
150. Lapainis T, Rubakhin SS, Sweedler JV (2009) Capillary electrophoresis with electrospray ionization mass spectrometric detection for single-cell metabolomics. Anal Chem 81(14):5858–5864
151. Kim J et al (2012) GC-TOF-MS- and CE-TOF-MS-based metabolic profiling of cheonggukjang (fast-fermented bean paste) during fermentation and its correlation with metabolic pathways. J Agric Food Chem 60(38):9746–9753
152. Sugimoto M et al (2012) Changes in the charged metabolite and sugar profiles of pasteurized and unpasteurized Japanese sake with storage. J Agric Food Chem 60(10):2586–2593
153. Yassine MM et al (2012) Identification of weak and strong organic acids in atmospheric aerosols by capillary electrophoresis/mass spectrometry and ultra-high-resolution Fourier transform ion cyclotron resonance mass spectrometry. Anal Chem 84(15):6586–6594
154. Sakagami H et al (2013) Metabolomic profiling of sodium fluoride-induced cytotoxicity in an oral squamous cell carcinoma cell line. Metabolomics 10(2):270–279
155. Kwon HJ, Ohmiya Y (2013) Metabolomic analysis of differential changes in metabolites during ATP oscillations in chondrogenesis. Biomed Res Int 2013:213972
156. Sugimoto M et al (2012) Non-targeted metabolite profiling in activated macrophage secretion. Metabolomics 8(4):624–633
157. Hayashi K et al (2011) Use of serum and urine metabolome analysis for the detection of metabolic changes in patients with stage 1-2 chronic kidney disease. Nephro Urol Mon 3:164–171
158. Shima N et al (2011) Influences of methamphetamine-induced acute intoxication on urinary and plasma metabolic profiles in the rat. Toxicology 287(1–3):29–37
159. Bardsley WG, Ashford JS, Hill CM (1971) Synthesis and oxidation of aminoalkyl-onium compounds by pig kidney diamine oxidase. Biochem J 122(4):557–567

Chapter 22

Capillary Electrophoresis in Food and Foodomics

Clara Ibáñez, Tanize Acunha, Alberto Valdés, Virginia García-Cañas, Alejandro Cifuentes, and Carolina Simó

Abstract

Quality and safety assessment as well as the evaluation of other nutritional and functional properties of foods imply the use of robust, efficient, sensitive, and cost-effective analytical methodologies. Among analytical technologies used in the fields of food analysis and foodomics, capillary electrophoresis (CE) has generated great interest for the analyses of a large number of compounds due to its high separation efficiency, extremely small sample and reagent requirements, and rapid analysis. The introductory section of this chapter provides an overview of the recent applications of capillary electrophoresis (CE) in food analysis and foodomics. Relevant reviews and research articles on these topics are tabulated including papers published in the period 2011–2014. In addition, to illustrate the great capabilities of CE in foodomics the chapter describes the main experimental points to be taken into consideration for a metabolomic study of the antiproliferative effect of carnosic acid (a natural diterpene found in rosemary) against HT-29 human colon cancer cells.

Key words Capillary electrophoresis, CE-MS, Food bioactivity, Food safety, Food traceability, Foodomics, Food quality, Metabolomics

1 Introduction

Food safety assessment and food quality control are major concerns of modern society. There is also a growing interest to improve health and general well-being of consumers through diet beyond the provision of the basic nutritional requirements. In this sense, regulatory authorities are requiring fully substantiated health claims linked to the so-called functional foods. Analysis of exogenous compounds (agrochemicals, environmental contaminants, veterinary drugs, etc.) is also a major concern in food safety. Apart from the negative impact on human health, food contamination has also major economic costs. Quality and safety assessment as well as the evaluation of other nutritional and functional properties of foods imply the use of robust, efficient, sensitive, and cost-effective analytical methodologies.

Philippe Schmitt-Kopplin (ed.), *Capillary Electrophoresis*: Methods and Protocols, Methods in Molecular Biology, vol. 1483,
DOI 10.1007/978-1-4939-6403-1_22,

Foods are very complex matrices; moreover, many food components undergo numerous reactions in the course of food processing and storage. Hence, the use of advanced analytical instrumentation for food analysis is needed. Comparison of different analytical platforms employed in food analysis has been described before [1–6]. Among them, capillary electrophoresis (CE) is a versatile technique that has generated great interest due to its high separation efficiency, extremely small sample and reagent requirements, and rapid analysis. CE has demonstrated to be a very useful and complementary analytical tool, especially when (highly) polar and charged metabolites are analyzed and sample volume is limited. Targeted analysis is currently carried out for quality and safety assessments, involving a combination of procedures of sample preparation and the subsequent CE analysis of a given number of compounds (DNA, proteins, small molecules) from a complex mixture [7–9]. As an alternative strategy to target analysis, the development and use of profiling technologies present the potential to improve the number of analytes that can be assessed simultaneously in a single analysis. In this context, foodomics, defined as a new discipline that studies the food and nutrition domains through the application and integration of advanced omics technologies in order to improve consumers' well-being and confidence [3, 7, 10], can be regarded as a useful analytical approach in food science and nutrition research. As it has been shown in various published reports, the use of CE in foodomics offers enormous opportunities to obtain valuable detailed information that can be directly correlated to food quality, safety, and other features related to food processing, storage, authenticity assessment, etc. The main applications of CE in food analysis and foodomics in the period 2011–2014 are presented in this work. Recent results on food quality and safety, nutritional value, storage, bioactivity, as well as applications of CE for monitoring food interactions and food processing have been reviewed. These applications regarding the analysis of foods and food components using capillary electromigration methods are tabulated (*see* Table 1).

Since the introduction of foodomics, capillary electrophoresis-mass spectrometry (CE-MS) has found great application in the study of the health effects of food ingredients, e.g., on the proliferation of various cancer cells, where CE-MS has demonstrated to be as valuable as other high-performance analytical techniques [148–153]. Next, the experimental and methodological description on the use of CE-MS for metabolomics is provided in detail. In this study CE-MS is used to investigate the changes induced in the metabolite fingerprinting of human colon cancer cells (i.e., HT-29 cells) after the treatment with a bioactive compound with antiproliferative activity and potential use as functional food ingredient. Time-of-flight (TOF) mass analyzer is used for the CE-MS

Table 1
Summary of CE-based methods developed to analyze compounds relevant to food science and foodomics in the period 2011–2014

	Sample	Sample preparation	Topic of interest	Analytical platform	Ref.
Amino acids, biogenic amines, other hazardous amines					
Cypromazine, melamine	Dairy products	Extraction with trichloroacetic acid, water, and chloroform	FS	MEKC-UV	[11]
Melamine	Milk powder, gluten, chicken feed, cookies	Centrifugation, SPE	FS	MEKC-UV	[12]
Melamine	Milk	Ultrasonic-assisted extraction	FS	CE-UV	[13]
Ala, Arg, Asp, Cys, Glu, Lys, Met, Pro, Thr, Ser	Wine	DTAF/microwave-assisted derivatization	FQ, FS, FT	CE-LIF	[14]
Ornithine, alanine, GABA, alloisoleucine, citrulline, pyroglutamic acid	Olive oil	Butanol derivatization	FQ, FS	CE-Q/IT MS/MS	[15]
Arg, Val, Thr	Health drink	FITC derivatization	FQ	CE-LIF	[16]
Phe, Tyr, cadaverine, histamine, tryptamine, spermidine, putrescine	Wine, fruit molasses	FITC derivatization	FS	MEKC-LIF	[17]
Histamine, 2-phenylethylamine, tyramine	Wines	Filtration	FQ	ITP-CZE-UV	[18]
Putrescine, cadaverine, histamine, tyramine, spermine, spermidine	Meat (pork, beef, poultry)	Extraction with trichloroacetic acid	FQ	ITP-conductivity detection	[19]
Melamine and related by-products	Milk powder	Ultrasonic-assisted extraction	FS	CEC-UV CEC-TOF MS	[20]
Methylamine, ethylamine, *n*-propylamine, *n*-butylamine, *n* pentylamine, *n*-hexylamine	Wine	MeCy5-OSu derivatization	FS	CE-LIF	[21]

(continued)

Table 1
(continued)

	Sample	Sample preparation	Topic of interest	Analytical platform	Ref.
Spermine, spermidine, histamine, Cad, phenylethylamine, tyramine, tryptamine	Tap water	SPE, filtration	FQ, FS	CZE-amperometric detection	[22]
Ala, Arg, Asp, GABA, Glu, Gly, His, Leu, Ile, Lys, Met, Phe, Pro, Ser, Thr, Tyr, Val, Cys	Royal jelly products	Extraction with ethanol	FQ	CE-Q MS/MS	[23]
Histidine	Meat, meat products, fish, and fish products	Extraction with methanol	FQ	CITP-conductivity detector	[24]
Lys, Arg, Val, Thr, Ala, Phe, Glu, Trp, Asp	Gourd seed milks	Extraction with water and FITC derivatization	FQ	CE-LIF; CE-LED-induced fluorescence	[25]
Peptides					
Phosphopeptides	Milk powder	Digestion with trypsin	Foodomics	t-ITP-CE-TOF MS	[26]
Profiling of tryptic digests of water-soluble proteins	*Bacillus thuringiensis* (Bt)-transgenic, native nontransgenic maize varieties	Extraction with water and digestion with bovine pancreatic trypsin immobilized on agarose gel	FS, FT	CZE-UV	[27]
Bioactive peptides	Hypoallergenic infant milk formulas	Dilution with water, centrifugation, SPE	FB, FS	CZE-TOF MS	[28]
Proteins					
Glutelin protein fraction	Rice	Extraction with NaOH	FQ	CE-UV	[29]

Protein profiling	Maize, and soybeans	Extraction with ACN:water mixture with 0.3% acetic acid	FS, FT	CE-UV	[30]
β-Lactoglobulin, β-lactalbumin	Milk, skimmed milk powder	Dilution, centrifugation, precipitation of casein	FQ, FS	Immunoaffinity CE-UV, and immunoaffinity CE-MALDI-TOF MS	[31]
Lysozyme, conalbumin, ovalbumin β-Lactoglobulin A, β -lactoglobulin B, β-lactalbumin	Hen egg white, milk powder	Filtration Centrifugation, filtration	FQ, FS	CE-UV	[32]
Two proteins (MW of 70.2 and 85.4 kDa) and one ribosomal protein (MW of 16.3 kDa)	*Listeria monocytogenes* and *Staphylococcus aureus*	Cell disruption, filtration	FS	CE-UV	[33]
Casein fractions and derived peptides	Goat milk, goat milk cheese	Solubilization with urea buffer	FQ	CE-UV	[34]
Protein profiling	Soybean, olive seeds	Extraction with water:ACN (4:1, v/v) Extraction with Tris-HCl buffer	FQ, FT	EKC-UV	[35]
Protein profiling	Olive	Extraction with chloroform:methanol, precipitation, and solubilization with Tris-HCl buffer	FQ, FT	CGE-UV	[36]
β-Lactoglobulin	Infant foods	On-capillary derivatization	FQ, FS	CE-LIF	[37]
Protein profiling	Genetic modified maize	Extraction with water Extraction with urea and DTT Extraction with Tris, NaCl, and CHAPS	FQ, FS	CGE (chip)-LIF	[38]
Histamine	Tuna fish	Extraction with ethanol	FQ, FS	CZE-UV	[39]

(continued)

Table 1
(continued)

	Sample	Sample preparation	Topic of interest	Analytical platform	Ref.
Phenols, polyphenols, pigments, and lipids					
Tyrosol, hydroxytyrosol, oleuropein glycoside, ferulic acid, *p*-coumaric acid, cinnamic acid, *p*-hydroxybenzoic acid, gallic acid, caffeic acid, luteolin, apigenin, vanillic acid, 3,4-dihydroxybenzoic acid	Extra-virgin olive oil	Online pre-concentration (stacking)	FQ, FT, FB	CE-UV	[40]
Ferulic acid, caffeic acid, gallic acid, and (+) -catechin	White wine	Filtration	FQ, FB	CZE-amperometric detection	[41]
Sinapic acid, ferulic acid, *p*-coumaric acid, caffeic acid	Broccoli, broccolini, Brussels sprouts, cabbage, cauliflower	SPE	FB	CZE-UV	[42]
Caffeic acid hexose, catechin glucoside, catechin, (Epi)afzelechin-(epi)catechin isomer A and B, procyanidin B_2, 2-hydroxy-3-O-β-d-glucopyranosyl-benzoic acid, (epi)afzelechin (epi)catechin-O-di methyl gallate, epicatechin-O-3,4-dimethylgallate, swertiamacroside isomer A and B, rutin, hyperin, dihydroxy-trimethoxyisoflavan, and 5,7,4′-trimethoxyflavan	Buckwheat	Extraction with ethanol:water (4:1, v/v), sonication	FB	CE-TOF MS	[43]
Hydroxytyrosol, tyrosol, vanillic acid	Olive oil	Dilution with propanol	FQ, FT, FB	NACE-UV-FL	[44]
Hydroxytyrosol, tyrosol, vanillic acid, cinnamic acid, caffeic acid	Olive oil	LLE with ethanol	FQ, FT, FB	NACE-UV-FL	[45]

Epicatechin gallate, epigallocatechin gallate, epicatechin, epigallocatechin, gallic acid, gallocatechin gallate, caffeine	Tea	Extraction with water	FB	MEKC-UV	[46]
2-(4-Hydroxyphenyl) ethanol, resveratrol, epicatechin, catechin, veratric acid, homovanillic acid, vanillin, cinnamic acid, sinapic acid, quercetin, homogentisic acid, syringic acid, ferulic acid, fisetin, *p*-coumaric acid, quercetin, caffeic acid, 4-hydroxybenzoic acid, gallic acid, and 3,4-dihydroxybenzoic acid	Wine	Filtration	FQ, FT, FB	CE-UV	[47]
Kaempferol and quercetin	Broccoli	SPE	FB	LVSS-CZE-UV	[48]
Daidzin, genistin, daidzein, genistein, formononetin, biochanin A, glycitein	Soy drink	LLE with ethanol	FB	CZE-UV; CZE-Q MS	[49]
Crocetin (β-d-glycosyl)-(β-d-gentiobiosyl) ester, crocetin di-(β-d-gentiobiosyl) ester, picrocrocin, safranal	Saffron (*Crocus sativus*)	Extraction with BGE (disodium phosphate, sodium tetraborate, and SDS)	FB, FT	MEKC-UV	[50]
Lysophosphatidic acid, phosphatidylcholine, lysophosphatidylethanolamine, phosphatidylethanolamine, phosphatidylinositol, phosphatidic acid and phosphatidylglycerol	Olive fruit, olive oil	Extraction with chloroform:methanol:water Dilution with hexane, extraction with ethanol, and water	FB, FT	NACE-Q/IT MS/MS	[51]
Rutin	Buckwheat sprouts	Extraction with water:acetone (1:1, v/v), filtration, evaporation	FB	CE-PDA	[52]

(continued)

Table 1
(continued)

	Sample	Sample preparation	Topic of interest	Analytical platform	Ref.
Citrus flavonoids, troxerutin, and ascorbic acid	Food supplements and pharmaceuticals	Extraction with DMSO	FB	CZE-DAD	[53]
Omega-3 and omega-6	Oil and beef muscle	Extraction with chloroform:methanol (1:1, v/v) and saponification with KOH	FQ	CZE-UV/DAD	[54]
Isoflavone	Soy-based foods	Extraction with hexane and QuEChERS	FB	CE-Q MS	[55]
p-Coumaric, caffeic, ferulic, 3,4-dihydroxyphenylacetic, vanillic, and 4-hydroxyphenilacetic acids	Virgin olive oil	Extraction with ethanol	FB, FQ	NACE-DAD	[56]
DNAs					
Genetically modified yeasts	Yeasts from wine	DNA extraction, amplification with *Multiplex* PCR	FS, FT	CGE-LIF	[57]
DNA fragments	*Listeria monocytogenes, Salmonella enterica Escherichia coli* O157	DNA extraction and amplification with *Multiplex* PCR	FS	NGS-CE-UV	[58]
Target DNA sequences	GM maize lines	DNA extraction, denaturation	FS, FT	(qc)-PCR-CGE-LIF	[59]
Genomic DNA	GM soybean seed	DNA extraction, amplification	FS, FT	CGE-UV	[60]
Specific DNA sequences (cow, sheep, goat, buffalo)	Dairy products	DNA extraction, and amplification with *Multiplex* PCR	FQ, FS, FT	CGE	[61]
Specific DNA sequences (chicken, turkey, pork)	Heat-treated meat mixtures	DNA extraction, amplification	FQ, FS, FT	CGE-LIF	[62]
Specific DNA fragments	Maize, barley, soybean, rape, sunflower, alfalfa	DNA extraction, and amplification by TBP strategy	FS, FT	CGE-LIF	[63]

Specific DNA fragments *Salmonella enterica*, *Listeria monocytogenes*, *Campylobacter jejuni*, *Staphylococcus aureus*, *Bacillus cereus*, *Clostridium perfringens*, *Escherichia coli* O157:H7, *Yersinia enterocolitica*, *Vibrio parahaemolyticus*, *Enterobacter sakazakii*	Ten foodborne pathogenic bacteria	DNA extraction, amplification	FS	CE-single strand conformation polymorphism	[64]
Species-specific sequences *Yersinia enterocolitica*, *Vibrio parahaemolyticus*, *Escherichia coli* O157:H7, *Staphylococcus aureus*, *Shigella flexneri*, *Listeria monocytogenes*, *Campylobacter jejuni*, *Clostridium perfringens*, *Bacillus cereus*, *Salmonella enterica*	Inoculated milk	DNA isolation, and amplification by multiplex displacement amplification (MDA)	FS	CE-single strand conformation polymorphism	[65]
Genotyping of the wine spoilage yeast *Dekkera/Brettanomyces bruxellensis*	Wine spoilage yeast *Dekkera/Brettanomyces bruxellensis*	DNA extraction, and amplification by intron splice site PCR amplification	FQ	CGE-LIF	[66]
Polymorphic tandem repeat regions of *L. monocytogenes*	*L. monocytogenes*	Amplification of tandem repeat regions	FS	CGE-LIF	[67]
Specific DNA fragments	Colon cancer SW480 cells, blood lymphocytes	RNA isolation, transcription to cDNA, amplification	FS, FT	CGE-LIF	[68]
Cyprinidae-related products	Cyprinidae fish species	PCR-RFLP	FT, FQ	CGE (chip)	[69]
Cronobacter spp.	Milk powder, instant noodles, fermented bread, beef and egg cakes	DNA extraction and amplification	FS	CE-LIF	[70]
Vitamins					

(continued)

Table 1
(continued)

	Sample	Sample preparation	Topic of interest	Analytical platform	Ref.
Thiamine hydrochloride (B1), riboflavin (B2), nicotinic acid (B3), pyridoxine hydrochloride (B6), and cyanocobalamine (B12), and vitamin C (ascorbic acid)	Cornflour and fortified corn flakes	Extraction with methanol	FQ	MEKC-UV	[71]
Vitamin C	Tomato	Extraction with phosphoric acid	FQ	CZE-UV	[72]
Riboflavin, folic acid, niacinamide	Health drink	Dilution and filtration; Dilution, filtration, and FITC derivatization	FQ	CE-LIF	[16]
Thiamine, nicotinamide, pyridoxine, riboflavin, folic acid	Bacterial growth media, *Ilex paraguariensis* leaves	Filtration, online preconcentration Extraction with water, dilution with NaH_2PO_4, online preconcentration	FQ	MEKC-UV	[73]
Tocopherols	Vegetable oils	SPE	FQ	NACE-UV-FL	[74]
Vitamins B3, C, B1, B2, B5, B6, B8, B9, B12, PP	Energy drinks, vitamin tablets, and fluit pulp powders	Extraction with ethanol	FQ	MECK-UV	[75]
Riboflavin	Cereal grains	SRMM or sweeping	FB	CE-LIF	[76]
Nicotinic acid and nicotinamide	Vitamin functional drinks, vitamins,water, russula alutacea, and instant dry yeast	Extraction with HCl	FQ	CZE-UV	[77]
Carbohydrates					
Saccharose, lactose, lactulose, epilactose, maltotriose, maltose, galactose, glucose, arabinose, mannose, fructose, xylose, ribose	Orange juice, red wine; rice brand, condensed milk coffee, and breakfast cereals	Dilution of the juice with water Extraction with acid solution	FQ	MEKC-UV	[78]
Glucose, lactose, sucrose, fructose	Glucose, lactose, sucrose, fructose standards	Dilution with water	FQ	CE-DAD	[79]

Glucose, fructose, galactose, mannose, ribose, sucrose, lactose	Fruit juices, cola drinks, milk, red and white wines, yoghurts, honey, foodstuff additive	Dilution with water:ACN (1:1, v/v)	FQ, FS	CE-C^4D	[80]
Fructose, glucose, sucrose	Multifloral honey	Dilution with water	FQ, FS	CE-DAD	[81]
Fructose, glucose, sucrose	Tomato, pepper, muskmelon, winter squash, orange	Dilution of the juice with water	FQ	CE-DAD	[82]
D-Mannose, D-ribose, D-glucose, L-rhamnose, D-glucuronic acid, D-galacturonic acid, glucosamine, D-xylose, D-galactose, larabinose, D-fucose, maltose, lactose	Herbal (*Lycipus lucidus Turcz*), chinese jujube (*Zizyphus jujuba*), beer, milk	Extraction or dilution with water, and PMP derivatization	FQ	CZE-UV	[83]
Galactose, glucose, mannose, ribose, lyxose, xylose, arabinose, maltose, N-acetylgalactosamine, N-acetylglucosamine, gentiobiose, melibiose, cellobiose, lactose	Maple syrup and maple sugar	PMP derivatization	FQ	CE-DAD	[84]
Fructose, glucose, lactose, sucrose, ribose, xylose, maltose, mannose, galactose	Fructose, glucose, ribose, xylose, mannose, lactose, galactose, maltose, sucrose stantards	Dilution with water	FQ	CE-pulsed amperometric detection	[85]
Fructose, glucose, lactose, sucrose	Red wine, apple juice	Dilution with water	FQ	CE-UV	[86]
Sucrose, lactose, glucose, fructose, ribose	High-energy drinks	Dilution with water, sonication	FQ	CZE-C^4D	[87]
Small organic and inorganic compounds					
Orthophosphates, pyrophosphates, tripolyphosphates, nitrites, and nitrates	Meat, seafood products	Extraction with water	FS	cITP-conductivity detector	[88]
Quinine	Beverages	Sonication and dilution in H_2SO_4	FS	CITP-CZE-DAD	[89]

(continued)

Table 1
(continued)

	Sample	Sample preparation	Topic of interest	Analytical platform	Ref.
Glycine betaine, trigonelline, proline betaine, total content of carnitines	Seed oils and extra virgin olive oils	Extraction with methanol:chloroform (2:1, v/v), wash with methanol:chloroform:water (2:1:0.8, v/v/v), aqueous-phase derivatization with butanol	FQ, FT	CE-Q/IT MS/MS	[90]
Formaldehyde, acetaldehyde, propanal, butanal, pentanal, hexanal, glutaradehyde, 2,3-butanedione, methylgloxal	Wines, oils, water-soaked products	Filtration, TBA derivatization	FQ, FS	CE-AD	[91]
Formaldehyde, acetaldehyde	Wines, waterishlogged products	Filtration, TBA derivatization	FQ, FS	mini-CE-AD	[92]
Namely, sinapaldehyde, syringaldehyde, coniferaldehyde, vanillin	Whiskey	Online preconcentration	FQ	CE-UV	[93]
Sodium	Milk, milk products	Extraction with water and acidification with oxalic acid	FS	CZE-UV	[94]
Co, Zn, Cu, Ni, and Cd	Juices	Extraction with carboxylic group functionalized magnetic nanoparticles and re-extraction with acid solution	FS	CE-UV	[95]
Perchlorate	Cow's milk, water, red wine	Electrokinetic injection of analytes across a disposable supported liquid membrane	FS	CE-C^4D	[96]
Lactic acid, malic acid, tartaric acid, citric acid	Fruits, juices, nectars, wines, beer	Injection direct	FQ	CE-UV	[97]

Nitrate, nitrite, oxalate	Kale (*B. oleracea* var. *acephala*), sultana pea (*Pisum sativum* var. saccharatum)	Extraction with water Extraction with HCl	FS	CE-DAD	[98]
Glucosamine	Nutritional supplements	Extraction with water, and in-capillary derivatization with *o*-phthalaldehyde	FQ	CE-PDA	[99]
Caffeine	Energy drinks	Centrifugation and dilution with buffer	FS	MEEKC-DAD	[100]
4-Bromophenol, 2,4,6-triBromophenol, 2,4 diBromophenol, 2-Bromophenol, 2,6-diBromophenol	Seafood	Homogenization with H_2SO_4, distillation extraction, concentration	FQ	CZE-pulsed amperometric detection	[101]
Sotolon	Maple-flavored food additive	Extraction with water	FQ	CZE-pulsed amperometric detection	[102]
Glucosamine and chondroitin sulfate	Dietary supplements	Extraction with water	FQ	CITP-conductivity detector	[103]
Melamine, ammelide, ammeline, and cyanuric acid	Milk products	Protein precipitation with HCl and SPE	FS	MECK-UV	[104]
Toxins, contaminants, pesticides, and residues					
Sulfadiazine, sulfamerazine, sulfapyridine, sulfamethazine, sulfisoxazole, sulfadimethoxine, sulfaquinoxaline, sulfamonomethoxine, sulfathiazole	Porcine liver and kidney	SPE, online concentration	FS	CEC-TOF MS	[105]
Sulfamethazine, sulfamerazine, sulfathiazole, sulfacarbamide, sulfachloropyridazine, sulfamethoxazole, sulfaguanidine	Poultry tissue	Deproteinization with ACN, centrifugation, SPE	FS	MEKC-UV	[106]

(continued)

Table 1
(continued)

	Sample	Sample preparation	Topic of interest	Analytical platform	Ref.
Oxacillin, penicillin V, penicillin G, nafcillin, ampicillin, amoxicillin	Porcine liver, kidney	Extraction with ACN, SPE	FS	NSM-W/O--MEEKC- 3D UV-vis	[107]
Colchicine	Milk	Deproteinization with HCl, LLE with dichloromethane:isopropanol (95:5, v/v), evaporation, dilution with phosphate buffer	FS	CZE, NACE, MEKC-UV	[108]
Marbofloxacin, CIP, danofloxacin, ENR, sarafloxacin, difloxacin, oxolinic acid, flumequine	Bovin, porcine plasm	SPE	FS	CE-UV	[109]
Isoproturon, linuron, iduron	Green vegetable, rice	Matrix solid-phase dispersion extraction	FS	CE-ECL	[110]
Saxitoxin, decarbamoylsaxitoxin	Shellfish	Extraction with acetic acid solution, filtration, immunoreaction	FS	Immunoaffinity CE-EC	[111]
Quinolone enrofloxacin, ciprofloxacin	Milk	Deproteinization with HCl solution, centrifugation, SPE	FS	CE-UV	[112]
Tetracycline, oxytetracycline, doxycycline	Milk	Extraction with matrix solid-phase dispersion	FS	CZE-UV	[113]
Albendazole, fenbendazole, mebendazole, thiabendazole, albendazole sulfoxide, albendazole sulfone, oxfendazole, fenbendazole sulfone, 2-amino-albendazole sulfone, 5-hydroxy thiabendazole	Swine tissue	Extraction with ACN, magnetic solid-phase extraction	FS	FASS-CZE-DAD	[114]

Methomyl, propoxur, carbofuran, carbaryl, isoprocarb, promecarb	Fruit juices	Filtration	FS	REPSM-MEKC-PDA	[115]
Metolcarb	Rice, cucumber	Homogenization with methanol and filtration	FS	Immunoaffinity CE-LIF	[116]
2,4-Dichlorophenol, 2,4,5-trichlorophenol, 4 tert-butyl-phenol, pentachlorophenol, bisphenol-A, 4-tert-butyl benzoic acid	Honey	LLE with hexane, QuEChERS	FS	PNP-CE-Q MS	[117]
Brevetoxin B	Shellfish	Extraction with methanol, filtration, immunoreaction	FS	Immunoaffinity CE-EC	[118]
Citrinin, a nephrotoxic, hepatotoxic mycotoxin	Red yeast rice, monascus color	Selective extraction and cleanup by immunoaffinity column	FS	CZE-UV	[119]
Ochratoxin A	Mould strains	Extraction with chloroform, filtration, evaporation	FS	MEKC-UV	[120]
Sulfonamides and their acetylated metabolites	Shrimp, sardine, and anchovy	Accelerated solvent extraction with ACN	FS	CZE-DAD	[121]
Polycyclic aromatic hydrocarbons	Isio 4®oil	SPE	FS	CZE-LIF	[122]
Polycyclic aromatic hydrocarbons	Bovine milk	Hydrolisis with b-glucuronidase, extraction with ACN, SPE	FS	CZE-UV	[123]
Patulin	Apple juices	Dispersive liquid-liquid microextraction	FS	MECK-DAD	[124]
Patulin	Apple juices	Extraction with ethyl acetate	FS	CZE-UV	[125]
Zearalenone	Poultry feed and cereals	Extraction with methanol and dicholoromethane, SPE	FS	CZE-UV	[126]
Glyphosate and glufosinate	Water, soybean, and broccoli	Extraction with water, FITC derivatization	FS	CE-LIF (chip)	[127]
Amprolium	Eggs	Extraction with water, SPE, and FASI preconcentration	FQ, FS	CE-Q/IT MS/MS	[128]

(continued)

Table 1
(continued)

	Sample	Sample preparation	Topic of interest	Analytical platform	Ref.
Anthelmintic benzimidazoles	Eggs	Extraction with ethyl acetate, hexane and SPE; extraction with water and SPE; QuEChERS and SPE	FS	CE-Q MS	[129]
Brevetoxin-B	Shellfish	Extraction with methanol	FS	CE-immunoassay	[118]
Arsenic compounds: As (III), As (V), DMA, MMA, AsB, AsC, 3-NHPAA, 4-NPAA,o-ASA (o-arsanilic acid) and p-UPAA	Herbal plants and chicken meat	Extraction with water	FS	CE-ICP MS	[130]
Sulfonamide residues: Sulfamethazine, sulfadiazine, and sulfathiazole	Milk	Protein precipitation with HCl, and SPE	FQ, FS	CE-UV/DAD	[131]
Food additives					
Citrate, tartrate, malate, succinate, adipate, acetate, propionate, lactate, benzoate, sorbate, dehydroacetate, ascorbate, gluconate	Wine, health drink, yogurt, pickled ginger	Dilution with water, filtration	FQ, FS	CZE-DAD	[132]
Methyl, ethyl, propyl, and butyl parabens	Sweetener	Filtration	FS	CEC-UV	[133]
Benzoic acid, sorbic acid	Beverages, vinegar, fruit jam	Dilution with buffer, filtration	FS	CZE-UV-Vis	[134]

Sudan I (1-(phenylazo)-2-naphthalenol) Sudan II (1-[(2,4-dimethylphenyl) azo]-2-naphthalenol) Sudan III (1-[[4-(phenylazo)phenyl] azo]-2-naphthalenol) Sudan IV (1-[[2-methyl-4-[(2-methylphenyl)-azo]phenyl] azo]-2-naphthalenol)	Chilli tomato sauces	Extraction with acetone:dichloromethane:methanol (3:2:1, v/v/v), evaporation	FS	MEKC-UV MEKC-Q/IT MS/MS	[135]
Sudan I (1-(phenylazo)-2-naphthalenol) Sudan II (1-[(2,4-dimethylphenyl) azo]-2-naphthalenol) Sudan III (1-[[4-(phenylazo)phenyl] azo]-2-naphthalenol) Sudan IV (1-[[2-methyl-4-[(2-methylphenyl)-azo]phenyl] azo]-2-naphthalenol)	Chilli tomato sauces, chilli powder	Extraction with acetone:dichloromethane:methanol (3:2:1, v/v/v), evaporation	FS	MEKC-Q/IT MS/MS	[136]
Benzoyl peroxide, benzoic acid	Wheat flour	Dilution with methanol, reduction with potassium iodide solution, filtration	FS	CZE-UV	[137]
Hydroxyproline	Meat products	Digestion, filtration, reaction with fluorescamine reagent, evaporation	FQ	CE-UV	[138]
Hydroxyproline	Milk powder, liquid milk, milk drink, soymilk powder	Hydrolysis, dilution, in-capillary derivatization	FQ	MEKC-LIF	[139]
Neotame	Nonalcoholic beverage	Dilution with water or extraction with formic acid:triethylamine:water (4:125:5000, v/v/v), and SPE	FQ	CZE-UV	[140]
2-Methylimidazole and 4-Methylimidazole	Color caramel	Dilution with water	FS	CZE-UV	[141]

(continued)

Table 1
(continued)

	Sample	Sample preparation	Topic of interest	Analytical platform	Ref.
Aspartame, cyclamate, saccharin, and acesulfame K	Tabletop sweetener tablet, confectionary sweets, soft drink samples	Dilution with water	FQ	CE-conductivity detector	[142]
Aspartame, cyclamate, saccharin, and acesulfame-K	Lemon tea sachet	Dilution with water	FQ	CZE-UV	[143]
Chiral compounds					
Amino acid enantiomers	Food supplements	FMOC derivatization	FQ	Chiral selector CEC-UV	[144]
Thirteen α-amino acid enantiomeric pairs	Amino acids	FITC derivatization	FQ	Chiral selectors CE-DAD	[145]
Enantiomers of lipoic acid	Food supplements	Extraction with ethanol	FQ	Chiral selector CE-UV	[146]
A-hydroxy acids and their enantiomers	Fruit juices	Dilution with water, SPE	FQ	Ligand exchange CE-UV	[147]
Foodomics					
Metabolite profiling	GM tomato varieties and traditional tomato cultivars	Extraction with methanol:chloroform:water (3:1:1, v/v/v), centrifugation	FS, FT	CE-TOF MS	[148]
Metabolite profiling	Dietary polyphenol-treated HT-29 cells	SPE, ultrafiltration, and methanol deproteinization	FB	CE-TOF MS	[149, 150]

Metabolite profiling	Dietary polyphenol-treated HT-29 cells	Ultrafiltration	FB	CE-TOF MS	[151, 152]
Metabolite profiling	Dietary polyphenol-treated K562 cells	Ultrafiltration		CE-TOF MS	[153]
Metabolite profiling	Avocado fruits	Extraction with methanol	FT	CZE-IT MS	[154]

FB food bioactivity, *FS* food safety, *FT* food traceability, *FQ* food quality, *LVSS* large-volume sample stacking, *NSM* normal stacking mode, *FASS* field-amplified sample stacking, *REPSM* reversed electrode polarity stacking mode, *PMP* 1-phenyl-3-methyl-5-pyrazolone, *SRMM* stacking in reverse migrating micelles, *DTAF* 5-(4,6-dichlorotriazinyl)amino-fluorescein, *FASI*: field-amplified sample injection, *t-ITP* transient-isotachophoresis
Topics of interest: food bioactivity, food safety (FS), food quality (FQ), food traceability (FT), foodomics

coupling due to its high scan speed and high mass resolution and accuracy, what perfectly fits with the narrow and fast peaks provided by CE and the needs of a metabolomic study.

2 Materials

2.1 Reagents

2.1.1 Reagents for Sample Preparation

1. Human colon adenocarcinoma HT-29 cell line (American Type Culture Collection, LGC Promochem, UK).
2. Dimethyl sulfoxide (DMSO) (Sigma-Aldrich, St. Louis, MO, USA).
3. McCoy's 5A cell culture media (Lonza, Barcelona, Spain).
4. Penicillin-streptomycin mixture (5000 IU/mL penicillin G, 5 mg/mL streptomycin) (Lonza).
5. Heat-inactivated fetal calf serum (Biowest, Nuaillé, France).
6. Carnosic acid as pure standard (Sigma-Aldrich).
7. Phosphate-buffered saline (PBS) solution: 138 mM Sodium chloride, 2.7 mM potassium chloride, and 10 mM sodium hydrogen phosphate, at pH 7.4 (Lonza).
8. Trypsin-Versene (Lonza).
9. Trypan blue (0.4%, w/v) 0.81% sodium chloride, 0.06% potassium phosphate (Sigma-Aldrich).
10. Liquid nitrogen (Carburos Metalicos-Air Products Group, Barcelona, Spain).
11. Metabolite internal standards (IDs): Tyramine, DL-methionine sulfone (Sigma-Aldrich).
12. Water from Milli-Q system (Millipore, Bedford, MA, USA).

2.1.2 Reagents for CE-ESI-TOF MS Analysis

1. MS-grade water (Scharlau, Barcelona, Spain).
2. MS-grade formic acid (Sigma-Aldrich).
3. MS-grade 2-propanol (Labscan, Gliwice, Poland).
4. Sodium hydroxide (NaOH) (Panreac, Barcelona, Spain).
5. Metabolite commercial standards (Sigma-Aldrich) for quality control (QC) mixture: Spermine, spermidine, putrescine, cadaverine, *N*-acetylspermine, ornithine, lysine, arginine, S-adenosylmethionine, adenine, tyramine, *N*-acetyl-putrescine, S-adenosylhomocysteine, homocysteine, cysteine, *N*-acetyl-ornithine, cytidine, methionine, adenosine, methyl-thio-adenosine, DL-methionine sulfone, glutathione, oxidized glutathione.

2.1.3 Preparation of Solutions

1. Culture media solution: Add 50 mL heat-inactivated fetal calf serum and 5 mL penicillin-streptomycin mixture to 450 mL McCoy's 5A media in a cell culture flask.

2. Carnosic acid (CA) (100 mM): Dissolve CA in DMSO to obtain a final concentration of 33.22 (mg/mL) (*see* **Note 1**).
3. Metabolite extraction solvent with IDs at 125 μM concentration: Prepare 0.91 mg/mL tyramine and 0.62 mg/mL DL-methionine sulfone solution in Milli-Q water.
4. QC mixture: Mix 56 μL MS-grade water and 2 μL 5 mM solutions of putrescine, cadaverine, *N*-acetylspermine, ornithine, lysine, arginine, S-adenosyl-methionine, adenine, tyramine, *N*-acetyl-putrescine, S-adenosyl-homocysteine, cysteine, *N*-acetyl-ornithine, cytidine, methionine, adenosine, methyl-thio-adenosine, and DL-methionine sulfone. Finally add 4 μL 2.5 mM solutions of glutathione, oxidized glutathione, spermine, spermidine, and homocysteine.
5. Sodium hydroxide (1 M): Dissolve 4 g of sodium hydroxide in 95 mL of Milli-Q water. Then reach a final volume of 100 mL using a volumetric flask.
6. Sodium hydroxide (0.1 M): Dilute 1 mL 1 M NaOH in 9 mL Milli-Q water
7. Sodium formate (10 mM) for MS calibration: Mix 200 μL 1 M NaOH and 39.8 μL formic acid and make up volume to 10 mL with 2-propanol:water (50:50, v/v).
8. Formic acid (3 M): Mix 200 mL MS-grade water with 11.31 mL formic acid in a volumetric flask and reach a final volume of 250 mL with water.
9. Sheath liquid (2-propanol-water (50:50, v/v): Mix 5 mL of MS-grade 2-propanol with 5 mL MS-grade water.

2.2 Consumables and Equipment

2.2.1 Consumables and Equipment for Sample Preparation

1. Light microscope (ID3, Carl Zeiss, Jena, Germany).
2. Tissue culture flasks 100 mL volume (Sarstedt, Barcelona, Spain).
3. P150 tissue culture plates (Sarstedt).
4. Neubauer counting chamber (Brand, Wertheim, Germany).
5. Vortex (JP Selecta, Barcelona, Spain) to prepare commercial standard solutions.
6. Rotina 380R centrifuge (Hettich, MA, USA).
7. Ultrasonic bath (JP Selecta, Barcelona, Spain).
8. Ball mill MM 400 (Retsch, Haan, Germany).
9. Glass beads (212–300 μm) (Sigma-Aldrich).
10. 2 mL Microcentrifuge screw tubes.
11. PTFE adapter rack for ten reaction vials 1.5 and 2.0 mL (Ref: 22.008.0008) (Retsch).
12. Amicon Ultra 3 kDa 0.5 mL centrifugal devices from Millipore (Billerica).

2.2.2 Consumables and Equipment for CE-ESI-TOF MS Analysis

1. Uncoated fused silica capillary (80 cm length, 50 μm i.d.) (Composite Metal Services, Worcester, England).
2. High-performance capillary electrophoresis (CE) system model P/ACE 5500 (Beckman, Fullerton, CA, USA) controlled by a PC equipped with System Gold software (Beckman).
3. TOF MS instrument (micrOTOF model) (Bruker Daltonics, Bremen, Germany).
4. Cole Palmer syringe pump (model 74900-00-05) (Vernon Hills, IL, USA).
5. Glass syringe (2.5 mL volume) (SGE, Milton Keynes, UK).
6. Orthogonal electrospray ionization (ESI) interface (model G1607A) (Agilent Technologies, Palo Alto, CA, USA).

2.2.3 Software and Bioinformatic Tools

1. DataAnalysis 4.0 software (Bruker Daltoniks).
2. Data file format converter: Trapper (free available at http://tools.proteomecenter.org/wiki/index.php?title=Software:trapper).
3. Free access databases used for identification [155–157].
4. Software for statistical analysis: STATISTICA v.7 (Statsoft, Tulsa, OK, USA).

3 Methods

3.1 Cell Culture Preparation Protocol

1. Grow colon adenocarcinoma HT-29 cells in 10 mL culture media inside a culture flask at 37 °C in humidified atmosphere and 5% CO_2.
2. When cells reach ~50% confluence (cells fill ~50% flask), discard culture media and place cells in a 15 mL Falcon tube with 4 mL trypsin and 4 mL cell culture media solution.
3. Centrifuge at 500 × *g* for 3 min, discard the supernatant, and suspend the cell pellet in 4 mL culture media solution.
4. Seed cells at 10,000 cells/cm^2 onto six independent P150 tissue culture dishes: Take 0.5 mL cell suspension, add 19.5 mL cell culture media, and incubate overnight at 37 °C (*see* **Note 2**).
5. Add 5.96 μL 100 mM CA solution to three of the culture dishes to obtain 9.9 μg/mL final concentration of CA in the cell plates and incubate all six cell cultures (CA-treated and non-treated) for 48 h at 37 °C.

3.2 Obtainment of Ten Million Cells from Cell Culture Dishes

1. Aspire growth medium from culture plates, add 2 mL trypsin solution, and rapidly aspire it.
2. Dispense 5 mL trypsin solution covering the monolayer of cells and incubate cells at 37 °C for 15 min.

3. Transfer cells suspended in trypsin to 15 mL Falcon tubes. Add 3 mL trypsin more to culture dish to collect maximum number of cells and transfer these 3 mL to the same 15 mL Falcon tube (*see* **Note 3**).
4. Centrifuge at 300 × *g* for 5 min, discard the supernatants, and add 1 mL PBS to each pellet ($n = 6$) to suspend the cells (*see* **Note 4**).
5. Cell counting: Dilute 5 μL of cell suspension (obtained in the previous step) in 15 μL PBS and add 20 μL trypan blue commercial solution. Mix well by gentle pipetting within the pellet using a micropipette and place the suspension on Neubauer counting chamber. Count the cells in the central square and in the four squares at the corners using a light microscope. Count separately viable (opaque) and nonviable (blue-stained) cells (*see* **Note 5**). Repeat this procedure to obtain the average number of cells from at least three different squares of Neubauer chamber (*see* **Note 6**) and calculate the number of cells/mL and the volume of cell suspension to have 10×10^6 cells (*see* **Note 7**).
6. Transfer the volume required to have 10×10^6 cells from the PBS cell suspension previously obtained (Subheading 3.2, **step 4**) to 2 mL microcentrifuge screw tubes to obtain six independent tubes (three non-treated and three CA-treated cells) containing 10×10^6 cells each.
7. Centrifuge for 10 min at 500 × *g* to obtain the cell pellets containing 10×10^6 cells.

3.3 Metabolite Extraction Procedure

1. Add 0.3 g glass beads and 300 μL metabolite extraction solvent containing the IDs to each screw tube ($n = 6$).
2. Perform three cycles of metabolite quenching and cell disruption applying the three following steps: First submerge a rack with the six cell suspension tubes in liquid nitrogen (*see* **Note 8**) for 3 min. Then carefully take the rack with the tubes and thaw on ultrasonic bath at 50 Hz for 5 min. The third step consists of placing the tubes inside the PTFE adapter racks and applying 30 Hz frequency for 3 min using a ball mill. Repeat three times these steps.
3. Centrifuge the tubes at 24,000 × *g* for 10 min at 4 °C.
4. Filter 200 μL supernatant (cellular content) from each tube by using 3 kDa molecular weight filters programming the centrifuge at 14,000 × *g* for 40 min at 20 °C.
5. Store fraction less than 3 kDa (metabolic fraction) in screw tubes at −80 °C until CE-MS analysis.

3.4 CE-ESI-TOF MS Methodology

1. Condition all new capillaries by flushing with 0.1 M NaOH for 20 min, followed by MS-grade water for 20 min and background electrolyte (BGE) (3 M formic acid) for 5 min (*see* **Note 9**).
2. Introduce the capillary through the interface (ESI) and set the sheath-flow configuration to establish the electrical contact at the ESI tip. Program 0.24 mL/min sheath liquid flow rate in the syringe pump menu.
3. Create an analysis method with the following CE-TOF MS parameters: CE voltage set at +27 kV, CE temperature at 25 °C, positive ionization mode MS, MS capillary voltage set at 4 kV, acquisition *m/z* range from 50 to 600 *m/z*, dry nitrogen gas heated at 200 °C delivered at 4 L/min and maintained at 0.4 bar.
4. Perform TOF MS external calibration by introducing 10 mM sodium formate before each injection. For internal calibration record signal obtained using the same solution at the end of each sample file for 2 min. Ions used for calibration are 90.9766, 158.9641, 226.9515, 294.9389, 362.9263, 430.9138, 498.9012, and 566.8886 *m/z* (Fig. 1).

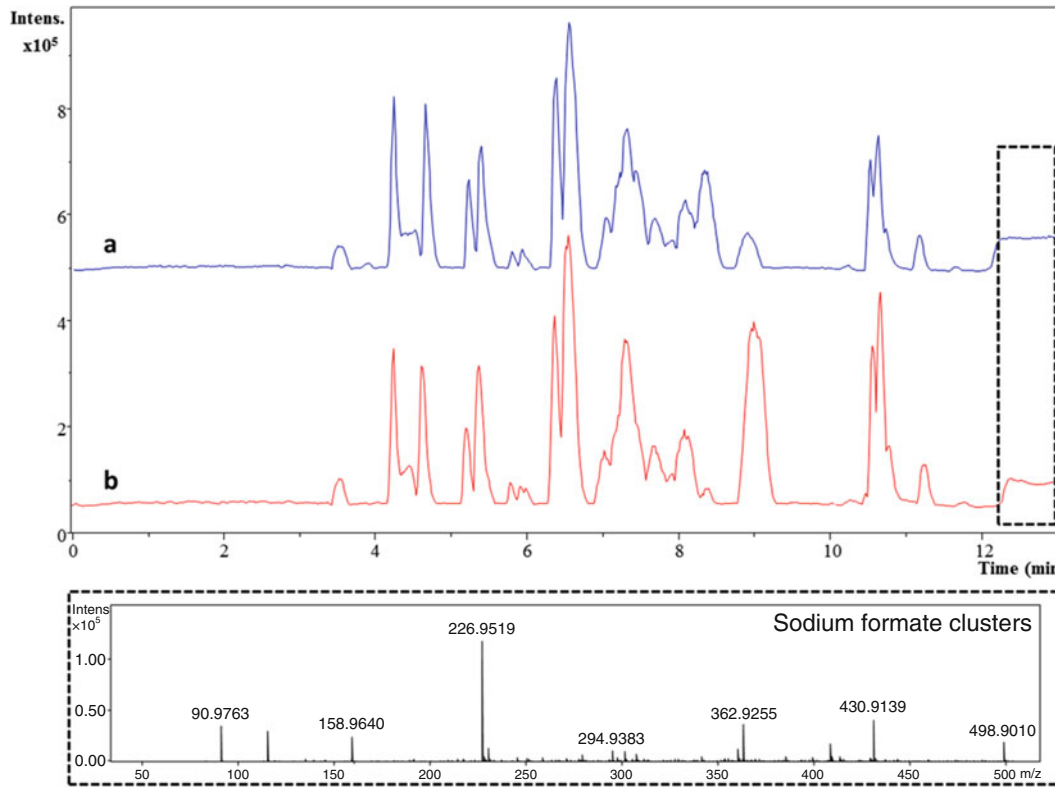

Fig. 1 CE-ESI-TOF MS base peak electropherograms (BPE) of the cytosolic fraction from (**a**) control HT-29 colon cancer cells and (**b**) treated with carnosic acid. Calibrant acquisition is framed at the end of the two electropherograms using a dashed line rectangle. (**c**) An example of MS spectra from the framed area showing the experimental clusters used for calibration

5. Inject the sample for 80 s at 0.5 psi (34.5 mbar) and apply the CE-MS method described above. Obtain the metabolic profiles of control and CA-treated cells (Fig. 1).
6. Inject each sample to obtain three CE-MS replicates. Check the suitability of the results using DataAnalysis 4.0 software.
7. Each three injections change BGE vial and inject QC mixture (Fig. 2).
8. After each injection and the subsequent external calibration, condition the capillary for 5 min with BGE.

3.5 Data Processing

1. Use DataAnalysis 4.0 software to check the suitability of your data by extracting known ions such as internal standards and ions from the QC (Fig. 2) to calculate deviation intra and inter day.
2. Export ".d" CE-MS data to the MS exchange format "mzXML" using Trapper bioinformatic tool. Select the pathways where sample data files are stored in the PC, select "peak

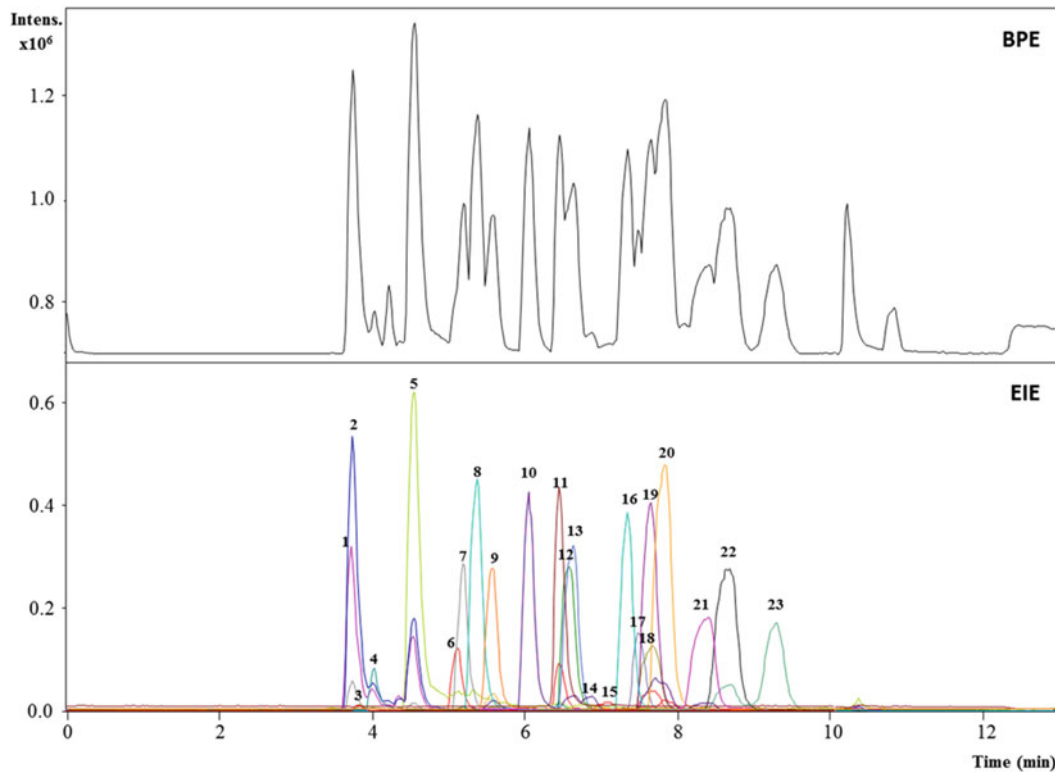

Fig. 2 CE-ESI-TOF MS base peak chromatogram (BPE) of quality control mixture and extracted ion chromatograms (EIE) of the 23 metabolite standards: 1, spermine; 2, spermidine; 3, putrescine; 4, cadaverine; 5, *N*-acetyl-spermine; 6, ornithine; 7, lysine; 8, arginine; 9, S-adenosyl-methionine; 10, adenine; 11, tyramine; 12, *N*-acetyl-putrescine; 13, S-adenosyl-homocysteine; 14, homocysteine; 15, cysteine; 16, *N*-acetyl-ornithine; 17, cytidine; 18, methionine; 19, adenosine; 20, methyl-thio-adenosine; 21, ethionine sulfone; 22, oxidized glutathione; 23, glutathione

picking" option to centroid your data, and click start to begin with the conversion.

3. Process exported centroided mzXML data with MZmine program (*see* **Note 10**). Set the threshold of electropherograms (*see* **Note 11**). Use wavelet transform algorithm to detect the masses with a wavelet window size set at 50% and normalize migration time between replicates setting minimum standard intensity at 5×10^4 a.u.. For deconvolution use "baselina cut-off" algorithm setting the minimum peak height at 3×10^2 a.u. Then align the replicates and samples applying the "Join aligner" algorithm with m/z tolerance set at 0.01 and weight for m/z set at 90. Finally perform adduct and complex search within your detected peaks and export the resulting data table to csv format.
4. Import the csv table in Excel and remove the metabolic signals showing high variability within the same group of samples (i.e., control and treated cells) from CE-MS data set. Transpose the data table to get samples arranged in rows and high-confident metabolic signals in columns.
5. Open the transposed data table using STATISTICA program.
6. Inspect your data variability by means of principal component analysis (PCA). If necessary remove high-variable metabolic signals and/or outlier samples.
7. Detect significantly different molecular features due to CA treatment applying an analysis of variance method (i.e., ANOVA, *t*-test, Kruskal-Wallis) and setting p-value at 0.05.

3.6 Identification of Potential Biomarkers

1. Match the experimental m/z value of the metabolites showing significant differences ($p < 0.05$) with m/z values contained in different databases: Human Metabolome Database, METLIN, and KEGG, with a mass accuracy window of 10 ppm (Table 2).
2. Use Generate-Molecular Formula editor (DataAnalysis 4.0) to compare the isotopic pattern of the theoretical formulas obtained from the databases with the experimental isotopic pattern of each of the metabolites differentially expressed.
3. Inject metabolite standards to corroborate tentative identifications, in the same analytical conditions and spiked (if possible) in cell culture samples (*see* **Note 12**).
4. Associate metabolite expression (up or down expression) to CA treatment and study the most affected cellular pathways (Fig. 3).

Table 2
Tentative identification of metabolites differentially expressed in HT-29 cells after CA treatment sorted according to their migration time

Metabolite ID	*m/z*	Ion	Formula	Error (ppm)	Identification	Standard coinjection	HMDB identifier	Expression
1	131.118	M+H	$C_6H_{14}N_2O$	-2.9	*N*-acetyl-putrescine	YES	HMDB02064	DOWN
2	104.070	M+H	$C_4H_9NO_2$	-6.7	γ-Aminobutyric acid	YES	HMDB00650	DOWN
3	298.096	M+H	$C_{11}H_{15}N_5O_3S$	-3.8	Methyl-thio-adenosine	YES	HMDB01173	DOWN
4	179.049	M+H	$C_5H_{10}N_2O_3S$	4.5	Cysteinyl-glycine[a]	NO	HMDB28775	UP
5	307.086	M+2H	$C_{20}H_{32}N_6O_{12}S_2$	8.5	Oxidized glutathione	YES	HMDB03337	DOWN
6	308.092	M+H	$C_{10}H_{17}N_3O_6S$	1.8	Reduced glutathione	YES	HMDB00125	UP
7	244.094	M+H	$C_9H_{13}N_3O_5$	5.5	Cytidine	YES	HMDB00089	DOWN

[a]Cysteine-glycine was tentatively identified due to the lack of standard

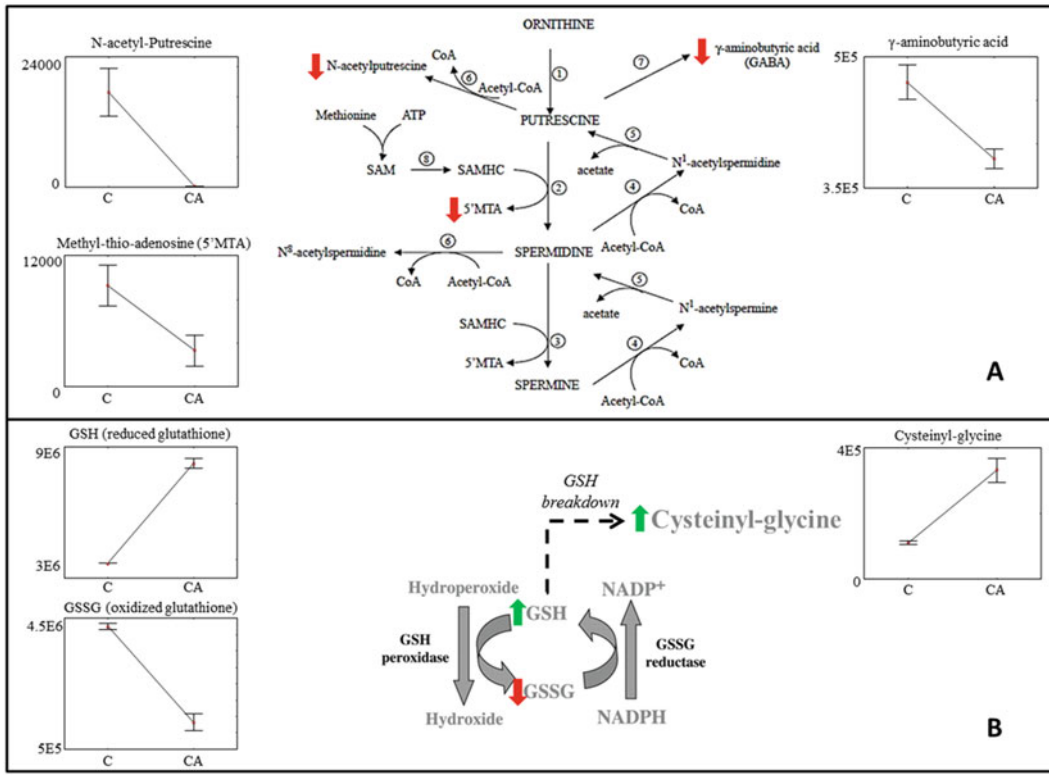

Fig. 3 Main pathways within HT29 metabolome altered after the CA treatment. CA brings about modifications on polyamine pathway (**a**) by the down-expression of N-acetylputrescine, methyl-thio-adenosine, and γ-aminobutyric acid. CA also alters glutathione metabolism (**b**) by a down-expression of oxidized glutathione that gives rise to increased levels of reduced glutathione and cysteinyl-glycine. Down- and up-expressed metabolites are marked with *red* and *green* arrows, respectively. Whisker plots of average metabolite areas (±SD) in control- (**c**) and carnosic acid-treated (CA) cells are also shown for significantly different metabolites involved in A and B pathways. Enzymes involved in polyamine pathway are ornithine decarboxylase (1), spermidine synthase (2), spermine synthase (3), acetyl-CoA: spermidine/spermine N 1-acetyltransferase (4), polyamine oxidase (5), spermidine N 8-acetyltransferase (6), amine oxidase plus aldehyde dehydrogenase (7), S-adenosylmethionine decarboxylase (8)

4 Notes

1. CA molecule is easily degradable and photosensitive. For this reason avoid light and high temperature when preparing CA solution. Divide the resulting solution in several aliquots and store them at −80 °C.
2. Volume of 0.5 mL cell suspension is estimated with the microscope to obtain a final density of cells up to 10,000 cells/cm^2. Thus, this volume has to be estimated in each study.
3. A final volume of 8 mL trypsin is added to the culture dish to collect cells and can be added in one step before incubation (Subheading 3.2). However to divide trypsin addition in two

steps (add 5 mL trypsin, then incubate, and add 3 mL trypsin) is more advisable to obtain the maximum recovery of cells from the culture dish.

4. PBS volume is estimated in order to obtain a 10×10^6 cell suspension.
5. In order to follow a routine on how to count the cells, it is important to establish a procedure to not count more than one time each cell. To do so, one possibility is to count the cells touching the midline of the triple line, on the top and left of each square (of the Neubauer chamber). Do not count cells touching the midline of the triple line, on the bottom or right side of the square.
6. The total count of cells must be around 100. If not, adjust the dilution of cell suspension by modifying PBS volume. It is important to note that a half of the total volume of the final solution to count cells has to consist of trypan blue (commercially available at 0.4%). Namely 0.2% final trypan blue concentration is necessary to count cells.
7. The formulas for calculation are the following ones:

   Cells/mL = average number of cell counted × 104 × dilution factor [8] (dilution factor can change depending on the result obtained from cell counting (*see* **Note 2**).

   Total cells = cells/mL × vol. of original suspension.

   Another relevant parameter if for example proliferation under given conditions is under scrutiny is the viability of cells described below:

   % Viability = (number of viable cells counted/total number of cells counted) × 100.
8. Liquid nitrogen must be carefully used because contact may produce burns. Always use security glasses and gloves to work with it. The use of a rack or container with a handle or handgrip is recommended to submerge the tubes.
9. Low-pH BGE promotes positive charge of analytes and is recommended to avoid analyte adsorption onto the inner capillary wall.
10. Every parameter in data processing must be carefully optimized for each experiment and instrument. MZmine has the advantage to present a very visual interface which is very recommendable for CE-MS data processing due to higher migration time deviations compared to LC- or GC-MS and moreover data processing experience is not necessary to visually check the results.
11. There are many ways to estimate the minimum intensity from which peaks are detected in data process. One of the most common estimations of the threshold is to divide the lower signal intensity (low-abundant species) by 3.

12. Migration time or intensity of standards could be different from the values obtained in the samples if standards are injected alone. Salts, viscosity, and other matrix properties contribute to migration time and intensity values of metabolites.

Acknowledgments

This work was supported by an AGL2011-29857-C03-01 project (Ministerio de Educacion y Ciencia, Spain). A.V. thanks the Ministerio de Economía y Competitividad for his FPI predoctoral fellowship. T.A. thanks the Capes Foundation, Ministry of Education of Brazil, for her predoctoral fellowship (proc. nº: BEX 1532/13-8).

References

1. LeDoux M (2011) Analytical methods applied to the determination of pesticide residues in foods of animal origin. A review of the past two decades. J Chromatogr A 1218:1021–1036
2. García-Cañas V, Simó C, Herrero M, Ibáñez E, Cifuentes A (2012) Present and future challenges in food analysis: foodomics. Anal Chem 84:10150–10159
3. Herrero M, Simó C, García-Cañas V, Ibáñez E, Cifuentes A (2012) Foodomics: MS-based strategies in modern food science and nutrition. Mass Spectrom Rev 31:49–69
4. Ellis DI, Brewster VL, Dunn WB, Allwood JW, Golovanovc AP, Goodacre R (2012) Fingerprinting food: current technologies for the detection of food adulteration and contamination. Chem Soc Rev 41:5706–5727
5. Monakhova YB, Kuballa T, Lachenmeier DW (2013) Chemometric methods in NMR spectroscopic analysis of food products. J Anal Chem 68:755–766
6. Ibáñez C, García-Cañas V, Valdés A, Simó C (2013) Novel MS-based approaches and applications in food metabolomics. TrAC 52:100–111
7. Herrero M, García-Canñas V, Simó C, Cifuentes A (2010) Recent advances in the application of capillary electromigration methods for food analysis and foodomics. Electrophoresis 31:205–228
8. Castro-Puyana M, García-Canñas V, Simó C, Cifuentes A (2012) Recent advances in the application of capillary electromigration methods for food analysis and Foodomics. Electrophoresis 33:147–167
9. García-Cañas V, Simó C, Castro-Puyana M, Cifuentes A (2014) Recent advances in the application of capillary electromigration methods for food analysis and foodomics. Electrophoresis 35:147–169
10. Cifuentes A (2009) Food analysis and foodomics. J Chromatogr A 1216:7109–7110
11. Li X, Hu J, Han H (2011) Determination of cypromazine and its metabolite melamine in milk by cationselective exhaustive injection and sweepingcapillary micellar electrokinetic chromatography. J Sep Sci 34:323–330
12. Wu W-C, Tsai I-L, Sun S-W, Kuo C-H (2011) Using sweeping-micellar electrokinetic chromatography to determine melamine in food. Food Chem 128:783–789
13. Lv Y-K, Sun Y-N, Wang L-M, Jia C-L, Sun H-W (2011) A simple and high-throughput method of ultrasonic extraction-capillary electrophoresis for determination of melamine in milk. Anal Meth 3:2557–2561
14. Mandrioli R, Morganti E, Mercolini L, Kenndler E, Raggi MA (2011) Fast analysis of amino acids in wine by capillary electrophoresis with laser-induced fluorescence detection. Electrophoresis 32:2809–2815
15. Sánchez-Hernández L, Marina ML, Crego AL (2011) A capillary electrophoresis-tandem mass spectrometry methodology for the determination of non-protein amino acids in vegetable oils as novel markers for the detection of adulterations in olive oils. J Chromatogr A 1218:4944–4951
16. Zhao D, Lu M, Cai Z (2012) Separation and determination of B vitamins and essential

amino acids in health drinks by CE-LIF with simultaneous derivatization. Electrophoresis 33:2424–2432

17. Uzaşçı S, Başkan S, Erim FB (2012) Biogenic amines in wines and pomegranate molasses-A non-ionic micellar electrokinetic chromatography assay with laser-induced fluorescence detection. Food Anal Meth 5:104–108
18. Ginterová P, Marák J, Staňová A, Maier V, Ševčík J, Kaniansky D (2012) Determination of selected biogenic amines in red wines by automated on-line combination of capillary isotachophoresis-capillary zone electrophoresis. J Chromatogr B 904:135–139
19. Jastrzębska A (2012) A comparative study for determination of biogenic amines in meat samples by capillary isotachophoresis with two electrolyte systems. Eur Food Res Technol 235:563–572
20. Huang H-Y, Lin C-L, Jiang S-H, Singco B, Cheng Y-J (2012) Capillary electro chromatography-mass spectrometry determination of melamine and related triazine by-products using poly(divinyl benzene-alkene-vinylbenzyl trimethylammonium chloride) monolithic stationary phases. Anal Chim Acta 719:96–103
21. Fu N-N, Zhang H-S, Wang H (2012) Analysis of short-chain aliphatic amines in food and water samples using a near infrared cyanine 1-(ε-succinimydyl-hexanoate)-1′-methyl-3,3,3′,3′-tetramethyl-indocarbocyanine-5,5′-disulfonate potassium with CE-LIF detection. Electrophoresis 33:3002–3007
22. Li W-L, Ge J-Y, Pan Y-L, Chu Q-C, Ye J-N (2012) Direct analysis of biogenic amines in water matrix by modified capillary zone electrophoresis with 18-crown-6. Microchim Acta 177:75–80
23. Akamatsu S, Mitsuhashi T (2013) Development of a simple analytical method using capillary electrophoresis tandem mass spectrometry for product identification and simultaneous determination of free amino acids in dietary supplements containing royal jelly. J Food Compost Anal 30:47–51
24. Jastrzębska A, Piasta A, Filipiak-Szok A, Szłyk E (2013) Optimization of capillary isotachophoretic method for histidine determination in protein matrices. Anal Lett 46:1364–1378
25. Enzonga J, Ong-Meang V, Couderc F, Boutonnet A, Poinsot V, Tsieri MM, Silou T, Bouajila J (2013) Determination of free amino acids in African gourd seed milks by capillary electrophoresis with light-emitting diode induced fluorescence and laser-induced fluorescence detection. Electrophoresis 34:2632–2638
26. Heemskerk AA, Busnel JM, Schoenmaker B, Derks RJ, Klychnikov O, Hensbergen PJ, Deelder AM, Mayboroda OA (2012) Ultra-low flow electrospray ionization-mass spectrometry for improved ionization efficiency in phosphoproteomics. Anal Chem 84:4552–4559
27. Sázelova P, Kašička V, Leon C, Ibáñez E, Cifuentes A (2012) Capillary electrophoretic profiling of tryptic digests of water soluble proteins from Bacillus thuringiensis-transgenic and non-transgenic maize species. Food Chem 134:1607–1615
28. Català-Clariana S, Benavente F, Giménez E, Barbosa J, Sanz-Nebot V (2013) Identification of bioactive peptides in hypoallergenic infant milk formulas by CE-TOF-MS assisted by semiempirical model of electromigration behavior. Electrophoresis 34:1886–1894
29. Baxter G, Zhao J, Blanchard C (2011) Salinity alters the protein composition of rice endosperm and the physicochemical properties of rice flour. J Sci Food Agric 91:2292–2297
30. Latoszek A, García-Ruiz C, Marina ML, de la Mata FJ, Gómez R, Rasines B, Cifuentes A, Poboży E, Trojanowicz M (2011) Modification of resolution in capillary electrophoresis for protein profiling in identification of genetic modification in foods. Croat Chem Acta 84:375–382
31. Gasilova N, Gassner AL, Girault HH (2012) Analysis of major milk whey proteins by immunoaffinity capillary electrophoresis coupled with MALDI-MS. Electrophoresis 33:2390–2398
32. Chen L, Zeng R, Xiang L, Luo Z, Wang Y (2012) Polydopamine-*graft*-PEG antifouling coating for quantitative analysis of food proteins by CE. Anal Meth 4:2852–2859
33. Trudeau K, Vu KD, Shareck F, Lacroix M (2012) Capillary electrophoresis separation of protein composition of γ-irradiated food pathogens *Listeria monocytogenes* and *Staphylococcus aureus*. PLoS One 7:e32488
34. Masotti F, Battelli G, De Noni I (2012) The evolution of chemical and microbiological properties of fresh goat milk cheese during its shelf life. J Dairy Sci 95:4760–4767
35. Montealegre C, Rasines B, Gómez R, de la Mata FJ, García-Ruiz C, Marina ML (2012) Characterization of carboxylate-terminated carbosilane dendrimers and their evaluation as nanoadditives in capillary electrophoresis for vegetable protein profiling. J Chromatogr A 1234:16–21
36. Montealegre C, García MC, del Río C, Marina ML, García-Ruiz C (2012) Separation of olive proteins by capillary gel electrophoresis. Talanta 97:420–424b

37. Garrido-Medina R, Puerta A, Pelaez-Lorenzo C, Rivera-Monroy Z, Guttman A, Diez-Masa JC, de Frutos M (2013) Capillary electrophoresis with laser-induced fluorescence detection of proteins from two types of complex sample matrices: food and biological fluids. Meth Protocols 984:207–225
38. Pobozy E, Filaber M, Koc A, Garcia-Reyes JF (2013) Application of capillary electrophoretic chips in protein profiling of plant extracts for identification of genetic modifications of maize. Electrophoresis 34:2740–2753
39. Vitali L, Valese AC, Azevedo MS, Gonzaga LV, Costa AC, Piovezan M, Vistuba JP, Micke GA (2013) Development of a fast and selective separation method to determine histamine in tuna fish samples using capillary zone electrophoresis. Talanta 106:181–185
40. Ballus CA, Meinhart AD, Bruns RE, Godoy HT (2011) Use of multivariate statistical techniques to optimize the simultaneous separation of 13 phenolic compounds from extra-virgin olive oil by capillary electrophoresis. Talanta 83:1181–1187
41. Moreno M, Sanchez Arribas A, Bermejo E, Zapardiel A, Chicharro M (2011) Analysis of polyphenols in white wine by CZE with amperometric detection using carbon nanotube-modified electrodes. Electrophoresis 32:877–883
42. Lee ISL, Boyce MC, Breadmore MC (2011) A rapid quantitative determination of phenolic acids in Brassica oleracea by capillary zone electrophoresis. Food Chem 127:797–801
43. Verardo V, Gomez-Caravaca AM, Segura-Carretero A, Caboni MF, Fernandez-Gutierrez A (2011) Development of a CE-ESI-microTOF-MS method for a rapid identification of phenolic compounds in buckwheat. Electrophoresis 32:669–673
44. Godoy-Caballero MP, Acedo-Valenzuela MI, Duran-Meras I, Galeano-Diaz T (2012) Development of a non-aqueous capillary electrophoresis method with UV-visible and fluorescence detection for phenolics compounds in olive oil. Anal Bioanal Chem 403:279–290
45. Godoy-Caballero MP, Galeano-Diaz T, Acedo-Valenzuela MI (2012) Simple and fast determination of phenolic compounds from different varieties of olive oil by nonaqueous capillary electrophoresis with UV-visible and fluorescence detection. J Sep Sci 35:3529–3539
46. Papieva IS, Kirsanov DO, Legin AV, Kartsova LA, Alekseeva AV, Vlasov YG, Bhattacharyya N, Sarkar S, Bandyopadkhyay R (2011) Analysis of tea samples with a multisensor system and capillary electrophoresis. Rus J Appl Chem 84:964–971
47. Franquet-Griell H, Checa A, Núñez O, Saurina J, Hernandez-Cassou S, Puignou L (2012) Determination of polyphenols in Spanish wines by capillary zone electrophoresis. Application to wine characterization by using chemometrics. J Agric Food Chem 60:8340–8349
48. Lee ISL, Boyce MC, Breadmore MC (2012) Extraction and on-line concentration of flavonoids in *Brassica oleracea* by capillary electrophoresis using large volume sample stacking. Food Chem 133:205–211
49. Bustamante-Rangel M, Delgado-Zamarreno MM, Carabias-Martinez R, Dominguez-Alvarez J (2012) Analysis of isoflavones in soy drink by capillary zone electrophoresis coupled with electrospray ionization mass spectrometry. Anal Chim Acta 709:113–119
50. Gonda S, Parizsa P, Surányi G, Gýmánt G, Vasas G (2012) Quantification of main bioactive metabolites from saffron (Crocus sativus) stigmas by a micellar electrokinetic chromatographic (MEKC) method. J Pharm Biomed Anal 66:68–74
51. Montealegre C, Sánchez-Hernández L, Crego A, Marina ML (2013) Determination and characterization of glycerophospholipids in olive fruit and oil by nonaqueous capillary electrophoresis with electrospray-mass spectrometric detection. J Agric Food Chem 61:1823–1832
52. Koyama M, Nakamura C, Nakamura K (2013) Changes in phenols contents from buckwheat sprouts during growth stage. J Food Sci Technol 50:86–93
53. Široká J, Martincová A, Pospíšilová M, Polášek M (2013) Assay of citrus flavonoids, Troxerutin, and ascorbic acid in food supplements and pharmaceuticals by capillary zone electrophoresis. Food Anal Methods 6:1561–1567
54. Soliman LC, Donkor KK, Church JS, Cinel B, Prema D, Dugan MER (2013) Separation of dietary omega-3 and omega-6 fatty acids in food by capillary electrophoresis. J Sep Sci 36:3440–3448
55. Bustamante-Rangel M, Delgado-Zamarreño MM, Pérez-Martín L, Carabias-Martínez R (2013) QuEChERS method for the extraction of isoflavones from soy-based foods before determination by capillary electrophoresis-electrospray ionization-mass spectrometry. Microchem J 108:203–209
56. Godoy-Caballero MP, Culzoni MJ, Galeano-Díaz T, Acedo-Valenzuela MI (2013) Novel combination of non-aqueous capillary electrophoresis and multivariate curve resolution-alternating least squares to determine phenolic

acids in virgin olive oil. Anal Chim Acta 763:11–19

57. León C, García-Cañas V, González R, Morales P, Cifuentes A (2011) Fast and sensitive detection of genetically modified yeasts in wine. J Chromatogr A 1218:7550–7556
58. Zhang S, Jiang C, Jia L (2011) Tetrabutylammonium phosphate-assisted separation of multiplex polymerase chain reaction products in non-gel sieving capillary electrophoresis. Anal Biochem 408:284–288
59. Holck AL, Pedersen BO (2011) Simple, sensitive, accurate multiplex quantitative competitive PCR with capillary electrophoresis detection for the determination of genetically modified maize. Eur Food Res Technol 233:951–991
60. Jiang C, Xu S, Zhang S, Jia L (2012) Chitosan functionalized magnetic particle-assisted detection of genetically modified soybeans based on polymerase chain reaction and capillary electrophoresis. Anal Biochem 420:20–25
61. Gonçalves J, Pereira F, Amorim A, van Asch B (2012) New method for the simultaneous identification of cow, sheep, goat, and water buffalo in dairy products by analysis of short species-specific mitochondrial DNA targets. J Agric Food Chem 60:10480–10485
62. Hernández-Chávez JF, González-Córdova AF, Rodríguez-Ramírez R, Vallejo-Cordoba B (2011) Development of a polymerase chain reaction and capillary gel electrophoresis method for the detection of chicken or turkey meat in heat-treated pork meat mixtures. Anal Chim Acta 708:149–154
63. Gavazzi F, Casazza AP, Depedro C, Mastromauro F, Breviario D (2012) Technical improvement of the TBP (tubulin-based polymorphism) method for plant species detection, based on capillary electrophoresis. Electrophoresis 33:2840–2851
64. Oh MH, Hwang HW, Chung B, Paik HD, Han S, Kang SM, Ham JS, Kim HW, Seol KH, Jang A, Jung GY (2012) Simultaneous detection of 10 foodborne pathogens using capillary electrophoresis-based single strand conformation polymorphism. Korean J Food Sci Ani Resour 32:241–246
65. Chung B, Shin GW, Na J, Oh MH, Jung GY (2012) Multiplex quantitative foodborne pathogen detection using high resolution CE-SSCP coupled stuffer-free multiplex ligation-dependent probe amplification. Electrophoresis 33:1477–1481
66. Vigentini I, De Lonrenzis G, Picozzi C, Imazio S, Merico A, Galafassi S, Piskur J, Poschino R (2012) Intraspecific variations of Dekkera/Brettanomyces bruxellensis genome studied by capillary electrophoresis separation of the intron splice site profiles. Int J Food Microbiol 157:6–15
67. Miya S, Takahashi H, Kamimura C, Nakagawa M, Kuda T, Kimura B (2012) Highly discriminatory typing method for Listeria monocytogenes using polymorphic tandem repeat regions. J Microbiol Methods 90:285–291
68. Valdés A, García-Cañas V, Cifuentes A (2013) CGE-laser induced fluorescence of double-stranded DNA fragments using GelGreen dye. Electrophoresis 34:1555–1562
69. Chen CH, Hsieh CH, Hwang DF (2013) PCR-RFLP analysis using capillary electrophoresis for species identification of Cyprinidae-related products. Food Control 33:477–483
70. Ruan J, Li M, Liu YP, Li YQ, Li YX (2013) Rapid and sensitive detection of Cronobacter spp. (previously Enterobacter sakazakii) in food by duplex PCR combined with capillary electrophoresis-laser-induced fluorescence detector. J Chromatogr B Anal Technol Biomed Life Sci 921–922:15–20
71. Truica GI, Teodor E, Dumitru E, Radu GL (2012) Quantification of ascorbic acid and B-complex vitamins in corn flour and corn flakes. Rev Chim 63:445–450
72. Tortajada-Genaro LA (2012) Determination of L-ascorbic acid in tomato by capillary electrophoresis. J Chem Educ 89:1194–1197
73. Dziomba S, Kowalski P, Baczek T (2012) Field-amplified sample stacking-sweeping of vitamins B determination in capillary electrophoresis. J Chromatogr A 1267:224–230
74. Galeano-Diaz T, Acedo-Valenzuela MI, Silva-Rodriguez AJ (2012) Determination of tocopherols in vegetable oil samples by non-aqueous capillary electrophoresis (NACE) with fluorimetric detection. Food Compos Anal 25:24–30
75. Da Silva DC, Visentainer JV, de Souza NE, Oliveira CC (2013) Micellar electrokinetic chromatography method for determination of the ten water-soluble vitamins in food supplements. Food Anal Meth 6:1592–1606
76. Chen J, Sun J, Liu S (2013) Determination of riboflavin in cereal grains by capillary electrophoresis with laser-induced fluorescence detection with on-line concentration. Anal Lett 46:887–899
77. Mu G, Luan F, Liu H, Gao Y (2013) Use of experimental design and artificial neural network in optimization of capillary electrophoresis for the determination of nicotinic acid and nicotinamide in food compared with high-performance liquid chromatography. Food Anal Meth 6:191–200

78. Meinhart AD, Ballus CA, Bruns RE, Lima Pallone JA, Godoy HT (2011) Chemometrics optimization of carbohydrate separations in six food matrices by micellar electrokinetic chromatography with anionic surfactant. Talanta 85:237–244
79. Sarazin C, Delaunay N, Costanza C, Eudes V, Mallet JM, Gareil P (2011) New avenue for mid-UV-range detection of underivatized carbohydrates and amino acids in capillary electrophoresis. Anal Chem 83:7381–7387
80. Tuma P, Malkova K, Samcova E, Stulik K (2011) Rapid monitoring of mono- and disaccharides in drinks, foodstuffs and foodstuff additives by capillary electrophoresis with contactless conductivity detection. Anal Chim Acta 698:1–5
81. Rizelio VM, Tenfen L, da Silveira R, Gonzaga LV, Oliveira Costa AC, Fett R (2012) Development of a fast capillary electrophoresis method for determination of carbohydrates in honey samples. Talanta 93:62–66
82. Cebolla-Cornejo J, Valcarcel M, Herrero-Martinez JM, Rosello S, Nuez F (2012) High efficiency joint CZE determination of sugars and acids in vegetables and fruit. Electrophoresis 33:2416–2423
83. Wang T, Yang X, Wang D, Jiao Y, Wang Y, Zhao Y (2012) Analysis of compositional carbohydrates in polysaccharides and foods by capillary zone electrophoresis. Carbohydr Polym 88:754–762
84. Taga A, Kodama S (2012) Analysis of reducing carbohydrates and fructosyl saccharides in maple syrup and maple sugar by CE. Chromatographia 75:1009–1016
85. Sarazin C, Delaunay N, Costanza C, Eudes V, Gareil P, Vial J (2012) On the use of response surface strategy to elucidate the electrophoretic migration of carbohydrates and optimize their separation. J Sep Sci 35:1351–1358
86. Sarazin C, Delaunay N, Costanza C, Eudes V, Gareil P (2012) Application of a new capillary electrophoretic method for the determination of carbohydrates in forensic, pharmaceutical, and beverage samples. Talanta 99:202–206
87. Vochyánová B, Opekar F, Tůma P, Štulík K (2012) Rapid determinations of saccharides in high-energy drinks by short-capillary electrophoresis with contactless conductivity detection. Anal Bioanal Chem 404:1549–1554
88. Jastrzebska A (2011) Capillary isotachophoresis as rapid method for determination of orthophosphates, pyrophosphates, tripolyphosphates and nitrites in food samples. J Food Comp Anal 24:1049–1056
89. Mikus P, Marakova K, Veizerova L, Piestansky J (2011) Determination of quinine in beverages by online coupling capillary isotachophoresis to capillary zone electrophoresis with UV spectrophotometric detection. J Sep Sci 34:3392–3398
90. Sanchez-Hernandez L, Castro-Puyana M, Marina ML, Crego AL (2011) Determination of betaines in vegetable oils by capillary electrophoresis tandem mass spectrometry—application to the detection of olive oil adulteration with seed oils. Electrophoresis 32:1394–1401
91. Zhang JB, Li MJ, Li WL, Chu QC, Ye JJ (2011) A novel capillary electrophoretic method for determining aliphatic aldehydes in food samples using 2-thiobarbituric acid derivatization. Electrophoresis 32:705–711
92. Zhang D, Zhang J, Li M, Li W, Aimaiti G, Tuersun G, Ye J, Chu Q (2011) A novel miniaturised electrophoretic method for determining formaldehyde and acetaldehyde in food using 2-thiobarbituric acid derivatisation. Food Chem 129:206–212
93. Heller M, Vitali L, Leal O, Marcone A, Costa AC, Micke GA (2011) A Rapid sample screening method for authenticity control of whiskey using capillary electrophoresis with online preconcentration. Agric Food Chem 59:6882–6888
94. Masotti F, Erba D, De Noni I, Pellegrino L (2012) Rapid determination of sodium in milk and milk products by capillary zone electrophoresis. J Dairy Sci 95:2872–2881
95. Carpio A, Mercader-Trejo F, Arce L, Valcarcel M (2012) Use of carboxylic group functionalized magnetic nanoparticles for the preconcentration of metals in juice samples prior to the determination by capillary electrophoresis. Electrophoresis 33:2446–2453
96. Kuban P, Kiplagat IK, Bocek P (2012) Electrokinetic injection across supported liquid membranes: New sample pretreatment technique for online coupling to capillary electrophoresis. Direct analysis of perchlorate in biological samples. Electrophoresis 33:2695–2702
97. Golubenko AM, Nikonorov VV, Nikitina TG (2012) Determination of hydroxycarboxylic acids in food products by capillary electrophoresis. J Anal Chem 67:778–782
98. Erdogan BY, Onar AN (2012) Determination of nitrates, nitrites and oxalates in kale and sultana pea by capillary electrophoresis. J Food Drug Anal 20:532–538
99. Akamatsu S, Mitsuhashi T (2012) Development of a simple capillary electrophoretic determination of glucosamine in nutritional supplements using in-capillary derivatisation with o-phthalaldehyde. Food Chem 130:1137–1141

100. Liotta E, Gottardo R, Seri C, Rimondo C, Miksik I, Serpelloni G, Tagliaro F (2012) Rapid analysis of caffeine in "smart drugs" and "energy drinks" by microemulsion electrokinetic chromatography (MEEKC). Forensic Sci Int 220:279–283
101. Yue ME, Xu J, Li QQ, Hou WG (2012) Separation and determination of bromophenols in *Trachypenaeus curvirostris* and *Lepidotrigla microptera* by capillary zone electrophoresis. J Food Drug Anal 20:88–93
102. Taga A, Sato A, Suzuki K, Takeda M, Kodama S (2012) Simple determination of a strongly aromatic compound, sotolon, by capillary electrophoresis. J Oleo Sci 61:45–48
103. Václavíková E, Kvasnička F (2013) Isotachophoretic determination of glucosamine and chondroitin sulphate in dietary supplements. Czech J Food Sci 1:55–65
104. Vachirapatama N, Maitresorasun S (2013) Simultaneous determination of melamine, ammelide, ammeline and cyanuric acid in milk products by micellar electrokinetic chromatography. J Food Drug Anal 21:66–72
105. Cheng YJ, Huang SH, Singco B, Huang HY (2011) Analyses of sulfonamide antibiotics in meat samples by on-line concentration capillary electrochromatography-mass spectrometry. J Chromatogr A 1218:7640–7647
106. Kowalski P, Plenis A, Oledzka I, Konieczna L (2011) Optimization and validation of the micellar electrokinetic capillary chromatographic method for simultaneous determination of sulfonamide and amphenicol-type drugs in poultry tissue. J Pharm Biomed Anal 54:160–167
107. Huang HY, Liu WL, Hsieh SH, Shih YH (2011) On-line concentration sample stacking coupled with water-in-oil microemulsion electrokinetic chromatography. J Chromatogr A 1218:7663–7669
108. Bodoki E, Iacob BC, Oprean R (2011) Capillary electromigration techniques for the quantitative analysis of colchicine. Croat Chem Acta 84:383–391
109. Hermo MP, Nemutlu E, Barbosa J, Barrón D (2011) Multiresidue determination of quinolones regulated by the European Union in bovine and porcine plasma. Application of chromatographic and capillary electrophoretic methodologies. Biomed Chromatogr 25:555–569
110. Wang Y, Xiao L, Cheng M (2011) Determination of phenylureas herbicides in food stuffs based on matrix solid-phase dispersion extraction and capillary electrophoresis with electrochemiluminescence detection. J Chromatogr A 1218:9115–9119
111. Zhang X, Zhang Z (2012) Capillary electrophoresis-based immunoassay with electrochemical detection as rapid method for determination of saxitoxin and decarbamoylsaxitoxin in shellfish samples. J Food Compos Anal 28:61–68
112. Piñeiro MY, Garrido-Delgado R, Bauza R, Arce L, Valcarcel M (2012) Easy sample treatment for the determination of enrofloxacin and ciprofloxacin residues in raw bovine milk by capillary electrophoresis. Electrophoresis 33:2978–2986
113. Mu G, Liu H, Xu L, Tian L, Luan F (2012) Matrix solid-phase dispersion extraction and capillary electrophoresis determination of tetracycline residues in milk. Food Anal Meth 5:148–153
114. Hu XZ, Chen ML, Gao Q, Yu QW, Feng YQ (2012) Determination of benzimidazole residues in animal tissue samples by combination of magnetic solid-phase extraction with capillary zone electrophoresis. Talanta 89:335–341
115. Santalad A, Srijaranai S, Burakham R (2012) Reversed electrode polarity stacking sample preconcentration combined with micellar electrokinetic chromatography for the analysis of carbamate insecticide residues in fruit juices. Food Anal Meth 5:96–103
116. Liu C, Fang G, Deng Q, Zhang Y, Feng J, Wang S (2012) Determination of metolcarb in food by capillary electrophoresis immunoassay with a laser-induced fluorescence detector. Electrophoresis 33:1471–1476
117. Domínguez-Álvarez J, Rodríguez-Gonzalo E, Hernández-Méndez J, Carabias-Martínez R (2012) Programed nebulizing-gas pressure mode for quantitative capillary electrophoresis-mass spectrometry analysis of endocrine disruptors in honey. Electrophoresis 33:2374–2381
118. Zhang X, Zhang Z (2013) Capillary electrophoresis-based immunoassay for the determination of brevetoxin-B in shellfish using electrochemical detection. J Chromatogr Sci 51:107–111
119. Zhu D, Zhang H, Bing X (2013) Preparation of an immunoaffinity column for the clean-up of fermented food samples contaminated with citrinin. Food Add Cont 20:389–394
120. Luque MI, Córdoba JJ, Rodríguez A, Núñez F, Andrade MJ (2013) Development of a PCR protocol to detect ochratoxin A producing moulds in food products. Food Control 29:270–278
121. Sun H, Qi H, Li H (2013) Development of capillary electrophoretic method combined with accelerated solvent extraction for simultaneous

determination of residual sulfonamides and their acetylated metabolites in aquatic products. Food Anal Meth 6:1049–1055

122. Ferey L, Delaunay N, Rutledge DN, Huertas A, Raoul Y, Gareil P, Vial J (2013) Use of response surface methodology to optimize the simultaneous separation of eight polycyclic aromatic hydrocarbons by capillary zone electrophoresis with laser-induced fluorescence detection. J Chromatogr A 1302:181–190
123. Knobel G, Campiglia AD (2013) Determination of polycyclic aromatic hydrocarbon metabolites in milk by a quick, easy, cheap, effective, rugged and safe extraction and capillary electrophoresis. J Sep Sci 36:2291–2298
124. Víctor-Ortega MD, Lara FJ, García-Campaña AM, Olmo-Iruela M (2013) Evaluation of dispersive liquideliquid microextraction for the determination of patulin in apple juices using micellar electrokinetic capillary chromatography. Food Control 31:353–358
125. Güray T, Tuncel M, Uysal UD (2013) A rapid determination of patulin using capillary zone electrophoresis and its application to analysis of apple juices. J Chromatogr Sci 51:310–317
126. Güray T, Tuncel M, Uysal UD, Oncu-Kaya EM (2013) Determination of zearalenone by the capillary zone electrophoresis-UV detection and its application to poultry feed and cereals. J Liq Chromatogr Relat Technol 36:1366–1378
127. Wei X, Gao X, Zhao L, Peng X, Zhou L, Wang J, Pu Q (2013) Fast and interference-free determination of glyphosate and glufosinate residues through electrophoresis in disposable microfluidic chips. J Chromatogr A 1281:148–154
128. Martínez-Villalba A, Núñez O, Moyano E, Galceran MT (2013) Field amplified sample injection-capillary zone electrophoresis for the analysis of amprolium in eggs. Electrophoresis 34:870–876
129. Domínguez-Álvarez J, Mateos-Vivas M, García-Gómez D, Rodríguez-Gonzalo E, Carabias-Martínez R (2013) Capillary electrophoresis coupled to mass spectrometry for the determination of anthelmintic benzimidazoles in eggs using a QuEChERS with preconcentration as sample treatment. J Chromatogr A 1278:166–174
130. Liu L, He B, Yun Z, Sun J, Jiang G (2013) Speciation analysis of arsenic compounds by capillary electrophoresis on-line coupled with inductively coupled plasma mass spectrometry using a novel interface. J Chromatogr A 1304:227–233
131. Polo-Luque ML, Simonet BM, Valcárcel M (2013) Solid phase extraction-capillary electrophoresis determination of sulphonamide residues in milk samples by use of C18-carbon nanotubes as hybrid sorbent materials. Analyst 138:3786–3791
132. Yoshikawa K, Saito S, Sakuragawa A (2012) Simultaneous analysis of acidulants and preservatives in food samples by using capillary zone electrophoresis with indirect UV detection. Food Chem 127:1385–1390
133. Bottoli CBG, Gutierrez-Ponce MJS, Aguiar VS, de Aquino WM (2011) Determination of parabens in sweeteners by capillary electrochromatography. J Pharm Sci 47:779–785
134. Zhang X, Xu S, Sun Y, Wang Y, Wang C (2011) Simultaneous determination of benzoic acid and sorbic acid in food products by CE after on-line preconcentration by dynamic pH junction. Chromatographia 73:1217–1221
135. Fukuji TS, Castro-Puyana M, Tavares MFM, Cifuentes A (2011) Fast determination of Sudan dyes in chilli tomato sauces using partial filling micellar electrokinetic chromatography. J Agric Food Chem 59:11903–11909
136. Fukuji TS, Castro-Puyana M, Tavares MFM, Cifuentes A (2012) Sensitive and fast determination of Sudan dyes in chilli powder by partial-filling micellar electrokinetic chromatography- tandem mass spectrometry. Electrophoresis 33:705–712
137. Mu G, Liu H, Gao Y, Luan F (2011) Determination of benzoyl peroxide, as benzoic acid, in wheat flour by capillary electrophoresis compared with HPLC. J Sci Food Agric 4:960–964
138. Mazorra-Manzano A, Torres-Llanez M, Gonzalez-Córdova MJ, González-Córdova AF, Vallejo-Cordoba B (2012) A capillary electrophoresis method for the determination of hydroxyproline as a collagen content index in meat products. Food Anal Method 5:46–470
139. Dong YL, Yan N, Li X, Zhou XM, Zhou L, Zhang HJ, Chen XG (2012) Rapid and sensitive determination of hydroxyproline in dairy products using micellar electrokinetic chromatography with laser-induced fluorescence detection. J Chromatogr A 1233:156–160
140. Hu F, Xu L, Luan F, Liu H, Gao Y (2013) Determination of neotame in non-alcoholic beverage by capillary zone electrophoresis. J Sci Food Agric 93:3334–3338
141. Petruci JF, Pereira EA, Cardoso AA (2013) Determination of 2-methylimidazole and 4-methylimidazole in caramel colors by capillary electrophoresis. J Agric Food Chem 61:2263–2267

142. Stojkovic M, Mai TD, Hauser PC (2013) Determination of artificial sweeteners by capillary electrophoresis with contactless conductivity detection optimized by hydrodynamic pumping. Anal Chim Acta 787:254–259
143. Fernandes VNO, Fernandes LB, Vasconcellos JP, Jager AV, Tonin FG, de Oliveira MAL (2013) Simultaneous analysis of aspartame, cyclamate, saccharin and acesulfame-K by CZE under UV detection. Anal Methods 5:1524–1532
144. Dominguez-Vega E, Crego AL, Lomsadze K, Chankvetadze B, Marina ML (2011) Enantiomeric separation of FMOC-amino acids by nano-LC and CEC using a new chiral stationary phase, cellulose tris(3-chloro-4-methylphenylcarbamate. Electrophoresis 32:2700–2707
145. Giuffrida A, Caruso R, Messina M, Maccarrone G, Contino A, Cifuentes A, Cucinotta V (2012) Chiral separation of amino acids derivatised with fluorescein isothiocyanate by single isomer derivatives 3-monodeoxy-3-monoamino-β- and -γ-cyclodextrins: the effect of the cavity size. J Chromatogr A 1269:360–365
146. Kodama S, Taga A, Aizawa S-I, Kemmei T, Honda Y, Suzuki K, Yamamoto A (2012) Direct enantioseparation of lipoic acid in dietary supplements by capillary electrophoresis using trimethyl-β-cyclodextrin as a chiral selector. Electrophoresis 33:2441–2445
147. Kodama S, Aizawa S, Taga A, Yamamoto A, Honda Y, Suzuki K, Kemmei T, Hayakawa K (2013) Determination of α-hydroxy acids and their enantiomers in fruit juices by ligand exchange CE with a dual central metal ion system. Electrophoresis 34:1327–1333
148. Kusano M, Redestig H, Hirai T, Oikawa A, Matsuda F, Fukushima A, Arita M, Watanabe S, Yano M, Hiwasa-Tanase K, Ezura H, Saito K (2011) Covering chemical diversity of genetically-modified tomatoes using metabolomics for objective substantial equivalence assessment. PLoS One 6:e16989
149. Simó C, Ibáñez C, Gómez-Martínez A, Ferragut JA, Cifuentes A (2011) Is metabolomics reachable? Different purification strategies of human colon cancer cells provide different CE-MS metabolite profiles. Electrophoresis 32:1765–1777
150. Celebier M, Ibañez C, Simó C, Cifuentes A (2012) A Foodomics approach: CE-MS for comparative metabolomics of colon cancer cells treated with dietary polyphenols. Methods Mol Biol 869:185–195
151. Ibáñez C, Simó C, García-Cañas V, Ferragut JA, Cifuentes A (2012) CE/LC-MS multiplatform for broad metabolomic analysis of dietary polyphenols effect on colon cancer cells proliferation. Electrophoresis 33:2328–2336
152. Ibáñez C, Valdés A, García-Cañas V, Simó C, Celebier M, Rocamora L, Gómez A, Herrero M, Castro M, Segura-Carretero A, Ibáñez E, Ferragut JA, Cifuentes A (2012) Global foodomics strategy to investigate the health benefits of dietary constituents. J Chromatogr A 1248:139–153
153. Valdés A, Simó C, Ibáñez C, Rocamora L, Ferragut JA, García-Cañas V, Cifuentes A (2012) Effect of dietary polyphenols on K562 leukemia cells: a foodomics approach. Electrophoresis 33:2314–2327
154. Contreras-Gutiérrez PK, Hurtado-Fernández E, Gómez-Romero M, Hormaza JI, Carrasco-Pancorbo A, Fernández-Gutiérrez A (2013) Determination of changes in the metabolic profile of avocado fruits (Persea americana) by two CE-MS approaches (targeted and non-targeted). Electrophoresis 34:2928–2942
155. Wishart DS, Knox C, Guo AC, Eisner R, Young N, Gautam B, Hau DD, Psychogios N, Dong E, Bouatra S, Mandal R, Sinelnikov I, Xia J, Jia L, Cruz JA, Lim E, Sobsey CA, Shrivastava S, Huang P, Liu P, Fang L, Peng J, Fradette R, Cheng D, Tzur D, Clements M, Lewis A, De Souza A, Zuniga A, Dawe M, Xiong Y, Clive D, Greiner R, Nazyrova A, Shaykhutdinov R, Li L, Vogel HJ, Forsythe I (2009) HMDB: a knowledgebase for the human metabolome. Nucleic Acids Res 37:D603–D610
156. Smith CA, O'Maille G, Want EJ, Qin C, Trauger SA, Brandon TR, Custodio DE, Abagyan R, Siuzdak G (2005) METLIN: a metabolite mass spectral database. Ther Drug Monit 27:747–751
157. Kanehisa M, Goto S (2000) KEGG: Kyoto encyclopedia of genes and genomes. Nucleic Acids Res 28:27–30

Chapter 23

Capillary Electrophoresis in Wine Science

Christian Coelho, Franck Bagala, Régis D. Gougeon, and Philippe Schmitt-Kopplin

Abstract

Capillary electrophoresis appeared to be a powerful and reliable technique to analyze the diversity of wine compounds. Wine presents a great variety of natural chemicals coming from the grape berry extraction and the fermentation processes. The first and more abundant after water, ethanol has been quantified in wines via capillary electrophoresis. Other families like organic acids, neutral and acid sugars, polyphenols, amines, thiols, vitamins, and soluble proteins are electrophoretically separated from the complex matrix.

Here, we will focus on the different methodologies that have been employed to conduct properly capillary electrophoresis in wine analysis.

Two examples informing on wine chemistry obtained by capillary electrophoresis will be detailed. They concern polyphenol analysis and protein profiling. The first category is a well-developed quantitative approach important for the quality and the antioxidant properties conferred to wine. The second aspect involves more research aspects dealing with microbiota infections in the vineyard or in the grape as well as enological practices.

Key words Capillary electrophoresis, Wine compounds, Polyphenols, Proteins, Sulfur compounds

1 Introduction

Numerous applications of capillary electrophoresis have grown since its first introduction in 1981 by Jorgenson and Lukacs [1]. They concern a variety of fields like pharmaceutical, food, or biological sciences requiring powerful and reliable analyses in complex matrices. Among them, wine presents a great variety of aromatic and nonvolatile compounds mixed within a highly diverse—yet partly unknown—oligomeric and macromolecular pool made of polysaccharides, proteins, and condensed tannins. Such diversity has been revealed with electrophoresis techniques involving conductimetric, amperometric, and photometric detection in the last two decades. Table 1 provides a non-exhaustive classification of the various wine compounds that have been separated by capillary electrophoresis with their analytical conditions including electrolyte

Philippe Schmitt-Kopplin (ed.), *Capillary Electrophoresis: Methods and Protocols*, Methods in Molecular Biology, vol. 1483, DOI 10.1007/978-1-4939-6403-1_23,

Table 1
Capillary electrophoresis parameters applied to the detection and quantification of wine compounds

Family	Wine active compounds	Electrolyte	Capillary	Injection mode	Detection	LOD	References
Alcohols	Ethanol	Barbital buffer 20 mM, sodium dodecyl sulfate 200 mM at pH 8.6	Fused silica capillary 25 μm, L = 33.5 cm	Hydrodynamic at 300 mBar	UV at 510 nm	–	[6]
Phenols	Hydroxytyrosol, tyrosol	Phosphate 25 mM, borate 10 mM at pH 8.8	Silica capillary tube 75 μm, L = 50 cm	Hydrodynamic at 3.45 kPa during 7 s	UV 206 nm	100–200 μg/L	[14]
Phenolic acids	Gallic acid, coumaric acid, vanillic acid, salicylic acid, hydroxybenzoic acid	Phosphate 25 mM, borate 10 mM at pH 8.8	Silica capillary tube 75 μm, L = 50 cm	Hydrodynamic at 3.45 kPa during 7 s	UV 217 nm	25–45 μg/L	[14]
	Caffeic acid	Phosphate 25 mM, borate 10 mM at pH 8.8 Borax 35 mM at pH 8.9	Silica capillary tube 75 μm, L = 50 cm Silica capillary tube 75 μm, L = 70 cm	Hydrodynamic at 3.45 kPa during 7 s Vacuum injection during 1 s	UV 217 nm UV 250 nm	286 μg/L 30 μg/L	[14] [21]
	Protocatechuic acid	Phosphate 25 mM, borate 10 mM at pH 8.8	Silica capillary tube 75 μm, L = 50 cm	Hydrodynamic at 3.45 kPa during 7 s	UV 206 nm	114 μg/L	[14]
	Gentisic acid	Phosphate 25 mM, borate 10 mM at pH 8.8	Silica capillary tube 75 μm, L = 50 cm	Hydrodynamic at 3.45 kPa during 7 s	UV 206 nm	80 μg/L	[14]
Phenolic aldehydes	Vanillin acid, syringaldehyde, coniferaldehyde, sinapaldehyde	Borate buffer 50 mM at pH 9.3	Silica capillary tube 50 μm, L = 53.5 cm	Hydrodynamic at 50 mBar during 4 s	UV 348, 362, 404 & 422 nm	150–275 μg/L	[24]

Stilbenes	Trans and cis resveratrol	Phosphate 25 mM, borate 10 mM at pH 8.8 75 mM sodium dodecyl sulfate, 30 mM boric acid, 30 mM dibasic phosphate, 15% acetonitrile at pH 9.2	Silica capillary tube 75 µm, L=50 cm Fused silica capillary 50 µm, L=37 cm	Hydrodynamic at 3.45 kPa during 7 s Hydrodynamic at 0.5 psi during 3 s	UV 206 & 312 nm UV 314 nm	18–50 µg/L 23–34 µg/L	[14] [3], [22]
Flavonols	Kaempferol, quercetin, luteolin, naringenin	Borax 35 mM at pH 8.9	Silica capillary tube 75 µm, L=70 cm	Vacuum injection during 1 s	UV 250 nm	50–100 µg/L	[21]
	Myricetin	Borax 35 mM at pH 8.9	Silica capillary tube 75 µm, L=70 cm	Vacuum injection during 1 s	UV 250 nm	600 µg/L	[21]
Flavanols	Catechin, epicatechin, epicatechin gallate	Phosphate 25 mM, borate 10 mM at pH 8.8	Silica capillary tube 75 µm, L=50 cm	Hydrodynamic at 3.45 kPa during 7 s	UV 206 nm	33–65 µg/L	[21]
Vitamins and cofactors	Riboflavin, flavin adenine dinucleotide, flavin mononucleotide	30 mM phosphate buffer at pH 9.8	Uncoated fused silica capillary tube 75 µm, L=92 cm	Hydrodynamic at 50 mbar during 10 s	Laser Induced Fluorescence with a 442 nm wavelength laser	0.5 µg/L	[35], [36]
Amino acids	Histidine, arginine, glycine, alanine, proline, valine, phenylalanine, tyrosine, tryptophane	20 mM of sodium dodecyl sulfate, 100 mM boric acid at pH 9.3	Fused silica capillary tube 50 µm, L=75 cm	Hydrodynamic injection at 0.8 psi during 10 s	Laser induced fluorescence with a 488 nm wavelength laser	–	[7]
Biogene amines	Spermidine, putrescine, cadaverine, histamine, spermine, putrescine, cadaverine, histamine, phenylethylamine, tyramine	100 mM boric acid, 50 mM SDS, 10% acetonitrile at pH 8.9 25 mM citric acid at pH 2.0	Coated capillary tube 50 µm, L=75 cm	Hydrodynamic during 5 s Mol/L G/mol Hydrodynamic at 50 mbar during 7 s	UV 254 nm MS (Ion trap, time of flight, and ESI)	5–200 µg/L 10–70 µg/L	[8] [17], [18]

(continued)

Table 1
(continued)

Family	Wine active compounds	Electrolyte	Capillary	Injection mode	Detection	LOD	References
Thiols	Glutathione	50 mM phosphate buffer at pH 7.0	Fused silica capillary tube 50 µm, L = 120 cm	Hydrostatic injection at 50 mbar during 3 s	Laser-induced fluorescence with a 410 nm wavelength laser	20 pg/L	[15]
Sulfur compounds		Working buffer with pH ranging between pH 1.66 and 10.55	Polyetheretherketone tubing capillary 100 µm, L = 50 cm	Hydrodynamic injection	Conductivity detector		[31]
Neutral sugars	Glucose, galactose, xylose, arabinose, mannose, ribose, rhamnose	50 mM borate buffer, 30% acetonitrile at pH 10.3	Uncoated fused silica capillary tube 50 µm, L = 77 cm	Hydrostatic injection at 50 mbar during 3 s under 3.45 kPa	UV at 200 nm		[4]
Acid sugars	Glucuronic acid, galacturonic acid, gluconic acid	5 mM β-resorcylic acid, 1 mM Tetradecyltrimethyl ammonium hydroxide at pH 3.0	Fused silica capillary 75 µm, L = 60 cm	Hydrostatic injection during 30 s	Indirect UV at 214 nm	5 mg/L	[11]

Organic acids	Tartaric acid, malic acid, citric acid, succinic acid, acetic acid, lactic acid	7 mM 2-N-morpholino-ethanesulfonic acid ; 0.5 mM tetradecyltrimethylammonium bromide and 30 % methanol at pH 6 200 mM phosphate buffer at pH 7.5 10 mM 3,5-dinitrobenzoic acid, 0.5 mM cetyltrimethylammonium bromide at pH 3.6	Polymide-clad fused silica capillary 75 µm, L = 67 cm Polyacrylamide fused coated capillary 50 µm, L = 50 cm Fused silica capillary 75 µm, L = 57 cm	Hydrostatic injection during 10–20 s Hydrostatic injection at 0.035 bar during 20 s Hydrostatic injection at 0.5 psi during 3 s	Conductivity Direct UV at 200 nm Indirect UV at 254 nm	– – 0.64–1.55 mg/L	[5] [37] [12]
Soluble proteins and polypeptides		100 mM tris(hydroxymethyl) aminoethane at pH 8.0 0.3 M borate buffer at pH 8.5 0.12 M Tris/HCl, SDS 1 % at pH 6.6	Uncoated fused silica capillary 75 µm, L = 57 cm Deactivated fused silica capillary 50 µm with a nonpolar surface, L = 24 cm Fused silica capillary 100 µm, L = 47 cm	Hydrostatic injection at 0.5 psi during 5 s Hydrostatic injection at 5 psi during 2–4 s Hydrostatic injection at 0.5 psi during 40s	UV at 214 nm UV at 200 and 280 nm UV at 214 nm	– – –	[25], [26] [27] [9]
Cations	Potassium, sodium, lithium, calcium, magnesium, barium	Imidazolium-based ionic liquid 0,03 mM at pH 5	Fused silica capillary tube 50 µm, L = 50 cm	Hydrodynamic injection	UV indirect at 207 and 209 nm	0.5–2 mg/L	[13]

composition and pH, capillary parameters, injection/detection modes, and limit of detection of each molecules.

Wine is a subtle matrix due to its direct acidic and ethanolic constitution. Low pH requires the use of alkaline buffer to facilitate the migration of phenolic type of wine constituents except strong organic acids. The presence of ethanol directly affects the viscosity of the electrolyte inside the capillary and modifies the electroosmotic flow of wine compounds facilitating the migration and improving analyte solubility [2]. However such organic modification of the electrolyte by ethanol renders unique the analysis of wine constituents not necessarily applicable to non-ethanolic samples like must, for instance.

1.1 Background Electrolyte Compositions

Phosphate or borate buffers with appropriated ionic strength and pH are mostly used electrolytes to separate a large class of wine compounds: flavonoids and non-flavonoids, amines, polypeptides, neutral sugars, vitamins, and cofactors. Wine polypeptides and soluble proteins have also been separated with tris(hydroxymethyl)aminoethane.

For the separation of acid sugars and organic acids, β-resorcylic acid, 2-(N-morpholino) ethanesulfonic acid, and dinitrobenzoic acid appeared to be good background electrolytes. However, additional organic flow modifiers, acting as cationic surfactant (tetradecyltrimethylammonium hydroxide, tetradecyltrimethylammonium bromide, or cetyltrimethylammonium bromide), have to be added to the buffer in order to reverse the electroosmotic flow and facilitate the separation of wine analytes.

Alternative methods also used other organic modifiers, such as methanol or acetonitrile, in order to alter the relative order of solute migration or selectivity [3–5].

Other electrophoretic methodologies were based on sodium dodecyl sulfate for the preparation of the electrolyte [6–9]. In this case, sodium dodecyl sulfate was used above its critical micellar concentration in order to build spherical micelles with the negatively charged sulfate groups pointing at the surface, thus providing additional partition between the pseudo-stationary phase and the electrolyte buffer for wine compounds. Such micellar electrokinetic chromatography clearly exhibited enhanced selectivity [6, 7, 10].

1.2 Detection of Wine Compounds

Wine electrophoresis mostly employs UV detection, either in the direct mode if wine compounds absorb in the UV or have been modified to present chromophores or in the indirect mode if wine compounds do not absorb UV radiation, as in the case of the detection of cations, acid sugars, and organic acids [11–13]. Conductimetry has also proven to efficiently detect wine organic acids [5]. Concerning important biologically peptides, amines, proteins, and vitamins that are present at trace levels in wine, laser-induced fluorescence appeared to be a powerful detector [7, 14, 15]. Very low limits of detection were reached, down to 20 pg/L

in the case of glutathione [15]. Mass spectrometry has also been coupled to capillary electrophoresis for the detection of phenolic compounds in red wines [16], biogenic amines [17, 18], and protein contents [19, 20]. The only limitation when using this detection is that the running buffer should be volatile and compatible to electrospray, ion trapping, and time-of-flight implementations.

2 Applications of Capillary Electrophoresis to Wine Research

Capillary electrophoresis provides high resolution, is fast and simple technique, consumes very few reagents and samples, and requires minimum preparation of sample even in complex matrices. It can advantageously replace usual separative techniques like gas chromatography for volatile compounds [6], or liquid chromatography for flavonoids [21]. It can even go further in the separation of isomers in the case of sugars [4] or stilbene analyses [3, 22, 23]. Among wine compounds that have been precisely quantified in the last decades, flavonoids and non-flavonoid polyphenols take a large place in wine analyses [3, 14, 16, 21–24]. Peptides and proteins started to be explored but were not so much exploited to deepen wine research [9, 19, 20, 25–27]. Due to the difficulty to separate such analytes (or cationic analytes in general) new suitable capillary modification is the first stage to perform to reduce analyte—capillary interactions.

2.1 Enantiomeric Analysis

Qualitative observation on L-arabinose and D-galacturonic acid contents, obtained from Riesling wine electropherograms, enabled to differentiate vintages due to differences in fermentation routes, infection processes by *Botrytis cinerea* during the grape maturation, and enzyme treatments occurring during winemaking [4].

Trans-resveratrol and *cis*-resveratrol present in red wines are easily distinguishable by electrophoresis [3, 22]. Table 2 indicates concentrations for each enantiomer in red wines. *Trans*-resveratrol is the most abundant isomer, with concentrations ranging from 1 to 25.5 μmol/L. Generally *trans*- and *cis*-resveratrol is present in grapes in their glycosylated forms and aglycones can be released after hydrolysis during fermentation. Differences in concentrations can be attributed to the cultivar, the growing region, and the yeast strains. In general Merlot and Pinot Noir wines exhibited the highest contents of resveratrol. The highest resveratrol amount of 25.5 μmol/L was obtained for the Oregon Pinot Noir. *Trans*- and *cis*-Piceid, the glycosylated forms of resveratrol, has also been identified in red wines [23].

2.2 Quantitative Analysis: Polyphenolic Contents in Wines

Wines present a large amount of phenolic compounds that can be readily oxidized by significant amounts of oxygen. The total amount of phenolics is quickly obtained by the Folin-Ciocalteu colorimetric assessment, usually expressed as a concentration in mg of gallic acid equivalent per liter. Global concentrations spanning

Table 2
Resveratrol concentration in red wine, from [3]

Variety or name	Maker	Vintage	Trans[a]	Cis[a]	Total
California					
Cabernet	J. Lohr-Cypress	1994	2.41 ± 0.16	ND	2.41
Zinfandel	Karly–Pokerville	1996	3.26 ± 0.08	ND	3.26
Cabernet Sauvignon	Sutter Home	1995	1.73 ± 0.09	ND	1.73
Special Reserve Red	Mountain View	none	10.16 ± 0.57	4.29 ± 0.13	14.45
Cabernet Sauvignon	Hawk Crest	1995	1.90 ± 0.29	0.65 ± 0.01	2.56
Merlot	Saintsbury	1996	1.90 ± 0.13	0.68 ± 0.10	2.58
Pinot Noir	Parducci	1996	7.93 ± 0.26	2.44 ± 0.07	10.37
Cabernet Sauvignon	Frey Mendocino	1995	0.99 ± 0.10	ND	0.99
Oregon					
Pinot Noir	Bethel Heights	1996	25.49 ± 2.34	ND	25.49
Washington					
Merlot	Paul Thomas	1995	11.78 ± 0.38	3.34 ± 0.07	15.12
France					
Cotes-Du-Rhone	George Duboeuf	1993	7.62 ± 0.62	1.18 ± 0.07	8.79
Beaujolais Villages	George Duboeuf	1996	6.52 ± 0.16	2.98 ± 0.11	9.50
Bordeaux	Chauteau Larose	1994	7.60 ± 0.31	1.66 ± 0.07	9.26
Bordeaux	Christian Moueix	1995	12.71 ± 0.89	2.37 ± 0.15	15.08
Chile					
Merlot	Sunrise-Concha Toro	1997	5.80 ± 0.29	2.52 ± 0.05	8.32
Cabernet Sauvignon	Castillero del Diablo	1996	4.02 ± 0.16	1.19 ± 0.06	5.21
Spain					
Tinto Reserva Pendes	Mont Marcal	1989	5.66 ± 0.15	0.69 ± 0.02	6.35
Red Navarra	Guelbenzu	1995	10.10 ± 0.27	1.47 ± 0.123	11.57
Australia					
Shiraz	Rosemount Estate	1997	6.78 ± 0.29	2.46 ± 0.08	9.24
Cabernet Sauvignon	Rosemount Estate	1995	6.40 ± 0.29	1.42 ± 0.07	7.82
Argentina					
Cabernet Sauvignon	Santa Julia	1995	5.11 ± 0.37	ND	5.11
Cabernet Sauvignon	Santa Julia	1995	6.78 ± 0.30	ND	6.78
Italy					

(continued)

Table 2
(continued)

Variety or name	Maker	Vintage	Trans[a]	Cis[a]	Total
Vino Nobile	Montepalciano	1991	2.88 ± 0.20	ND	2.88
Chianti Classico	Castello D'alboa	1995	4.99 ± 0.23	0.83 ± 0.03	5.82
Valpolicella Classico	Zenato	1994	5.06 ± 0.33	0.75 ± 0.03	5.82
Portugal					
Porto	Warre's	None	2.26 ± 0.10	0.70 ± 0.02	2.95

ND not detected

[a]Values for *trans*- and *cis*-resveratrol represent micromolar concentrations ± SD of the mean of three determinations

from 200 to 2000 mg/L were found, respectively, in white and red wines [28]. Simultaneously, individual polyphenolic identification and quantification could be achieved by means of a reliable analytical separative tool such as capillary electrophoresis. The key factor for the polyphenolic compounds to be separated is based on their charge-to-mass ratio, which is totally dependent on the electrolyte buffer pH and ionic strength.

Most of polyphenols have pKa comprised between 7 and 12, and in the presence of an appropriate buffer electrolyte with pH above 8, all phenolic substrates should be completely or partially ionized [29]. For that purpose, phosphate and borate buffers were mostly used for electrophoretic separations in wine. However, modification of the buffer ionic strength could affect the resolution and the analytical times [21].

As flavonoids and non-flavonoids are chromophoric structures, thanks to their aromatic rings, they are easily detectable spectrophotometrically with a diode array detector in the ultraviolet region.

2.3 Recent Advances in the Sulfur Chemistry of Wines

The diversity of yet-unknown sulfur compounds in wines has been described previously by ultrahigh-resolution FTICR-MS [30]. However, these results also emphasized the need for selective ionization strategies in order to overcome ion suppressions in the electrospray. Capillary electrokinetic fractionation (CEkF) was thus investigated as a simple and robust approach for semi-preparative and analytical sample analysis based on p*K*a-dependant pH-driven electrophoretic mobility [31]. Capillary electrokinetic fractionation/mass spectrometry (CEkF/MS): Technology setup and application to metabolite fractionation from complex samples coupled at line with ultrahigh-resolution mass spectrometry. In this study, CEkF was optimized with contactless conductivity detection and coupled on/at line to electrospray ionization (ESI) mass spectrometry (MS). A semi-empirical model was proposed, based

on the correlation between sample/medium pH regulating the partial charge and thus the electrokinetic loading of the capillary and intensity (I) of the highly resolved single-mass signals of the analytes as obtained after flow injection of the electrokinetically filled capillary into electrospray ion cyclotron-Fourier transform/mass spectrometry (ICR-FT/MS). According to the model, an empirical function ($I=f(\mathrm{pH})$) could be derived to calculate the acid dissociation constant (pKa) of various model compounds based on their pH-dependant MS intensity profiles. Using the ultrahigh resolution of ICR-FT/MS, the pKa model was further illustrated in real samples through the structure prediction of important compounds in wine for two different wine samples only differing by their age in bottle. The established CEkF was successfully used to selectively fractionate sulfur compounds from the complex wine samples, and it showed that S-containing compounds dominated the low-pH fractionations, especially in the old vintage, thus suggesting a specific stability of S-conjugated compounds over time. Moreover, the sulfur compounds found in low-pH fractionations were typically located in the van Krevelen area of sulfonated phenols and anthocyanins. The visualization indicated that CEkF conducted at extreme low pH preferentially orientates to sulfur compounds, which are highly polar and can be dissociated at extreme low pH. The proposed CEkF method is thus able to extract compounds with high polarity from highly complex matrices.

2.4 Peptides and Proteins in Wines: What Can Be Learnt by Capillary Electrophoresis?

Many macromolecules and proteins in particular tend to adsorb to the inner capillary surface of the capillary due to electrostatic and hydrophobic interactions. Adsorption leads to analytical problems (zone broadening, non-reproducible migration times, errors in quantification …). Two different approaches are offered to the analyst. The first consists in changing the chemistry of the electrolyte by changing its pH or its ionic strength or by adding specific additives. The second strategy involves a modified coating of the fused silica surface that in some cases appeared to be the most suitable strategy for the analysis of such biomolecules [32].

Analyses of variations in the concentrations of biomolecules (proteins, peptides, natural products) that occur either naturally or in response to environmental or genetic influences can provide important insights into complex biological processes. Wine is a complex system requiring a separation step before quantification of variations in the individual components. Several isolation methods have been tested: ultrafiltration, dialysis, and centrifugation [9, 27]. Centrifugation filter devices appeared to be the most convenient for isolate and concentrate wine proteins [9].

For wine samples, the large number of different proteins present and the small concentrations at which they can exist make such experiments difficult. SDS-PAGE has proven to be a powerful tool for the profiling of protein expression [33]. Combining isoelectric

focusing for charge-based separation to SDS-PAGE for size-based separation enabled to have hundreds of separated proteic components [34]. Improvements could be achieved by using capillary electrophoresis, which offers many advantages for the separation of a wide variety of molecules.

The first parameter, which conditions the proteinaceous pool of wine, has been shown to be the grape variety from which the wine has been elaborated. Very little difference was noted for wines coming from the same grape variety. However, the protein profiles differ slightly from a cooler growing region compared to a warmer one. The cooler one displayed fewer and smaller protein peaks [9, 27]. However, enological practices occurring during winemaking appeared to have little impact on the protein content. Skin contact, for instance, has been proven to increase the protein concentration without changing the profile of wine.

Capillary electrophoresis enabled to determine that the pool of high-molecular-weight proteins were more specifically involved in haze formation mechanism in white wines [27].

3 Materials and Equipment

3.1 Wine Polyphenol Quantification [14]

1. Analytes: Tyrosol, *cis*-resveratrol, *trans*-resveratrol, catechin, epicatechin, hydroxytyrosol, sinapic acid, epicatechin gallate, syringic acid, *o*-coumaric acid, *p*-coumaric acid, vanillic acid, gentisic acid, *p*-hydroxybenzoic acid, salicylic acid, caffeic acid, gallic acid, protocatechuic acid.
2. Sample: White wines (grape variety: *Chardonnay*, *Riesling* and *Cabernet Blanc*, *Greco di Tufo*, *Pinot Grigio*, *Verdicchio*, vintages: 2007 and 2008) from Argentina, Brazil, and Italy; rosé wine from Italia (vintage 2008); red wines (grape variety: *Pinot*, *Cabernet Sauvignon*, *Barbera*, *Montepulciano*, vintages: 2006 and 2008) from Brazil, Chile, Portugal, and Italy
3. Sample preparation: A liquid/liquid extraction with diethyl ether was carried twice in the dark and under nitrogen atmosphere. The diethyl extract was dried and resuspended in the electrophoretic buffer with 10% of methanol.
4. CE instrument and capillary: Beckman P/ACE Station 5000 Software equipped with a Diode Array Detector. Uncoated fused silica capillary tube of 75 μm with effective and total lengths of 50 and 57 cm, respectively.
5. CE buffer: The buffer was obtained by mixing H_3BO_3 (100 mmol/L) and Na_2HPO_4 (100 mmol/L) and NaOH (2 mol/L) to reach the final composition of phosphate 25 mmol/L, borate 10 mmol/L, and a fixed pH of 8.8.

3.2 Analysis of Wine Proteins and Polypeptides [9]

1. Analytes: Standard proteins from 14.2 to 205 kDa are used as molecular weight markers: α-lactalbumin (14.2 kDa), carbonic anhydrase (29 kDa), ovalbumin (45 kDa), bovine serum albumin (66 kDa), phosphorylase b (97.4 kDa), β-galactosidase (116 kDa), mysosin (205 kDa).
2. Sample: White wine from Tenerife island and red wines from Tenerife, Lanzarote, and Gran Canaria islands. Grape varieties used to produce these wines are *Listan*, *Negro*, and *Negramoll*.
3. Sample preparation: The wine is pre-concentrated by using centrifugal filter devices with a centrifugation for 30 min at 13,000 × *g* and a molecular weight membrane cutoff of 10 kDa. The retentate is transferred to an Eppendorf vial after a new centrifugation for 3 min at 1000 × *g*. The retentate is dissolved in the electrophoretic buffer by adding Orange G Reference Marker and 2-mercaptoethanol. The final solution is stirred and heated at 100 °C for 10 min in a closed microfuge vial, prior to cooling for 3 min and filtering with a 0.22 μm filter.
4. CE instrument and capillary: Beckman P/ACE Station 5510 Software equipped with a Diode Array Detector. Coated fused silica capillary tube of 100 μm with effective and total lengths of 40 cm and 47 cm, respectively.
5. CE buffer: Tris/HCl/sodium dodecyl sulfate 1%, at pH 6.6.

4 Methods

4.1 Wine Polyphenol Analysis

1. The capillary is pre-rinsed with ultrapure water for 1.5 min and electrophoretic buffer for 1.5 min. Before each measuring, the capillary is rinsed with a solution of HCl (0.1 mol/L) for 1.5 min, NaOH (0.1 mol/L) for 1.5 min, and ultrapure water for 1.5 min.
2. Inject the sample hydrodynamically for 7 s with 3.45 kPa.
3. Run sample under 15 kV with running buffer and detect peaks at the specific wavelength corresponding to the maximum of absorption of each wine analytes, in order to improve sensitivity.
4. Figure 1 shows an electropherogram for a diethyl ether extract white wine.
5. Calibration is used for the determination of the analyte concentration from integrated peak area. Concentrations of calibrated samples spanned from 1 to 50 mg/L.

4.2 Wine Protein Analysis

1. The new capillary is pre-conditioned with HCl (1 mol/L) for 10 min. The capillary is daily conditioned with HCl (1 mol/L) for 5 min and electrophoretic buffer for 10 min. After each injection, the capillary is rinsed with a solution of HCl

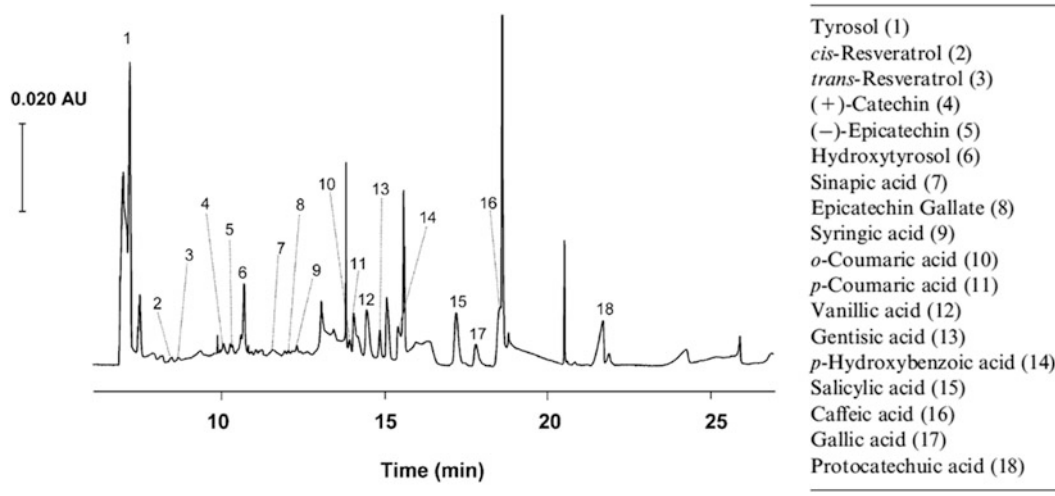

Fig. 1 Electropherogram of a white wine diethyl ether extract, with its 18 identified polyphenols. Conditions: uncoated fused silica capillary of 57 cm total length (500 cm of effective length) with 75 μm of inner diameter. The electrophoretic buffer is a mixture of phosphate 25 mmol/L and borate 10 mmol/L, at pH 8.8. UV detection. Injection for 7 s at a pressure of 3.45 kPa. Figure adapted from [14]

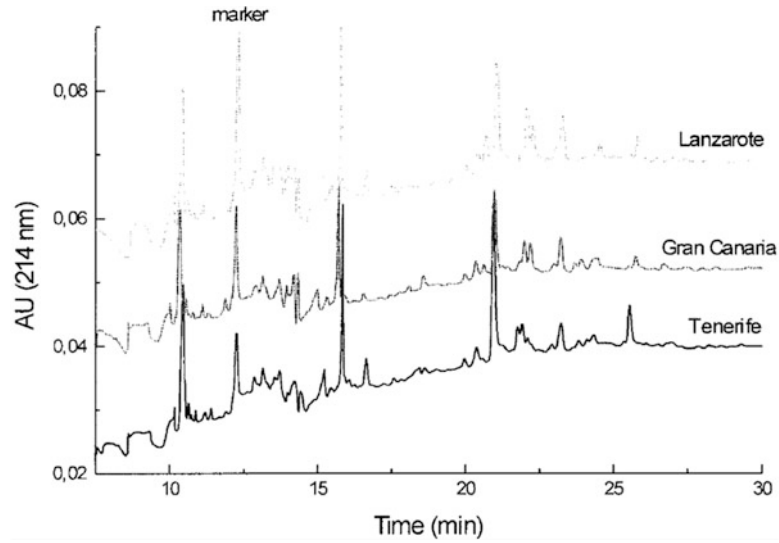

Fig. 2 Protein profiling of three red wines from Lanzarote, Gran Canaria, and Tenerife islands after a concentration step using centrifugal filter devices. Conditions: Coated capillary of 47 cm total length (40 cm of effective length) with 100 μm of inner diameter. The electrophoretic buffer is a mixture of Tris/HCl/ sodium dodecyl sulfate 1 %, at pH 6.6. Detection at 214 nm. Injection for 40 s using N2 pressure (0.5 psi). Standard protein migration times are ranging from 15.2 min (corresponding to 14.2 kDa) to 27. 5 min (corresponding to 205 kDa). Figure adapted from [9]

(0.1 mol/L) for 1 min and the electrophoretic buffer for 5 min. At the end of each day, the capillary is rinsed with water for 5 min, HCl (0.1 mol/L) for 5 min, and the buffer for 5 min.

2. Inject the sample hydrodynamically for 40 s with 0.5 psi at the cathode.
3. Run sample under –14.1 kV with running buffer and detect peaks at 214 nm.
4. Figure 2 shows sucha a protein profiling of three red wines from Lanzarote, Gran Canaria, and Tenerife islands.
5. Standard proteins are treated with sodium dodecyl sulfate and 2-mercaptoethanol like the wine proteins and injected at the beginning of each running day. Orange G is added to all injected samples as marker in order to calculate the relative migration time t_M (protein migration time/Orange G migration time). The molecular weights (MW) of unknown wine proteins are calculated from the linear regression equation of $\log MW = 1/t_M$.

References

1. Jorgenson JW, Lukacs KD (1981) Zone electrophoresis in open-tubular glass capillaries. Anal Chem 53:1298–1302
2. VanOrman BB, Liversidge GG, McIntire GL, Olefirowicz TM, Ewing AG (1990) Effects of buffer composition on electroosmotic flow in capillary electrophoresis. J Microcolumn Sep 2:176–180
3. Gu X, Creasy L, Kester A, Zeece M (1999) Capillary electrophoretic determination of resveratrol in wines. J Agric Food Chem 47:3223–3227
4. Noe CR, Lachmann B, Möllenbeck S, Richter P (1999) Determination of reducing sugars in selected beverages by capillary electrophoresis. Z Lebensm Unters Forsch 208:148–152
5. Huang X, Luckey JA, Gordon MJ, Zare RN (1989) Quantitative determination of low molecular weight carboxylic acids by capillary zone electrophoresis/conductivity detection. Anal Chem 61:766–770
6. Collins TS, Miller CA, Altria KD, Waterhouse AL (1997) Development of a rapid method for the analysis of ethanol in wines using capillary electrophoresis. Am J Enol Vitic 48:280–284
7. Nouadje G, Siméon N, Dedieu F, Nertz M, Puig P, Couderc F (1997) Determination of twenty eight biogenic amines and amino acids during wine aging by micellar electrokinetic chromatography and laser-induced fluorescence detection. J Chromatogr A 765:337–343
8. Kovács Á, Simon-Sarkadi L, Ganzler K (1999) Determination of biogenic amines by capillary electrophoresis. J Chromatogr A 836:305–313
9. Rodríguez-Delgado M, Malovaná S, Montelongo F, Cifuentes A (2002) Fast analysis of proteins in wines by capillary gel electrophoresis. Eur Food Res Technol 214:536–540
10. Hsieh M-C, Lin C-H (2004) On-line identification of trans-resveratrol in red wine using a sweeping technique combined with capillary electrophoresis/77 K fluorescence spectroscopy. Electrophoresis 25:677–682
11. de Valme García Moreno M, Castro Mejías R, Natera Marín R, García Barroso C (2002) Analysis of sugar acids by capillary electrophoresis with indirect UV detection. Application to samples of must and wine. Eur Food Res Technol 215:255–259
12. Peres RG, Moraes EP, Micke GA, Tonin FG, Tavares MFM, Rodriguez-Amaya DB (2009) Rapid method for the determination of organic acids in wine by capillary electrophoresis with indirect UV detection. Food Control 20:548–552
13. Qin W, Wei H, Li SFY (2003) 1,3-Dialkylimidazolium-based room-temperature ionic liquids as background electrolyte and coating material in aqueous capillary electrophoresis. J Chromatogr A 985:447–454
14. Minussi RC, Rossi M, Bologna L, Cordi LV, Rotilio D, Pastore GM, Durán N (2003) Phenolic compounds and total antioxidant potential of commercial wines. Food Chem 82:409–416
15. Lavigne V, Pons A, Dubourdieu D (2007) Assay of glutathione in must and wines using capillary electrophoresis and laser-induced flu-

orescence detection: changes in concentration in dry white wines during alcoholic fermentation and aging. J Chromatogr A 1139:130–135
16. Vanhoenacker G, De Villiers A, Lazou K, De Keukeleire D, Sandra P (2001) Comparison of high-performance liquid chromatography—mass spectroscopy and capillary electrophoresis—mass spectroscopy for the analysis of phenolic compounds in diethyl ether extracts of red wines. Chromatographia 54:309–315
17. Simó C, Moreno-Arribas MV, Cifuentes A (2008) Ion-trap versus time-of-flight mass spectrometry coupled to capillary electrophoresis to analyze biogenic amines in wine. J Chromatogr A 1195:150–156
18. Santos B, Simonet BM, Ríos A, Valcárcel M (2004) Direct automatic determination of biogenic amines in wine by flow injection-capillary electrophoresis-mass spectrometry. Electrophoresis 25:3427–3433
19. Simó C, Elvira C, González N, San Román J, Barbas C, Cifuentes A (2004) Capillary electrophoresis-mass spectrometry of basic proteins using a new physically adsorbed polymer coating. Some applications in food analysis. Electrophoresis 25:2056–2064
20. Zhao SS, Zhong X, Tie C, Chen DD (2012) Capillary electrophoresis-mass spectrometry for analysis of complex samples. Proteomics 12:2991–3012
21. Wang S-P, Huang K-J (2004) Determination of flavonoids by high-performance liquid chromatography and capillary electrophoresis. J Chromatogr A 1032:273–279
22. Gu X, Chu Q, O'Dwyer M, Zeece M (2000) Analysis of resveratrol in wine by capillary electrophoresis. J Chromatogr A 881:471–481
23. Brandolini V, Maietti A, Tedeschi P, Durini E, Vertuani S, Manfredini S (2002) Capillary electrophoresis determination, synthesis, and stability of resveratrol and related 3-O-β-d-glucopyranosides. J Agric Food Chem 50:7407–7411
24. Panossian A, Mamikonyan G, Torosyan M, Gabrielyan E, Mkhitaryan S (2001) Analysis of aromatic aldehydes in brandy and wine by high-performance capillary electrophoresis. Anal Chem 73:4379–4383
25. Luguera C, Moreno-Arribas V, Pueyo E, Polo MC (1997) Capillary electrophoretic analysis of wine proteins. Modifications during the manufacture of sparkling wines. J Agric Food Chem 45:3766–3770
26. Luguera C, Moreno-Arribas V, Pueyo E, Bartolome B, Polo MC (1998) Fractionation and partial characterization of protein fractions present at different stages of the production of sparkling wines. Food Chem 63:465–471
27. Dizy M, Bisson LF (1999) White wine protein analysis by capillary zone electrophoresis. Am J Enol Vitic 50:120–127
28. Waterhouse AL (2002) Wine phenolics. Ann N Y Acad Sci 957:21–36
29. Herrero-Martínez JM, Sanmartin M, Rosés M, Bosch E, Ràfols C (2005) Determination of dissociation constants of flavonoids by capillary electrophoresis. Electrophoresis 26:1886–1895
30. Roullier-Gall C, Boutegrabet L, Gougeon RD, Schmitt-Kopplin P (2014) A grape and wine chemodiversity comparison of different appellations in Burgundy: vintage vs terroir effects. Food Chem 152:100–107
31. He Y, Harir M, Chen G, Gougeon RD, Zhang L, Huang X, Schmitt-Kopplin P (2014) Capillary electrokinetic fractionation mass spectrometry (CEkF/MS): technology setup and application to metabolite fractionation from complex samples coupled at-line with ultrahigh-resolution mass spectrometry. Electrophoresis 35:1965–1975
32. Schmalzing D, Piggee CA, Foret F, Carrilho E, Karger BL (1993) Characterization and performance of a neutral hydrophilic coating for the capillary electrophoretic separation of biopolymers. J Chromatogr A 652:149–159
33. Dorrestein E, Ferreira RB, Laureano O, Teixeira AR (1995) Electrophoretic and FPLC analysis of soluble proteins in four portuguese wines. Am J Enol Vitic 46:235–242
34. Cilindre C, Jégou S, Hovasse A, Schaeffer C, Castro AJ, Clément C, Van Dorsselaer A, Jeandet P, Marchal R (2008) Proteomic approach to identify champagne wine proteins as modified by Botrytis cinerea infection. J Proteome Res 7:1199–1208
35. Cataldi TRI, Nardiello D, Scrano L, Scopa A (2002) Assay of riboflavin in sample wines by capillary zone electrophoresis and laser-induced fluorescence detection. J Agric Food Chem 50:6643–6647
36. Cataldi TRI, Nardiello D, De Benedetto GE, Bufo SA (2002) Optimizing separation conditions for riboflavin, flavin mononucleotide and flavin adenine dinucleotide in capillary zone electrophoresis with laser-induced fluorescence detection. J Chromatogr A 968:229–239
37. Saavedra L, Barbas C (2003) Validated capillary electrophoresis method for small-anions measurement in wines. Electrophoresis 24:2235–2243

Index

A

Acids 11, 53, 54, 56, 57, 60, 63–65, 67, 68, 70, 71, 81–85, 94, 99–102, 111–120, 122, 123, 125, 126, 134–137, 139–145, 157, 161, 163, 171, 172, 174, 175, 187, 189, 198–201, 213, 218–227, 232, 237, 238, 241–243, 246, 250–268, 271, 283, 284, 287, 288, 292, 296, 301–305, 315, 340–359, 366, 372, 374, 376, 377, 379, 380, 384–387, 395, 398, 400, 401, 409–411, 413–416, 419, 420, 423, 426, 427, 438–454, 456, 458–460, 462–464, 473, 475–478, 480–488, 490, 491, 494, 497, 498, 510–512, 514, 515, 518, 519
Actinides 217
Acylamino acids 288
Alditols 301, 303, 314, 315
Amino acids ..... v, 24, 53, 56, 57, 60, 99–101, 115, 250–268, 271, 283, 284, 287, 303, 305, 366–369, 374, 376, 377, 385, 438–440, 446, 450, 451, 488, 511
Aminoalcohols 32–33
Aminoglycosides 77, 79–84, 87, 88

B

Background electrolyte (BGE) 29, 41, 54, 55, 58, 61, 63, 65–68, 71, 72, 77, 81, 82, 84, 111–127, 135, 155–157, 160–164, 177, 198, 199, 207, 239, 241, 252, 259, 263–266, 269, 270, 277–280, 283, 284, 287–293, 295, 297, 303, 305, 315, 366, 367, 370, 372, 373, 379, 382, 384–386, 388, 395, 401, 402, 409, 410, 413, 419, 422, 439, 442, 444–446, 450, 452, 453, 460, 461, 494, 514
Bacterial aggregation 394, 398, 402
Bases 126, 140, 144, 145, 183, 239, 296, 304, 315, 349, 385, 388, 462–464
Bile salts 79, 96, 288
Bioanalytical applications 122–125, 250–268, 271
Biological samples 41, 43, 147, 169, 174, 266, 339, 370, 371, 383, 464
Bromine 207–208
Butanol 43, 47, 48, 92, 95, 97, 98, 100–103, 473, 482

C

Capillary electrophoresis (CE) ..... v, 3, 4, 11, 17, 32, 33, 77, 91, 99, 103, 111–127, 134–145, 155, 158–160, 162–165, 168–172, 174–178, 181–193, 197–205, 207, 210, 213, 218–228, 240–242, 245, 250–268, 271, 277–293, 295–297, 301–304, 312–316, 322, 324, 326, 328, 339–353, 355–357, 359, 365–374, 376, 378, 379, 382–389, 394–402, 404, 405, 407–413, 415–419, 421, 422, 424, 426–428, 430, 434, 437, 452–455, 460, 461, 464, 472, 492, 509–521
Capillary electrophoresis–mass spectrometry (CE–MS) 41, 53–57, 59, 61, 63, 65–68, 70–73, 155, 265, 267, 288, 369, 372, 402, 404, 452, 454–457, 460, 464, 472, 493, 495, 496, 499
Capillary zone electrophoresis (CZE) ..... v, 9, 10, 21, 30–33, 77, 80, 82, 83, 98, 99, 134, 155–165, 170, 199, 202, 217–229, 231–235, 237–246, 251–262, 305–307, 309, 322, 323, 325–326, 340–346, 350, 352, 366–368, 380, 395–397, 401, 424, 439, 441, 450, 473–478, 480–489
Carboxylated sugars 291, 313
Charge density 30, 65, 146, 278, 280, 349, 355, 357, 359, 365–367
Charged polysaccharides 348, 357
Chiral selector 39, 120, 139, 142, 143, 259, 263, 277–290, 294, 296, 367, 372, 379, 380, 488
Chiral separations 97, 98, 156, 251, 259–263
Chlorine 198, 202–203, 208–211
Coatings 53–58, 60–62, 64–68, 70–73, 119, 120, 127, 134–139, 142, 144, 148, 160, 164, 185, 187, 213, 290, 295, 370, 373, 383, 387, 398, 400, 402, 404, 518
Complexing agents 30, 78, 199, 218, 219, 224
Cyclodextrins (CDs) 78, 83, 95, 98, 101, 115, 117, 120, 122, 125, 126, 139, 140, 142, 147–150, 155, 200, 205, 263, 264, 278, 283, 285–286, 288–290, 293–295, 297, 314, 318, 372, 379, 408, 413, 424

D

Derivatization 37–50, 80, 82–84, 99–101, 203, 237, 263, 265, 266, 268, 271, 279, 284, 303–325, 328, 341, 343, 345, 354, 368, 369, 371, 372, 379, 455, 458–460, 464, 473–475, 480–483, 485, 487, 488
Dithiocarbamates 408, 411–412, 421–422, 433
Dyes 144, 263, 312, 320, 408–410, 419–421

Philippe Schmitt-Kopplin (ed.), *Capillary Electrophoresis: Methods and Protocols*, Methods in Molecular Biology, vol. 1483, DOI 10.1007/978-1-4939-6403-1, © Springer Science+Business Media New York 2016

E

Effective mobility 8, 9, 11–14, 16, 17, 22, 33, 55, 59, 61, 278, 279, 281
Electrokinetic chromatography (EKC) 77, 79–84, 87, 88, 91, 92, 94–106, 117, 118, 125, 126, 156, 170, 251, 277, 279, 284, 287, 288, 366, 367, 379, 413, 514
Electromigration techniques 114, 156, 366, 394, 397
Electroosmotic flow (EOF) 5, 6, 9, 17, 55, 61, 62, 65, 67, 73, 78, 80, 92–94, 96, 97, 99, 117, 118, 156, 199, 204, 231, 235, 240, 263, 278, 280, 281, 284, 288, 290, 293, 294, 296, 315, 368, 370, 373, 374, 377–380, 383, 384, 387, 394, 397, 398, 412, 514
Electroosmotic flow (EOF) velocity 56, 65
Electrophoretic mobility 9, 16, 23, 30, 32, 55, 59, 61, 62, 68, 78, 80, 92, 94, 105, 112, 119, 135, 136, 142, 201, 277, 278, 280, 282, 283, 347–351, 355–359, 366, 367, 374, 378, 380, 382, 394, 398, 399, 409, 517
Electrospray ionization (ESI) 99, 119, 134, 155–165, 227, 245, 252–256, 258, 260, 262, 266–268, 345, 369, 492, 517
Enantiomer separation 96, 277–293, 295–297
Endocrine disruptors 102, 408, 413–414, 424–426
Environmental organic pollutants 408
Explosives 246, 408, 417–418, 426–429

F

Fatty acids 100, 101, 452–465
Fluorescein isothiocyanate (FITC) 42, 99, 252–255, 257, 260–262, 473, 474, 480, 485, 488
Fluorine 133
Food bioactivity 489
Food omics 437, 472–489
Food quality 471, 472, 489
Food safety 471, 489
Food samples 41
Food traceability 489
Formaldehyde releasers 32–33

G

Gentamicin 80–83, 85, 87
Glycoconjugates 301, 303, 342, 346, 349–350
Glycosaminoglycans oligosaccharides 304, 316
Glycosides 283, 302, 303, 316, 321, 324, 328, 476
Glycosylamines 314, 316–321, 323–325, 328

H

Hyaluronan (HA) 340, 341, 343, 344, 346, 348–353, 355–357, 359
Hydrodynamic injection 4, 5, 99, 103, 104, 126, 162, 204, 237, 297, 388, 424
Hydrophobic interaction 55, 60, 65, 134, 384, 518

I

In-capillary 38, 41, 43, 45, 82, 201–203, 237, 263, 313, 483, 487
Inductively coupled plasma mass spectrometry 168–172, 174–178
Intact cell analysis 403–404
Interface 5, 6, 47, 65, 92, 99, 100, 113, 116, 120, 124, 127, 156, 158, 159, 168–174, 182, 201, 226, 227, 241, 265, 398, 446, 460, 492, 494, 499
Iodine 199, 203–204, 210–213
Ionic liquids (IL) 43, 96, 98, 131, 133, 137, 143, 199–200, 204, 205, 220, 229–231, 283, 513

K

Kanamycin 80, 83

L

Lanthanides 168, 219, 224–226, 239–242

M

Mass spectrometric (MS) detection 55, 99, 112, 120–122, 126, 155, 156, 159, 227, 263, 403
Mass spectrometry (MS) ..... v, 38, 39, 67, 71, 111–127, 155–165, 168–172, 174–178, 226, 227, 241, 245, 252–256, 258, 260, 263–268, 278, 288, 304, 311, 312, 314, 315, 321, 369, 399, 400, 403, 438, 472, 515, 517
Matrix-assisted laser desorption/ionization mass spectrometry (MALDI MS) 312, 397, 402–404
MEKC. *See* Micellar electrokinetic chromatography (MEKC)
Metabolomics 250, 372, 437, 452–455, 460, 461, 464, 472, 490
Metal ions 197–200, 217–229, 231–235, 237–246, 264, 271, 284, 367, 380, 397–399
Metal ligand interactions 217
Method development 22, 34, 277, 289–290, 303, 366, 367, 372–384
Micellar electrokinetic chromatography (MEKC) ..... v, 17, 38, 77, 79–84, 87, 88, 93, 138–142, 156, 170, 251–262, 277, 284, 288, 289, 307, 308, 310, 325–327, 340, 343–345, 347, 352–355, 366–368, 378–380, 383, 413, 418, 425, 428, 439, 473, 477, 480, 483–485, 487, 514
Microemulsion 91, 92, 94–106, 277, 287, 289, 290, 368
Microwave-accelerated derivatization 37
Migration mode 280–283
Mobility-scale 3
Mobility simulation 21
Model 21, 22, 24–26, 29, 43, 44, 57, 118, 201, 202, 221, 280, 322, 348–351, 356, 367, 371, 375, 376, 381, 382, 386, 492, 517, 518

Molar mass distribution....339
Monosaccharides.... 301–304, 312–316, 320, 322, 324, 326, 328, 342

N

Neutral sugars....303, 304, 312, 315, 317, 319, 512, 514
Nitrogen....197, 213, 266, 268, 271, 490, 493, 494, 499, 519
Nonaqueous capillary electrophoresis.... 111–127, 229
Non-targeted....437, 439, 440, 442, 444, 445, 447, 451–465

O

Oligosaccharides....133, 283, 301–304, 312–316, 322, 324, 326, 328, 340, 342, 347, 352–355, 379, 446
o-Phthaldialdehyde (OPA)....41, 81, 84, 85, 88, 252, 258, 369, 483

P

Paraquat and diquat.... 408, 412, 422
Peptide analysis 53–57, 59, 61, 63, 65–68, 70–73, 365–374, 376, 378, 379, 382–389
Peptides....v, 21, 22, 24, 25, 30, 53–57, 59, 61, 63, 65–68, 70–73, 122, 133, 155, 159, 163, 164, 251, 268, 270, 302, 365–374, 376, 378, 379, 382–389, 474, 475, 514, 515, 518–519
Pesticides 30, 408, 410–412, 421–422, 433, 483
Phenolic pollutants....408
Phenoxy acids....408, 410–411, 421, 422
Phosphorus....168, 198, 201–202, 207
Phthalates....102, 198, 408, 409, 419
Polycyclic aromatic hydrocarbons.... 102, 408, 418–419, 485
Polyphenols 135, 476, 488, 489, 515–521
Pre-capillary 263
Problem solutions....172
Proteins 21, 22, 55–57, 61, 62, 69, 73, 100, 136, 155, 159, 163, 164, 169, 175, 250, 253, 258, 265, 266, 268, 270, 278, 283, 301, 347, 366, 368, 371, 398, 399, 403, 472, 474, 475, 483, 486, 509, 513–515, 518–522
Pseudo-stationary phase 77, 78, 80, 93, 94, 97–99, 277, 279, 287, 289
Pseudostationary phase....367, 378

R

Random degradation 347
Reductive amination.... 304, 312–314
Resolution ....v, 14, 53–57, 59, 61, 63, 65–68, 70–73, 79, 83, 96, 105, 124, 133, 135–137, 139, 141, 142, 147–150, 156, 171, 199, 208, 240, 265, 267, 278, 290, 295, 303, 366–368, 372, 373, 377–384, 394, 490, 515, 517
Rhizosphere.... 181–185, 187–193

S

Semi-empirical model 517
Separation optimization 4, 7–9, 11–17, 84, 95–98, 121
Sialic acids 63, 302, 303, 306, 313, 319, 320
Single cell analysis 182
Single cell sampling....182, 189
Small ions....197–205, 207, 210, 213
Speciation.... 118, 125, 168, 169, 174–178, 203, 438
s-triazines 30, 32, 33
Sugar acids.... 25, 27–28, 302, 304, 313, 315, 319
Sugar phosphates.... 302, 446, 453
Sulfur....198, 201, 206, 207, 517–518
Sulfur compounds....512
Sulphated sugars....303

T

Targeted....99, 189, 302, 376, 400, 402, 405, 439–447, 449–465, 472
Tobramycin....83
Toxins.... 365, 408, 414–417, 426, 428, 483
Transition metal ions.... 225, 228, 240

U

Ultrasound-accelerated derivatization 37
Uronic acids....303, 320
UV detection....37, 45, 49, 95, 99, 103, 138, 159, 160, 191, 198, 199, 201–206, 208, 218–221, 224, 228, 237, 267, 269, 293, 303–305, 314–316, 327, 328, 368, 369, 408, 416, 426, 429, 514, 521

W

Wine analysis 509–521
Wine metabolites 517